

## ABSTRACT

Title of Document: SYNTHESIS AND REACTIVITY OF  
MONOHYDROCARBYL PALLADIUM(IV)  
COMPLEXES USING H<sub>2</sub>O<sub>2</sub> AS OXIDANT IN  
PROTIC SOLVENTS

Williamson Njoroge Oloo, Ph.D., 2011

Directed By: Associate Professor Andrei N. Vedernikov,  
Department of Chemistry and Biochemistry

Mild, and selective transition metal catalyzed processes for the functionalization of C–H bonds utilizing environmentally benign and inexpensive O<sub>2</sub> and/ or H<sub>2</sub>O<sub>2</sub> oxidants are extremely attractive, as they render these transformations more atom economical and practical for large-scale syntheses. Our approach towards this end involves optimizing the oxidation and C–X reductive elimination steps of the proposed catalytic cycle using tridentate facially chelating ligands, which include 1-hydroxy-1,1-di(2-pyridyl)methoxide, a derivative of di(2-pyridyl)ketone (dpk) and 6-(2-pyridinoyl)pyridine-2-carboxylic acid (ppc).

Oxidation of the dpk- and the ppc-ligated palladacycles with H<sub>2</sub>O<sub>2</sub> in water and acetic acid solvents produces the corresponding monohydrocarbyl Pd(IV) complexes quantitatively. The mechanism of oxidation of these complexes was

investigated, and was proposed to involve addition of H<sub>2</sub>O<sub>2</sub> across the C=O bond of the ligand, followed by heterolytic cleavage of the O–O bond via nucleophilic attack of Pd(II) onto the hydroperoxo adduct.

The dpk- and ppc-ligated monohydrocarbyl Pd(IV) complexes undergo C–O reductive elimination at room temperature in acetic acid and/ or water to produce the corresponding phenols and/ or aryl acetates quantitatively. Mechanistic studies led us to propose a C–O reductive elimination reaction that proceeds either from a 5-coordinate intermediate, produced upon dissociation of the pyridine group of the dpk chelate or from a 6-coordinate Pd(IV) species.

Addition of HX (X=Cl, Br, and I) to aqueous solutions of the dpk-supported hydroxo-ligated monohydrocarbyl Pd(IV) complexes leads to quantitative formation of C–X bond-coupling products. Some of the corresponding X-ligated monohydrocarbyl Pd(IV) complexes were isolated from these solutions (X=Cl and Br), and could be independently prepared by oxidation of the hydrocarbyl Pd(II) precursors with the corresponding *N*-halogenosuccinimides (NXS).

Palladium catalyzed C–H functionalization reactions were performed in the presence of tridentate, facially chelating bis(6-methyl-2-pyridyl)methanesulfonate ligand. Substituted 2-phenylpyridine substrates underwent predominantly C–C coupling reactions with minor C–O coupling products produced, while 2-benzyl- and 2-phenoxy-pyridine substrates that form 6-membered palladacycles produced the corresponding C–O coupling products selectively in high yields. These reactions were significantly slower in the absence of the ligand, and no reactions took place in the absence of Pd(OAc)<sub>2</sub>.

SYNTHESIS AND REACTIVITY OF MONOHYDROCARBYL PALLADIUM(IV)  
COMPLEXES USING HYDROGEN PEROXIDE AS OXIDANT IN PROTIC  
SOLVENTS

By

Williamson Njoroge Oloo

Dissertation submitted to the Faculty of the Graduate School of the  
University of Maryland, College Park, in partial fulfillment  
of the requirements for the degree of  
Doctor of Philosophy  
2011

Advisory Committee:  
Associate Professor Andrei Vedernikov, Chair  
Professor Michael Doyle  
Professor Bryan Eichhorn  
Professor Daniel Falvey  
Professor Gregory Jackson

© Copyright by  
Williamson Njoroge Oloo  
2011

## Dedication

Dedicated to those struggling against oppression and aggression.

Thus far has the Lord brought me.....

## Acknowledgements

I start by thanking my former lab mates, Dr. Jing Zhang, Dr. Eugene Khaskin, Pratheep Khanthapura, and especially Dr. Julia Khusnutdinova, who offered tremendous help during my most difficult, first and second years in Grad school. I am also grateful to my current lab mates, Anna Sberegaeva, Shrinwantu Pal, Xiaohang Liu, Yang Wen, and Dr. Daoyong Wang. I really cherish the time I had with you all.

I greatly appreciate working with great undergraduate and High school students, including Huong-Thu Tran, John Jubar, Jilian Neifeld, Gillian Anku, William Sama, and Anshu Mano. I hope you learnt from me as much as I learnt from you all.

I am grateful to Dr. Yiu Fai Lam and Dr. Yinde Wang for assisting me in the NMR experiments, and for being available at night and in the weekends to fix the instruments so that my experiments could be completed in time. I also thank Dr. Peter Zavalij for running the X-ray diffraction experiments, and for being available even at times in the weekend to run my urgent samples.

I thank my undergraduate Mentor, Roger Young. He has been like father to me since my undergraduate years, and I would not be what I am without his help. I owe so much to him. I also thank David Jasper, who established a scholarship foundation that paid for my undergraduate tuition.

I am grateful to my family members, including Doreen Selly Oloo and her husband Anthony Dale, and Steve Oloo, and my friend Raphael Kamau. You have all made my life easier during my time in the graduate school. I am grateful to my father,

Shadrach Oloo for everything he has given me, and my mother Beth Oloo, for all the sacrifices she has made to make it possible for me to be what I am today.

I am also thankful to my great friends who have supported me throughout my time in the graduate school, including Rennisha Wickham for being a great friend and offering encouragement in tough times, Dominique Downing, Melantha Jackson, and Geraldine Echebiri. I especially thank Andrea Andrew for being a great friend, and assisting me through my dissertation write up.

I am thankful to my committee members and to my advisor, Dr. Andrei Vedernikov. He has given me the time and space to mature as a scientist, and given me many valuable life's lessons, and for that I am very grateful.

# Table of Contents

Dedication.....	ii
Thus far has the Lord brought me.....	iii
Acknowledgements.....	iv
Table of Contents.....	vi
List of Tables.....	xi
List of Figures.....	xiv
List of Schemes.....	xxi
List of Abbreviations.....	xxvii
Chapter 1: Oxidative Palladium Catalyzed Functionalization of C–H Bonds.....	1
1.1 Introduction.....	1
1.2 Palladium Catalyzed Oxygenation of C–H Bonds.....	4
1.2.1 Utilization of Iodine-Based Reagents as Oxidants for the C–H Bond Oxygenation Reactions.....	4
1.2.2 Utilization of Peroxie-based Reagents as Oxidants for the Palladium Catalyzed Oxygenation of C–H Bonds.....	12
1.2.3 Utilization of O <sub>2</sub> as Oxidant for Palladium Catalyzed Oxygenation Reactions.....	17
1.3 Palladium Catalyzed Halogenation of C–H bonds.....	20
1.4 Our Approach and Goal.....	26
Chapter 2: Synthesis of Monohydrocarbly Pd(IV) Complexes.....	31
2.1 Introduction.....	31
2.2 Preparation and Reactivity of Acetato-bridged Palladacycles <b>49-57</b> .....	43
2.2.1 Preparation of Acetato-bridged Palladacycles <b>49-57</b> .....	43
2.2.2 Attempted Aerobic Oxidation of Acetato-bridged Palladacycles.....	46
2.3 Preparation and Reactivity of dpms-ligated Palladacycles <b>58-60</b> .....	47
2.3.1 Preparation of Complexes <b>58-60</b> .....	47
2.3.2 Attempted Aerobic Oxidation of dpms-ligated Palladacycles <b>58-60</b> .....	48
2.3.3 Attempted Oxidation of Acetato-bridged Palladacycles <b>49-57</b> with H <sub>2</sub> O <sub>2</sub> .....	49
2.3.4 Reactivity of dpms-ligated Palladacycles <b>58-60</b> Towards Oxidation with H <sub>2</sub> O <sub>2</sub> .....	51

2.4 Preparation of dpk-ligated Palladacycles <b>66-74</b> .....	55
2.4.1 Preparation of dpk-ligated Palladacycles <b>66</b> and <b>67</b> .....	55
2.4.2 Preparation of dpk-ligated Palladacycles <b>68-71</b> .....	57
2.4.3 Preparation of dpk-ligated Palladacycles <b>72</b> and <b>73</b> .....	59
2.4.4 Preparation of dpk-ligated Palladacycles <b>74</b> .....	59
2.5 Oxidation of dpk-ligated Palladacycles <b>66-74</b> with H <sub>2</sub> O <sub>2</sub> in Water .....	61
2.5.1 Oxidation of Complexes <b>66</b> and <b>67</b> to Monohydrocarbyl Pd(IV) Complexes <b>75</b> and <b>76</b> with H <sub>2</sub> O <sub>2</sub> in Water .....	61
2.5.2 Oxidation of Complexes <b>66</b> and <b>67</b> to Monohydrocarbyl Pd(IV) Complexes <b>75</b> and <b>82</b> with H <sub>2</sub> O <sub>2</sub> in Acetic Acid .....	69
2.5.3 Oxidation of Complexes <b>68-71</b> to Monohydrocarbyl Pd(IV) Complexes <b>83-86</b> with H <sub>2</sub> O <sub>2</sub> in Water .....	75
2.5.4 Oxidation of Complex <b>69</b> to Monohydrocarbyl Pd(IV) Complexes <b>84</b> and <b>92</b> with H <sub>2</sub> O <sub>2</sub> in Acetic Acid .....	84
2.5.5 Oxidation of Complexes <b>72</b> and <b>73</b> to Monohydrocarbyl Pd(IV) Complexes <b>93</b> and <b>94</b> with H <sub>2</sub> O <sub>2</sub> in Water and Acetic Acid .....	86
2.5.6 Oxidation of Complex <b>74</b> to Monohydrocarbyl Pd(IV) Complex <b>96</b> with H <sub>2</sub> O <sub>2</sub> in Water .....	94
2.6 Mechanism of Oxidation of Hydrocarbyl Pd(II) Complexes with H <sub>2</sub> O <sub>2</sub> .....	97
2.6.1 Introduction .....	97
2.6.2 Kinetics Study of the Reaction of Organopalladium(II) Complexes <b>66</b> and <b>67</b> with H <sub>2</sub> O <sub>2</sub> in Water .....	102
2.6.3 Kinetics Study of the Reaction of Organopalladium(II) Complexes <b>68-71</b> with H <sub>2</sub> O <sub>2</sub> in Water .....	120
2.6.4 <sup>1</sup> H NMR Study of the Reaction of Organopalladium(II) Complexes <b>72</b> and <b>73</b> with H <sub>2</sub> O <sub>2</sub> in Water .....	126
2.7 Summary and conclusion .....	127
2.8 Experimental .....	129
2.8.1 General .....	129
2.8.2 Computational details .....	129
2.8.3 Acetate-bridged Palladacycles .....	130
2.8.4 Preparation of dpms-ligated Palladacycles .....	138
2.8.5 Preparation of dpk-ligated Palladacycles .....	141
2.8.6 Preparation of Monohydrocarbyl Pd(IV) Complexes .....	151
Chapter 3: Reactivity of Monohydrocarbyl Pd(IV) Complexes in Various Solvents	
.....	178
3.1 Introduction .....	178
3.2 C–O Reductive Elimination Reactivity at Monohydrocarbyl Pd(IV) Complexes <b>14-17</b> in Various Solvents .....	186
3.2.1 C–O Reductive Elimination Reactivity at Monohydrocarbyl Pd(IV) Complexes <b>14-17</b> in Water .....	186
3.2.2 C–O Reductive Elimination Reactivity at Monohydrocarbyl Pd(IV) Complexes <b>15</b> in Acetic Acid .....	200

3.3 C–O Reductive Elimination Reactivity at Monohydrocarbyl Pd(IV) Complexes <b>31</b> and <b>32</b> in Various Solvents .....	201
3.3.1 C–O Reductive Elimination Reactivity at Monohydrocarbyl Pd(IV) Complexes <b>31</b> and <b>32</b> in Acetic Acid .....	201
3.3.2 C–O Reductive Elimination Reactivity at Monohydrocarbyl Pd(IV) Complex <b>31</b> in Water .....	214
3.3.3 C–O Reductive Elimination Reactivity at Monohydrocarbyl Pd(IV) Complexes <b>31</b> and <b>32</b> in Water in the Presence of Base.....	221
3.4 C–O Reductive Elimination Reactivity at Monohydrocarbyl Pd(IV) Complexes <b>37</b> and <b>38</b> in Acetic Acid Solvent .....	226
3.5 C–O Reductive Elimination Reactivity at Monohydrocarbyl Pd(IV) Complexes <b>46</b> and <b>53</b> .....	227
3.5.1 C–O Reductive Elimination Reactivity at Monohydrocarbyl Pd(IV) Complexes <b>46</b> in Water and Acetic Acid Solvents.....	227
3.5.2 C–O Reductive Elimination Reactivity at Monohydrocarbyl Pd(IV) Complexes <b>46</b> in Solid State .....	229
3.5.3 C–O Reductive Elimination Reactivity at Monohydrocarbyl Pd(IV) Complexes <b>53</b> in Water and Acetic Acid Solvents.....	230
3.6 C–O Reductive Elimination Reactivity at Monohydrocarbyl Pd(IV) Complexes <b>59</b> in Water.....	232
3.7 Summary and Conclusions of C–O Reductive Elimination Reactions at Monohydrocarbyl Pd(IV) Complexes.....	235
3.7 Experimental.....	238
3.8.1 General.....	238
3.8.2 Computational details.....	238
3.8.3 Characterization of products of reductive elimination.....	239
3.8.4 Kinetic experiments .....	249
Chapter 4: Synthesis and Reactivity of Monohydrocarbyl Pd(IV)–X in Water (X=Cl, Br, and I).....	263
4.1 Introduction.....	263
4.2 C–Cl Bond Formation at Monohydrocarbyl Pd(IV) Alkoxides in Water in the Presence of HCl .....	271
4.2.1 C–Cl Bond Formation at 2-Aroylpyridine-derived Monohydrocarbyl Pd(IV) Alkoxides <b>9</b> and <b>15</b> in Water in the Presence of HCl.....	271
4.2.2 C–Cl Bond Formation at 2-Phenoxy pyridine-derived Monohydrocarbyl Pd(IV) Alkoxides <b>18</b> in Water in the Presence of HCl.....	275
4.2.3 C–Cl Bond Formation at 2-Tolylpyridine-derived Monohydrocarbyl Pd(IV) Alkoxide <b>24</b> in Water in the Presence of HCl.....	279
4.3 C–Br Bond Formation at Monohydrocarbyl Pd(IV) Alkoxides in Water in the Presence of HBr .....	293
4.3.1 C–Br Bond Formation at 2-Aroylpyridine-derived Monohydrocarbyl Pd(IV) Alkoxides <b>9</b> and <b>15</b> in Water in the Presence of HBr.....	293
4.3.2 C–Br Bond Formation at 2-Phenoxy pyridine-derived Monohydrocarbyl Pd(IV) Alkoxides <b>18</b> in Water in the Presence of HBr.....	297

4.3.3 C–Br Bond Formation at 2-Tolylpyridine-derived Monohydrocarbyl Pd(IV) Alkoxides <b>24</b> in Water in the Presence of HBr.....	301
4.4 C–I Bond Formation at Monohydrocarbyl Pd(IV) Alkoxides in Water in the Presence of HI.....	307
4.4.1 C–I Bond Formation at 2-Tolylpyridine-derived Monohydrocarbyl Pd(IV) Alkoxide <b>24</b> in Water in the Presence of HI.....	307
4.4.2 C–I Bond Formation at 2-Aroylpyridine-derived Monohydrocarbyl Pd(IV) Alkoxides <b>15</b> in Water in the Presence of HI.....	311
4.4.3 C–I Bond Formation at 2-Phenoxypyridine-derived Monohydrocarbyl Pd(IV) Alkoxides <b>15</b> in Water in the Presence of HI.....	313
4.5 Attempted C–F Bond Formation at Monohydrocarbyl Pd(IV) Alkoxides in Water in the Presence of HCl.....	315
4.5.1 Attempted C–F Bond Formation at 2-Tolylpyridine-derived Monohydrocarbyl Pd(IV) Alkoxide <b>24</b> in Water, in the Presence of HF.....	315
4.6 Mechanism of C–X Reductive Elimination From Monohydrocarbyl Pd(IV) Alkoxides in Water, in the Presence of HX.....	317
4.7 Summary and Conclusions.....	320
4.8 Experimental.....	323
Chapter 5: PPC Ligand-enabled Functionalization of C–Pd Bonds With H <sub>2</sub> O <sub>2</sub> in Acetic Acid.....	329
5.1 Introduction.....	329
5.2 Preparation of Palladacycles Supported by ppc Ligand, <b>15–19</b> .....	338
5.3 Reactivity of Palladacycles Supported by ppc Ligand, <b>15–19</b> with H <sub>2</sub> O <sub>2</sub> in Acetic Acid.....	341
5.3.1 Reactivity of Complex <b>15</b> with H <sub>2</sub> O <sub>2</sub> in Acetic Acid at Room Temperature.....	342
5.3.2 Reactivity of Complex <b>16</b> with H <sub>2</sub> O <sub>2</sub> in Acetic Acid at Room Temperature.....	356
5.3.3 Reactivity of Complex <b>17</b> with H <sub>2</sub> O <sub>2</sub> in Acetic Acid at Room Temperature.....	363
5.3.4 Reactivity of Complex <b>18</b> with H <sub>2</sub> O <sub>2</sub> in Acetic Acid at Room Temperature.....	371
5.3.5 Reactivity of Complex <b>19</b> with H <sub>2</sub> O <sub>2</sub> in Acetic Acid at Room Temperature.....	378
5.4 Summary and Conclusions.....	384
5.5 Application of the ppc Ligand Towards C–H Bond Activation.....	387
5.6 Application of the ppc Ligand Towards Catalytic C–H Bond Functionalization.....	392
5.6 Experimental.....	395
Chapter 6: Ligand-Enabled Oxidative Palladium Catalyzed Functionalization of Aromatic C–H Bonds.....	409
6.1 Introduction.....	409

6.2 Results and Discussion .....	419
6.3 Summary and Conclusion .....	432
6.4 Experimental .....	433
Chapter 7: Conclusion.....	435
7.1 Summary and Conclusion.....	435
7.2 Future Work .....	438
NMR Spectra .....	439
Bibliography .....	495

## List of Tables

Table 2.1. Ratio of the presumed <i>cis</i> - and <i>trans</i> - isomers of complexes <b>49</b> and <b>50</b> , as determined by <sup>1</sup> H NMR spectroscopy in CDCl <sub>3</sub> at 22 °C. ....	44
Table 2.2. Ratio of the presumed <i>cis</i> - and <i>trans</i> - isomers of complexes <b>51-54</b> as determined by <sup>1</sup> H NMR spectroscopy in CDCl <sub>3</sub> at 22 °C. ....	45
Table 2.3. Ratio of the presumed <i>cis</i> - and <i>trans</i> - isomers of complexes <b>55</b> and <b>56</b> , as determined by <sup>1</sup> H NMR spectroscopy in dmsd-d <sub>6</sub> at 22 °C. ....	45
Table 2.4. Selected <sup>1</sup> H NMR peaks for complex <b>66</b> . ....	57
Table 2.5. Selected <sup>1</sup> H NMR peaks for complex <b>69</b> . ....	58
Table 2.6. Oxidation of 0.010 M D <sub>2</sub> O solution of complexes <b>68-71</b> with 1.5 equivalent of H <sub>2</sub> O <sub>2</sub> at 3 °C, showing the ratio of the major and minor products. ....	79
Table 2.7. Oxidation of 0.010 M D <sub>2</sub> O solution of complex <b>69</b> with H <sub>2</sub> O <sub>2</sub> , showing the ratio of the major product <b>84</b> and minor product <b>88</b> as a function of [H <sub>2</sub> O <sub>2</sub> ] and temperature. ....	80
Table 2.8. Oxidation of 0.010 M D <sub>2</sub> O solution of complex <b>69</b> with 2.0 eq of H <sub>2</sub> O <sub>2</sub> at 17°C, showing the ratio of the major product <b>84</b> and minor product <b>88</b> as a function of pD. ....	81
Table 2.9. Selected <sup>1</sup> H NMR chemical shifts for complexes <b>69</b> , <b>84</b> , and <b>88</b> in D <sub>2</sub> O at room temperature. ....	83
Table 2.10. Selected <sup>1</sup> H NMR signals of complex <b>72</b> and <b>93</b> in water at room temperature. ....	87
Table 2.11. Selected <sup>1</sup> H NMR signals of complex <b>73</b> and <b>94</b> in water at room temperature. ....	91
Table 2.12. Selected <sup>1</sup> H NMR signals of complex <b>74</b> and <b>96</b> in D <sub>2</sub> O at room temperature. ....	94
Table 2.13. Oxidation of complex <b>67</b> with H <sub>2</sub> O <sub>2</sub> in water, showing the concentration of the intermediate “ <b>X</b> ” as a function of H <sub>2</sub> O <sub>2</sub> concentration and temperature. ....	107
Table 2.14. Selected <sup>1</sup> H NMR chemical shifts for complexes <b>67</b> , <b>76</b> , and intermediate “ <b>X</b> ” in D <sub>2</sub> O at 0°C. ....	108
Table 2.15. The rate constants for the oxidation of complex <b>67</b> at 3 °C with various concentrations of H <sub>2</sub> O <sub>2</sub> . ....	114
Table 2.16. Time for 50% conversion of complex <b>67</b> in acetic acid at 6 °C, in the presence and absence of benzoquinone additive. ....	116
Table 2.17. Time for 50 % conversion of complex <b>67</b> in buffered aqueous acidic, basic and non-buffered conditions. ....	119

Table 2.18. Correlation between the observed first order rate constants and the $\sigma_m$ for oxidation of various 4-substituted phenylpyridine dpk-derived palladacycles with excess $H_2O_2$ at 3 °C under pseudo-first order conditions.....	121
Table 2.19. Observed first order rate constants for the depletion of complex <b>69</b> in acetic acid at 3 °C, in the presence and absence of benzoquinone additive. ....	122
Table 2.20. Oxidation of 0.010 M $D_2O$ solutions of complex <b>69</b> with excess $H_2O_2$ at 3 °C in the presence of various additives. ....	126
Table 3. 1. Observed first order rate constants for C–O reductive elimination at complex <b>15</b> in $D_2O$ in the presence of various additives at 22 °C in water. ....	190
Table 3. 2. Observed first order rate constants for C–O reductive elimination at complexes <b>14-17</b> in water in the presence 4.0 equivalents of tfa- $d_1$ at 22 °C.....	191
Table 3. 3. Observed first order rate constants for C–O reductive elimination at complexes <b>14-17</b> in water at 22 °C. ....	198
Table 3. 4. $^1H$ NMR yields of phenol and aryl acetate from C–O reductive elimination reactions at complexes <b>31</b> and <b>32</b> in acetic acid at 63°C. ....	202
Table 3. 5. Observed first order rate constants for the C–O reductive elimination reaction at complex <b>31</b> in AcOD at 56°C in the presence and absence of 5.0 equivalents of tfa additive.....	204
Table 3. 6. Observed first order rate constants for the C–O reductive elimination reaction at complex <b>31</b> in AcOD at 56°C in the presence and absence of 5.0 equivalents of LiOAc additive. ....	205
Table 3. 7. Observed first order rate constants for the C–O reductive elimination reaction at complex <b>31</b> in AcOD at 48°C in the presence and absence of 5.0 equivalents of pyridine additive.....	206
Table 3. 8. Time (min) for the 50% conversion of complex <b>31</b> in the C–O reductive elimination reaction at complex <b>31</b> in AcOD at 48°C in the presence and absence of 28% of water. ....	207
Table 3. 9. summary of the influence of various additives on the rate of C–O reductive elimination from acetic acid solutions of complex <b>31</b> . ....	207
Table 3. 10. Observed first order rate constants for C–O reductive elimination from acetic acid solutions of complex <b>31</b> (OOCCF <sub>3</sub> ) at various temperatures. ....	210
Table 3. 11. Observed first order rate constants for the C–O reductive elimination reaction at complexes <b>31</b> and <b>32</b> in AcOD at 50°C. ....	213
Table 3. 12. The time for 50 % conversion of a 0.010 M $D_2O$ solution of complex <b>31</b> at 70°C in the presence of 1-3 equivalent trifluoroacetic acid. ....	217

Table 3. 13. The C–O reductive elimination reaction of 0.010 M D <sub>2</sub> O solution of complex <b>31</b> at 70°C in the presence of 1 equivalent of trifluoroacetic acid and 20 % of complex <b>39</b> .	218
Table 3. 14. Observed first order rate constants for C–O reductive elimination at complex <b>31</b> in water in the presence of various equivalents of NaOH at 50°C.	224
Table 4. 1. <sup>1</sup> H NMR yields of the aryl chloride <b>25</b> and phenol <b>26</b> products relative to the amount of HCl used.	280
Table 4. 2. Fraction of the aryl bromide <b>42</b> and phenol <b>25</b> relative to the amount of HBr added according to <sup>1</sup> H NMR analysis.	302
Table 4. 3. Observed first order rate constants for the C–X reductive elimination reactions in water at room temperature (X = OH, Cl, and Br).	318
Table 6. 1. Palladium catalyzed C–H bond functionalization using H <sub>2</sub> O <sub>2</sub> as terminal oxidant in the presence of various ligands.	422
Table 6. 2. Palladium catalyzed <i>ortho</i> C–H bond functionalization of compound <b>12</b> in acetic acid using H <sub>2</sub> O <sub>2</sub> as terminal oxidant in the presence of Me <sub>2</sub> -dmops ligand, showing relative fractions of C–C and C–O coupling products as a function of temperature.	424
Table 6. 3. Palladium catalyzed <i>ortho</i> C–H bond functionalization of compound <b>12</b> in acetic acid using H <sub>2</sub> O <sub>2</sub> as terminal oxidant in the presence of Me <sub>2</sub> -dmops ligand, showing the conversion of compound <b>12</b> and yield of compound <b>20</b> as a function of catalyst loading.	424
Table 6. 4. Palladium catalyzed <i>ortho</i> C–H bond functionalization in acetic acid using H <sub>2</sub> O <sub>2</sub> as terminal oxidant in the presence of Me <sub>2</sub> -dmops ligand.	425

## List of Figures

Figure 2.1. ORTEP drawing (50 % probability ellipsoid) of complex <b>63</b> .....	53
Figure 2.2. ORTEP drawing (50 % probability ellipsoid) of complex <b>74</b> .....	60
Figure 2.3. ORTEP drawing (50 % probability ellipsoid) of complex <b>75</b> .....	62
Figure 2.4. ORTEP drawing (50 % probability ellipsoid) of complex <b>79</b> .....	66
Figure 2.5. pH of the solution of 0.0052 mM solution of <b>75</b> in water vs added volume of 0.1000 M NaOH. ....	68
Figure 2.6. Acetic acid solutions of (a) complex <b>66</b> ; (b) complex <b>81</b> at room temperature. ....	70
Figure 2.7. Acetic acid solutions of (a) complex <b>75</b> ; (b) complex <b>81</b> at room temperature. ....	71
Figure 2.8. Room temperature solutions of mixed AcOD/D <sub>2</sub> O solvent system (1:1) of (a) Complex <b>66</b> ; (b) solution of complex <b>66</b> after oxidation with 3 eq H <sub>2</sub> O <sub>2</sub> at room temperature (c) complex <b>75</b> ; (d) complex <b>81</b> generated in acetic acid.....	72
Figure 2.9. Room temperature AcOD solution of (a) complex <b>67</b> , (b) complex <b>82</b> ...	74
Figure 2.10. Room temperature AcOD solutions of (a) complex <b>76</b> ; (b) complex <b>82</b> . ....	75
Figure 2.11. ORTEP drawing (50 % probability ellipsoid) of complex <b>91</b> .....	77
Figure 2.12. <sup>1</sup> H NMR spectra of (a) 0.010 M D <sub>2</sub> O solution of complex <b>69</b> at 25 °C, (b) D <sub>2</sub> O solution of complexes <b>84</b> (major) and <b>88</b> (minor), (c) D <sub>2</sub> O solution of the oxapalladacycle <b>108</b> at the end of the reaction. ....	78
Figure 2.13. (a) Plot for the oxidation of 0.010 M D <sub>2</sub> O solution of complex <b>69</b> in water with 1.5 eq H <sub>2</sub> O <sub>2</sub> at 3 °C showing the fraction of the starting complex <b>69</b> , the major product <b>84</b> , and the minor product <b>88</b> as a function of reaction time; (b) Plot for the oxidation of 0.010 M D <sub>2</sub> O solution of complex <b>68</b> in water with 1.5 eq H <sub>2</sub> O <sub>2</sub> at 3 °C Oxidation showing the fraction of the Pd(II) precursor <b>68</b> , the major product <b>83</b> , and the minor product <b>87</b> , as a function of time. ....	79
Figure 2.14. (a) ORTEP drawing (50% probability ellipsoids) of dication <b>91</b> in <b>91(OOCCF<sub>3</sub>)<sub>2</sub>H<sub>2</sub>O</b> , and proposed structures for (b) <b>84</b> , the major product of oxidation, and (c) <b>88</b> , the minor product of oxidation.....	82
Figure 2.15. (a) Acetic acid solution of complex <b>69</b> ; (b) Acetic acid solution of complex <b>69</b> after addition of 3.0 equivalents of H <sub>2</sub> O <sub>2</sub> at 22°C, showing products <b>84</b> (minor) and <b>92</b> (major); (c) Acetic acid solution of complex <b>69</b> two days later, after addition of 5.0 equivalents of pyridine- <i>d</i> <sub>5</sub> , showing the corresponding phenol and aryl acetate products. ....	85

Figure 2.16. $^1\text{H}$ NMR of complex <b>93</b> in $\text{dms}\text{-d}_6$ at room temperature.....	89
Figure 2.17. ORTEP drawing (50 % probability ellipsoid) of complex <b>93</b> .....	89
Figure 2.18. Room temperature acetic acid solutions of (a) complex <b>73</b> ; (b) complex <b>73</b> , 2 minutes after addition of 3 eq $\text{H}_2\text{O}_2$ , showing complexes <b>95</b> (minor) and <b>94</b> (major) (c) complex <b>73</b> , 10 minutes after addition of $\text{H}_2\text{O}_2$ , showing complex <b>94</b> ; (d) complex <b>73</b> at the end of reaction, showing the aryl acetate as the major product of decomposition.....	93
Figure 2.19. (a) $\text{D}_2\text{O}$ solution of complex <b>74</b> at $0^\circ\text{C}$ ; (b) $\text{D}_2\text{O}$ solution of complex <b>96</b> at $0^\circ\text{C}$ .....	95
Figure 2.20. (a) Change of UV-visible spectra of 0.010 M $\text{D}_2\text{O}$ solutions of complex <b>74</b> upon addition of 10.0 equivalents of $\text{H}_2\text{O}_2$ at $0^\circ\text{C}$ (1.0 cm cuvette was used). (b) Change in absorbance as a function of time at the wavelength of 420 nm, over a period of 60 minutes .....	96
Figure 2.21. $^1\text{H}$ NMR spectra in $\text{D}_2\text{O}$ taken at $3^\circ\text{C}$ for (a) complex <b>66</b> ; (b) complex <b>66</b> , 18 minutes after addition of 10.0 eq of $\text{H}_2\text{O}_2$ , together with an intermediate “Y” and Pd(IV) product <b>75</b> ; and (c), at the end of reaction, showing Pd(IV) complex <b>75</b> .....	104
Figure 2.22. Plot for the oxidation of complex <b>66</b> with 10.0 eq $\text{H}_2\text{O}_2$ in $\text{D}_2\text{O}$ at $3^\circ\text{C}$ , showing the fraction of starting Pd(II) complex <b>66</b> , the intermediate complex, and the product <b>75</b> as a function of time.....	104
Figure 2.23. $^1\text{H}$ NMR taken in $\text{D}_2\text{O}$ at $3^\circ\text{C}$ for (a) complex <b>67</b> ; (b) complex <b>67</b> , 10 minutes after addition of 20.0 eq of $\text{H}_2\text{O}_2$ , together with intermediate “X” and Pd(IV) product <b>76</b> ; and (c), at the end of reaction, showing Pd(IV) complex <b>76</b> .....	105
Figure 2.24. Plot for the oxidation of complex <b>67</b> with 20.0 eq $\text{H}_2\text{O}_2$ in $\text{D}_2\text{O}$ at $3^\circ\text{C}$ , showing the fraction of starting Pd(II) complex <b>67</b> , the intermediate complex, and the product <b>76</b> as a function of time.....	106
Figure 2.25. ESI-MS spectrum of an aqueous solution 0.010 M complex <b>67</b> , 18 seconds after adding 20.0 equivalents of $\text{H}_2\text{O}_2$ in water at $0^\circ\text{C}$ .....	107
Figure 2.26. Representative kinetic plots of $\ln([\mathbf{67}]_0/[\mathbf{67}]_t)$ vs time for reaction mixtures containing aqueous solutions of 0.010 M complex <b>67</b> with various equivalents of $\text{H}_2\text{O}_2$ at $3^\circ\text{C}$ (a-b) 10.0 equivalents of $\text{H}_2\text{O}_2$ was used (c-d) 15.0 equivalents of $\text{H}_2\text{O}_2$ was used. ....	112
Figure. 2.27. Kinetics modeling plots for the reaction between 0.010 M $\text{D}_2\text{O}$ solutions of complex <b>67</b> with (a) 20.0 equivalents of $\text{H}_2\text{O}_2$ , and (b) 15.0 equivalents of $\text{H}_2\text{O}_2$ at $3^\circ\text{C}$ . The plots include concentration of complex <b>67</b> (blue circles/ diamonds), intermediate “X” (red circles/ diamonds), and complex <b>76</b> (green circles/ diamonds) as a function of time. The experimental concentrations are presented as circles while the modeled concentrations are presented as diamonds. ....	113

Figure 2.28. Representative kinetics plots of $\ln([\text{Pd(II)}]_o/[\text{Pd(II)}]_t)$ vs. time for the oxidation of 0.010 M solutions of complexes <b>69</b> and <b>71</b> with ~ 7.0 equivalents of $\text{H}_2\text{O}_2$ in $\text{D}_2\text{O}$ at 3 °C. ....	120
Figure 2.29. Hammett plot for the oxidation of 4-substituted phenylpyridine dpk-derived palladacycles <b>68-71</b> with excess $\text{H}_2\text{O}_2$ at 3 °C under pseudo-first order conditions. ....	121
Fig. 2.30. (a) A Kinetic plot for $\ln([\mathbf{69}]_o/[\mathbf{69}]_t)$ vs time plot for the oxidation of 0.010 M complex <b>69</b> with ~6 equivalents of $\text{H}_2\text{O}_2$ in 1.0 ml $\text{D}_2\text{O}$ at 3 °C at pD = 4.99 (b) Kinetic plot for $\ln([\mathbf{69}]_o/[\mathbf{69}]_t)$ vs time plot for the oxidation of 0.010 M complex <b>69</b> with ~25 equivalents of $\text{H}_2\text{O}_2$ in 1.0 ml $\text{D}_2\text{O}$ at 3 °C at pD = 8.88. ....	125
Figure 3. 1. Plot for the C–O reductive elimination reaction of 0.010 M $\text{D}_2\text{O}$ solutions of complexes (a) <b>15</b> and <b>19</b> and (b) <b>17</b> and <b>21</b> at 22 °C. ....	187
Figure 3. 2. ORTEP drawings (50% probability ellipsoids) of Pd(II) aryloxide cation <b>23</b> in <b>23(OAc)</b> . ....	187
Figure 3. 3. First order kinetic plots for the decomposition of $\text{D}_2\text{O}$ solutions of complexes (a) <b>15</b> and (b) <b>14</b> in the presence of 4.0 equivalents of trifluoroacetic acid at 22 °C ....	191
Figure 3. 4. The DFT-calculated Gibbs energy reaction profile for C–O reductive elimination reaction at complex <b>15</b> in gas phase and aqueous solutions in parenthesis (kcal/mol) leading to corresponding palladacyclic aryloxide <b>23</b> . ....	196
Figure 3. 5. First order kinetic plots for the decomposition of aqueous solutions of complexes (a) <b>15</b> and (b) <b>17</b> at 22 °C. ....	198
Figure 3. 6. Hammett plot for the decomposition of aqueous solutions of complexes <b>14-17</b> at 22 °C. ....	199
Figure 3. 7. First order kinetic plot for the decomposition of complex <b>31</b> in AcOD/ $\text{D}_2\text{O}$ solvent mixture (5:2) at 49 °C ....	207
Figure 3. 8. First order kinetic plots for the decomposition of acetic acid solutions of complex <b>31</b> at (a) 47.5°C and (b) 56.5°C. ....	210
Figure 3. 9. Eyring plot for decomposition of complex <b>31(OOCCF<sub>3</sub>)</b> in acetic acid. ....	211
Figure 3. 10. First order kinetic plots for the C–O reductive elimination reaction at complex <b>31</b> in $\text{D}_2\text{O}$ at 70°C, in the presence of (a) 1.0 equivalent and (b) 3.0 equivalents of trifluoroacetic acid. ....	216
Figure 3. 11. First order kinetic plots for the C–O reductive elimination reaction at complex <b>31</b> in $\text{D}_2\text{O}$ at 70°C, in the presence of 1.0 equivalent of trifluoroacetic acid and 20 % of complex <b>39</b> . ....	218

Figure 3. 12. First order kinetic plots for the C–O reductive elimination reaction of aqueous solutions of complex <b>31</b> at 50°C in the presence of (a) 2.0 equivalents of NaOH and (b) 4.0 equivalents of NaOH .....	224
Figure 3. 13. <sup>1</sup> H NMR spectra of D <sub>2</sub> O solutions of (a) complex <b>59</b> ; (b) complex <b>59</b> ~ 11 hours after addition of H <sub>2</sub> O <sub>2</sub> , with “X” present, (c) complex <b>59</b> after one week, in the presence of both “X” and “Y”. The reaction was carried out at 22°C.....	233
Figure 3. 14. Plot showing the fraction of complex <b>59</b> and product “X” as a function of time over ~ 12 hours period.....	233
Figure 4. 1. Room temperature <sup>1</sup> H NMR spectra of (a) complex <b>9</b> in D <sub>2</sub> O; (b) complex <b>9</b> in D <sub>2</sub> O upon addition of HCl, showing an additional set of signals belonging to an intermediate; (c) the reaction mixture after C–Cl reductive elimination, showing product <b>11</b> .....	273
Figure 4. 2. Room temperature <sup>1</sup> H NMR spectra of (a) complex <b>15</b> in D <sub>2</sub> O, (b) the reaction mixture after C–Cl reductive elimination showing product <b>16</b> together with a symmetrical dpk-ligated Pd(II) product.....	275
Figure 4. 3. Room temperature <sup>1</sup> H NMR spectra of (a) complex <b>18</b> in D <sub>2</sub> O, (b) complex <b>18</b> in D <sub>2</sub> O upon addition of HCl, showing an additional set of signals belonging to an intermediate complex; (c) <sup>1</sup> H NMR of the reaction mixture after decomposition, showing the C–Cl reductive elimination product <b>19</b> together with a symmetrical dpk-ligated Pd(II) product in the presence of pyridine-d <sub>5</sub> , which was added to free any Pd-coordinated products.....	277
Figure 4. 4. (a) The aqua-ligated Pd(IV) complex <b>28</b> prepared via protonation of complex <b>24</b> with trifluoroacetic acid; (b) ORTEP drawing (50 % probability ellipsoid) of complex <b>30</b> .....	278
Figure 4. 5. Room temperature <sup>1</sup> H NMR spectra of (a) complex <b>24</b> in D <sub>2</sub> O, (b) complex <b>24</b> in D <sub>2</sub> O upon addition of HCl; (c) the reaction mixture after decomposition in the presence of pyridine-d <sub>5</sub> , showing C–Cl elimination product <b>25</b> and Pd(II) derived complexes.....	280
Figure 4. 6. (a) <sup>1</sup> H NMR of aqua-ligated Pd(IV) complex <b>28</b> in D <sub>2</sub> O at room temperature; (b) <sup>1</sup> H NMR of chloro-ligated Pd(IV) complex <b>29</b> in D <sub>2</sub> O at room temperature. ....	283
Figure 4. 7. Room temperature <sup>1</sup> H NMR spectra of (a) complex <b>24</b> in D <sub>2</sub> O, (b) complex <b>24</b> in D <sub>2</sub> O upon addition of HCl; (c) complex <b>29</b> in D <sub>2</sub> O....	285
Figure 4. 8. A kinetic plot for the depletion of <b>29</b> in water at 22°C in ln(C <sub>0</sub> /C) vs. time coordinates. ....	287
Figure 4. 9. A kinetic plot for the depletion of <b>29</b> in water in the presence of 2.0 equivalents of HCl at 22 °C in ln(C <sub>0</sub> /C) vs. time coordinates. ....	290

Figure 4. 10. Room temperature $^1\text{H}$ NMR spectra of (a) complex <b>29</b> in $\text{D}_2\text{O}$ , (b) complex <b>29</b> in $\text{D}_2\text{O}$ 6 hours after addition of 5.0 equivalents of pyridine, showing signals of a new species, presumably complex <b>32</b> . .....	292
Figure 4. 11. Room temperature $^1\text{H}$ NMR spectra of (a) complex <b>9</b> in $\text{D}_2\text{O}$ , (b) complex <b>9</b> in $\text{D}_2\text{O}$ upon addition of $\text{HBr}$ , showing additional signals belonging to an intermediate; (c) $^1\text{H}$ NMR of the reaction mixture after decomposition, showing the product of $\text{C}-\text{Br}$ elimination, <b>34</b> . .....	294
Figure 4. 12. Room temperature $^1\text{H}$ NMR spectra of (a) complex <b>15</b> in $\text{D}_2\text{O}$ , (b) the reaction mixture after decomposition, now in $\text{dms}\text{-d}_6$ in the presence of pyridine- $\text{d}_5$ , showing the presence of $\text{C}-\text{Br}$ elimination product <b>37</b> and a symmetrical dpk-ligated $\text{Pd}(\text{II})$ product. ....	296
Figure 4. 13. Room temperature $^1\text{H}$ NMR spectra of (a) complex <b>18</b> in $\text{D}_2\text{O}$ , (b) complex <b>18</b> in $\text{D}_2\text{O}$ upon addition of $\text{HBr}$ showing additional signals belonging to an intermediate, (c) $^1\text{H}$ NMR of the reaction mixture after decomposition, now in $\text{dms}\text{-d}_6$ in the presence of pyridine- $\text{d}_5$ , showing the presence of $\text{C}-\text{Br}$ elimination product <b>38</b> in the presence of (dpk) $\text{Pd}(\text{II})$ containing products.....	298
Figure 4. 14. Room temperature $^1\text{H}$ NMR spectra of (a) complex <b>24</b> in $\text{D}_2\text{O}$ , (b) complex <b>24</b> in $\text{D}_2\text{O}$ upon addition of $\text{HBr}$ showing the presence of additional set of signals belonging to an intermediate; (c) $^1\text{H}$ NMR of the reaction mixture after decomposition, now in $\text{dms}\text{-d}_6$ in the presence of pyridine- $\text{d}_5$ , showing the presence of $\text{C}-\text{Br}$ elimination product <b>42</b> in the presence of a symmetrical dpk-ligated $\text{Pd}(\text{II})$ product.....	303
Figure 4. 15. Room temperature $^1\text{H}$ NMR spectra of complexes (a) $28(\text{OOC}\text{CF}_3)_2$ , (b) <b>(28)Br<sub>2</sub></b> , and (c) <b>(28)Cl<sub>2</sub></b> , in $\text{D}_2\text{O}$ .....	305
Figure 4. 16. (a) Room temperature $^1\text{H}$ NMR spectrum of aqua-ligated $\text{Pd}(\text{IV})$ complex <b>(28)Br<sub>2</sub></b> in $\text{D}_2\text{O}$ at room temperature; (b) $^1\text{H}$ NMR of bromo-ligated(IV) complex <b>45</b> in $\text{D}_2\text{O}$ at room temperature. ....	306
Figure 4. 17. Kinetic plot for the depletion of <b>45</b> in water at $22^\circ\text{C}$ in the coordinates $\ln(\text{C}_0/\text{C})$ vs. time. ....	307
Figure 4. 18. Room temperature $^1\text{H}$ NMR spectra of (a) the hydroxo-ligated $\text{Pd}(\text{IV})$ complex <b>24</b> in $\text{D}_2\text{O}$ ; (b) the reaction solution upon decomposition of complex <b>24</b> in water in the presence of $\text{HI}$ , now in $\text{dms}\text{-d}_6$ in the presence of pyridine, showing the $\text{C}-\text{I}$ elimination product <b>46</b> . ....	309
Figure 4. 19. Room temperature $^1\text{H}$ NMR spectra of (a) the hydroxo-ligated $\text{Pd}(\text{IV})$ complex <b>15</b> in $\text{D}_2\text{O}$ ; (b) the reaction solution upon decomposition of complex <b>25</b> in water in the presence of $\text{HI}$ , now in $\text{dms}\text{-d}_6$ in the presence of pyridine- $\text{d}_5$ , showing the aryl iodide <b>51</b> and (dpk) $\text{Pd}(\text{II})$ containing products.....	312
Figure 4. 20. Room temperature $^1\text{H}$ NMR spectrum of (a) the hydroxo-ligated $\text{Pd}(\text{IV})$ complex <b>18</b> in $\text{D}_2\text{O}$ , (b) the reaction solution upon decomposition of complex <b>18</b> , now in $\text{dms}\text{-d}_6$ showing $\text{C}-\text{I}$ elimination product <b>53</b> . ...	314

Figure 4. 21. Room temperature $^1\text{H}$ NMR spectrum of (a) the hydroxo-ligated Pd(IV) complex <b>24</b> in $\text{D}_2\text{O}$ , (b) the reaction solution upon decomposition of complex <b>24</b> in water in the presence of HF, showing oxapalladacycle <b>31</b> .	316
Figure 4. 22. Hammett plot for the decomposition of aqueous solutions of complexes <b>23</b> , <b>58-60</b> at $22^\circ\text{C}$ .	319
Figure 5. 1. ORTEP drawing (50 % probability ellipsoids) of complex <b>18</b>	339
Figure 5. 2. Complex <b>19</b> , showing the hydrogen atoms $\text{H}_a$ and $\text{H}_b$ .	339
Figure 5. 3. Room temperature $^1\text{H}$ NMR spectrum of (a) complex <b>15</b> in $\text{AcOH-d}_4$ (b) complex <b>25</b> in $\text{AcOH-d}_4$ . The minor signals belong to products of decomposition.	343
Figure 5. 4. NOE experiment of complex <b>25</b> , showing the hydrogen atoms $\text{H}_a$ and $\text{H}_b$ .	345
Figure 5. 5. Room temperature $^1\text{H}$ NMR spectra of (a) Acetic solution of complex <b>25</b> , (b) acetic acid solution of a mixture of products of decomposition, aryl acetate <b>38</b> and inorganic product <b>30</b> .	353
Figure 5. 6. (a) Kinetics plot for the reaction mixture containing 0.010 M acetic acid solution of complex <b>15</b> and 5 eq of $\text{H}_2\text{O}_2$ , showing the fraction of the starting complex <b>15</b> , the organopalladium(IV) complex <b>25</b> , and aryl acetate product <b>38</b> , as a function of time; (b) Plot for the $\ln([\mathbf{25}]_o/[\mathbf{25}]_t)$ vs. time in acetic acid at room temperature.	354
Figure 5. 7. $^1\text{H}$ NMR spectra of acetic acid solution of (a) complex <b>16</b> and (b) complex <b>26</b> at room temperature. This spectrum also shows some products of decomposition.	357
Figure 5. 8. Room temperature $^1\text{H}$ NMR spectra for: (a) Acetic solution of complex <b>26</b> (b) acetic acid solution of products of decomposition, including aryl acetate <b>45</b> and inorganic product <b>30</b> .	361
Figure 5. 9. $^1\text{H}$ NMR spectra of acetic acid solution of (a) complex <b>17</b> and (b) a mixture of complexes <b>17</b> and <b>48</b> at room temperature.	364
Figure 5. 10. ESI-MS spectrum of acetic acid solution of a mixture of complexes <b>17</b> and $\text{H}_2\text{O}_2$ at room temperature.	364
Figure 5. 11. Room temperature $^1\text{H}$ NMR spectra for (a) Acetic solution of organopalladium(IV) complex <b>48</b> in the presence of organopalladium(II) precursor <b>17</b> ; (b) acetic acid solution of the products of decomposition, including the aryl acetate <b>53</b> , phenol <b>52</b> , and inorganic product <b>30</b> , in the presence of pyridine- $\text{d}_5$ added to free coordination products.	369

Figure 5. 12. Room temperature $^1\text{H}$ NMR spectra of acetic acid solution of (a) complex <b>18</b> and (b) a mixture of complexes <b>54</b> and <b>55</b> at room temperature. ....	372
Figure 5. 13. ESI–MS analysis of an acetic acid solution of complex <b>18</b> upon addition of $\text{H}_2\text{O}_2$ .....	372
Figure 5. 14. Room temperature $^1\text{H}$ NMR spectra for the, (a) Acetic solution of complex <b>55</b> and <b>56</b> ; (b) acetic acid solution of products of decomposition, including the aryl acetate <b>61</b> , phenol <b>60</b> , and inorganic product <b>30</b> . ....	377
Figure 5. 15. $^1\text{H}$ NMR spectra of acetic acid solution of (a) complex <b>19</b> and (b) a mixture of complexes <b>62</b> and <b>63</b> at room temperature. ....	379
Figure 5. 16. ESI–MS analysis of an acetic acid solution of complex <b>19</b> upon addition of $\text{H}_2\text{O}_2$ .....	379
Figure 5. 17. Room temperature $^1\text{H}$ NMR spectra for (a) Acetic solution of complex <b>63</b> and <b>64</b> ; (b) acetic acid solution of products of decomposition, including the aryl acetate <b>68</b> , phenol <b>67</b> , after addition of pyridine- $\text{d}_5$ to the reaction solution.....	383
Figure 5. 18. ORTEP drawing (50 % probability ellipsoids) of complex 30 .....	388

## List of Schemes

Scheme 1.1 .....	5
Scheme 1.2 .....	7
Scheme 1.3 .....	8
Scheme 1.4 .....	9
Scheme 1.5 .....	10
Scheme 1.6 .....	11
Scheme 1.7 .....	14
Scheme 1.8 .....	15
Scheme 1.9 .....	15
Scheme 1.10 .....	16
Scheme 1.11 .....	18
Scheme 1.12 .....	18
Scheme 1.13 .....	19
Scheme 1.14 .....	22
Scheme 1.15 .....	23
Scheme 1.16 .....	23
Scheme 1.17 .....	24
Scheme 1.18 .....	25
Scheme 1.19 .....	26
Scheme 1.20 .....	27
Scheme 1.21 .....	30
Scheme 2.1 .....	31
Scheme 2.2 .....	31
Scheme 2.3 .....	37
Scheme 2.4 .....	42
Scheme 2.5 .....	53
Scheme 2.6 .....	55
Scheme 2.7 .....	57
Scheme 2.8 .....	59

Scheme 2.9 .....	59
Scheme 2.10 .....	61
Scheme 2.11 .....	64
Scheme 2.12 .....	64
Scheme 2.13 .....	65
Scheme 2.14 .....	67
Scheme 2.15 .....	68
Scheme 2.16 .....	68
Scheme 2.17 .....	69
Scheme 2.18 .....	73
Scheme 2.19 .....	78
Scheme 2.20 .....	84
Scheme 2.21 .....	86
Scheme 2.22 .....	86
Scheme 2.23 .....	92
Scheme 2.24 .....	94
Scheme 2.25 .....	95
Scheme 2.26 .....	98
Scheme 2.27 .....	99
Scheme 2.28 .....	100
Scheme 2.29 .....	101
Scheme 2.30 .....	102
Scheme 2.31 .....	103
Scheme 2.32 .....	110
Scheme 2.33 .....	111
Scheme 2.34 .....	113
Scheme 2.35 .....	114
Scheme 3. 1 .....	178
Scheme 3. 2 .....	180
Scheme 3. 3 .....	181
Scheme 3. 4 .....	182

Scheme 3. 5.....	184
Scheme 3. 6.....	186
Scheme 3. 7.....	189
Scheme 3. 8.....	200
Scheme 3. 9.....	201
Scheme 3. 10.....	202
Scheme 3. 11.....	203
Scheme 3. 12.....	214
Scheme 3. 13.....	220
Scheme 3. 14.....	221
Scheme 3. 15.....	222
Scheme 3. 16.....	225
Scheme 3. 17.....	226
Scheme 3. 18.....	228
Scheme 3. 19.....	228
Scheme 3. 20.....	229
Scheme 3. 21.....	231
Scheme 3. 22.....	231
Scheme 3. 23.....	232
Scheme 4. 1.....	263
Scheme 4. 2.....	265
Scheme 4. 3.....	266
Scheme 4. 4.....	267
Scheme 4. 5.....	268
Scheme 4. 6.....	268
Scheme 4. 7.....	269
Scheme 4. 8.....	271
Scheme 4. 9.....	271
Scheme 4. 10.....	273
Scheme 4. 11.....	274
Scheme 4. 12.....	275

Scheme 4. 13.....	277
Scheme 4. 14.....	279
Scheme 4. 15.....	281
Scheme 4. 16.....	282
Scheme 4. 17.....	282
Scheme 4. 18.....	286
Scheme 4. 19.....	287
Scheme 4. 20.....	288
Scheme 4. 21.....	291
Scheme 4. 22.....	293
Scheme 4. 23.....	293
Scheme 4. 24.....	295
Scheme 4. 25.....	295
Scheme 4. 26.....	297
Scheme 4. 27.....	299
Scheme 4. 28.....	299
Scheme 4. 29.....	301
Scheme 4. 30.....	303
Scheme 4. 31.....	305
Scheme 4. 32.....	306
Scheme 4. 33.....	307
Scheme 4. 34.....	310
Scheme 4. 35.....	311
Scheme 4. 36.....	312
Scheme 4. 37.....	313
Scheme 4. 38.....	315
Scheme 4. 39.....	319
Scheme 4. 40.....	320
Scheme 4. 41.....	321
Scheme 5. 1.....	329
Scheme 5. 2.....	330

Scheme 5. 3.....	331
Scheme 5. 4.....	333
Scheme 5. 5.....	334
Scheme 5. 6.....	335
Scheme 5. 7.....	335
Scheme 5. 8.....	336
Scheme 5. 9.....	340
Scheme 5. 10.....	341
Scheme 5. 11.....	342
Scheme 5. 12.....	344
Scheme 5. 13.....	344
Scheme 5. 14.....	346
Scheme 5. 15.....	347
Scheme 5. 16.....	348
Scheme 5. 17.....	348
Scheme 5. 18.....	349
Scheme 5. 19.....	350
Scheme 5. 20.....	351
Scheme 5. 21.....	352
Scheme 5. 22.....	354
Scheme 5. 23.....	355
Scheme 5. 24.....	356
Scheme 5. 25.....	358
Scheme 5. 26.....	358
Scheme 5. 27.....	360
Scheme 5. 28.....	361
Scheme 5. 29.....	363
Scheme 5. 30.....	366
Scheme 5. 31.....	367
Scheme 5. 32.....	368
Scheme 5. 33.....	370
Scheme 5. 34.....	371
Scheme 5. 35.....	374

Scheme 5. 36.....	375
Scheme 5. 37.....	376
Scheme 5. 38.....	377
Scheme 5. 39.....	378
Scheme 5. 40.....	380
Scheme 5. 41.....	381
Scheme 5. 42.....	382
Scheme 5. 43.....	383
Scheme 5. 44.....	388
Scheme 5. 45.....	389
Scheme 5. 46.....	390
Scheme 5. 47.....	391
Scheme 5. 48.....	392
Scheme 5. 49.....	393
Scheme 6. 1.....	410
Scheme 6. 2.....	410
Scheme 6. 3.....	411
Scheme 6. 4.....	414
Scheme 6. 5.....	414
Scheme 6. 6.....	415
Scheme 6. 7.....	415
Scheme 6. 8.....	416
Scheme 6. 9.....	416
Scheme 6. 10.....	417
Scheme 6. 11.....	429
Scheme 6. 12.....	430
Scheme 6. 13.....	431
Scheme 7. 1.....	437

## List of Abbreviations

Ac	acetyl
Acac	acetylacetonate
Ac <sub>2</sub> O	acetic anhydride
AcOH	acetic acid
Ar	Aryl
Boc	<i>tert</i> -butoxycarbonyl
BQ	benzoquinone
Bu	butyl
Bpy	bipyridine
Cp	cyclopentadienyl
DMSO	dimethyl sulfoxide
Dppe	1,2-Bis(diphenylphosphino)ethane
FG	functional group
H <sub>2</sub> hpda	4-hydroxypyridine-2,6-dicarboxylic acid
I	Iodide
Me	Methyl
NBS	<i>N</i> -bromosuccinimide
NCS	<i>N</i> -chlorosuccinimide
NIS	<i>N</i> -iodosuccinimide
OAc	acetate
Ph	phenyl
Phpy	phenylpyridine
R	alkyl
Rt	room temperature
TFA	trifluoroacetic acid
THF	tetrahydrofuran
X	halide
XRD	X-ray diffraction

# Chapter 1: Oxidative Palladium Catalyzed Functionalization of C–H Bonds

## 1.1 Introduction

Transition metal catalyzed processes for the construction of C–C and C–Heteroatom bonds (Heteroatom= O, F, N, Cl, Br, and I) represent essential tools for synthetic organic chemistry. Mild and selective transformations of this type will find widespread use as key steps in target-oriented syntheses to afford natural products, advanced materials, pharmaceutical compounds, and other high-value commercial products. Traditional approaches for the installation of C–C and C–heteroatom bonds rely on prefunctionalized starting materials for both reactivity and selectivity, thus leading to additional costly steps to the overall synthesis of a molecule. Procedures which involve direct C–H bond functionalization are therefore attractive as they will not only improve atom economy and increase the overall efficiency of multistep synthetic sequences, but they will also render the transformations more economically favorable.<sup>1,2</sup>

Direct C–H bond functionalization reactions are limited by several challenges. These include (i) the inert nature of most C–H bonds as a result of their high bond strengths (85-105 kcal/mol) and low polarity. This leads to a large kinetic barrier associated with the C–H cleavage step, required prior to or during functionalization reactions. Transition metal catalysts serve to increase the rates of reactions of C–H bonds by many orders of magnitude. This is because they are capable of breaking C–H bonds and form C–M bonds, which in most cases can be converted to new

functional groups under milder conditions;<sup>3,4</sup> (ii) the requirement to control site selectivity in molecules that contain diverse C–H bonds. Many strategies have been employed to improve selectivity of various C–H bond functionalization reactions, including the use of substrates that contain weaker, or activated C–H bonds (eg. 3° or benzylic/ allylic systems),<sup>5</sup> use of Lewis acids as directing groups,<sup>6,7</sup> use of arene groups bearing intramolecular coupling partners,<sup>8,9</sup> use of heteroarene substrates with highly activated C–H bonds (e.g. indoles and pyrroles),<sup>10-14</sup> catalyst-based control of selectivity by tuning the sterics or electronics of the ancillary ligands at the metal,<sup>15</sup> and the use of substrates that contain coordinating ligands as directing groups. The directing groups, which can include N-donor groups such as pyridine, O-donor groups such as ketones, esters, amides, etc, bind to the metal center and selectively deliver the catalyst to a proximal C–H bond.<sup>16-20</sup> Therefore, the “Holy Grail” of C–H activation research is not only to find new C–H activation reactions, but to also develop reagents that are capable of selectively functionalizing the C–H bonds. Although a few organic and main group reagents have been developed with the potential of meeting this goal, much of the activity in this field has been in transition metal chemistry.<sup>4</sup>

Among transition metal catalysts that have been developed for C–H bond functionalization reactions, palladium complexes have stood out as attractive homogenous catalysts for both laboratory and industrial applications due to several reasons.<sup>1,2</sup> First, C–H functionalization at Pd centers can be used to construct many types of bonds, including C–oxygen, C–halogen, C–sulfur, C–nitrogen, and C–C bonds, where few other metals show such diverse bond construction capability.<sup>5,21-23</sup>

This versatility is proposed to result mainly from the compatibility of many Pd(II) catalysts with many oxidants, as well as the ability to selectively functionalize cyclopalladated intermediates. Palladium complexes are also attractive homogenous catalysts because palladium participates in cyclometalation reactions with a wide range of directing groups, and readily promotes C–H activation at both  $sp^2$  and  $sp^3$  C–H bonds.<sup>24</sup> Finally, most oxidative palladium catalyzed reactions can be performed under ambient conditions, making them attractive for practical applications in organic synthesis.<sup>24</sup>

Most common Pd-catalyzed bond-forming processes have been proposed to involve the Pd(0)/Pd(II) catalytic cycle in the presence of benzoquinone, copper (II) salts, or molecular oxygen usually as stoichiometric oxidants.<sup>25,26</sup> Potential Pd(II)/Pd(IV) cycles have received little attention for a long time due to the difficulty in isolating Pd(IV) complexes.<sup>27-29,30</sup> However recently, the Pd(II)/Pd(IV) catalytic cycle has been implicated in a variety of C–C and C–heteroatom bond forming processes in the presence of oxidants such as  $\text{PhI}(\text{OAc})_2$ <sup>31</sup>,  $\text{NCS}$ <sup>32</sup> and Oxone.<sup>33</sup> The oxidants convert hydrocarbyl Pd(II) intermediates to their Pd(IV) analogues, which consequently undergo reductive elimination reactions to form C–O,<sup>34-36</sup> C–N<sup>37,38</sup>, C–C,<sup>39,40</sup> C–Cl,<sup>41</sup> and C–F<sup>42</sup> bonds, which were difficult to access via the traditional Pd(0)/Pd(II) catalysis. Apart from the construction of new types of bonds, the development of Pd(II)/Pd(IV) catalysis has also eliminated problems associated with the Pd(0)/Pd(II) catalysis, which include  $\beta$ -hydride elimination, palladium-black decomposition from Pd(II) species, and the necessity to conduct the reactions under air and moisture free conditions. Moreover, the Pd(II)/Pd(IV) catalysis allows for

tolerance of various functional groups, including aryl halides, ether, benzylic hydrogens, nitro groups, enolizable ketones, oximes and amides.<sup>43</sup> Also, the necessity to fine-tune ligands in order to facilitate reductive elimination from Pd(II) species<sup>44</sup> is no longer necessary since most Pd(IV) complexes readily undergo reductive elimination.

## 1.2 Palladium Catalyzed Oxygenation of C–H Bonds

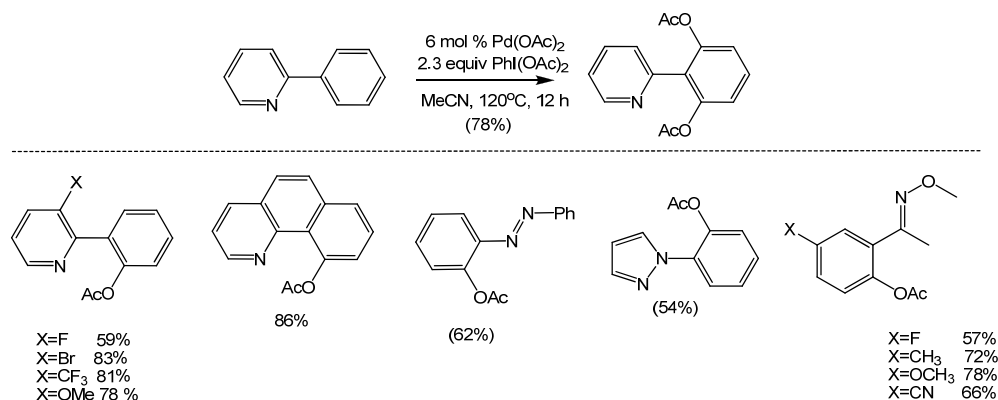
### 1.2.1 Utilization of Iodine-Based Reagents as Oxidants for the C–H Bond

#### Oxygenation Reactions

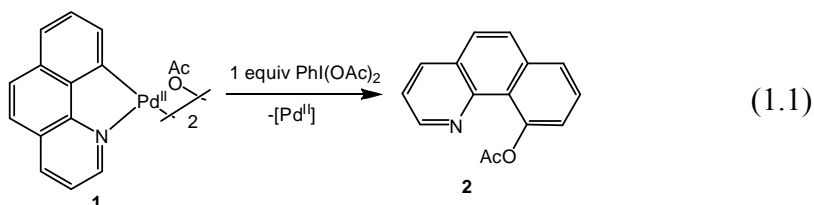
Palladium catalyzed C–H bond oxygenation reactions have undergone significant development during the past 10 years.<sup>45,46</sup> The palladium catalyzed acetoxylation of benzene was first reported in 1966 by Triggs and co-workers.<sup>47</sup> In 1971, another example of aromatic C–H acetoxylation using  $K_2Cr_2O_7$  as oxidant was reported by Henry and co-workers, where the intermediacy of Pd(IV) complexes was proposed.<sup>48</sup> Crabtree also reported palladium catalyzed acetoxylation of aromatic C–H bonds using  $PhI(OAc)_2$  as the terminal oxidant, where he also proposed the intermediacy of Pd(IV) complexes.<sup>49</sup> In 2004, Sanford optimized the procedure developed by Crabtree for the acetoxylation of aromatic C–H bonds using  $PhI(OAc)_2$  as oxidant.<sup>50</sup> She applied a strategy that involves the use of directing groups to selectively acetoxylate *ortho* C–H bonds of the aromatic compounds. This procedure has since been used for the *ortho* C–H bond acetoxylation of several aromatic compounds with various nitrogen-based directing groups such as imines, oxime

ethers, azobenzene derivatives, and nitrogen heterocycles (eg pyrazoles and isoxazolines) (Scheme 1.1).

**Scheme 1.1**

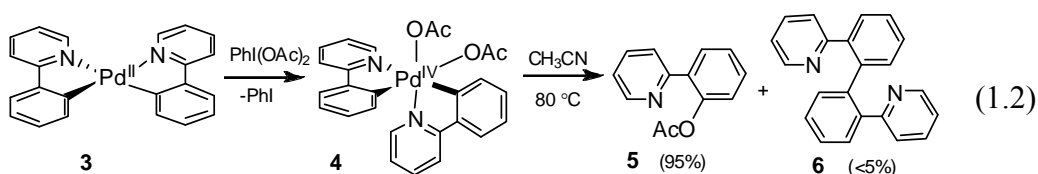


When the solvent of these reactions was changed from acetic acid to alcohol, aryl ether products were produced in high yields. Sanford proposed that in situ reaction of the alcohol solvent with PhI(OAc)<sub>2</sub> affords PhI(OR)<sub>2</sub> which functions as the oxidant in these transformations.

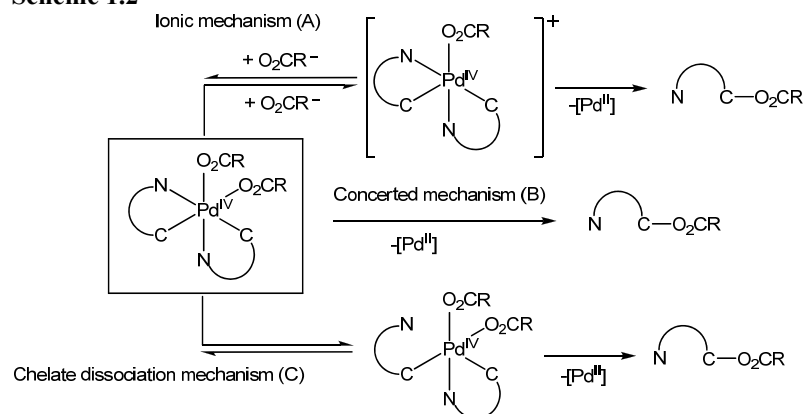


The mechanism of these oxidative C–H bond oxygenation reactions was explored by Sanford and co-workers. The reactions were shown to proceed with similar rates using either Pd(OAc)<sub>2</sub> or palladacycle **1** (eq. 1.1) as the catalyst, suggesting that **1** is a kinetically competent intermediate in these reactions. In addition, **1** was shown to react directly with PhI(OAc)<sub>2</sub> to afford the acetoxyated product, thus providing evidence against a Pd(0)/Pd(II) process (eq. 1.1).<sup>50</sup> Additional studies for the oxidative Pd-catalyzed C–H bond acetoxylation reaction using

benzo[*h*]quinoline and 2-*ortho*-tolylpyridine as substrates revealed a zero-order dependence on [PhI(OAc)<sub>2</sub>] in several solvents such as benzene, AcOH/Ac<sub>2</sub>O, and MeCN. Large primary deuterium intermolecular kinetic isotope effects (between 3.6 and 4.3) were also observed, indicating that cyclopalladation is the rate-limiting step of the catalytic cycle. A rate-limiting C–H bond activation step prevented study of the subsequent steps following cyclopalladation, thus limiting these studies to the synthesis and study of model complexes.



In the study of model complexes, Pd(IV) complex **4** was synthesized via the reaction of biaryl Pd(II) complex **3** with PhI(OAc)<sub>2</sub> (eq. 1.2). Earlier attempts to isolate stable O-ligated organopalladium(IV) complexes and study their reactivity towards C–O bond formation were complicated by their low stability and their propensity to undergo side reactions such as C–C bond forming reductive elimination.<sup>51-56</sup> Complex **4** was however stable at ambient temperature, and underwent clean C–O bond reductive elimination to form the acetoxylated product **5** upon thermolysis. The stability and reactivity of complex **4** enabled detailed studies of the C–O bond forming reductive elimination from Pd(IV) complexes.

**Scheme 1.2**

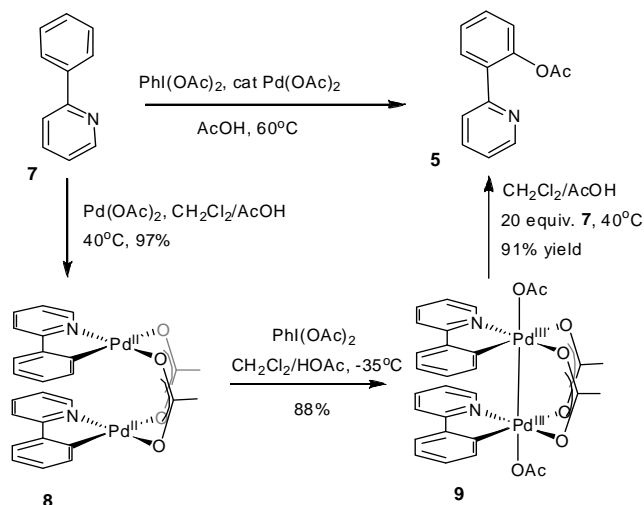
According to Scheme 1.2 above, three mechanisms were considered in the study of the C–O reductive elimination reaction from complex **4**: the ionic mechanism (A), which involves preliminary dissociation of a carboxylate ligand, followed by reductive elimination from a 5-coordinate palladium complex; the concerted mechanism (B), where reductive elimination takes place from a 6-coordinate palladium complex; and the chelate dissociation mechanism (C), which involves preliminary chelate dissociation followed by reductive elimination from a 5-coordinate palladium(IV) intermediate. On the basis of experimental observations, mechanism C was proposed, which involves preliminary chelate dissociation, followed by C–O reductive elimination from a pentacoordinate Pd(IV) complex.<sup>57</sup>

Later, theoretical studies on the C–O reductive elimination reaction from complex **4** were performed by Liu and co-workers. These studies favored mechanism B on Scheme 1.2 above, where the C–O reductive elimination reaction takes place from a 6-coordinate palladium species.<sup>43</sup> This mechanism was supported by a close match between calculated and experimental activation free energy barriers. The theoretical model also correctly predicted the solvent and substituent effects observed experimentally.

However, a recent detailed study led Sanford and co-workers to conclude that the C–O reductive elimination reaction proceeds via mechanism A in Scheme 1.2, which involves pre-equilibrium dissociation of an acetate ligand, followed by rate limiting C–O reductive elimination from a 5-coordinate cationic intermediate.<sup>58</sup> This revised mechanism was proposed based on additional experimental observations, including the rapid exchange of the bound and free carboxylate ligands, which indicates that dissociation of carboxylate ligand from the Pd(IV) complex is possible. These studies indicate that the mechanism of C–O bond-forming reductive elimination from Pd(IV) complexes is still not well understood.

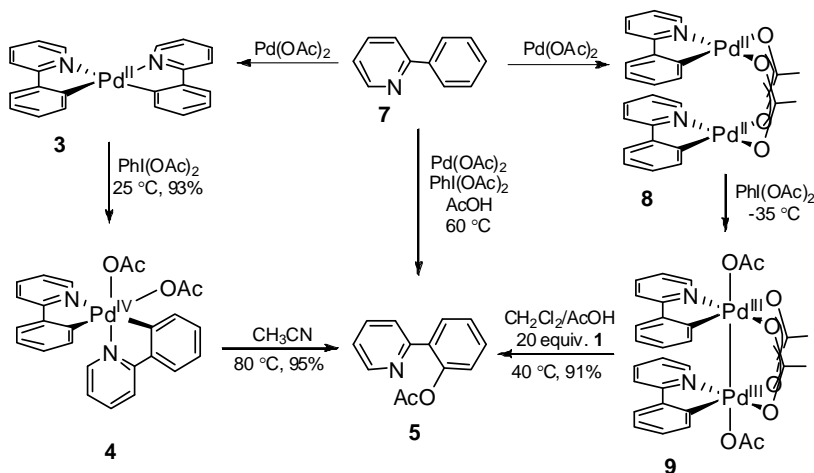
The intermediacy of Pd(III) complexes in the palladium catalyzed C–H acetoxylation reaction with PhI(OAc)<sub>2</sub> as oxidant has also been proposed.<sup>59</sup> The dimeric Pd(III) complex **9** (Scheme 1.3) was independently synthesized via oxidation of complex **8** with PhI(OAc)<sub>2</sub> at low temperature. Upon thermolysis, C–O reductive elimination was observed in high yields, demonstrating the feasibility of C–O bond formation from dimeric Pd(III) complexes. Complex **8** was also shown to be a kinetically competent intermediate in catalytic C–H bond functionalization reactions.

**Scheme 1.3**



As a result of the study of model stoichiometric organometallic reactions of isolated Pd(IV) and Pd(III) complexes, two mechanisms for the palladium catalyzed oxygenation of C–H bonds with  $\text{PhI}(\text{OAc})_2$  have thus been put forward. As presented in Scheme 1.4 below, the proposed mechanisms involve C–H bond activation of compound **7** to generate a cyclopalladated complex **8** or **3**. Palladacycle **3** may undergo two electron oxidation to generate Pd(IV) intermediate **4**, whereas **8** can generate a Pd(III) intermediate **9** via 1-electron oxidation of each palladium center. C–O reductive elimination from either of these high valent palladium complexes releases the product **5** and regenerates the catalyst.

**Scheme 1.4**

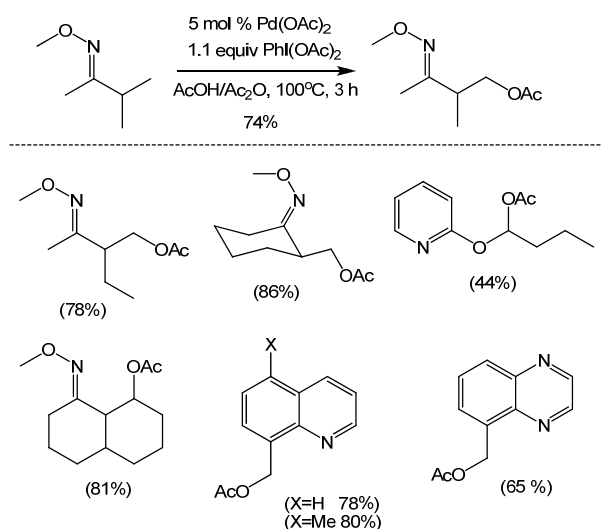


It is however not possible to identify the nature of the high oxidation state palladium intermediates in the oxidative C–H functionalization reactions due to rate-limiting cyclopalladation.<sup>60</sup> As a result, there is currently no basis to distinguish between the involvement of mononuclear Pd(IV) or dinuclear Pd(III) species as intermediates in the catalytic cycle involving  $\text{PhI}(\text{OAc})_2$  as oxidant. Thus, current research efforts are aimed at determining the nature of the intermediates involved in these transformations, finding out which reaction mechanism is operative, and using

the understanding of the reaction mechanism to improve the efficiency of these reactions, and even make the reactions more environmentally benign.

Palladium catalyzed acetoxylation of  $sp^3$  C–H bonds using  $\text{PhI}(\text{OAc})_2$  as the terminal oxidant has also been performed (Scheme 1.5). These reactions also rely on metal-coordinating groups for regioselective C–H functionalization. Both benzylic and unactivated  $sp^3$  C–H bonds were converted to the corresponding alkyl acetates, and no products from  $\beta$ -hydride elimination were observed. The reactions proceed with high selectivity for primary *vs.* secondary C–H bonds, and compounds that form 5-membered palladacycles were favored over those that form 6-membered palladacycles. In this system, the functionalization of secondary and tertiary C–H bonds was not efficient. Still, secondary C–H bonds adjacent to activating groups were acetoxylation (see Scheme 1.5).

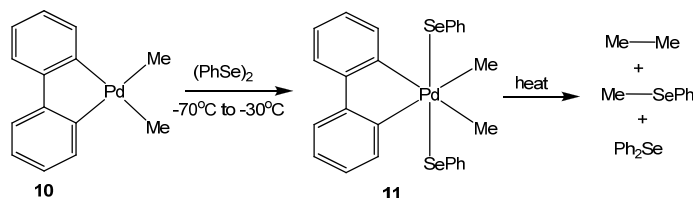
**Scheme 1.5**



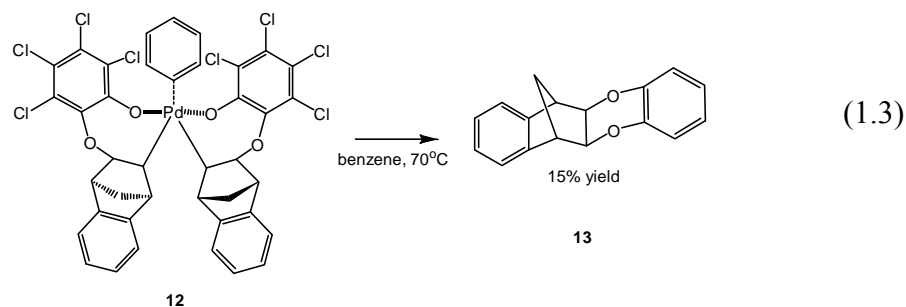
In contrast to the aryl C–H bond oxygenation reactions, there is little information on the putative intermediates involved in the alkyl C–H bond oxygenation reactions, although the intermediacy of  $\text{Pd}(\text{IV})$  complexes has been

proposed. Isolable alkyl Pd(IV) complexes capable of undergoing C–heteroatom reductive elimination were first reported by Canty and co-workers.<sup>51</sup> In this work, oxidation of a (bipy)PdMe<sub>2</sub> complex **10** (Scheme 1.6) with diphenyl diphenylselenide was reported to cleanly produce *trans* (bipy)Pd(SePh)<sub>2</sub>Me<sub>2</sub> **11**, which was characterized by XRD. This complex underwent carbon-selenium bond formation upon thermolysis in solution.<sup>55</sup> Related complexes derived from the oxidation of dimethylpalladium(II) compounds with diaryol peroxides were detected by NMR spectroscopy, but reductive elimination led to C–C coupling.<sup>51</sup> This report supports the intermediacy of Pd(IV) complexes in the palladium catalyzed acetoxylation of sp<sup>3</sup> C–H bonds.

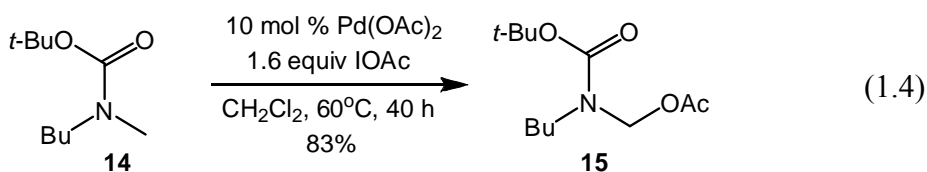
**Scheme 1.6**



An example of sp<sup>3</sup> C–O reductive elimination from an alkyl Pd(IV) complex was demonstrated by Yamamoto and co-workers.<sup>61</sup> In this report, the Pd(IV) complex **12** (eq. 1.3) was prepared by the stoichiometric reaction between tetrachloro-1,2-benzoquinone and a palladium(0) precursor. Thermolysis of complex **12** led to the bisoxygenated compound **13**, among other products. This reaction proved that C–O reductive elimination from alkyl Pd(IV) complexes is a feasible pathway, and supports the intermediacy of Pd(IV) complexes in the palladium catalyzed acetoxylation of sp<sup>3</sup> C–H bonds with PhI(OAc)<sub>2</sub> as oxidant, described previously.



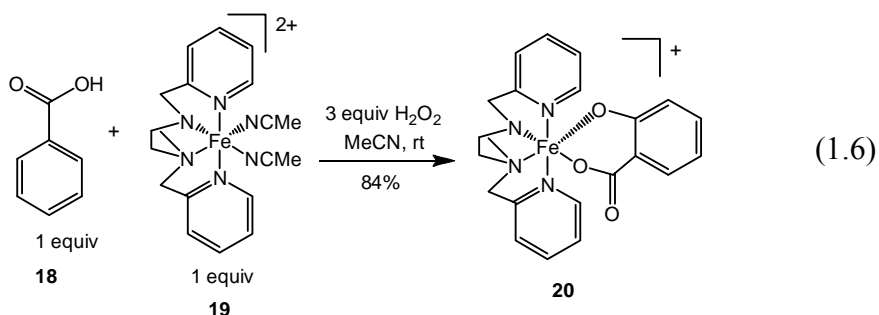
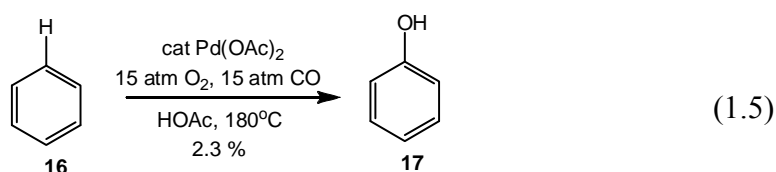
Apart from iodine(III) oxidants, iodine(I) oxidants have also been applied in the palladium catalyzed acetoxylation of  $sp^3$  C–H bonds. The IOAc oxidant was used in the palladium catalyzed acetoxylation of *N*-methylamine derivatives (eq. 1.4).<sup>62</sup> This oxidant is generated in situ by the reaction of  $I_2$  with either  $PhI(OAc)_2$  or  $AgOAc$ . In this system, no reaction was observed when either  $PhI(OAc)_2$  or  $I_2$  was used independently. High selectivity for the functionalization of  $N-CH_3$  over  $N$ -aryl substituents was observed. The mechanism of this reaction was proposed to involve amide directed C–H activation, followed by oxidation to Pd(IV), C–I bond-forming reductive elimination, followed by nucleophilic displacement of  $I^-$  by  $OAc^-$  under the reaction conditions. However, direct C–OAc elimination to generate the acetoxyated products was not ruled out.



### 1.2.2 Utilization of Peroxie-based Reagents as Oxidants for the Palladium Catalyzed Oxygenation of C–H Bonds

Hypervalent iodine oxidants are expensive and produce stoichiometric amount of toxic waste products. Oxidation reactions that utilize inexpensive and environmentally benign oxidants such as molecular oxygen and/ or hydrogen

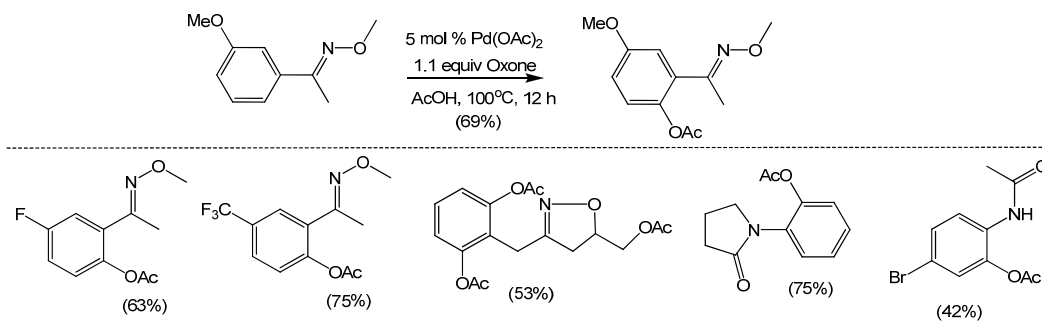
peroxide are extremely attractive as they render the resulting transformations “greener” and more practical for large scale synthesis.<sup>33</sup> Such transformations however remain a significantly challenging task.<sup>63-67</sup> An early result on the palladium catalyzed hydroxylation of benzene **16** using molecular oxygen was reported by Fujiwara and co-workers in 1990.<sup>68</sup> This transformation was however conducted under harsh reaction conditions and low yields were produced (eq. 1.5). In another study, Rybak-Akimova and Que reported the *ortho*-hydroxylation of benzoic acid **18** with H<sub>2</sub>O<sub>2</sub> in the presence of a stoichiometric amount of a reactive iron complex [Fe(II)(BPMEN)(CH<sub>3</sub>CN)<sub>2</sub>](ClO<sub>4</sub>)<sub>2</sub> **19** (eq. 1.6).<sup>69</sup>



Recently, more efficient palladium catalyzed reactions have been developed for the oxygenation of sp<sup>3</sup> and sp<sup>2</sup> C–H bonds using various peroxide-based oxidants. In 2005, Sanford and co-workers reported palladium catalyzed acetoxylation of aromatic C–H bonds using Oxone as terminal oxidant in acetic acid. The inorganic peroxide was proposed to oxidize Pd(II) to Pd(IV) while the solvent was proposed to be the source of oxygen functionality. Substrates with a variety of directing groups

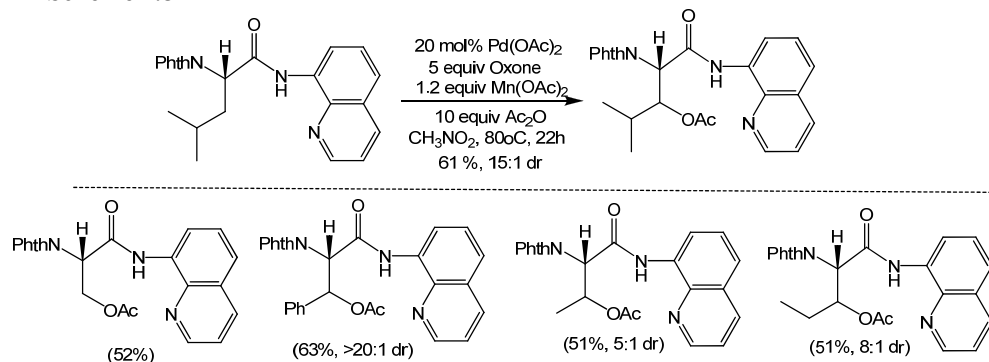
including oxime ethers, amides, and isoxazolines reacted in acetic acid solvent to afford aryl esters,<sup>70</sup> and aryl ethers when the reactions were performed in alcohol solvents (Scheme 1.7).<sup>33</sup>

**Scheme 1.7**



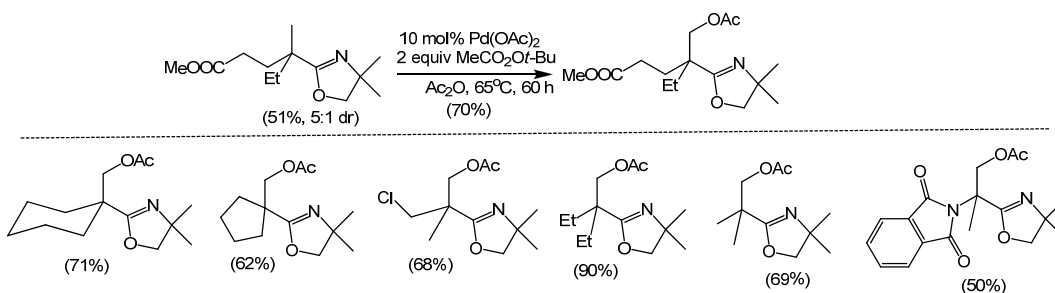
While Oxone was an effective oxidant for the oxygenation of aromatic C–H bonds, only modest activity was observed when this oxidant was used for the oxygenation of aliphatic C–H bonds.<sup>33</sup> The combination of Oxone with Mn(OAc)<sub>2</sub> however promoted efficient oxygenation of secondary sp<sup>3</sup> C–H bonds in amidoquinolines (Scheme 1.8).<sup>71</sup> It was proposed that the reaction between Mn(OAc)<sub>2</sub> and Oxone affords Mn<sub>3</sub>O(OAc)<sub>7</sub>, which then functions as a Lewis acid to increase the reactivity of the Pd(II) catalyst. A C–H functionalization mechanism that involves chelation-assisted C–H activation to produce a cyclopalladacycle, followed by oxidation to Pd(IV) by Oxone in the presence of acetic anhydride was proposed. Reductive elimination from the Pd(IV) species releases the product and regenerates the catalyst.

**Scheme 1.8**



*Tert*-butyl peroxyacetate has also been used as terminal oxidant for the palladium catalyzed oxygenation of aliphatic C–H bonds (Scheme 1.9).<sup>72</sup> Acetic anhydride was an important additive in this reaction since low yields were obtained in its absence. Oxazolines were used as directing groups, and the reaction conditions applied were compatible with ketals, imides, esters, and alkyl chlorides. The authors suggested a mechanism that involves cyclopalladation, followed by oxidation by the peroxyester to produce a Pd(IV) intermediate that ultimately undergoes C–O bond-forming reductive elimination to release the product and regenerate the catalyst.

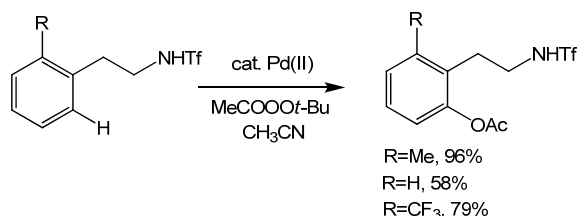
**Scheme 1.9**



The *tert*-butyl peroxyacetate oxidant has also been utilized in the acetoxylation of aromatic C–H bonds. In 2010, Jin-Quan Yu and co-workers reported a palladium catalyzed acetoxylation of phenylalanine and ephedrine derivatives with *tert*-butyl peroxyacetate as terminal oxidant in dichloroethane solvent (Scheme

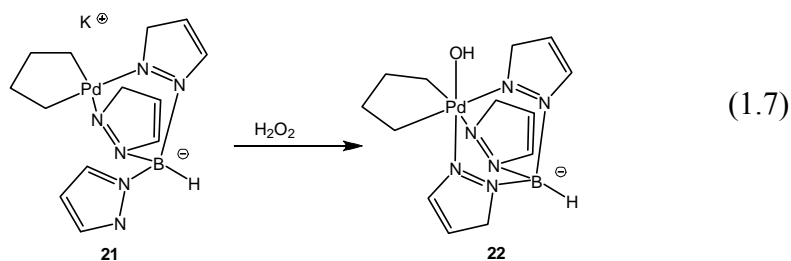
1.10).<sup>73</sup> In this transformation, additives such as DMF, acetonitrile, acetic acid and acetic anhydride were used to increase the product yields. The role of the additives as well as the mechanism of this reaction were not discussed.

**Scheme 1.10**



Although the intermediacy of Pd(IV) complexes in the palladium catalyzed C–H acetoxylation reactions utilizing peroxo-based reagents as oxidants has been proposed, the putative Pd(IV) intermediates have never been detected in these systems. In addition, stoichiometric reactions between cyclopalladated complexes with peroxide-based oxidants have led to oxygen atom insertion into of the C–Pd bonds in most cases, to produce the corresponding oxapalladacycles.<sup>74-80</sup> Although the mechanisms of these oxapalladation reactions were proposed to involve Pd(IV) intermediates, no such intermediates were detected in these reactions. However the ability of peroxo-based oxidants to oxidize hydrocarbyl Pd(II) complexes to their Pd(IV) analogues was demonstrated by Canty and co-workers (eq. 1.7).<sup>81</sup> In this report, the tris(pyrazol-1-yl)borate-ligated Pd(II) complex **21** underwent oxidation with H<sub>2</sub>O<sub>2</sub> to produce the corresponding Pd(IV) complex **22**. Although the C–O reductive elimination reactivity of this complex was not discussed, this report demonstrates that oxidation of hydrocarbyl Pd(II) complexes with H<sub>2</sub>O<sub>2</sub> to the corresponding Pd(IV) analogs is possible. The report thus lends support to the

intermediacy of Pd(IV) complexes in the palladium catalyzed oxygenation reactions using peroxide based reagents as oxidants.



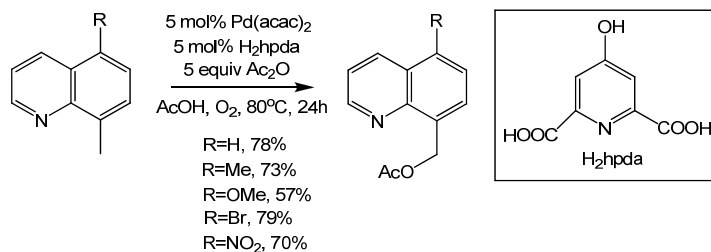
The challenges of the palladium catalyzed C–H oxygenation reactions utilizing peroxo-based reagents as oxidants lie in the efficiency, selectivity, and the substrate scope of these reactions. Most of these reactions, especially those involving aromatic C–H functionalization proceed with low yields, and require the presence of directing groups to induce *ortho* C–H bond selectivity. Thus future studies should broaden the substrate scope of these reactions and remove the requirement for chelate directed C–H activation. In addition, it would be more desirable if these reactions are conducted in water, utilizing oxidants such as H<sub>2</sub>O<sub>2</sub> and/ or molecular oxygen, since these reagents are more abundant, inexpensive, and more benign to the environment.

### 1.2.3 Utilization of O<sub>2</sub> as Oxidant for Palladium Catalyzed Oxygenation Reactions

Molecular oxygen, which is a more attractive oxidant than the peroxide-based oxidants, has also been used as a terminal oxidant in palladium catalyzed oxygenation of both aliphatic and aromatic C–H bonds. In the acetoxylation of aliphatic C–H bonds, our group reported a quinoline-directed oxygenation of benzylic C–H bonds using dioxygen as the terminal oxidant (Scheme 1.11).<sup>82</sup> This transformation proceeded with Pd(acac)<sub>2</sub> as the catalyst in conjunction with a 2,6-pyridinedicarboxylate ligand in AcOH/Ac<sub>2</sub>O under an atmosphere of oxygen. The

reaction was compatible with a wide array of substituents, including all halides, some of which are usually not tolerated under the Pd(0)/Pd(II) catalytic conditions. The possibility of Pd(II)/Pd(IV) catalytic cycle, where dioxygen oxidizes Pd(II) to Pd(IV) was suggested.

**Scheme 1.11**



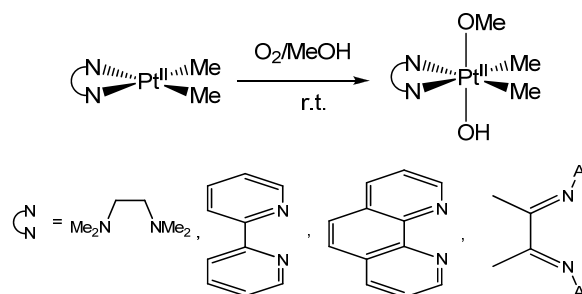
Palladium catalyzed *ortho*-hydroxylation of potassium benzoates with dioxygen as the terminal oxidant in DMF, DMA and DMP was recently reported by Yu and co-workers (Scheme 1.12).<sup>83</sup> In this transformation, benzoquinone and bases such as KOAc and K<sub>2</sub>HPO<sub>4</sub> were found to increase the product yields. Labeling studies using <sup>18</sup>O<sub>2</sub> and H<sub>2</sub><sup>18</sup>O supported a direct oxygenation of the arylpalladium intermediates instead of an acetoxylation/hydrolysis sequence. The possibility of a Pd(II)/Pd(IV) redox pathway was also proposed, where dioxygen could function as the terminal oxidant to oxidize Pd(II) to Pd(IV). Oxygen incorporation from H<sub>2</sub>O or H<sub>2</sub>O<sub>2</sub> formed through a Pd(0)/Pd(II) catalysis was ruled out through the labeling studies.

**Scheme 1.12**



Palladium(IV) intermediates in the palladium catalyzed aerobic C–H functionalization reactions have not been observed in solution. In addition, the aerobic oxidation of hydrocarbyl Pd(II) complexes to their Pd(IV) analogues has never been reported. The oxidation of hydrocarbyl Pt(II) complexes to their Pt(IV) analogues has however been reported. Ligand enabled aerobic oxidation of dimethyl Pt(II) complexes to the Pt(IV) analogues has been reported by Bercaw (Scheme 1.13),<sup>84,85</sup> while that for monohydrocarbyl Pt(II) complexes was reported by Vedernikov.<sup>86</sup> Considering that platinum complexes are frequently considered as models for the reactivity of palladium complexes, the isolation of hydrocarbyl Pt(IV) complexes via the oxidation of hydrocarbyl Pt(II) complexes with dioxygen suggests that aerobic oxidation of hydrocarbyl Pd(II) complexes to generate the corresponding Pd(IV) analogues might be possible. This presents an opportunity to develop aerobic palladium catalyzed C–H functionalization reactions that proceed via the Pd(II)/Pd(IV) redox cycle. In addition, the reactivity of hydrocarbyl Pt(II) complexes towards oxidation with molecular oxygen supports the intermediacy of Pd(IV) complexes in the C–H bond oxygenation reactions described in Schemes 1.11 and 1.12 described previously.

**Scheme 1.13**



Given that there are very few palladium catalyzed C–H functionalization reactions where dioxygen is used as the terminal oxidant, and these reactions have a

very narrow substrate scope, future studies should broaden the substrate scope of these reactions and also remove the requirement for chelate directed C–H activation.

### 1.3 Palladium Catalyzed Halogenation of C–H bonds

Recently, a variety of procedures that involve direct functionalization of aromatic C–H bonds have been developed.<sup>24</sup> Most of these procedures utilize *N*- or *O*-donor atoms as directing groups to selectively functionalize the *ortho* C–H bond. Of particular importance are the procedures developed for selective halogenation of aromatic C–H bonds, given that aryl halides are important components of a variety of biologically active molecules, natural products, and pharmaceuticals,<sup>87</sup> and also serve as precursors to organometallic reagents such as organolithium<sup>88</sup> and Grignard reagents.<sup>89</sup>

The most common synthetic approaches to halogenated arenes are electrophilic aromatic substitution reactions using reagents such as *N*-halosuccinimides,<sup>90-92</sup> X<sub>2</sub>,<sup>93</sup> peroxides/ HX,<sup>94-96</sup> peroxides/ MX,<sup>97-100</sup> or hypervalent iodine reagents/ MX (M= Li, Na, or K).<sup>101,102</sup> These transformations however suffer from several challenges, including limited substrate scope due to the requirement for activated arenes, side reactions that include overhalogenation, and multiple regioisomeric products are usually obtained, resulting in decreased yields and the requirement for tedious separations.<sup>32,103</sup> Another procedure for the preparation of halogenated arenes is the directed *ortho*-lithiation reaction followed by halogen quenching.<sup>104</sup> This technique is limited by the requirement for strong bases, which in turn results in low functional group tolerance, and a narrow scope of suitable

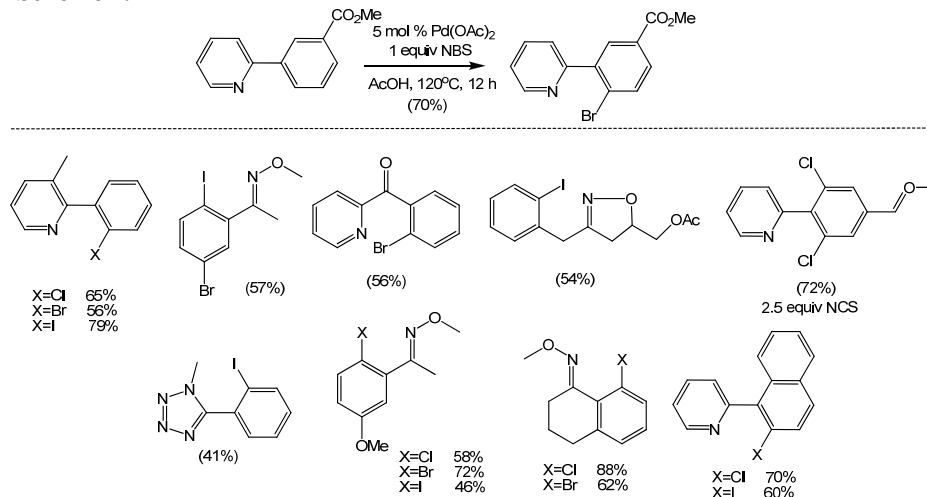
directing groups.<sup>32</sup> As a result, the development of more efficient, selective, and environmentally friendly transition metal catalyzed procedures for halogenation of C–H bonds would be highly desirable.

Examples of transition metal catalyzed C–halogen forming reactions are rare, mainly because the reverse aryl halide oxidative addition is thermodynamically favored at most metal centers.<sup>105</sup> However, several examples of stoichiometric C–halogen reductive elimination reactions at Pd(II) centers under oxidizing conditions using oxidants such as X<sub>2</sub>,<sup>106-111</sup> CuX<sub>2</sub>,<sup>111-113</sup> or PhICl<sub>2</sub>,<sup>111</sup> have been reported.

The stoichiometric C–halogen reductive elimination reaction at Pd(II) utilizing Cl<sub>2</sub> as oxidant was developed into a catalytic C–H chlorination reaction in 1970 by Fahey and co-workers.<sup>114,115</sup> In this report, the palladium catalyzed *ortho*-chlorination of azobenzenes with Cl<sub>2</sub> as oxidant generated a mixture of mono-, di-, tri-, and tetra-chlorinated products. However the use of Cl<sub>2</sub> as oxidant and the lack of selectivity of this system limited its application in organic synthesis. More practical methods for the halogenation of C–H bonds using electrophilic halogenating reagents are therefore the focus of current research efforts.

In 2001, the N–iodosuccinimide oxidant was applied in the palladium catalyzed *ortho*-iodination of benzoic acids by Kodama and co-workers.<sup>116</sup> This system inspired Sanford and co-workers to develop a procedure for the palladium catalyzed *ortho* chlorination and bromination of benzo[*h*]quinoline utilizing *N*-chlorosuccinimide and *N*-bromosuccinimide as oxidants.<sup>117</sup> This reaction has since been applied to a wide array of substrates with various directing groups such as pyridines, oxime ethers, isoquinolines, amides, and isoxazolines (Scheme 1.14).<sup>32,50</sup>

Scheme 1.14

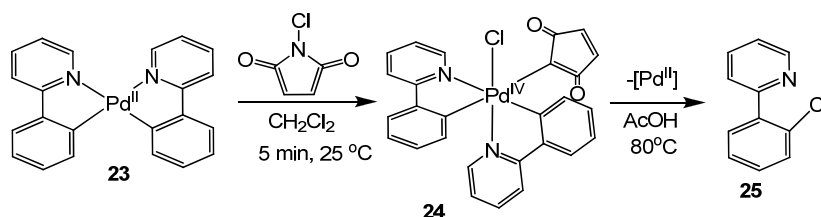


The mechanism of palladium catalyzed halogenation utilizing *N*-halosuccinimides as oxidants has recently been studied. Using 2-tolylpyridine as a model compound and NCS as oxidant, the palladium catalyzed chlorination of aromatic C–H bonds was found to be first order in [Pd] and zero order in NCS. A large intermolecular kinetic isotope effect ( $K_H/K_D = 4.4$ ) was also observed. On the basis of these experimental observations, C–H bond activation was proposed to be the rate-limiting step of this reaction. Consequently, it was not possible to determine the structure of the palladium intermediate complexes involved in these reactions. As a result, model studies were conducted in order to gain insight into the reactivity of the steps following the cyclopalladation reaction in the catalytic cycle.

In the model studies, stoichiometric oxidation of a Pd(II) model complex (phpy)<sub>2</sub>Pd(II) **23** with NCS was performed to produce the corresponding Pd(IV) complex **24** (Scheme 1.15). Complex **24** underwent C–Cl reductive elimination upon thermolysis at 80°C to produce the corresponding aryl chloride **25** in high yield. These studies indicate that NCS is a sufficiently strong oxidant to promote oxidation

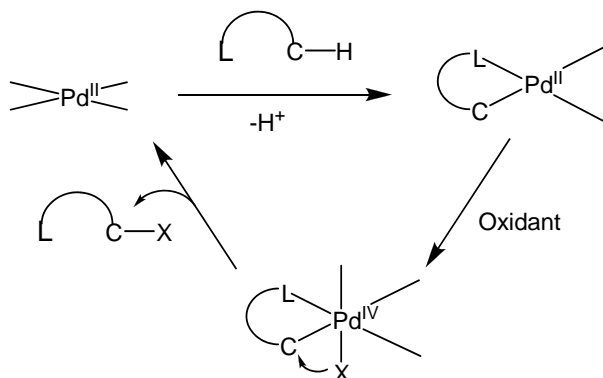
of Pd(II) to Pd(IV) in this model system, and the viability of C–Cl bond-forming reductive elimination from Pd(IV) was also demonstrated.<sup>118</sup>

**Scheme 1.15**



As a result of the model studies, Sanford and co-workers proposed a palladium catalyzed C–H halogenation mechanism that involves ligand-directed C–H bond activation to produce a cyclopalladated complex.<sup>50</sup> This palladacycle undergoes two-electron oxidation with NCS to produce a Pd(IV) intermediate, which in turn undergoes C–X reductive elimination to release the product and regenerate the catalyst (scheme 1.16).<sup>50</sup>

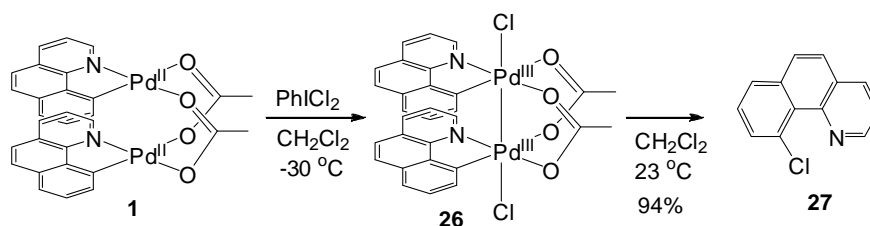
**Scheme 1.16**



The intermediacy of Pd(III) complexes in the catalytic C–H bond chlorination reactions with NCS has also been considered. The reaction of the acetato-bridged palladacycle **1** with PhICl<sub>2</sub> at low temperature was observed to produce a dimeric Pd(III) complex **26**,<sup>59</sup> which underwent high yielding C–Cl reductive elimination upon thermolysis (Scheme 1.17). The oxidation of complex **1** with NCS indicates that

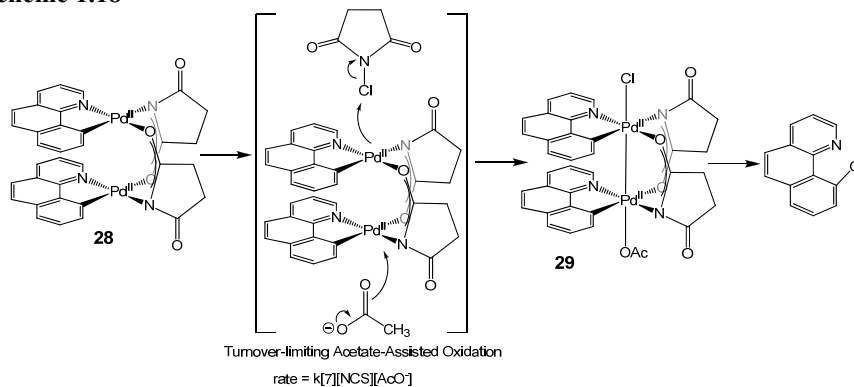
this oxidant is sufficiently strong to oxidize dimeric Pd(II) complexes to their Pd(III) analogues, while the C–Cl reductive elimination from complex **26** indicates that the dimeric Pd(III) complexes are chemically viable intermediates in the catalytic chlorination reactions. The kinetic viability of dimeric Pd(III) complexes in the catalytic chlorination reactions was also demonstrated, where complex **26** catalyzed the chlorination of benzo[*h*]quinoline in the presence of either PhICl<sub>2</sub> or NCS as oxidants. The structure of the high valent intermediates in the catalytic halogenation reactions was however not determined due to a rate limiting C–H activation step.<sup>60</sup>

**Scheme 1.17**



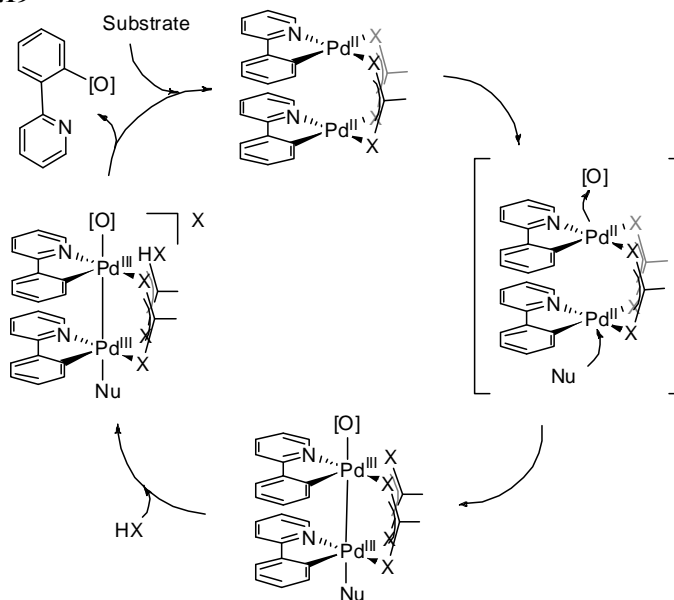
In 2010, Ritter and co-workers discovered a palladium catalyzed aromatic C–H bond chlorination reaction that takes place via rate limiting oxidation step, thus enabling the detection of the high valent palladium complexes (Scheme 1.18).<sup>46</sup> In this system, the succinamate bridged dimer **28** was proposed to be the resting state of the catalyst, while the rate law for this reaction was established as rate =  $k[\mathbf{28}][\text{NCS}][\text{OAc}^-]$ . On the basis of the rigid dinuclear structure of **28**, and the measured first order dependence on the concentration of **28**, acetate, and NCS oxidant, a rate-limiting oxidation of **28** with nucleophilic assistance by acetate was proposed. This oxidation reaction was proposed to produce the dimeric Pd(III) intermediate **29**.

**Scheme 1.18**



Complex **29** was independently synthesized via oxidation of complex **28** with acetyl hypochlorite at  $-78^{\circ}\text{C}$ , and characterized via  $^1\text{H}$  NMR at  $-90^{\circ}\text{C}$ . Upon warming the solution to room temperature, C–Cl and C–O reductive elimination reactions were observed to generate the corresponding products in 84 % and 0.5 % yield respectively; a similar product distribution was observed during catalysis. As a result, the mechanism depicted in Scheme 1.19 was proposed as the mechanism for the palladium catalyzed chlorination of aromatic C–H bonds utilizing NXS as the terminal oxidant (X=Cl, Br, and I). This mechanism involves C–H bond activation to produce a dimeric Pd(II) complex. This complex undergoes nucleophile assisted oxidation with NXS to produce a dimeric Pd(III) intermediate, which undergoes acid catalyzed C–X reductive elimination to produce the functionalized product and regenerate the active catalyst. This system allowed for the study of the structure of the intermediate complex, but the intermediate was not detected in solution due to its instability under the catalytic reaction conditions.

**Scheme 1.19**



As a result of the study of stoichiometric organometallic reactions described above, two mechanisms for the palladium catalyzed C–H halogenation reactions have been put forward; a mechanism involving Pd(II)/Pd(IV) redox couple and another involving Pd(II)/Pd(III) redox couple. Which of these cycles closely resembles the operative catalytic cycle has not been determined since most of these reactions operate via rate limiting C–H bond activation step and thus its not possible to determine the identity of the high oxidation state palladium intermediate. As a result, current research efforts are aimed at understanding the mechanism of these C–H halogenation reactions, with the aim of developing more selective and efficient catalysts. In addition, the study of these reaction mechanisms might enable the development of more environmentally friendly C–H bond halogenation reactions.

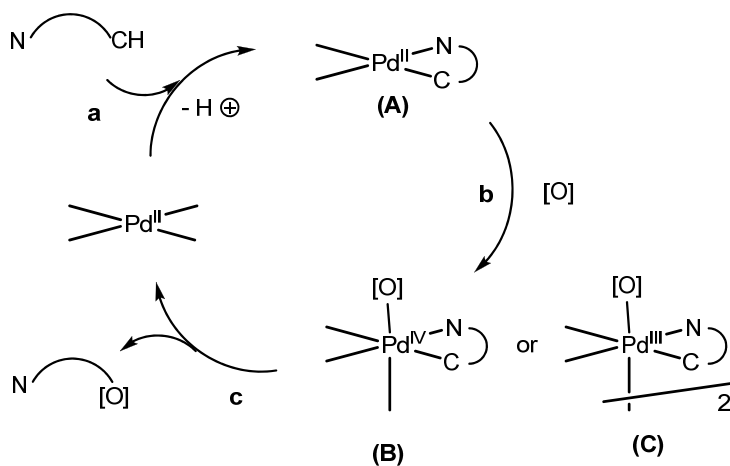
#### 1.4 Our Approach and Goal

Given that very few palladium catalyzed C–H bond functionalization reactions utilizing molecular oxygen and/ or hydrogen peroxide oxidants have been developed,

our ultimate goal is to develop mild, efficient, and environmentally friendly catalytic C–H functionalization reactions utilizing molecular oxygen or hydrogen peroxide as terminal oxidants.

Our approach will involve the study and optimization of the steps in the proposed catalytic cycle presented in Scheme 1.20 below.

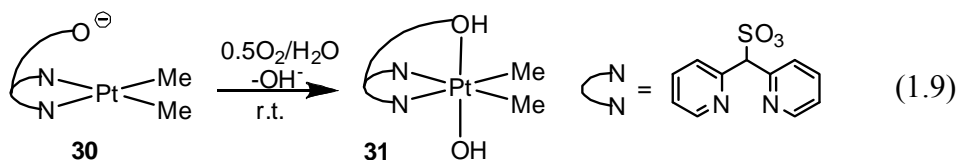
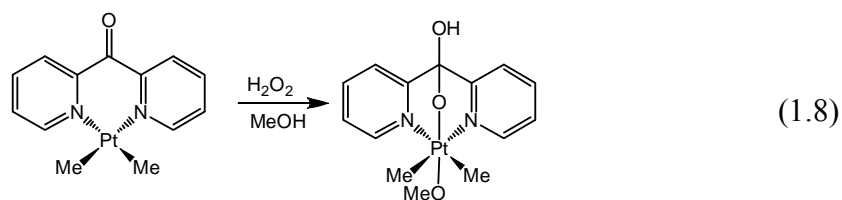
**Scheme 1.20**



According to Scheme 1.20, the C–H bond functionalization reaction is proposed to proceed via (a) C–H bond activation to produce cyclopalladated species **A**. Stoichiometric ligand-directed C–H activation reactions to produce cyclopalladacyclic complexes have been demonstrated in literature.<sup>3,119</sup> The following step (b) involves oxidation of the palladacycle to produce a high-valent palladium intermediate **B** or **C**. The oxidation of organopalladium(II) compounds to generate monomeric Pd(IV)<sup>118</sup> or dimeric Pd(III)<sup>46</sup> complexes has been demonstrated using strong oxidants such as  $\text{PhI}(\text{OAc})_2$ . The functionalization of C–Pd bonds using peroxide based oxidants such as MCPBA,<sup>74-77</sup> *tert*-butylhydroperoxide in the presence of a vanadium catalyst,<sup>120</sup> and hydrogen peroxide in the presence of an iron catalyst<sup>121</sup> have also been demonstrated. Most of these reactions were proposed to proceed via

Pd(IV) intermediates, although these species were not detected in the solution. The tris(pyrazol-1-yl)borate ligand-enabled oxidation of organopalladium(II) complexes to their Pd(IV) analogues using H<sub>2</sub>O<sub>2</sub> has also been demonstrated.<sup>122</sup> The last step (c) involves product release via C–X reductive elimination. This step has also been demonstrated from both monomeric Pd(IV),<sup>57,59</sup> and dimeric Pd(III)<sup>59</sup> complexes.

Given that oxidation of monohydrocarbyl Pd(II) complexes to their Pd(IV) analogues utilizing O<sub>2</sub> and/ or H<sub>2</sub>O<sub>2</sub> as oxidant is rare, our plan involves the use of facially chelating tridentate ligands to aid in this transformation. Stoichiometric studies have shown that bidentate ligands which can adopt a tridentate, facially chelating coordination mode enable oxidation of hydrocarbyl M(II) complexes (M=Pt or Pd) utilizing H<sub>2</sub>O<sub>2</sub><sup>123</sup> or molecular oxygen<sup>86</sup>. For example, the tris(pyrazol-1-yl)borate ligand has been used to enable the oxidation of a hydrocarbyl Pd(II) complex to its Pd(IV) analogue using H<sub>2</sub>O<sub>2</sub> as oxidant (eq. 1.7), while the dpk ligand enabled the oxidation of a (dpk)PtMe<sub>2</sub> complex to its Pt(IV) analogue using H<sub>2</sub>O<sub>2</sub> as oxidant in methanol (eq. 1.8).<sup>123</sup> The 2-dipyridylmethanesulfonate (dpms) ligand has also been used to enable functionalization of C–Pt bonds using dioxygen as oxidant (eq. 1.9). These potentially tridentate ligands are proposed to enable oxidation of M(II) to M(IV) species with relatively less reactive oxidants because the pendant third arm can lower the activation energy of oxidation by incipient formation of the third M–O bond upon oxidation to the M(IV) species.<sup>85,124</sup> Additionally, since this is an intramolecular event, it occurs without the entropy penalty involved with coordinating a free ligand.<sup>125</sup>

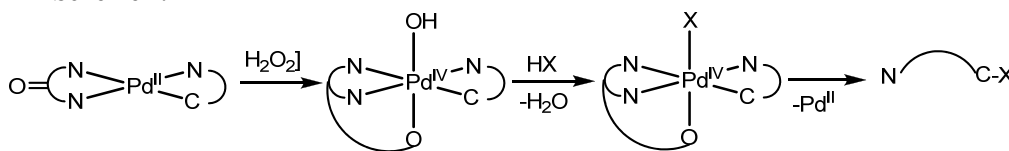


Our approach involves utilizing bidentate, potentially tridentate facially chelating ligands to enable oxidation of monohydrocarbyl Pd(II) complexes with  $O_2$  and/ or  $H_2O_2$ , and also stabilize the resulting high oxidation state palladium complexes. These reactions will enable us to study the oxidation reaction utilizing dioxygen and/ or  $H_2O_2$  oxidants, and the reductive elimination reaction from the resulting Pd(IV) species. The understanding of the mechanism of oxidation of Pd(II) complexes with these oxidants, and C–O reductive elimination from the resulting high valent Pd complexes will enable us to optimize these steps, with the ultimate goal of developing a suitable palladium catalyzed C–H bond oxygenation reaction utilizing  $O_2$  and/ or  $H_2O_2$  as oxidant.

In addition, we also plan to develop palladium catalyzed C–H bond halogenation reactions utilizing  $O_2$  and/ or  $H_2O_2$  in HX solvents (X=Cl, Br, and I). Most of these halogenation reactions currently require oxidants such as  $X_2$ , NXS, and  $PhIX_2$ , which produce stoichiometric amounts of waste products. Thus, the use of  $O_2$  and/ or  $H_2O_2$  in water will render these transformations more atom economical, and thus more applicable to large scale synthesis.<sup>33,126</sup>

In order to develop more environmentally friendly procedures for the halogenation of aromatic C–H bonds, our approach will involve synthesis of model halogeno-ligated monohydrocarbyl Pd(IV) complexes capable of undergoing C–halogen bond reductive elimination, utilizing environmentally friendly oxidants in water. Most hydrocarbyl halogeno-ligated Pd(IV) and Pd(III) complexes have been prepared using oxidants such as NXS<sup>118,127</sup> and PhIX<sub>2</sub><sup>59,118</sup> (X=Cl and Br). A more atom-economical procedure for the preparation of model halogeno-ligated monohydrocarbyl Pd(IV) complexes would involve ligand enabled oxidation of organopalladium(II) complexes with H<sub>2</sub>O<sub>2</sub> in water, with subsequent reaction of the Pd(IV) hydroxo species with HX acids (X=Cl, Br, and I) ( Scheme 1.21). C–X bond-forming reductive elimination reaction from the halogeno-ligated monohydrocarbyl Pd(IV) complexes will also be studied.

**Scheme 1.21**

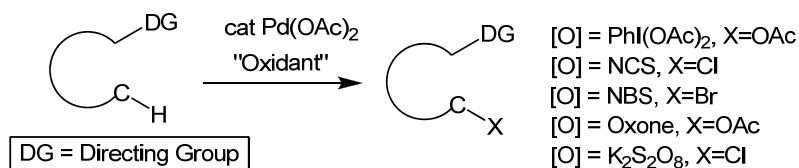


In summary, we plan to develop “green” procedures for palladium catalyzed aromatic C–H bond oxygenation and halogenation reactions utilizing environmentally benign oxidants such as O<sub>2</sub> and/ or H<sub>2</sub>O<sub>2</sub>. Our approach involves study of stoichiometric organometallic reactions to optimize each step involved in the catalytic cycle presented in Scheme 1.20 above. Since oxidation of C–Pd bonds utilizing dioxygen and/ or H<sub>2</sub>O<sub>2</sub> is challenging, we plan to use bidentate, potentially tridentate ligands to enable this transformation.

## Chapter 2: Synthesis of Monohydrocarbyl Pd(IV) Complexes

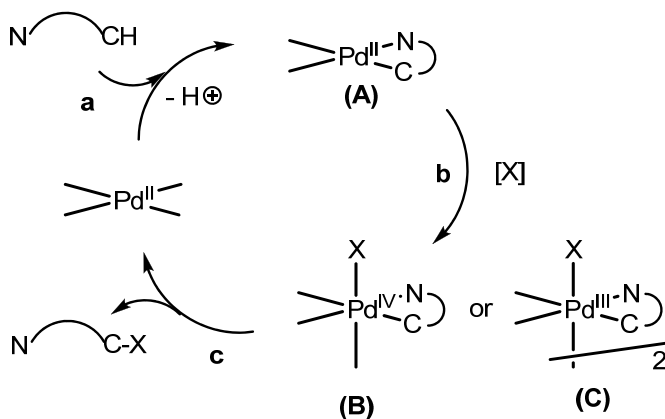
### 2.1 Introduction

**Scheme 2.1**



Directed, palladium catalyzed C(sp<sup>2</sup>)-H bond functionalization utilizing strong oxidants has undergone significant development during the past 10 years (Scheme 2.1).<sup>24</sup> Some oxidants used in these transformations include I<sup>III</sup> based reagents such as PhI(OAc)<sub>2</sub>,<sup>128</sup> NXS (X=Br, Cl, or I),<sup>32</sup> and peroxide based oxidants such as Oxone,<sup>33</sup> which are required in stoichiometric quantities to oxidize Pd(II) to either monomeric Pd(IV) or dimeric Pd(III) species. The proposed mechanism of these oxidative C-H bond functionalization reactions is presented in Scheme 2.2 below.

**Scheme 2.2**

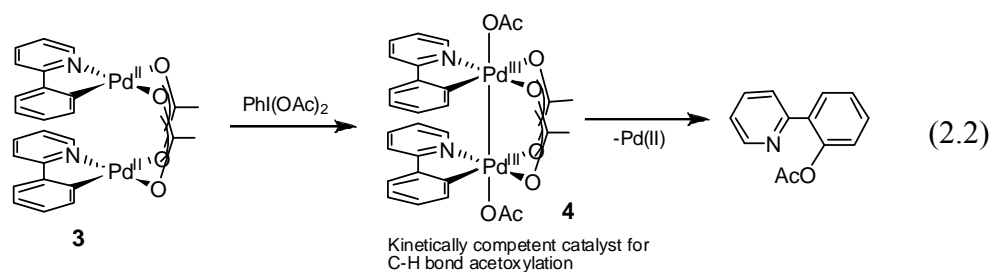
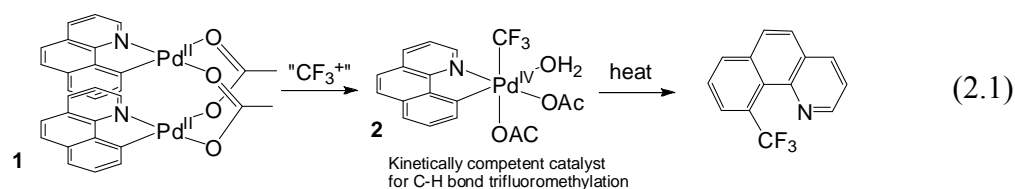


In the mechanism presented in this Scheme, Pd-catalyzed directed oxidative C–H bond functionalization reactions have been proposed to proceed via initial C–H bond activation at the Pd(II) center to generate a cyclopalladated intermediate **A**.<sup>129</sup> Complex **A** could undergo two-electron oxidation to produce a monomeric Pd(IV) complex **B** or one-electron oxidation at each palladium center to produce a dimeric Pd(III) complex **C**, depending on the nature of the ancillary ligands present at the metal center. C–X bond-forming reductive elimination from either complex **B** or **C** releases the product and regenerates the Pd(II) catalyst.

The intermediacy of complex **A** in oxidative palladium catalyzed oxygenation reactions has been supported experimentally.<sup>50</sup> Sanford and co-workers observed that the palladium catalyzed C–H bond acetoxylation of benzo[*h*]quinoline substrate proceeds with similar rate constants when either Pd(OAc)<sub>2</sub> or the acetate-bridged benzo[*h*]quinoline-derived palladacycle **1** is used as catalyst in the presence of PhI(OAc)<sub>2</sub> oxidant. The stoichiometric reaction of complex **1** with PhI(OAc)<sub>2</sub> was also observed to produce the corresponding acetoxyated product. These observations indicate that complex **1** is a chemically viable intermediate in these reactions. Additional mechanistic studies indicated that the catalytic C–H bond functionalization reaction takes place via rate-limiting cyclopalladation, step **a**.<sup>49,50</sup> As a result, it is not possible to study the oxidation step **b** and subsequent C–X bond reductive elimination step **c** in Scheme 2.2. Consequently, these studies have been limited to the synthesis and study of the reactivity of model complexes.

The study of model complexes has shown that oxidation of arylpalladium(II) complexes to produce either mononuclear Pd(IV) or dinuclear Pd(III) complexes with

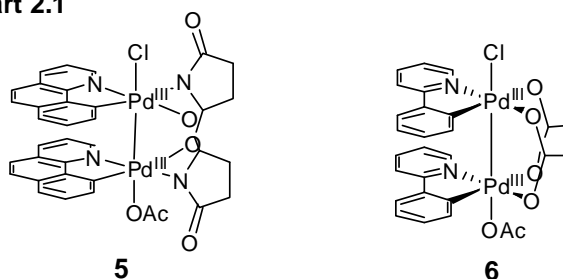
hypervalent iodine oxidants is feasible, and the C–X reductive elimination (X=OAc or Cl) reaction upon thermolysis of these high valent palladium complexes has also been demonstrated (equation 2.1 and 2.2 below). These studies indicate that the mononuclear Pd(IV) and dinuclear Pd(III) complexes are chemically viable intermediates in the oxidative palladium catalyzed C–H bond functionalization reactions. A monomeric Pd(IV) complex has also been shown to be kinetically competent intermediate in the palladium catalyzed transformations. The mononuclear Pd(IV) complex **2** (eq. 2.1) was shown to catalyze trifluoromethylation of benzo[*h*]quinoline substrates at a faster rate than the Pd(OAc)<sub>2</sub> catalyst under similar conditions, and similar product yields were also obtained.<sup>130</sup> These results demonstrate the kinetic competence of complex **2** in the palladium catalyzed trifluoromethylation reactions, and also confirm the potential viability of this complex as a catalytic intermediate in the palladium catalyzed transformation.



The kinetic competency of dinuclear Pd(III) complexes as intermediates in catalytic reactions has been demonstrated numerous times. In one example, complex

**4** (eq. 2.2) was shown to be kinetically competent in the palladium catalyzed acetoxylation of phenylpyridine-derived complexes.<sup>131</sup> Dinuclear Pd(III) complexes **5** and **6** have also been shown to be chemically and kinetically competent intermediates in the palladium catalyzed *ortho*-chlorination of benzo[*h*]quinoline and phenylpyridine substrates respectively.<sup>46,59</sup>

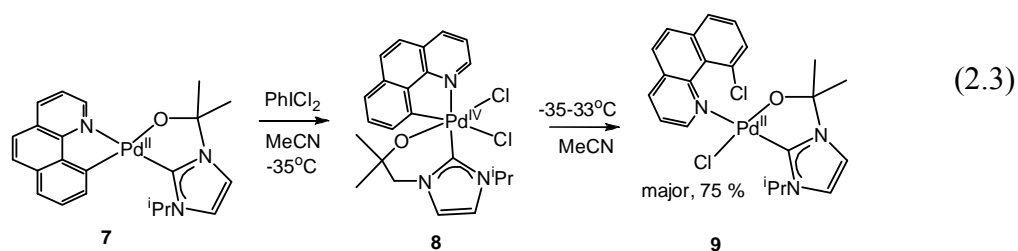
**Chart 2.1**



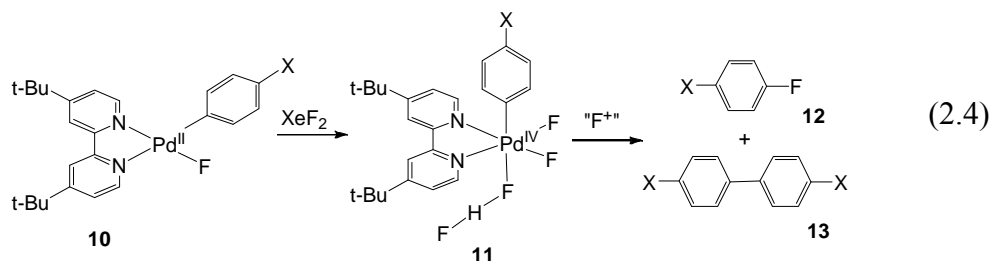
These studies indicate that either monomeric Pd(IV) or dimeric Pd(III) complexes could be active intermediates in oxidative palladium catalyzed C–H bond functionalization reactions depending on the auxiliary ligands and reaction conditions. However these studies have no demonstrated relevance to catalysis because there is no basis to discriminate between the potential mechanisms involving oxidation to either dinuclear Pd(III) or mononuclear Pd(IV) intermediates since it is not possible to study these intermediate complexes due to rate-limiting cyclopalladation reaction. Consequently, the study of model complexes only provides insights into the reactivity of high oxidation state palladium centers which may be relevant to the oxidative catalytic transformations. These insights are important because any advanced knowledge of the possible pathways of oxidation and C–O reductive elimination from high oxidation state palladium complexes might be very beneficial in the design of more selective, efficient, and environmentally benign palladium catalyzed functionalization reactions.<sup>132</sup>

While a number of model dinuclear Pd(III) and mononuclear dihydrocarbyl Pd(IV) complexes have been prepared and their reactivity towards C–X bond formation studied, few monohydrocarbyl Pd(IV) model complexes have been prepared and the study of their reactivity conducted. The difficulty to prepare and isolate stable monohydrocarbyl Pd(IV) complexes stems from the fact that these complexes are too reactive. The presence of multiple hydrocarbyl ligands on the palladium coordination sphere of isolable Pd(IV) complexes often leads to unwanted C–C bond forming side reactions that make the study of C–X reductive elimination reactions from these complexes challenging, thus demonstrating the need to prepare monohydrocarbyl Pd(IV) complexes. In addition, monohydrocarbyl Pd(IV) complexes are relevant intermediates in oxidative palladium catalyzed C–H functionalization reactions since the ligands on the palladium coordination sphere of the proposed Pd(IV) catalytic intermediates are usually represented by sticks, implying the possibility of either mono- or dihydrocarbyl Pd(IV) species. Given that polyhydrocarbyl Pd(IV) complexes have been studied several times, it is therefore important to prepare and study the reactivity of monohydrocarbyl Pd(IV) complexes.

Very few monohydrocarbyl Pd(IV) complexes had been prepared before our work. One such Pd(IV) monohydrocarbyl complex is **8** (eq. 2.3), which was prepared by oxidation of the Pd(II) complex **7** with PhICl<sub>2</sub> at low temperature. Complex **8** is stabilized by a carbene, an alkoxide, and two chloride ligands, and is stable for at least one week at room temperature. It however undergoes C–Cl reductive elimination upon thermolysis.<sup>133</sup>



Another monohydrocarbonyl Pd(IV) complex **11** was prepared by oxidation of the Pd(II) complex **10** with XeF<sub>2</sub> (eq. 2.4). Complex **11** is stabilized by multiple fluoride ligands, and undergoes high yielding C–F reductive elimination in the presence of F<sup>+</sup> sources such as XeF<sub>2</sub>, *N*-fluorosulfanamide, and 1-fluoro-2,4,6-trimethylpyridinium tetrafluoroborate; only trace amounts of C–F bond coupling products are observed in the absence of F<sup>+</sup> sources.<sup>134</sup>

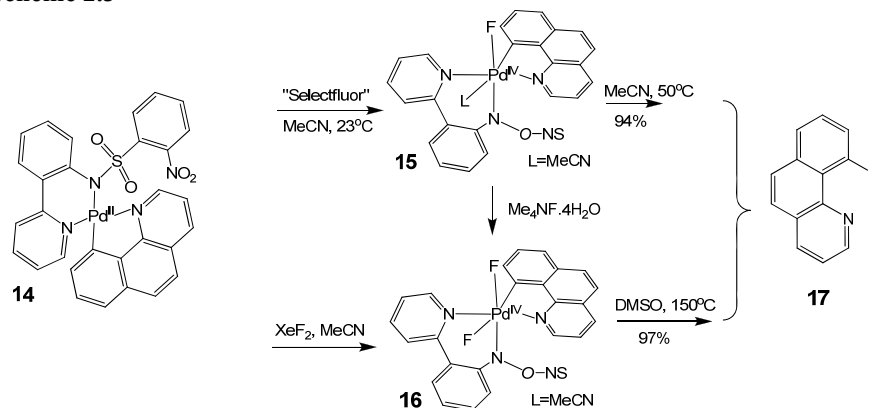


entry	"F <sup>+</sup> "	12	13
1	None	Trace	35%
2	XeF <sub>2</sub>	92%	4%
3	(PhSO <sub>2</sub> ) <sub>2</sub> NF	83%	<1%

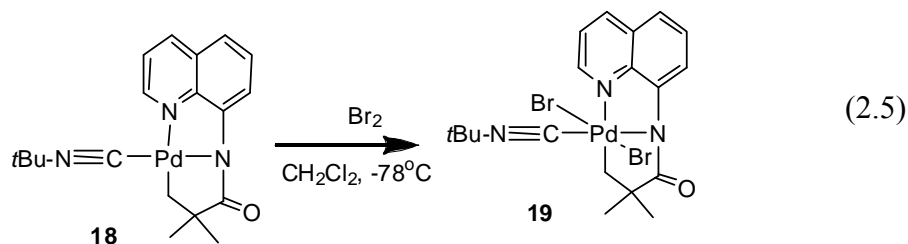
Another fluoro-ligated monohydrocarbonyl Pd(IV) complex **15** (Scheme 2.3) was prepared by oxidation of complex **14** with Selectfluor, but the difluoro-ligated Pd(IV) complex **16** was produced when XeF<sub>2</sub> was used as the oxidant instead. These Pd(IV) monohydrocarbonyls are stabilized by the anionic pyridyl sulfonamide and fluoride ligands. The difluoride complex **16** is thermally more stable than the

monofluoride complex **15**, but both complexes undergo C–F bond-forming reductive elimination in various solvents upon thermolysis.<sup>135</sup>

Scheme 2.3



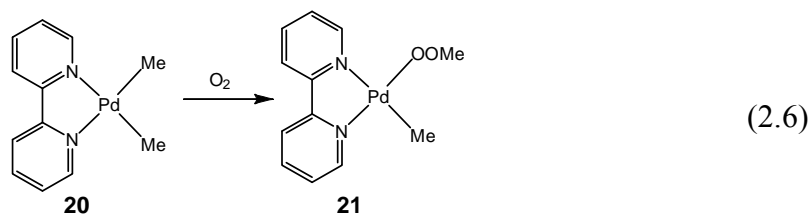
Daugulis and co-workers also prepared the monohydrocarbyl Pd(IV) complex **19** (eq. 2.5) by oxidation of complex **18** with Br<sub>2</sub>. This complex is stabilized by a dianionic tridentate NNC, and bromide ligands. The reactivity of this complex was however not studied because it was too reactive and decomposed at 0°C within hours in solution.<sup>136</sup>



These monohydrocarbyl-Pd(IV) complexes can be viewed as models of potential intermediates in Pd(II)/Pd(IV) mediated C–F and C–Cl functionalization reactions.<sup>135,137-141</sup> However Pd(IV) monohydrocarbyls have never been shown to undergo C–O reductive elimination. This is mainly because most isolable O-ligated monohydrocarbyl Pd(IV) complexes possess other heteroatomic ligands such as halogens in the palladium coordination sphere, leading to side reactions such as C–

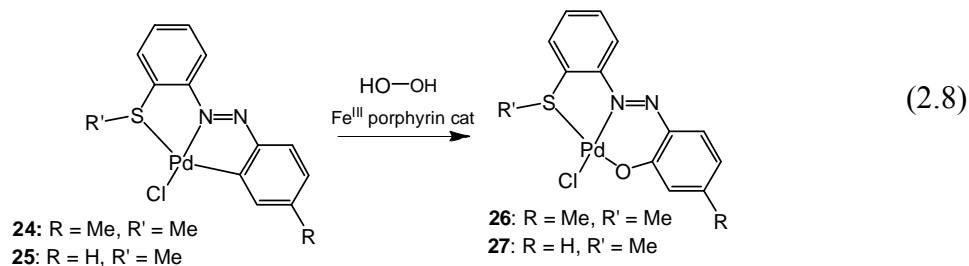
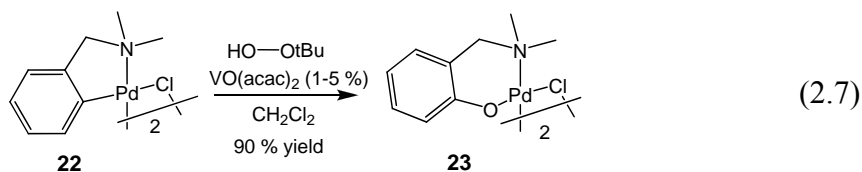
halogen reductive elimination. C–O reductive elimination from these Pd(IV) monohydrocarbyls would therefore be more effective in the absence of other heteroatoms on the Pd coordination sphere except oxygen. An even more attractive goal would be to prepare the monohydrocarbyl Pd(IV) complexes using O<sub>2</sub> and/ or H<sub>2</sub>O<sub>2</sub> as terminal oxidants, as this will ultimately lead to the development of “green” Pd-catalyzed transformations.

The reaction of hydrocarbyl Pd(II) complexes with molecular oxygen has been demonstrated.<sup>142</sup> Goldberg and co-workers observed insertion of molecular oxygen into the Pd–C bond of a (bpy)PdMe<sub>2</sub> complex **20** to form (bpy)PdMe(OOMe) complex **21** (eq. 2.6). Kinetic studies of this reaction supported the involvement of a radical chain mechanism, where the chain propagation was proposed to proceed via a stepwise associative homolytic substitution at the Pd center of **20** via a pentacoordinate Pd(III) intermediate. Aerobic oxidation of Pd(II) complexes to their Pd(IV) analogues has however never been reported.

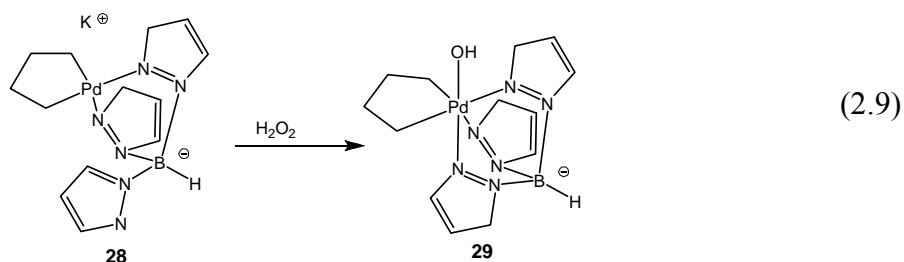


Oxygenation of C–Pd bonds using hydroperoxide based oxidants has also been observed. Van Koten and co-workers reported oxygenation of the C–Pd bond of cyclopalladated benzylamine complex **22** using *tert*-butyl peroxide as oxidant in the presence of a vanadium catalyst (eq. 2.7).<sup>120</sup> Bandyopadhyay and co-workers also reported insertion of oxygen atom into the Pd–C bond of cyclopalladated azobenzene derivatives **24** and **25** using H<sub>2</sub>O<sub>2</sub> as oxidant in the presence of Fe(III) porphyrin

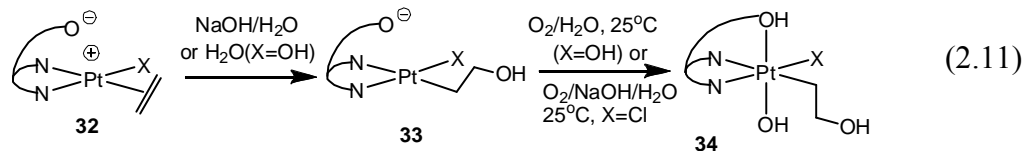
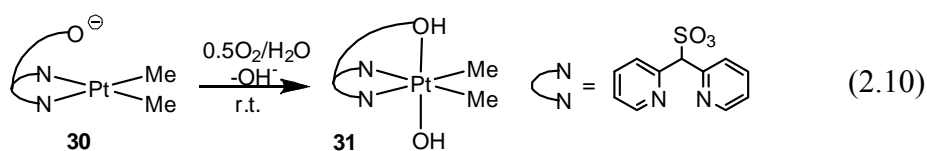
catalysts (eq. 2.8).<sup>121</sup> These oxapalladation reactions were proposed to take place via Pd(IV) intermediates, but these intermediates were not detected in solution.



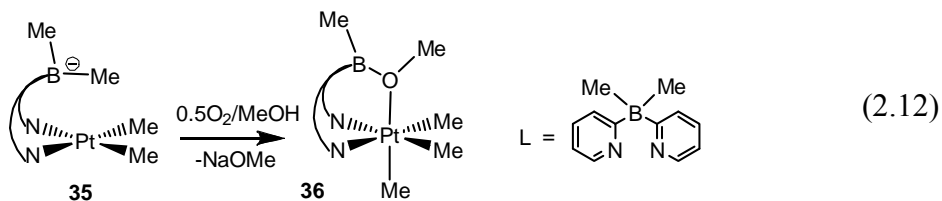
The oxidation of hydrocarbyl Pd(II) complexes to their Pd(IV) analogues in the absence of additives had only been demonstrated once before our work. In a 1996 report by Canty, a tris(pyrazolyl)borate-ligated diorganopalladium(II) complex **28** reacted with H<sub>2</sub>O<sub>2</sub> to produce the corresponding hydroxodiorganopalladium(IV) analogue **29** (eq. 2.9).<sup>81,122</sup> This was the first time H<sub>2</sub>O<sub>2</sub> was used to oxidize a hydrocarbyl Pd(II) complex to the corresponding hydrocarbyl Pd(IV) species. This oxidation reaction was presumably enabled by the tris(pyrazolyl)borate ligand, which was also important in the stabilization of the corresponding Pd(IV) species. These results indicate that similar bidentate, but potentially tridentate, facially ligands may enable oxidation of organopalladium (II) complexes with dioxygen or hydrogen peroxide, and also stabilize the resulting organopalladium(IV) complexes.



The ability of facially chelating tridentate ligands to enable oxidation of M(II) species by O<sub>2</sub> has also been demonstrated (M=Pt or Pd). Vedernikov and co-workers found that the 2-dypyridylmethanesulfonate (dpms) ligand enables aerobic oxidation of a dimethyl-Pt(II) complex **30** to the hydroxydimethyl Pt(IV) complex **31** (eq. 2.10).<sup>86</sup> This ligand combines two moderately good pyridine donors and a tethered labile *sulfonate* group.<sup>86</sup> The sulfonate arm can lower the activation energy of oxidation by incipient formation of the Pt–O bond upon oxidation to the octahedral Pt(IV) species.<sup>85,124</sup> The dpms ligand also enabled aerobic oxidation of a hydroxoPt(II) ethylene complex **32** to produce the corresponding 2-hydroxyethylPt(IV) complex **34** (eq. 2.11).<sup>143</sup>



The dimethyl(2-pyridyl)borate ligand has also been observed to enable aerobic oxidation of a dimethylPt(II) complex **35** to its Pt(IV) analogue **36** (eq. 2.12). Similar to the dpms ligand, this anionic, potentially facially chelating tridentate ligand tuned the reactivity of Pt(II) towards oxidation with dioxygen.<sup>144</sup>



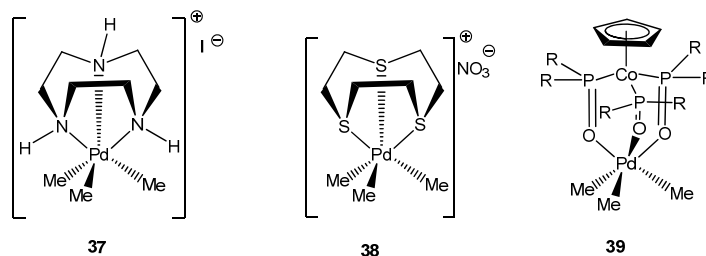
These N-donor tridentate ligands are proposed to enable oxidation of M(II) to M(IV) species with relatively less reactive oxidants because the pendant third arm can lower the activation energy of oxidation by incipient formation of the third Pd–X bond (X=O or N) upon oxidation to the M(IV) species.<sup>85,124</sup> Since this is an intramolecular event, it occurs without the entropy penalty involved with coordinating a free ligand.<sup>125</sup> Furthermore, coordination of the anionic third arm also provides stability to the octahedral Pd(IV) product and in most cases enables its isolation.<sup>86</sup>

The ability of  $\kappa^3$  ligands to stabilize the Pd(IV) products has been demonstrated. Canty characterized a series of trimethylPd(IV) complexes with various ligands and established that Pd(IV) complexes with bidentate ligands are less stable than those with tridentate ligands, where bidentate-ligated complexes had to be stored below  $-20^\circ\text{C}$ , while those with tridentate ligands were stable as solids at ambient temperature.<sup>145</sup> The enhanced stability of tridentate ligands was proposed to partly result from the requirement for dissociation of one donor group of the tripod ligand prior to reductive elimination.

Apart from the dpms and the dimethyl(2-pyridyl)borate ligands discussed above, scorpionate ligands such as bis(pyrazol-1-yl)borate and the neutral tris(pyrazol-1-yl)methane have also been used to stabilize Pd(IV) complexes.<sup>146</sup> A thermally stable trimethylPd(IV) complex **37** was synthesized by Vedernikov and co-workers using the facially chelating triazacyclononane ligand (see scheme 2.4 below).<sup>147</sup> This compound was thermally very stable, decomposing in the solid state at  $152\text{--}154^\circ\text{C}$ . It eliminates ethane upon thermolysis in dmsO at  $140^\circ\text{C}$ . Another

trimethyl-Pd(IV) complex **38** that was stable at room temperature was prepared using a facially chelating tridentate ligand 1,4,7-trithiacyclononane (tcn).<sup>148</sup> Considering that Pd(IV) complexes have a strong preference for N-donor ligands,<sup>149</sup> it is remarkable that complex **38**, which is exclusively stabilized by S-donor ligands displays such stability at room temperature. A stable trialkyl-Pd(IV) complex **39** stabilized exclusively through O-donor ligands was also synthesized using the facially chelating, tridentate ligand ( $L^- = [\text{CpCo}^{150}_3]$ ).<sup>150</sup> The unusual stability of complexes **37**, **38** and **39** demonstrates the excellent stabilizing capability of facially chelating tridentate ligands.

**Scheme 2.4**

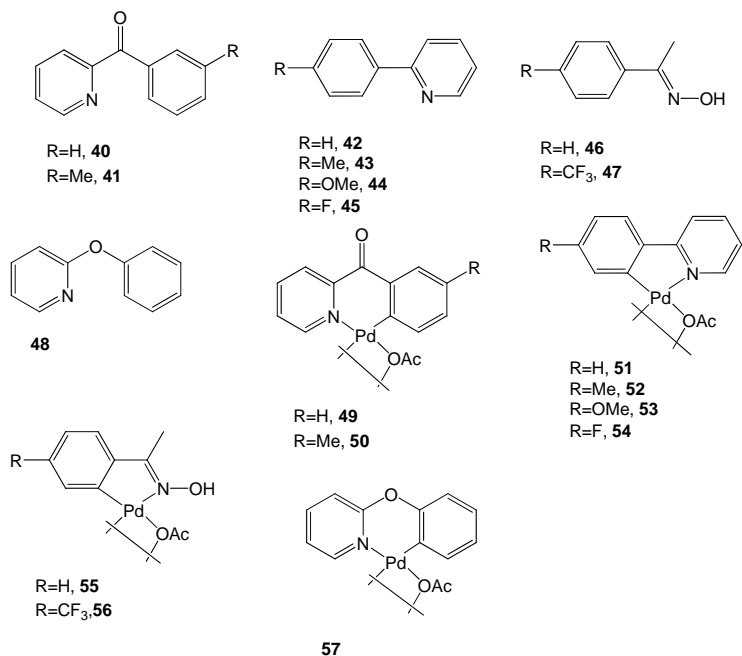


Therefore, considering that potentially facially chelating tridentate ligands have been shown to enable oxidation of M(II) complexes to their M(IV) analogues (M=Pt or Pd) using either dioxygen or hydrogen peroxide, and these ligands have been shown to stabilize the resulting M(IV) complexes at the same time, we plan to use similar facially chelating tridentate ligands to enable oxidation of monohydrocarbyl Pd(II) complexes to their Pd(IV) analogues using either dioxygen or hydrogen peroxide as oxidants, and also to stabilize the resultant monohydrocarbyl Pd(IV) complexes.

## 2.2 Preparation and Reactivity of Acetato-bridged Palladacycles 49-57

### 2.2.1 Preparation of Acetato-bridged Palladacycles 49-57

Chart 2.2



We started our study by synthesizing the acetate-bridged palladacycles **49-57** and analyzing their reactivity towards dioxygen. Oxidation of X-bridged palladacycles has been demonstrated before, but stronger oxidants such as  $\text{PhI}(\text{OAc})_2$ ,<sup>50,59</sup> and *m*-CPBA,<sup>74</sup> or less reactive oxidants such as tert-butyl hydroperoxide in the presence of vanadium catalysts,<sup>120</sup> were required in these oxidation reactions; no oxidation of X-bridged palladacycles has been reported with either dioxygen or  $\text{H}_2\text{O}_2$  as oxidants. Thus complexes **49-57** were synthesized and exposed to dioxygen in acetic acid solvent.

The 2-arylpiperidine-derived acetato-bridged palladacycles **49** and **50** were prepared according to literature.<sup>151</sup> The substrate **40** or **41** was combined with 1.0 equivalent of  $\text{Pd}(\text{OAc})_2$  in acetic acid, the resulting solution was refluxed for 3 hours,

concentrated to produce dark yellow precipitate, and the precipitate was filtered off to produce the target compounds in good yields. The identity of compound **49** was confirmed by comparing its NMR spectra to literature, while the identity of compound **50** was confirmed by NMR and its purity was confirmed by elemental analysis. Proton NMR spectroscopy revealed the presence of two species, presumably *cis*- and *trans*- isomers whose ratio was determined by integration of the NMR spectra (Table 2.1).

**Table 2.1.** Ratio of the presumed *cis*- and *trans*- isomers of complexes **49** and **50**, as determined by  $^1\text{H}$  NMR spectroscopy in  $\text{CDCl}_3$  at  $22^\circ\text{C}$ .

Entry	Complex	R	Major	Minor	Yield (%)
1	<b>49</b>	-H	95	5	83
2	<b>50</b>	-Me	94	6	96

Phenylpyridine-derived dinuclear acetato-bridged palladacycles were prepared by a modified literature procedure.<sup>127</sup> A substituted phenylpyridine derivative **42-45** and  $\text{Pd}(\text{OAc})_2$  (1.0 eq.) were combined in acetic acid and the solution was either refluxed for 4 hours or stirred at  $80^\circ\text{C}$  for 12 hours. The solutions were concentrated to produce yellow precipitate, which was filtered off to produce the target complexes **51-54** in high yields. The complexes were isolated as a mixture of two species, presumably *cis*- and *trans*- isomers whose ratios were determined via  $^1\text{H}$  NMR integration (Table 2.2). The identity of the products was confirmed by NMR spectroscopy while the purity was confirmed by elemental analysis.

**Table 2.2.** Ratio of the presumed *cis*- and *trans*- isomers of complexes **51-54** as determined by <sup>1</sup>H NMR spectroscopy in CDCl<sub>3</sub> at 22 °C.

Entry	Complex	R	Major	Minor	Yield (%)
1	<b>51</b>	-H	92	8	92
2	<b>52</b>	-Me	86	14	95
3	<b>53</b>	-OMe	82	18	85
4	<b>54</b>	-F	86	14	79

The acetato-bridged palladacycles **55** and **56** derived from substituted acetophenone oxime derivatives were prepared by stirring an acetic acid solution of palladium acetate (1.00 mmol) and a substituted acetophenone oxime derivative **46** or **47** (1.05 mmol) at 80 °C for 8 hours. Concentration of the resulting solution produced deep yellow precipitate, which was filtered off to produce the target complex in high yield. The identity of the complexes was confirmed by NMR spectroscopy while the purity was confirmed by elemental analysis. Proton NMR spectroscopy revealed the presence of two species, presumably *cis*- and *trans*- isomers whose ratio could be determined by integration of the NMR spectra.

**Table 2.3.** Ratio of the presumed *cis*- and *trans*- isomers of complexes **55** and **56**, as determined by <sup>1</sup>H NMR spectroscopy in dmsd-d<sub>6</sub> at 22 °C.

Entry	Complex	R	Major	Minor	Yield (%)
1	<b>55</b>	-H	68	32	96
2	<b>56</b>	-CF <sub>3</sub>	79	21	92

Phenoxyppyridine-derived acetate-bridged palladacycle **57** was prepared by a modified literature procedure,<sup>152</sup> where Phenoxyppyridine and Pd(OAc)<sub>2</sub> (1.0 eq.) were stirred in acetic acid at 50 °C for 12 hours to produce the target complex as a light yellow precipitate, which was filtered off. The identity of the complex was confirmed by comparing its spectra to that reported in literature. Proton NMR revealed the presence of two species, presumably *cis*- and *trans*- isomers whose ratio was determined to be 92 % to 8 % according to <sup>1</sup>H NMR integration in CDCl<sub>3</sub> solvent at 22 °C.

### 2.2.2 Attempted Aerobic Oxidation of Acetato-bridged Palladacycles

Aerobic oxidation of the acetato-bridged palladacycles **49-57** was attempted in acetic acid solvent. A study by Goldberg and co-workers revealed that molecular O<sub>2</sub> could insert into a Pd(II)–C bond of a dimethyl-Pd(II) complex to produce a Pd(II)–alkylperoxide species via a radical chain mechanism.<sup>142</sup> Therefore, we subjected our palladacyclic reaction mixtures to aerobic oxidation.

We used 3 complexes as representative samples to study the oxidation of OAc-bridged palladacycles with dioxygen. Complex **49** was used as representative sample for arylpyridine complexes, **55** was used as representative sample for acetophenone oxime-derived complexes, and complex **52** was used as representative sample for R-phenylpyridine-derived complexes. 0.02 mmoles of the OAc-bridged palladacyclic complexes were combined with 1.0 ml of deuterated acetic acid, 10 % acetic anhydride by volume was added to the solution containing complex **55** to prevent hydrolysis of the oxime moiety, and these reaction mixtures were purged with dioxygen for 10 minutes. The reaction mixtures were then transferred to J. Young

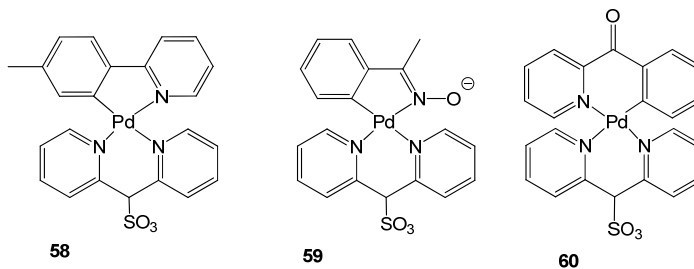
NMR tubes and oxygen was purged into the tubes for an additional 10 minutes.  $^1\text{H}$  NMR spectra were collected at the start of the reactions, and the J. Young NMR tubes were heated in oil-bath at  $100^\circ\text{C}$ ; additional  $^1\text{H}$  NMR spectra were taken periodically. After 3 days, no products of oxidation were detected by either  $^1\text{H}$  NMR spectroscopy or ESI-MS.

As a result, dpms-ligated complexes were prepared and subjected to aerobic oxidation. There have been a number of literature reports on the oxidation of Pt(II) hydrocarbyls with dioxygen enabled by anionic facially chelating ligands, including the dpms ligand. As mentioned before, Vedernikov and co-workers observed ligand-enabled aerobic oxidation of Pt(II) to Pt(IV) hydrocarbyl complexes using the 2-dipyridylmethanesulfonate (dpms) ligand. This anionic bidentate ligand enabled the aerobic oxidation reactions because it has the potential to adopt a facially chelating tridentate coordination mode which can stabilize the octahedral geometry, and thus facilitate oxidation of a  $\text{M}^{\text{II}}$  to  $\text{M}^{\text{IV}}$  monohydrocarbyl with relatively less reactive oxidants.<sup>126</sup> As a result, we expected the dpms ligand to enable aerobic oxidation of Pd(II) monohydrocarbyls to the Pd(IV) analogues.

### 2.3 Preparation and Reactivity of dpms-ligated Palladacycles 58-60

#### 2.3.1 Preparation of Complexes 58-60

**Chart 2.3**



The preparation and characterization of complex **58** was performed by Zhang and co-workers (Zhang, unpublished results). Complexes **59** and **60** were prepared by combining the acetato-bridged palladacycles **55** or **49** with the dpms ligand (1.05 eq.) in water and methanol solvents respectively at ambient conditions. These complexes were isolated as white solids, and their identity was confirmed by NMR spectroscopy and electrospray ionization mass spectrometry, while their purity was confirmed by elemental analysis.

### 2.3.2 Attempted Aerobic Oxidation of dpms-ligated Palladacycles **58-60**

Complexes **58** and **59** were used as representative samples for this oxidation reaction. Vedernikov and Zhang obtained promising results when they observed aerobic oxidation of the dpms complex of cyclopalladated tolylpyridine **58** in acetic acid at 110 °C, albeit at a very low yield of ~ 5 % (Zhang, unpublished results). However when a 0.010 M acetic acid solution of complex **59** was refluxed for 48 hours, no products of oxidation were detected by <sup>1</sup>H NMR or ESI-MS analysis. These results indicate that aerobic oxidation of Pd-C(sp<sup>2</sup>) bonds using the dpms ligand is too slow under these conditions. As a result H<sub>2</sub>O<sub>2</sub>, which is a stronger oxidant, was used.

Oxidation of organopalladium(II) compounds with H<sub>2</sub>O<sub>2</sub> has been reported before. In one study, Bandyopadhyay and co-workers reported the oxapalladation of cyclopalladated azobenzenes with H<sub>2</sub>O<sub>2</sub> in the presence of an Iron(III) porphyrin catalyst (eq. 2.8).<sup>121</sup> Canty and co-workers also reported the oxidation of a diorganopalladium(II) compound to the corresponding hydroxo-diorganopalladium

(IV) analogue using H<sub>2</sub>O<sub>2</sub> (eq. 2.9) in the presence of an ionic tris(pyrazolyl)borate ligand.<sup>81,122</sup>

Considering the successful oxidation of a dihydrocarbyl Pd(II) complex using H<sub>2</sub>O<sub>2</sub> in the presence of a tridentate ligand reported by Canty and co-workers (eq. 2.9) and the aerobic oxidation of organoplatinum(II) complexes in the presence of facially chelating tridentate ligands reported by Vedernikov and co-workers, we expected to achieve oxidation of monohydrocarbyl Pd(II) complexes to their monohydrocarbyl Pd(IV) analogues using H<sub>2</sub>O<sub>2</sub> in the presence of dpms, which is a tridentate, facially chelating ligand.

However, we started our studies by determining whether the oxidation of acetate-bridged palladacycles would be facile using H<sub>2</sub>O<sub>2</sub> in the absence of ligands. Oxygenation of Cl-bridged palladacycles utilizing hydroperoxide based oxidants was achieved by Van Koten and co-workers only in the presence of vanadium catalysts (eq. 2.7), while efficient oxidation of X-bridged palladacycles utilizing hydroperoxide based oxidants in the absence of additives or ligands has never been achieved.

### 2.3.3 Attempted Oxidation of Acetato-bridged Palladacycles **49-57** with H<sub>2</sub>O<sub>2</sub>

We used 4 complexes as representative samples to study the oxidation of OAc-bridged palladacycles with H<sub>2</sub>O<sub>2</sub>. Complex **49** was used as representative complex for aroylpyridine-derived complexes, **55** was used as representative sample for acetophenone oxime-derived complexes, complex **52** was used as representative sample for R-phenylpyridine-derived complexes, and complex **57** were oxidized with H<sub>2</sub>O<sub>2</sub> in acetic acid. Thus, 0.02 mmoles of complexes **49-57** in 0.8 ml of deuterated

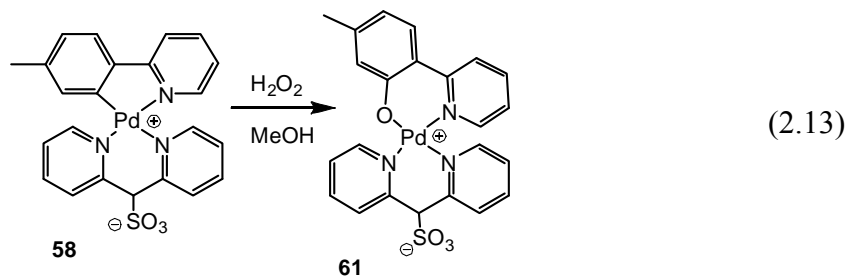
acetic acid were transferred to NMR tubes.  $^1\text{H}$  NMR spectra were collected at the start of the reactions and 10.0 equivalents of 30 % HOOH were added. The resulting solutions were stirred for 2.5 hours at room temperature. Upon addition of  $\text{H}_2\text{O}_2$ , the reaction mixture of complex **55** dissolved to produce a brown solution, while the reaction mixtures of the other 3 complexes remained heterogeneous. After stirring for 2.5 hours at room temperature, pyridine- $\text{d}_5$  was added to the reaction solutions to free any coordinated products of oxidation and  $^1\text{H}$  NMR was taken; addition of 5.0 eq of pyridine led to complete dissolution of all the complexes in acetic acid.  $^1\text{H}$  NMR analysis of the reaction solution of complex **49** revealed ~ 15 % conversion and the presence of 8 % phenol and 4 % aryl acetate.  $^1\text{H}$  NMR analysis of complex **52** revealed the presence of the reactants with no other species in the solution.  $^1\text{H}$  NMR analysis of complex **55** revealed < 5 % conversion to the corresponding phenol and aryl acetate, while that of complex **57** showed no other species in solution except the Pd(II) precursor.

Oxidation was only observed from the 2-benzoylpyridine derived palladacycle **49** to produce the corresponding phenol and aryl acetate products. This reaction presumably proceeds via high oxidation state palladium intermediates which were not detected by  $^1\text{H}$  NMR analysis. Given that reactivity was observed with a complex which possesses the C=O bond, this indicates that this group might be necessary for the oxidation of organopalladium(II) complexes with  $\text{H}_2\text{O}_2$ . Presumably, the C=O group undergoes hydration to produce a facially chelating ligand which in turn enables oxidation of Pd(II) to high oxidation state palladium complexes, which subsequently undergoes C–O bond coupling to generate the oxidized products.

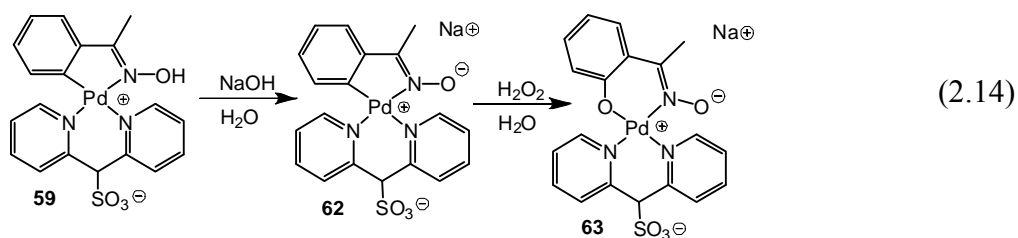
As a result, the oxidation reactions are expected to be facile in the presence of the dpms ligand, which is a bidentate N-donor ligand with the potential to adopt a facially chelating tridentate coordination mode. Besides, the dpms ligand has been shown to facilitate oxidation of organoplatinum(II) complexes with dioxygen.<sup>86</sup>

#### 2.3.4 Reactivity of dpms-ligated Palladacycles **58-60** Towards Oxidation with $H_2O_2$

When a methanolic solution of complex **58** and  $H_2O_2$  were combined, Zhang and co-workers observed near quantitative oxygen insertion into the C-Pd bond at ambient conditions to produce the corresponding oxapalladacycle **61** (Zhang, unpublished results). However no Pd(IV) intermediates were detected in this reaction. Inspired by this result, the oxidation of complexes **59-60** with  $H_2O_2$  was attempted. In the oxidation of complex **59**, a 0.010 M methanolic solution of the complex was combined with 2.0 equivalents of  $H_2O_2$  at ambient conditions. Formation of the corresponding oxapalladacycle **63** among other unidentified products was observed via both  $^1H$  NMR and ESI-MS analysis. The reaction of 0.010 mmoles of complex **60** in 1.0 ml of methanol with  $H_2O_2$  was also investigated. This complex was poorly soluble in methanol. 5.0 equivalents of  $H_2O_2$  were added to the reaction mixture and the resulting mixture was stirred at room temperature for 12 hours. After 12 hours, no changes to the reaction mixture were visually observed or detected by  $^1H$  NMR. The slow reactivity is probably due to the poor solubility of this complex in methanol.



With these results in hand, we attempted the oxidation reactions in water. When 0.010 mmoles of complexes **58-60** were combined with 5.0 equivalents of  $\text{H}_2\text{O}_2$  in  $\text{D}_2\text{O}$  at ambient conditions, no changes were observed by  $^1\text{H}$  NMR over 12 hours. We hypothesized that the slow reactivity of these complexes was due to their poor solubility in water. As a result, we decided to improve the solubility of complex **59** by preparing its anionic analogue and subjecting this solution towards oxidation with  $\text{H}_2\text{O}_2$ . An aqueous reaction mixture of 0.010 mmoles of complex **59** was prepared and 1.0 equivalent of  $\text{NaOD}$  was added to this reaction mixture. Addition of the base led to complete dissolution of the white precipitate to produce a colorless solution. The dissolution resulted probably due to formation of an anionic Pd(II) complex **62** produced upon deprotonation of the oxime moiety as shown below (see eq. 2.14). Addition of 3.0 equivalents of  $\text{H}_2\text{O}_2$  resulted in formation of the corresponding oxapalladacycle **63** cleanly according to both  $^1\text{H}$  NMR and ESI-MS. The  $\text{H}_2\text{O}_2$  was added in 1.0 equivalent batches in 10 minute intervals because decomposition of  $\text{H}_2\text{O}_2$  is fast in basic aqueous solutions. Complex **63** was fully characterized, including NMR spectroscopy, ESI-MS, and X-ray diffraction (Fig. 2.1), while its purity was confirmed using elemental analysis.



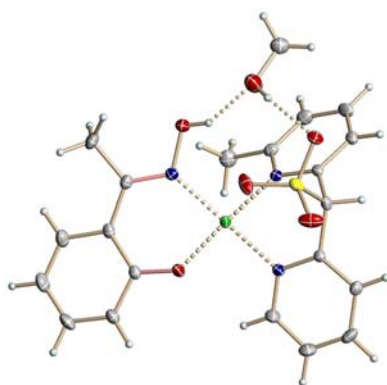
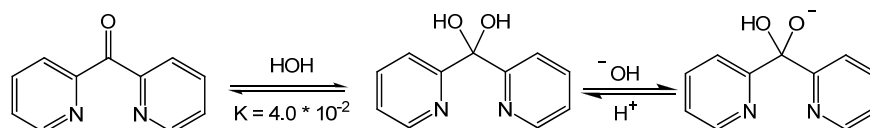


**Figure 2.1.** ORTEP drawing (50 % probability ellipsoid) of complex **63**

The slow reactivity of complexes **58-60** in neutral water, and the lack of detection of Pd(IV) intermediates during the oxidation of basic aqueous solution of complex **59** led us to attempt the oxidation reactions using the 2-dipyridylketone (dpk) ligand. We expect the complexes containing the dpk ligand to be cationic, and thus more soluble in hydroxylic solvents such as water and methanol. Better solubility of these complexes is expected to result in faster and cleaner oxidation reactions, and access to the deprotonated form of the solvated dpk ligand is expected to stabilize the resulting Pd(IV) complexes and allow for their detection in solution. In its hydrated and deprotonated form, the alkoxide is expected to stabilize the Pd(IV) center better than sulfonate group of the dpms since it is more basic, and thus allow for isolation of the Pd(IV) complexes.

**Scheme 2.5**

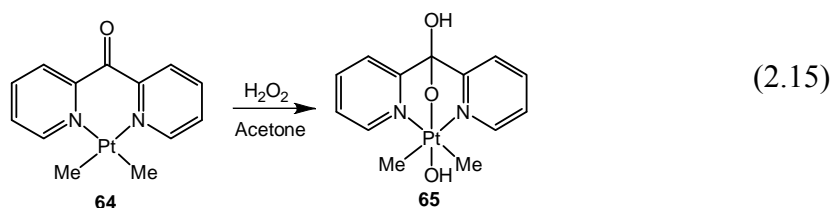


Hydration of the dpk complexes of platinum and palladium has been demonstrated previously. Uncoordinated dpk ligand has been shown to readily undergo addition of nucleophiles such as water to give its hydrated *gem*-diol form,<sup>153</sup>

dpk.H<sub>2</sub>O, where the equilibrium constant for this reaction was calculated to be  $K(\text{dpk.H}_2\text{O}/\text{dpk}) = 4.0 \times 10^{-2}$ .<sup>154</sup> The conversion of this sp<sup>2</sup> hybridized C atom in dpk to sp<sup>3</sup> in dpk.H<sub>2</sub>O was shown to be facilitated by metal coordination to the N-sites, where the equilibrium constant  $K(\text{dpk.H}_2\text{O}/\text{dpk}) = 3.0$  when the dpk ligand is complexed to cis-[Pt(D<sub>2</sub>O)<sub>2</sub>]<sup>2+</sup>. The equilibrium constant is much larger in the case of Pd, where literature has proposed near complete conversion to the hydrate form whenever dpk is bonded to Pd(II).<sup>155</sup>

Because the C=O bond of the dpk ligand in metal-coordinated dpk complexes is very susceptible to attack by nucleophiles, we expect H<sub>2</sub>O<sub>2</sub> to attack the dpk ligand and bring the oxidant in close proximity to Pd(II), and thus facilitate oxidation of hydrocarbyl Pd(II) complexes, and at the same time produce an anionic tridentate ligand with a facially chelating mode that will stabilize the resulting Pd(IV) species.<sup>125</sup>

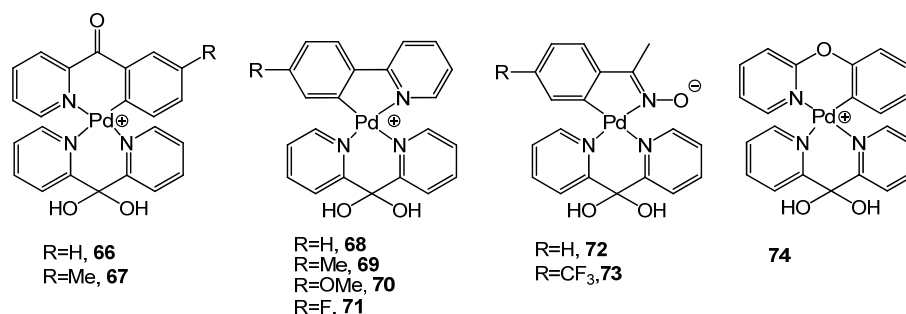
The ability of the dpk ligand to enable oxidation of hydrocarbyl Pt(II) complexes with H<sub>2</sub>O<sub>2</sub> and to stabilize the corresponding hydrocarbyl Pt(IV) complexes has been demonstrated. Puddephatt and co-workers oxidized a dpkPt(II)Me<sub>2</sub> complex **64** with H<sub>2</sub>O<sub>2</sub> in acetone and obtained the corresponding dpkPt(IV)Me<sub>2</sub>(OH) complex **65** (eq. 2.15).<sup>123</sup> This oxidation reaction was enabled by the dpk ligand while the deprotonated dpk hydrate stabilized the resulting Pt(IV) species. We expect a similar reactivity in our system, where the dpk ligand will enable the oxidation reaction and stabilize the resulting monohydrocarbyl-Pd(IV) complexes.



## 2.4 Preparation of dpk-ligated Palladacycles 66-74

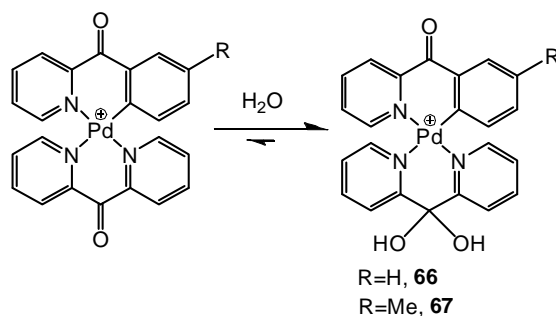
### 2.4.1 Preparation of dpk-ligated Palladacycles 66 and 67

Chart 2.4



The 2-arylpyridine (aryl = benzoyl or 3-methyl benzoyl) derived dpk-based palladacycles **66** and **67** were prepared by combining the acetate bridged palladacycle **49** or **50** and dpk ligand (1.05 eq.) in acetic acid under ambient conditions. The target complexes were obtained as white precipitate by trituration of the reaction solutions with diethyl ether. The identity of the complexes was confirmed using NMR spectroscopy and ESI-mass spectrometry, while the purity was confirmed by elemental analyses.

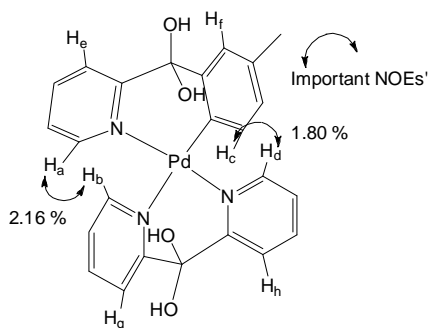
Scheme 2.6



Analysis of the  $^1\text{H}$  NMR spectrum of complex **66** revealed two species in solution with a 95:5 % ratio, while the ESI-MS analysis of the solution revealed two mass envelopes; one at  $m/z = 472.0203$  which was assigned to complex **66** (Calculated for **66**,  $\text{C}_{23}\text{H}_{16}\text{N}_3\text{O}_2^{106}\text{Pd} = 472.0277$ ), and another at  $m/z = 490.0432$  which was assigned to complex **66** with an additional  $\text{H}_2\text{O}$  molecule (calculated for  $\text{C}_{23}\text{H}_{18}\text{N}_3\text{O}_3^{106}\text{Pd} = 490.0383$ , the product of addition of  $1\text{H}_2\text{O}$  across a  $\text{C}=\text{O}$  bond). This indicates that the species observed by  $^1\text{H}$  NMR are the hydrated and dehydrated forms of complex **66**. Using  $^{13}\text{C}$  NMR in  $\text{D}_2\text{O}$ , the identity of the major complex was assigned as the  $\text{C}=\text{O}$  hydrated complex, where a peak at 95.6, characteristic of a hydrate,  $\text{C}(\text{OH})_2$  was observed. In addition, two low-field carbon shifts at 182.0 and 194.4 characteristic of  $\text{C}=\text{O}$  were observed. These signals were assigned to the carbonyl carbons of the acetate and the benzoylpyridine moiety in the complex.

Literature has shown that hydration of dpk ligand becomes more facile upon coordination to  $\text{Pd}(\text{II})$ , and thus the major complex is expected to be hydrated.<sup>154</sup>

*Selective 1D-difference NOE experiments ( $\text{D}_2\text{O}$ ) for complex **66***



The structure of complex **66** in solution was confirmed by Selective 1D-difference NOE experiments. In the 1D difference NOE experiment, positive NOE was observed between  $\text{H}_a$  and  $\text{H}_b$  (2.16 %), and between the  $\text{H}_c$  and  $\text{H}_d$  (1.80 %) (mixing time of 0.6s, delay time 3s).

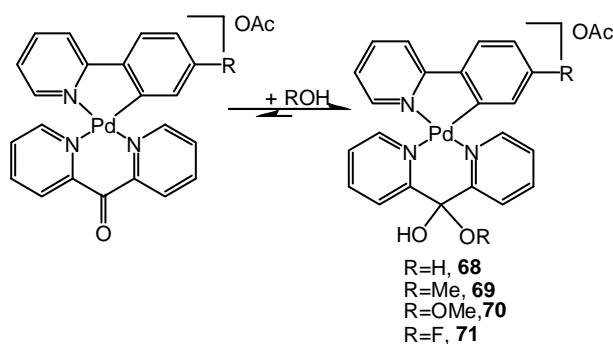
Complete peak assignment was accomplished via  $^1\text{H}$  and  $^{13}\text{C}$  NMR,  $^1\text{H}$ - $^1\text{H}$  COSY,  $^1\text{H}$ - $^{13}\text{C}$  HMBC,  $^1\text{H}$ - $^{13}\text{C}$  HSQC, 1D Selective NOE and 1D Selective TOCSY experiments. Selected  $^1\text{H}$  NMR peaks are presented in the table below:

**Table 2.4.** Selected  $^1\text{H}$  NMR peaks for complex **66**.

H	H <sub>a</sub>	H <sub>b</sub>	H <sub>c</sub>	H <sub>d</sub>	H <sub>e</sub>	H <sub>f</sub>	H <sub>g</sub>	H <sub>h</sub>
(ppm)	8.38	7.61	6.83	7.41	8.12	7.37	8.06	8.04

#### 2.4.2 Preparation of dpk-ligated Palladacycles **68-71**

**Scheme 2.7**

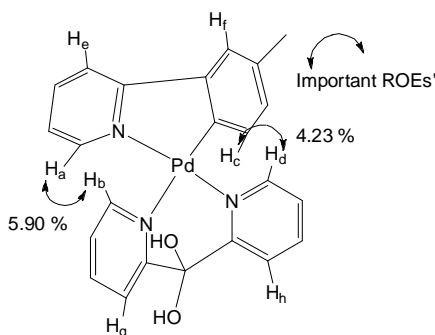


Complexes **68-71** were prepared by combining the acetato-bridged palladacycle **51-54** with the dpk ligand (1.05 eq.) in either dichloromethane (complexes **68-70**) or acetic acid (complex **71**). The target compounds were obtained as white precipitate by trituration of the solutions with either thf or diethyl ether. The identity of the complexes **68-71** was confirmed by NMR spectroscopy and ESI-Mass spectrometry, while the purity was confirmed by elemental analysis.

The complexes were shown by  $^{13}\text{C}$  NMR spectroscopy to have a hydrated carbonyl group of the dpk ligand as expected. The  $^{13}\text{C}$  NMR spectrum of complex **69** in  $\text{D}_2\text{O}$  showed a peak at 95.6 ppm characteristic of a hydrate,  $\text{C}(\text{OH})_2$ , and the

presence of only one C=O peak at 181.9 ppm assigned to the carbonyl group of the acetate counterion. This composition was also confirmed by electrospray ionization mass spectrometry. The ESI-MS of complex **69** in water shows the presence of signals derived from both the hydrated and non-hydrated complexes. Similar observations were made for complexes **68**, **70** and **71**.

*Selective 1D-difference NOE experiments (D<sub>2</sub>O) for complex 69*



The structure of complex **69** in solution was confirmed by Selective 1D-difference NOE experiments. In the 1D difference NOE experiment, positive NOE was observed between H<sub>a</sub> and H<sub>b</sub> (5.90 %), and between the H<sub>c</sub> and H<sub>d</sub> (4.23 %) (mixing time of 0.6s, delay time 4s).

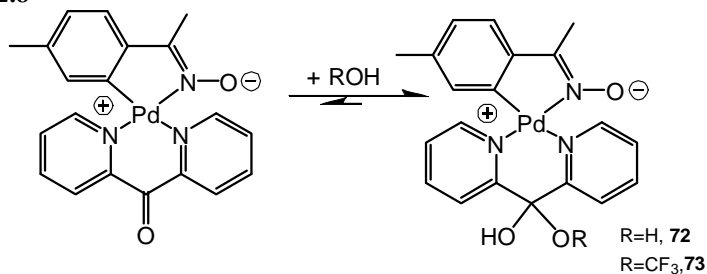
Complete peak assignment was accomplished via <sup>1</sup>H and <sup>13</sup>C NMR, <sup>1</sup>H-<sup>1</sup>H COSY, <sup>1</sup>H-<sup>13</sup>C HMBC, <sup>1</sup>H-<sup>13</sup>C HSQC, 1D Selective NOE and 1D Selective TOCSY experiments. Selected <sup>1</sup>H NMR peaks are presented in the table below:

**Table 2.5.** Selected <sup>1</sup>H NMR peaks for complex **69**.

H	H <sub>a</sub>	H <sub>b</sub>	H <sub>c</sub>	H <sub>d</sub>	H <sub>e</sub>	H <sub>f</sub>	H <sub>g</sub>	H <sub>h</sub>
(ppm)	7.68	7.80	6.28	7.92	7.47	7.16	7.89	7.80

### 2.4.3 Preparation of dpk-ligated Palladacycles **72** and **73**

Scheme 2.8

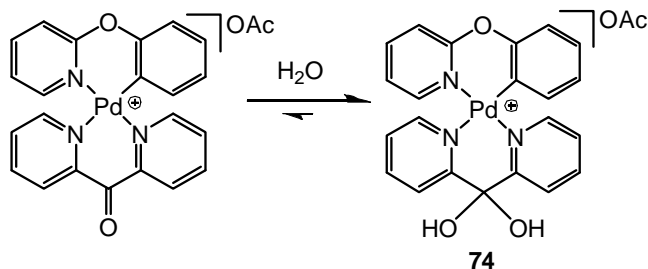


Complexes **72** and **73** were prepared by combining the acetato-bridged palladacycle **55** or **56** with the dpk ligand (1.05 eq.) in methanol under ambient conditions. The target compounds were obtained as white precipitate by trituration of the reaction mixtures with diethyl ether. The identity of the complexes was established using NMR spectroscopy and ESI-mass spectrometry, while the purity was confirmed by elemental analysis.

The <sup>1</sup>H NMR analysis of these complexes in deuterated acetic acid or methanol showed only one singlet in the aliphatic region integrating as 3 hydrogens, indicating absence of the acetate counterion. This analysis indicates that these compounds were isolated as zwitterions with a deprotonated OH<sup>-</sup> group of the oxime moiety. However a small amount of acetic acid was observed in both the <sup>1</sup>H NMR spectra (integrating to <1H) and elemental analysis of complexes **72** and **73**.

### 2.4.4 Preparation of dpk-ligated Palladacycles **74**

Scheme 2.9



Complex **74** was prepared by combining the acetato-bridged palladacycle **57** and with the dpk ligand (1.05 eq.) in acetic acid under ambient conditions. The target complex was obtained as white precipitate by trituration of the reaction solution with diethyl ether. The identity of the complex was determined using NMR spectroscopy, X-ray diffraction and ESI-mass spectrometry, while the purity was confirmed by elemental analysis.

$^1\text{H}$  NMR analysis of complex **74** in chloroform displayed a high-field singlet at 1.97 ppm assigned to the acetate counterion. X-ray quality crystals of complex **74** could be grown by layering a dichloromethane solution of the complex with diethyl ether in the freezer. According to the X-ray diffraction, the hydrated dpk ligand is coordinated to Pd in N-N mode. The geometry around palladium is square planar as expected for a Pd(II) compound. The Pd-N bond-length *trans* to the aryl ligand is elongated (2.142 Å) relative to the Pd-N bond-length *trans* to the pyridine group of the phenoxypyridine ligand (2.063 Å), as expected due to the higher *trans* influence of the phenyl ligand. Each of the two six-membered rings forms a boat conformation. The complex is also cationic, and one acetate ligand was observed for every Pd atom.

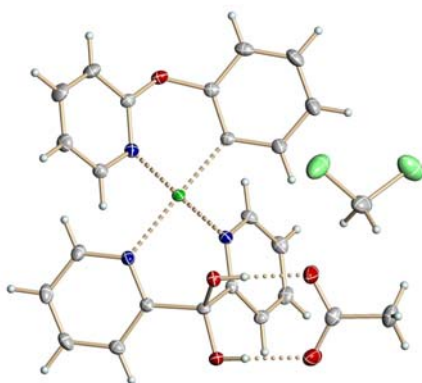


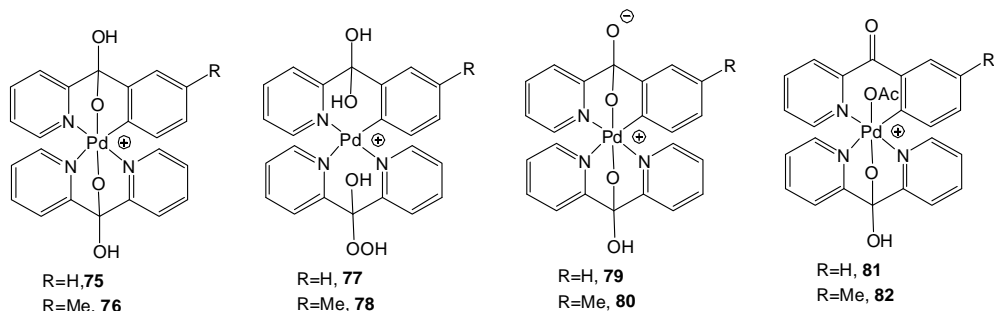
**Figure 2.2.** ORTEP drawing (50 % probability ellipsoid) of complex **74**

## 2.5 Oxidation of dpk-ligated Palladacycles **66-74** with $H_2O_2$ in Water

### 2.5.1 Oxidation of Complexes **66** and **67** to Monohydrocarbyl Pd(IV) Complexes **75**

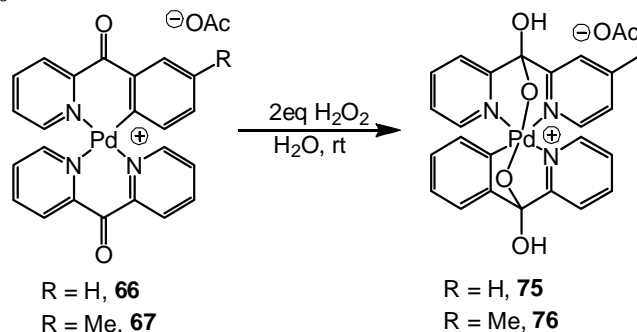
### and **76** with $H_2O_2$ in Water

Chart 2.5



The oxidation of complexes **66** and **67** was expected to yield stable Pd(IV) complexes due to the presence of two tridentate facially chelating ligands derived from the hydrated 2-arylpyridine, and the hydrated dpk ligand.

Scheme 2.10



The dpk ligand-supported arylpyridine-derived palladacycle **66** or **67** (0.01 mmol) was dissolved in 1.0 ml of  $D_2O$  and 2.0 equivalents of  $H_2O_2$  was added, leading to immediate formation of a deep yellow solution and gradual appearance of new peaks by  $^1H$  NMR. The new products, identified as the corresponding Pd(IV) complexes **75** and **76** were formed quantitatively in less than 2 hours at room temperature. These compounds were isolated by removal of water, and were characterized using NMR, electrospray ionization mass spectrometry (ESI-MS), and

X-ray diffraction analysis of complex **75**. The  $^1\text{H}$  NMR spectrum of complex **75** in  $\text{D}_2\text{O}$ , deuterated acetic acid or methanol revealed the presence of 16 partially overlapping multiplets in the aromatic region integrating as 1H each, indicative of a  $C_1$  symmetric structure. X-ray quality crystals of complex **75** were grown by slow diffusion of diethyl ether into a cold methanolic solution of the complex **75**.

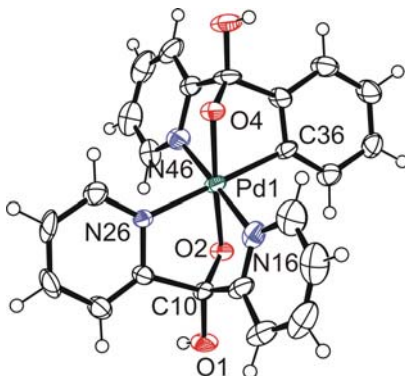
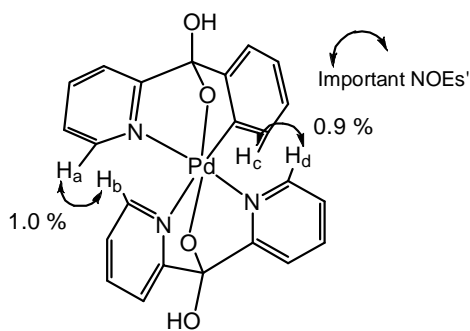


**Figure 2.3.** ORTEP drawing (50 % probability ellipsoid) of complex **75**

The structure of these complexes in solution was confirmed by  $^1\text{H}$ ,  $^{13}\text{C}$ , and 1D selective NOE spectroscopy.

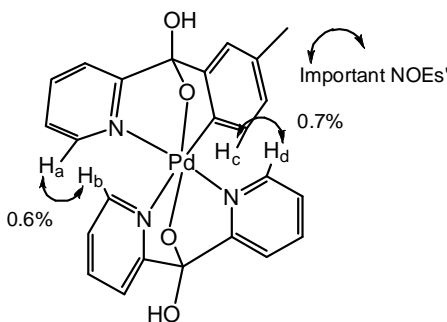
*Selective 1D-difference NOE experiments ( $\text{AcOH-d}_4$ ) for **75***



The structure of complex **75** in solution was confirmed by  $^1\text{H}$  and  $^{13}\text{C}$  NMR, and 1D NOE experiments. In the 1D difference NOE experiment, positive NOE was

observed between H<sub>a</sub> and H<sub>b</sub> (1.0 %) and between H<sub>c</sub> and H<sub>d</sub> (0.9 %) (mixing time of 0.8s, delay time 5s).

*Selective 1D-difference NOE experiments (AcOH-d<sub>4</sub>) for 76*



The structure of complex **76** in solution was also confirmed by <sup>1</sup>H and <sup>13</sup>C NMR, and 1D NOE experiments. In the 1D difference NOE experiment, positive NOE was observed between H<sub>a</sub> and H<sub>b</sub> (0.6 %) and between H<sub>c</sub> and H<sub>d</sub> (0.7 %) (mixing time of 0.8s, delay time 5s).

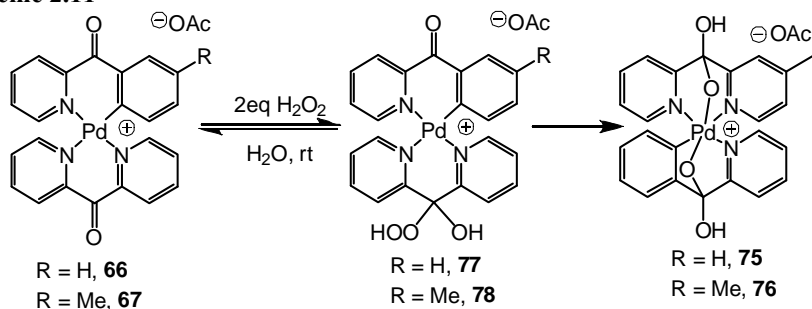
Complex **75** was isolated from the aqueous solution by removal of the solvent under vacuum to afford a brown solid. The complex decomposes when left under vacuum for a long time. Complex **75** is also not stable in the solid state at room temperature. It is however stable in water for over 1 week at room temperature, and is also stable in water up to 90°C, but when heated at this temperature for over 30 minutes, it decomposes to produce a black solid.

Complex **75** could be characterized by <sup>1</sup>H NMR spectroscopy in such solvents as water, methanol and acetic acid. However, when the complex is dissolved in dimethyl sulfoxide, a complex <sup>1</sup>H NMR results indicating the presence of multiple species.

The isolation of these relatively stable cationic Pd(IV) complexes **75** and **76** is intriguing because the cationic nature of Pd(IV) complexes has been reported to lead to decreased stability, and higher reactivity in reductive elimination reactions.<sup>156</sup>

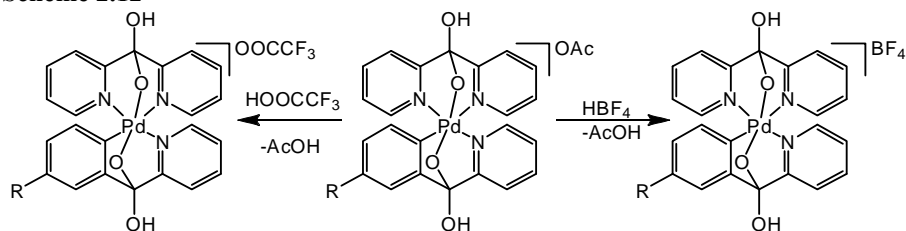
Since access to these Pd(IV) complexes by aerobic oxidation was not successful, facile oxidation by H<sub>2</sub>O<sub>2</sub> was proposed to take place in part due to the ability of a coordinated dpk ligand to add nucleophilic H<sub>2</sub>O<sub>2</sub> across the C=O of the dpk ligand, so accommodating the oxidizing hydroperoxo group in close proximity to a reducing Pd(II) center as shown in Scheme 2.11.

**Scheme 2.11**



*Synthesis of BF<sub>4</sub> and OOCF<sub>3</sub> salts of complexes 75 and 76*

**Scheme 2.12**

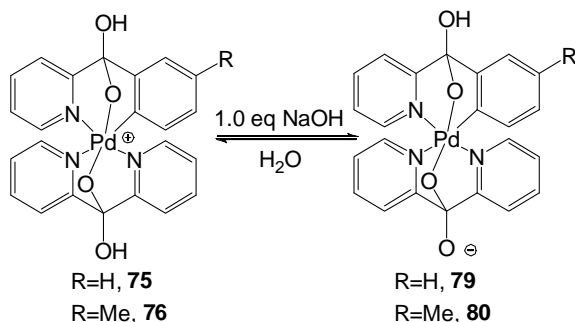


The isolation of complexes **75** and **76** was greatly facilitated by precipitation of the cations in the form of the corresponding less soluble OOCF<sub>3</sub><sup>-</sup> and BF<sub>4</sub><sup>-</sup> salts. Addition of 10-20 eq of either tetrafluoroboric or trifluoroacetic acid to an aqueous solution of **75** or **76** resulted in immediate precipitation of yellow solid (in the case or

trifluoroacetic acid) or orange solid (in the case of tetrafluoroboric acid). Solutions of **75**(OOCCF<sub>3</sub>), **75**(BF<sub>4</sub>), **76**(OOCCF<sub>3</sub>), and **76**(BF<sub>4</sub>) in dms-*d*<sub>6</sub> exhibited two additional broad singlets in the downfield region. In particular, the solution of **75**(OOCCF<sub>3</sub>) in dms-*d*<sub>6</sub> exhibited broad singlets at 8.82 and 9.11 ppm integrating as 1H each, which were assigned to the protons of two OH groups present in cation **75**<sup>+</sup>. The ESI-MS of both complexes showed the presence of a single cationic complex with the same m/z ratio as the corresponding acetate. The mass spectra of **75**(X) and **76**(X) dissolved in methanol (X = OAc or OOCCF<sub>3</sub>) or dms-*d*<sub>6</sub> (X = OOCCF<sub>3</sub> or BF<sub>4</sub>) showed the presence of the cation **75**<sup>+</sup> or **76**<sup>+</sup> as the sole Pd-containing species. The isolated yields are: **75**(OOCCF<sub>3</sub>), 83 %; **75**(BF<sub>4</sub>), 83 %; **76**(OOCCF<sub>3</sub>), 87 %; **76**(BF<sub>4</sub>), 92 %.

Preparation of Zwitterionic complexes **79** and **80**

Scheme 2.13



The zwitterionic analogues of complexes **75** and **76** were also prepared. To an aqueous solution of complex **75** or **76** (0.10 mmol) was added ~1 eq NaOH, leading to precipitation of an orange solid. The reaction mixture was filtered and the residue was washed with a small amount of cold water to afford the target compounds in 70% for **79** and 71% for **80** after drying at room temperature for a few hours. <sup>1</sup>H NMR

spectra taken in methanol- $d_4$  revealed a simple complex with 16 multiplets, with excess water of crystallization present. Residual water could not be completely removed since both complexes **79** and **80** decompose when placed under vacuum at room temperature. For samples dried under vacuum for an extended period, the  $^1\text{H}$  NMR spectra in methanol reveal appearance of additional peaks over time, and eventually disappearance of the peaks of **79** or **80**.

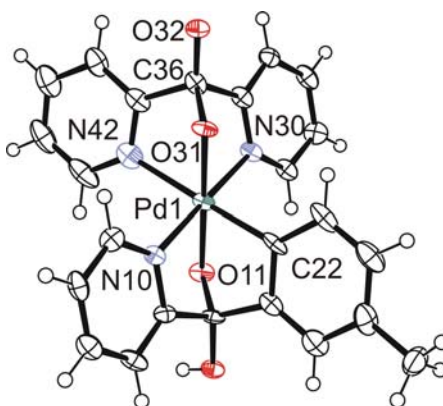
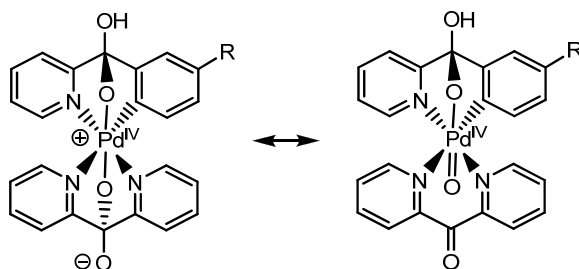


**Figure 2.4.** ORTEP drawing (50 % probability ellipsoid) of complex **79**

X-ray quality crystals of complexes **79** and **80** were grown from alkaline solutions of the complexes. The C36-O32 (1.326(5) Å) and Pd1-O31 (1.974(3) Å) bonds in the zwitterionic complex **80** were observed to be  $\sim 0.02$ - $0.07$  Å shorter than the matching bonds in the cation **76**, with C10-O1 (1.393(7) Å) and Pd1-O2 (2.011(4) Å), respectively. This bond shortening may be indicative of a resonance contribution of Pd(IV) oxo complex featuring C=O and Pd(IV)=O fragments and no formal charge separation, as shown in Scheme 2.14

Scheme 2.14



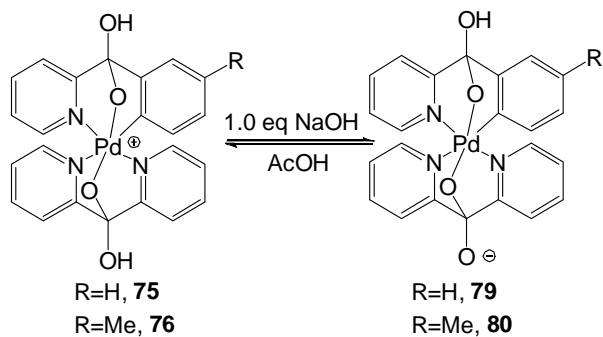
Both **79** and **80** dissolve in the presence of one equivalent of aqueous alkali metal hydroxide to form clear solutions.

Complexes **79** and **80** are not stable in the solid state at room temperature and undergo slow decomposition. For complex **79**, ~ 10 % decomposition was observed at room temperature in 7 days according to <sup>1</sup>H NMR spectroscopy in methanol. However, the complex is stable in the solid state at low temperature, at -20°C.

The zwitterionic complexes are sparingly soluble in H<sub>2</sub>O. In methanol, complex **79** is soluble, but undergoes decomposition, where 50% decomposition had taken place in ~ 108 minutes. The complex is more soluble in trifluoroethanol and the decomposition rate is slower, where only 20 % decomposition was observed in 150 minutes. Complex **79** dissolves slowly in dmsol producing multiple peaks by <sup>1</sup>H NMR, indicating decomposition and formation of multiple products. Similar decomposition pattern was also observed for complex **80**.

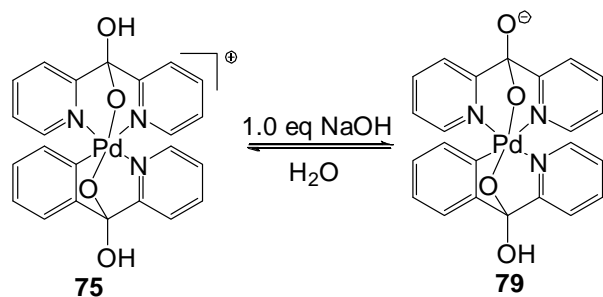
The deprotonation of complexes **75** and **76** to produce **79** and **80** (see below) respectively is reversible: when either **79** or **80** is dissolved in acetic acid-*d*<sub>4</sub>, complete protonation occurs leading to formation of **75** or **76**, according to <sup>1</sup>H NMR analysis. Comparison of the <sup>1</sup>H NMR spectra obtained for **79** or **80** in deuterated acetic acid matches exactly the <sup>1</sup>H NMR spectrum of **75** or **76** in the same solvent.

Scheme 2.15



Potentiometric determination of  $pK_a$  for complex **75**

Scheme 2.16



The  $pK_a$  of complex **75** was determined by titration of an aqueous solution of complex **75** (6.6 mg of complex in 2.0466 g of  $\text{H}_2\text{O}$  at  $22^\circ\text{C}$ ) with 0.1000 N NaOH solution.

The results of the titration are given in figure 2.5 below:

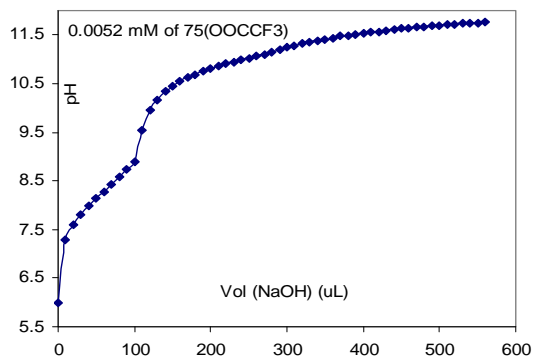


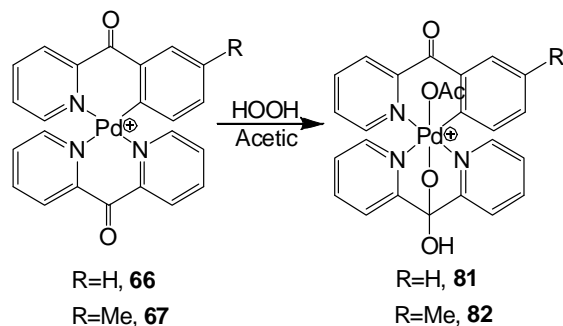
**Figure 2.5.** pH of the solution of 0.0052 mM solution of **75** in water vs added volume of 0.1000 M NaOH.

The first bend ( $pH = 8.73$ ,  $vol = 90 \mu\text{L}$ ) shows the point where precipitate formation (complex **79**) took place. Dissolution of the precipitate occurred gradually until addition of  $290 \mu\text{L}$  ( $pH = 11.9$ ), where the solution was completely clear. Hence, for  $pK_a$  calculations the range of the  $pH$  from 6.00 to 8.73 was considered. In these calculations it was assumed that each portion of the base added contributed to two processes only,  $[\text{OH}^-]$  increase (reflected in the  $pH$  change) and **[79]** increase. The  $K_a$  values were calculated at each point as  $K_a = [\text{79}][\text{H}^+]/[\text{75}]$ , where the total amount of **79** and **75** in solution = initial amount of **75** used.

An average was calculated and the  $pK_a$  for **75** was found to be  $8.14 \pm 0.02$  and  $8.16 \pm 0.02$  in two independent titrations.

### 2.5.2 Oxidation of Complexes **66** and **67** to Monohydrocarbyl Pd(IV) Complexes **75** and **82** with $\text{H}_2\text{O}_2$ in Acetic Acid

**Scheme 2.17**



The addition of 3.0 equivalents of  $\text{H}_2\text{O}_2$  to an acetic acid solution of complex **66** resulted in an exothermic reaction and color change of the solution from light to deep yellow.  $^1\text{H}$  NMR monitoring of the reaction revealed generation of a single product with 16 multiplets in less than 5 minutes (Fig. 2.6). The  $^1\text{H}$  NMR chemical shifts of the product are generally significantly shifted downfield, where the aromatic

signals in the Pd(II) precursor **66** cover a range of 6.7-8.4 ppm while the aromatic signals for complex **81** cover a range of 7.1-8.7 ppm. This downfield shift of all the aromatic hydrogens indicates a more deshielded environment, and would signify coordination of the ligands to a more electrophilic central atom, supporting the assignment of complex **81** as a Pd(IV) species. ESI-MS analysis of the reaction immediately upon addition of H<sub>2</sub>O<sub>2</sub> revealed two major peaks at m/z = 506.0323 corresponding to complex **66** plus 2OH groups (assigned to complex **75**) and 548.0321 corresponding to complex **66** plus 1 OH and 1 OAc groups (assigned to complex **81**).

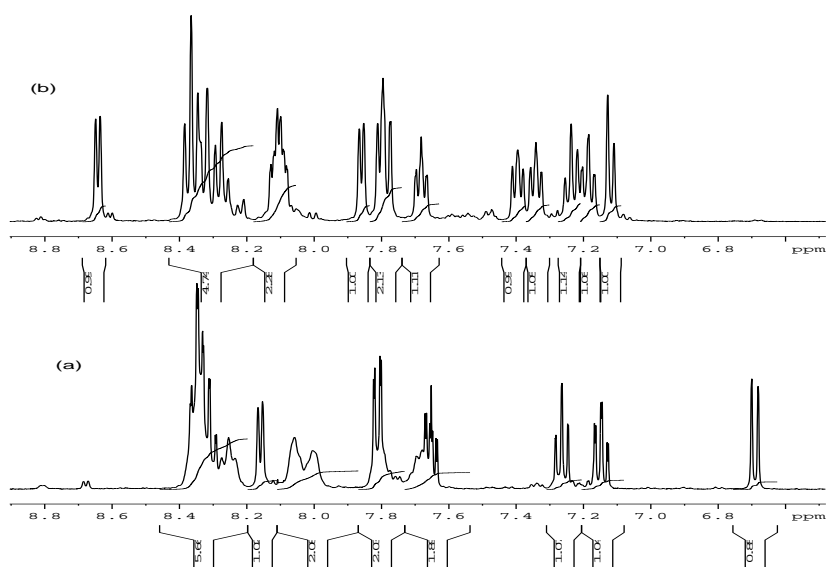


**Figure 2.6.** Acetic acid solutions of (a) complex **66**; (b) complex **81** at room temperature.

When a 0.010 M acetic acid solution of complex **81** was left at room temperature for 2 days, a mixture of the corresponding phenol **106** and aryl acetate **108** products were observed in 41 to 57 % yields respectively. This decomposition pattern signifies the presence of a Pd(IV) center bearing a hydroxide and an acetato

ligand. The phenol **106** was identified by comparison of its  $^1\text{H}$  NMR spectrum to literature,<sup>157</sup> while the aryl acetate was prepared by acetoxylation of the phenol **106** in a AcOH/Ac<sub>2</sub>O mixture. Its identity was confirmed via NMR and ESI–MS analysis.

Since ESI–MS reveals the presence of two species in solution while the  $^1\text{H}$  NMR reveals the presence of one predominant species in solution, additional  $^1\text{H}$  NMR experiments were conducted to determine the identity of the product of oxidation. In the first test, complex **75** was dissolved in acetic acid and the  $^1\text{H}$  NMR compared to that of the product of oxidation. The  $^1\text{H}$  NMR pattern of the two complexes were significantly different, indicating that the predominant product of oxidation is not complex **75**, and it was assigned to complex **81**, based on the ESI–MS analysis.

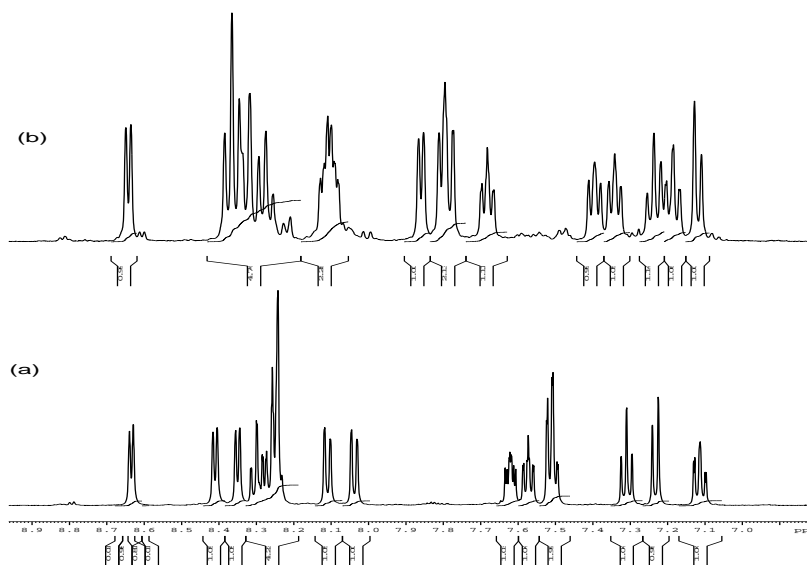


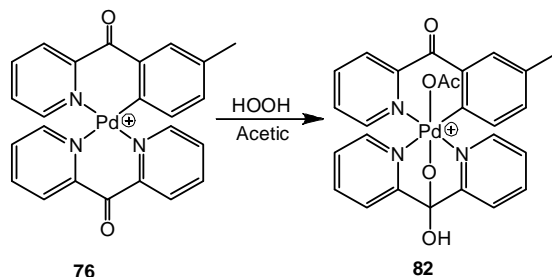
**Figure 2.7.** Acetic acid solutions of (a) complex **75**; (b) complex **81** at room temperature.

In a second test, complex **66** and H<sub>2</sub>O<sub>2</sub> were combined in a mixture of deuterated acetic acid and water in order to determine whether two products will be



acetic acid to produce the corresponding phenol **106** and aryl acetate **108** in less than 12 hours.

Scheme 2.18



The addition of 3.0 equivalents of  $\text{H}_2\text{O}_2$  to an acetic acid solution of complex **67** resulted in an exothermic reaction and color change of the solution from light to deep yellow.  $^1\text{H}$  NMR monitoring of the reaction revealed generation of a single product with 15 multiplets in less than 5 minutes (see figure below). The  $^1\text{H}$  NMR chemical shifts of the product are generally significantly shifted downfield, where the aromatic signals in the Pd(II) precursor **67** cover a range of 6.5-9.4 ppm while the aromatic signals for complex **82** cover a range of 7.0-9.6 ppm. This downfield shift of the aromatic hydrogens indicates a more deshielded environment, and would also signify coordination of the ligands to a more electrophilic central atom, supporting the assignment of compound **82** as a Pd(IV) species. ESI-MS analysis of the reaction immediately upon addition of  $\text{H}_2\text{O}_2$  revealed two major peaks at  $m/z = 520.0472$  corresponding to complex **67** plus 2OH groups (assigned to complex **76**) and 562.0611 corresponding to complex **67** plus 1 OH and 1 OAc groups (assigned to complex **82**). When an acetic acid solution of the product of oxidation was left at room temperature for 2 days, a mixture of the corresponding phenol **107** and aryl acetate **109** products were observed in 39% to 57% yields respectively. This decomposition pattern signifies the presence of Pd(IV) center bearing a hydroxide



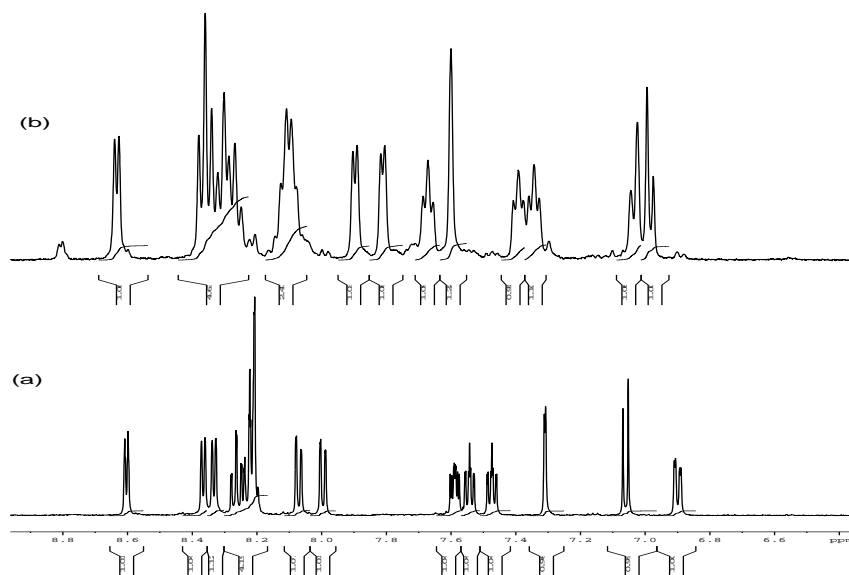
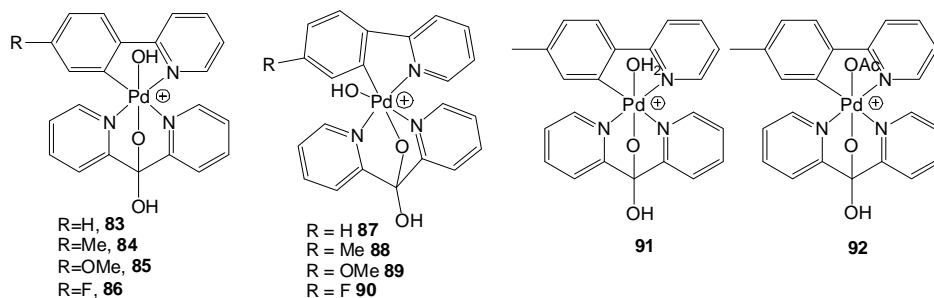


**Figure 2.10.** Room temperature AcOD solutions of (a) complex **76**; (b) complex **82**.

This analysis indicates that oxidation of complex **67** with  $\text{H}_2\text{O}_2$  in acetic acid produces complex **82**, which undergoes C–O bond-forming reductive elimination in acetic acid to produce the corresponding phenol **107** and aryl acetate **109** in less than 12 hours.

### 2.5.3 Oxidation of Complexes **68-71** to Monohydrocarbyl Pd(IV) Complexes **83-86** with $\text{H}_2\text{O}_2$ in Water

**Chart 2.6**



Oxidation of complexes **68-71** with 1.5 eq of  $\text{H}_2\text{O}_2$  in water at room temperature led to formation of a deep yellow solution, which became lighter as the

reaction progressed, ultimately producing the corresponding oxapalladacycles quantitatively. When the oxidation reaction was performed with 10.0 equivalents of H<sub>2</sub>O<sub>2</sub> and monitored by <sup>1</sup>H NMR at 3 °C, clean quantitative formation of the corresponding Pd(IV) products **83-86** was observed. These complexes are stable at this temperature for at least 2 hours.

The identity of complexes **83-86** was confirmed by NMR spectroscopy and ESI-MS. An attempt to isolate complex **84** was not successful. When aqueous solution of complex **84** was dried under vacuum at 0 °C, an orange solid was obtained, which contained a mixture of Pd(IV) complex **84** and the corresponding oxapalladacycle **107**. This indicates that complex **84** decomposes in the solid state under vacuum to generate the product of C-O bond coupling. As a result, isolation of the trifluoroacetate salt of complex **84** was attempted. This is because the isolation of complexes **75** and **76** was greatly facilitated by precipitation of the cations in the form of the corresponding less soluble OOCF<sub>3</sub> and BF<sub>4</sub> salts. Therefore excess trifluoroacetic acid was added into aqueous solution of complex **84** at 0 °C and the resulting solution was dried under vacuum at 0 °C. An orange precipitate was obtained which gave a simple <sup>1</sup>H NMR pattern in D<sub>2</sub>O with 15 multiplets. The <sup>1</sup>H NMR pattern of this complex was similar to that of complex **84** except that the high field signal belonging to the acetate counterion was absent. Analysis of this complex by ESI-MS gave an m/z ratio similar to the cation of complex **84**. In order to determine the identity of this complex, X-ray quality crystals were grown from an aqueous solution of complex **84** layered onto aqueous trifluoroacetic acid at -20°C.

X-ray quality crystals of an aqua ligated Pd(IV) complex identified as complex **92** were obtained.

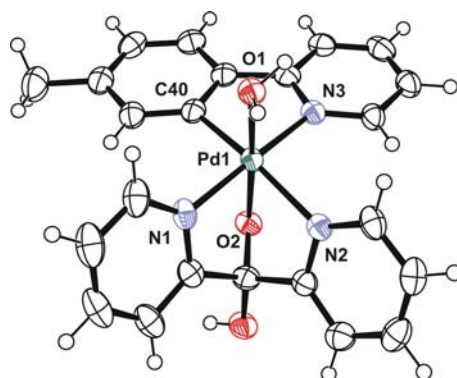
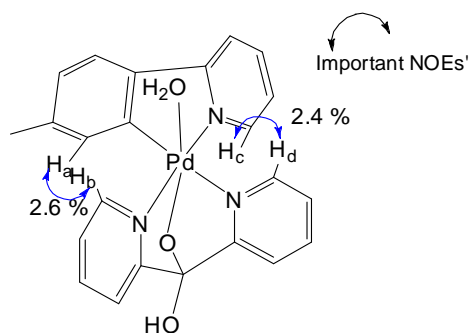


**Figure 2.11.** ORTEP drawing (50 % probability ellipsoid) of complex **91**

This compound was characterized by NMR, ESI-MS and its purity was confirmed by elemental analysis. Its solution state structure was confirmed by 1D difference NOE experiment.

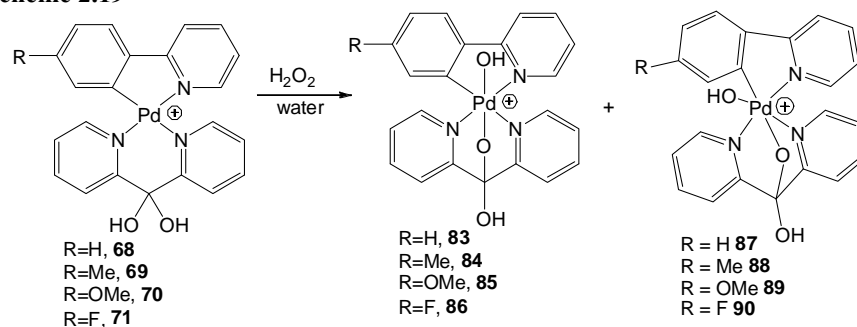
*Selective 1D-difference NOE experiment ( $D_2O$ ) for **91***



In the 1D difference NOE experiment, positive NOE was observed between H<sub>a</sub> and H<sub>b</sub> (2.6 %) and between H<sub>c</sub> and H<sub>d</sub> (2.4 %) (mixing time of 0.8s, delay time 5s). This indicates that the solid state structure is maintained in solution.

*<sup>1</sup>H NMR characterization of a mixture of complex 68-71 and H<sub>2</sub>O<sub>2</sub>*

Scheme 2.19



Analysis of the <sup>1</sup>H NMR spectra of a mixture containing one of the complexes **68-71** and 1.5 equivalents of H<sub>2</sub>O<sub>2</sub> in water at 3-22 °C revealed gradual formation of two products (see fig. 2.12 and 2.13 below). Both products are stable at 3 °C for over 2 hours, but they undergo decomposition by C–O bond elimination at higher temperatures.

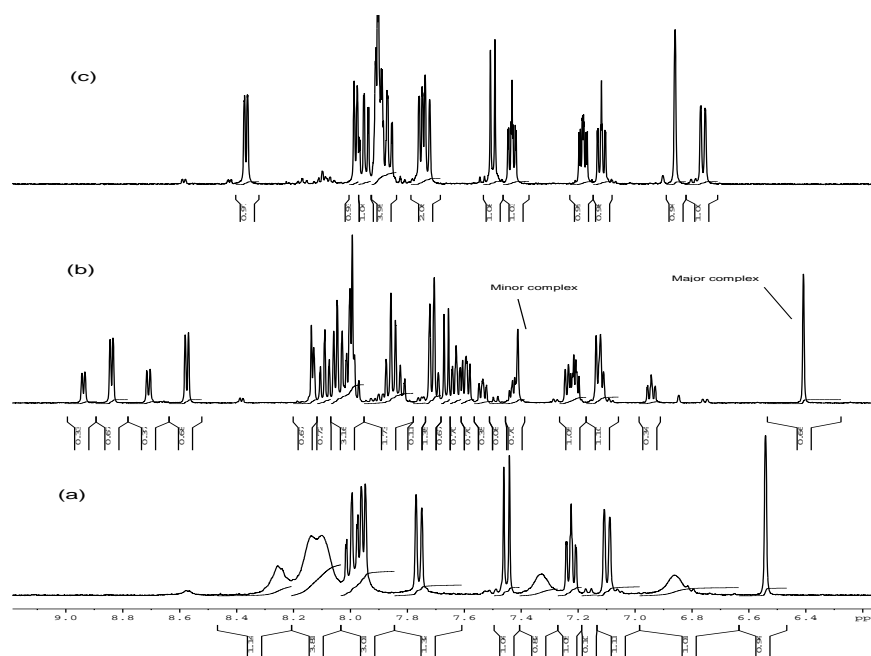


**Figure 2.12.** <sup>1</sup>H NMR spectra of (a) 0.010 M D<sub>2</sub>O solution of complex **69** at 25 °C, (b) D<sub>2</sub>O solution of complexes **84** (major) and **88** (minor), (c) D<sub>2</sub>O solution of the oxapalladacycle **108** at the end of the reaction.

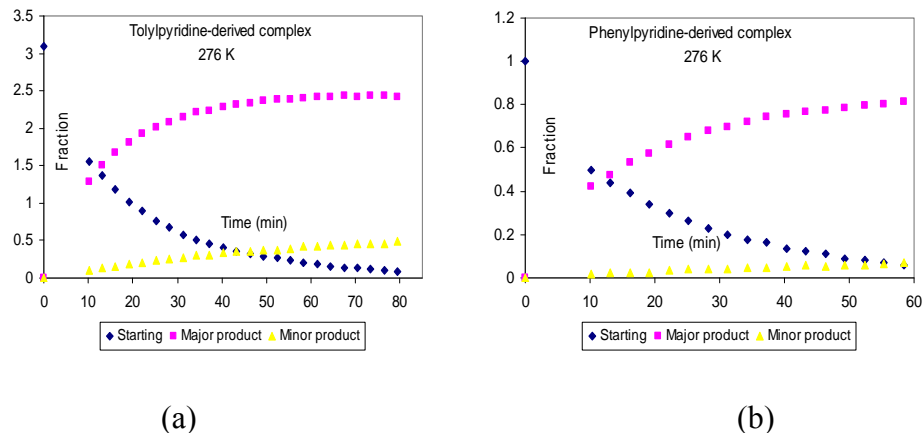


**Figure 2.13.** (a) Plot for the oxidation of 0.010 M  $D_2O$  solution of complex **69** in water with 1.5 eq  $H_2O_2$  at 3 °C showing the fraction of the starting complex **69**, the major product **84**, and the minor product **88** as a function of reaction time; (b) Plot for the oxidation of 0.010 M  $D_2O$  solution of complex **68** in water with 1.5 eq  $H_2O_2$  at 3 °C Oxidation showing the fraction of the Pd(II) precursor **68**, the major product **83**, and the minor product **87**, as a function of time.

The ratio of the two products formed upon combining 0.010 M aqueous solutions of complexes **68-71** with 1.5 eq  $H_2O_2$  varied depending on the nature of the substrate used. The ratio of these two products as a function of the substrate is presented in table 2.6 below.

**Table 2.6.** Oxidation of 0.010 M  $D_2O$  solution of complexes **68-71** with 1.5 equivalent of  $H_2O_2$  at 3 °C, showing the ratio of the major and minor products.

1.5 eq HOOH, 276 K		
Substrate	Major product (%)	Minor product (%)
R=H, <b>68</b>	92	8
R=Me, <b>69</b>	83	17
R=OMe, <b>70</b>	80	20
R=F, <b>71</b>	95	5

In this analysis, more electron-rich substrates such as complex **69** exhibited a higher fraction of the minor product while electron-poorer substrates such as complex **71** exhibited a lower fraction of the minor product.

The ratio of the two products formed upon oxidation of 0.010 M D<sub>2</sub>O solution of complex **69** with 1.5 and 10.0 equivalents of H<sub>2</sub>O<sub>2</sub> at 3-25 °C was also found to be dependent on the amount of H<sub>2</sub>O<sub>2</sub> used and the temperature at which the reaction was carried out (table 2.7).

**Table 2.7.** Oxidation of 0.010 M D<sub>2</sub>O solution of complex **69** with H<sub>2</sub>O<sub>2</sub>, showing the ratio of the major product **84** and minor product **88** as a function of [H<sub>2</sub>O<sub>2</sub>] and temperature.

1.5 eq HOOH			10.0 eq HOOH		
Temp	Major product	Minor product	Temp	Major product	Minor product
3 °C	83	17	3 °C	96	4
10 °C	73	27	10 °C	89	11
25 °C	61	39	25 °C	86	14

\*The product ratio was taken after complete conversion of complex **69**, and before > 5 % oxapalladacycle was present. The time for complete conversion is dependent upon the amount of H<sub>2</sub>O<sub>2</sub> used and the temperature at which the reaction is carried out.

The ratio of the two products of oxidation, complexes **84** and **88** was also found to be dependent on the pH of the solution. For example, when the oxidation of complex **69** was carried out in buffered D<sub>2</sub>O solutions of various pD values, the ratio of complexes **84** to **88** was observed to change significantly (Table 2.8).

**Table 2.8.** Oxidation of 0.010 M D<sub>2</sub>O solution of complex **69** with 2.0 eq of H<sub>2</sub>O<sub>2</sub> at 17°C, showing the ratio of the major product **84** and minor product **88** as a function of pD.

pD	Major (%)	Minor (%)
4.86	91	8
5.97	85	14
6.82	76	23
7.37	79	21
8.99	87	12

\*The pH meter was calibrated using pH scale but D<sub>2</sub>O solutions were used, and therefore pD = pH + 0.41.<sup>159</sup>

In an effort to determine whether the two products can interconvert as the temperature changes, various experiments were performed at one temperature and exposed to a different temperature to observe whether there would be any change in the ratio of the two products of oxidation. In the first experiment, a 0.010 M aqueous solution of complex **69** was combined with 1.5 equivalents of H<sub>2</sub>O<sub>2</sub> at 25 °C and a product ratio of 61:39 was observed by <sup>1</sup>H NMR. This solution was transferred to another NMR instrument whose temperature was set to 3 °C and <sup>1</sup>H NMR was collected after 2 hrs; a product ratio of 67:33 was observed. Similarly, when the oxidation reaction was performed at 3 °C with 10.0 eq HOOH, a product ratio of 96: 4 was observed. Upon warming the solution to 25 °C, the product ratio decreased to 92: 8, while cooling it back to 3 °C further decreased the ratio to 91:9. In all these experiments, care was taken to avoid accumulation of the corresponding oxapalladacycle to greater than 5 %. These experiments indicate that isomerization of the two complexes takes place, but the rate of isomerization is too slow.

### Identity of the Major and Minor products of oxidation

In order to determine the identity of the two products resulting from combining complex **69** and H<sub>2</sub>O<sub>2</sub> in water, the <sup>1</sup>H NMR signals for both products were assigned and 1D Selective NOE experiment was performed.

The selective NOE analysis of the major product **84** reveals positive NOE enhancement between the H<sub>a</sub> (*ortho*-H<sub>a</sub> of the tolylpyridine ligand) and H<sub>b</sub> (*ortho*-H<sub>b</sub> of the dpk ligand) resonances (2.6 %) and between H<sub>c</sub> (*ortho*-H<sub>c</sub> of the tolylpyridine) and H<sub>d</sub> (*ortho*-H<sub>d</sub> of the dpk ligand) resonances (2.4%). In the minor product **88** however, NOE was only observed between H<sub>c</sub> (*ortho*-H<sub>c</sub> on the pyridyl fragment of the tolylpyridine ligand) and H<sub>d</sub> (*ortho*-H<sub>d</sub> of the dpk ligand) resonances (6.7 %).

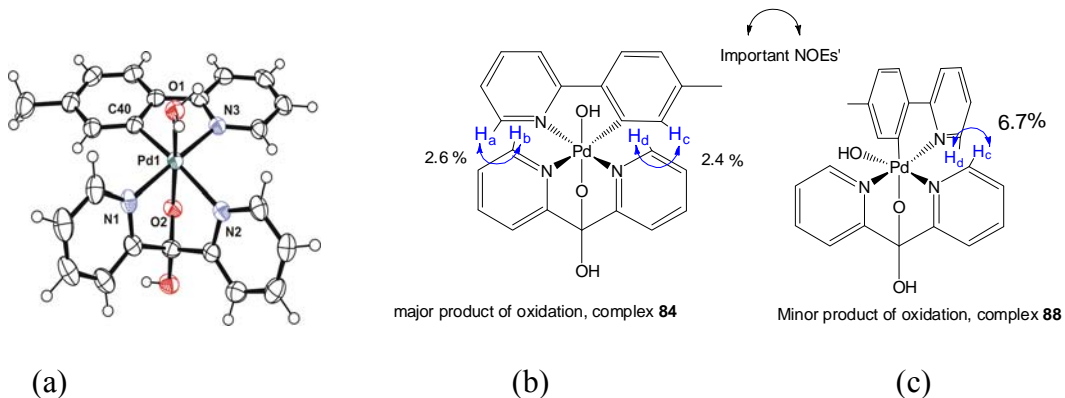


**Figure 2.14.** (a) ORTEP drawing (50% probability ellipsoids) of dication **91** in **91**(OOCF<sub>3</sub>)<sub>2</sub>·H<sub>2</sub>O, and proposed structures for (b) **84**, the major product of oxidation, and (c) **88**, the minor product of oxidation.

In order to determine the structure of complex **88**, the <sup>1</sup>H NMR chemical shifts for complexes **69**, **84** and **88** were assigned and compared. In the assignment of the chemical shifts, <sup>1</sup>H and <sup>13</sup>C NMR, <sup>1</sup>H-<sup>1</sup>H COSY, <sup>1</sup>H-<sup>13</sup>C HMBC, <sup>1</sup>H-<sup>13</sup>C HSQC, 1D Selective NOE, and 1D Selective TOCSY experiments were used. The

overlapping signals were assigned using 1D Selective TOCSY experiments. The selected  $^1\text{H}$  NMR chemical shifts are presented in the table below:

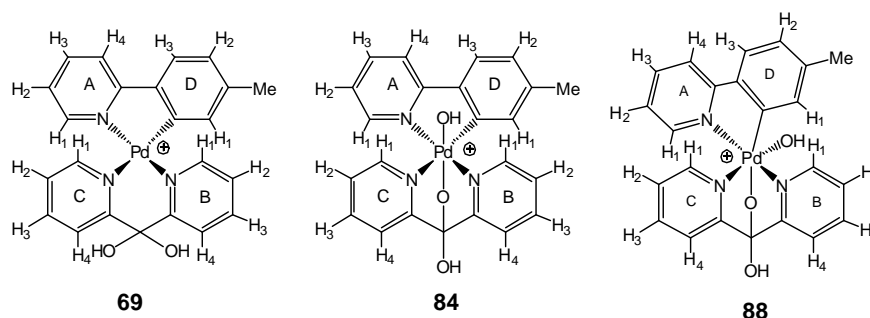


**Table 2.9.** Selected  $^1\text{H}$  NMR chemical shifts for complexes **69**, **84**, and **88** in  $\text{D}_2\text{O}$  at room temperature.

	D		A		B		C	
	1	3	1	4	1	4	1	4
<b>69</b>	6.28	7.17	7.70*	7.47	7.93	7.80*	7.80*	7.89
<b>84</b>	6.43	7.68	8.07	8.01*	8.61	7.74	8.87	7.87
<b>88</b>	7.41	7.71*	8.71	8.14*	7.24	7.71*	8.94	7.87

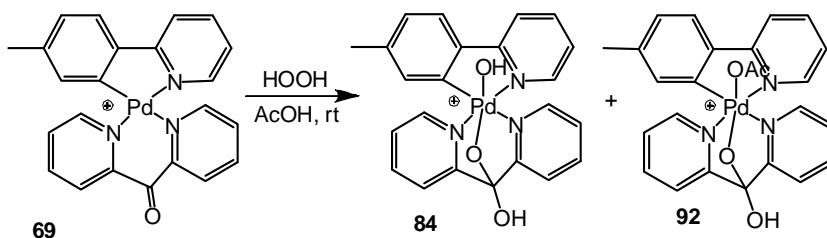
\* Indicates signals that overlap with other signals, and therefore the chemical shift value given is midpoint between the two overlapping signals to give an idea of where the signal is located.

The 1D difference NOE experiment for complex **84** reveals positive NOE enhancement between the *ortho*-H signals of the four ligand fragments around palladium. However, the 1D difference NOE experiment for complex **88** reveals positive NOE enhancement between the *ortho*-H signals of the two pyridyl fragments of the dpk and tolylpyridine ligands. The lack of NOE signal enhancement between the *ortho*-H of the aryl fragment of the tolylpyridine ligand and the pyridyl fragment of the dpk ligand indicates that these two fragments are not in close proximity, and might suggest a different binding mode where the aryl fragment is *trans* to an

alkoxide as proposed in complex **88**. The different binding modes between complexes **84** and **88** might also account for the significant difference in their  $^1\text{H}$  NMR chemical shifts.

#### 2.5.4 Oxidation of Complex **69** to Monohydrocarbyl Pd(IV) Complexes **84** and **92** with $\text{H}_2\text{O}_2$ in Acetic Acid

Scheme 2.20



The oxidation of complex **69** in water cleanly generated a mixture of complexes **84** and **88**. However the addition of 3.0 equivalents of  $\text{H}_2\text{O}_2$  to a 0.010 M deuterated acetic acid solution of complex **69** at room temperature led to appearance of two sets of  $^1\text{H}$  NMR signals different from the starting Pd(II) precursor **69**. Analysis of this reaction solution by ESI-MS revealed a mass envelope with  $m/z = 492.0684$  corresponding to the mass of complex **69** plus 2 OH groups which was assigned to complex **84**, and  $m/z = 534.0674$  corresponding to the mass of complex **69** plus 1 OH and 1 OAc groups which was assigned to complex **92**. The oxidation reaction was slow with  $\sim 60\%$  conversion in  $\sim 30$  minutes. The two reaction products ultimately decomposed to the corresponding phenol **110** in 25 % yield and aryl acetate **111** in 71 % yield, identified by means of ESI-MS and  $^1\text{H}$  NMR spectroscopy (see figure 2.15 below). The identity of the phenol **110** was confirmed by comparison of its NMR spectrum to literature,<sup>160</sup> while the identity of the aryl acetate was confirmed by independent synthesis of the compound via acetoxylation of the phenol

**110** in AcOH/Ac<sub>2</sub>O solvent mixture. Its identity was confirmed by NMR spectroscopy and ESI-MS.

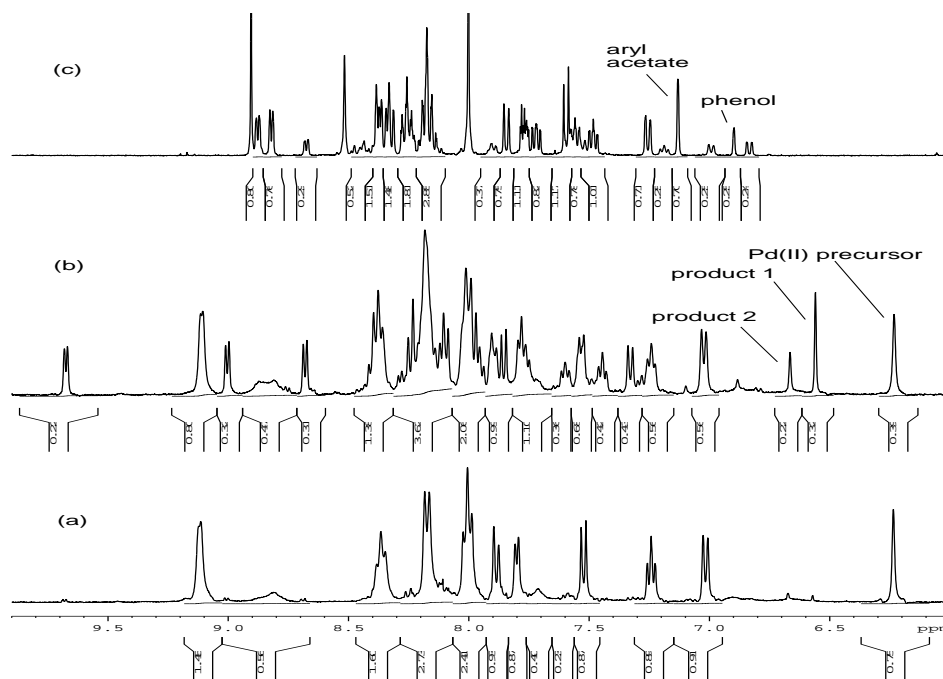
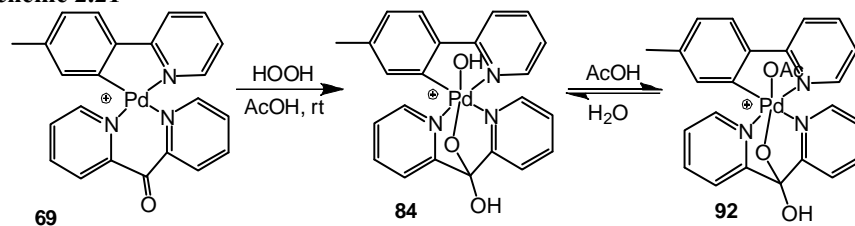


**Figure 2.15.** (a) Acetic acid solution of complex **69**; (b) Acetic acid solution of complex **69** after addition of 3.0 equivalents of H<sub>2</sub>O<sub>2</sub> at 22°C, showing products **84** (minor) and **92** (major); (c) Acetic acid solution of complex **69** two days later, after addition of 5.0 equivalents of pyridine-*d*<sub>5</sub>, showing the corresponding phenol and aryl acetate products.

This analysis indicates that the oxidation of complex **69** with H<sub>2</sub>O<sub>2</sub> in acetic acid produces complexes **84** and **92**. This oxidation reaction in acetic acid is relatively slow, but ultimately the corresponding phenol and aryl acetate are produced in a combined quantitative yield.

Complex **92** is probably produced via ligand exchange from complex **84** as shown below. Both complexes are observed by <sup>1</sup>H NMR and ESI-MS, and the formation of both phenol and aryl acetate products supports the existence of both complexes **84** and **92** in solution.

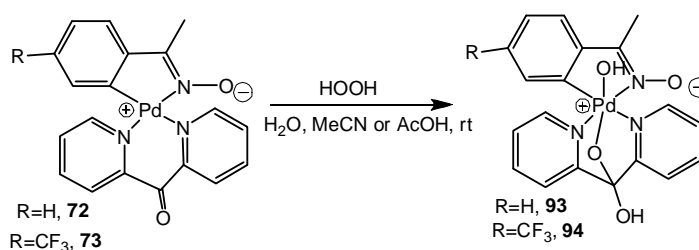
**Scheme 2.21**



### 2.5.5 Oxidation of Complexes **72** and **73** to Monohydrocarbyl Pd(IV) Complexes **93**

and **94** with  $\text{H}_2\text{O}_2$  in Water and Acetic Acid

**Scheme 2.22**



#### Oxidation of complex **72** in water

The addition of 2.0 equivalents of aqueous  $\text{H}_2\text{O}_2$  to a reaction mixture containing 0.02 mmoles of complex **72** in 1.0 ml of  $\text{D}_2\text{O}$  at room temperature resulted in the dissolution of the poorly water-soluble complex to form a deep brown solution. When this reaction was monitored by  $^1\text{H}$  NMR, clean formation of a single product identified as complex **93** with 12 multiplets in the aromatic region and 1 singlet in the aliphatic region was observed within 10 minutes. Complex **93** exhibits narrow  $^1\text{H}$  NMR signals in deuterated acetic acid, which are significantly different from those of the starting organopalladium(II) precursor **72**, which exhibits broad signals in acetic acid solvent, indicating loss of fluxional behavior upon oxidation. In addition, the  $^1\text{H}$  NMR signals belonging to both the methyl group and the aromatic hydrogens of

complex **72** are shifted downfield relative to the organopalladium(II) precursor **72**, indicating a more deshielded environment (see table 2.10 below). ESI-MS analysis of this solution after some time displayed two major peaks at  $m/z = 440.0248$ , corresponding to an increase of the mass of the Pd(II) precursor by + 16, assigned to the oxapalladacycle **112**, and  $m/z = 458.0376$ , corresponding to the mass of the Pd(II) precursor with two additional OH groups, assigned to complex **93**.

**Table 2.10.** Selected  $^1\text{H}$  NMR signals of complex **72** and **93** in water at room temperature.

Entry	Complex	Ortho-H (ppm)	Methyl group (ppm)
1	<b>72</b>	6.43	2.31
2	<b>93</b>	6.97	2.35

Complex **93** was isolated from the corresponding aqueous solution via fast removal of the solvent under vacuum to afford a brown solid. However when the solid was left under vacuum for longer than 20 minutes, additional peaks appeared in the  $^1\text{H}$  NMR spectrum collected in deuterated methanol, acetic acid or dmsO, indicating decomposition.

#### Oxidation of complex **72** in acetic acid

When a 0.010 M acetic acid solution of complex **72** was combined with 3.0 equivalents of  $\text{H}_2\text{O}_2$ , a new set of 12 multiplets was observed by  $^1\text{H}$  NMR spectroscopy; no intermediates were observed. The  $^1\text{H}$  NMR spectrum of this product of oxidation was identical to that of complex **93**, produced upon oxidation of complex **72** in water.

### Oxidation of complex 72 in acetonitrile

Complex **93** could also be prepared in acetonitrile solvent. A mixture of 0.1 mmoles of complex **72** in 2.0 ml acetonitrile was combined with 10.0 equivalents of H<sub>2</sub>O<sub>2</sub> at 0°C, resulting in the formation of a deep red reaction mixture accompanied by formation of brown precipitate. This reaction mixture was stirred at 0°C for 30 minutes after which it was concentrated, filtered, and the solid was washed with a small amount of cold diethyl ether. <sup>1</sup>H NMR spectrum of this solid in deuterated methanol or acetic acid was identical to that of complex **93**, produced upon oxidation of complex **72** with H<sub>2</sub>O<sub>2</sub> in water.

The identical <sup>1</sup>H NMR patterns of the products of oxidation in water, acetic acid, and acetonitrile indicate that the same product **93** is generated upon oxidation of complex **72** with H<sub>2</sub>O<sub>2</sub> in these solvents. Complex **93** was characterized by NMR spectroscopy and ESI mass spectrometry, while its elemental composition was confirmed by elemental analysis. The <sup>1</sup>H NMR spectrum of this complex in dms<sub>o</sub>-d<sub>6</sub> reveals the presence of three singlets, one in the low-field region at 7.96 ppm, and two in the high-field region at 1.36 ppm and 2.06 ppm. The singlet at 7.96 ppm integrating as 1H was assigned to the –OH group on the dpk ligand. This –OH signal in Pd(IV) complexes **75** and **76** in dms<sub>o</sub>-d<sub>6</sub> solvent shows up at a similar range of 8.7-8.8 ppm. The high field signal at 1.36 ppm integrating as 1H was assigned to the –OH group coordinated onto the Pd(IV) center. Similar –OH signals coordinated to Pt(IV) center are usually observed in the high field region.<sup>123</sup> The other singlet at 2.06 ppm that integrates as 3H was assigned to the methyl group of the acetophenone oxime moiety. Complete assignment of the chemical shifts was accomplished using <sup>1</sup>H and

$^{13}\text{C}$  NMR,  $^1\text{H}$ - $^1\text{H}$  COSY,  $^1\text{H}$ - $^{13}\text{C}$  HSQC,  $^1\text{H}$ - $^{13}\text{C}$  HMBC, and 1D selective TOCSY and 1D selective NOE experiments.

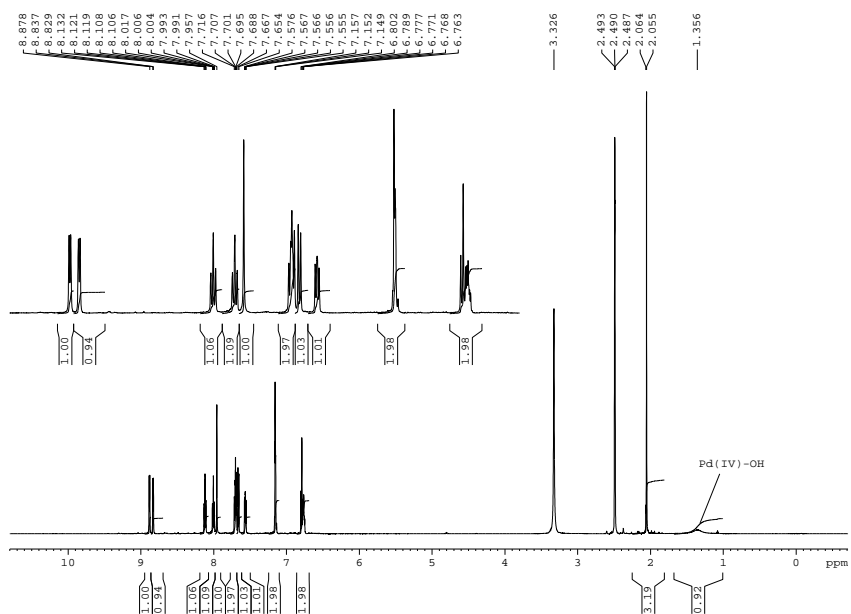


**Figure 2.16.**  $^1\text{H}$  NMR of complex **93** in  $\text{dms0-d}_6$  at room temperature.

X-ray quality crystals of complex **93** could be grown by layering a cold methanolic solution of complex **93** with diethyl ether.

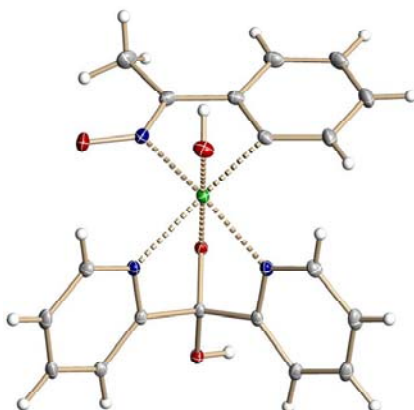
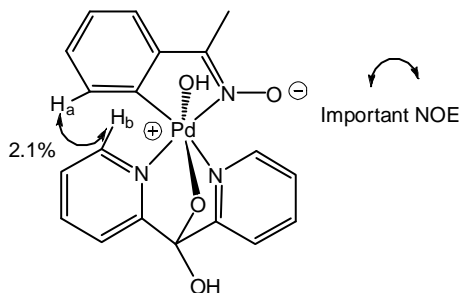


**Figure 2.17.** ORTEP drawing (50 % probability ellipsoid) of complex **93**

*Selective 1D-difference NOE experiments (D<sub>2</sub>O) for Complex 93*



In the 1D difference NOE experiment, positive NOE enhancement was observed between H<sub>a</sub> and H<sub>b</sub> (2.1 %) (mixing time of 4.0s, delay time 5s). This confirms that the solid state structure is maintained in solution.

Complex **93** is not stable in the solid state at room temperature. When left at room temperature for several days, new peaks appear in the <sup>1</sup>H NMR spectrum in deuterated methanol or acetic acid solvents. After 4 weeks, the <sup>1</sup>H NMR and ESI-MS analysis revealed complete decomposition to generate the corresponding phenol and inorganic complex cleanly. This complex is however stable at -20°C.

*Oxidation of complex 73 with H<sub>2</sub>O<sub>2</sub> in water*

When a mixture of 0.02 mmoles of a trifluoromethyl analogue of **72**, complex **73** in 1.0 ml of D<sub>2</sub>O was combined with 2.0 equivalents of H<sub>2</sub>O<sub>2</sub> at room temperature, dissolution of the poorly water soluble complex to form a deep red solution was observed. <sup>1</sup>H NMR analysis of this reaction revealed formation of a single product with 11 multiplets cleanly within 10 minutes. Analysis of the reaction solution by ESI-MS during oxidation at room temperature revealed two major peaks at m/z = 508.0008 assigned to the oxapalladacycle **113** and 526.0276 assigned to the monohydrocarbyl Pd(IV) complex **94**.

$^1\text{H}$  NMR analysis of the oxidation reaction revealed formation of a new species with an  $^1\text{H}$  NMR pattern that is significantly different from that of the starting organopalladium(II) precursor **73**. In particular, the  $^1\text{H}$  NMR spectrum of the Pd(II) precursor exhibits broad multiplets in acetic acid solvent indicative of a fluxional behavior, while the product of oxidation **94** exhibits 11 sharp multiplets. In addition, both the methyl group and the aromatic hydrogens in the product of oxidation, complex **94** are shifted downfield relative to the organopalladium(II) precursor **73**, indicative of a more deshielded environment.

**Table 2.11.** Selected  $^1\text{H}$  NMR signals of complex **73** and **94** in water at room temperature.

Entry	Complex	Ortho-H (ppm)	Methyl group (ppm)
1	<b>73</b>	6.71	2.27
2	<b>94</b>	7.17	2.34

Complex **94** was isolated as a brown solid from the corresponding aqueous solution by fast removal of the solvent under vacuum. However when the solid was left under vacuum for longer than 20 minutes, additional peaks were observed in the  $^1\text{H}$  NMR indicating decomposition.

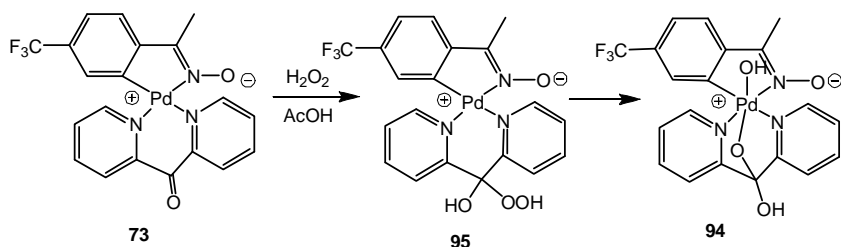
#### Oxidation of complex **73** in acetonitrile

The oxidation of 0.01 mmoles of complex **73** in 1.0 ml deuterated acetonitrile solvent with 5.0 eq of  $\text{H}_2\text{O}_2$  resulted in formation of a reaction mixture consisting of deep red solution and deep yellow solid. Diethyl ether was added into the reaction mixture to afford more precipitate, which was filtered off and washed with a small

amount of cold diethyl ether to afford the target complex **94**. The  $^1\text{H}$  NMR spectrum of the solid in methanol or acetic acid was identical to that of complex **94** generated upon oxidation of complex **73** with  $\text{H}_2\text{O}_2$  in water.

Oxidation of complex **73** in acetic acid

Scheme 2.23



The addition of  $\text{H}_2\text{O}_2$  to an acetic acid solution of complex **73** resulted in a slightly different reactivity to that of complex **72**. Upon addition of 3.0 eq of  $\text{H}_2\text{O}_2$  to an acetic acid solution of complex **73**, an exothermic reaction with concomitant color change from colorless to deep brown was observed.  $^1\text{H}$  NMR analysis of this reaction solution 2 minutes after addition of the oxidant revealed complete disappearance of the starting Pd(II) precursor **73** and the presence of two new complexes. Consecutive  $^1\text{H}$  NMR spectra at room temperature revealed gradual disappearance of one of the products with simultaneous increase of the other, leading to the formation of one major product in  $> 90\%$  yield  $\sim 10$  minutes after addition of  $\text{H}_2\text{O}_2$ . The ESI-MS analysis of the reaction solution after addition of hydrogen peroxide revealed two major mass envelopes, at  $m/z = 508.0008$  assigned to oxapalladacycle **113**, and  $526.0276$  which may be assigned to the Pd(IV) complex **94** and/ or an adduct of **73** with  $\text{H}_2\text{O}_2$ , **95**. The  $^1\text{H}$  NMR of the major product was identical to that of complex **94** produced upon oxidation of complex **73** with  $\text{H}_2\text{O}_2$  in either water or acetonitrile.

Considering the ESI-MS analysis, the intermediate complex **95** was proposed to be a product of addition of H<sub>2</sub>O<sub>2</sub> across the C=O bond of the dpk ligand, which precedes formation of the Pd(IV) complex **94**.

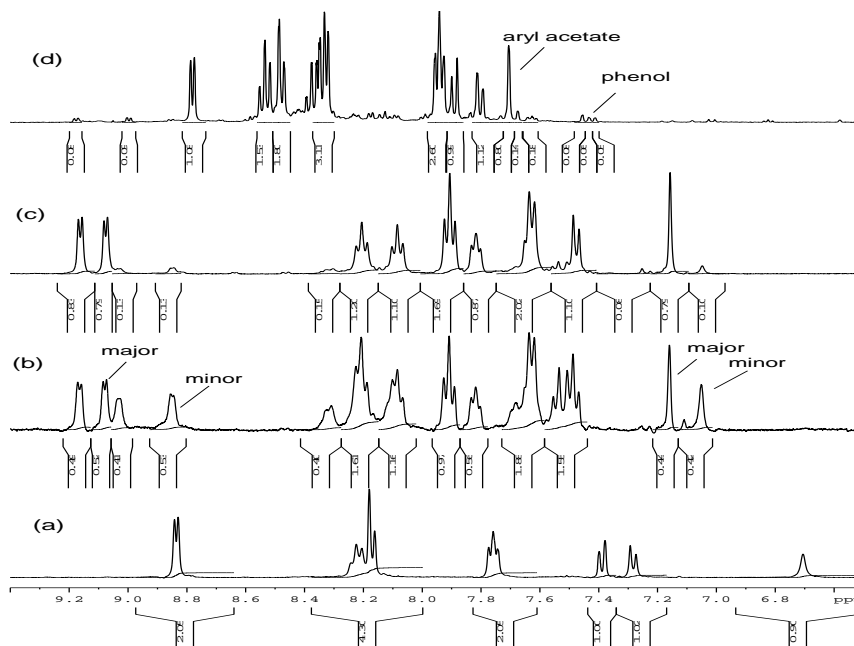
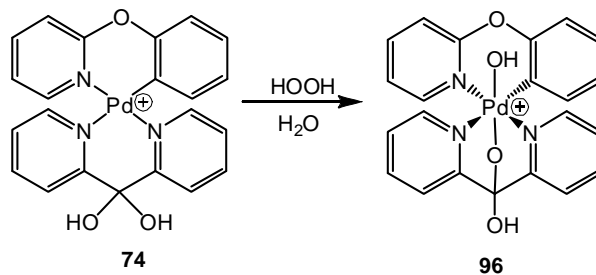


**Figure 2.18.** Room temperature acetic acid solutions of (a) complex **73**; (b) complex **73**, 2 minutes after addition of 3 eq H<sub>2</sub>O<sub>2</sub>, showing complexes **95** (minor) and **94** (major) (c) complex **73**, 10 minutes after addition of H<sub>2</sub>O<sub>2</sub>, showing complex **94**; (d) complex **73** at the end of reaction, showing the aryl acetate as the major product of decomposition.

The adduct of H<sub>2</sub>O<sub>2</sub> addition across the C=O bond of the dpk ligand **95** was most likely detected due to the more electron-deficient nature of complex **73** relative to complex **72**. The presence of the “CF<sub>3</sub>” group in **73** would make the C=O bond more electrophilic thus increasing the rate of the addition reaction, while slowing down the rate of the subsequent oxidation of Pd(II) to Pd(IV).

2.5.6 Oxidation of Complex **74** to Monohydrocarbyl Pd(IV) Complex **96** with H<sub>2</sub>O<sub>2</sub>  
in Water

Scheme 2.24



The addition of 1.5 equivalents of H<sub>2</sub>O<sub>2</sub> to a 0.010 M D<sub>2</sub>O solution of complex **74** at room temperature resulted in color change from colorless to deep yellow. <sup>1</sup>H NMR monitoring of the reaction revealed slow disappearance of the starting complex and appearance of an intermediate species which eventually led to formation of two products. A clean <sup>1</sup>H NMR spectrum of the intermediate could be obtained when 10.0 equivalents of H<sub>2</sub>O<sub>2</sub> was used at 0°C. The <sup>1</sup>H NMR pattern of the intermediate species was significantly different from that of the Pd(II) precursor **74**, with the resonance of the *ortho*-H of the aryl fragment of the phenoxypyridine ligand in the intermediate complex significantly shifted upfield relative to that of complex **74** (Fig. 2.19).

**Table 2.12.** Selected <sup>1</sup>H NMR signals of complex **74** and **96** in D<sub>2</sub>O at room temperature.

Entry	Complex	Ortho-H <sub>aryl</sub> (ppm)
1	<b>74</b>	6.68
2	<b>96</b>	6.35

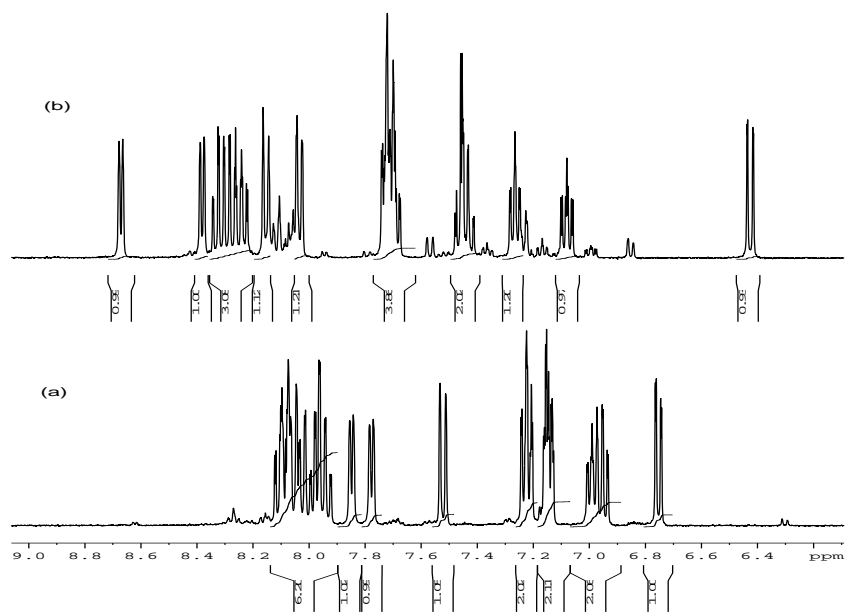
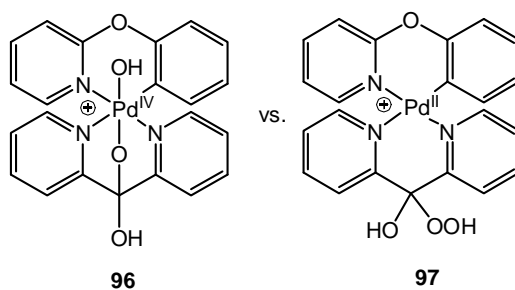


**Figure 2.19.** (a) D<sub>2</sub>O solution of complex **74** at 0°C; (b) D<sub>2</sub>O solution of complex **96** at 0°C.

Analysis of the reaction solution by ESI-MS immediately after addition of H<sub>2</sub>O<sub>2</sub> revealed two major peaks at  $m/z = 476.0264$  assigned to the oxapalladacycle **114**, and 494.0294 which can be assigned to the H<sub>2</sub>O<sub>2</sub> adduct **97** and monohydrocarbyl-Pd(IV) complex **96**.

**Scheme 2.25**



In order to confirm the identity of the complex **96**, several experiments were conducted. First, a 0.010 M aqueous solution of complex **74** was combined with 10.0 eq of HOOH at 3°C because at this temperature, complex **96** is stable and doesn't decompose for several hours, and this reaction was monitored by <sup>1</sup>H NMR. A similar

experiment was set up and monitored by UV-vis spectroscopy. We hypothesized that a Pd(IV) complex would display a Ligand to Metal charge transfer band on the visible range of the UV-vis spectrum, while the peroxy adduct is not expected to display any LMCT bands.

When the reaction of 0.010 M D<sub>2</sub>O solution of complex **74** with 10.0 equivalents of H<sub>2</sub>O<sub>2</sub> at 3°C was monitored by <sup>1</sup>H NMR, gradual disappearance of complex **74** was observed with > 95 % conversion after 60 minutes; < 5% decomposition was observed at this temperature.

A similar reaction was monitored by UV-vis analysis. A 0.010 M, 3.0 ml H<sub>2</sub>O solution of complex **74** was prepared and placed in a cuvette at 0°C for 30 minutes. The cuvette was placed in a cell holder of a spectrophotometer and UV-vis spectrum was collected at 0°C. The cuvette was placed at 0°C, 10.0 eq of H<sub>2</sub>O<sub>2</sub> was added to the solution at this temperature, and consecutive UV-vis spectra were collected at regular intervals at 0°C for at least 60 minutes.

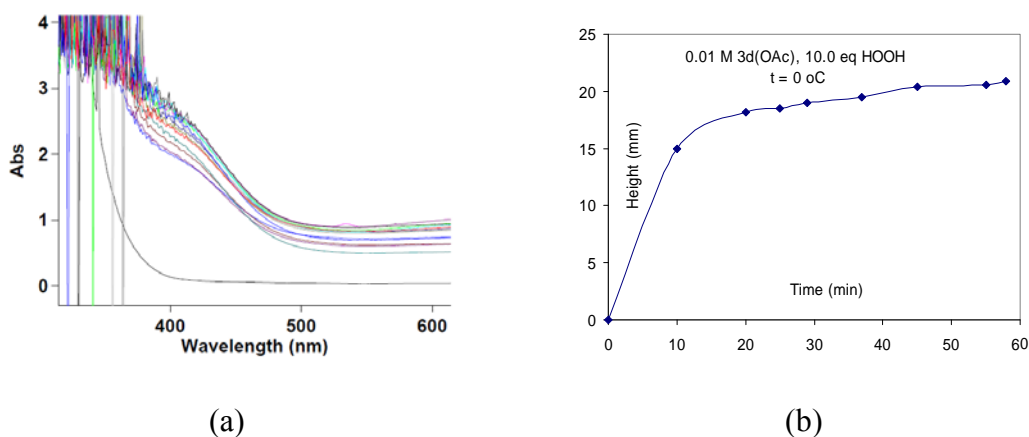
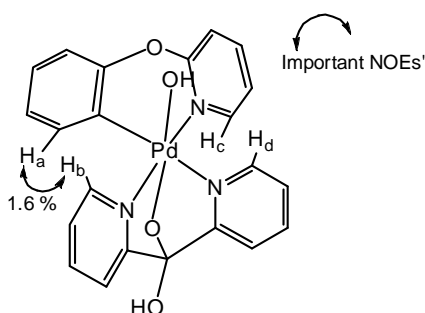


**Figure 2.20.** (a) Change of UV-visible spectra of 0.010 M D<sub>2</sub>O solutions of complex **74** upon addition of 10.0 equivalents of H<sub>2</sub>O<sub>2</sub> at 0°C (1.0 cm cuvette was used). (b) Change in absorbance as a function of time at the wavelength of 420 nm, over a period of 60 minutes

According to the UV-vis spectral analysis, an absorption band gradually developed around 425 nm during the reaction of complex **74** with 10.0 eq of H<sub>2</sub>O<sub>2</sub> (see fig. 2.20) at 0°C. Since <sup>1</sup>H NMR monitoring of this experiment revealed gradual reaction of complex **74** with 10.0 eq H<sub>2</sub>O<sub>2</sub> at 3°C with > 95 % conversion after 60 minutes and < 5 % decomposition, the absorption band at ~ 425 nm was assigned to the product of the reaction, and since the band occurs at the LMCT range, the band was assigned to the Pd(IV) complex **96**. This complex was characterized by <sup>1</sup>H NMR, <sup>13</sup>C NMR, and ESI-MS.

*Selective 1D-difference NOE experiments (D<sub>2</sub>O) for **96***



In the 1D difference NOE experiment of complex **96**, NOE was observed between H<sub>a</sub> and H<sub>b</sub> (1.6 %)(mixing time of 0.8s, delay time 5s).

2.6 Mechanism of Oxidation of Hydrocarbonyl Pd(II) Complexes with H<sub>2</sub>O<sub>2</sub>

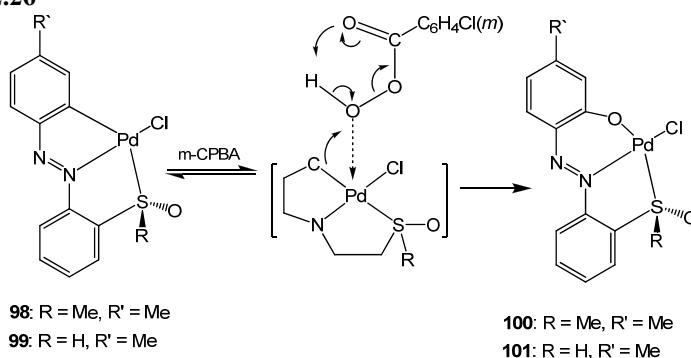
2.6.1 Introduction

Pd-catalyzed oxidative C–H bond functionalization reactions take place in the presence of various oxidants, including ArIX<sub>2</sub><sup>59,161,162</sup> (Ar = aryl groups such as phenyl, X = functional groups such as Cl and OAc), NXS<sup>32</sup> (X = Halogens such as Cl, Br, and I), organic and inorganic peroxides such as Oxone<sup>33</sup>, tBu-peroxides<sup>72</sup> etc. The oxidation step has been studied for various oxidants such as PhIX<sub>2</sub> (X = OAc or Cl)

and NXS (X = Cl, Br, and I) using various model complexes.<sup>118</sup> However the oxidation of organopalladium(II) complexes using peroxide based oxidants has not been studied due to the difficulty of accessing stable high oxidation state palladium complexes using peroxide based oxidants.

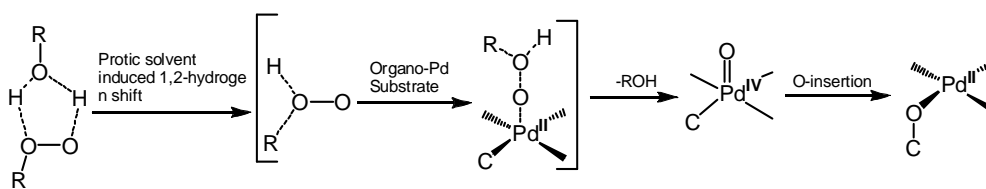
Several experiments for the stoichiometric oxidation of organopalladium(II) complexes with peroxy-based oxidants have been performed. In one study, Chakravorty and co-workers performed detailed kinetic studies on the mechanism of oxygenation of 2-(alkylsulfinyl)azobenzenes with *meta*-perchlorobenzoic acid as oxidant.<sup>76</sup> In this study, an overall second order rate law was established, first order on the substrate and first order on the oxidant. The activation process exhibited a small enthalpy and large negative entropy. The large negative entropy of activation is indicative of an associative transition state where the association was proposed to involve the metal center and the *m*-CPBA peroxy oxygen in the transition state as shown in Scheme 2.26 below. This was proposed to be followed by heterolytic cleavage of the O–O bond, where the facile nature of this cleavage is reflected on the small enthalpy of activation (<10Kcal/mol). This mechanism was also supported by the experimental observation where more electron-rich substrates undergo oxidation faster than electron-poor substrates.

**Scheme 2.26**



A later mechanistic study on the oxygenation of cyclopalladated *N,N*-dimethylbenzylamine complexes by *tert*-butyl hydroperoxide in the presence of VO(acac)<sub>2</sub> that leads to oxygen insertion into the Pd–C bond was reported by Van Koten and co-workers in 1993.<sup>120</sup> Kinetic studies of this reaction revealed that the rate of oxygenation is strongly enhanced by increasing the nucleophilicity of the metal center. On the basis of the kinetic studies and solvent effects observed, a mechanism of oxygenation reaction that begins with a 1,2-proton shift in the hydroperoxide (ROOH) to form an alcohol oxide species (RHO–O) was proposed. This *tert*-butyl alcohol oxide is proposed to be the actual oxygen donating agent in this reaction by transferring an oxenoid oxygen atom to Pd(II), leading to formation of a transient Pd(IV) oxo species and a neutral alcohol leaving group. This is followed by insertion of oxygen into the Pd–C bond (Scheme 2.27).

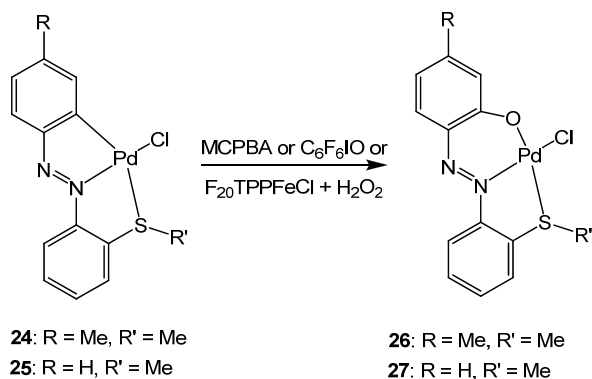
**Scheme 2.27**



In this oxidation reaction, the mechanism of the actual oxygen insertion step was proposed as an S<sub>N</sub>2 end-on attack of the d<sub>z</sub><sup>2</sup> HOMO of the palladium center on the σ\* LUMO of the O–O bond of either the *tert*-butyl alcohol oxide (oxygenations with TBHP in *t*-BuOH) or vanadium alkyl peroxide (vanadium catalyzed oxygenations with TBHP). This mechanism is similar to the oxidative addition of dihalogens to square-planar d<sup>8</sup> metal complexes which has been shown to proceed via end-on, nucleophilic attack of the metal on the σ\* LUMO of the X–X bond and concomitant splitting of an X<sup>−</sup> anion as the leaving group. The mechanism was

supported by the experimental observation where the rate of oxygenation increased strongly with the nucleophilicity of the metal center. The formation of the Pd(IV) oxo species was proposed as the rate-determining step.

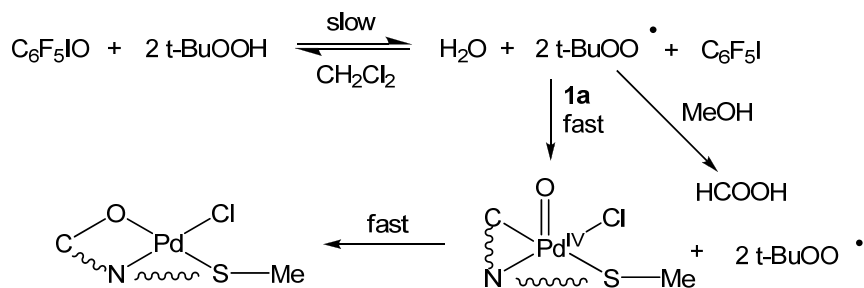
**Scheme 2.28**



To achieve a wider application of the selective C–Pd bond oxidation, especially towards industrial and pharmaceutical samples containing multiple functionalities, the use of bio-friendly and inexpensive oxidants such as H<sub>2</sub>O<sub>2</sub> would be very useful. Bandyopadhyay and co-workers achieved a successful C–Pd bond functionalization using H<sub>2</sub>O<sub>2</sub> in the presence of *meso*-tetrakis(pentafluorophenyl)porphyrinatoiron(III) chloride, which is an iron(III)porphyrin catalyst.<sup>121</sup> In these studies, they proposed the generation of an oxoiron(IV) porphyrin cation radical by the reaction of F<sub>20</sub>TPP–FeCl and H<sub>2</sub>O<sub>2</sub> in the presence of excess H<sub>2</sub>O<sub>2</sub>. This oxoiron(IV) porphyrin radical abstracts a hydrogen atom from H<sub>2</sub>O<sub>2</sub> to generate a hydroperoxy radical, which was proposed to be the major reactive species. The oxidation mechanism could be similar to the mechanism proposed for the oxygen atom insertion into the Pd–C bond of cyclopalladated 2-(alkylthio)azobenzene complexes using the t-BuOO· radical oxidant (Scheme 2.29),<sup>163</sup> which was proposed to occur via initial direct attack of the t-BuOO· radical

at Pd<sup>II</sup> to make an oxopalladium(IV) complex with the generation of a t-BuO· radical. The oxopalladium(IV) species reacts further via oxygen atom insertion into the Pd–C bond while the t-BuO· radical abstracts a hydrogen atom from another molecule of t-BuOOH, which will attack another Pd(II) molecule and so the oxygenation cycle is repeated.

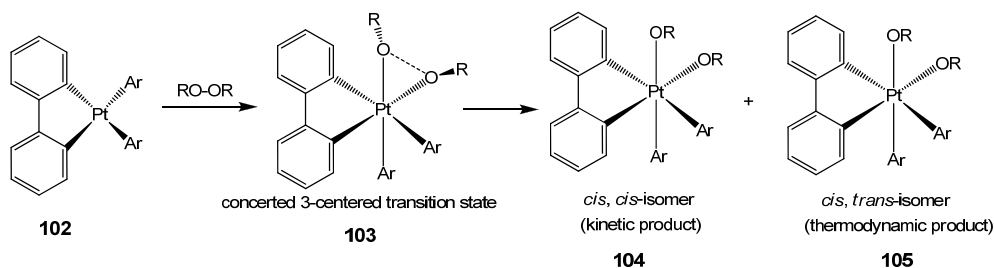
**Scheme 2.29**



There have been extensive studies on the oxidation of organoplatinum(II) complexes with H<sub>2</sub>O<sub>2</sub>. These studies are relevant because platinum complexes are frequently considered to have similar reactivity with palladium complexes bearing identical ligand environment under similar conditions. Rashidi and co-workers performed kinetic investigations into the mechanism of cleavage of the O–O bond in hydrogen peroxide and dibenzoyl peroxide oxidants by arylplatinum(II) complexes of the form (bpy)PtAr<sub>2</sub> (Ar = Ph, *p*-MeC<sub>6</sub>H<sub>4</sub>, *p*-MeOC<sub>6</sub>H<sub>4</sub>).<sup>164</sup> These kinetic reactions were found to observe a second order rate law, with a first order dependence in the substrate and first order dependence in the peroxide oxidant. The activation produced a small enthalpy and large negative entropy, indicative of an associative transition state. The reaction was not sensitive towards solvent polarity differences, thus ruling out the possibility of an S<sub>N</sub>2-type mechanism in which the transition state involves the formation of a cationic intermediate. Reproducible kinetic data and the fact that

radical scavengers did not affect the reaction rate ruled out the possibility of a radical mechanism. As a result, a mechanism of oxidation involving a concerted three-centered transition state involving the two oxygen atoms of the peroxide moiety and the metal was proposed (Scheme 2.30). This association was consistent with the large negative entropy of activation and also with the simple second-order rate law that was observed. The rate of oxidation reaction was also found to increase with increasing electron-density at platinum, providing support for the proposed mechanism. The predominant formation of the *trans* isomer was explained by a possible rapid isomerization of the kinetic *cis* complex to the thermodynamically favored *trans* complex.

**Scheme 2.30**

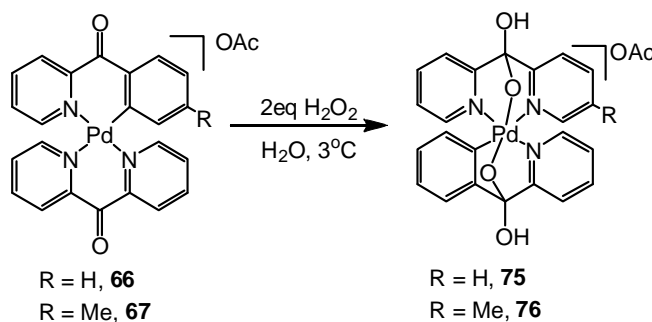


### 2.6.2 Kinetics Study of the Reaction of Organopalladium(II) Complexes **66** and **67** with H<sub>2</sub>O<sub>2</sub> in Water

In this work, we performed detailed kinetic analyses on the oxidation of organopalladium(II) complexes to the corresponding organopalladium(IV) complexes using H<sub>2</sub>O<sub>2</sub> in water. The substrates studied are derived from substituted 2-benzoylpyridine and substituted 2-phenylpyridine. The oxidation reactions were performed under pseudo-first order conditions at low temperature since the reactions are too fast at room temperature. We began to study the reaction of benzoylpyridine-

derived Pd(II) complexes with various equivalents of H<sub>2</sub>O<sub>2</sub> in water at 3 °C according to the following equation:

**Scheme 2.31**



*<sup>1</sup>H NMR characterization of reaction mixtures containing complex **66** and 10.0 eq H<sub>2</sub>O<sub>2</sub> in water at 3 °C*

When a mixture of complex **66** with 10.0 eq H<sub>2</sub>O<sub>2</sub> was monitored by <sup>1</sup>H NMR at 6 °C, three sets of signals were observed: (a) Signals belonging to the reactant complex **66** which disappeared gradually; (b) Signals belonging to the Pd(IV) product **75** which grew gradually; (c) signals belonging to a reaction intermediate “**Y**” which appeared upon addition of H<sub>2</sub>O<sub>2</sub> and remained relatively steady throughout the reaction, but eventually disappeared at the end of reaction (Fig 2.21 and 2.22). At the end of the oxidation reaction, complex **75** was the only species present in solution according to both <sup>1</sup>H NMR and ESI-MS analysis. The maximum amount of the intermediate produced in this reaction is 17 %.

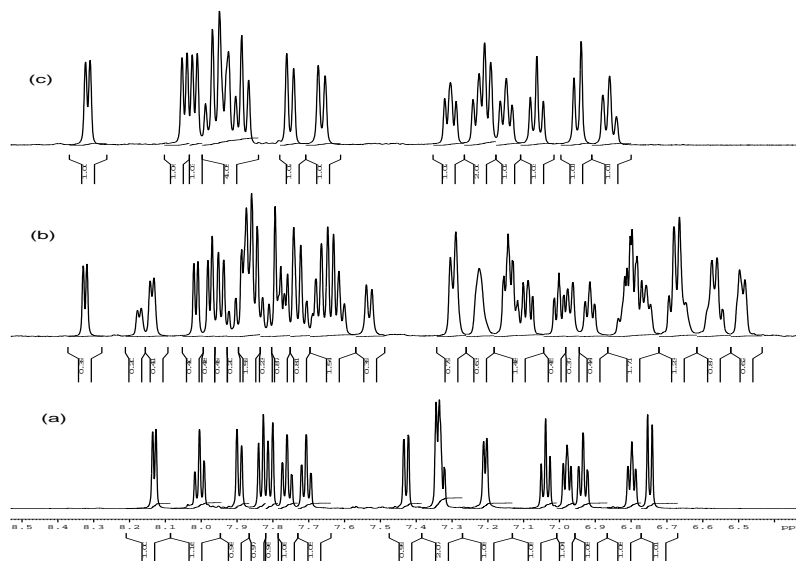


**Figure 2.21.**  $^1\text{H}$  NMR spectra in  $\text{D}_2\text{O}$  taken at  $3^\circ\text{C}$  for (a) complex **66**; (b) complex **66**, 18 minutes after addition of 10.0 eq of  $\text{H}_2\text{O}_2$ , together with an intermediate “Y” and Pd(IV) product **75**; and (c), at the end of reaction, showing Pd(IV) complex **75**.

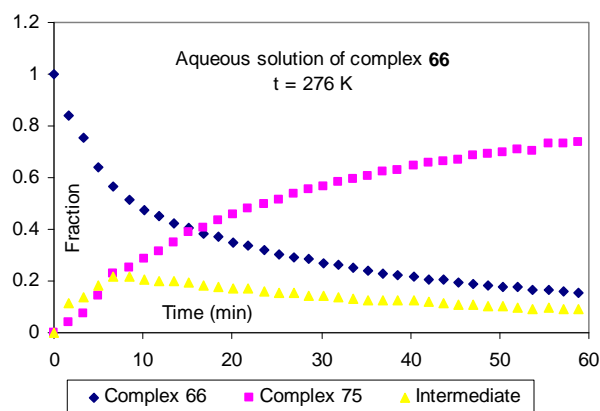


**Figure 2.22.** Plot for the oxidation of complex **66** with 10.0 eq  $\text{H}_2\text{O}_2$  in  $\text{D}_2\text{O}$  at  $3^\circ\text{C}$ , showing the fraction of starting Pd(II) complex **66**, the intermediate complex, and the product **75** as a function of time.

A similar characterization for the reactivity of complex **67** with  $\text{H}_2\text{O}_2$  was monitored by both  $^1\text{H}$  NMR and ESI-MS.

*<sup>1</sup>H NMR characterization of reaction mixtures containing complex 67 and 1.0 - 40.0 eq H<sub>2</sub>O<sub>2</sub> in water at 3 °C and 22 °C*

The observations made in this oxidation reaction are similar to those made in the oxidation of complex **66** under similar conditions. Mixtures of 0.010 M D<sub>2</sub>O solutions of complex **67** and 1.0 - 40.0 equivalents of H<sub>2</sub>O<sub>2</sub> were monitored by <sup>1</sup>H NMR spectroscopy at temperatures ranging from 3-22 °C. In these experiments, three sets of signals were observed: (a) Signals belonging to the reactant complex **67** which disappeared gradually; (b) Signals belonging to the Pd(IV) product **76** which grew gradually; (c) signals belonging to a reaction intermediate “X” which appeared upon addition of H<sub>2</sub>O<sub>2</sub> and remained steady throughout the reaction and eventually disappeared at the end of reaction (Fig. 2.23 and 2.24). At the end of the oxidation reaction, complex **76** was the only species present in solution according to both <sup>1</sup>H NMR and ESI-MS analysis.

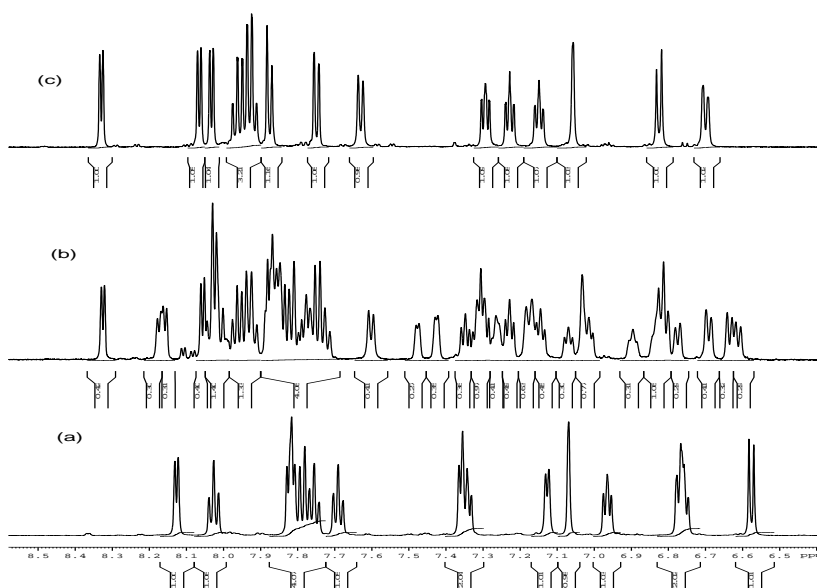


**Figure 2.23.** <sup>1</sup>H NMR taken in D<sub>2</sub>O at 3 °C for (a) complex **67**; (b) complex **67**, 10 minutes after addition of 20.0 eq of H<sub>2</sub>O<sub>2</sub>, together with intermediate “X” and Pd(IV) product **76**; and (c), at the end of reaction, showing Pd(IV) complex **76**.

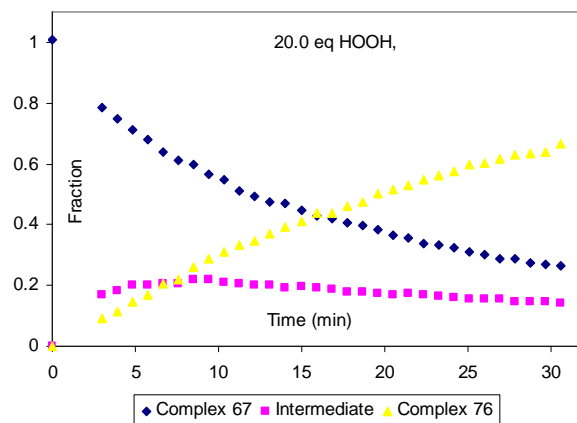


**Figure 2.24.** Plot for the oxidation of complex **67** with 20.0 eq  $\text{H}_2\text{O}_2$  in  $\text{D}_2\text{O}$  at  $3^\circ\text{C}$ , showing the fraction of starting Pd(II) complex **67**, the intermediate complex, and the product **76** as a function of time.

In order to understand the nature of the intermediate complex observed in the  $^1\text{H}$  NMR experiments, ESI-MS analysis of the oxidation reaction was performed.

*ESI-MS characterization of a mixture of complex **67** with 10.0 eq  $\text{H}_2\text{O}_2$  in water at 273 K*

A 0.010 M solution of complex **67** in 1.0 ml of water was combined with 10.0 equivalents of  $\text{H}_2\text{O}_2$  in an ice-water bath at  $0^\circ\text{C}$ . Analysis of this solution by ESI-MS 18 seconds after mixing revealed the following major peaks ( $m/z$ , positive mode): 1) 486.0448, assigned to the Pd(II) precursor **67**; 2) 504.0525 assigned to product of hydration of the Pd(II) precursor **67**; 3) 520.0472 assigned to complex **76** and/ or complex **78** (see fig. 2.25).

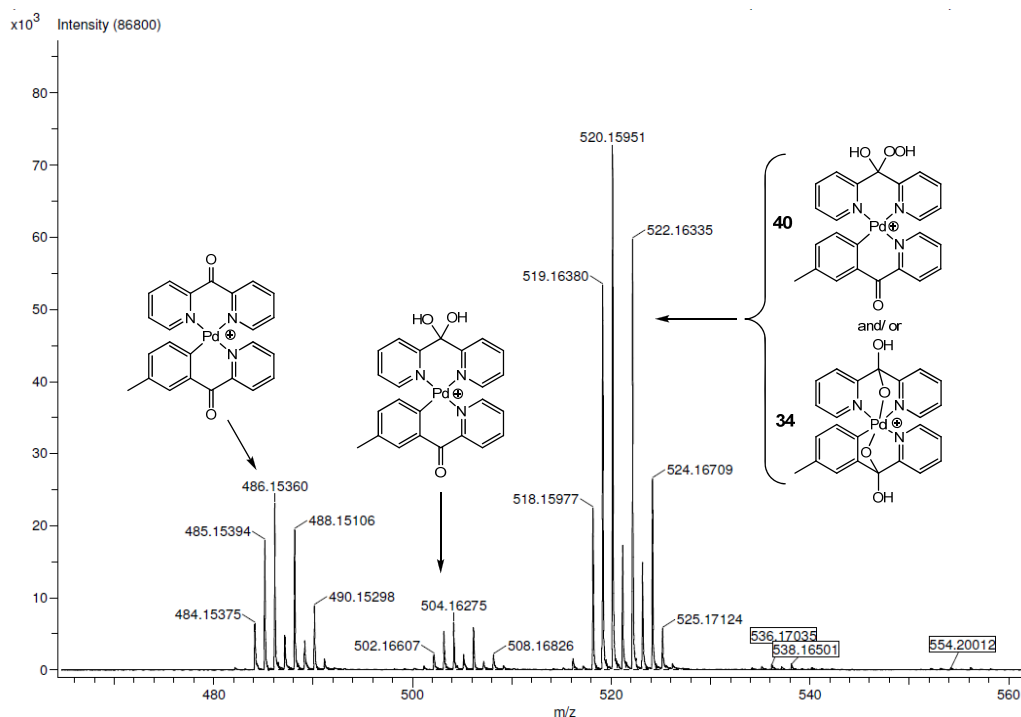


**Figure 2.25.** ESI-MS spectrum of an aqueous solution 0.010 M complex **67**, 18 seconds after adding 20.0 equivalents of  $\text{H}_2\text{O}_2$  in water at  $0^\circ\text{C}$ .

The maximum fraction of the intermediate “**X**” formed was dependent on the temperature and the amount of  $\text{H}_2\text{O}_2$  added. A higher concentration of the intermediate was observed when the reaction was conducted at lower temperatures and when a higher concentration of  $\text{H}_2\text{O}_2$  was used (see table 2.13 below).

**Table 2.13.** Oxidation of complex **67** with  $\text{H}_2\text{O}_2$  in water, showing the concentration of the intermediate “**X**” as a function of  $\text{H}_2\text{O}_2$  concentration and temperature.

$\text{H}_2\text{O}_2$ (eq)	Temp (K)	Intermediate X (%)
1.0	295	2 %
1.0	276	12 %
20.0	276	27 %
40.0	276	33 %

In order to determine the identity of the intermediate complex “X”, some of its  $^1\text{H}$  NMR resonances were assigned and compared to similar set of signals belonging to the Pd(II) precursor **67** and the Pd(IV) product **76**. Peak assignment for complexes **67** and **76** was based on  $^1\text{H}$  NMR,  $^1\text{H}$ - $^1\text{H}$  COSY,  $^1\text{H}$ - $^{13}\text{C}$  HSQC,  $^1\text{H}$ - $^{13}\text{C}$  HMBC, 1D Selective NOE, and 1D Selective TOCSY. The assignment of overlapping signals was possible using 1D Selective TOCSY pulse program.

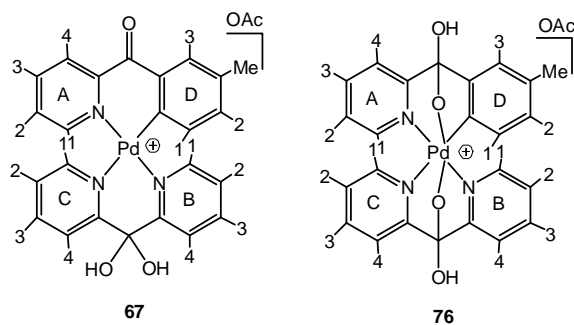


**Table 2.14.** Selected  $^1\text{H}$  NMR chemical shifts for complexes **67**, **76**, and intermediate “X” in  $\text{D}_2\text{O}$  at  $0^\circ\text{C}$ .

	A				B				C			
	1	2	3	4	1	2	3	4	1	2	3	4
<b>67</b>	8.20	7.35	8.02	7.93	7.42	6.90	7.76	7.84	7.49	7.05	7.79	7.86
<b>“X”</b>	8.22	7.32	8.01	7.94	7.45	6.96	7.80	7.85	7.53	7.10	7.83	7.90
<b>76</b>	8.06	7.15	7.92	7.63	8.03	7.23	7.96	7.75	8.33	7.29	7.94	7.87

\*The  $^1\text{H}$  NMR chemical shifts were analyzed towards the end of the reaction with 64 % complex **76**, 18 % complex **67**, and 18 % “X” present.

It can be observed that the chemical shifts of the signals belonging to the intermediate “X” are very similar to those belonging to complex **67** and different from complex **76**. This indicates that the intermediate “X” is structurally and electronically more similar to complex **67** than to complex **76**. The difference in the

$^1\text{H}$  NMR pattern of complex **67** and **76** probably arises from the electrophilic nature of the latter as a result of the Pd(IV) center relative to the Pd(II) center of complex **67**, and thus the similarity of the  $^1\text{H}$  NMR pattern of the intermediate “**X**” and that of the Pd(II) precursor **67** suggests the presence of a similar central atom in both complexes **67** and “**X**”. This analysis led us to propose the structure of the intermediate complex as a Pd(II) species having a similar chemical environment to the Pd(II) precursor **67**. Thus the intermediate “**X**” was assigned to the adduct of addition of  $\text{H}_2\text{O}_2$  across the C=O bond of the dpk ligand of complex **67**, complex **78**.

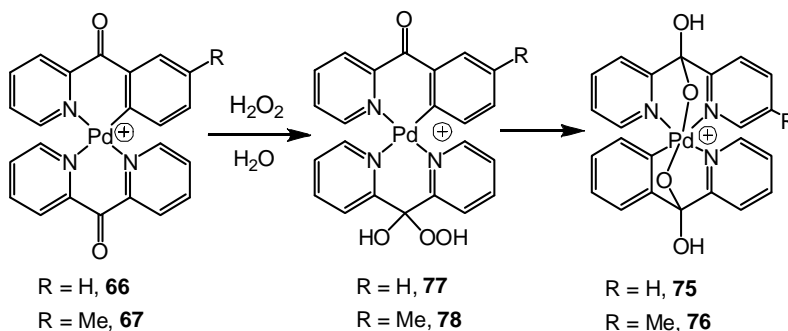
In addition, the ESI-MS analysis revealed formation of a compound with  $m/z = 520.0472$  corresponding to the mass of the Pd(II) precursor **67** plus 34 (two OH groups), which was assigned to either complex **78** (intermediate “**X**”) and/ or complex **76** (Fig. 2.25). According to the  $^1\text{H}$  NMR analysis of this reaction, the concentration of complex **76** is not significant 18 seconds after addition of  $\text{H}_2\text{O}_2$  while the concentration of the intermediate is substantial. As a result, the  $m/z = 520.0472$  was also assigned to the intermediate complex of  $\text{H}_2\text{O}_2$  addition across C=O, complex **78**. This assignment is also supported by the facile hydration of the C=O group of the dpk ligand (rate =  $4.0 * 10^{-2}$  in water),<sup>154</sup> especially upon coordination to a Pd(II) atom,<sup>154</sup> which increases the efficiency of the hydration reaction. Moreover,  $\text{H}_2\text{O}_2$  being a stronger nucleophile than  $\text{H}_2\text{O}$  is expected to increase the favorability of the addition reaction.

The fraction of complex **78** in the reaction mixture is expected to be affected by the concentration of  $\text{H}_2\text{O}_2$  in solution, and considering that it is an unstable intermediate which decomposes to the Pd(IV) product **76**, its fraction is also expected

to be affected by the temperature of the solution. Indeed, upon addition of 1.0 equivalents of  $\text{H}_2\text{O}_2$  to an aqueous solution of complex **67** at  $3^\circ\text{C}$ , a 12 % fraction of complex **78** is produced, but this fraction increases to 33 % when 40.0 equivalents of  $\text{H}_2\text{O}_2$  are used. In addition, the fraction of complex **78** is lower at higher temperatures as expected because its reactivity towards oxidation to produce the Pd(IV) complex **76** increases at higher temperatures. This was demonstrated when a 12 % maximum fraction of complex **78** was produced when of 1.0 equivalents of  $\text{H}_2\text{O}_2$  was added to an aqueous solution of complex **67** at  $3^\circ\text{C}$ , but this fraction decreases to only 2 % at  $22^\circ\text{C}$  under similar conditions.

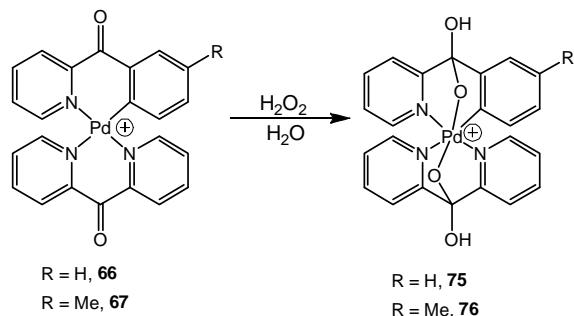
As a result of the analysis of the ESI-MS and  $^1\text{H}$  NMR experiments, we propose that the intermediate complex “X” produced upon addition of  $\text{H}_2\text{O}_2$  to an aqueous solution of either complex **66** or **67** is an adduct of  $\text{H}_2\text{O}_2$  addition across the  $\text{C}=\text{O}$  bond of the coordinated dpk ligand such as **78**, and this complex decomposes to produce the observed Pd(IV) product according to the equation below.

**Scheme 2.32**

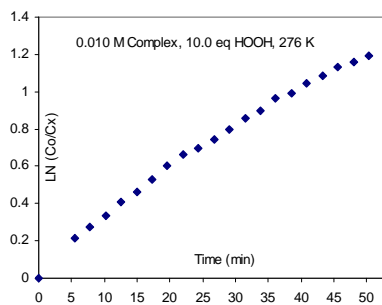


Kinetics study for the oxidation of 0.010 M complex **67** in water with  $H_2O_2$

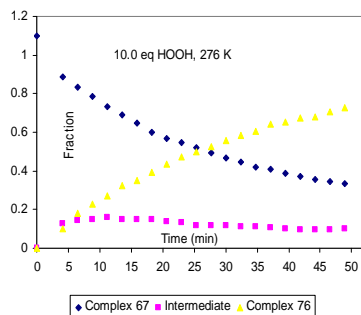
Scheme 2.33



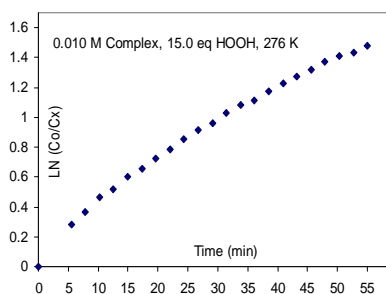
In order to understanding of the mechanism of the oxidation reaction, several kinetic experiments were performed. A 0.010 M aqueous solution of complex **67** was combined with 10.0-20.0 equivalents of  $H_2O_2$  at 3 °C, and this reaction was monitored by  $^1H$  NMR spectroscopy; 10.0-20.0 equivalents of  $H_2O_2$  were used in order to give pseudo-first order conditions. The rate of disappearance of the starting complex **67** at 3 °C K was analyzed as  $\ln([67]_0/[67]_t)$  vs time, where  $[67]_0$  refers to the initial concentration of the organopalladium(II) complex **67**, while  $[67]_t$  refers to the concentration of the organopalladium(II) complex **67** at time t. The kinetic plots were found to be non-linear.



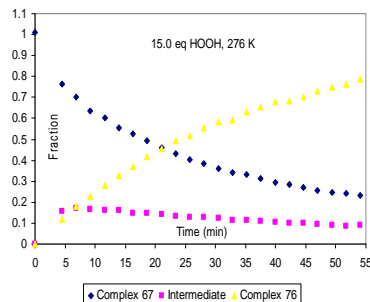
(a)



(b)



(c)



(d)

**Figure 2.26.** Representative kinetic plots of  $\ln([\mathbf{67}]_0/[\mathbf{67}]_t)$  vs time for reaction mixtures containing aqueous solutions of 0.010 M complex **67** with various equivalents of  $\text{H}_2\text{O}_2$  at 3 °C (a-b) 10.0 equivalents of  $\text{H}_2\text{O}_2$  was used (c-d) 15.0 equivalents of  $\text{H}_2\text{O}_2$  was used.

These plots indicate that the reaction does not follow a simple pseudo-first order rate law. The lack of simple second order kinetics would indicate a complex oxidation reaction mechanism. This is expected due to the observation of an intermediate complex which we propose is an adduct of  $\text{H}_2\text{O}_2$  addition across the C=O bond of the dpk ligand. Either addition of  $\text{H}_2\text{O}_2$  to the C=O bond or the actual oxidation of Pd(II) to Pd(IV) could be the rate determining step in our system, or the two processes could have similar rates, leading to the complex kinetics. In order to study this oxidation system, kinetics modeling was performed. The kinetics modeling was performed by Dr. Andrei Vedernikov. Selected results are presented in fig. 2.27.

In the kinetics modeling described in figure 2.27, experimental data for the reaction mixtures containing 0.010 M  $\text{D}_2\text{O}$  solutions of complex **67** with 10.0 and 15.0 equivalents of  $\text{H}_2\text{O}_2$  are modeled using Scheme 2.34. The rate constants  $k_1$ ,  $k_{-1}$ ,  $k_2$ ,  $k_3$ ,  $k_4$ ,  $k_{-4}$  were varied to produce the best least-square fit to the experimental data. Numerical integration was used to find the desired concentrations of **67** (blue diamonds in the plot), **76** (green diamonds in the plot), and **78** (red diamonds in the

plot) based on the rate constant values guessed and initial concentrations of **67**, **76** and **78**. The quality of the final fit (diamonds) is shown in fig. 2.27.

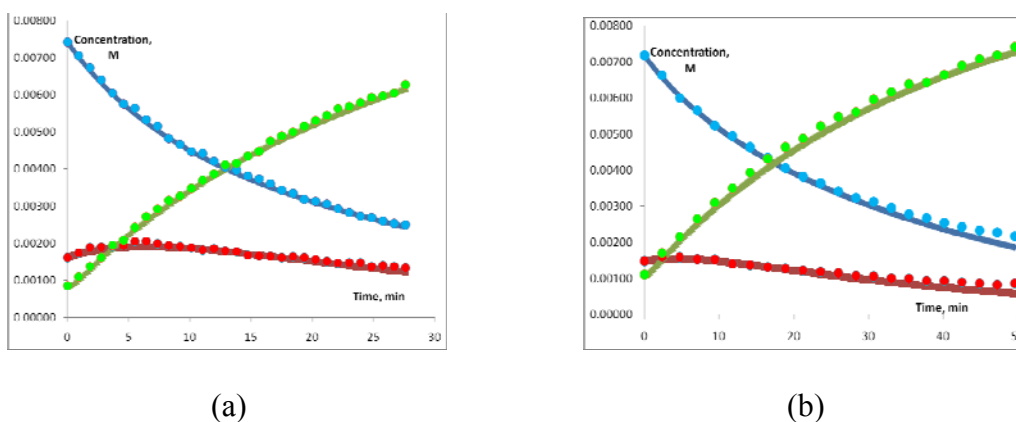
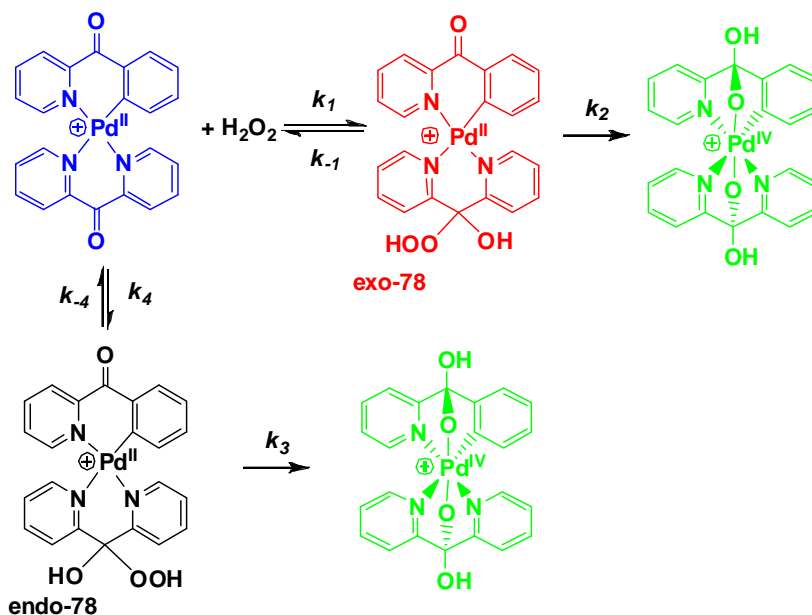


**Figure. 2.27.** Kinetics modeling plots for the reaction between 0.010 M D<sub>2</sub>O solutions of complex **67** with (a) 20.0 equivalents of H<sub>2</sub>O<sub>2</sub>, and (b) 15.0 equivalents of H<sub>2</sub>O<sub>2</sub> at 3°C. The plots include concentration of complex **67** (blue circles/diamonds), intermediate “X” (red circles/diamonds), and complex **76** (green circles/diamonds) as a function of time. The experimental concentrations are presented as circles while the modeled concentrations are presented as diamonds.

**Scheme 2.34**



According to figure 2.27, there is a near perfect fit of the experimental and the calculated values. The rate constants for the oxidation reactions found in three



Consistent with this formal consideration, results of our kinetics modeling give  $k_2 = 0$  and large  $k_3$  value. In addition, complex **endo-78** does not exist in sufficient concentration to be detected by NMR spectroscopy and the intermediate observed experimentally is therefore **exo-78**, which is unreactive towards product formation but exists in equilibrium with the Pd(II) precursor **67**. When higher concentrations of  $H_2O_2$  are used in the oxidation reaction, the fraction of **exo-78** increases since the increase in  $H_2O_2$  concentration will push the equilibrium between complexes **67** and **exo-78** forwards towards complex **exo-78**. Moreover, when the oxidation reaction is performed at higher temperatures, the rate of formation of the Pd(IV) complex **76** is expected to increase, and this will in-turn increase both the rate of depletion of complex **67** and the rate of reversible interconversion of complexes **67** and **exo-78**. Indeed at 22 °C, the fraction of complex **exo-78** was lower than at 3 °C.

Having analyzed the identity of the intermediate, we next sought to study the mechanism of oxidation of Pd(II) to Pd(IV). Van Koten and co-workers have proposed formation of an alcohol oxide which initially coordinates onto Pd(II). This is followed by nucleophilic attack of the Pd(II)  $d_z^2$  orbitals onto the  $\sigma^*$  O–O LUMO in a rate-determining step to form a Pd(IV) complex. Bandyopadhyay proposed formation of  $\cdot OOH$  radicals from  $HO_2H$  by a Fe(III) porphyrin catalyst. This  $\cdot OOH$  radical is attacked by Pd(II), ultimately leading to the formation of a Pd(IV) complex in a rate-determining step. In the oxidation of Pd(II) to Pd(IV) using *m*-CPBA, Bandyopadhyay proposed heterolytic cleavage of O–O bond of the peroxide oxidant in a concerted fashion, leading to formation of oxapalladacycles without formation of any Pd(IV) intermediate. In the oxidation of organoplatinum(II) complexes to

dihydroxy-organoplatinum(IV) complexes with H<sub>2</sub>O<sub>2</sub>, Rashidi and co-workers proposed a concerted three-centered transition state involving the two oxygen atoms of the peroxide group and the metal. Therefore we started our analysis by determining whether radicals are involved in the oxidation reaction.

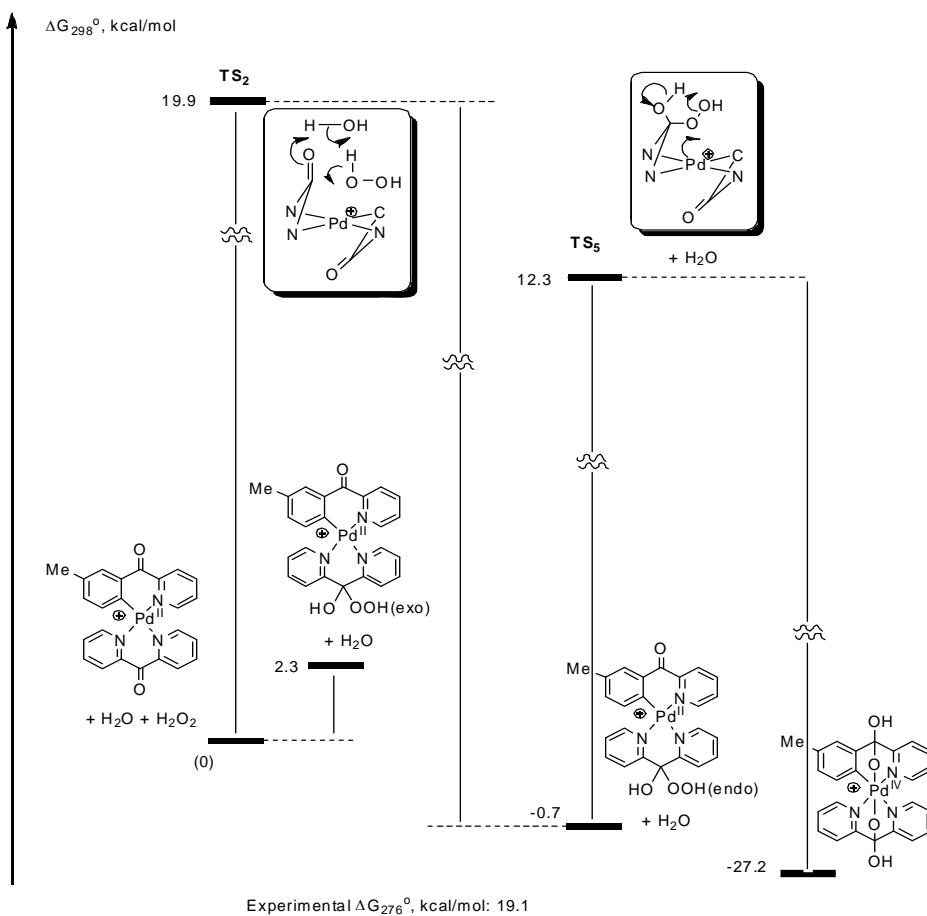
In order to rule out participation of ·OH or ·OOH free radicals in the oxidation of the organopalladium(II) complexes, the oxidation of complex **67** was performed in the presence of benzoquinone, which is a known radical reaction inhibitor.<sup>165</sup> A 0.010 M aqueous solution of complex **67** was combined with 5.0 eq of benzoquinone and 10.0 eq of H<sub>2</sub>O<sub>2</sub> was added to the solution. This reaction was monitored by <sup>1</sup>H NMR at 6 °C. Since the time for 50% conversion in the absence of benzoquinone was found to be ~ 17 minutes while the time for 50 % conversion in the presence of benzoquinone was ~ 18 minutes, the radical inhibitor was found not to inhibit the oxidation reaction, ruling out the participation of radicals in this reaction.

**Table 2.16.** Time for 50% conversion of complex **67** in acetic acid at 6 °C, in the presence and absence of benzoquinone additive.

Additive	50 % conversion
No additive	17 min
5.0 eq benzoquinone	18 min

As a result of the lack of inhibition of the oxidation reaction by benzoquinone radical inhibitor, a 2-electron oxidation mechanism was considered in the oxidation of Pd(II) to Pd(IV) by H<sub>2</sub>O<sub>2</sub>. This oxidation reaction was studied computationally using the DFT (see scheme 2.36 below, all data is for the aqueous phase reactions). The theoretical calculations were performed by Dr. Andrei Vedernikov.

Scheme 2.36



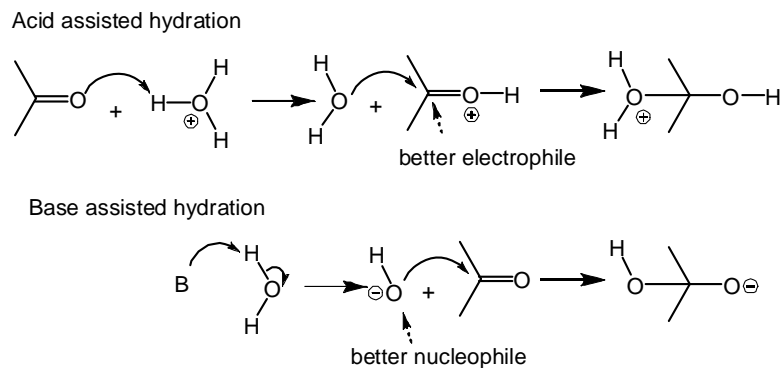
Consistent with our experimental results, the oxidation reaction might involve two steps: (i) addition of HOOH across the C=O bond of the dpk ligand, and (ii) oxidation of Pd(II) to Pd(IV). According to theoretical calculations, the rate-determining step for the oxidation of 2-benzoylpyridine derived dpk complexes with H<sub>2</sub>O<sub>2</sub> is the addition of H<sub>2</sub>O<sub>2</sub> across the C=O bond of the dpk ligand. This addition reaction has a lower barrier when its transition state includes one water molecule involved in a concerted proton transfer from H<sub>2</sub>O<sub>2</sub> to the dpk carbonyl oxygen atom. The calculated  $\Delta G^{\ddagger}$  of 19.9 kcal/mol closely matches the experimental value of 19.1 kcal/mol at 3°C. The theoretical calculations were performed using density functional theory (DFT) method,<sup>166</sup> specifically functional PBE,<sup>167</sup> implemented in an original

program package “Priroda”.<sup>168</sup> The basis set was 311-split for main group elements with one additional polarization *p*-function for hydrogen, additional two polarization *d*-functions for elements of higher periods.

The DFT was also used to study the mechanism for the oxidation of Pd(II) to Pd(IV) with H<sub>2</sub>O<sub>2</sub>. The lowest energy transition state for this step was found to involve proton assisted heterolytic cleavage of the O–O bond of the peroxide moiety in a cyclic transition state involving 5 atoms (Scheme 2.36). In this mechanism, 2-electrons from the doubly occupied *d*<sub>z<sup>2</sup> orbital of the Pd(II) atom attack the  $\sigma^*$  orbital of the O–O bond of the peroxide moiety leading to cleavage of this bond with the assistance from the proton of the neighboring hydroxide group. Proton transfer and eventual closure of the second pair of chelate rings lead to formation of the six-coordinate Pd(IV) cation **76**. The calculated  $\Delta G^\ddagger$  for this step was found to be 12.3 kcal/mol, which is lower than that for the addition of H<sub>2</sub>O<sub>2</sub> across the C=O bond of the dpk ligand.</sub>

Additional experiments were performed to test the calculated mechanism. Experiments were set up to monitor the effect of acids and bases on the rate of oxidation of aqueous solutions of complex **67** with H<sub>2</sub>O<sub>2</sub>. It is known that base accelerates the rate of hydration of ketones and aldehydes by deprotonating H<sub>2</sub>O and making a better nucleophile, OH<sup>-</sup>.<sup>169</sup> Acid also accelerates the rate of hydration of ketones and aldehydes by protonating the C=O moiety and making it a better electrophile.<sup>169</sup> With a rate-limiting addition of HOOH onto the C=O bond, the oxidation reaction is expected to be accelerated under both acidic and basic conditions.

**Scheme 2.37**



Thus two 0.010 M aqueous solutions of complex **67** buffered at pD = 8.50 and 5.03 were combined with 10.0 eq of H<sub>2</sub>O<sub>2</sub> and the reactions were monitored by <sup>1</sup>H NMR at 6°C. The time for 50% conversion in the absence of a buffer (pD = 5.72) is ~ 17 minutes while the time for 50 % conversion at pD = 8.50 ~ 17 minutes. The time for 50 % conversion at pD = 5.03 was found to be ~ 15.5 minutes. These results indicate that both acidic and basic conditions do not have significant effect on the rate of the oxidation reaction (see table 2.17 below).

**Table 2.17.** Time for 50 % conversion of complex **67** in buffered aqueous acidic, basic and non-buffered conditions.

Additive	50 % conv	50 % product	Max. Intermediate
No additive (pD = 5.72)	17 min	22 min	17 %
pD = 8.50	17 min	19 min	17 %
pD = 5.03	15.5 min	20 min	19 %

In summary, these results indicate that the reaction between H<sub>2</sub>O<sub>2</sub> and complex **67** is not affected by radical inhibitors, acidic or basic conditions.

The lack of acceleration of this oxidation reaction by acid or base is surprising since acidic and basic reactions conditions are known to increase the rate of hydration

of the C=O moiety. These results might indicate that the rate of addition of H<sub>2</sub>O<sub>2</sub> across the C=O bond of coordinated dpk is not affected in the studied pH range.

### 2.6.3 Kinetics Study of the Reaction of Organopalladium(II) Complexes 68-71 with H<sub>2</sub>O<sub>2</sub> in Water

In order to study the mechanism of oxidation of complexes **68-71**, the kinetics of this reaction was studied. Representative plots of  $\ln([\text{Pd(II)}]_0/[\text{Pd(II)}]_t)$  vs. time for a mixture of 0.010 M aqueous solution of complexes **69** and **71** and ~ 7-12 eq H<sub>2</sub>O<sub>2</sub> at 3 °C are given in figure 2.28 below. The pseudo-first order plots for these oxidation reactions are linear. The rates for these oxidation reactions with various substituents on the 2-phenylpyridine ligand are presented in table 2.18 below.

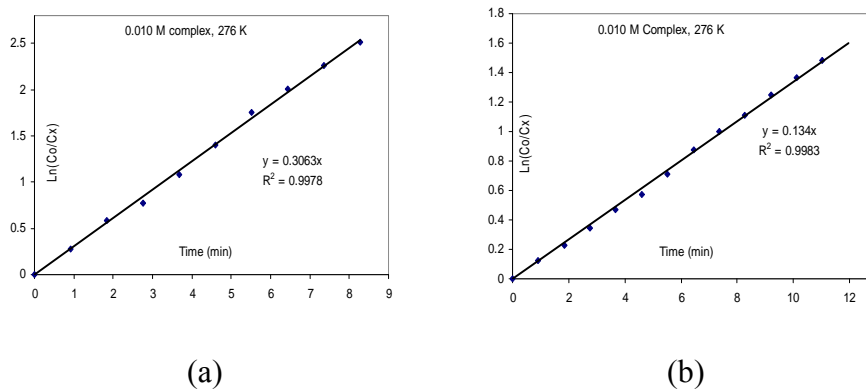


**Figure 2.28.** Representative kinetics plots of  $\ln([\text{Pd(II)}]_0/[\text{Pd(II)}]_t)$  vs. time for the oxidation of 0.010 M solutions of complexes **69** and **71** with ~ 7.0 equivalents of H<sub>2</sub>O<sub>2</sub> in D<sub>2</sub>O at 3 °C.

**Table 2.18.** Correlation between the observed first order rate constants and the  $\sigma_m$  for oxidation of various 4-substituted phenylpyridine dpk-derived palladacycles with excess  $\text{H}_2\text{O}_2$  at 3 °C under pseudo-first order conditions.

R	[Pd(II)]	[HOOH]	$K_{\text{obs}}$ ( $\text{min}^{-1}$ )	$\sigma_m$
-F	$4.85 * 10^{-3}$	$39.9 * 10^{-3}$	$(1.18 \pm 0.02) * 10^{-1}$	.337
-H	$5.78 * 10^{-3}$	$40.8 * 10^{-3}$	$(3.09 \pm 0.13) * 10^{-1}$	0
-Ome	$2.93 * 10^{-3}$	$37.9 * 10^{-3}$	$(4.63 \pm 0.06) * 10^{-1}$	0.115
-Me	$5.61 * 10^{-3}$	$40.6 * 10^{-3}$	$(1.37 \pm 0.01) * 10^{-1}$	-0.069

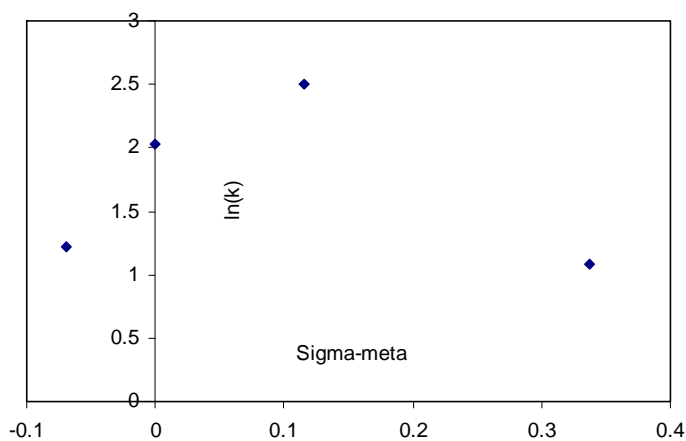


**Figure 2.29.** Hammett plot for the oxidation of 4-substituted phenylpyridine dpk-derived palladacycles **68-71** with excess  $\text{H}_2\text{O}_2$  at 3 °C under pseudo-first order conditions.

The Hammett plot shows a change in the slope of the plot with two intersecting lines, which is indicative of a change in the rate-determining step as a function of the substituents.

In order to rule out participation of  $\cdot\text{OH}$  radicals in the oxidation of the organopalladium(II) complexes, the oxidation of complex **69** was performed in the presence of benzoquinone, which is a known inhibitor of radical reactions. Thus

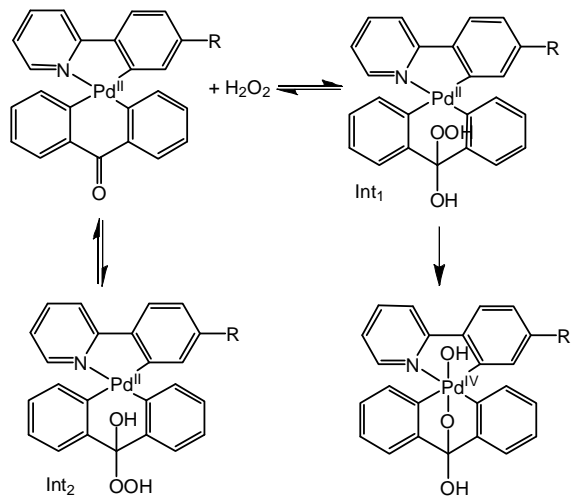
0.010 M aqueous solution of complex **69** was combined with 3.0 eq of benzoquinone and ~7.0 equivalents of H<sub>2</sub>O<sub>2</sub> was added to the solution. This reaction was monitored by <sup>1</sup>H NMR at 3 °C. The observed pseudo-first order rate constant for the oxidation reaction in the absence of benzoquinone was found to be indistinguishable to the pseudo-first order rate constant in the presence of benzoquinone, indicating the absence of radicals.

**Table 2.19.** Observed first order rate constants for the depletion of complex **69** in water at 3 °C, in the presence and absence of benzoquinone additive.

Additive	k <sub>obs</sub> (min <sup>-1</sup> )
No additive	0.121 ± 0.003
5.0 eq benzoquinone	0.125 ± 0.006

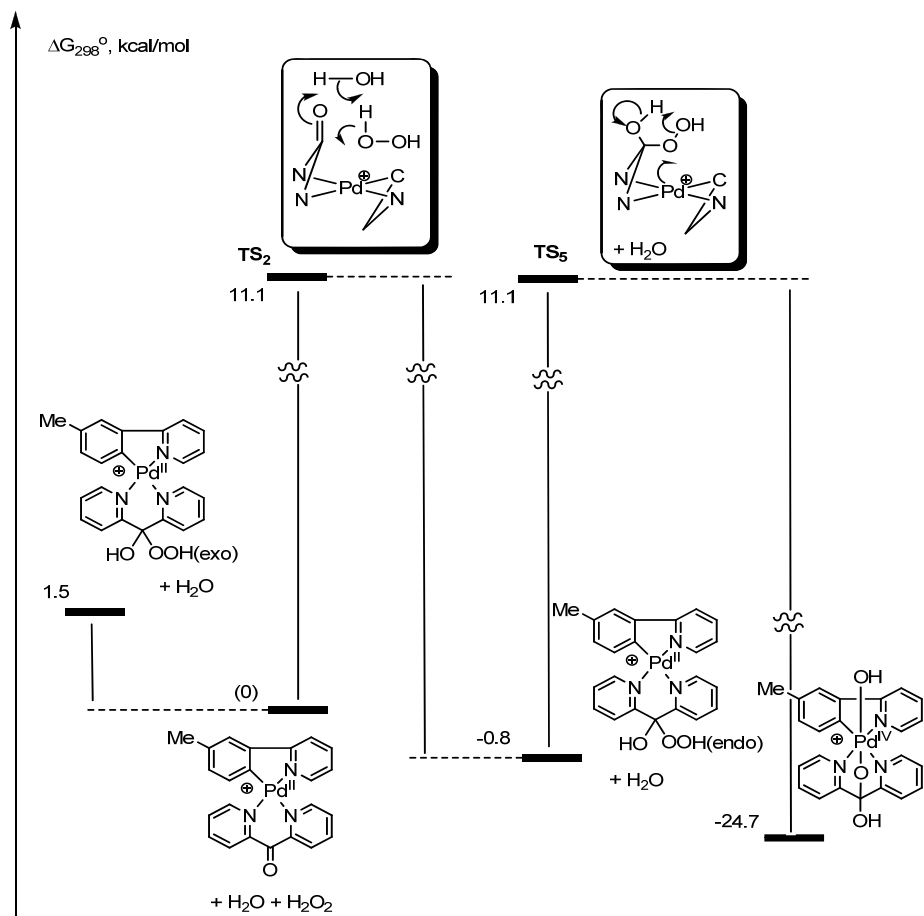
This analysis indicates that radicals are not involved in this oxidation reaction. Therefore a 2-electron mechanism of oxidation was considered. Similar to the oxidation of complexes **66** and **67** with H<sub>2</sub>O<sub>2</sub> in water, a two-step oxidation mechanism was proposed. The first step is proposed to involve addition of H<sub>2</sub>O<sub>2</sub> across the C=O bond of the dpk ligand to produce a hydroperoxo adduct. The second step involves nucleophilic attack of Pd(II) onto the O–O bond in the hydroperoxide adduct that results into heterolytic cleavage of the bond to generate the observed Pd(IV) products, according to Scheme 2.38. Attempts to detect the hydroperoxo adduct were unfruitful. In particular, when the oxidation reactions of complexes **69** and **71** were performed in water with various equivalents of H<sub>2</sub>O<sub>2</sub> at various temperatures, no intermediates were detected in these reactions.

Scheme 2.38



This reaction was studied by DFT calculations (Scheme 2.39).

Scheme 2.39



According to the DFT calculations, the two steps involved in the oxidation reaction have similar Gibbs free energy. As a result, any change in substrates or reaction conditions could change the rate-determining step of the reaction. Thus the experimental observation of a curved Hammett plot for the oxidation of 2-phenylpyridine derived palladacycles is not surprising.

The experimentally observed Hammett plot gives a negative  $\rho$  value for electron-withdrawing substituents and a positive  $\rho$  value for electron-donating substituents. A negative  $\rho$  value indicates that there is a build up of positive charge at the transition state, and this would support the oxidation step being the rate-determining step. However a positive  $\rho$  value for electron-donating substituents indicates a build up of negative charge in the transition state. Since attack of the C=O bond by H<sub>2</sub>O<sub>2</sub> leads to development of positive charge at the oxygen atom of the hydrogen peroxide moiety and negative charge at the oxygen atom of the carbonyl moiety, the extent to which the charges develop determines the  $\rho$  value observed; in this case more negative than positive charge develops at the transition state.

Thus, the mechanism proposed through DFT calculations where the energy of both steps involved in the oxidation reaction are close agrees with experimental observations. This is because when the energies of both steps are close, various factors could change the rate-determining step of the oxidation reaction, and this is the case where electronic factors were observed to change the rate-determining steps according to Hammett analysis.

The effect of pH was also analyzed on the rate of this oxidation reaction. As discussed above, both acids and bases are expected to increase the rate of hydrolysis

of C=O bond, and these factors are expected to increase the rate of addition of H<sub>2</sub>O<sub>2</sub> across the C=O bond. As a result, if the rate-determining step of the oxidation reaction is addition of H<sub>2</sub>O<sub>2</sub> across the C=O bond, then acidic and basic pH are expected to increase the rate of the oxidation reaction.

The effect of pH in the oxidation of the organopalladium(II) complexes with H<sub>2</sub>O<sub>2</sub> was investigated. Two 0.010 M aqueous solutions of complex **69** buffered at pD = 8.88 and 4.86 were prepared. ~ 5.0 eq. of H<sub>2</sub>O<sub>2</sub> was added to the solutions and the reactions were monitored by <sup>1</sup>H NMR at 3 °C. The plots for ln([**69**]<sub>o</sub>/[**69**]<sub>t</sub>) vs time plot for these reactions are presented below. These plots were found to be non-linear, and thus the time for 50 % conversion are presented in table 2.20 below.

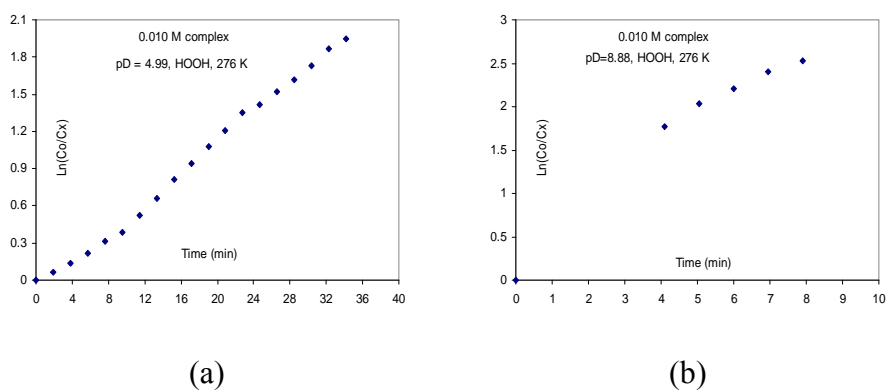


**Fig. 2.30.** (a) A Kinetic plot for  $\ln([\mathbf{69}]_o/[\mathbf{69}]_t)$  vs time plot for the oxidation of 0.010 M complex **69** with ~6 equivalents of H<sub>2</sub>O<sub>2</sub> in 1.0 ml D<sub>2</sub>O at 3 °C at pD = 4.99 (b) Kinetic plot for  $\ln([\mathbf{69}]_o/[\mathbf{69}]_t)$  vs time plot for the oxidation of 0.010 M complex **69** with ~25 equivalents of H<sub>2</sub>O<sub>2</sub> in 1.0 ml D<sub>2</sub>O at 3 °C at pD = 8.88.

According to the kinetics of oxidation of aqueous solutions of 2-phenylpyridine derived palladacycles with H<sub>2</sub>O<sub>2</sub> in acidic and basic conditions, the reaction is accelerated at high pH, and inhibited at low pH (table 2.20).

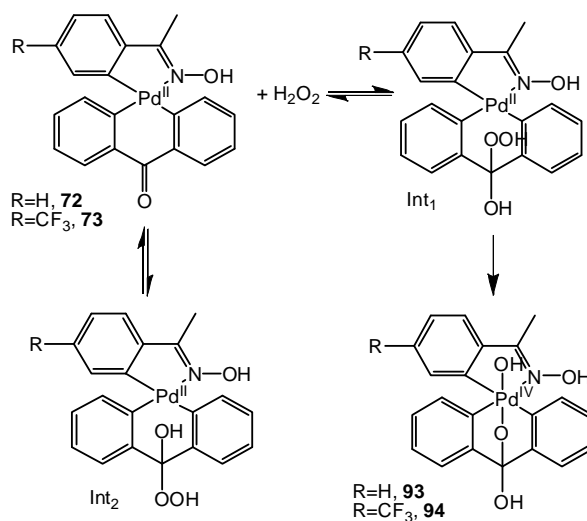
**Table 2.20.** Oxidation of 0.010 M D<sub>2</sub>O solutions of complex **69** with excess (>6 equivalents) H<sub>2</sub>O<sub>2</sub> at 3 °C in the presence of various additives.

Additive	50 % conversion (mins)	Complex <b>84</b>	Complex <b>88</b>
No additive (pD = 7.32)	6.0	76 %	24 %
3.0 eq benzoquinone	8.0	87 %	13 %
pD = 4.99	16	96 %	4 %
pD = 8.88	<2	94 %	6 %

2.6.4 <sup>1</sup>H NMR Study of the Reaction of Organopalladium(II) Complexes **72** and **73** with H<sub>2</sub>O<sub>2</sub> in Water

A similar two-step oxidation scheme could be considered for the oxidation of complexes **72** and **73**.

**Scheme 2.40**



When aqueous solutions of complexes **72** and **73** were combined with 2.0 equivalents of H<sub>2</sub>O<sub>2</sub> at ambient conditions, quantitative formation of complexes **93** and **94** were observed and no intermediates were detected in these reactions.

Similarly, when an acetic acid solution of complex **72** was combined with 2.0 equivalents of H<sub>2</sub>O<sub>2</sub>, quantitative formation of complex **93** was observed with no intermediates detected. However when an acetic acid solution of the more electron-deficient complex **73** was combined with 2.0 equivalents of H<sub>2</sub>O<sub>2</sub>, an intermediate was detected. This intermediate led to formation of complex **94** under the reaction conditions. It is possible that the adduct of H<sub>2</sub>O<sub>2</sub> addition across the C=O bond of the dpk ligand was detected when complex **73** was used as substrate due to its electron-deficient nature. An electron-deficient complex would make the C=O bond of the dpk ligand more electrophilic and thus increase the rate of the addition reaction. In addition, an electron-deficient complex would make the Pd<sup>II</sup> center less nucleophilic towards attacking the  $\sigma^*$  orbitals of the O–O bond of the oxidant, and thus a high rate of formation of the hydroperoxo adduct and a lower rate of depletion would increase the concentration of this adduct leading to its detection by <sup>1</sup>H NMR.

### 2.7 Summary and conclusion

In summary, the ligand enabled oxidation of monohydrocarbyl Pd(II) complexes **66-74** with H<sub>2</sub>O<sub>2</sub> in water and acetic acid has been achieved to generate the corresponding Pd(IV) monohydrocarbyls. The Pd(IV) complexes bearing two facially chelating ligands were found to be more stable than those bearing one facially chelating ligand.

The mechanism of oxidation of the organopalladium(II) complexes with H<sub>2</sub>O<sub>2</sub> has been studied. This mechanism has been proposed to involve two steps: (i) addition of H<sub>2</sub>O<sub>2</sub> across the C=O bond of the dpk ligand to produce a hydroperoxo adduct, (ii) heterolytic O–O bond cleavage in the hydroperoxo adduct to produce the

Pd(IV) products. The adduct of addition of  $\text{H}_2\text{O}_2$  across the  $\text{C}=\text{O}$  bond of the dpk ligand has been detected in reactions involving the 2-benzoylpyridine-derived complexes in water and acetophenone oxime-derived complexes in acetic acid. The rate-determining step in these oxidation reactions was found to vary as a function of the substrate used and the reaction conditions.

## 2.8 Experimental

### 2.8.1 General

All manipulations were carried out under ambient atmosphere unless otherwise noted. All reagents for which synthesis is not given are commercially available from Aldrich, Acros, Alfa-Aesar or Pressure Chemicals, and were used as received without further purification.  $^1\text{H}$  (400 MHz or 500 MHz) and  $^{13}\text{C}$  NMR (100 MHz or 125 MHz) spectra were recorded on a Bruker AVANCE 400 or Bruker DRX-500. Chemical shifts are reported in ppm and referenced to residual solvent resonance peaks. High Resolution Mass Spectrometry (HRMS) experiments were performed using a JEOL AccuTOF-CS instrument. Elemental analyses were carried out by either Chemisar Laboratories Inc., Guelph, Canada, or Columbia Analytical Services, Tucson, AZ.

### 2.8.2 Computational details.

Theoretical calculations in this work have been performed using density functional theory (DFT) method,<sup>166</sup> specifically functional PBE,<sup>167</sup> implemented in an original program package “Priroda”.<sup>168</sup> In PBE calculations relativistic Stevens-Basch-Krauss (SBK) effective core potentials (ECP)<sup>170-172</sup> optimized for DFT-calculations have been used. Basis set was 311-split for main group elements with one additional polarization *p*-function for hydrogen, additional two polarization *d*-functions for elements of higher periods. Full geometry optimization has been performed without constraints on symmetry. For all species under investigation frequency analysis has been carried out. All minima have been checked for the

absence of imaginary frequencies. All transition states possessed just one imaginary frequency. Using the method of Intrinsic Reaction Coordinate, reactants, products and the corresponding transition states were proven to be connected by a single minimal energy reaction path.

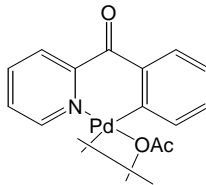
All the species under investigation were next modeled with the Jaguar program package with the same functional (PBE)<sup>173</sup> and LACVP relativistic basis set with two polarization functions. These results showed the same trends as with Priroda calculations and the essentially same reaction parameters. The solvation of all complexes in Scheme 5 in water was modeled using a Poisson-Boltzmann continuum solvation model (PBF).

### 2.8.3 Acetate-bridged Palladacycles

#### *Preparation of complexes 49 and 50*

Compounds **49** and **50** were prepared by the following general procedure. The substrate **40** or **41** was combined with 1.0 equivalent of Pd(OAc)<sub>2</sub> in acetic acid. The resulting acetic acid solution was refluxed for 3 hours. The solution was filtered through Celite while hot to remove Pd black and concentrated to afford precipitate. The precipitate was filtered off and washed with a small amount of diethyl ether to afford the target compounds in good yields. The identity of compound **49** was confirmed by comparing its NMR spectra to literature, while the identity of compound **50** was confirmed by NMR and its purity was confirmed by elemental analysis.

**Complex 49 (82.8 % yield)**

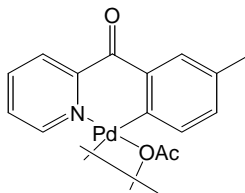


The identity of complex **49** was confirmed by comparing its spectrum to that published in literature.<sup>7</sup>

<sup>1</sup>H NMR (CDCl<sub>3</sub>, 22°C), δ: 2.07 (s, 3H), 6.81-6.87 (m, 2H), 6.97 (td, *J*=7.8, 1.2 Hz, 1H), 7.13 (ddd, *J*=7.5, 5.6, 1.8 Hz, 1H), 7.42 (dd, *J*=7.6, 1.4 Hz, 1H), 7.79-7.86 (m, 2H), 8.28 (d, *J*=5.4 Hz, 1H).

<sup>13</sup>C NMR (CDCl<sub>3</sub>, 22°C), δ: 24.7, 124.8, 125.7, 126.8, 128.8, 130.6, 132.8, 134.2, 138.8, 143.5, 150.8, 152.0, 181.7, 190.6

**Complex 50 (96.0 % yield)**



<sup>1</sup>H NMR (CDCl<sub>3</sub>, 22°C), δ: 2.03 (s, 3H), 2.22 (s, 3H), 6.69 (vs, 2H), 7.10 (ddd, *J*=7.5, , 5.5, 1.9 Hz, 1H), 7.26 (s, 1H), 7.81 (td, *J*=7.4, 1.5 Hz, 1H), 7.85 (dd, *J*=7.9, 1.3 Hz, 1H), 8.27 (dd, *J*=5.3, 0.8 Hz, 1H).

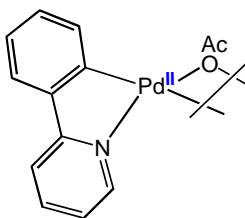
<sup>13</sup>C NMR (CDCl<sub>3</sub>, 22°C), δ: 20.6, 24.7, 125.7, 126.7, 129.1, 132.0, 132.5, 134.1, 134.2, 138.6, 139.9, 150.9, 152.1, 181.6, 190.6.

Anal. Found (Calcd for C<sub>15</sub>H<sub>13</sub>NO<sub>3</sub>Pd): C, 49.54 (49.81); H, 3.71 (3.62); N, 3.77 (3.87).

### Preparation of 2-phenylpyridine derived complexes **51** – **54**

Phenylpyridine-derived dinuclear acetato-bridged palladacycles were prepared by a modified literature procedure. A substituted phenylpyridine derivative **42-45** (1.05 mmoles) and Pd(OAc)<sub>2</sub> (1.00 mmoles) were combined in acetic acid and the solution was either refluxed for 4 hours or stirred at 80°C overnight. The resulting solution was filtered through Celite while hot to remove Pd black. Concentration of the reaction solutions produced yellow precipitate of the target complexes. The reaction mixtures were triturated with diethyl ether to afford more products. Filtration of the resulting reaction mixtures afforded the target complexes as yellow residue which were washed with a small amount of diethyl ether and dried under vacuum at room temperature. The target compounds **51-54** were isolated as a mixture of two species, presumably *cis*- and *trans*- isomers whose ratios were determined via <sup>1</sup>H NMR integration. The identity of the products was confirmed by NMR spectroscopy while the purity was confirmed by elemental analysis.

#### Complex **51** (90.3 % yield)

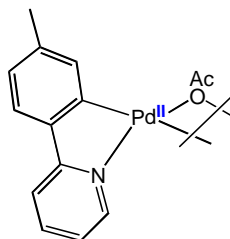


The identity of complex **51** was confirmed by comparing its spectrum to that published in literature.<sup>174</sup>

<sup>1</sup>H NMR (CDCl<sub>3</sub>, 22°C), δ: 2.25 (s, 3H), 6.42 (t, *J*=6.5Hz, 1H), 6.76–6.85 (m, 3H), 6.89 (d, *J*=7.5 Hz, 1H), 7.06 (d, *J*=7.8 Hz, 1H), 7.34 (td, *J*=7.8, 1.4 Hz, 1H), 7.84 (d, *J*=5.5 Hz, 1H),

$^{13}\text{C}$  NMR ( $\text{CDCl}_3$ ,  $22^\circ\text{C}$ ),  $\delta$ : 25.04, 117.3, 121.2, 122.5, 124.0, 128.6, 132.0, 137.7, 144.6, 150.2, 152.1, 164.3, 181.8.

**Complex 52 (94.7 % yield)**

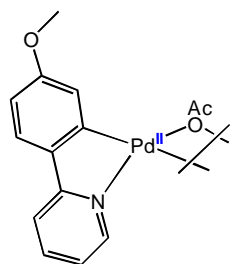


The identity of complex **52** was confirmed by comparing its spectrum to that published in literature.<sup>174</sup>

$^1\text{H}$  NMR ( $\text{CDCl}_3$ ,  $22^\circ\text{C}$ ),  $\delta$ : 2.17 (s, 3H), 2.25 (s, 3H), 6.49 (td,  $J=6.5$ , 0.9 Hz, 1H), 6.56 (d,  $J=7.7$  Hz, 1H), 6.62 (s 1H), 6.72 (d,  $J=7.8$  Hz, 1H), 6.99 (d,  $J=8.0$  Hz, 1H), 7.33 (td,  $J=7.9$ , 1.5 Hz, 1H), 7.86 (td,  $J=5.8$ , 0.8 Hz, 1H).

$^{13}\text{C}$  NMR ( $\text{CDCl}_3$ ,  $22^\circ\text{C}$ ),  $\delta$ : 22.2, 25.3, 117.3, 120.3, 122.4, 125.0, 132.7, 137.6, 138.6, 141.9, 150.0, 152.0, 164.7, 181.9.

**Compound 53 (84.9 % yield)**



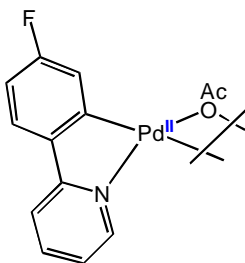
Complex **53** was prepared using the general procedure described above, and was isolated in 84.9 % yield as a mixture of two isomers in 82:18 ratio as determined by  $^1\text{H}$  NMR integration.

Major Isomer:  $^1\text{H}$  NMR ( $\text{CDCl}_3$ ,  $22^\circ\text{C}$ ),  $\delta$ : 2.24 (s, 3H), 3.73 (s, 3H), 6.31 (dd,  $J=8.3$ , 2.4 Hz, 1H), 6.38 (vs, 1H), 6.44 (td,  $J=6.6$ , 0.8 Hz, 1H), 6.76 (d,  $J=8.5$  Hz, 1H), 6.92 (d,  $J=8.1$  Hz, 1H), 7.31 (td,  $J=7.8$ , 1.3 Hz, 1H), 7.82 (d,  $J=5.2$  Hz, 1H).

$^{13}\text{C}$  NMR ( $\text{CDCl}_3$ ,  $22^\circ\text{C}$ ),  $\delta$ : 25.0, 55.3, 110.5, 116.2, 166.8, 119.8, 123.6, 137.5, 137.6, 149.7, 153.9, 164.4, 181.8.

Anal. Found (Calcd,  $\text{C}_{14}\text{H}_{13}\text{NO}_3\text{Pd}$ ): C, 47.90 (48.09); H, 3.63 (3.75); N, 3.96 (4.01).

**Complex 54 ( 79.2 % yield)**



Complex **54** was prepared by the general procedure described above, and was isolated in 79.2 % yield as a mixture of two isomers in 86:14 ratio as determined by  $^1\text{H}$  NMR integration.

Major Isomer:  $^1\text{H}$  NMR ( $\text{CDCl}_3$ ,  $22^\circ\text{C}$ ),  $\delta$ : 2.26 (s, 3H), 6.47 (td,  $J=8.3$ , 2.4 Hz, 1H), 6.51 (dd,  $J=9.0$ , 2.4 Hz, 1H), 6.65 (td,  $J=6.6$ , 1.1 Hz, 1H), 6.85 (dd,  $J=8.8$ , 5.3 Hz, 1H), 7.00 (d,  $J=8.1$  Hz, 1H), 7.42 (td,  $J=7.7$ , 1.5 Hz, 1H), 7.90 (dd,  $J=5.8$ , 0.8 Hz, 1H).

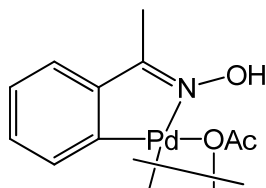
$^{13}\text{C}$  NMR ( $\text{CDCl}_3$ ,  $22^\circ\text{C}$ ),  $\delta$ : 25.0, 111.2 (d,  $J=23$  Hz), 117.5, 118.5 (d,  $J=19$  Hz), 121.1, 123.7 (d,  $J=9$  Hz), 138.1, 149.9, 154.4 (d,  $J=5.5$  Hz), 160.0, 162.0, 163.7, 182.2.

Anal. Found (Calcd, C<sub>10</sub>H<sub>10</sub>FNO<sub>2</sub>Pd): C, 46.16 (46.24); H, 2.91 (2.99); N, 4.05 (4.15).

*Preparation of acetophenone oxime-derived complexes 55 and 56*

The acetato-bridged palladacycles **55** and **56** were prepared by combining palladium acetate and a substituted acetophenone oxime derivative **46** or **47** (1.05 eq.) were combined in acetic acid and stirred 80 °C for 8 hours. The resulting solution was filtered through Celite while hot to remove Pd black. Concentration of the resulting solution produced precipitate of the target compound, which was filtered off and the residue was washed with a small amount of diethyl ether to afford the target complexes; complex **55** was isolated as a yellow solid while complex **56** was isolated as an orange solid. The identity of the compounds was confirmed by NMR spectroscopy while the purity was confirmed by elemental analysis. Proton NMR spectroscopy revealed the presence of two species, presumably *cis*- and *trans*-isomers whose ratio could be determined by integration of the NMR spectra.

**Complex 55 ( 96% yield)**



Complex **55** was isolated in 96.0 % yield as a mixture of two isomers in 32:68 ratio as determined by <sup>1</sup>H NMR integration.

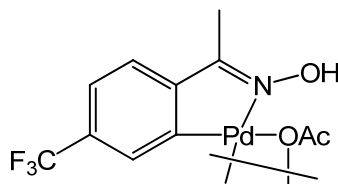
Major isomer:  $^1\text{H}$  NMR (DMSO- $d_6$ , 22°C),  $\delta$ : 1.90(s, 3H), 2.12 (s, 3H), 6.79 (td,  $J=7.0$ , 1.2 Hz, 1H), 7.03 (td,  $J=7.4$ , 1.1 Hz, 1H), 7.09 (dd,  $J=6.8$ , 1.1 Hz, 1H), 7.71 (d,  $J=7.6$  Hz, 1H), 12.10 (s, 1H).

Minor isomer:  $^1\text{H}$  NMR (DMSO- $d_6$ , 22°C),  $\delta$ : 1.90(s, 3H), 2.22 (s, 3H), 6.99 (t,  $J=7.1$  Hz, 1H), 7.12 (t,  $J=7.3$ , Hz, 1H), 7.22 (d,  $J=7.1$  Hz, 1H), 7.58 (d,  $J=7.7$  Hz, 1H), 12.10 (s, 1H)

$^{13}\text{C}$  NMR (DMSO, 22°C) for both isomers,  $\delta$ : 11.5, 12.2, 22.3, 124.3, 124.9, 125.4, 126.0, 128.0, 131.6, 132.4, 144.4, 146.5, 149.5, 154.7, 162.1, 165.7.

Anal. Found: C, 40.34; H, 4.06; N, 4.36; Calculated for  $\text{C}_{20}\text{H}_{22}\text{N}_2\text{O}_6\text{Pd}_2$ ; C, 40.09; H, 3.70; N, 4.67.

**Complex 56 ( 92% yield)**



Complex **56** was isolated in 96.0 % yield as a mixture of two isomers in 21:79 ratio as determined by  $^1\text{H}$  NMR integration.

Major isomer:  $^1\text{H}$  NMR (DMSO- $d_6$ , 22°C),  $\delta$ : 1.90(s, 3H), 2.16 (s, 3H), 7.28 (d,  $J=7.9$  Hz, 1H), 7.38 (d,  $J=7.8$  Hz, 1H), 8.08 (s, 1H), 12.32 (s, 1H).

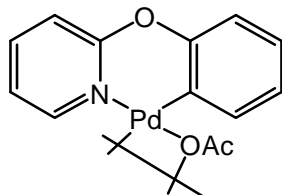
Minor isomer:  $^1\text{H}$  NMR (DMSO- $d_6$ , 22°C),  $\delta$ : 1.90(s, 3H), 2.25 (s, 3H), 7.39 (d,  $J=7.9$  Hz, 1H), 7.46 (d,  $J=7.8$  Hz, 1H), 7.94 (s, 1H), 12.32 (s, 1H)

$^{13}\text{C}$  NMR (DMSO- $d_6$ , 22°C) for both isomers,  $\delta$ : 13.0, 22.5, 123.2, 124.6, 124.9, 125.0, 125.3, 126.4, 126.7, 128.5, 151.5, 154.9, 156.3, 173.8.

Anal. Found: C, 36.16; H, 3.14; N, 3.49. Calculated for  $\text{C}_{22}\text{H}_{20}\text{F}_6\text{N}_2\text{O}_6\text{Pd}_2$ ; C, 35.94; H, 2.74; N, 3.81.

**Complex 57, (90% yield)**

Phenoxyppyridine-derived acetate-bridged palladacycle **57** was prepared by a modified literature procedure.<sup>152</sup> Phenoxyppyridine (1.05 mmoles) and Pd(OAc)<sub>2</sub> (1.0 mmoles) were combined in acetic acid and stirred at 50 °C for 12 hours. The reaction mixture was filtered and the residue was washed with a small amount of diethyl ether to afford the target compound as light yellow crystals in 90 % yield. The identity of the product was confirmed by comparing its spectra to those reported in literature. Proton NMR revealed the presence of two species, presumably *cis*- and *trans*-isomers whose ratio was determined to be 92 % to 8 % according to <sup>1</sup>H NMR integration in CDCl<sub>3</sub> solvent at 22 °C.



Complex **57** was prepared according to literature, except that the solution was heat at 50 °C for 6 hours to increase yield.<sup>152</sup>

<sup>1</sup>H NMR (AcOH-d<sub>4</sub>, 22°C), δ: 2.06(s, 3H), 6.61 ( d, *J*=8.1 Hz, 1H), 6.67 (d, *J*=7.6 Hz, 1H), 6.70 to 6.77 (m, 2H), 6.88 (t, *J*=7.4 Hz, 1H), 6.97 (d, *J*=8.3 Hz, 1H), 6.69 (t, *J*=7.7 Hz, 1H), 8.02 (d, *J*=5.8 Hz, 1H).

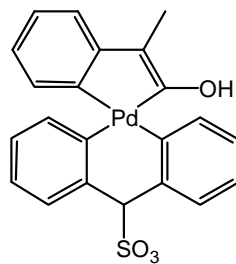
<sup>13</sup>C<sup>95</sup> NMR (CDCl<sub>3</sub>, 22°C), δ: 24.5, 114.3, 115.2, 117.7, 118.5, 123.0, 124.9, 134.2, 139.8, 148.9, 149.4, 157.4, 181.2.

#### 2.8.4 Preparation of dpms-ligated Palladacycles

Complexes **58** and **61** have been characterized by Zhang and Vedernikov in unpublished results.<sup>175</sup>

The preparation and characterization of complex **58** was performed by Zhang and co-workers (Zhang, unpublished results). Complex **59** was prepared by combining the acetato-bridged palladacycle **55** (1.00 mmol) with an aqueous solution of the dpms ligand (1.05 mmol.) at ambient conditions. Stirring the reaction mixture at room temperature for several hours gradually produced a white precipitate. After 12 hours, the precipitate was filtered off and washed with a small amount of cold water to afford the pure target complex. Complex **60** was prepared by combining methanolic solution of the dpms ligand (1.05 mmol.) with the acetate-bridged palladacycle **49** (1.00 mmol). The resulting reaction mixture was stirred at room temperature for 6 hours, where gradual formation of white precipitate was observed. At the end of the reaction, diethyl ether was added to the reaction mixtures to afford more white precipitate. The precipitate was filtered off and washed with a small amount of cold diethyl ether to afford pure the target complex **60**. The identity of the complexes **58-60** was confirmed by NMR spectroscopy and electrospray ionization mass spectrometry, while the purity was confirmed by elemental analysis.

#### ***Complex 59 (82%)***



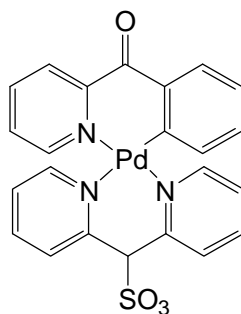
$^1\text{H}$  NMR (AcOH- $d_4$ , 22°C),  $\delta$ : 2.43 (s, 3H), 6.43 (s, 1H), 6.82 (d,  $J=7.6$  Hz, 1H), 7.04 (dt,  $J=7.4$ , 1.4 Hz, 1H), 7.14 (dt,  $J=7.5$ , 0.8 Hz, 1H), 7.33 (dd,  $J=7.5$ , 1.3 Hz, 1H), 7.56 (t,  $J=6.2$  Hz, 2H), 7.93 (d,  $J=7.5$  Hz, 2H), 8.06 (t,  $J=7.4$  Hz, 2H), 8.99 (s, 2H).

$^{13}\text{C}$  NMR (AcOH- $d_4$ , 22°C),  $\delta$ : 12.1, 126.0, 127.1, 130.0, 130.4, 134.5, 141.1, 143.6, 158.5, 177.4.

ESI-MS of solution of **59**<sup>+</sup> in methanol,  $m/z = 489.9776$ . Calculated for  $\text{C}_{19}\text{H}_{18}\text{N}_3\text{O}_4\text{S}^{106}\text{Pd}$ , 490.0053.

Anal. Found: 46.48; H, 3.75; N, 8.32; Calculated for  $\text{C}_{19}\text{H}_{17}\text{N}_3\text{O}_3\text{PdS}$ : C, 46.59; H, 3.50; N, 8.58.

**Complex 60 (89%)**



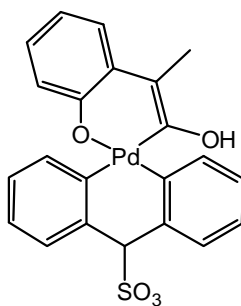
$^1\text{H}$  NMR (AcOH- $d_4$ , 22°C),  $\delta$ : 7.12 (dd,  $J=7.4$ , 1.4 Hz, 1H), 7.15 (td,  $J=6.8$ , 1.6 Hz, 1H), 7.19 (td,  $J=6.9$ , 1.4 Hz, 1H), 7.28 (ddd,  $J=7.7$ , 5.6, 1.4 Hz, 1H), 7.34 (ddd,  $J=7.6$ , 5.5, 1.4 Hz, 1H), 7.61 (ddd,  $J=7.6$ , 5.8, 1.7 Hz, 1H), 7.67 (d,  $J=5.0$ , 1.7 Hz, 1H), 7.72 (dd,  $J=7.4$ , 1.4 Hz, 1H), 7.82 (dd,  $J=5.8$ , 1.0 Hz, 1H), 7.97-8.05 (m, 4H), 8.21 (td,  $J=7.8$ , 1.4 Hz, 1H), 8.24 (td,  $J=7.8$ , 1.2 Hz, 1H), 8.60 (d,  $J=5.4$  Hz, 1H).

$^{13}\text{C}$  NMR (222, trifluoroethanol-d, 22°C),  $\delta$ : 128.4, 128.6, 130.2, 130.3, 131.1, 131.7, 133.1, 134.5, 135.0, 142.0, 142.2, 142.6, 145.5, 147.3, 150.9, 151.8, 153.7, 195.6

ESI-MS of solution of **59**<sup>+</sup> in methanol,  $m/z = 538.0621$ , Calculated for  $\text{C}_{23}\text{H}_{18}\text{N}_3\text{O}_4\text{S}^{106}\text{Pd}$ , = 538.0053.

Anal. Found: C, 51.11; H, 3.04; N, 7.57; Calculated for  $\text{C}_{23}\text{H}_{17}\text{N}_3\text{O}_4\text{PdS}$ : C, 51.36; H, 3.19; N, 7.81.

### Complex 63



$^1\text{H}$  NMR (AcOH-d<sub>4</sub>, 22°C),  $\delta$ : 2.43 (s, 3H), 6.44 (s, 1H), 6.82 (dd,  $J=6.6$ , 1.0 Hz, 1H), 7.08 (dt,  $J=7.5$ , 1.5 Hz, 1H), 7.14 (dt,  $J=7.5$ , 1.1 Hz, 1H), 7.33 (dd,  $J=7.5$ , 1.5 Hz, 1H), 7.56 (dt, 6.6, 1.1 Hz, 2H), 7.93 (dd,  $J=7.7$ , 1.0 Hz, 2H), 8.06 (t,  $J=7.7$ , 2H), 8.88 (s, 2H).

$^{13}\text{C}$  NMR (AcOH-d<sub>4</sub>, 22°C),  $\delta$ : 15.5, 116.5, 120.6, 122.9, 124.4, 124.6, 127.8, 128.4, 130.6, 133.0, 140.4, 140.5, 149.2, 152.1, 152.6, 153.2, 160.4, 163.1.

ESI-MS of solution of **63.H**<sup>+</sup> in water,  $m/z = 505.9259$ . Calculated for  $\text{C}_{19}\text{H}_{18}\text{N}_3\text{O}_5\text{S}^{106}\text{Pd}$ , 506.0002.

Anal. Found: C, 43.69; H, 3.37; N, 7.72; Calculated for  $\text{C}_{19}\text{H}_{19}\text{N}_3\text{O}_6\text{PdS}$  (with one water molecule): C, 43.56; H, 3.66; N, 8.02

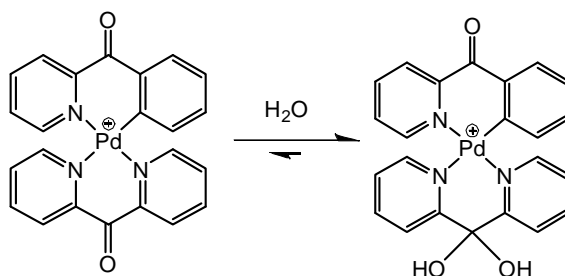
### 2.8.5 Preparation of dpk-ligated Palladacycles

#### 2-Aroylpyridine Derived Complexes **66** and **67**

In the preparation of the 2-arylpdpyridine (aroyl = benzoyl or 3-methyl benzoyl) derived dpk-based palladacycles **66** and **67**, the acetate bridged palladacycle (1.00 mmol) **49** or **50** and dpk ligand (1.05 mmoles) were combined in acetic acid. Upon stirring the reaction mixture at room temperature under ambient conditions for 30 minutes, the precipitate dissolved and produced a clear solution, which was stirred at room temperature for an additional 60 minutes. Concentration of the solution and trituration with diethyl ether afforded white crystals of the target compounds. The resulting reaction mixtures were filtered and the residues washed with a small amount of cold diethyl ether to afford the target compound **66** in 93 % yield and complex **67** in 92 % yield. The identity of the complexes was established using NMR spectroscopy and ESI-mass spectrometry, while the purity was confirmed by elemental analyses.

#### Complex **66**

Scheme S1. 1



<sup>1</sup>H NMR (D<sub>2</sub>O, 22°C), δ: 1.89 (s, 3H), 6.95 (d, *J*=7.6 Hz, 1H), 7.03 (td, *J*=6.6, 1.2 Hz, 1H), 7.16 (td, *J*=7.6, 1.5 Hz, 1H), 7.21 (td, *J*=6.6, 1.1 Hz, 1H), 7.26 (t, *J*=7.5 Hz, 1H), 7.37 (d, *J*=5.2, 1H), 7.52 (d, *J*=5.1, 1H), 7.57 (td, *J*=6.6, 1.3 Hz, 1H), 7.65 (dd, *J*=7.7, 1.2 Hz, 1H), 7.94 (td, *J*=7.8, 1.3 Hz, 1H), 7.99 (td, *J*=7.8, 1.3 Hz, 1H),

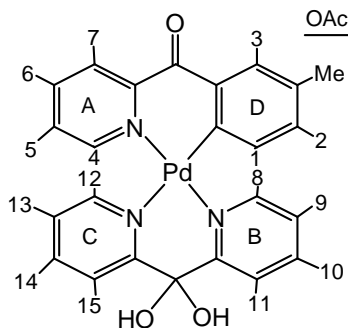
8.03 to 8.07 (m, 2H), 8.11 (d,  $J=7.6$ , 1H), 8.24 (td,  $J=7.8$ , 1.2 Hz, 1H), 8.34 (d,  $J=5.3$ , 1H).

$^{13}\text{C}$  NMR ( $\text{D}_2\text{O}$ ,  $22^\circ\text{C}$ ),  $\delta$ : 23.9, 95.6, 122.5, 122.6, 126.1, 126.5, 126.6, 126.7, 128.7, 129.6, 133.0, 134.5, 138.0, 141.2, 141.3, 141.8, 150.4, 151.6, 151.9, 153.6, 154.7, 158.1, 158.5, 182.0, 194.4.

ESI-MS spectrum of solution of  $66^+$  in  $\text{H}_2\text{O}$ , positive mode,  $m/z = 472.0203$ , 490.0432, Calculated for  $66$ ,  $\text{C}_{23}\text{H}_{16}\text{N}_3\text{O}_2^{106}\text{Pd}$ , 472.0286;  $\text{C}_{23}\text{H}_{18}\text{N}_3\text{O}_3^{106}\text{Pd}$  (the product of addition of  $1\text{H}_2\text{O}$  across a  $\text{C}=\text{O}$  bond), 490.0392.

Anal. Found (Calcd for a singly  $\text{C}=\text{O}$ -hydrated adduct with one molecule of acetic acid of crystallization)  $\text{C}_{27}\text{H}_{25}\text{N}_3\text{O}_7\text{Pd}$ : C, 53.14 (53.17); H, 3.90 (4.13); N, 6.84 (6.89).

### Complex 67



$^1\text{H}$  NMR ( $\text{D}_2\text{O}$ , 276 K),  $\delta$ : 1.97 (s, 3H, OAc-3H), 2.26 (s, 3H, Me-3H), 6.83 (d,  $J=7.7$  Hz, 1H, H-1), 7.01 (dd,  $J=7.8$ , 1.3 Hz, 1H, H-2), 7.03 (ddd,  $J=7.8$ , 5.8, 1.6 Hz, 1H, H-9), 7.23 (ddd,  $J=7.9$ , 5.3, 1.2 Hz, 1H, H-13), 7.37 (vs, 1H, H-3), 7.41 (d,  $J=5.5$  Hz, 1H, H-12), 7.59 (ddd,  $J=7.9$ , 5.7, 1.5 Hz, 1H, H-5), 7.61 (d,  $J=5.1$  Hz, 1H, H-12), 7.95 (td,  $J=7.9$ , 1.5 Hz, 1H, H-10), 8.00 (td,  $J=7.9$ , 1.5 Hz, 1H, H-14), 8.04 (d,  $J=7.9$  Hz, 1H, H-11), 8.06 (d,  $J=7.8$  Hz, 1H, H-15), 8.12 (d,  $J=7.9$  Hz, 1H, H-7), 8.27 (td,  $J=7.9$ , 1.5 Hz, 1H, H-6), 8.38 (d,  $J=5.5$  Hz, 1H, H-4).

$^{13}\text{C}$  NMR ( $\text{D}_2\text{O}$ ,  $22^\circ\text{C}$ ),  $\delta$ : 19.9, 22.8, 97.2, 122.1, 122.2, 125.6, 126.0, 126.2, 128.3, 129.2, 133.8, 136.2, 137.5, 140.6, 140.7, 141.4, 147.9, 150.1, 151.3, 153.2, 154.4, 157.6, 158.1, 180.8, 194.1.

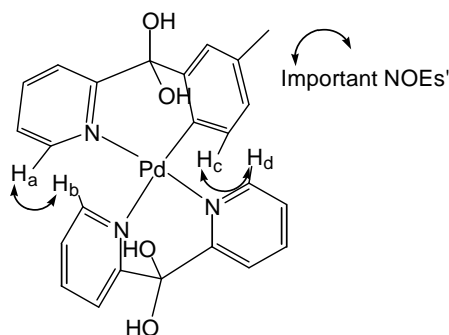
ESI-MS spectrum of solution of **67** $^+$  in  $\text{H}_2\text{O}$ , positive mode,  $m/z = 486.0527$ , 504.0575, Calculated for **67**,  $\text{C}_{24}\text{H}_{18}\text{N}_3\text{O}_2^{106}\text{Pd} = 486.0443$ ;  $\text{C}_{24}\text{H}_{20}\text{N}_3\text{O}_3^{106}\text{Pd}$  (a product of addition of  $1\text{H}_2\text{O}$  across a  $\text{C}=\text{O}$  bond) = 504.0589;

Anal. Found (Calcd for a singly  $\text{C}=\text{O}$ -hydrated adduct with one molecule of acetic acid of crystallization,  $\text{C}_{28}\text{H}_{27}\text{N}_3\text{O}_7\text{Pd}$ ): C, 53.89 (53.90); H, 4.42 (4.36); N, 6.56 (6.73).

Analysis of the  $^1\text{H}$  and  $^{13}\text{C}$  NMR data also allowed to assign this species as the hydrated species, similar to complex **66**.

The  $^1\text{H}$  NMR and elemental analysis data for this complex also indicate the presence of a residual acetic acid molecule. Attempts to remove the excess solvent under vacuum while heating the complex at  $40 - 50^\circ\text{C}$  resulted in decomposition to produce a deeper colored (green) complex which was only partially soluble in water.

*Selective 1D-difference NOE experiments ( $\text{D}_2\text{O}$ ) for **67***



The structure of **67** in solution was confirmed by Selective 1D-difference NOE experiments, while the peak assignment was accomplished via  $^1\text{H}$  and  $^{13}\text{C}$

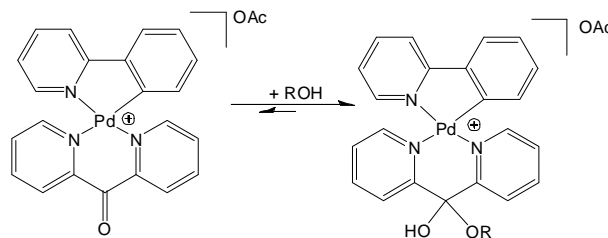
NMR,  $^1\text{H}$ - $^1\text{H}$  COSY,  $^1\text{H}$ - $^{13}\text{C}$  HMBC,  $^1\text{H}$ - $^{13}\text{C}$  HSQC, 1D Selective NOE and 1D Selective TOCSY experiments. In the selective NOE experiments, irradiation of a resonance at 8.10 ppm (*ortho*-H<sub>a</sub> of pyridyl fragment of the benzoylpyridine) showed enhancement (positive NOE) of a doublet at 7.36 ppm (*ortho*-H<sub>b</sub> of the dpk ligand, 2.16 %), and irradiation of a resonance at 6.49 ppm (*ortho*-H<sub>c</sub> of aryl fragment of the 2-(3-methyl)benzoylpyridine) showed enhancement (positive NOE) of a doublet at 7.14 ppm (*ortho*-H<sub>d</sub> of the dpk ligand, 1.80 %) (mixing time of 0.6s, delay time of 3s).

#### *2-Aroylpyridine Derived Complexes 66 and 67*

Complexes **68-70** were prepared in dichloromethane. The acetato-bridged palladacycle **51-53** (1.00 mmol) was combined with a dichloromethane solution of dpk ligand (1.05 mmol.) to form a clear solution. After stirring the solution at room temperature for 1 hour, the target compound was precipitated via concentration of the solution and trituration with either thf or hexanes. Filtration of the reaction mixtures afforded the target compounds **68-70** as white solids in good yields. Complex **71** was prepared by combining the acetate-bridged palladacyclic complex **54** (1.00 mmol.) and dpk ligand (1.05 mmol.) in acetic acid as solvent. The complex was isolated via removal of acetic acid solvent and addition of tetrahydrofuran to the residue to dissolve free dpk ligand. Filtration of the reaction mixture afforded the target compound as white solid in good yield. The identity of the complexes **68-71** was confirmed by NMR spectroscopy and ESI-Mass spectrometry, while the purity was confirmed by elemental analysis.

**Complex 68 (91.5 % yield)**

**Scheme S1. 2**



$^1\text{H}$  NMR ( $\text{D}_2\text{O}$ , 276 K),  $\delta$ : 1.89 (s, 3H), 6.75 (d,  $J=7.8$  Hz, 1H), 6.90 (bs, 1H), 7.14 (t,  $J=7.8$  Hz, 1H), 7.23-7.27 (m, 2H), 7.37 (bs, 1H), 7.56 (d,  $J=7.8$  Hz, 1H), 7.83 (d,  $J=7.8$  Hz, 1H), 7.93 (bs, 1H), 7.98 (d,  $J=5.6$  Hz, 1H), 8.01 (t,  $J=7.8$  Hz, 1H), 8.03-8.10 (m, 3H), 8.22 (bs, 1H), 8.28 (bs, 1H).

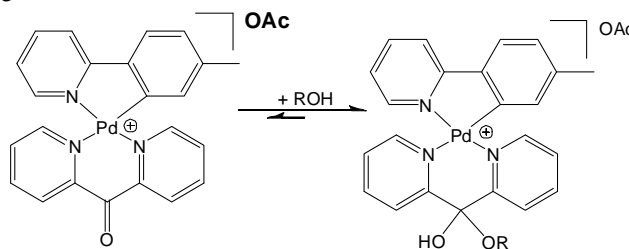
$^{13}\text{C}$  NMR ( $\text{MeOH-d}_4$ , 22°C),  $\delta$ : 24.2, 100.5, 121.1, 124.5, 125.0, 125.3, 126.9, 127.4, 127.6, 131.1, 135.1, 141.6, 141.8, 141.9, 147.6, 151.1, 152.8, 156.2, 156.4, 159.4, 159.8, 167.8, 180.3 (OAc)

ESI-MS of solution of  $\mathbf{68}^+$  in water, positive mode,  $m/z = 444.0264$  and 462.0403. Calculated for  $\mathbf{68}^+$ ,  $\text{C}_{22}\text{H}_{16}\text{N}_3\text{O}^{106}\text{Pd}$ : 444.0328;  $(\mathbf{68}+\text{H}_2\text{O})^+$   $\text{C}_{22}\text{H}_{18}\text{N}_3\text{O}_2^{106}\text{Pd}$ : 462.0434

Anal. Found (Calcd for a C=O-hydrated adduct,  $\text{C}_{24}\text{H}_{21}\text{N}_3\text{O}_4\text{Pd}$ ): C, 55.29 (55.24); H, 4.20 (4.06); N, 7.83 (8.05).

**Complex 69, (95.4 % yield)**

**Scheme S1. 3**



$^1\text{H}$  NMR (MeOH- $d_4$ , 22°C),  $\delta$ : 1.89 (s, 3H), 2.26 (s, 3H), 6.58 (s, Hz, 1H), 7.05 (d,  $J=7.8$  Hz, 1H), 7.30 (t,  $J=6.4$  Hz, 1H), 7.60 (d,  $J=7.8$  Hz, 1H), 7.67 (m, 2H), 8.00 (d,  $J=7.8$  Hz, 1H), 8.06 (t,  $J=7.8$  Hz, 1H), 8.14 to 8.19 (m, 5H), 8.86 (d,  $J=4.8$  Hz, 1H), 8.94 (d,  $J=4.8$  Hz, 1H).

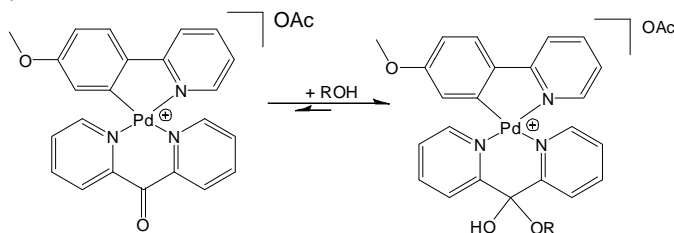
$^{13}\text{C}$  NMR (MeOH- $d_4$ , 22°C),  $\delta$ : 23.2, 25.5, 101.8, 122.0, 125.3, 125.8, 126.2, 126.4, 128.6, 128.9, 137.0, 142.7, 142.9, 143.0, 143.2, 146.0, 152.2, 154.0, 157.4, 157.6, 160.7, 161.2, 169.1, 181.4

ESI-MS of solution of  $69^+$  in methanol, positive mode,  $m/z = 458.0563$ , 490.0853. Calculated for  $\text{C}_{23}\text{H}_{18}\text{N}_3\text{O}^{106}\text{Pd}$ , 458.0494;  $\text{C}_{23}\text{H}_{20}\text{N}_3\text{O}_2^{106}\text{Pd}$  (meoh adduct), 490.0756.

Anal. Found (Calcd for  $\text{C}_{25}\text{H}_{23}\text{N}_3\text{O}_4\text{Pd}$  (hydrated complex): C, 56.04 (56.03); H, 4.27 (4.33); N, 7.70 (7.84).

**Compound 70 (85.5 % yield)**

**Scheme S1.4**



$^1\text{H}$  NMR ( $\text{D}_2\text{O}$ , 276 K),  $\delta$ : 1.66 (s, 3H), 3.42 (s, 3H), 5.89 (vs, 1H), 6.43 (t,  $J=5.9$  Hz, 1H), 6.50 (dd,  $J=8.5$ , 2.2 Hz, 1H), 6.89 (t,  $J=6.7$  Hz, 1H), 7.02 (t,  $J=6.1$  Hz, 1H), 7.17 (d,  $J=8.6$  Hz, 1H), 7.36 (d,  $J=8.1$  Hz, 1H), 7.62-7.67 (m, 3H), 7.77-7.83 (m, 3H), 7.88-7.92 (m, 2H).

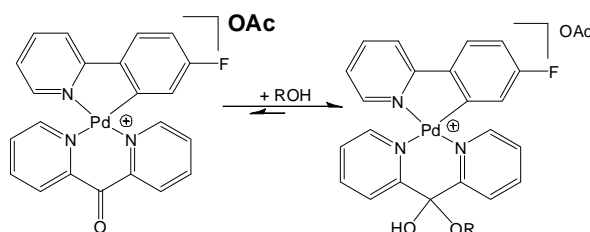
$^{13}\text{C}$  NMR (MeOH- $d_4$ , 22°C),  $\delta$ : 24.3, 55.9, 100.5 (Pyr<sub>2</sub>OH), 111.7, 120.4, 121.0, 123.3, 124.6, 125.0, 126.6, 127.4, 127.6, 140.1, 141.4, 141.8, 142.0, 150.7, 152.8, 156.2, 157.9, 159.4, 159.9, 161.6, 167.7, 180.3 (OAc)

ESI-MS of solution of **70** in water, positive mode,  $m/z$  = 474.0318 and 492.0423. Calculated for **70**<sup>+</sup>, C<sub>23</sub>H<sub>18</sub>N<sub>3</sub>O<sub>2</sub><sup>106</sup>Pd: 474.0434; (**70**+H<sub>2</sub>O)<sup>+</sup> C<sub>23</sub>H<sub>20</sub>N<sub>3</sub>O<sub>3</sub><sup>106</sup>Pd: 492.0539

Anal. Found (Calcd for a singly C=O-hydrated adduct with one extra H<sub>2</sub>O molecule, C<sub>25</sub>H<sub>23</sub>N<sub>3</sub>O<sub>5</sub>Pd): C, 52.53 (52.69); H, 3.90 (4.42); N, 7.44 (7.37).

**Complex 71 (75.6 % yield)**

Scheme S1. 5



$^1\text{H}$  NMR (D<sub>2</sub>O, 276 K),  $\delta$ : 1.66 (s, 3H), 6.22 (dd,  $J=9.2$ , 2.3 Hz, 1H), 6.70 (td,  $J=8.8$ , 2.4 Hz, 1H), 6.78 (t,  $J=6.2$  Hz, 1H), 6.96 (t,  $J=6.5$  Hz, 1H), 7.11 (t,  $J=6.2$  Hz, 1H), 7.33 (dd,  $J=8.6$ , 5.4 Hz, 1H), 7.51 (d,  $J=8.0$  Hz, 1H), 7.71-7.74 (m, 3H), 7.81-7.84 (m, 2H), 7.88 (d,  $J=7.9$  Hz, 1H), 8.07 (d,  $J=5.2$  Hz, 1H), 8.12 (d,  $J=5.2$  Hz, 1H).

$^{13}\text{C}$  NMR (MeOH- $d_4$ , 22°C),  $\delta$ : 24.2, 100.5 (Pyr<sub>2</sub>OH), 113.7 (d,  $J=24$  Hz), 121.2, 121.5 (d,  $J=20.3$  Hz), 124.5, 124.7, 125.1, 127.0 (d,  $J=8.4$  Hz), 127.5, 127.9, 141.9 (d,  $J=18.8$ ), 142.2, 143.9, 151.0, 152.9, 155.9, 158.6 (d,  $J=5.3$  Hz), 159.3, 159.8, 162.6, 164.6, 166.8, 180.0 (OAc).

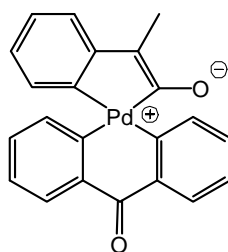
ESI-MS of solution of **71** in water, positive mode,  $m/z = 462.0111$  and  $480.0257$ . Calculated for **71**<sup>+</sup>,  $C_{22}H_{15}FN_3O^{106}Pd$ : 462.0234; (18 + H<sub>2</sub>O)  $C_{22}H_{17}FN_3O_2^{106}Pd$ : 480.0340

Anal. Found (Calcd for a hydrated complex with 1 molecule of acetic acid of crystallization,  $C_{26}H_{24}FN_3O_6Pd$ ): C, 51.80 (52.05); H, 4.46 (4.03); N, 7.16 (7.00).

### *Preparation of complexes 72 and 73*

In the preparation of complexes **72** and **73**, a methanolic solution of the dpk ligand (0.11 mmol) and acetato-bridged palladacycle (0.1 mmol, 1 eq) **55** or **56** were combined at ambient conditions. Upon stirring the reaction solution for ~ 10 minutes, white precipitate was observed to gradually develop. The reaction mixture was stirred for a total of 60 minutes. The resulting mixture was concentrated and triturated with diethyl ether. The white precipitate was filtered off and washed with a small amount of diethyl ether to afford the target compound **72** in 90 % and **73** in 78 %.

### *Complex 72, (90% yield)*



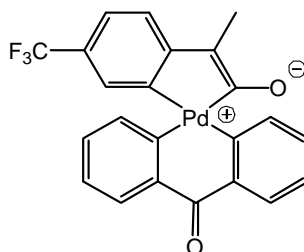
<sup>1</sup>H NMR (AcOH-d<sub>4</sub>, 22°C),  $\delta$ : 2.31 (s, 3H), 6.44 (d,  $J=7.1$ , 1H), 6.96 (t,  $J=7.3$  Hz, 1H), 7.11 (t,  $J=7.9$  Hz, 1H), 7.23 (d,  $J=7.0$  Hz, 1H), 7.82 (t,  $J=5.6$  Hz, 2H), 6.14 (d, 2H), 8.25 (t,  $J=7.3$ , 2H), 8.95 (d,  $J=4.4$ , 2H)

<sup>13</sup>C NMR (AcOH-d<sub>4</sub>, 22°C),  $\delta$ : 10.7, 48.7, 125.2, 126.0, 128.4, 128.7, 132.6, 140.2, 143.2, 152.2, 153.4, 188.0.

ESI-MS of solution of **(72)<sup>+</sup>** in H<sub>2</sub>O, m/z = 424.0182 and 442.0356.  
Calculated for C<sub>19</sub>H<sub>16</sub>N<sub>3</sub>O<sub>2</sub><sup>106</sup>Pd, 424.0277; (hydrated ligand ketone)  
C<sub>19</sub>H<sub>18</sub>N<sub>3</sub>O<sub>3</sub><sup>106</sup>Pd, 442.0380.

Anal. Found: C, 52.24; H, 4.12; N, 8.64; Calcd. for C<sub>21</sub>H<sub>19</sub>N<sub>3</sub>O<sub>4</sub>Pd: C, 52.13;  
H, 3.96; N, 8.69.

**Complex 73, (78% yield)**



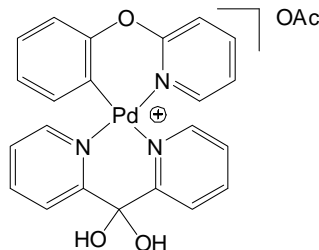
<sup>1</sup>H NMR (MeOH-d<sub>4</sub>, 22°C), δ: 2.29 (s, 3H), 6.93 (s, Hz, 1H), 7.28 (d, *J*=7.9 Hz, 1H), 7.35 (dd, *J*=7.8, 0.8 Hz, 1H), 7.55 (m, 1H), 7.62 (m, 1H), 8.04 (m, 2H), 8.14 (m, 2H), 8.93 (d, *J*=5.3 Hz, 1H), 9.34 (d, *J*=5.2 Hz, 1H).

<sup>13</sup>C NMR (MeOH-d<sub>4</sub>, 22°C), δ: 9.8, 20.0, 98.5, 121.3, 121.8, 123.1, 124.2, 125.7, 127.7, 139.1, 140.1, 150.7, 152.5, 153.8, 156.9, 157.3, 158.6, 163.4, 174.8.

ESI-MS of solution of **(73)<sup>+</sup>** in H<sub>2</sub>O, m/z = 492.0031 and 510.0261.  
Calculated for C<sub>20</sub>H<sub>15</sub>N<sub>3</sub>F<sub>3</sub>O<sub>2</sub><sup>106</sup>Pd, 492.0151; (hydrated ligand ketone)  
C<sub>20</sub>H<sub>17</sub>F<sub>3</sub>N<sub>3</sub>O<sub>3</sub><sup>106</sup>Pd, 510.0257

Anal. Found: C, 47.83; H, 3.22; N, 7.72; Calculated for C<sub>22</sub>H<sub>18</sub>F<sub>3</sub>N<sub>3</sub>O<sub>4</sub>Pd: C, 47.89; H, 3.29; N, 7.61.

**Complex 74, (93 % yield)**



Complex **74** was prepared by a procedure similar to that of complexes **66** and **67**. The acetato-bridged palladacycle (1.00 mmol) **57** and the dpk ligand (1.05 mmoles) were combined in acetic acid. Upon stirring the reaction mixture for ~ 20 minutes at ambient conditions, the precipitate dissolved to produce a clear, colorless solution. The solution was stirred at room temperature under ambient conditions for a total of 90 minutes. Concentration of the solution and trituration with diethyl ether afforded white crystals of the target compound. The resulting mixture was filtered and the residue was washed with a small amount of cold diethyl ether. The target compound **74** was produced in 93 % yield as a white solid. The identity of the complex was established using NMR spectroscopy, X-ray diffraction and ESI-mass spectrometry, while the purity was confirmed by elemental analysis.

$^1\text{H}$  NMR ( $\text{D}_2\text{O}$ ,  $22^\circ\text{C}$ ),  $\delta$ : 1.89(s, 3H), 6.67 (dd,  $J=7.6$ , 1.0 Hz, 1H), 6.81 (t,  $J=6.2$  Hz, 1H), 6.91 (td,  $J=7.1$ , 0.7 Hz, 1H), 7.14 (td,  $J=7.6$ , 0.6 Hz, 1H), 7.11 to 7.14 (m, 2H). 7.19 (td,  $J=7.5$ , 1.0 Hz, 1H), 7.44 (d,  $J=7.2$  Hz, 1H), 7.52 (d,  $J=5.1$ Hz, 1H), 7.67 (d,  $J=5.0$  Hz 1H); 7.85 to 7.91 (m, 2H), 7.96 to 8.02 (m, 2H), 8.05 to 8.09 (m, 2H).

$^{13}\text{C}^{95}$  NMR (MeOH- $\text{d}_4$ ,  $22^\circ\text{C}$ ),  $\delta$ : 23.6, 117.0, 117.3, 117.4, 120.6, 122.1, 124.0, 125.0, 126.5, 127.1, 127.3, 127.6, 130.6, 141.6, 141.7, 144.1, 151.1, 151.9, 153.1, 156.6, 158.9, 159.0, 161.8, 179.3.

ESI-MS of solution of **74**<sup>+</sup> in acetic acid, m/z observed: 460.0203. Calculated for C<sub>22</sub>H<sub>16</sub>N<sub>3</sub>O<sub>2</sub><sup>106</sup>Pd, 460.0277.

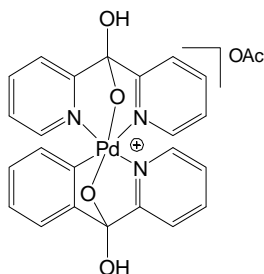
Anal. Found: C, 52.53; H, 3.55; N, 6.94: Calculated for C<sub>26</sub>H<sub>25</sub>N<sub>3</sub>O<sub>7</sub>Pd (solvated complex with one acetic acid molecule): C, 52.23; H, 4.21; N, 7.03.

### 2.8.6 Preparation of Monohydrocarbyl Pd(IV) Complexes

#### *Synthesis of MonohydrocarbylPd(IV) Complexes 75 and 76*

The complexes bearing acetate counterion were prepared by combining an aqueous solution of the Pd(II) precursor with 10.0 equivalents of H<sub>2</sub>O<sub>2</sub>, and the resulting solutions were stirred at room temperature for 3 hours. Removal of water under vacuum produced the target complex as dark orange solid.

#### **Complex 75(OAc)**



<sup>1</sup>H NMR (D<sub>2</sub>O, 22°C), δ: 1.91 (s, 3H), 7.11 (t, *J*=7.2 Hz, 1H), 7.20 (d, *J*=7.9 Hz, 1H), 7.31 (t, *J*=7.3 Hz, 1H), 7.41 (t, *J*=6.4 Hz, 1H), 7.44 to 7.49 (m, 2H), 7.55 (t, *J*=6.2, 1H), 7.92 (d, *J*=7.7, 1H), 7.99 (d, *J*=7.7 Hz, 1H), 8.12 (d, *J*=7.7 Hz, 1H), 8.16 to 8.23 (m, 3H), 8.27 (d, *J*=5.6 Hz, 1H), 8.30 (d, *J*=5.6 Hz, 1H), 8.56 (d, *J*=5.1, 1H).

<sup>1</sup>H NMR (AcOH-d<sub>4</sub>, 22°C), δ: 2.06 (s, 3H), 7.08 (td, *J*=7.8, 1.5 Hz, 1H), 7.21 (d, *J*=8.0 Hz, 1H), 7.28 (t, *J*=7.3 Hz, 1H), 7.47 to 7.49 (m, 2H), 7.55 (td, *J*=6.7, 1.2 Hz, 1H), 7.60 (td, *J*=5.8, 2.2 Hz, 1H), 8.01 (d, *J*=7.3 Hz, 1H), 8.09 (d, *J*=7.4 Hz, 1H),

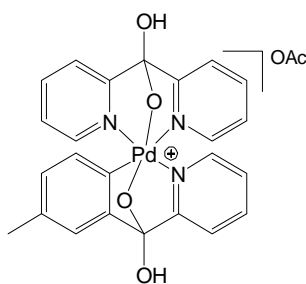
8.20 to 8.25 (m, 3H), 8.27 (td,  $J=7.7, 0.9$  Hz, 1H), 8.32 (d,  $J=5.5$  Hz, 1H), 8.39 (d,  $J=5.5$  Hz, 1H), 8.61 (d,  $J=5.1$  Hz, 1H).

$^{13}\text{C}$  NMR ( $\text{D}_2\text{O}$ ,  $22^\circ\text{C}$ ),  $\delta$ : 23.2, 104.8, 122.7, 122.8, 124.1, 125.5, 127.1, 127.2, 128.1, 129.1, 130.5, 131.2, 142.9, 144.3, 144.5, 147.7, 149.2, 149.9, 150.4, 157.6, 159.3, 162.3, 165.1, 180.6.

ESI-MS of solution of  $75^+$  in methanol or acetic acid, positive mode,  $m/z = 506.0323$ . Calculated for  $75^+$ ,  $\text{C}_{23}\text{H}_{18}\text{N}_3\text{O}_4^{106}\text{Pd}$ : 506.0350.

Complex **75** was isolated from the aqueous solution by removal of the solvent under vacuum to afford a brown solid. However if the solid is left under vacuum for a long time, decomposition takes place as indicated by appearance of new peaks in  $^1\text{H}$  NMR spectrum in various solvents such as deuterated acetic acid or methanol. Complex **75** is unstable in the solid state. When left at room temperature for several hours, new peaks are observed in the  $^1\text{H}$  NMR spectrum of the product taken in deuterated methanol or acetic acid, indicating decomposition.

### **Complex 76(OAc)**



$^1\text{H}$  NMR ( $\text{D}_2\text{O}$ , 295 K),  $\delta$ : 1.95 (s, 3H), 2.34 (s, 3H), 6.95 (,  $J=7.8$  Hz, 1H), 7.07 (d,  $J=7.8$  Hz, 1H), 7.30 (s, 1H), 7.41 (t,  $J=6.4$  Hz, 1H), 7.49 (ddd,  $J=7.9, 5.4, 1.0$  Hz, 1H), 7.55 (ddd,  $J=7.8, 5.5, 1.0$  Hz, 1H), 7.90 (d,  $J=7.8$  Hz, 1H), 7.99 (d,

$J=7.8$  Hz, 1H), 8.12 ( $\delta$ ,  $J=7.8$  Hz, 1H), 8.17-8.23 (m, 3H), 8.27 (d,  $J=5.5$  Hz, 1H), 8.29 (d,  $J=5.5$  Hz, 1H), 8.57 (d,  $J=5.2$  Hz, 1H).

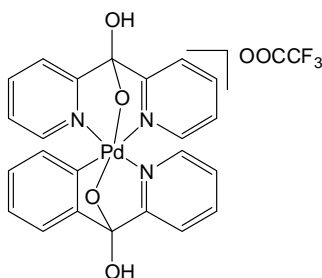
$^{13}\text{C}$  NMR ( $\text{D}_2\text{O}$ ,  $22^\circ\text{C}$ ),  $\delta$ : 20.0, 22.6, 103.8, 121.7, 123.1, 124.9, 126.1, 126.2, 127.1, 129.1, 130.5, 138.8, 142.0, 143.4, 143.5, 148.2, 148.9, 149.4, 158.3, 161.4, 180.2

ESI-MS of solution of  $76^+$  in methanol or acetic acid, positive mode,  $m/z = 520.0472$ . Calculated for  $76$ ,  $\text{C}_{24}\text{H}_{20}\text{N}_3\text{O}_4^{106}\text{Pd}$ : 520.0498.

#### *Preparation of Complexes 75X and 76X (X=OOCF<sub>3</sub> or BF<sub>4</sub>)*

Complexes bearing trifluoroacetate or tetrafluoroborate counterions were prepared by adding an excess amount of either trifluoroacetic acid or tetrafluoroboric acid to aqueous reaction solutions of the complexes bearing an acetate counterion. This lead to formation of either deep yellow or dark orange precipitate. These reaction mixtures were concentrated further, and the precipitate was filtered off and washed with a small amount of cold water.

#### **Complex 75(OOCF<sub>3</sub>)**



$^1\text{H}$  NMR ( $\text{DMSO-d}_6$ ,  $22^\circ\text{C}$ ),  $\delta$ : 7.05 to 7.07 (m, 2H), 7.22 (td,  $J=7.1$ , 1.3 Hz, 1H), 7.33 (dd,  $J=7.4$ , 1.5 Hz, 1H), 7.49 (td,  $J=6.7$ , 1.4 Hz, 1H), 7.59 to 7.62 (m, 2H),

7.88 (d,  $J=7.3$  Hz, 1H), 7.95 (d,  $J=7.1$  Hz, 1H), 8.07 (d,  $J=5.2$  Hz, 1H), 8.17 (d,  $J=5.2$  Hz, 1H), 8.23 to 8.31 (m, 4H), 8.43 (d,  $J=5.0$  Hz, 1H), 8.83 (brs, 1H), 9.13 (brs, 1H)

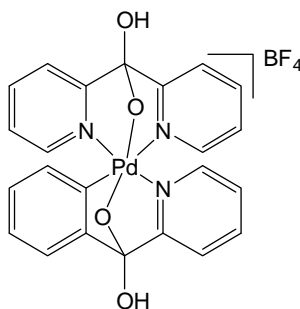
$^{13}\text{C}$  NMR (DMSO- $d_6$ , 22°C),  $\delta$ : 103.8, 105.2, 116.4, 118.4, 121.6, 121.7, 123.0, 124.1, 125.9, 126.1, 127.0, 127.2, 129.1, 129.3, 141.8, 143.1, 143.3, 147.7, 148.6, 148.9, 149.3, 156.1, 157.5, 157.7, 160.4, 163.5, 166.7

ESI-MS of solution of **75(OOCCF<sub>3</sub>)** in dimethyl sulfoxide or methanol, positive mode,  $m/z = 506.0326$ . Calculated for **75<sup>+</sup>**, C<sub>23</sub>H<sub>18</sub>N<sub>3</sub>O<sub>4</sub><sup>106</sup>Pd: 506.0350.

Anal. Found (Calcd for a complex with 3.5 molecules of water of hydration, C<sub>25</sub>H<sub>25</sub>F<sub>3</sub>N<sub>3</sub>O<sub>9.5</sub>Pd): C, 44.02 (43.97); H, 3.59 (3.69); N, 5.96 (6.15).

Attempts at removing water of hydration at higher temperatures under vacuum led to decomposition.

#### **Complex 75(BF<sub>4</sub>)**



$^1\text{H}$  NMR (DMSO- $d_6$ , 22°C),  $\delta$ : 7.03 to 7.10 (m, 2H), 7.23 (td,  $J=7.1, 1.6$  Hz, 1H), 7.35 (dd,  $J=7.5, 1.5$  Hz, 1H), 7.49 (td,  $J=7.7, 1.4$  Hz, 1H), 7.58 to 7.62 (m, 2H), 7.88 (d,  $J=7.4$  Hz, 1H), 7.95 (d,  $J=7.7$  Hz, 1H), 8.07 (d,  $J=7.8$  Hz, 1H), 8.17 (d,  $J=5.3$  Hz, 1H), 8.23 to 8.30 (m, 4H), 8.44 (d,  $J=5.0$  Hz, 1H), 8.66 (brs, 1H), 8.95 (brs, 1H).

$^{13}\text{C}$  NMR (DMSO- $d_6$ , 22°C),  $\delta$ : 103.8, 105.2, 121.6, 123.0, 124.2, 126.0, 126.1, 127.0, 127.2, 129.1, 129.2, 141.8, 143.0, 143.3, 147.8, 148.6, 148.9, 149.3, 156.1, 160.4, 163.5, 166.6.

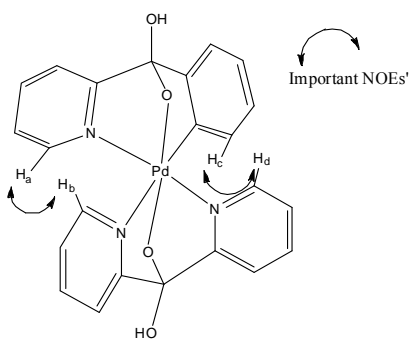
ESI-MS of solution of **75**(BF<sub>4</sub>) in dimethyl sulfoxide or methanol, positive mode, m/z = 506.0321. Calculated for **75**<sup>+</sup>, C<sub>23</sub>H<sub>18</sub>N<sub>3</sub>O<sub>4</sub><sup>106</sup>Pd: 506.0350.

Anal. Found (Calcd for a complex with 1 molecule of water of hydration, C<sub>23</sub>H<sub>20</sub>BF<sub>4</sub>N<sub>3</sub>O<sub>5</sub>Pd): C, 45.47 (45.16); H, 3.06 (3.30); N, 6.81 (6.87).

An <sup>1</sup>H NMR signal produced by the water of hydration was observed in the spectrum recorded in dms<sup>o</sup>-d<sub>6</sub>.

Attempts at removing water of hydration at higher temperature under vacuum led to decomposition.

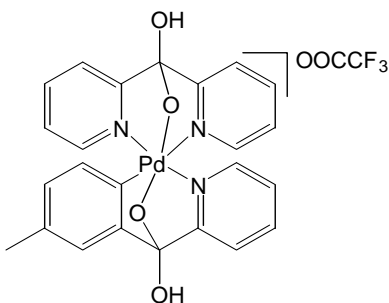
*Selective 1D-difference NOE experiments (AcOH-d<sub>4</sub>) for 75*



The structure of complex **75** in solution was confirmed by <sup>1</sup>H and <sup>13</sup>C NMR, and 1D NOE experiments. In the 1D difference NOE experiment, NOE was observed between the *ortho*-H<sub>a</sub> of pyridyl fragment of the benzoylpyridine ligand and that of the *ortho*-H<sub>b</sub> of pyridyl fragment of the dpk ligand and also the *ortho*-H<sub>c</sub> of the aryl fragment of benzoylpyridine ligand and the *ortho*-H<sub>b</sub> of the pyridyl fragment of dpk ligand. Irradiation of a resonance at 8.63 ppm (*ortho*-H<sub>a</sub> of pyridyl fragment of the benzoylpyridine) showed enhancement (positive NOE) of a doublet at 8.41 ppm (*ortho*-H<sub>b</sub> of the dpk ligand, 1.0 %), and irradiation of a resonance at 8.35 ppm (*ortho*-H<sub>c</sub> of aryl fragment of the benzoylpyridine) showed enhancement (positive

NOE) of a doublet at 7.23 ppm (*ortho*-H<sub>d</sub> of the dpk ligand, 0.9 %) (mixing time of 0.8s, delay time 5s).

**Complex 76(OOCCF<sub>3</sub>)**



<sup>1</sup>H NMR (DMSO-d<sub>6</sub>, 22°C), δ: 2.29 (s, 3H), 6.87 (dd, *J*=8.3, 1.7 Hz, 1H), 6.95 (d, *J*=8.0 Hz, 1H), 7.16 (s, 1H), 7.49 (ddd, *J*=7.9, 5.5, 1.4 Hz, 1H), 7.58-7.61 (m, 2H), 7.86 (d, *J*=7.6 Hz, 1H), 7.94 (d, *J*=7.8 Hz, 1H), 8.06 (d, *J*=7.7 Hz, 1H), 8.17 (d, *J*=5.5 Hz, 1H), 8.22-8.26 (m, 3H), 8.28 (td, *J*=7.7, 1.2 Hz, 1H), 8.43 (d, *J*=5.2 Hz, 1H), 8.78 (brs, 1H), 9.11 (brs, 1H).

<sup>13</sup>C NMR (DMSO-d<sub>6</sub>, 22°C), δ: 28.3, 103.7, 105.1, 121.6, 122.9, 124.6, 125.8, 125.9, 126.9, 128.8, 129.3, 136.6, 141.7, 142.9, 143.2, 147.7, 148.5, 148.9, 149.0, 153.2, 160.4, 163.6, 166.7.

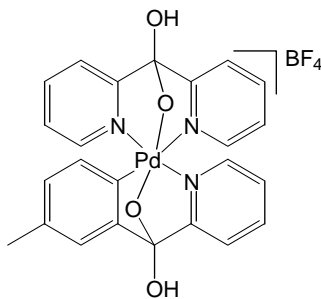
ESI-MS of solution of **76(OOCCF<sub>3</sub>)** in methanol, acetic acid or dms, positive mode, *m/z* = 520.0472. Calculated for **76**<sup>+</sup>, C<sub>24</sub>H<sub>20</sub>N<sub>3</sub>O<sub>4</sub><sup>106</sup>Pd: 520.0498.

Anal. Found (Calcd for a complex with 0.5 molecule of water of hydration, C<sub>26</sub>H<sub>22</sub>F<sub>3</sub>N<sub>3</sub>O<sub>6.5</sub>Pd): C, 48.34 (48.50); H, 3.08 (3.44); N, 6.50 (6.53).

An <sup>1</sup>H NMR signal produced by the water of hydration was observed in the spectrum recorded in dms-d<sub>6</sub>.

Attempts at removing water of hydration at higher temperature under vacuum led to decomposition.

**Complex 76(BF<sub>4</sub>)**



<sup>1</sup>H NMR (DMSO-d<sub>6</sub>, 22°C), δ: 2.28 (s, 3H), 6.87 (dd, *J*=8.2, 0.6 Hz, 1H), 6.95 (d, *J*=8.1 Hz, 1H), 7.15 (d, *J*=2.0 Hz 1H), 7.49 (dd, *J*=6.6, 1.6 Hz, 1H), 7.58-7.62 (m, 2H), 7.86 (dq, *J*=7.9, 0.6 Hz, 1H), 7.94 (dq, *J*=7.9, 0.9 Hz, 1H), 8.06 (dt, *J*=7.7, 1.0 Hz, 1H), 8.17 (dq, *J*=5.8, 0.6 Hz, 1H), 8.22-8.31 (m, 4H), 8.43 (dt, *J*=5.2, 0.5 Hz, 1H), 8.76 (s, 1H), 9.07 (s, 1H).

<sup>13</sup>C NMR (DMSO-d<sub>6</sub>, 22°C), δ: 20.4, 103.7, 105.1, 121.6, 122.9, 124.6, 125.9, 126.0, 127.0, 128.8, 129.4, 136.6, 141.8, 143.0, 143.3, 147.7, 148.5, 149.0, 153.2, 160.4, 163.5, 166.7,

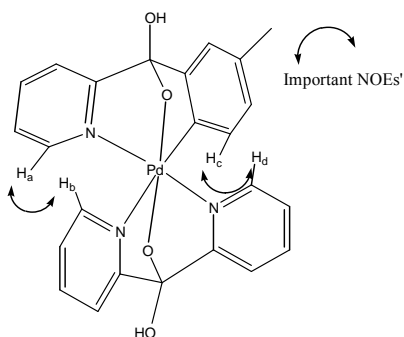
ESI-MS of solution of **76(BF<sub>4</sub>)** in methanol, acetic acid or dmsol, positive mode, *m/z* = 520.0472. Calculated for **76**<sup>+</sup>, C<sub>24</sub>H<sub>20</sub>N<sub>3</sub>O<sub>4</sub><sup>106</sup>Pd: 520.0498.

Anal. Found (Calcd for a complex with 2.0 molecule of H<sub>2</sub>O, C<sub>24</sub>H<sub>24</sub>BF<sub>4</sub>N<sub>3</sub>O<sub>6</sub>Pd): C, 44.53 (44.78); H, 3.69 (3.76); N, 6.47 (6.53).

An <sup>1</sup>H NMR signal produced by the water of hydration was observed in the spectrum recorded in dmsol-d<sub>6</sub>.

Attempts at removing water of hydration at higher temperature under vacuum led to decomposition.

### Selective 1D-difference NOE experiments (MeOD) for **76**

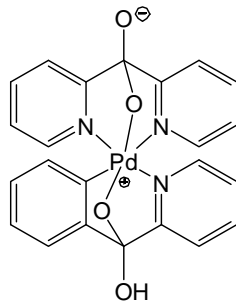


The structure of **76** in solution was confirmed by  $^1\text{H}$  and  $^{13}\text{C}$  NMR,  $^1\text{H}$ - $^1\text{H}$  COSY,  $^1\text{H}$ - $^{13}\text{C}$  HMBC,  $^1\text{H}$ - $^{13}\text{C}$  HSQC, 1D Selective NOE and 1D Selective TOCSY experiments. In the 1D difference NOE experiment, NOE was observed between the *ortho*- $H_a$  of pyridyl fragment of the benzoylpyridine ligand and that of the *ortho*- $H_b$  of pyridyl fragment of the dpk ligand and between the *ortho*- $H_c$  of the aryl fragment of benzoylpyridine ligand and the *ortho*- $H_d$  of the pyridyl fragment of dpk ligand. Irradiation of a resonance at 8.58 ppm (*ortho*- $H_a$  of pyridyl fragment of the benzoylpyridine) showed enhancement (positive NOE) of a doublet at 8.31 ppm (*ortho*- $H_b$  of the dpk ligand, 2.16 %), and irradiation of a resonance at 7.06 ppm (*ortho*- $H_c$  of aryl fragment of the 2-(3-methyl)benzoylpyridine) showed enhancement (positive NOE) of a doublet at 8.31 ppm (*ortho*- $H_d$  of the dpk ligand, 0.72 %) (mixing time of 0.6s, delay time 3s).

### Preparation of Zwitterionic complexes **79** and **80**

These complexes were produced by addition of 1.0 equivalent of NaOH to aqueous solutions of complexes **75** (OOCF<sub>3</sub>) and **76** (OOCF<sub>3</sub>) under ambient conditions.

### Complex 79



$^1\text{H}$  NMR (MeOD<sub>4</sub>, 22°C),  $\delta$ : 6.99 (td,  $J=7.6$ , 1.4 Hz, 1H), 7.20 (t,  $J=7.4$  Hz, 1H), 7.23 (d,  $J=7.9$  Hz, 1H), 7.37 (td,  $J=6.5$ , 1.4 Hz, 1H), 7.39 – 7.43 (m, 2H), 7.47 (td,  $J=6.3$ , 1.5 Hz, 1H), 7.92 (d,  $J=7.7$  Hz, 1H), 7.98 (d,  $J=7.8$  Hz, 1H), 8.12 – 8.17 (m, 4H), 8.26 (d,  $J=5.6$  Hz, 1H), 8.35 (d,  $J=5.6$  Hz, 1H), 8.52 (d,  $J=5.3$  Hz, 1H).

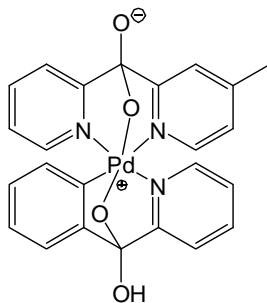
$^{13}\text{C}$  NMR (trifluoroethanol d<sub>1</sub>, 22°C),  $\delta$ : 107.6, 122.7, 123.1, 124.3, 124.5, 124.9, 125.5, 126.3, 126.8, 127.2, 128.2, 129.1, 130.5, 130.9.

Anal. Found (Calcd for a complex with 3.5 molecules of H<sub>2</sub>O, C<sub>23</sub>H<sub>24</sub>N<sub>3</sub>O<sub>7.5</sub>Pd): C, 48.76 (48.56); H, 4.08 (4.25); N, 7.39 (7.39).

ESI-MS of solution of **79** in methanol, positive mode,  $m/z = 506.0323$ .

Calculated for **75**<sup>+</sup>, C<sub>23</sub>H<sub>18</sub>N<sub>3</sub>O<sub>4</sub><sup>106</sup>Pd: 506.0350.

### Complex 80



$^1\text{H}$  NMR (MeOD<sub>4</sub>, 22°C),  $\delta$ : 2.33 (s, 3H), 6.81 (ddd,  $J=8.1$ , 2.5, 0.6 Hz, 1H), 7.08 (d,  $J=8.1$  Hz, 1H), 7.24 (vs, 1H), 7.35 (dd,  $J=6.6$ , 1.3 Hz, 1H), 7.35 (dd,  $J=6.6$ ,

1.3 Hz, 1H), 7.46 (dd,  $J=6.4, 1.4$  Hz, 1H), 7.90 (dq,  $J=7.9, 0.6$  Hz, 1H), 7.99 (dq,  $J=7.8, 0.9$  Hz, 1H), 8.11 – 8.17 (m, 4H), 8.26 (d,  $J=5.6$  Hz, 1H), 8.33 (d,  $J=5.6$  Hz, 1H), 8.52 (dt,  $J=5.1, 1.1$  Hz, 1H).

$^{13}\text{C}$  NMR (MeOD<sub>4</sub>, 2°C),  $\delta$ : 21.1, 108.1, 109.4, 123.0, 123.4, 124.5, 126.1, 126.2, 126.4, 127.0, 130.4, 130.6, 138.5, 142.4, 143.6, 143.8, 148.8, 150.0, 150.3, 155.2, 165.4, 168.3, 169.5.

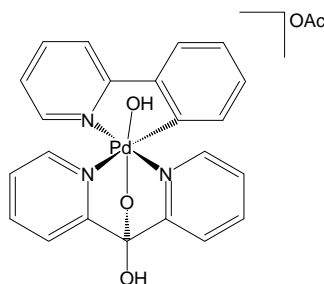
Anal. Found (Calcd for a complex with 9.5 molecules of H<sub>2</sub>O, C<sub>24</sub>H<sub>38</sub>N<sub>3</sub>O<sub>13.5</sub>Pd): C, 41.63 (41.72); H, 5.75 (5.54); N, 5.99 (6.08).

ESI-MS of solution of **80** in acidified methanol or acetic acid, positive mode,  $m/z = 520.0472$ . Calculated for **80**<sup>+</sup>, C<sub>24</sub>H<sub>20</sub>N<sub>3</sub>O<sub>4</sub><sup>106</sup>Pd: 520.0498.

#### *Preparation of complexes 83-87 in water*

These complexes were prepared by dissolution of the Pd(II) precursors in water in ice-water bath at 0°C, and addition of ~ 10.0 equivalents of H<sub>2</sub>O<sub>2</sub> into these aqueous solutions at 0°C. It was not possible to isolate these complexes due to their low stability, and thus they were characterized using NMR spectroscopy and electrospray ionization mass spectrometry.

#### **Complex 83**



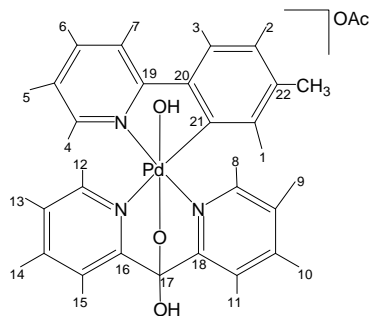
$^1\text{H}$  NMR ( $\text{D}_2\text{O}$ , 276 K),  $\delta$ : 1.72 (s, 3H), 6.70 (d,  $J= 8.6$  Hz, 1H), 8.18 (td,  $J= 8.0, 1.5$  Hz, 1H), 7.29-7.37 (m, 2H), 7.62-7.71 (m, 2H), 7.77 (d,  $J= 7.3$  Hz, 1H), 7.86 (dd,  $J= 7.8, 1.5$  Hz, 1H), 7.91 (d,  $J= 7.8$  Hz, 1H), 8.07-8.17 (m, 5H), 8.63 (d,  $J= 5.6$  Hz, 1H), 8.91 (d,  $J= 5.1$  Hz, 1H).

$^{13}\text{C}$  NMR ( $\text{D}_2\text{O}$ , 276 K),  $\delta$ : 23.6, 104.3, 122.4, 123.0, 123.4, 126.4, 127.3, 128.4, 128.9, 129.4, 130.4, .

ESI-MS of solution of  $\mathbf{83}^+$  in water, positive mode,  $m/z = 478.0546$ .  
Calculated for  $\mathbf{83}^+$ ,  $\text{C}_{22}\text{H}_{18}\text{N}_3\text{O}_3^{106}\text{Pd}$ : 478.0383

This complex is too unstable and thus elemental analysis could not be performed.

#### **Complex 84**



$^1\text{H}$  NMR ( $\text{D}_2\text{O}$ , 5°C),  $\delta$ : 1.69 (s, 3H, Ar- $\text{CH}_3$ ), 2.12 (s, 3H, OAc- $\text{CH}_3$ ), 6.43 (s, 1H, H-1), 7.15 (d,  $J= 7.7$  Hz, 1H, H-2), 7.24 (td,  $J= 5.9, 3.1$  Hz, 1H, H-6), 7.62 (ddd,  $J= 7.9, 5.3, 1.0$  Hz, 1H, H-13), 7.66 (td,  $J= 6.7, 1.4$  Hz, 1H, H-9), 7.68 (d,  $J= 7.8$  Hz, 1H, H-3), 7.74 (d,  $J= 7.9$ , 1H, H-11), 7.87 (d,  $J= 7.9$ , 1H, H-15), 8.00 – 8.02 (m, 2H, H-5 and -7), 8.06 (td,  $J= 7.8, 1.2$  Hz, 1H, H-14), 8.07 (d,  $J= 6.0$ , 1H, H-4), 8.12 (td,  $J= 7.8, 1.0$  Hz, 1H, H-10), 8.61 (d,  $J= 5.7$ , 1H, H-8), 8.87 (d,  $J= 5.1$ , 1H, H-12).

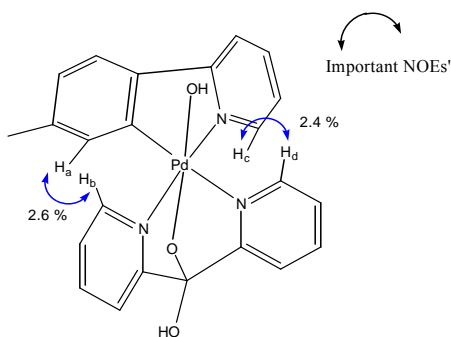
$^{13}\text{C}$  NMR ( $\text{D}_2\text{O}$ , 5°C),  $\delta$ : 21.4 (C- $\text{CH}_3$ ), 23.1 (Oac- $\text{CH}_3$ ), 104.0 (C-17), 122.0 (C-15), 122.7 (C-11), 125.6 (C-5), 127.0 (C-13), 127.6 (C-3), 128.6 (C-9), 129.8 (C-

2), 130.1 (C-1), 138.7 (C-20), 142.4 (C-14), 143.0 (C-6), 143.9 (C-10), 145.7 (C-22), 146.9 (C-8), 147.6 (C-12), 148.7 (C-4), 158.4 (C-16), 160.0 (C-21), 161.2 (C-18), 162.1 (C-19), 181.3 (Oac-C)

ESI-MS of solution of **84**<sup>+</sup> in water, m/z observed: 492.0684. Calculated for C<sub>22</sub>H<sub>18</sub>N<sub>3</sub>O<sub>4</sub><sup>106</sup>Pd, m/z = 492.0548.

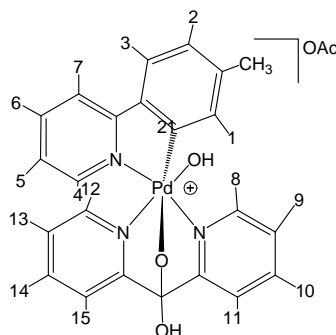
This complex is too unstable and thus elemental analysis could not be performed.

*Selective 1D-difference NOE experiments (D<sub>2</sub>O) for 84*



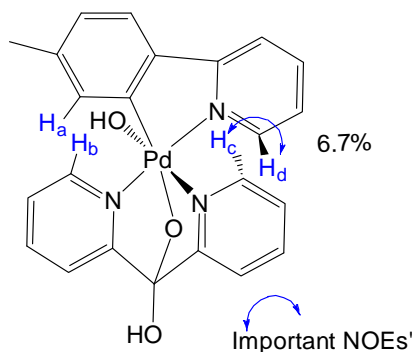
In the 1D difference NOE experiment, NOE was observed between the *ortho*-H<sub>a</sub> of the tolylpyridine ligand and that of the *ortho*-H<sub>b</sub> of the dpk ligand and between the *ortho*-H<sub>c</sub> of the tolylpyridine and *ortho*-H<sub>d</sub> of the dpk ligand. Irradiation of a resonance at 8.87 ppm (*ortho*-H<sub>d</sub> of the dpk ligand) showed enhancement (positive NOE) of the doublet at 8.07 ppm (*ortho*-H<sub>c</sub> on the pyridyl fragment of the tolylpyridine ligand, 2.4 %) (mixing time of 0.8s, delay time 5s) and irradiation of a resonance at 8.61 ppm (*ortho*-H<sub>b</sub> of the dpk ligand) showed enhancement (positive NOE) of the singlet at 6.43 ppm (*ortho*-H<sub>a</sub> on the phenyl fragment of tolylpyridine ligand, 2.6%) (mixing time of 0.8s, delay time 5s).

### Minor Complex 88



$^1\text{H}$  NMR ( $\text{D}_2\text{O}$ ,  $5^\circ\text{C}$ ),  $\delta$ : 1.69 (s, 3H, Ar- $\text{CH}_3$ ), 2.14 (s, 3H, OAc- $\text{CH}_3$ ), 6.94 (ddd,  $J=7.7, 5.8, 1.6$  Hz, 1H, H-9), 7.12 (m, 1H, H-2), 7.24 (d,  $J=5.9$  Hz, 1H, H-8), 7.41 (s, 1H, H-1), 7.43 (td,  $J=5.5, 3.5$  Hz, 1H, H-5), 7.48 (ddd,  $J=7.7, 4.9, 1.6$  Hz, 1H, H-13), 7.69–7.73 (m, 2H, H-11 and H-3), 7.82 (td,  $J=7.8, 1.4$  Hz, 1H, H-10), 7.87 (d,  $J=7.2$  Hz, 1H, H-15), 7.99 (td,  $J=7.8, 1.3$  Hz, 1H, H-14), 8.13–8.15 (m, 2H, H-6 and H-7), 8.71 (d,  $J=5.9$  Hz, 1H, H-4), 8.94 (d,  $J=5.3$  Hz, 1H, H-12).

#### Selective 1D-difference NOE experiments ( $\text{D}_2\text{O}$ ) for 88

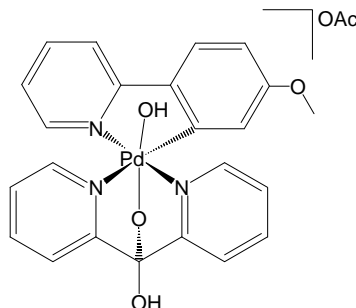


In the 1D difference NOE experiment, NOE was observed between the *ortho*- $\text{H}_c$  of the tolylpyridine ligand and that of the *ortho*- $\text{H}_d$  of the dpk ligand. Irradiation of a resonance at 8.94 ppm (*ortho*- $\text{H}_d$  of the dpk ligand) showed enhancement (positive

NOE) of the doublet at 8.71 ppm (*ortho*-H<sub>c</sub> on the pyridyl fragment of the tolylpyridine ligand, 6.7 %) (mixing time of 0.8s, delay time 5s).

This complex is too unstable and thus elemental analysis could not be performed.

### Complex 85



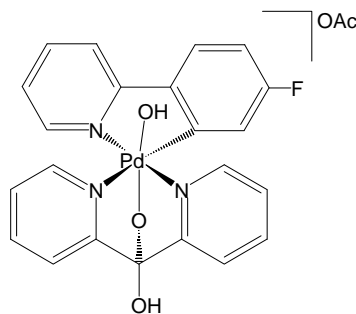
<sup>1</sup>H NMR (D<sub>2</sub>O, 276 K), δ: 1.66 (s, 3H), 3.58 (s, 3H), 6.10 (vs, 1H), 6.88 (d, *J*= 9.2 Hz, 1H), 7.15 (t, *J*= 6.7 Hz, 1H), 7.60 (t, *J*= 6.7 Hz, 1H), 7.64 (t, *J*= 6.5 Hz, 1H), 7.71-7.76 (m, 2H), 7.85 (d, *J*= 8.0 Hz, 1H), 7.90 (d, *J*= 8.3 Hz, 1H), 7.96 (t, *J*= 7.5 Hz, 1H), 8.00 (d, *J*= 6.0 Hz, 1H), 8.02 (td, *J*= 7.9, 1.2 Hz, 1H), 8.09 (t, *J*= 7.6 Hz, 1H), 8.58 (d, *J*= 5.6 Hz, 1H), 8.84 (d, *J*= 5.2 Hz, 1H).

<sup>13</sup>C NMR (D<sub>2</sub>O, 276 K), δ: 23.3, 56.0, 104.0, 113.4, 116.5, 122.1, 122.3, 122.7, 124.8, 127.1, 128.6, 128.8, 134.0, 142.4, 142.8, 144.0, 146.9, 147.6, 148.5, 158.3, 160.2, 161.3, 161.8, 162.0, 181.7.

ESI-MS of solution of **85**<sup>+</sup> in water, positive mode, *m/z* = 508.0589.  
Calculated for **85**<sup>+</sup>, C<sub>23</sub>H<sub>20</sub>N<sub>3</sub>O<sub>4</sub><sup>106</sup>Pd, *m/z* = 508.0489

This complex is too unstable and thus elemental analysis could not be performed.

### Complex 86



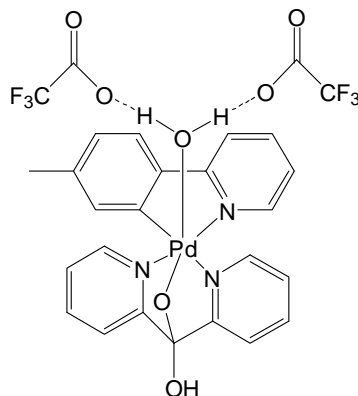
$^1\text{H}$  NMR ( $\text{D}_2\text{O}$ , 276 K),  $\delta$ : 1.91 (s, 3H), 6.66 (dd,  $J$ = 8.1, 2.2 Hz, 1H), 7.34 (td,  $J$ = 8.6, 2.2 Hz, 1H), 7.51 (td,  $J$ = 6.6, 1.9 Hz, 1H), 7.85 (td,  $J$ = 6.6, 1.0 Hz, 1H), 7.89 (td,  $J$ = 6.6, 1.5 Hz, 1H), 7.96 (dd,  $J$ = 7.9, 1.0 Hz, 1H), 8.08-8.12 (m, 2H), 8.23-8.31 (m, 4H), 8.35 (td,  $J$ = 7.9, 1.0 Hz, 1H), 8.82 (d,  $J$ = 5.5 Hz, 1H), 5.09 (d,  $J$ = 5.2 Hz, 1H).

$^{13}\text{C}$  NMR ( $\text{D}_2\text{O}$ , 276 K),  $\delta$ : 23.1, 104.1, 116.5 (d,  $J$ =22.4 Hz), 117.9 (d,  $J$ =25.6 Hz), 122.2, 122.9, 123.2, 126.0, 127.2, 128.9, 129.0 (d,  $J$ =10.9 Hz), 138.2, 142.6, 143.2, 144.1, 146.9, 147.5, 148.8, 158.2, 159.0, 161.1, 161.3, 161.7, 163.8, 181.4.

ESI-MS of solution of  $\mathbf{86}^+$  in water, positive mode,  $m/z$  = 496.0324.  
Calculated for  $\mathbf{86}^+$ ,  $\text{C}_{22}\text{H}_{17}\text{FN}_3\text{O}_3$   $^{106}\text{Pd}$ ,  $m/z$  = 496.0289

This complex is too unstable and thus elemental analysis could not be performed.

**Complex 91(OOCCF<sub>3</sub>)<sub>2</sub>**



<sup>1</sup>H NMR (D<sub>2</sub>O, 3°C), δ: 2.10 (s, 3H), 6.42 (s, 1H), 7.13 (d, *J* = 7.9 Hz, 1H), 7.22 (ddd, *J* = 11.3, 5.7, 3.6 Hz, 1H), 7.60 (ddd, *J* = 7.8, 5.3, 1.0 Hz, 1H), 7.63 (ddd, *J* = 7.7, 5.9, 1.4 Hz, 1H), 7.66 (d, *J* = 7.9 Hz, 1H), 7.72 (d, *J* = 7.9 Hz, 1H), 7.86 (d, *J* = 7.9 Hz, 1H), 8.00-8.01 (m, 2H), 8.04 (td, *J* = 7.8, 1.4 Hz, 1H), 8.06 (d, *J* = 6.0 Hz, 1H), 8.10 (td, *J* = 7.8, 1.0 Hz, 1H), 8.59 (d, *J* = 5.8 Hz, 1H), 8.87 (d, *J* = 4.9 Hz, 1H).

<sup>13</sup>C NMR (D<sub>2</sub>O, 3°C), δ: 21.4, 104.4, 115.3, 117.6, 122.1, 122.9, 125.7, 127.1, 127.8, 128.8, 130.0, 130.1, 138.6, 142.4, 143.1, 144.0, 145.9, 147.0, 147.7, 148.8, 158.0, 160.3, 161.0, 162.0, 163.5.

Anal. Found (Calculated for C<sub>27</sub>H<sub>23</sub>F<sub>6</sub>N<sub>3</sub>O<sub>8</sub>Pd with one water molecule of hydration): C, 43.71 (43.95); H, 3.18 (3.14); N, 5.61 (5.69).

ESI-MS of a solution of **91(OOCCF<sub>3</sub>)<sub>2</sub>** in dmsO, *m/z* = 492.0622. Calculated for **84<sup>+</sup>**, C<sub>23</sub>H<sub>20</sub>N<sub>3</sub>O<sub>3</sub><sup>106</sup>Pd = 492.0548.

X-ray quality crystals could be produced as described below. 40.0 mg of complex **69(OAc)** was placed in a vial and 1.5 ml of H<sub>2</sub>O was added. The mixture was warmed to completely dissolve the solid. The pale yellow solution was placed in ice-water bath at 0°C. After 10 minutes, 5 drops of 30 % HOOH were added to the cold solution and it was left in ice-water bath for 2 hours. Afterward, 3 drops of

HOCCF<sub>3</sub> were added to another 0.2 ml H<sub>2</sub>O solution, and the oxidation solution was carefully layered onto the aqueous HOCCF<sub>3</sub> solution. The resulting solution was layered with ~ 4.0 ml of tetrahydrofuran and was placed in the freezer at -20°C. Deep red crystals were observed after ~ 12 hours.

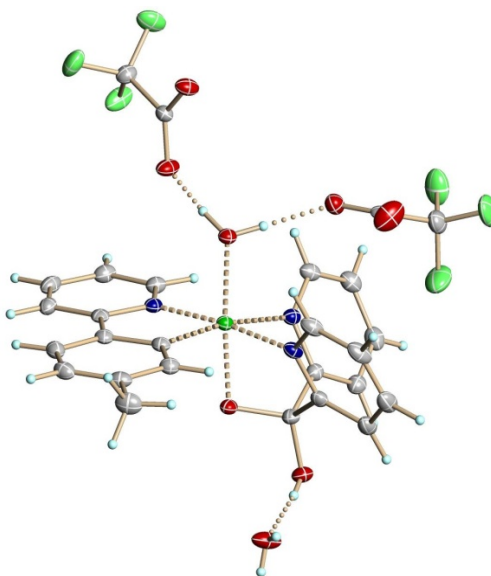
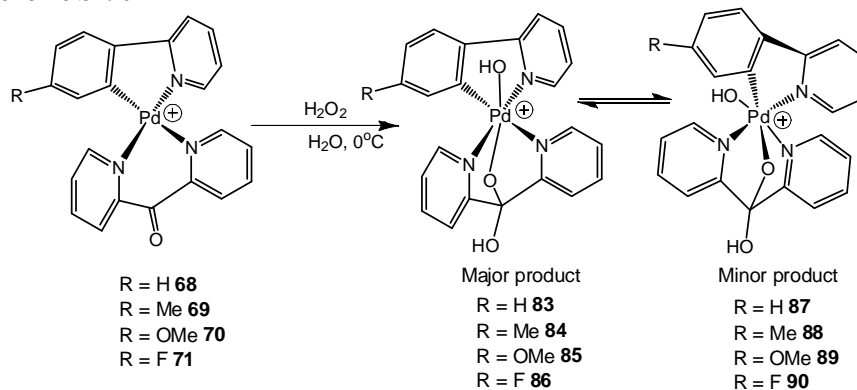


**Figure S1. 1.** ORTEP drawing (50% probability ellipsoids) of dication **91** in **91(OOCCF<sub>3</sub>)<sub>2</sub>·H<sub>2</sub>O**,

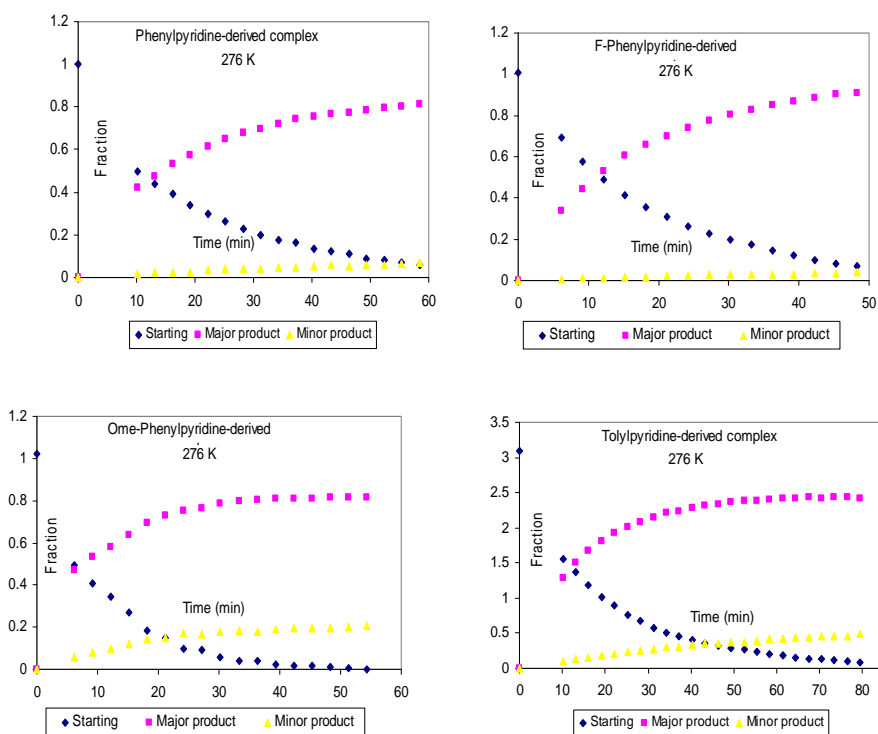
*<sup>1</sup>H NMR analysis for the oxidation of complex 68-71 with H<sub>2</sub>O<sub>2</sub> in water*

**Scheme S1. 6**



Careful analysis of the <sup>1</sup>H NMR spectrum upon oxidation of complexes **68-71** with 1.5 equivalents H<sub>2</sub>O<sub>2</sub> in water at room temperature revealed formation of a

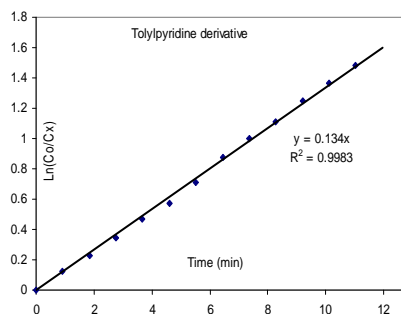
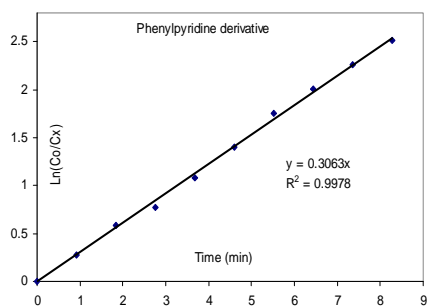
second, minor product of oxidation (see below). In particular, 0.010 mmoles of the substituted phenylpyridine-dpk derivative was dissolved in 1.0 ml of deuterated water, 1.0  $\mu$ l of dioxane was added as internal standard and the solution was added into an NMR tube. The tube was inserted into the NMR probe at 3  $^{\circ}$ C and  $^1$ H NMR was taken after 10 minutes. 1.5 mmoles of 30%  $\text{H}_2\text{O}_2$  in water was added to the solution and consecutive  $^1$ H NMR spectra were collected at regular intervals. Data taken for the first 5 minutes was not included because it takes approximately 5-10 minutes for the temperature of the solution to equilibrate with the temperature of the NMR probe. Plots for the fraction of the starting Pd(II) precursor **68-71**, the major Pd(IV) complex **83-86**, and the minor product **87-90** are presented below:



**Figure S1. 2.** Plots showing fraction of Pd(II) complexes **68-71**, major complexes **83-86**, and minor complexes **87-90**, as a function of time, upon combination of aqueous solutions of complexes **68-71** with 1.5 eq of  $\text{H}_2\text{O}_2$  at 3  $^{\circ}$ C.

*Kinetics study for the oxidation of complexes 68-71 in water*

The kinetics of oxidation of compounds **68-71** at 3 °C was studied under pseudo-first order conditions. 0.010 mmol of the substituted phenylpyridine dpk-derived complex was dissolved in 1.0 ml of deuterated water, 1.0  $\mu$ l of dioxane was added as internal standard and the solution was placed into an NMR tube. The tube was inserted into the NMR probe set at 3 °C and  $^1\text{H}$  NMR was taken after 10 minutes. 4.5 mmoles of 30%  $\text{H}_2\text{O}_2$  in water was added to the solution and consecutive  $^1\text{H}$  NMR spectra were collected at regular intervals. Data taken for the first 5 minutes was not included because it takes approximately 10 minutes for the temperature of the solution to equilibrate with the temperature of the NMR probe (Since the solution before addition of  $\text{H}_2\text{O}_2$  was already  $\sim 17$  °C, it took  $< 5$  minutes for the resulting solution to attain the required temperature). Plots of  $\ln([\text{Pd(II)}]_0/[\text{Pd(II)}]_t)$  vs. time for the oxidation of complexes **68-71** in deuterated water at 3 °C are given below.



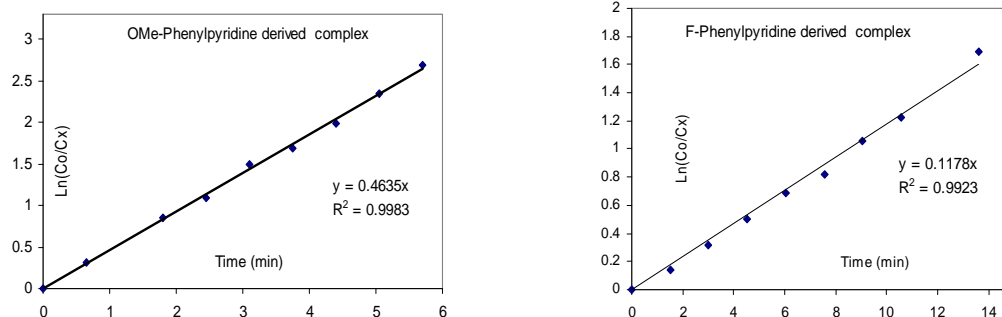


**Figure S1. 3.** First order plots for the oxidation of 0.010 mmoles of complexes **68-71** in 1.0 ml D<sub>2</sub>O with >8 equivalents of H<sub>2</sub>O<sub>2</sub>.

**Table S. 1.** Correlation between the rate constant in min<sup>-1</sup> and the  $\sigma_m$  for oxidation of various R-substituted phenylpyridine dpk-derived palladacycles with excess H<sub>2</sub>O<sub>2</sub> at 3 °C under pseudo-first order conditions. The initial concentrations of the reactants are calculated from the first data point collected by <sup>1</sup>H NMR and used in the analysis

R	[Pd(II)]	[HOOH]	K <sub>obs</sub> (min <sup>-1</sup> )	$\sigma_m$
-F ( <b>71</b> )	4.85 * 10 <sup>-3</sup>	39.9 * 10 <sup>-3</sup>	(1.18 ± 0.02) * 10 <sup>-1</sup>	.337
-H ( <b>68</b> )	5.78 * 10 <sup>-3</sup>	40.8 * 10 <sup>-3</sup>	(3.09 ± 0.13) * 10 <sup>-1</sup>	0
-Ome ( <b>70</b> )	2.93 * 10 <sup>-3</sup>	37.9 * 10 <sup>-3</sup>	(4.63 ± 0.06) * 10 <sup>-1</sup>	0.115
-Me ( <b>69</b> )	5.61 * 10 <sup>-3</sup>	40.6 * 10 <sup>-3</sup>	(1.37 ± 0.01) * 10 <sup>-1</sup>	-0.069

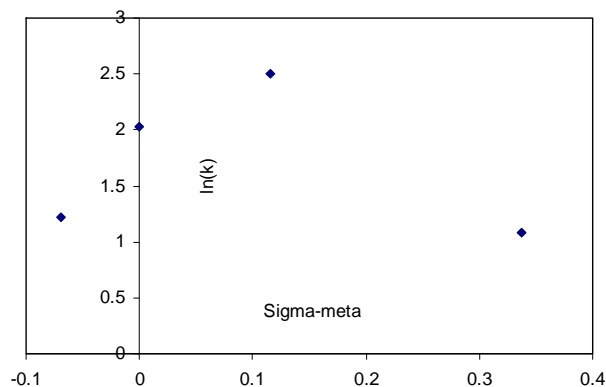


**Figure S1. 4.** Hammett plot for the oxidation of complexes **68-71** with excess H<sub>2</sub>O<sub>2</sub> in D<sub>2</sub>O at 3°C.

Due to the unexpected nature of the hammet plot, this experiment was repeated under the same conditions, but 0.040 mmoles of  $\text{H}_2\text{O}_2$  was used instead. Plots of  $\ln([\text{Pd(II)}]_o/[\text{Pd(II)}]_t)$  vs. time for the oxidation of complexes **68-71** in deuterated water at 3 °C using 4.0 mmoles of  $\text{H}_2\text{O}_2$  are given below.

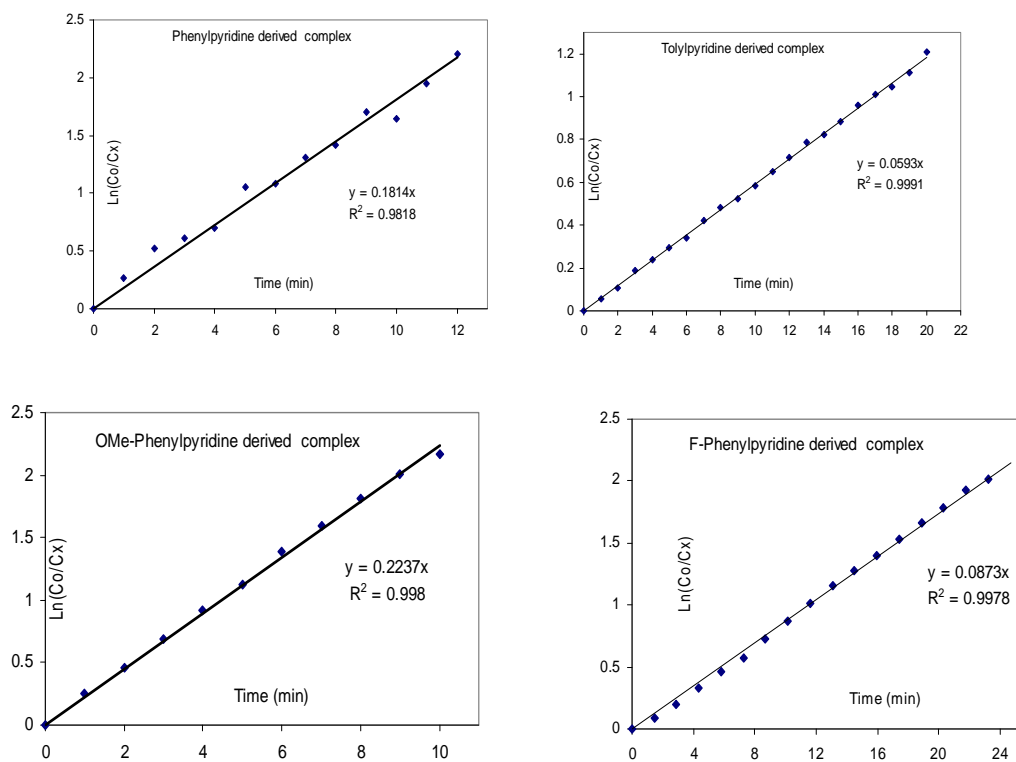


**Figure S1. 5.** First order plots for the oxidation of 0.010 mmoles of complexes **68-71** in 1.0 ml  $\text{D}_2\text{O}$  with >6 equivalents of  $\text{H}_2\text{O}_2$ .

**Table S. 2.** Correlation between the rate constant in  $\text{min}^{-1}$  and the  $\sigma_m$  for oxidation of various R-substituted phenylpyridine dpk-derived palladacycles with excess  $\text{H}_2\text{O}_2$  at  $3^\circ\text{C}$  under pseudo-first order conditions. The initial concentrations of the reactants are calculated from the first data point collected by  $^1\text{H}$  NMR and used in the analysis.

R	[Pd(II)]	[HOOH]	$K_{\text{obs}}$ ( $\text{min}^{-1}$ )	$\sigma_m$
-F	$6.30 * 10^{-3}$	$36.3 * 10^{-3}$	$(0.910 \pm 0.02) * 10^{-1}$	.337
-H	$4.35 * 10^{-3}$	$34.3 * 10^{-3}$	$(1.71 \pm 0.13) * 10^{-1}$	0
-Ome	$4.93 * 10^{-3}$	$34.9 * 10^{-3}$	$(2.19 \pm 0.06) * 10^{-1}$	0.115
-Me	$7.87 * 10^{-3}$	$37.9 * 10^{-3}$	$(0.993 \pm 0.01) * 10^{-1}$	-0.069

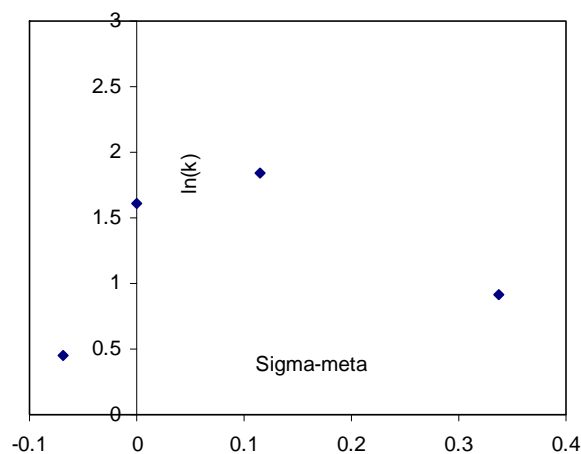


**Figure S1. 6.** Hammett plot

*Influence of pH on the ratio of complexes 84 and 88 produced*

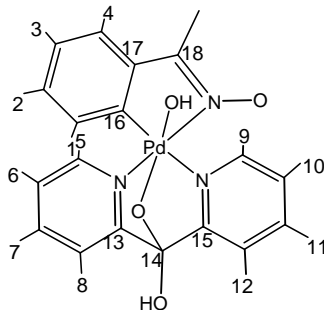
The *pH*-potentiometric titrations were performed with OAKTON Waterproof pH Testr BNC pH-meter at  $22^\circ\text{C}$ . To calibrate the glass-reference electrode pair, potassium biphthalate (pH 4.00, 0.05M), potassium phosphate monobasic-NaOH (pH 7.00, 0.05M), and potassium-carbonate-potassium borate-KOH (pH 10.00, 0.05M) buffer solutions were used. For the titrations, 1.0 M NaOD solution and neat deuterated acetic acid were used. 0.05 mmoles of complex **69** was dissolved in 5.0 ml

of D<sub>2</sub>O at 22 °C, in a vial equipped with a magnetic stirring bar. A 2.0 ml portion of this solution was titrated with 1.0 M NaOD solution at room temperature using a microsyringe while the pH was monitored with the pH meter until the pH of 8.47 (pD = 8.88) was attained. Another 2.0 ml portion of the solution was titrated with neat deuterated acetic acid solution at room temperature using a microsyringe while the pH was monitored with the pH meter until the pH of 4.58 (pD = 4.99) was attained. The pH of the solution was read from the pH meter after 2 minutes to ensure complete stabilization. 1.0 ml of the solution at either pD = 8.88 or 4.99 was placed into an NMR tube and placed in the NMR probe set at 17 °C. <sup>1</sup>H NMR was taken at after 10 minutes to ensure equilibration of the temperature of the NMR solution with the NMR probe. The tube was ejected from the instrument, 2.0 μl of H<sub>2</sub>O<sub>2</sub> was quickly added, the solution was shaken and inserted back into the probe at 17 °C. Consecutive <sup>1</sup>H NMR spectra were collected until quantitative conversion of complex **69** to the Pd(IV) complexes **84** and **88** had occurred. The ratio of complex **84** to complex **88** was recorded at the various pD values.

*Preparation of complexes 93 and 94 in acetonitrile*

Complexes **93** and **94** were prepared in acetonitrile. 0.10 mmoles of complex **72** or **73** was added to 5.0 ml of acetonitrile at 0 °C, and 10.0 equivalents of H<sub>2</sub>O<sub>2</sub> were added to the reaction mixture. The mixture was stirred at 0 °C for 2 hours, after which it was concentrated and triturated with diethyl ether. The resulting precipitate was filtered off and washed with a small amount of cold diethyl ether to afford pure target complex.

### Complex 93



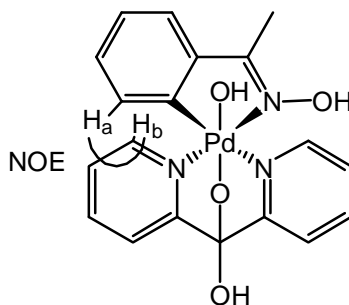
$^1\text{H}$  NMR ( $\text{D}_2\text{O}$ ,  $22^\circ\text{C}$ ),  $\delta$ : 2.32 (s, 3H, Oac- $\text{CH}_3$ ), 3.34 (s, 3H, - $\text{CH}_3$ ), 6.99 (d,  $J=7.6$  Hz, 1H, H-1), 7.04 (dt,  $J=6.8$ , 1.4 Hz, 1H, H-2), 7.35 (dt,  $J=6.9$ , 1.3, 0.6 Hz, 1H, H-3), 7.42 (dd,  $J=7.5$ , 1.4 Hz, 1H, H-4), 7.64 (dt, 6.4, 1.1 Hz, 1H, H-10), 7.56 (dt,  $J=6.5$ , 1.0 Hz, 1H, H-6), 7.87 (d,  $J=7.8$ , 2H, H-8 and -12), 8.10 (dt,  $J=7.8$ , 1.2 Hz, 1H, H-11), 8.19 (dt, 7.8, 1.0 Hz, 1H, H-7), 8.79 (d,  $J=5.3$  Hz, 1H, H-5), 8.90 (d,  $J=5.0$  Hz, 1H, H-9).

$^{13}\text{C}$  NMR ( $\text{D}_2\text{O}$ ,  $22^\circ\text{C}$ ),  $\delta$ : 13.2 (OAc- $\text{CH}_3$ ), 104.1 (C-14), 120.8 (C-8), 122.1 (C-12), 126.2 (C-10), 127.4 (C-4), 128.0 (C-6), 128.5 (C-2), 128.8 (C-3), 130.3 (C-1), 141.6 (C-11), 143.0 (C-17, 17), 147.9 (C-5), 148.5 (C-9), 155.0 (C-18), 159.2 (C-15), 161.8 (C-13), 163.4 (C-16)

ESI-MS of oxidation solution of  $\mathbf{93}^+$  in water,  $m/z$  458.0376. Calculated for Pd(IV) complex  $\text{C}_{19}\text{H}_{18}\text{N}_3\text{O}_4^{106}\text{Pd}$ ; 458.0332

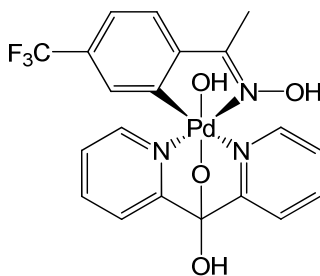
Anal. Found: C, 47.47; H, 4.16; N, 8.01; Calculated for complex with 1 residual water molecule and  $\frac{1}{2}$  molecule of acetic acid; C, 47.49; H, 4.18; N, 8.31.

Selective 1D-difference NOE experiments (D<sub>2</sub>O) for **93**



In the 1D difference NOE experiment, NOE was observed between the *ortho*-H<sub>a</sub> on the phenyl fragment of the oxime ligand and that of the *ortho*-H<sub>b</sub> on the dpk ligand. Irradiation of a resonance at 8.79 ppm (*ortho*-H<sub>b</sub> on the dpk ligand) showed enhancement (positive NOE) of a doublet at 6.99 ppm (*ortho*-H<sub>b</sub> on the phenyl fragment of the oxime ligand, 2.1%) (mixing time of 4.0s, delay time 5s).

**Complex 94**

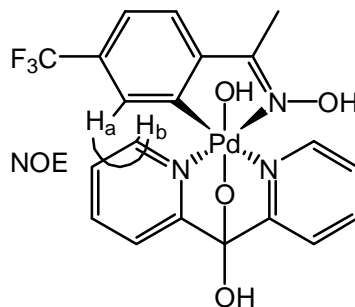


<sup>1</sup>H NMR (D<sub>2</sub>O, 22°C), δ: 2.03 (s, 3H), 2.31 (s, 3H), 7.16 (s, 1H), 7.53 (d, *J*=7.9 Hz, 1H), 7.64 (t, *J*=6.5 Hz, 1H), 7.69 (d, *J*=8.0 Hz 1H), 7.76 (dt, *J*=6.5, 1.0 Hz 1H), 7.87-7.90 (m, 2H), 8.10 (dt, *J*=7.8, 1.2 Hz, 1H), 8.21 (dt, *J*=7.8, 1.0 Hz, 1H), 8.82 (d, *J*=5.5, Hz, 1H), 8.91 (d, *J*=5.2, Hz, 1H).

<sup>13</sup>C NMR (D<sub>2</sub>O, 22°C), δ: 12.6, 20.9, 103.6, 120.2, 121.7, 122.5, 124.3, 125.4, 125.6, 125.7, 126.2, 127.2, 127.4, 127.6, 141.1, 142.6, 146.6, 147.0, 147.6, 152.6, 158.1, 160.8, 161.2, 177.5.

ESI-MS of solution of **94**<sup>+</sup> in water,  $m/z = 526.0276$ . Calculated for Pd(IV) complex  $C_{20}H_{17}N_3F_3O_4^{106}Pd$ , 526.0206

*Selective 1D-difference NOE experiments (D<sub>2</sub>O) for 94*

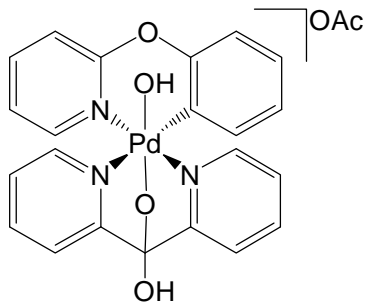


In the 1D difference NOE experiment, NOE was observed between the *ortho*-H<sub>a</sub> on the phenyl fragment of the oxime ligand and that of the *ortho*-H<sub>b</sub> on the dpk ligand. Irradiation of a resonance at 8.82 ppm (*ortho*-H<sub>b</sub> on the dpk ligand) showed enhancement (positive NOE) of a singlet at 7.16 ppm (*ortho*-H<sub>a</sub> on the phenyl fragment of the oxime ligand, 7.4%) (mixing time of 0.6s, delay time 4s).

*Preparation of complex 96*

Complex **96** was prepared in water. 0.01 mmoles of complex **74** was dissolved in 1.0 ml of D<sub>2</sub>O in ace-water bath at 0°C, and 10.0 equivalents of H<sub>2</sub>O<sub>2</sub> was added to the solution. The resulting yellow solution was stirred at this temperature for 60 minutes. Complex **96** was characterized via NMR spectroscopy and electrospray mass ionization spectrometry in solution since it was too reactive to be isolated.

**Complex 96**



$^1\text{H}$  NMR ( $\text{D}_2\text{O}$ ,  $5^\circ\text{C}$ ),  $\delta$ : 1.82(s, 3H), 6.27 (d,  $J=8.4$  Hz, 1H) 6.92 (td,  $J=7.7$ , 1.5 Hz, 1H), 7.10 (t,  $J=6.7$  Hz, 1H), 7.26 to 7.32 (m, 2H), 7.53 to 7.60 (m, 4H), 7.89 (d,  $J=7.9$ , 1H). 8.01 (d,  $J=7.9$  Hz, 1H), 8.09 (dt,  $J=7.7$ , 1.0 Hz, 1H), 8.13 (dt,  $J=7.7$ , 1.0 Hz, 1H), 8.18 (t,  $J=7.9$  Hz, 1H), 8.22 (d,  $J=5.7$  Hz 1H), 8.51 (d,  $J=4.9$  Hz 1H).

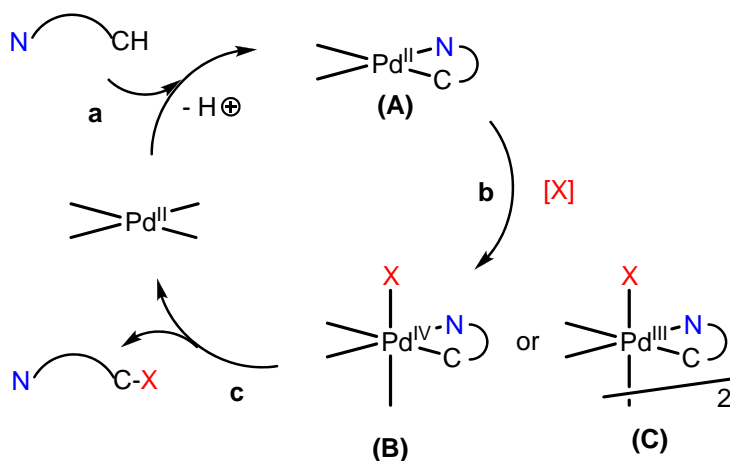
$^{13}\text{C}$  NMR ( $\text{D}_2\text{O}$ ,  $5^\circ\text{C}$ ),  $\delta$ : 22.1, 104.4, 118.5, 120.7, 122.4, 122.5, 123.4, 127.0, 127.4, 128.0, 130.0, 132.7, 133.2, 142.6, 144.1, 145.6, 147.2, 147.8, 147.9, 148.4, 158.0, 158.7, 159.3, 161.2, 179.6

ESI-MS of solution of **96** in water,  $m/z$  observed: 494.0294. Calculated for  $\text{C}_{22}\text{H}_{18}\text{N}_3\text{O}_4^{106}\text{Pd}$ ,  $m/z = 494.0332$ .

## Chapter 3: Reactivity of Monohydrocarbyl Pd(IV) Complexes in Various Solvents

### 3.1 Introduction

Scheme 3. 1

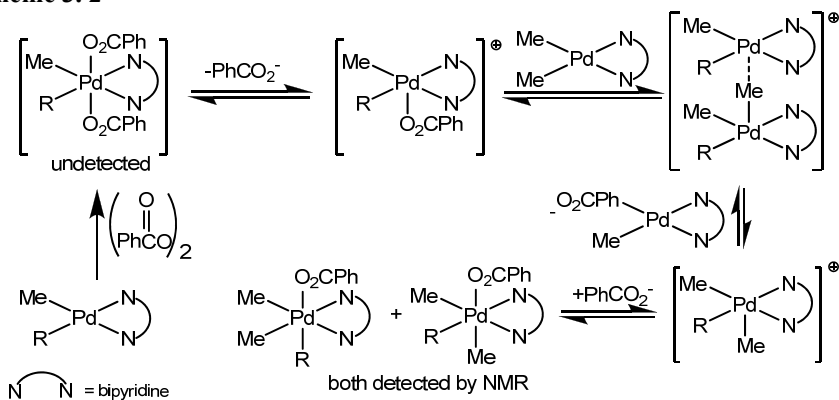


Oxidative palladium catalyzed C-H bond functionalization reactions have been proposed to proceed via C-H bond activation to produce organopalladium(II) intermediates (step a). These intermediates undergo oxidation to generate high oxidation state palladium species of monomeric palladium(IV) or dimeric palladium(III) structure (step b), which in turn undergo C-O reductive elimination to release the functionalized product and regenerate the catalyst (step c). The C-H bond activation reaction has been studied in detail,<sup>3,17,63</sup> but the subsequent steps of oxidation and C-O reductive elimination from the high oxidation state palladium intermediates have not been studied in sufficient detail,<sup>57</sup> mainly because most oxidative palladium catalyzed reactions have been found to proceed via rate-limiting



at low temperatures. C–O bond forming reductive elimination from these Pd(IV) complexes was however accompanied with either C–C bond formation and/ or intermolecular alkyl exchange processes.<sup>51-54</sup> The instability of these O–ligated hydrocarbyl Pd(IV) complexes towards isolation in pure form and their tendency to undergo C–C bond forming and/ or intermolecular alkyl exchange reactions prevented detailed studies of the C–O reductive elimination reaction.

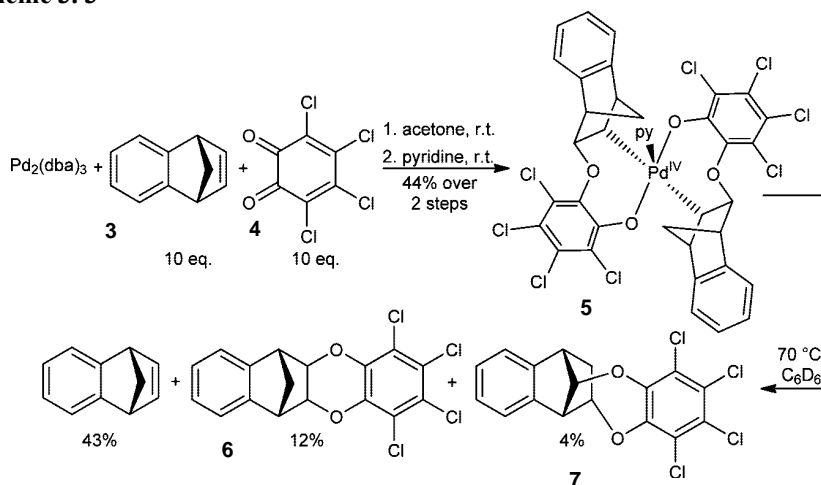
**Scheme 3.2**



The first isolated stable hydrocarbyl Pd(IV) complex containing O–donor ligands was reported by Yamamoto and co-workers in 2004 (Scheme 3.3).<sup>56,178</sup> This trigonal-bipyramidal complex **5** was formed via the reaction of  $\text{Pd}_2(\text{dba})_3$  with *O*-chloranil **4** and benzonorbornadiene **3**, and is stable in the absence of bidentate or tripodal donor spectator ligands. It contains two residues of *O*-chloranil and norbornene that form two 7-membered chelate rings. Complex **5** decomposes slowly over several days at ambient temperature in THF, but undergoes decomposition in  $\text{C}_6\text{D}_6$  at  $70^\circ\text{C}$  over several hours to give benzonorbornadiene **3** as the major organic product and two isomeric adducts between *O*-chloranil and benzonorbornadiene, **6** and **7**. The decomposition was inhibited by pyridine additives, while acid was found to significantly accelerate the decomposition in  $\text{CDCl}_3$ , where decomposition was

complete within 15 minutes at  $-40^{\circ}\text{C}$  upon exposure to  $\text{HCl}$  in  $\text{CDCl}_3$ . Detailed study of the  $\text{C-O}$  reductive elimination reaction from complex **5** was not possible because apart from products resulting from  $\text{C-O}$  coupling, other products resulting from side-reactions were also observed.

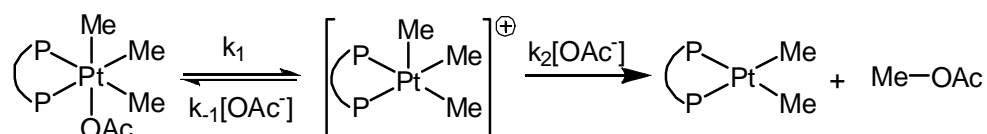
**Scheme 3.3**



The first detailed studies of  $\text{C-O}$  reductive elimination from organoplatinum(IV) complexes was reported by Goldberg and co-workers (Scheme 3.4). In this report, a series of  $\text{dppePt(IV)Me}_3\text{X}$  complexes ( $\text{X}=\text{OAc}$  or  $\text{OAr}$ ) were prepared and products resulting from both  $\text{C-O}$  and  $\text{C-C}$  bond forming reductive elimination upon thermolysis in various solvents were observed.<sup>179,180</sup> Different reaction conditions could be employed to favor one reaction pathway over the other. The mechanism of  $\text{C-O}$  reductive elimination was proposed to take place from a reactive 5-coordinate intermediate produced upon dissociation of an  $\text{OR}^-$  ligand. This was based on the observation that the rate of  $\text{C-O}$  reductive elimination was accelerated by polar solvents, which is indicative of an ionic or polar transition state, and by acids, which increase the rate of  $\text{C-O}$  reductive elimination by hydrogen bonding to  $\text{OR}$  and thus assist in  $\text{OR}^-$  dissociation. The rate of reductive elimination

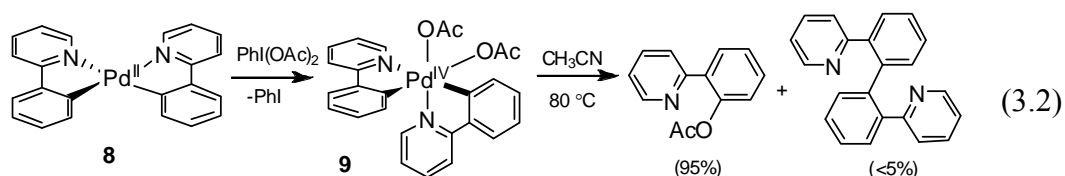
reaction was also found to increase with more electron-withdrawing aryloxides. These observations were proposed to be consistent with a mechanism that involves preliminary dissociation of the  $\text{OR}^-$  ligand leading to the development of a negative charge at oxygen. The exchange of aryloxides was extremely fast, where complete exchange was observed at temperatures below those required for reductive elimination, indicating a pre-equilibrium exchange of the  $\text{OR}^-$  ligand. Thus the mechanism of C–O reductive elimination was proposed to involve pre-equilibrium dissociation of the  $\text{OR}^-$  ligand, followed by rate-limiting  $\text{S}_{\text{N}}2$  attack of the ligand on the platinum-bound methyl group of the 5-coordinate cation (Scheme 3.4). A similar mechanism was proposed for one of the steps of the Shilov reaction. In this reaction, activation of methane generates a methyl platinum(II) intermediate, which undergoes oxidation by  $\text{H}_2\text{Pt(IV)Cl}_6$  to generate a methylPt(IV) transient species. The Pt(IV) complex in turn undergoes C–O reductive elimination with water acting as external nucleophile to produce methanol.<sup>181</sup> There have been additional reports on C–O reductive elimination from alkylPt(IV) complexes where the  $\text{S}_{\text{N}}2$  mechanism was proposed.<sup>182</sup> There have also been reports on C–O reductive elimination reactions from Pt(IV) complexes where a concerted 3-center mechanism was proposed.<sup>183</sup>

**Scheme 3. 4**



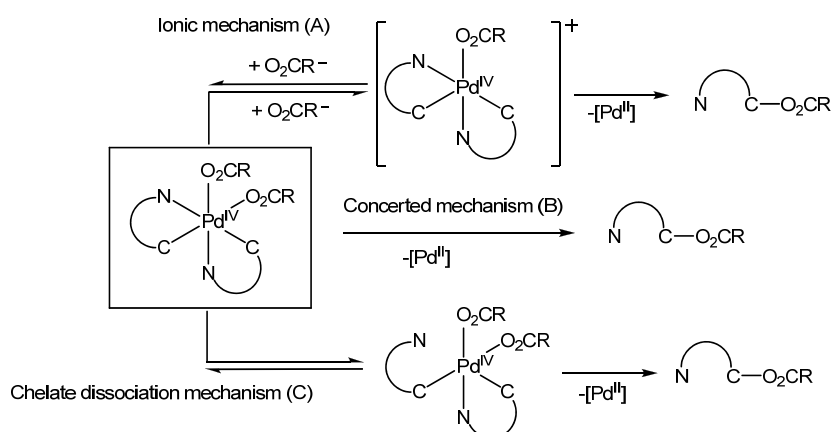
The first detailed studies of C–O reductive elimination from Pd(IV) complexes were reported by Sanford and co-workers in 2005.<sup>57</sup> In this report, a series of biaryl Pd(IV) complexes that were stable at ambient temperature but underwent C–

O bond reductive elimination upon thermolysis were prepared (eq. 3.2). The biaryl Pd(IV) complexes were accessed via oxidation of (N~C)<sub>2</sub>Pd(II) complex **8** (N~C= cyclometalated phenylpyridine ligand) with PhI(O<sub>2</sub>CR)<sub>2</sub> (R= substituted aromatic groups), where the benzoate-based O-donors were used in order to model catalytic arene oxygenation reactions.<sup>50</sup> The resultant Pd(IV) complex **9** is stabilized by rigid bidentate N~C ligands,<sup>184-188</sup> which also contribute two electron-donating σ-aryl ligands to the high oxidation state Pd complex. The rigid, chelating nature of the ligands also limits competing C~C bond forming reductive elimination reactions relative to the desired C~O coupling.



The C~O coupling reaction was subjected to a series of experimental analyses, including solvent effect studies, Eyring analysis, Hammett plot, and crossover studies. Three mechanisms were considered, including (A) the ionic mechanism where pre-equilibrium dissociation of a benzoate ligand was followed by reductive elimination from the resulting cationic 5-coordinate Pd(IV) intermediate;<sup>86,179,180,182,183,189</sup> (B) direct reductive elimination from the 6-coordinate Pd(IV) intermediate;<sup>190-196</sup> (C) dissociation of a pyridyl arm of one cyclometalated ligand followed by internal coupling from the resulting 5-coordinate complex<sup>197-199</sup> (Scheme 3.5). These mechanisms were considered because there is literature precedent for each in reductive elimination reactions from group 10 metal complexes.<sup>58</sup>

**Scheme 3. 5**



On the basis of experimental observations, a C–O coupling mechanism that involves preliminary chelate dissociation, followed by C–O reductive elimination from a pentacoordinate Pd(IV) complex, path C was proposed. This mechanism was supported by the absence of solvent effects, a near zero entropy value, negative cross-over studies, a slower rate of reaction rate when the more rigid bisbenzo[*h*]quinoline-derived Pd(IV) complex was used, and lack of incorporation of OAc when the reaction was performed in the presence of NBu<sub>4</sub>OAc.

Theoretical studies on this system by Liu and co-workers however favored mechanism B, where C–O reductive elimination takes place from a 6-coordinate palladium species.<sup>43</sup> This mechanism was supported by a close match between calculated and experimental activation free energy barriers. The theoretical model also correctly predicted the subtle solvent and substituent effects observed experimentally. The model also explained why the rate of reductive elimination from the bisphenylpyridine complex is significantly faster than that from bisbenzo[*h*]quinoline.

A recent detailed study led Sanford and co-workers to conclude that the C–O reductive elimination reaction proceeds via the ionic mechanism A, where pre-equilibrium dissociation of an acetate ligand is followed by rate limiting C–O reductive elimination.<sup>58</sup> This revised mechanism was proposed based on additional experimental observations, including the rapid exchange of the bound and free carboxylate ligands, which indicates that dissociation of carboxylate ligand from the Pd(IV) complex is possible. The rates of carboxylate exchange and C–O coupling were also observed to increase to similar extents upon addition of AcOH and AgOTf additives. These results support a mechanism of C–O reductive elimination that includes pre-equilibrium dissociation of the carboxylate ligand, followed by C–O coupling from a 5-coordinate intermediate. Through crossover studies, the non-exchangeable carboxylate ligand was found to selectively participate in the C–O reductive elimination reaction.

These mechanistic studies indicate that the mechanism of C–O reductive elimination from Pd(IV) complexes is not well understood. In addition, C–O reductive elimination from monohydrocarbyl Pd(IV) complexes has never been studied due to the difficulty in accessing these complexes and their tendency to undergo side reactions. As a result, it is important to prepare O-ligated monohydrocarbyl Pd(IV) complexes and study their reactivity towards C–O reductive elimination since these complexes are potential intermediates in palladium catalyzed C–H bond oxygenation reactions. Additionally, the study of the C–O reductive elimination reaction from monohydrocarbyl Pd(IV) complexes is important because any advanced knowledge of the possible C–O reductive elimination pathways might

be very beneficial in the design of more selective, efficient, and environmentally benign oxidative C–H bond functionalization reactions.

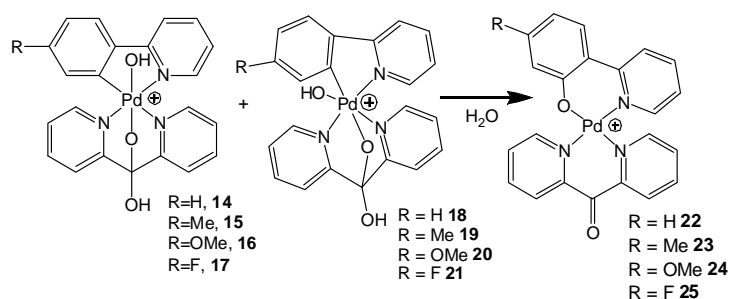
As a result, we prepared a number of monohydrocarbyl Pd(IV) complexes and studied their reactivity towards C–O reductive elimination in various solvents.

### 3.2 C–O Reductive Elimination Reactivity at Monohydrocarbyl Pd(IV) Complexes 14-17 in Various Solvents

#### 3.2.1 C–O Reductive Elimination Reactivity at Monohydrocarbyl Pd(IV) Complexes

##### 14-17 in Water

**Scheme 3. 6**



C–O reductive elimination from monohydrocarbyl Pd(IV) complexes **14-17** in water was studied. The decomposition of these complexes generates the corresponding oxapalladacycles **22-25** in >95 % yield. Aqueous solutions of complexes **14-17** were prepared *in-situ* by combining 0.010 M D<sub>2</sub>O solutions of complexes **10-13** with 5.0 equivalents of H<sub>2</sub>O<sub>2</sub> at 0°C. In the preparation of complexes **14-17**, complexes **18-21** were also observed as minor complexes. When monitored by <sup>1</sup>H NMR at 0 °C, no decomposition was observed for up to 2 hours, but when the temperature of these solutions was raised to 22 °C, clean C–O reductive

elimination was observed to generate the corresponding oxapalladacycles **22-25**. Representative plots for the C–O bond reductive elimination reactions from complex **15** and **17** are presented in figure 3.1 below.

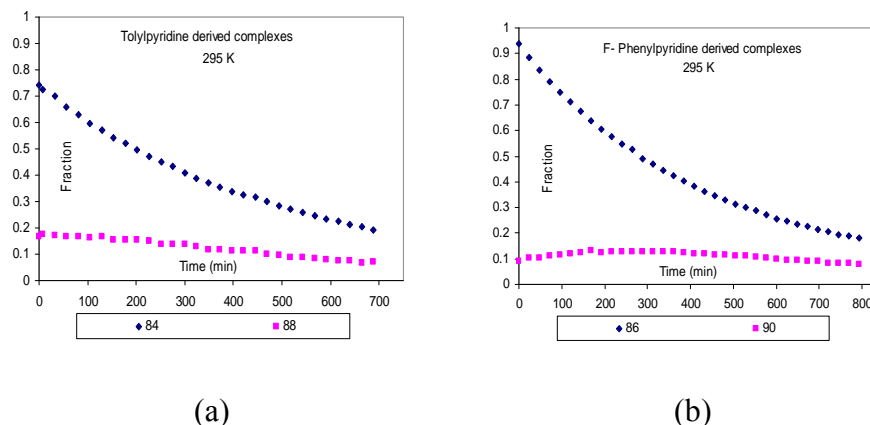


**Figure 3. 1.** Plot for the C–O reductive elimination reaction of 0.010 M D<sub>2</sub>O solutions of complexes (a) **15** and **19** and (b) **17** and **21** at 22 °C.

The product of C–O reductive elimination of complexes **15** and **19**, complex **23** was characterized completely by NMR spectroscopy, ESI-MS, and single crystal X-ray diffraction, while its purity was confirmed using elemental analysis. X-ray quality crystals of complex **23** were grown by slow evaporation of an acetone solution of the complex under air.

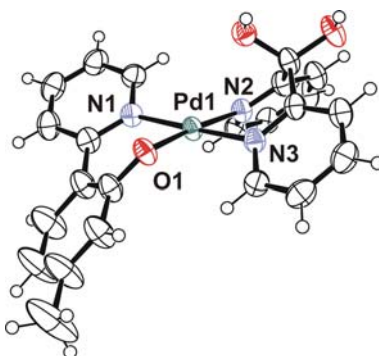
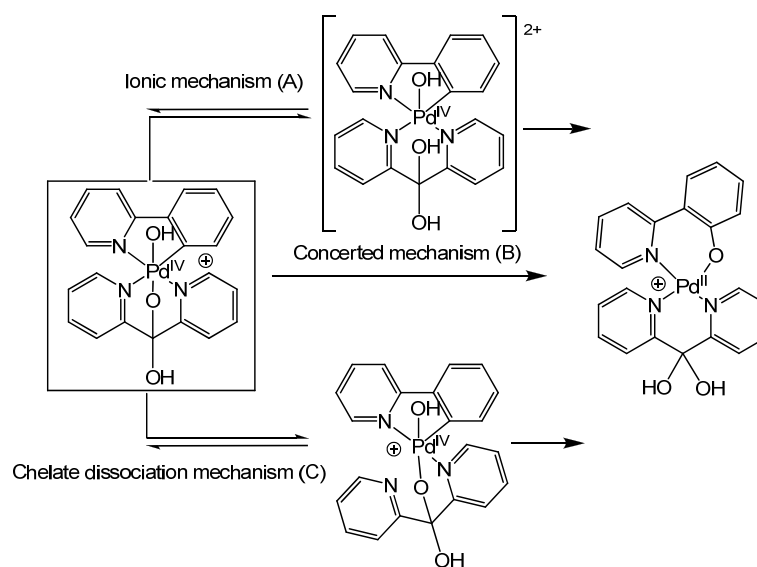


**Figure 3. 2.** ORTEP drawings (50% probability ellipsoids) of Pd(II) aryloxide cation **23** in **23(OAc)**.

Complex **25** was also characterized by NMR spectroscopy, electrospray mass spectrometry, and X-ray diffraction (see the experimental section). Complexes **22** and **24** were not isolated but converted to the corresponding phenols by hydrolysis of the oxapalladacycles with HCl at 70°C for 6 hours. The phenolic products were isolated from the aqueous solutions by extraction with diethyl ether. The identity of the known phenols was determined by comparison to literature while unknown phenols were identified via NMR spectroscopy and ESI mass spectrometry.

In the study of the mechanism of reductive elimination from the monohydrocarbyl Pd(IV) complexes derived from substituted phenylpyridine ligands **14-17**, the following pathways were considered: (i) ionic mechanism A, where preliminary dissociation of an alkoxide ligand produces a dicationic 5-coordinate Pd(IV) intermediate that undergoes C–O reductive elimination; (ii) concerted mechanism B, where C–O bond reductive elimination takes place from a cationic 6-coordinate Pd(IV) species; (iii) chelate dissociation mechanism C, where dissociation of a pyridine group of the dpk ligand takes place prior to C–O bond elimination from a cationic 5-coordinate species. These mechanisms were considered because there is literature precedent for each in reductive elimination reactions from group 10 metal centers. For example, the ionic mechanism A has been proposed for C(sp<sup>3</sup>)–O,<sup>86,179,180,182,183,189</sup> C(sp<sup>3</sup>)–halogen,<sup>200,201</sup> C(sp<sup>3</sup>)–N,<sup>202</sup> and C(sp<sup>2</sup>)–halogen<sup>203</sup> bond forming reductive elimination reactions from Pt(IV) center, the chelate dissociation mechanism B has been reported for some C–C bond forming reactions from Pt(IV) center,<sup>197-199</sup> while a concerted-type mechanism C has been implicated for C(sp<sup>2</sup>)–O,<sup>95,190-196</sup> C(sp<sup>2</sup>)–N,<sup>204</sup> and C(sp<sup>2</sup>)–S<sup>205,206</sup> reductive elimination from Pd(II) centers.

**Scheme 3. 7**



*Kinetics study for C–O reductive elimination from complex 15 in water in the presence of various additives*

We started by performing C–O reductive elimination studies of aqueous solutions of complex **15** in the presence of various additives, including trifluoroacetic acid, KOAc, and pyridine. Thus, 0.010 M aqueous solution of complex **15** was prepared by combining 0.010 M aqueous solution of complex **10** with 5.0 equivalents of H<sub>2</sub>O<sub>2</sub> in ice-water bath at 0 °C. The additive was added into the solution at 0 °C and the temperature of the resulting solution was raised to 22 °C. Consecutive <sup>1</sup>H NMR spectra were collected at regular intervals and the concentration of complex **15** was monitored as a function of time. The kinetic plots of ln([**15**]<sub>0</sub>/[**15**]<sub>t</sub>) as a function of time for the C–O reductive elimination reaction from complex **15** in D<sub>2</sub>O in the presence of the pyridine, trifluoroacetic acid and acetate anion at 22 °C were found to be linear. [**15**]<sub>0</sub> refers to the initial concentration of complex **15** while [**15**]<sub>t</sub> refers to

the concentration of complex **15** at time  $t$ . The observed first order rate constants are given in table 3.1 below.

**Table 3. 1.** Observed first order rate constants for C–O reductive elimination at complex **15** in D<sub>2</sub>O in the presence of various additives at 22 °C in water.

Entry	Additive	k (min <sup>-1</sup> )
1	none	(1.37 ± 0.02) · 10 <sup>-3</sup>
2	5.0 eq pyridine	(2.38 ± 0.04) * 10 <sup>-3</sup>
3	5.0 eq KOAc	(1.32 ± 0.01) * 10 <sup>-3</sup>
4	2.0 eq tfa	(3.45 ± 0.03) * 10 <sup>-3</sup>
5	4.0 eq tfa	(3.46 ± 0.04) * 10 <sup>-3</sup>

*Kinetics study for C-O reductive elimination from complex **14-17** in water in the presence of 4.0 equivalents of trifluoroacetic acid*

As a result of the mild acceleration of C–O bond coupling for complex **15** in the presence of trifluoroacetic acid, C–O reductive elimination reactions were carried out for complexes **14**, **16** and **17** in the presence of 4.0 equivalents of trifluoroacetic acid. 0.010 M D<sub>2</sub>O solutions of complexes **14**, **16** and **17** were combined with 5.0 equivalents of H<sub>2</sub>O<sub>2</sub> in ice-water bath at 0 °C. 4.0 equivalents of deuterated trifluoroacetic acid were added to the solutions and consecutive <sup>1</sup>H NMR spectra were collected at regular intervals at 22 °C. The kinetic plots of ln([Pd(IV)]<sub>0</sub>/[Pd(IV)]<sub>t</sub>) vs. time for these reactions were found to be linear. Representative plots are given below.

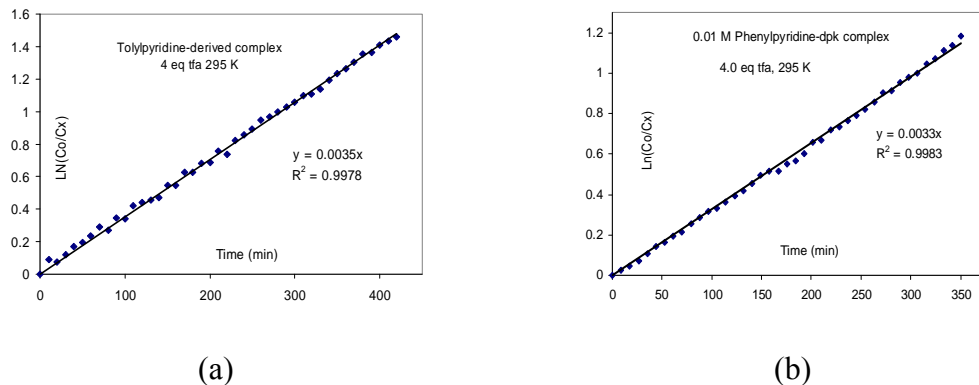


**Figure 3. 3.** First order kinetic plots for the decomposition of D<sub>2</sub>O solutions of complexes (a) **15** and (b) **14** in the presence of 4.0 equivalents of trifluoroacetic acid at 22 °C

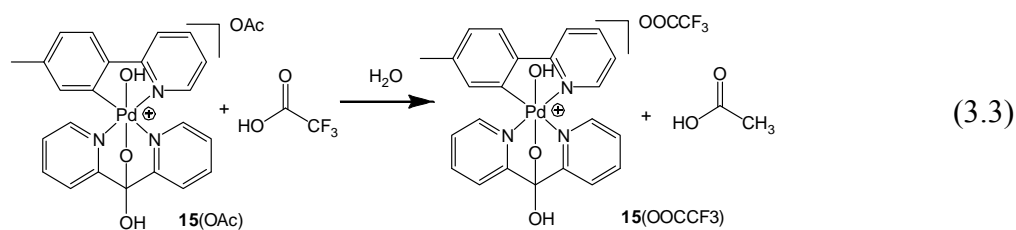
**Table 3. 2.** Observed first order rate constants for C–O reductive elimination at complexes **14-17** in water in the presence 4.0 equivalents of tfa-*d*<sub>1</sub> at 22 °C.

Entry	Complex	-R	$k_{\text{obs}}, \text{min}^{-1}$	$k_{\text{obs}}, \text{min}^{-1}$
			(no acid additive)	(4 eq tfa)
1	<b>14</b>	-H	$(1.65 \pm 0.02) \cdot 10^{-3}$	$(3.90 \pm 0.04) \cdot 10^{-3}$
2	<b>15</b>	-Me	$(1.37 \pm 0.02) \cdot 10^{-3}$	$(3.50 \pm 0.04) \cdot 10^{-3}$
3	<b>16</b>	-OMe	$(1.41 \pm 0.01) \cdot 10^{-3}$	$(2.16 \pm 0.05) \cdot 10^{-3}$
4	<b>17</b>	-F	$(1.74 \pm 0.01) \cdot 10^{-3}$	$(3.50 \pm 0.05) \cdot 10^{-3}$

The trifluoroacetic acid and LiOAc additives were used to probe a potential ionic mechanism A. C–O reductive elimination reactions that take place via preliminary dissociation of an ionic ligand have been observed to undergo rate acceleration in the presence of Bronsted acid additives. For example, Goldberg and co-workers observed acceleration of C–O and C–C reductive elimination reactions from diphosphine-ligated trihydrocarbylacetato Pt(IV) complexes in the presence of

Bronsted and Lewis acids, where the additives were proposed to speed up the reactions by accelerating the dissociation of the  $\text{OR}^-$  ligand.<sup>180</sup> Similarly, Sanford and co-workers observed acceleration of C–O reductive elimination from bipyridine ligated biaryldiacetato Pd(IV) complexes in the presence of Bronsted and Lewis acid additives.<sup>58</sup> As a result, rate acceleration of C–O reductive elimination from complexes **14-17** in the presence of Bronsted acids would indicate preliminary dissociation of  $\text{OR}^-$  group from the palladium coordination sphere prior by C–O bond formation from a 5-coordinate species. However the rate of C–O reductive elimination reactions from complexes **14-17** was not significantly accelerated by Bronsted acids. Approximately the same two-fold acceleration was observed when either 2.0 or 4.0 equivalents of trifluoroacetic acid were added. These observations are not in favor of an ionic mechanism A.

The minor acceleration brought about by trifluoroacetic acid could be due to a counterion effect. Given that only two-fold acceleration was observed irrespective of the concentration of trifluoroacetic acid used (2.0 vs 4.0 equivalent), we propose that the acid acts as a reagent in this system. As a reagent, trifluoroacetic acid protonates the acetate counterion and produces acetic acid and trifluoroacetate counterion instead (eq. 3.3). Since acetate is a stronger base compared to trifluoroacetate, the latter is expected to make a weaker ion pair interaction with the cationic complex **15**, and lead to a less stable and more reactive complex (this interaction is also affected by solvation, hydrogen bonding among other factors).



C–O reductive elimination reactions that proceed via preliminary dissociation of an anionic ligand have also been observed to be inhibited by exogenous anionic ligands in solution.<sup>180</sup> These anions drive the equilibrium between the 5- and the 6-coordinate complexes towards the 6-coordinate complex. This decreases the fraction of the reactive 5-coordinate complex in solution, which in turn decreases the rate of reaction. In a C–C reductive elimination reaction from  $\text{dppePt(IV)Me}_3(\text{OAr})$  complex that was proposed to take place via pre-equilibrium  $\text{OR}^-$  ligand dissociation, Goldberg and co-workers observed inhibition of the elimination reaction in the presence of exogenous aryloxide ligands.<sup>180</sup> Sanford and co-workers also observed inhibition of a C–O reductive elimination reaction from  $(\text{phenylpyridyl})_2\text{Pd(IV)OAc}_2$  that was proposed to take place via preliminary dissociation of an acetate ligand, by exogenous acetate anions.<sup>58</sup> As a result, inhibition of C–O reductive elimination from complexes **14-17** would indicate preliminary dissociation of the  $\text{OR}^-$  ligand, and thus favor the ionic mechanism A. The presence of 5.0 equivalents of acetate anions however had no effect on the rate of C–O reductive elimination from aqueous solutions of complex **15**, thus ruling out the ionic mechanism A (In this system, acetate anions were used instead of more basic  $\text{OH}^-$  or  $\text{OMe}^-$  because these stronger bases deprotonate complex **15** to produce the less a soluble zwitterionic analog).

In order to determine whether mechanism C is operative, where preliminary dissociation of the chelate prior to C–O reductive elimination from a 5-coordinate species takes place, the reductive elimination reaction was conducted in the presence of 5.0 equivalents of pyridine. Goldberg and co-workers studied a C–C reductive elimination system which was proposed to proceed via preliminary chelate

dissociation. They prepared *fac*-(PMe<sub>3</sub>)<sub>2</sub>Pt(IV)Me<sub>3</sub>(OAc) complex and investigated its C–C reductive elimination reaction in the presence of added phosphine ligand. They found that phosphine additives significantly inhibit the C–C reductive elimination reaction, indicating that phosphine ligand dissociation precedes the C–C coupling reaction.<sup>180</sup> Considering this report, inhibition of C–O reductive elimination from complex **15** in the presence of pyridine additive would indicate preliminary chelate dissociation preceding C–O bond coupling as the operative mechanism, C. However C–O reductive elimination from complex **15** in water was not inhibited by 5.0 equivalents of pyridine additive. As a result, this pathway was ruled out and pathway B was considered, where the reductive elimination reaction proceeds from a 6-coordinate species.

C–C reductive elimination reaction from biaryl Pd(IV) complexes that proceed via 6-coordinate species was reported by Sanford and co-workers.<sup>58</sup> In that system, both C–O and C–C reductive elimination reactions were possible, but each was favored under different reaction conditions. Reaction conditions that favor dissociation of an anionic ligand led to predominant C–O reductive elimination while reaction conditions that disfavor acetate ligand dissociation led to predominant C–C bond coupling. Exclusive experiments were however not designed to interrogate the proposed mechanism of C–C bond formation from 6-coordinate palladium complex.

In our system, the absence of rate acceleration in the presence of Bronsted acids and the lack of inhibition by exogenous acetate anions enabled us to rule out mechanism A. The absence of inhibition of the C–O reductive elimination reaction by pyridine additive enabled us to rule out mechanism C. Consequently, mechanism B

which involves C–O reductive elimination from a 6-coordinate species was proposed as the operative mechanism. This mechanism was also supported by theoretical calculations.

### *Theoretical Calculations*

The theoretical calculations were performed using density functional theory (DFT) method,<sup>1</sup> specifically functional PBE,<sup>2</sup> implemented in an original program package “Priroda”.<sup>3</sup> The basis set was 311-split for main group elements with one additional polarization *p*-function for hydrogen, additional two polarization *d*-functions for elements of higher periods.

In the DFT calculations, two pathways for the C–O reductive elimination reaction from complex **15** were considered. The first pathway involves reductive elimination from a 6-coordinate complex via the transition state **TS6** while the second pathway involves reductive elimination from a 5-coordinate Pd(IV) intermediate **26** via the transition state **TS5**. The barrier for reductive elimination from the 5-coordinate complex produced upon dissociation of a chelate arm was found to be higher than that from a 6-coordinate species, indicating that the former pathway via **TS5** is less competitive. In the **TS6**, the pyridyl nitrogen atom *trans*- to the aryl carbon is only partially dissociated with a Pd–N distance of 2.518 Å in **26** vs. 2.239 Å in **15**. Given that the chelate dissociation in the transition state **TS6** is not too significant, the reductive elimination reaction can be considered to take place from a 6-coordinate species, in agreement with our experimental observations.

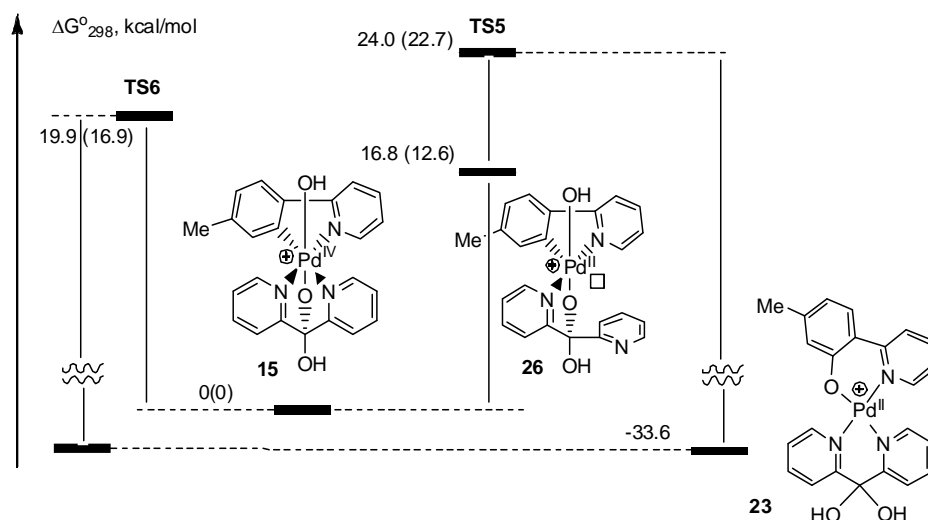
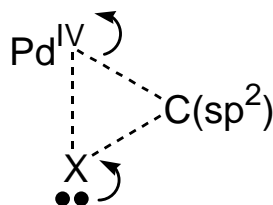


**Figure 3. 4.** The DFT-calculated Gibbs energy reaction profile for C–O reductive elimination reaction at complex **15** in gas phase and aqueous solutions in parenthesis (kcal/mol) leading to corresponding palladacyclic aryloxide **23**.

#### *C–O reductive elimination process: Substituent effects*

C(sp<sup>2</sup>)–O reductive elimination from hydrocarbyl Pd(IV) complexes has been proposed to proceed through a three-center, four-electron transition state (see scheme below).<sup>45</sup> Although the geometry of the coordination spheres of the complexes involved differs substantially, the process itself has been suggested to be comparable to related reductive elimination from Pd(II) complexes. The precise mechanistic picture of the process of reductive elimination from Pd(IV) is not yet fully understood because these complexes are too reactive to allow structure isolation and advanced mechanistic studies.



Up until now, the most common studied reaction that involves reductive elimination from Pd(IV) via a concerted 3-center 4-electron pathway is C(sp<sup>2</sup>)-O reductive elimination of aryl carboxylates from diaryl dicarboxylato Pd(IV) complexes.<sup>57,58</sup> In this system, experiments were designed to probe the electronic effect of carboxylate and arylpyridine ligands on the C-O reductive elimination reaction. Faster C-O reductive elimination reactions were observed when electron-rich benzoate ligands and electron-poor arylpyridine fragments were employed, indicating that the carboxylate ligand act as a nucleophilic coupling partner while the aryl ring acts as an electrophilic coupling partner in the C-O reductive elimination reaction.

We designed experiments to study the electronic effects of the arylpyridine fragment, where a series of complexes containing electronically varied arylpyridine ligands were prepared to place different electron-withdrawing and electron-donating substituents *meta*- to the Pd-bound carbon atom (complexes **14-17**).

*Kinetics study for the C-O reductive elimination reactivity from complexes 14-17 in water to study substituent effect*

Reductive elimination from complexes **14-17** to produce complexes **22-25** in D<sub>2</sub>O was monitored by <sup>1</sup>H NMR spectroscopy. 0.010 M D<sub>2</sub>O solutions of complexes **10-13** were combined with 5.0 eq of H<sub>2</sub>O<sub>2</sub> in ice-water bath at 0 °C to generate the Pd(IV) adducts in-situ, and 1.0 μl of dioxane was added as internal standard; these complexes were prepared *in-situ* since they are too reactive to be isolated. Upon formation of the Pd(IV) complexes, the temperature was raised to 22 °C to allow for

the C–O bond reductive elimination to take place, and consecutive  $^1\text{H}$  NMR spectra were collected at regular intervals. Representative plots of  $\ln([\text{Pd(IV)}]_0/[\text{Pd(IV)}]_t)$  as a function of time for the C-O reductive elimination reaction of complexes **14** and **17** in  $\text{D}_2\text{O}$  at 22 °C are given below;  $[\text{Pd(IV)}]_0$  refers to the initial concentration of the Pd(IV) reactant while  $[\text{Pd(IV)}]_t$  refers to the concentration of the Pd(IV) complex at a time,  $t$ . These plots were found to be linear.

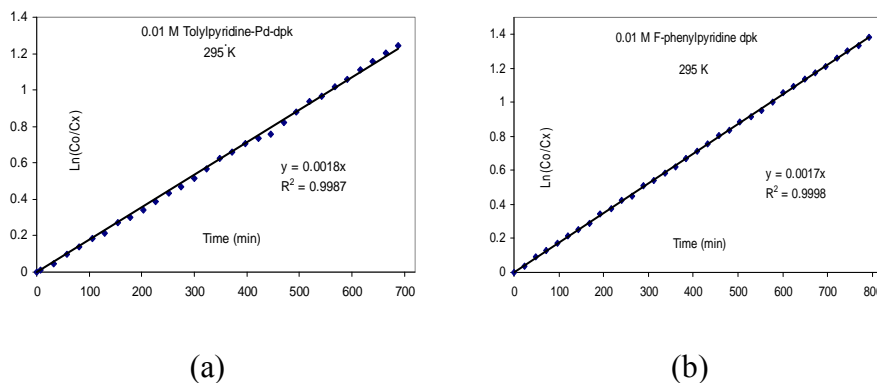


**Figure 3. 5.** First order kinetic plots for the decomposition of aqueous solutions of complexes (a) **15** and (b) **17** at 22 °C.

Reductive elimination from the Pd(IV) complexes was observed to follow 1<sup>st</sup> order kinetics with the following first order rate constants at 22 °C.

**Table 3. 3.** Observed first order rate constants for C–O reductive elimination at complexes **14-17** in water at 22 °C.

Entry	-R	Complex	$k$ ( $\text{min}^{-1}$ )
1	-H	<b>14</b>	$(1.65 \pm 0.02) \cdot 10^{-3}$
2	-Me	<b>15</b>	$(1.37 \pm 0.02) \cdot 10^{-3}$
3	-OMe	<b>16</b>	$(1.41 \pm 0.01) \cdot 10^{-3}$
4	-F	<b>17</b>	$(1.74 \pm 0.01) \cdot 10^{-3}$

The substituent effect was evaluated using the Hammett plot shown below. The  $\rho$  was found to be  $\sim 0$ , indicating the absence of substituent effects.

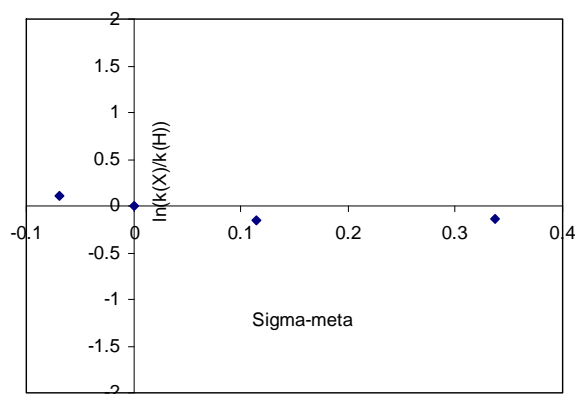


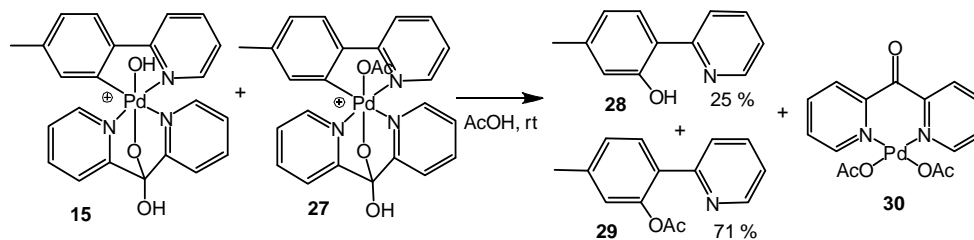
**Figure 3. 6.** Hammett plot for the decomposition of aqueous solutions of complexes **14-17** at 22 °C.

The observed near zero slope of the Hammett plot indicates no substituent effects of the aryl rings. This indicates that the C–O reductive elimination reaction is not sensitive to the electronics of the arylpyridine fragment. This is contrary to literature reports, where the aryl rings with electron-withdrawing groups have been found to accelerate C–O reductive elimination reactions, leading to the proposal that the carboxylate ligands act as the nucleophilic coupling partners while the aryl rings act as electrophilic coupling partners in these reactions.<sup>58</sup> As a result, we propose that the lack of substituent effects may be a result of a very exergonic reaction as a result of a significantly early transition state.

### 3.2.2 C–O Reductive Elimination Reactivity at Monohydrocarbyl Pd(IV) Complexes

#### 15 in Acetic Acid

**Scheme 3. 8**



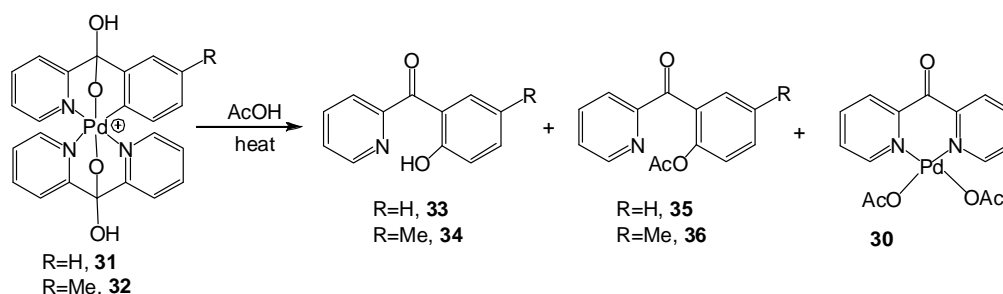
Reaction of complex **11** with  $\text{H}_2\text{O}_2$  in acetic acid generates a mixture of complexes **15** and **27** in 22% and 38 % respectively after 10 minutes, due to a slow oxidation reaction. Both complexes were observed by  $^1\text{H}$  NMR spectroscopy and detected via ESI–MS (see chapter 2 for characterization of these complexes). Complexes **15** and **27** decompose at room temperature to produce the corresponding phenol **28** in 25 % yield and aryl acetate **29** in 71 % yield. The identity of compound **28** was confirmed by comparison of the NMR spectra to literature publication,<sup>207</sup> while the identity of compound **29** and complex **30** were confirmed by independent synthesis.

3.3 C–O Reductive Elimination Reactivity at Monohydrocarbyl Pd(IV) Complexes **31** and **32** in Various Solvents

3.3.1 C–O Reductive Elimination Reactivity at Monohydrocarbyl Pd(IV) Complexes

**31** and **32** in Acetic Acid

**Scheme 3. 9**



The reactivity of Pd(IV) complexes **31** and **32** towards C–O reductive elimination was studied. Acetic acid solutions of 0.010 M complexes **31** and **32** were prepared, 1.0  $\mu\text{l}$  of 1,4 dioxane was added as internal standard, and the resulting yellow solutions were warmed to 63°C in a NMR tube. After 12 hours, the  $^1\text{H}$  NMR spectra of the resulting solutions were complex indicating the presence of multiple species in solution. However upon addition of a small amount of pyridine to free coordinated products, simple  $^1\text{H}$  NMR spectra resulted revealing clean formation of the corresponding phenol **33** and **34** and aryl acetate **35** and **36** products. When an acetic acid solution of complex **31** was warmed at 63°C in the presence of 10 % acetic anhydride by volume, the expected aryl acetate **35** was produced as the only product quantitatively. The identity of the compound **33** was confirmed by comparison of the NMR spectra to literature publications,<sup>157</sup> while the identity of compounds **34**, **35**, and **36** was confirmed by independent synthesis via acetoxylation of the

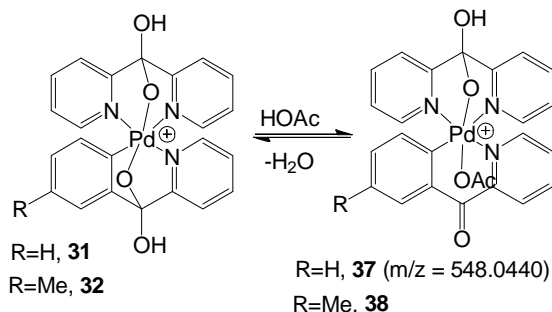
corresponding phenols in Ac<sub>2</sub>O/AcOH solvent mixture. These compounds were characterized by NMR spectroscopy and ESI-MS.

**Table 3. 4.** <sup>1</sup>H NMR yields of phenol and aryl acetate from C–O reductive elimination reactions at complexes **31** and **32** in acetic acid at 63°C.

Entry	Complex	Phenol	Aryl acetate
1	<b>31</b>	38	58
2	<b>32</b>	35	59

This experiment indicates that C–O reductive elimination from Pd(IV) complexes **31** and **32** is facile in acetic acid solvent. The formation of the aryl-acetate products may involve an acetato-ligated Pd(IV) complex, **37** or **38** (See Scheme 3.10). During the reductive elimination reaction from complex **31** in acetic acid, a mass envelope at  $m/z = 548.0440$  was observed by ESI-MS, which may be assigned to complex **37**, (Calculated for complex **37**, C<sub>25</sub>H<sub>21</sub>N<sub>3</sub>O<sub>5</sub><sup>106</sup>Pd = 548.0448). Complex **37** or **38** may form *in-situ* via chelate opening of complex **31** or **32** in acetic acid as shown below. The phenolic products **33** and **34** are produced via C–OH reductive elimination from complexes **31** and **32** respectively while the aryl acetate products **35** and **36** are produced via C–OAc reductive elimination from complexes **37** and **38** respectively.

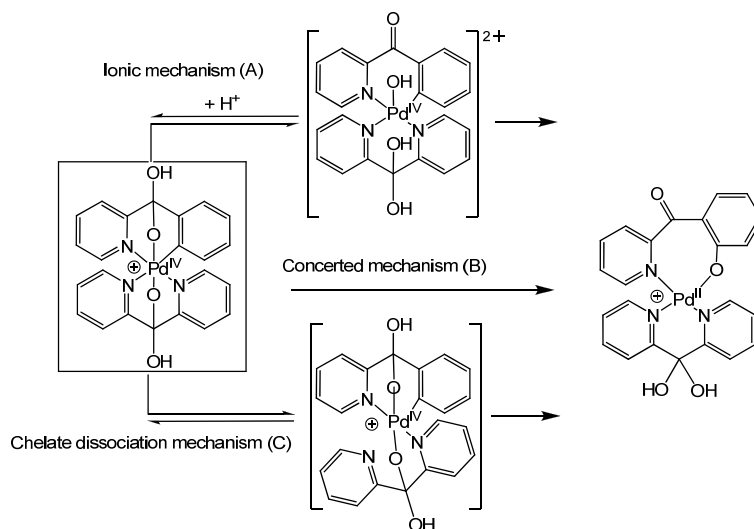
**Scheme 3. 10**



*Mechanistic Study of C–O Reductive Elimination from Monohydrocarbyl Pd(IV) Complexes Derived from 2-aryloxy-pyridine Ligands **31** and **32** in Acetic acid.*

In the study of the mechanism of reductive elimination from monohydrocarbyl Pd(IV) complexes derived from the 2-aryloxy-pyridine derived fragments **31** and **32**, the following pathways were considered: (I) ionic mechanism A, where the alkoxide ligand dissociates from the Pd coordination sphere, followed by C–O reductive elimination from a dicationic 5-coordinate species; (II) concerted mechanism B, where C–O bond reductive elimination takes place from a cationic 6-coordinate palladium species; (III) chelate dissociation mechanism C, where dissociation of the pyridyl arm of the dpk ligand trans to the phenyl ligand takes place prior to C–O reductive elimination from a cationic 5-coordinate species. These mechanisms were considered because there is literature precedent for each in the reductive elimination processes from group 10 metal centers. Several experiments were designed to determine the most favorable mechanism, including the study of the C–O reductive elimination reaction in the presence of various additives.

**Scheme 3. 11**



Reductive elimination of complex **31** in acetic acid in the presence of various additives was studied by  $^1\text{H}$  NMR.

*Trifluoroacetic acid (tfa) additive*

The decomposition of complex **31**( $\text{OOC}\text{CF}_3$ ) in acetic acid in the presence of 5.0 eq of trifluoroacetic acid was monitored by  $^1\text{H}$  NMR spectroscopy. A 0.010 M acetic acid solution of complex **31** was prepared and 5 eq of tfa was added to the solution followed by 1.0  $\mu\text{l}$  dioxane as internal standard. Consecutive  $^1\text{H}$  NMR spectra were collected at  $56^\circ\text{C}$ . Clean formation of the corresponding aryl acetate **35** and phenol **33** in 10 % and 28 % yields respectively was observed. The graph of  $\ln([\mathbf{31}]_0/[\mathbf{31}]_t)$  as a function of time for the C–O reductive elimination reaction of **31** in  $\text{AcOH-}d_4$  at  $56^\circ\text{C}$  in the presence of 5.0 equivalents of tfa was found to be linear, indicating an overall first order reaction. The first order rate constant for this reaction is presented in the table below.

**Table 3. 5.** Observed first order rate constants for the C–O reductive elimination reaction at complex **31** in AcOD at  $56^\circ\text{C}$  in the presence and absence of 5.0 equivalents of tfa additive.

Additive	$K_{\text{obs}}$ ( $\text{min}^{-1}$ )	Temp
5.0 eq tfa	$(9.09 \pm 0.18) * 10^{-3}$	$56^\circ\text{C}$
No additive	$(6.21 \pm 0.18) * 10^{-3}$	$56^\circ\text{C}$

This indicates that trifluoroacetic acid does not significantly influence the rate of C-O reductive elimination from complex **31**.

### *LiOAc additive*

The decomposition of complex **31(OOCCF<sub>3</sub>)** in acetic acid solvent in the presence of 5.0 eq of LiOAc was monitored by <sup>1</sup>H NMR spectroscopy. A 0.010 M acetic acid solution of complex **31** was prepared and 5 eq of LiOAc was added to the solution followed by 1.0 μl dioxane as internal standard. Consecutive <sup>1</sup>H NMR spectra were collected at 55°C. Clean formation of the corresponding aryl acetate and phenol products in 64 % and 28 % yields respectively was observed. The graph of ln([**31**]<sub>0</sub>/[**31**]<sub>t</sub>) vs. time for the C–O reductive elimination reaction of **31** in AcOH-*d*<sub>4</sub> at 55°C in the presence of 5.0 equivalents of LiOAc was found to be linear, indicating an overall first order reaction. The first order rate constant for this reaction is presented in the table below.

**Table 3. 6.** Observed first order rate constants for the C–O reductive elimination reaction at complex **31** in AcOD at 56°C in the presence and absence of 5.0 equivalents of LiOAc additive.

Additive	k (min <sup>-1</sup> )	Temp
5.0 eq LiOAc	(8.18 ± 0.06) * 10 <sup>-3</sup>	56°C
No additive	(6.21 ± 0.18) * 10 <sup>-3</sup>	56°C

The rate of C–O bond reductive elimination from an acetic acid solution of complex **31** in the presence of 5.0 equivalents of exogenous LiOAc is not inhibited.

### *Pyridine additive*

The decomposition of complex **31(OOCCF<sub>3</sub>)** in acetic acid solvent in the presence of 5.0 eq of pyridine additive was monitored by <sup>1</sup>H NMR spectroscopy. A

0.010 M acetic acid solution of complex **31** was prepared and 5 eq of pyridine was added to the solution followed by 1.0  $\mu\text{l}$  dioxane as internal standard. Consecutive  $^1\text{H}$  NMR spectra were collected at 48°C. Clean formation of the corresponding aryl acetate and phenol products in 72 % and 24 % yields respectively was observed. The graph of  $\ln([\mathbf{31}]_0/[\mathbf{31}]_t)$  vs. time for the C–O reductive elimination reaction of **31** in  $\text{AcOH-}d_4$  at 48°C in the presence of 5.0 equivalents of pyridine was found to be linear, indicating an overall first order reaction. The first order rate constant for this reaction is presented in the table below.

**Table 3. 7.** Observed first order rate constants for the C–O reductive elimination reaction at complex **31** in AcOD at 48°C in the presence and absence of 5.0 equivalents of pyridine additive.

<b>Additive</b>	<b><math>K_{\text{obs}}</math> (<math>\text{min}^{-1}</math>)</b>	<b>Temp</b>
5.0 eq pyr	$(4.3 \pm 0.1) * 10^{-4}$	48°C
No additive	$(2.7 \pm 0.3) * 10^{-3}$	48°C

Pyridine was observed to slow the reaction at least 10-fold.

#### *Water additive*

A 0.010 M acetic acid solution of complex **31(OOCCF<sub>3</sub>)** was prepared and 28 % of  $\text{D}_2\text{O}$  by volume was added into the solution followed by 1.0  $\mu\text{l}$  dioxane as internal standard. Consecutive  $^1\text{H}$  NMR spectra of the solution were collected at 48°C. Clean formation of the corresponding phenol was observed with a total yield of > 95 %; no aryl acetate product was detected by  $^1\text{H}$  NMR. The graph of  $\ln([\mathbf{31}]_0/[\mathbf{31}]_t)$  as a function of time for the C–O reductive elimination reaction of

complex **31** in AcOH- $d_4$  at 48°C in the presence of 28 % water is given below. This plot was found to be non-linear, as a result the time for 50 % conversion is given.

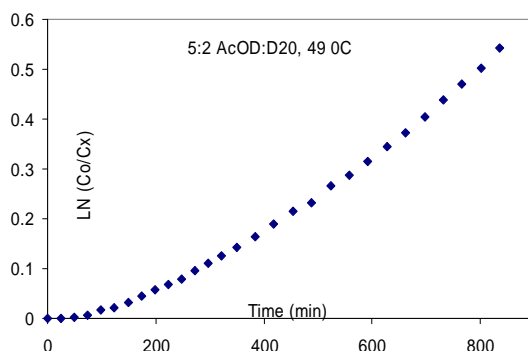


**Figure 3. 7.** First order kinetic plot for the decomposition of complex **31** in AcOD/D<sub>2</sub>O solvent mixture (5:2) at 49 °C

**Table 3. 8.** Time (min) for the 50% conversion of complex **31** in the C–O reductive elimination reaction at complex **31** in AcOD at 48°C in the presence and absence of 28% of water.

Additive	50 % conversion (min <sup>-1</sup> )	Temp
28 % water	210	48°C
No additive	265	48°C

This indicates that water slows down the rate of C–O coupling.

**Table 3. 9.** Summary of the influence of various additives on the rate of C–O reductive elimination from acetic acid solutions of complex **31**.

Entry	Additive	Effect on K <sub>obs</sub>
1.	5.0 eq Pyridine	Slows reaction rate 10-fold
2.	Water	Slows rate 3-fold
3.	LiOAc	No significant effect on rate
4.	tfa	No significant effect on rate

### *Discussion of the mechanism of C–O reductive elimination*

Bronsted acids have been observed to increase the rate of C–O reductive elimination reactions that proceed via preliminary dissociation of an anionic ligand, which is followed by reductive elimination from a 5-coordinate palladium species.<sup>58</sup> The acid has been proposed to accelerate the rate of ligand dissociation, which in turn accelerates the overall elimination reaction. However, trifluoroacetic did not have any noticeable effect on the rate of C–O reductive elimination from complex **31** in acetic acid. This is inconsistent with a mechanism that involves pre-equilibrium dissociation of an anionic ligand, and thus mechanism A was ruled out.

Exogenous anionic ligands have also been observed to inhibit C–O reductive elimination reactions that proceed via initial loss of an anionic ligand.<sup>57,180</sup> However LiOAc was found to have no effect on the rate of C–O reductive elimination from complex **31** in acetic acid, which is also inconsistent with a mechanism that involves pre-equilibrium dissociation of an anionic ligand prior to C–O bond reductive elimination from a 5-coordinate reactive species. This additional experimental observation enabled us to rule out mechanism A.

In a mechanism that involves dissociation of one arm of a chelate, additives of a neutral Lewis basic ligand have been found to inhibit such reactions. For example, Goldberg and co-workers found phosphine additives to inhibit C–C reductive elimination from (PMe)<sub>3</sub>Pt(IV)Me<sub>3</sub>(OAc) complexes that proceed from a 5-coordinate palladium intermediate produced upon preliminary dissociation of phosphine ligand.<sup>180</sup> In our studies, pyridine additive was used to probe whether pyridine ligand dissociation from the dpk chelate takes place prior to C–O reductive

elimination from the resulting 5-coordinate intermediate. Indeed, pyridine was found to inhibit C–O reductive elimination from complex **31** in acetic acid significantly. Water was also found to inhibit the C–O reductive elimination reaction. In this system, water was proposed to act as a neutral Lewis basic ligand similar to pyridine. These results indicate that the C–O reductive elimination reaction takes place from a 5-coordinate species formed upon chelate dissociation, mechanism C.

Reactions that proceed via preliminary dissociation of a neutral ligand have been reported to display high positive entropy values. For example in a series of diphosphino Pt(IV)Me<sub>4</sub> complexes that were proposed to undergo C–C reductive elimination from 5-coordinate intermediates produced via preliminary dissociation of a phosphine ligand, Goldberg and co-workers found these reactions to proceed with relatively high entropy of  $15 \pm 4$  eu. Thus, Eyring analysis was performed on the C–O reductive elimination from complex **31** in acetic acid to obtain the enthalpy and entropy parameters.

*Activation parameters for C–O bond reductive elimination of acetic acid solutions of complex **31(OOCCF<sub>3</sub>)***

0.010 M acetic acid solution of **31(OOCCF<sub>3</sub>)** was prepared and 1.0  $\mu$ l 1,4-dioxane was added as internal standard. The resulting yellow solution was monitored by <sup>1</sup>H NMR spectroscopy at various temperatures. Clean formation of the corresponding phenol and aryl acetate products was observed. The concentration of the Pd(IV) precursor **31** was monitored by integration of a single peak that did not overlap with other peaks using 1,4-dioxane as an internal standard. The color of the

solution changed from deep yellow to colorless as the reaction progressed. The disappearance of complex **31** was observed to follow first order kinetics. Representative plots of  $\ln([\mathbf{31}]_o/[\mathbf{31}]_t)$  as a function of time for the C–O reductive elimination of **31** in  $\text{AcOH-}d_4$  at various temperatures are given in figure 3.8 below.

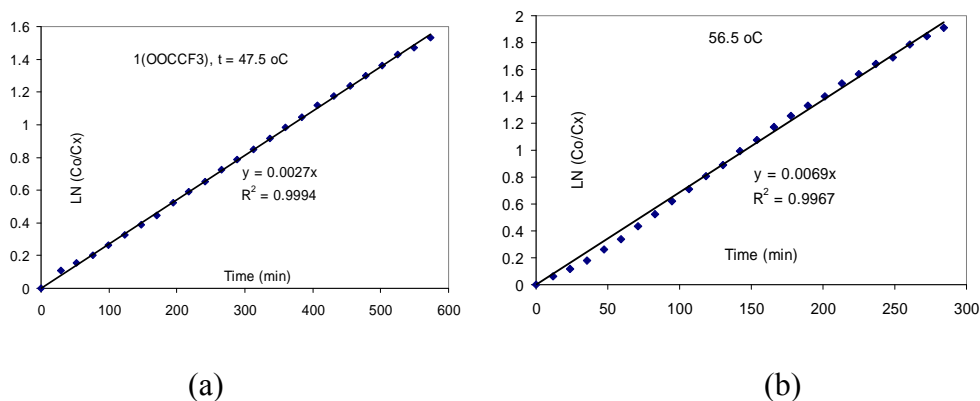


**Figure 3. 8.** First order kinetic plots for the decomposition of acetic acid solutions of complex **31** at (a) 47.5°C and (b) 56.5°C.

The first order rate constants  $k_{\text{red}}$  are given in the table below:

**Table 3. 10.** Observed first order rate constants for C–O reductive elimination from acetic acid solutions of complex **31**(OCCF<sub>3</sub>) at various temperatures.

Temperature (K)	$k_{\text{red}}, \text{min}^{-1}$
21.5	$(2.7 \pm 0.03) \cdot 10^{-3}$
22.5	$(6.9 \pm 0.14) \cdot 10^{-3}$
334	$(1.08 \pm 0.007) \cdot 10^{-2}$
346.5	$(3.67 \pm 0.158) \cdot 10^{-2}$

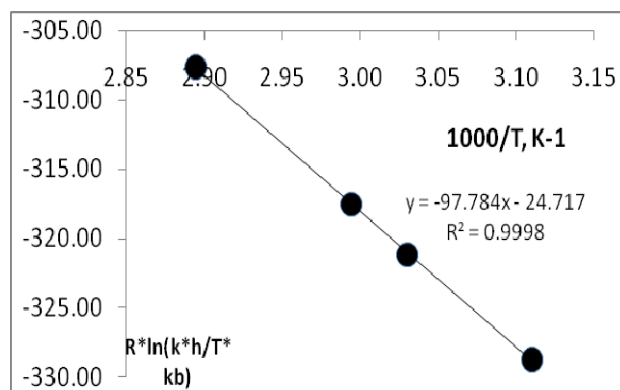


**Figure 3. 9.** Eyring plot for decomposition of complex **31**(OOCCF<sub>3</sub>) in acetic acid.

The activation parameters were found to be as follows:  $\Delta H^\ddagger = 23.4 \pm 0.2$  kcal/mol and  $\Delta S^\ddagger = -6 \pm 6$  cal/(mol·K).

Our earlier experimental observations led us to propose that C–O reductive elimination at complexes **31** and **32** in acetic acid takes place via preliminary dissociation of a chelate. The near zero entropy values observed are consistent with the proposed reaction mechanism involving preliminary chelate arm dissociation followed by C–O reductive elimination from a 5-coordinate palladium species.

#### *Substituent effects of the C–O reductive elimination from complexes 31 and 32*

Additional experiments were designed to probe the substituent effects. Sanford and co-workers observed a faster C–O reductive elimination reaction with electron-donating substituents on the benzoate ligands and electron-withdrawing substituents on the arylpyridine fragment, indicating that the carboxylate ligands act as the nucleophilic coupling partners while the aryl rings act as electrophilic coupling partners in the C–O reductive elimination reactions. Our earlier studies on C–O reductive elimination at complexes **14-17** in water found no substituent effects. Thus

we designed experiments to study the aroylpyridine electronic effects, where complexes **31** and **32** containing electronically varied aroylpyridine ligands were prepared to place different electron-withdrawing and electron-donating substituents *para*- to the Pd-bound carbon atom.

*Kinetics experiments to probe electronic effects on the rate of C–O reductive elimination from complexes 31 and 32 in AcOH-d<sub>4</sub>*

The rates of C–O reductive elimination from complexes **31** and **32** were determined under identical conditions. 0.010 M acetic acid solutions of complexes **31(OOCCF<sub>3</sub>)** and **32(OOCCF<sub>3</sub>)** were prepared and 1.0 μl dioxane was added as internal standard. C–O reductive elimination from these solutions was monitored by taking consecutive <sup>1</sup>H NMR spectra at regular intervals at 50°C. The disappearance of the starting complex **31** or **32** was monitored and observed to follow first order kinetics. The color of the solution changed from deep yellow to light yellow as the reaction progressed. At the end of the reaction, formation of phenol **33** in 38 % and **34** in 35 % yields, and aryl acetate **35** in 58 % and **36** in 59 % yields was observed. The graphs of  $\ln([\text{Pd(IV)}]_0/[\text{Pd(IV)}]_t)$  as a function of time for the C-O reductive elimination of **31** and **32** at 50°C in AcOH-*d*<sub>4</sub> are linear, indicating a first order reaction.

**Table 3. 11.** Observed first order rate constants for the C–O reductive elimination reaction at complexes **31** and **32** in AcOD at 50°C.

Complex	$K_{\text{obs}}$ ( $\text{min}^{-1}$ )	Temp ( $^{\circ}\text{C}$ )
R=H, <b>31</b>	$(3.19 \pm 0.04) * 10^{-3}$	50 $^{\circ}\text{C}$
R=Me, <b>32</b>	$(4.11 \pm 0.06) * 10^{-3}$	50 $^{\circ}\text{C}$

The rates of C–O reductive elimination from complexes **31** and **32** in acetic acid were found to be similar. This indicates that C–O reductive elimination from these complexes is not sensitive to the substituents on the aromatic ring. A similar lack of substituent electronic effect on the C–O reductive elimination reaction from complexes **14-17** in water was observed. This indicates that the process of C–O reductive elimination from substituted arylpyridine-derived complexes **14-17** in water and substituted arylpyridine-derived complexes **31** and **32** in acetic acid may be similar.

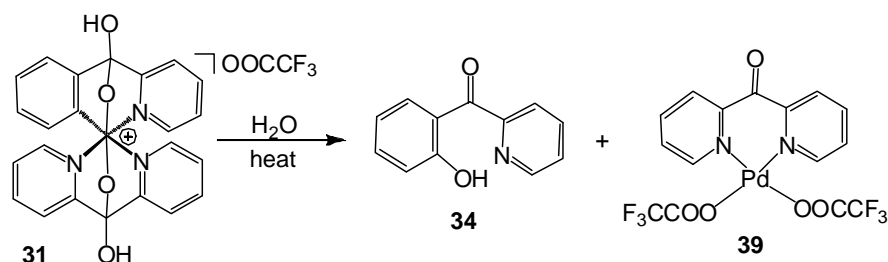
#### *Summary and Conclusion*

Our experimental observations suggest that C–O reductive elimination reactions at 2-arylpyridine derived complexes **14-17** in water proceed from a 6-coordinate Pd(IV) complex, while that at complexes **31** and **32** in acetic acid solvent proceeds from a 5-coordinate Pd(IV) intermediate generated via preliminary pyridine group dissociation. No substituent effects are observed in these C–O reductive elimination reactions.

### 3.3.2 C–O Reductive Elimination Reactivity at Monohydrocarbyl Pd(IV) Complex

#### 31 in Water

Scheme 3. 12



We started by attempting C–O reductive elimination at complex **31** in water. A 0.010 M aqueous solution of complex **31** was prepared and this reaction solution was monitored by <sup>1</sup>H NMR at various temperatures. When left in water at room temperature, no change in the <sup>1</sup>H NMR spectrum was observed for at least 2 days. When monitored at 70°C, only ~ 23 % conversion was observed after 12 hours. The presence of phenol was confirmed via both <sup>1</sup>H NMR and ESI–MS, but the yield of the phenol could not be determined due to overlapping signals in the <sup>1</sup>H NMR spectrum. When this reaction was attempted at 85°C, no change in the NMR was detected for ~ 30 minutes, but a mixture of white and black precipitate was observed when this reaction was carried out for longer times. After 12 hours, a small amount of acetic acid was added to dissolve the black and white precipitate and a small amount of pyridine was added to free any coordinated products. <sup>1</sup>H NMR analysis of the resulting solution indicated the presence of phenol among other unidentified products (the yield couldn't be determined due to too much overlap with unidentified peaks). The presence of the expected phenol was also confirmed by an ESI–MS peak at 200.0727 (calculated form phenol = 200.0131).

Due to slow reactivity of complex **31** in water, we sought to determine whether the C–O reductive elimination reaction would be faster in the presence of trifluoroacetic acid since Bronsted acids have been reported to accelerate C–O bond coupling reactions.<sup>58,180</sup>

*C–O Reductive Elimination at Complex **31** in Water with Various Equivalents of tfa*

C–O reductive elimination reaction was attempted in the presence of trifluoroacetic acid. A 0.010 M D<sub>2</sub>O solution of complex **31**(OOCCF<sub>3</sub>) was prepared by dissolving 0.010 mmoles of the complex in 1.0 ml of D<sub>2</sub>O and 20 % deuterated trifluoroacetic acid by volume was added to the solution. The reactivity of the resulting solution was monitored by <sup>1</sup>H NMR at room temperature at regular intervals in the presence of dioxane as internal standard. 50 % conversion of complex **31** was observed after 108 minutes and 84 % phenolic yield was observed at the end of reaction according to <sup>1</sup>H NMR analysis of the reaction solution after addition of pyridine to free coordinated products. This indicates that Bronsted acids accelerate C–O reductive elimination from complex **31** in water.

As a result of the observed acceleration of C–O reductive elimination from aqueous solutions of complex **31** in the presence of 20 % trifluoroacetic acid by volume, kinetic experiments were designed to probe the effect of acid concentration on the C–O coupling reaction. Thus 0.010 M D<sub>2</sub>O solutions of complex **31** were prepared and dioxane was added as internal standard. 1-3 equivalents of tfa-*d*<sub>1</sub> were added to the solutions and the reactions were monitored by <sup>1</sup>H NMR spectroscopy at 70°C. Dark brown precipitate was observed in the reaction mixtures as the reactions

progressed. At the end of the reaction, a small amount of deuterated acetic acid was added to dissolve the precipitate and pyridine was added to free any coordinated products. The total yield of the phenol was found to be between 70-73 % for multiple experiments, while another product with a yield of ~16-18 % could not be identified. The plots of  $\ln([\mathbf{31}]_0/[\mathbf{31}]_t)$  as a function of time for the C–O bond reductive elimination reactions from complex **31** in D<sub>2</sub>O at 70°C in the presence of 1-3 equivalents of tfa are non-linear, indicating product catalyzed reactions (Fig. 3.10).  $[\mathbf{31}]_0$  represents the initial concentration of complex **31** while  $[\mathbf{31}]_t$  represents the concentration of complex **31** at a time,  $t$ . Representative kinetic plots for  $\ln([\mathbf{31}]_0/[\mathbf{31}]_t)$  as a function of time for the C–O reductive elimination reaction of **31** in D<sub>2</sub>O at 70°C are given below.

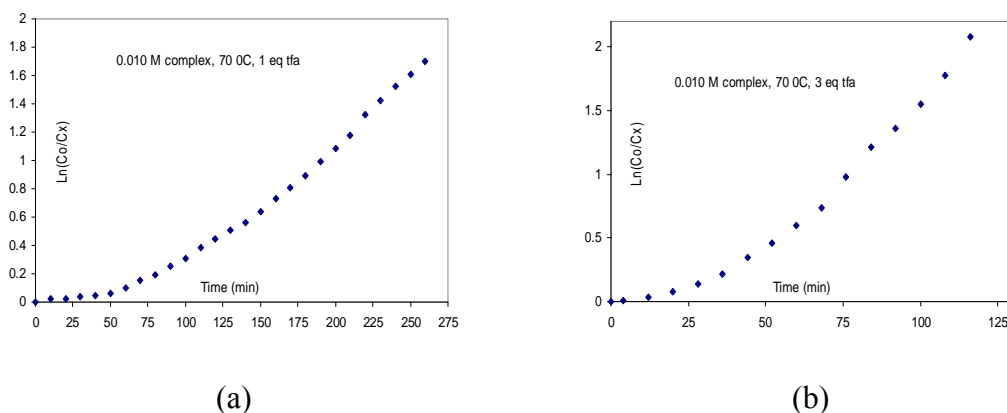


**Figure 3. 10.** First order kinetic plots for the C–O reductive elimination reaction at complex **31** in D<sub>2</sub>O at 70°C, in the presence of (a) 1.0 equivalent and (b) 3.0 equivalents of trifluoroacetic acid.

**Table 3. 12.** The time for 50 % conversion of a 0.010 M D<sub>2</sub>O solution of complex **31** at 70°C in the presence of 1-3 equivalent trifluoroacetic acid.

Acid concentration (M)	50 % conversion (min) at 70°C
0.01185	60
0.02	28
0.00625	150

The time for 50 % conversion of the starting material in the presence of various acid concentrations are presented in table 3.12. Higher acid concentration is observed to lead to proportional increase in the reaction rate, indicating that the C–O reductive elimination reaction is accelerated by acid. The non-linear first order plots indicate that the reaction is product catalyzed, and thus we designed a reaction to probe whether the inorganic product **39** catalyzes this reaction. A 0.010 M D<sub>2</sub>O solution of complex **31** was prepared and 1.0 μl dioxane was added as internal standard. 1.0 equivalent of tfa-*d*<sub>1</sub> and 20 % of additive **39** were added to the solution, and the resulting solution was monitored by <sup>1</sup>H NMR at 70°C. The plot of ln([**31**]<sub>0</sub>/[**31**]<sub>t</sub>) as a function of time for the C-O reductive elimination reaction of complex **31** in D<sub>2</sub>O in the presence of 1 eq of tfa and 20 % of complex **39** at 70 °C is given below.

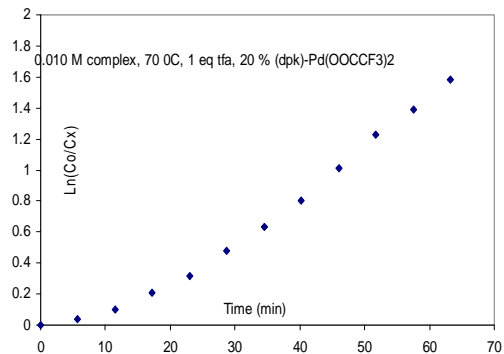


**Figure 3. 11.** First order kinetic plots for the C–O reductive elimination reaction at complex **31** in D<sub>2</sub>O at 70°C, in the presence of 1.0 equivalent of trifluoroacetic acid and 20 % of complex **39**.

**Table 3. 13.** C–O reductive elimination reaction of 0.010 M D<sub>2</sub>O solution of complex **31** at 70°C in the presence of 1.0 equivalent of trifluoroacetic acid and 20 % of complex **39**.

Entry	Acid concentration (M)	Additive	50 % conv.
1	0.00625	none	150 min
2	0.00625	0.2 eq	35 min

The plot of  $\ln([\mathbf{31}]_0/[\mathbf{31}]_t)$  vs. time for the C–O reductive elimination from aqueous solutions of complex **31** in the presence of both 1.0 equivalent of trifluoroacetic acid and complex **39** was found to be non-linear, indicating that the process is still autocatalytic. However the reaction was found to be ~ 4-fold faster in the presence of complex **39**, indicating that this product catalyzes the C–O reductive elimination reaction. In this kinetic analysis, the corresponding phenol was produced in 71 % yield together with an unidentified product in 17 % yield.

Complex **39** is proposed to accelerate the C–O bond coupling reaction as a Lewis acid in its cationic form, produced upon dissociation of an O<sub>2</sub>CCF<sub>3</sub> ligand.

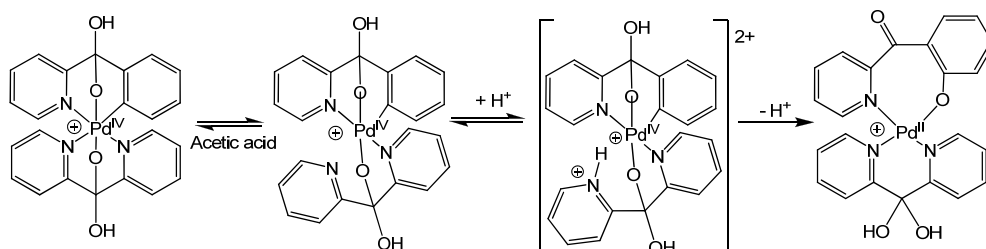
The acceleration of C–O bond reductive elimination by Lewis acids has been observed by Goldberg and Sanford.<sup>58,180</sup> Lewis acids are proposed to accelerate C–O reductive elimination reactions that proceed via preliminary dissociation of an OR<sup>-</sup> ligand by coordinating to the OR group and assisting in the dissociation of OR<sup>-</sup>. Thus, complex **39** accelerates the C–O coupling reaction probably by aiding in the dissociation of a ligand from the Pd(IV) center prior to C–O reductive elimination from a 5-coordinate intermediate.

*Unified Mechanism of C–O Reductive Elimination Reaction From Complexes 31 and 32 in Water and Acidic Media*

The mechanism of C–O reductive elimination from complexes **31** and **32** in water and acetic acid solvents was analyzed. It was observed that C–O reductive elimination from these complexes is too slow in neutral aqueous solutions while the reaction is faster in acidic solutions. This indicates that acid accelerates the C–O coupling reaction. In order to determine how acid accelerates the C–O reductive elimination reaction, the reaction was performed in acetic acid solution in the presence of various additives. In this study, the presence of pyridine additives was observed to cause a 10 fold inhibition of the reductive elimination reaction, indicating that the C–O reductive elimination from complex **31** proceeds via a 5-coordinate palladium intermediate produced upon preliminary chelate dissociation. Since C–O reductive elimination is fast in acidic solutions and slow in neutral solutions, acid is proposed to accelerate the reaction by shifting the equilibrium of pyridine arm dissociation by protonating the pyridine nitrogen as shown in Scheme 3.13.

Protonation of the pyridine group inhibits the reverse reaction and produces a dicationic species which is more reactive towards C–O reductive elimination. As a result, the overall rate of C–O coupling increases in the presence of acid.

**Scheme 3. 13**

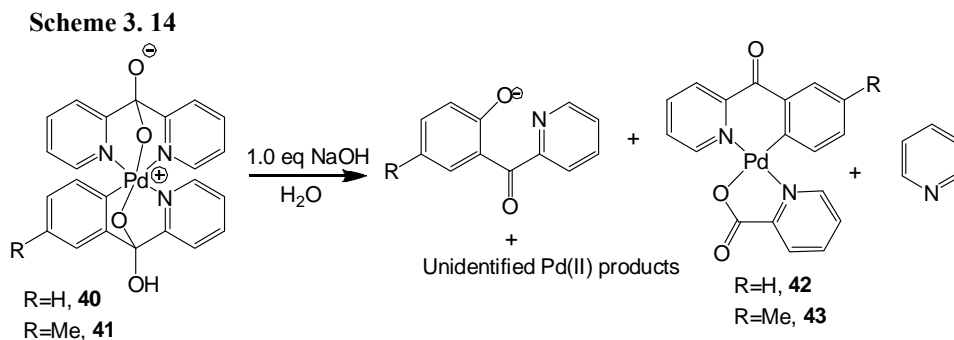


### *Summary and Conclusion*

In summary, C–O reductive elimination from aroylpyridine derived Pd(IV) complexes **31** and **32** is too slow in neutral aqueous solutions while the reaction is fast in acidic solutions. The mechanism of this reaction in acidic solutions was proposed to involve preliminary dissociation of the dpk chelate followed by C–O coupling from a 5-coordinate intermediate. Acid is proposed to accelerate the chelate dissociation.

### 3.3.3 C–O Reductive Elimination Reactivity at Monohydrocarbyl Pd(IV) Complexes

#### 31 and 32 in Water in the Presence of Base



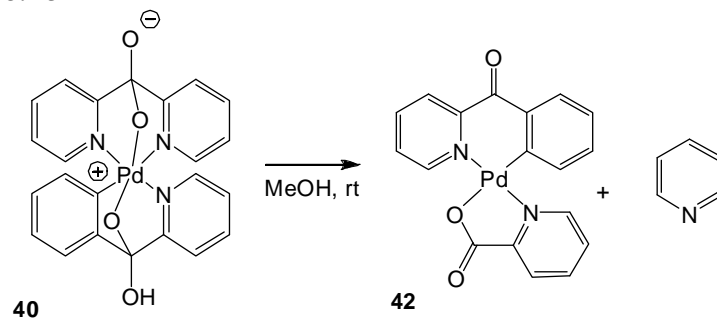
The zwitterionic complexes **40** and **41** were synthesized by addition of 1.0 equivalent of NaOH to aqueous solutions of complexes **31** and **32** respectively. The reactivity of aqueous solutions of these complexes towards C–O reductive elimination was studied. These complexes were found to be sparingly soluble in water. Heating a reaction mixture containing 0.010 mmoles of complex **31** in 1.0 ml of D<sub>2</sub>O at elevated temperatures resulted in decomposition to produce a black solid. However when 1.0 equivalent of NaOH was added to the reaction mixture of complex **40** and D<sub>2</sub>O, the precipitate dissolved to give a deep yellow solution. The <sup>1</sup>H NMR spectrum revealed 16 multiplets in the aromatic region, with a pattern significantly different from that of complex **31**. Heating a basic aqueous solution of complex **40** at 50°C for ~ 6 hours leads to formation of black solid. Addition of acetic acid to the reaction mixture at the end of the reaction to dissolve the precipitates revealed formation of the corresponding phenol **34** in 55 % yield, together with another product identified as a 2-benzoylpyridine-derived palladacycle supported by 2-picolinate ligand, complex **42** in 23 % yield. Complex **42** was also prepared by the decomposition of complex **40** in methanol.

ESI-MS analysis of the reaction solution in water in the negative mode, gave a major peak at  $m/z = 198.0550$ , calculated for the phenoxide  $C_{12}H_8NO_2 = 198.0555$ , while ESI-MS analysis of the acidified reaction solution in water in the positive mode, gave the following major peaks:  $m/z = 79.9102$  (calculated for protonated pyridine,  $C_5H_6N = 79.9610$ );  $200.0727$  (calculated for protonated phenol **34**<sup>+</sup>,  $C_{12}H_{10}NO_2 = 200.01315$ );  $410.9738$  (calculated for protonated complex **42H**<sup>+</sup>,  $C_{18}H_{13}N_2O_3^{106}Pd = 410.2261$ );  $402.9536$  (calculated for  $(dpk)Pd(OOCCF_3)^+$ ,  $C_{13}H_8N_2O_3F_3^{106}Pd = 402.9527$ ).

Complex **41** also undergoes decomposition in basic aqueous solutions to give the corresponding phenoxide in 49.9 % yield together with an unidentified complex (presumably complex **43**) in 20 % yield.

*Decomposition of complex 40 in methanol*

**Scheme 3. 15**



The zwitterionic complex **40** was dissolved in deuterated methanol at room temperature and  $^1H$  NMR spectra were collected at regular intervals over several days. New signals gradually appeared in the  $^1H$  NMR spectrum, while a white precipitate was observed to develop gradually. After 7 days at room temperature, the signals belonging to complex **40** had completely disappeared and a large amount of

white precipitate was present. The precipitate was filtered off, and its identity was determined as complex **42** via NMR spectroscopy and ESI-MS, while its composition was confirmed by elemental analysis. Due to the presence of the benzoylpyridine fragment, the picolinate ligand was proposed to originate from decomposition of the dpk fragment of complex **40**. The formation of this complex requires loss of pyridine, which was detected in the reaction solution by ESI-MS.

*Kinetics Experiments of Aqueous Solutions of **31** in the Presence of NaOH Additives*

Kinetics experiments were set up to study C–O reductive elimination reaction from basic aqueous solutions of complex **31**. 0.010 M D<sub>2</sub>O solutions of complex **31** were prepared and 2.0-6.0 equivalents of NaOD were added. Addition of less than 2.0 equivalents of base led to heterogeneous solutions which were not studied. 1,4-dioxane was added to the aqueous basic solutions of complex **31** as internal standard, and the resulting solutions were monitored by <sup>1</sup>H NMR spectroscopy at 50°C. Representative plots of  $\ln([31]_0/[31]_t)$  as a function of time for the C–O reductive elimination reaction of complex **31** in D<sub>2</sub>O at 50 °C in the presence of various equivalents of NaOD are given below.  $[31]_0$  refers to the initial concentration of complex **31** while  $[31]_t$  refers to the concentration of complex **31** at time,  $t$ .

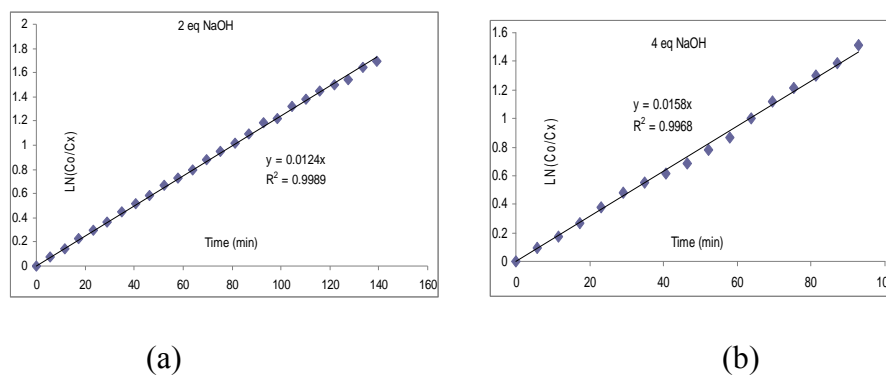


**Figure 3. 12.** First order kinetic plots for the C–O reductive elimination reaction of aqueous solutions of complex **31** at 50°C in the presence of (a) 2.0 equivalents of NaOH and (b) 4.0 equivalents of NaOH

In this kinetic study, the plots of  $\ln([\mathbf{31}]_o/[\mathbf{31}]_i)$  vs. time for the C–O reductive elimination of complex **31** in D<sub>2</sub>O at 50 °C are linear indicating a first order process. The observed first order rate constants were virtually identical when greater than 2.0 eq of base was used irrespective of the concentration of base used (see table 3.14 below).

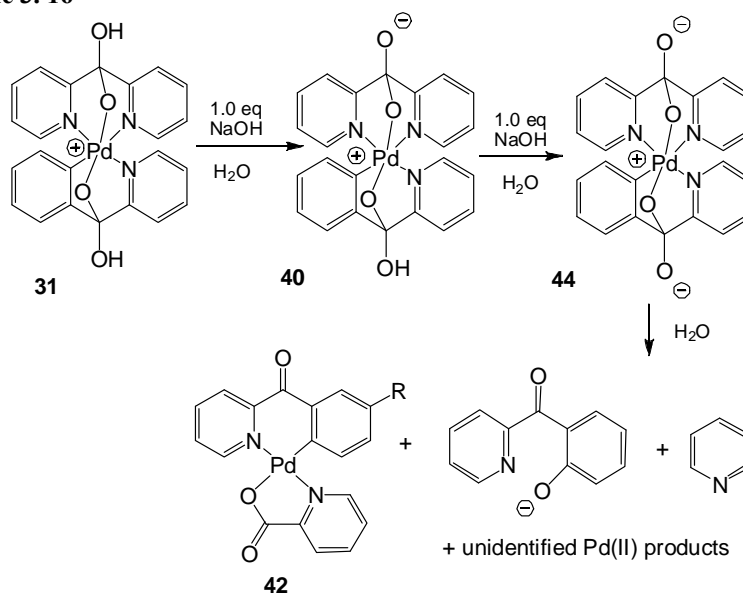
**Table 3. 14.** Observed first order rate constants for C–O reductive elimination at complex **31** in water in the presence of various equivalents of NaOH at 50°C.

Base concentration (M)	$k_{\text{obs}}$ (min <sup>-1</sup> )
0.020	1.29 ± 0.02
0.030	1.36 ± 0.04
0.040	1.64 ± 0.05
0.060	1.35 ± 0.05

The observation where the rate of reaction is independent of the amount of base used led us to propose that 2 equivalents of base are consumed in each of these reactions to produce common intermediate **44**. This proposed mechanism is supported

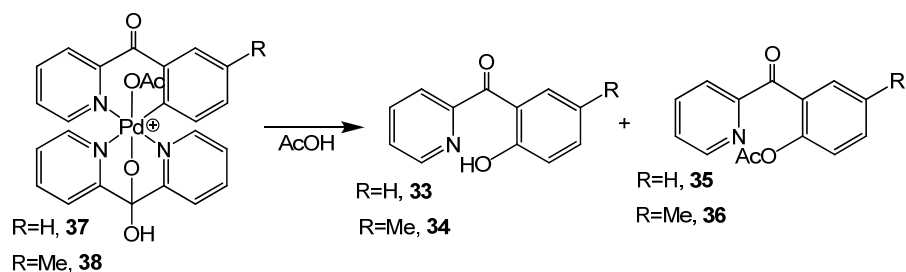
by the isolation of complex **40** from the reaction mixture when 1.0 eq of NaOH was used. Complex **40**, which is a poorly water soluble zwitterionic complex, was characterized by NMR, ESI-MS and X-ray diffraction, while its composition was confirmed by elemental analysis. Addition of one equivalent of NaOH to an aqueous reaction mixture containing complex **40** leads to dissolution of the poorly soluble zwitterionic complex to produce a complex that displays 16 multiplets in the aromatic region of the  $^1\text{H}$  NMR spectrum, complex **44**. This complex reacts to produce the corresponding phenoxide. However attempts to characterize complex **44** by ESI-MS in the negative mode were not successful as the species was not observed. This reaction suggests that the anionic complex **44** is more reactive towards C–O reductive elimination than the cationic complex **31** in water.

Scheme 3. 16



3.4 C–O Reductive Elimination Reactivity at Monohydrocarbyl Pd(IV) Complexes 37 and 38 in Acetic Acid Solvent

Scheme 3. 17



The combination of an acetic acid solution of complex **27** and 3.0 equivalents of HOOH led to clean formation of complex **37**. The identity of this complex was confirmed by both  $^1\text{H}$  NMR, ESI–MS and additional experimental observations previously described (Chapter 2). When a 0.010 M acetic acid solution of complex **37** was left at room temperature for 2 days, a mixture of the corresponding phenol **33** and aryl acetate **35** products were observed in 41% to 57 % yields respectively, after addition of pyridine in the reaction solutions to free coordinated products. The decomposition of this complex to produce both R–OH and R–OAc products indicates the presence of complexes with both –OH and –OAc ligated palladium(IV) centers in solution, since C–O reductive elimination from Pd(IV) complexes is believed to take place via a 3-center, 4-electron transition state. As a result, we propose that C–OAc reductive elimination from complex **37** produces that corresponding R–OAc product **35** while R–OR reductive elimination from the same complex, followed by protonation generates the phenol **33**.

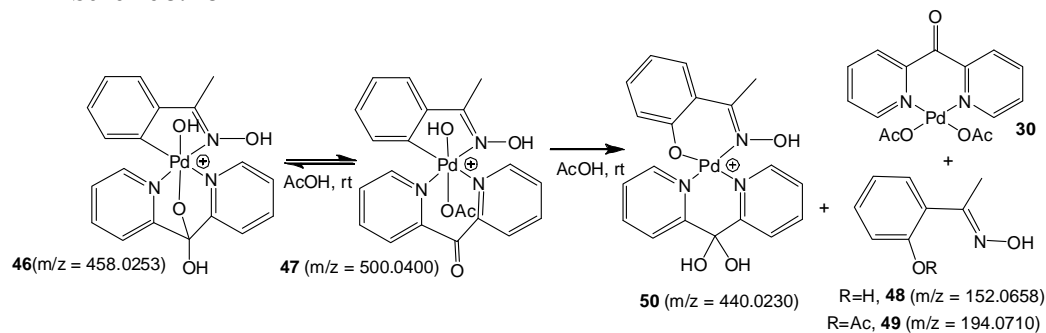
The reactivity of complex **38** in acetic acid was similar to that of complex **37**, where decomposition of this complex in acetic acid at room temperature for 2 days produced a mixture of the corresponding phenol **34** and aryl acetate **36** in 39% to 57% yields respectively. Similar to the reactivity of complex **37**, the C–OAc reductive elimination from complex **38** is responsible for generation of the aryl acetate **36** while C–OR reductive elimination followed by protonation generates the corresponding phenol **34**.

### 3.5 C–O Reductive Elimination Reactivity at Monohydrocarbyl Pd(IV) Complexes **46** and **53**

#### 3.5.1 C–O Reductive Elimination Reactivity at Monohydrocarbyl Pd(IV) Complexes **46** in Water and Acetic Acid Solvents

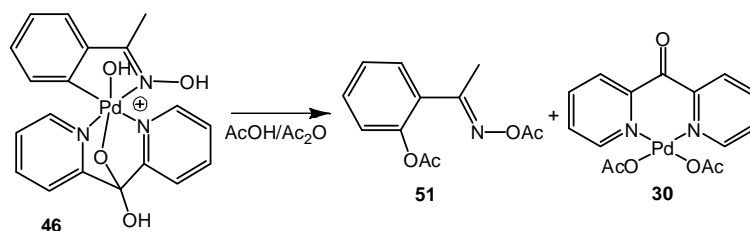
Complex **46** was prepared by combining a reaction mixture of complex **45** with H<sub>2</sub>O<sub>2</sub> in acetonitrile. It was isolated as a brown solid in pure form. When a 0.020 M aqueous solution of complex **46** was left in water for >90 minutes, new peaks were observed in the <sup>1</sup>H NMR spectrum accompanied by formation of a brown precipitate. Heating the solution accelerated the rate of decomposition and formation of the brown solid. The brown precipitate produced a complex <sup>1</sup>H NMR spectrum in deuterated acetic acid and methanol solvents, indicating the presence of multiple species in solution. ESI–MS analysis of a methanolic solution of the precipitate indicated the presence of the corresponding oxapalladacycle **50** among other unidentified products.

**Scheme 3. 18**



When an acetic acid solution of complex **46** was left at room temperature for several hours, a new species with 12 aromatic signals with a  $^1\text{H}$  NMR pattern similar to complex **46** was observed to develop gradually. ESI-MS analysis of the solution exhibited major peaks at 152.0658 assigned to the phenol **48**, 194.0130 assigned to the aryl acetate **49**, 440.0230 assigned to the corresponding oxapalladacycle **50**, 458.0253 assigned to the hydroxy-ligated Pd(IV) complex **46**, and 500.0400 assigned to acetato-ligated Pd(IV) complex **47**. This indicates that the additional product observed via  $^1\text{H}$  NMR may be the acetato-ligated Pd(IV) complex **47**, which ultimately decomposes to produce the aryl acetate product **49**. Complex **47** may be produced via chelate opening of complex **46** in acetic acid. After 3 hours, the fraction of complex **46** was  $\sim 39\%$ , the fraction of complex **47** was  $\sim 38\%$ , while complex **30** was  $\sim 10\%$ . At the end of the reaction, multiple new peaks appeared in the  $^1\text{H}$  NMR indicating multiple products.

**Scheme 3. 19**

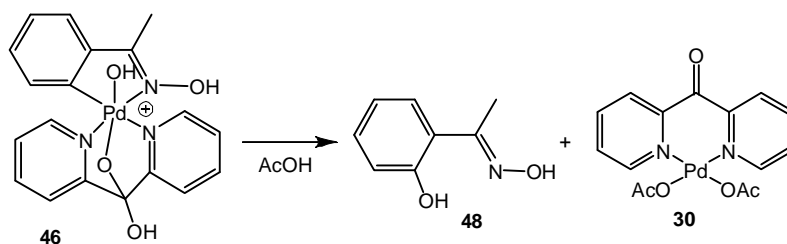


Given that the  $^1\text{H}$  NMR spectrum of the reaction solution after decomposition of complex **46** in acetic acid was complex indicating the presence of multiple products, while ESI-MS analysis of the reaction solution exhibited mass envelopes belonging to multiple products, including products of hydrolysis of the oxime moiety, acetic anhydride was added to the solution prior to decomposition in order to inhibit the hydrolysis of the oxime group and to simplify the reaction by generating a single organic product, the corresponding aryl acetate. As a result, decomposition of complex **46** in acetic acid solvent was performed in the presence of 10 % acetic anhydride by volume (Scheme 3.19). At the end of the reaction, the corresponding 2-acetoxyacetophenone oxime **51** was produced in >95 % yield (with acetoxyated N-OH group) together with dpk-Pd(OAc)<sub>2</sub> complex **30** as the only inorganic product (see figure below) within two days at room temperature. The organic product **51** was isolated by removal of solvent and extraction of the residue with diethyl ether. The identity of **51** was confirmed by independent synthesis using literature procedures for palladium catalyzed acetoxylation of aromatic C-H bonds using  $\text{PhI}(\text{OAc})_2$  as oxidant.<sup>50</sup>

### 3.5.2 C-O Reductive Elimination Reactivity at Monohydrocarbyl Pd(IV) Complexes

#### 46 in Solid State

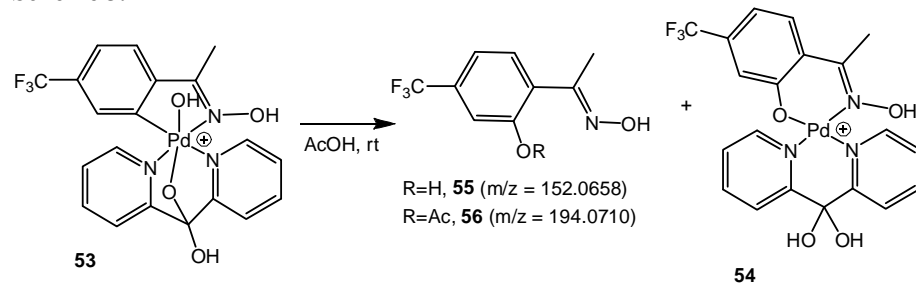
**Scheme 3. 20**



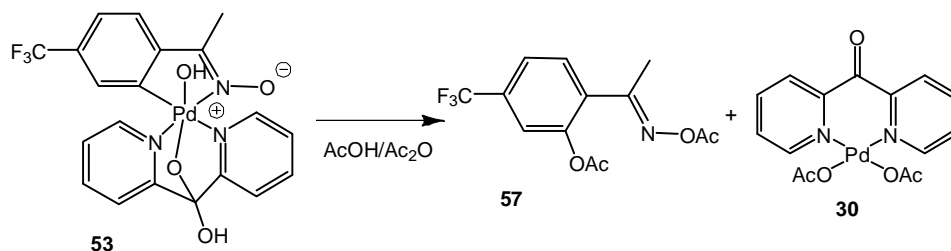
When complex **46** was left at room temperature in the solid state for over 4 weeks, the  $^1\text{H}$  NMR spectrum of the resulting solid in deuterated acetic acid revealed the corresponding phenolic product **48** and Pd(II) complex **30** as the only products in solution, after addition of pyridine- $d_5$  to free any coordinated products (Scheme 3.20). Phenol **48** was isolated by extraction of the solid with diethyl ether, and its identity was confirmed by comparison of its  $^1\text{H}$  NMR to that of 2-hydroxy acetophenone oxime published in literature. This indicates that complex **46** undergoes clean C–O reductive elimination in the solid state.

### 3.5.3 C–O Reductive Elimination Reactivity at Monohydrocarbyl Pd(IV) Complexes **53** in Water and Acetic Acid Solvents

Complex **53** was prepared by a procedure similar to that of complex **46**, where a reaction mixture of complex **52** in acetonitrile was combined with  $\text{H}_2\text{O}_2$ . This complex was isolated as a light orange solid in pure form. When a 0.02 M aqueous solution of complex **53** was left in water for >45 minutes, new peaks appeared in the  $^1\text{H}$  NMR spectrum accompanied by formation of a brown precipitate. Heating of the solution accelerated the rate of decomposition. The  $^1\text{H}$  NMR spectrum of the brown precipitate in deuterated acetic acid or methanol was complex, indicating the presence of multiple species in solution. ESI–MS analysis of a methanolic solution of the precipitate indicated the presence of the corresponding oxapalladacycle **54** among other unidentified products.

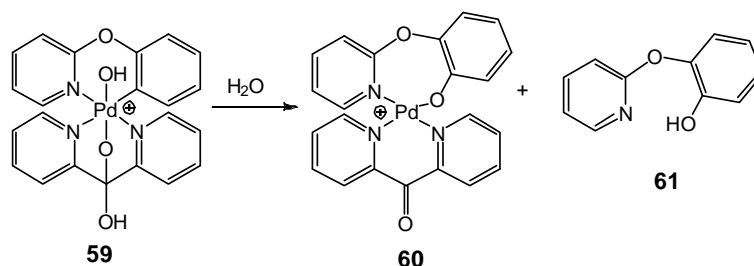
**Scheme 3. 21**

When an acetic acid solution of complex **53** was left at room temperature for several hours, multiple new peaks developed indicating the presence of multiple products by  $^1\text{H}$  NMR (Scheme 3.21). However, the addition of acetic anhydride to the reaction solution prior to decomposition afforded the corresponding aryl acetate product **57** in ~95 % yield (with acetoxyated N–OH group), and the Pd(II) complex **30** as the only inorganic product of decomposition (see Scheme 3.22 below). This reaction was too slow at room temperature, where 65 % decomposition was observed in ~ 16 hours. The organic product was isolated by removal of acetic acid solvent under vacuum, and extraction of the solid residue with diethyl ether. The identity of **57** was confirmed by independent synthesis via literature procedures for palladium catalyzed acetoxylation of aromatic C–H bonds using  $\text{PhI}(\text{OAc})_2$  as oxidant. It was characterized via NMR spectroscopy and ESI–MS analysis.

**Scheme 3. 22**

3.6 C–O Reductive Elimination Reactivity at Monohydrocarbyl Pd(IV) Complexes 59  
in Water

Scheme 3. 23



Complex **59** was prepared by combining a 0.010 M solution of complex **58** with 10.0 equivalents of H<sub>2</sub>O<sub>2</sub> in water at 0°C. Upon warming the solution to 22°C, <sup>1</sup>H NMR monitoring of the oxidation reaction revealed gradual disappearance of complex **59** and formation of one product “X” up to ~ 50 % yield in ~ 12 hours relative to an internal standard. However another product “Y” began to form after ~ 12 hours, with concomitant formation of brown solid (see figure 3.13 below). This reaction was too slow, taking > 1 week to come to completion, with product “X” at 22 % and product “Y” at 23 % at the end of the reaction, and a significant amount of brown precipitate was also present in solution. The pH of the solution dropped from ~ 6.0 at the start of the reaction to ~ 4.0 at the end of the reaction.

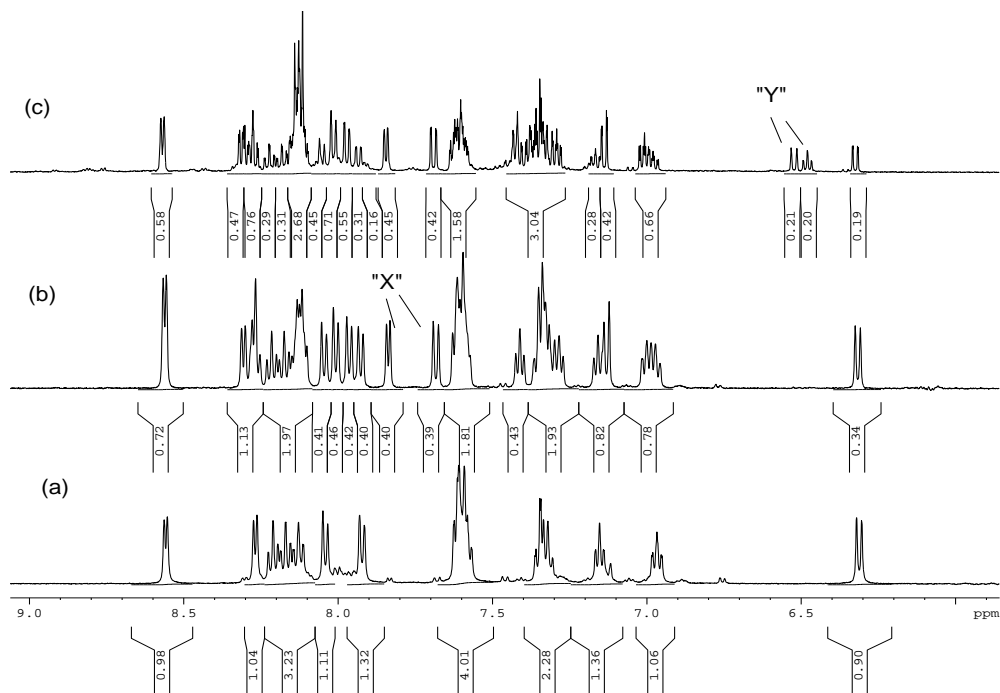


**Figure 3.13.** <sup>1</sup>H NMR spectra of D<sub>2</sub>O solutions of (a) complex **59**; (b) complex **59** ~ 11 hours after addition of H<sub>2</sub>O<sub>2</sub>, with "X" present, (c) complex **59** after one week, in the presence of both "X" and "Y". The reaction was carried out at 22°C.

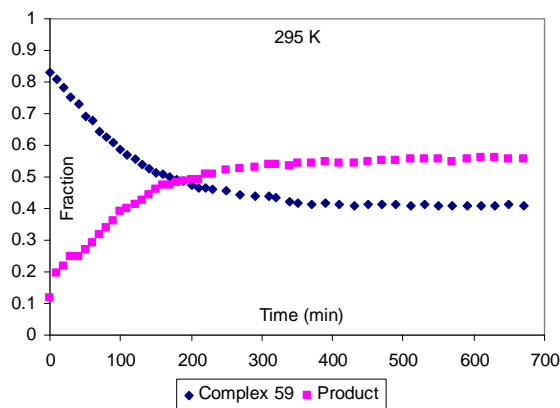


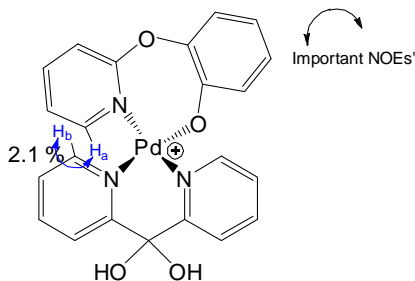
**Figure 3.14.** Plot showing the fraction of complex **59** and product "X" as a function of time over ~ 12 hours period.

Analysis of the aqueous reaction mixtures by ESI-MS after addition of methanol to dissolve the brown precipitate revealed three major mass envelopes at  $m/z = 188.0720$  which was assigned to the protonated phenol **61**,  $432.0264$  which

was assigned to the oxapalladacycle **60**, and 494.0294 which was assigned to the hydrated oxapalladacycle **60** or unreacted Pd(IV) complex **59** (see scheme 3.23 above).

When the reaction mixture at the end of the reaction was extracted with diethyl ether, the corresponding phenol **61** was isolated cleanly without acidification of the reaction mixture. The isolation of free phenol from the aqueous reaction mixtures produced upon decomposition of complex **59** in water indicates that phenol **61** is one of the products of C–O bond coupling from this reaction. Phenol may be formed via C–O reductive elimination from the Pd(IV) complex **59**, or via hydrolysis of an oxapalladacyclic product **60**. The presence of oxapalladacycle **60** is proposed based on production of oxapalladacycles during the decomposition of similar dpk ligated Pd(IV) complexes in water.

As a result, we designed experiments to determine the identity of the reaction products “X” and “Y”. We started by performing 1D selective difference NOE experiment on product “X” in order to determine whether this product was free phenol or a coordination complex, probably the oxapalladacycle **60** detected by ESI-MS at  $m/z = 432.0264$ .



In the 1D difference NOE experiment of product “X”, NOE enhancement was observed between the *ortho*-H<sub>a</sub> of the phenoxy-pyridine ligand and that of the *ortho*-

H<sub>b</sub> of the dpk ligand. The NOE experiment confirms that the product “X” is coordinated onto palladium, and that a pyridine based ligand, probably dpk is also coordinated. Since the only products observed by ESI–MS of the reaction solution are complex **59**, the oxapalladacyclic complex **60**, and the phenolic product **61**, we propose that product “X” is the corresponding oxapalladacycle **60**.

The second product of decomposition is proposed to be free phenol. This is because free phenol was obtained by extraction of the aqueous reaction solution with diethyl ether without acidification, indicating that it is one of the products observed by <sup>1</sup>H NMR. Moreover, the low pH of ~ 4.0 at the end of reaction would favor hydrolysis of the oxapalladacycle to generate free phenol.

### 3.7 Summary and Conclusions of C–O Reductive Elimination Reactions at

#### Monohydrocarbyl Pd(IV) Complexes

In summary, a number of monohydrocarbyl Pd(IV) complexes were prepared and their reactivity towards C–O reductive elimination studied. Arylpyridine derived complexes **14-18** were observed to undergo C–O bond coupling in aqueous solutions at room temperature to produce the corresponding oxapalladacycles **22-25**. C–O reductive elimination from complexes **14-18** in water was proposed to take place from a 6-coordinate palladium intermediate based on the observation that acid, exogenous anions, and pyridine additives do not influence the rate of the reductive elimination reaction. The electronics of the substituent effects on the aryl rings did not affect the rate of the C–O reductive elimination reactions.

The aroylpyridine derived complexes **31** and **32** undergo very slow C–O bond coupling in neutral aqueous solutions at room temperature. However the C–O reductive elimination reaction is accelerated in both basic and acidic media. In acidic media, the mechanism of C–O reductive elimination from these complexes was proposed to involve preliminary dissociation of the chelate to produce a 5-coordinate intermediate, which subsequently undergoes C–O reductive elimination. This mechanism was proposed based on the observation that pyridine additive significantly inhibits the C–O reductive elimination reaction in acetic acid. Acid was proposed to aid chelate dissociation by protonating the dissociated pyridine group. Protonation of the pyridine group slows down the reverse reaction and also produces a dicationic species which is more reactive towards C–O bond coupling, leading to a faster overall C–O reductive elimination reaction. Basic additives were proposed to accelerate the C–O bond coupling reaction by deprotonating the Pd(IV) complexes, resulting in formation of anionic intermediates. These intermediates are proposed to be more reactive towards C–O bond coupling than the cationic complexes **31** and **32** in water.

Oxime derived monohydrocarbyl Pd(IV) complexes **46** and **53** undergo slow C–O bond coupling reactions in water to produce the corresponding oxapalladacycles among other products. However the C–O coupling reactions are simple in the solid state and produce the corresponding phenols quantitatively. In acetic acid solvent, C–O coupling from complexes **46** and **53** produce the corresponding phenol and aryl acetate, among other products which presumably result from hydrolysis of the oxime moiety, while aryl acetates are produced quantitatively in the presence of acetic anhydride.

Phenoxy pyridine derived Pd(IV) complex **59** undergoes slow C–O bond coupling in water to produce the corresponding oxapalladacycle **60** and phenol **61**. The phenol **61** may also be produced by hydrolysis of the oxapalladacycle **60** as a result of acidification of the solution. Both products **60** and **61** are observed at the end of the reaction, and the phenol is isolated from the aqueous solutions without acidification.

In acetic acid solvent, the decomposition of alkoxo- and hydroxo-ligated Pd(IV) complexes was observed to produce the corresponding phenol and aryl acetate products. The aryl acetates may be produced by C–O reductive elimination from acetato-ligated Pd(IV) complexes which may form via chelate opening of alkoxo- and hydroxo-ligated Pd(IV) complexes in acetic acid.

Our next goal is to explore the ligand exchange reaction at the Pd(IV) center to produce compounds resulting from C–X reductive elimination reaction (X=Br, Cl, I, and F), while the ultimate goal is to develop environmentally benign, palladium catalyzed C–H bond functionalization reactions that produce C–X bond-coupling products (X=OR, Cl, Br, I, or F) utilizing H<sub>2</sub>O<sub>2</sub> as oxidant in water.

### 3.7 Experimental

#### 3.8.1 General

All manipulations were carried out under ambient atmosphere unless otherwise noted. All reagents for which synthesis is not given are commercially available from Aldrich, Acros, Alfa-Aesar or Pressure Chemicals, and were used as received without further purification.  $^1\text{H}$  (400 MHz or 500 MHz) and  $^{13}\text{C}$  NMR (100 MHz or 125 MHz) spectra were recorded on a Bruker AVANCE 400 or Bruker DRX-500. Chemical shifts are reported in ppm and referenced to residual solvent resonance peaks. High Resolution Mass Spectrometry (HRMS) experiments were performed using a JEOL AccuTOF-CS instrument. Elemental analyses were carried out by either Chemisar Laboratories Inc., Guelph, Canada, or Columbia Analytical Services, Tucson, AZ.

#### 3.8.2 Computational details.

Theoretical calculations in this work have been performed using density functional theory (DFT) method,<sup>166</sup> specifically functional PBE,<sup>167</sup> implemented in an original program package “Priroda”.<sup>168</sup> In PBE calculations relativistic Stevens-Basch-Krauss (SBK) effective core potentials (ECP)<sup>170-172</sup> optimized for DFT-calculations have been used. Basis set was 311-split for main group elements with one additional polarization *p*-function for hydrogen, additional two polarization *d*-functions for elements of higher periods. Full geometry optimization has been performed without constraints on symmetry. For all species under investigation frequency analysis has been carried out. All minima have been checked for the absence of imaginary frequencies. All transition states possessed just one imaginary frequency. Using the method of Intrinsic Reaction Coordinate, reactants, products and the corresponding

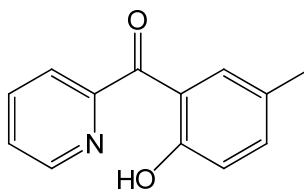
transition states were proven to be connected by a single minimal energy reaction path.

All the species under investigation were next modeled with the Jaguar program<sup>173</sup> package with the same functional (PBE) and LACVP relativistic basis set with two polarization functions. These results showed the same trends as with Priroda calculations and the essentially same reaction parameters. The solvation of all complexes in Scheme 5 in water was modeled using a Poisson-Boltzmann continuum solvation model (PBF).

### 3.8.3 Characterization of products of reductive elimination.

Compounds **33**,<sup>157</sup> **61**,<sup>152</sup> **62**,<sup>208</sup> **63**,<sup>21</sup> and **64**<sup>21</sup> are known.

#### ***Compound 34***

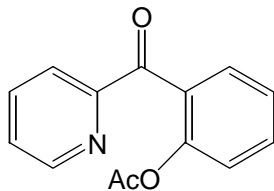


<sup>1</sup>H NMR (CDCl<sub>3</sub>, 22°C), δ: 2.25 (s, 3H), 6.94 (d, *J*=8.4 Hz 1H), 7.30 (dd, *J*=8.4, 2.0 Hz 1H), 6.49 (ddd, *J*=6.8, 4.9, 2.0 Hz 1H), 7.79 (vs, 1H), 7.89-7.91 (m, 2H), 8.72 (dt, *J*=4.8, 1.2 Hz 1H), 12.16 (s, 1H).

<sup>13</sup>C NMR (AcOH-*d*<sub>4</sub>, 22°C), δ: 20.7, 118.5, 119.1, 124.7, 126.2, 128.2, 137.6, 138.0, 148.4, 155.7, 161.6, 197.4.

ESI-MS of acidified methanolic solution of **34**·H<sup>+</sup>: found *m/z* = 214.0803; calculated for C<sub>13</sub>H<sub>12</sub>ON<sub>2</sub> = 214.0868.

**2-(2-acetoxybenzoyl)pyridine, 35**



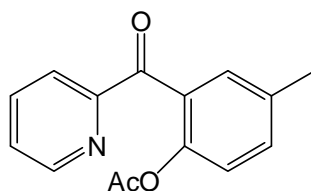
$^1\text{H}$  NMR ( $\text{CDCl}_3$ ,  $22^\circ\text{C}$ ),  $\delta$ : 1.94 (s, 3H), 7.22 (dd,  $J=8.3$ , 0.8 Hz 1H), 7.36 (td,  $J=7.6$ , 0.9 Hz 1H), 7.49 (ddd,  $J=7.6$ , 4.8, 1.2 Hz 1H), 7.57 (td,  $J=7.7$ , 1.6 Hz 1H), 7.71 (dd,  $J=7.7$ , 1.7 Hz 1H), 7.22 (td,  $J=7.7$ , 1.7 Hz 1H), 8.05 (d,  $J=7.8$  Hz 1H), 8.70 (d,  $J=4.7$  Hz 1H).

$^{13}\text{C}$  NMR ( $\text{AcOH-}d_4$ ,  $22^\circ\text{C}$ ),  $\delta$ : 124.2, 125.4, 126.7, 128.3, 131.4, 132.3, 134.0, 139.3, 149.7, 150.6, 155.1, 170.5, and 194.0

$^{13}\text{C}$  NMR ( $\text{CDCl}_3$ ,  $22^\circ\text{C}$ ),  $\delta$ : 20.8, 123.4, 124.0, 125.8, 126.8, 130.7, 131.6, 132.9, 137.2, 149.3, 149.5, 154.9, 169.0, and 193.9

ESI-MS of acidified methanolic solution of  $\mathbf{35}\cdot\text{H}^+$ : found  $m/z = 242.0855$ ;  
calculated for  $\text{C}_{14}\text{H}_{12}\text{NO}_3^+ = 242.0817$

**4-methyl-2-(pyridin-2-ylcarbonyl)phenyl acetate, 36**



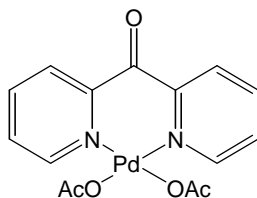
$^1\text{H}$  NMR ( $\text{AcOD}$ ,  $22^\circ\text{C}$ ),  $\delta$ : 1.87 (s, 3H), 2.39 (s, 3H), 7.11 (d,  $J=8.3$  Hz, 1H), 7.41 (dd,  $J=8.3$ , 2.0 Hz, 1H), 7.46 (vs, 1H), 7.64 (ddd,  $J=7.7$ , 4.6, 1.1 Hz, 1H), 7.95 (d,  $J=8.0$  Hz, 1H), 8.03 (td,  $J=7.9$ , 1.7 Hz, 1H), 8.76 (d,  $J=4.7$  Hz, 1H).

$^{13}\text{C}$  NMR ( $\text{AcOD}$ ,  $22^\circ\text{C}$ ),  $\delta$ : 20.5, 20.8, 123.9, 125.3, 128.1, 131.1, 132.4, 134.5, 136.7, 139.2, 148.3, 149.7, 155.1, 170.6, 194.2.

ESI-MS of acidified methanolic solution of **36·H<sup>+</sup>**: found  $m/z = 256.1039$ ;  
calculated for  $C_{15}H_{14}NO_3^+ = 256.0974$ .

**(dpk)Pd(OAc)<sub>2</sub>, 30**

184 mg (1.0 mmol) of dpk ligand was dissolved in 10 ml of acetic acid. 224 mg (1.0 mmol) of palladium diacetate was added to the solution, and the resulting reaction mixture was stirred at room temperature for 12 hours. After the reaction was complete, the resulting deep red solution was concentrated and triturated with diethyl ether, to give yellow crystals of (dpk)Pd(OAc)<sub>2</sub>. The reaction mixture was filtered and the residue was washed with a small amount of ether. Removal of solvent gave the pure product in 92 % yield.



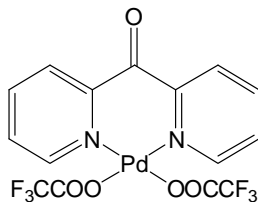
<sup>1</sup>H NMR (AcOH-*d*<sub>4</sub>, 22°C),  $\delta$ : 2.10 (s, 6H), 7.82 (m, 2H), 8.26-8.31 (m, 4H),  
8.77(m, 2H).

<sup>13</sup>C NMR (AcOH-*d*<sub>4</sub>, 22°C),  $\delta$ : 128.4, 130.5, 142.4, 149.1, 153.5, 182.2,  
185.2.

Anal. Found (Calc. for  $C_{15}H_{14}N_2O_5Pd$ ): C, 44.36 (44.08); H, 3.53 (3.45); N, 6.86  
(6.85).

ESI-MS of acetic acid solution of (dpk)Pd(OAc)<sup>+</sup> positive mode, found  $m/z =$   
348.9838; calculated for  $C_{13}H_{11}N_2O_3^{106}Pd^+ = 348.9810$

### Complex 39



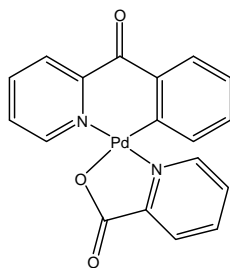
$^1\text{H}$  NMR (DMSO- $d_6$ , 22°C),  $\delta$ : 7.05 to 7.07 (m, 2H), 7.22 (dt,  $J=7.1$ , 1.3 Hz, 1H), 7.33 (dd,  $J=7.4$ , 1.5 Hz, 1H), 7.49 (dt,  $J=6.7$ , 1.4 Hz, 1H), 7.59 to 7.62 (m, 2H), 7.88 (d,  $J=7.3$  Hz, 1H), 7.95 (d,  $J=7.1$  Hz, 1H), 8.07 (d,  $J=5.2$  Hz, 1H), 8.17 (d,  $J=5.2$  Hz, 1H), 8.23 to 8.31 (m, 4H), 8.43 (d,  $J=5.0$  Hz, 1H), 8.83 (s, 1H), 9.13 (s, 1H)

$^{13}\text{C}$  NMR (DMSO- $d_6$ , 22°C),  $\delta$ : 103.8, 105.2, 116.4, 118.4, 121.6, 121.7, 123.0, 124.1, 125.9, 126.1, 127.0, 127.2, 129.1, 129.3, 141.8, 143.1, 143.3, 147.7, 148.6, 148.9, 149.3, 156.1, 157.5, 157.7, 160.4, 163.5, 166.7

ESI-MS of solution of  $(\text{dpk})\text{Pd}^{\text{II}}(\text{OOCF}_3)_2$  in water, positive mode,  $m/z = 403.02401$  Calculated for  $(\text{dpk})\text{Pd}^{\text{II}}(\text{OOCF}_3)^+$ ,  $\text{C}_{13}\text{H}_8\text{F}_3\text{N}_2\text{O}_3^{106}\text{Pd}$ : 402.95217.

Anal. Found (Calcd for a complex with 3.5 molecules of  $\text{H}_2\text{O}$ ,  $\text{C}_{25}\text{H}_{25}\text{F}_3\text{N}_3\text{O}_{9.5}\text{Pd}$ ): C, 44.02 (43.97); H, 3.59 (3.69); N, 5.96 (6.15).

### 2-Benzoylpyridine-derived palladacycle supported by 2-picolinate, 42



$^1\text{H}$  NMR ( $\text{CDCl}_3$ - $d$ , 22°C),  $\delta$ : 7.25 (t,  $J=7.5$  Hz, 1H), 7.36 (dt,  $J=7.4$ , 1.2 Hz, 1H), 7.47 (dt,  $J=6.6$ , 1.1 Hz, 1H), 7.56 (d,  $J=7.7$  Hz, 1H), 7.59 (dt,  $J=6.6$ , 1.2 Hz,

1H), 7.77 (dd,  $J=7.7$ , 1.1 Hz, 1H), 8.00 (dt,  $J=7.7$ , 1.1 Hz, 1H), 8.07 (dt,  $J=7.7$ , 1.2 Hz, 1H), 8.16 (d,  $J=5.4$  Hz, 1H), 8.25 (t,  $J=7.7$ , Hz, 2H), 9.21 (d,  $J=5.5$  Hz, 1H).

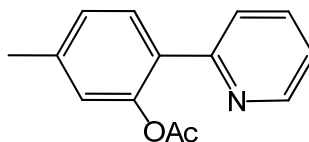
$^{13}\text{C}$  NMR ( $\text{CDCl}_3$ - $d$ , 22°C),  $\delta$ : 125.6, 125.9, 127.3, 127.5, 127.9, 128.5, 132.1, 135.0, 135.8, 139.7, 139.9, 149.4, 150.8, 151.4, 152.7, 156.2, 169.8, 191.3, 207.3.

ESI-MS of solution of **42**· $\text{H}^+$  in acetic acid, positive mode,  $m/z = 410.9782$ .  
Calculated for  $\text{C}_{18}\text{H}_{13}\text{N}_2\text{O}_3^{106}\text{Pd} = 410.9961$ .

Anal. Found (Calcd for hydrated complex with one water molecule,  $\text{C}_{18}\text{H}_{16}\text{N}_2\text{O}_5\text{Pd}$ ): C, 48.48 (48.39); H, 3.67 (3.61); N, 6.30 (6.27).

### Compound 29

Compound **29** was prepared by acetoxylation of the corresponding phenol, **63** in neat acetic anhydride. Removal of solvent afforded pure **29**.

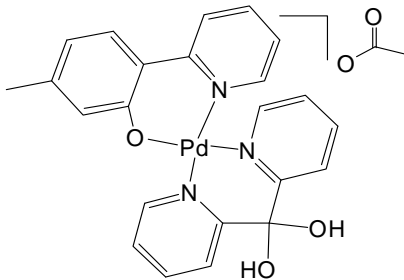


$^1\text{H}$  NMR ( $\text{AcOD}$ , 22°C),  $\delta$ : 2.13 (s, 3H), 2.42 (s, 3H), 7.10 (s, 1H), 7.24 (d,  $J=7.8$  Hz, 1H), 7.57 (d,  $J=7.8$  Hz, 1H), 7.60 (t,  $J=6.6$  Hz, 1H), 7.73 (d,  $J=7.8$  Hz, 1H), 8.11 (td,  $J=7.8$ , 1.5 Hz, 1H), 8.88 (d,  $J=5.2$  Hz, 1H).

$^{13}\text{C}$  NMR ( $\text{AcOD}$ , 22°C),  $\delta$ : 20.9, 21.3, 124.6, 124.7, 126.4, 128.3, 128.5, 131.7, 141.0, 142.9, 148.1, 149.1, 154.8, 170.8.

ESI-MS of solution of **29** in methanol,  $m/z$  observed: 228.1108, Calculated for  $\text{C}_{14}\text{H}_{14}\text{NO}_2$ ,  $m/z = 228.1025$ .

**Complex 23(OAc):**



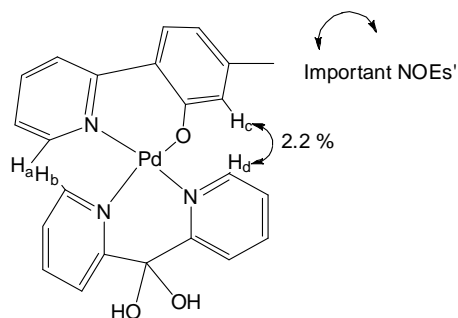
$^1\text{H}$  NMR (methanol- $d_4$ , 22°C),  $\delta$ : 1.90 (s, 3H), 2.42 (s, 3H), 6.87 (d,  $J=8.0$  Hz, 1H), 7.07 (s, 1H), 7.38 (ddd,  $J=7.3, 6.0, 1.5$  Hz, 1H), 7.50 (td,  $J=6.0, 2.6$  Hz, 1H), 7.69 (d,  $J=8.0$  Hz, 1H), 7.78 (ddd,  $J=7.0, 5.6, 2.0$  Hz, 1H), 8.00 (d,  $J=6.0$  Hz, 1H), 8.04 (d,  $J=8.2$  Hz, 1H), 8.12 (td,  $J=8.0, 1.6$  Hz, 1H), 8.16 – 8.26 (m, 4H), 8.36 (d,  $J=5.6$  Hz, 1H), 8.73 (d,  $J=5.6$  Hz, 1H);

$^{13}\text{C}$  NMR (methanol- $d_4$ , 22°C),  $\delta$ : 21.6, 24.1, 100.7, 121.7, 122.2, 125.0, 125.1, 125.2, 125.5, 127.6, 128.2, 128.8, 131.0, 142.0, 142.5, 142.7, 145.4, 152.0, 152.7, 154.1, 155.9, 157.2, 158.4, 163.0, 179.9.

ESI-MS of solution of **23** in methanol,  $m/z$  observed: 474.0541 and 506.0834. Calculated for  $\text{C}_{23}\text{H}_{18}\text{N}_3\text{O}_2^{106}\text{Pd}$ ,  $m/z = 474.0443$ , and  $\text{C}_{24}\text{H}_{22}\text{N}_3\text{O}_3^{106}\text{Pd}$  (a methanol adduct onto the C=O of dpk ligand) = 506.0705.

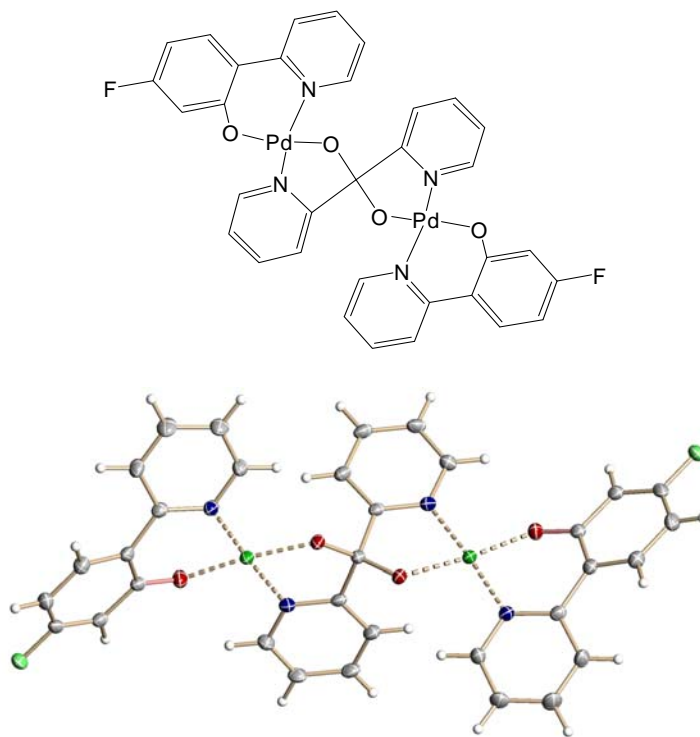
Anal. Found (Calcd. for  $\text{C}_{30}\text{H}_{33}\text{N}_3\text{O}_7\text{Pd}$  for the complex with one residual acetone molecule; it was recrystallized from acetone) C, 55.44 (55.13); H, 4.68 (4.79); N, 6.63 (6.89)

Selective 1D-difference NOE experiment ( $D_2O$ ) for **23(OAc)**



In the 1D difference NOE experiment, NOE was observed between the *ortho*-H<sub>c</sub> of the tolylpyridine ligand and the *ortho*-H<sub>d</sub> of the dpk ligand. Irradiation of a resonance at 8.56 ppm (*ortho*-H<sub>d</sub> of the dpk ligand) showed enhancement (positive NOE) of a singlet at 7.04 ppm (*ortho*-H<sub>c</sub> of the dpk ligand, 2.2%) (mixing time of 0.8s, delay time 5s).

**Complex 25(OAc):**



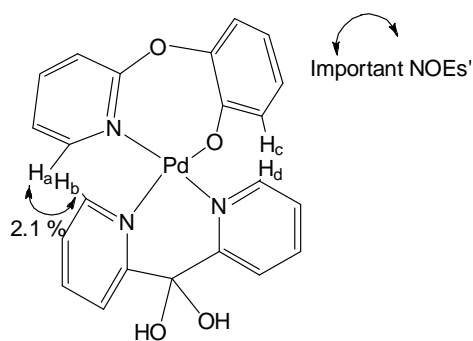
ORTEP drawing (50 % probability ellipsoid) of complex **25**.

$^1\text{H}$  NMR (Acetone- $d_4$ , 22°C),  $\delta$ : 6.45 (td,  $J=8.2$ , 2.8 Hz, 1H), 6.71 (dd,  $J=11.8$ , 2.6 Hz, 1H), 7.27 (ddd,  $J=7.5$ , 6.5, 1.5 Hz, 1H), 7.54 (ddd,  $J=7.5$ , 6.7, 1.0 Hz, 1H), 7.68 (dd,  $J=8.8$ , 7.1 Hz, 1H), 7.73 (d,  $J=7.7$  Hz, 1H), 7.95-8.03 (m, 3H), 8.62 (d,  $J=5.2$  Hz, 1H), 9.03 (d,  $J=6.0$  Hz, 1H).

$^{13}\text{C}$  NMR (Acetone- $d_4$ , 22°C),  $\delta$ : 104.2 (d,  $J=22.8$ ), 107.5 (d,  $J=19.8$ ), 121.9, 123.3, 124.3, 124.9, 133.5 (d,  $J=12.8$ ), 139.9, 140.5, 146.0, 151.5, 153.8, 176.7.

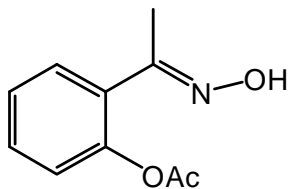
ESI-MS of solution of  $25^+$  in methanol,  $m/z$  observed: 790.9905, Calculated for  $\text{C}_{33}\text{H}_{23}\text{F}_2\text{N}_4\text{O}_4$   $^{106}\text{Pd}_2$ ,  $m/z = 790.9761$ .

*Selective 1D-difference NOE experiments ( $\text{D}_2\text{O}$ ) for 60*



In the 1D difference NOE experiment, NOE was observed between the *ortho*- $\text{H}_a$  of pyridyl fragment of the phenoxy pyridine ligand and that of the *ortho*- $\text{H}_b$  of pyridyl fragment of the dpk ligand. Irradiation of a resonance at 8.33 ppm (*ortho*- $\text{H}_a$  of pyridyl fragment of the phenoxy pyridine) showed enhancement (positive NOE) of a doublet at 8.12 ppm (*ortho*- $\text{H}_b$  of the dpk ligand, 2.1%) (mixing time of 4.0s, delay time 5s).

**Compound 49**

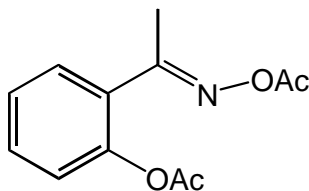


$^1\text{H}$  NMR ( $\text{CDCl}_3$ ,  $22^\circ\text{C}$ ),  $\delta$ : 2.22 (s, 3H), 2.41 (s, 3H), 6.89 (td,  $J=7.6$ , 1.2 Hz, 1H), 7.00 (dd,  $J=8.4$ , 1.3 Hz, 1H), 7.31 (td,  $J=7.8$ , 1.5 Hz, 1H), 7.44 (dd,  $J=8.0$ , 1.5 Hz, 1H), 11.2 (s, 1H).

$^{13}\text{C}$  NMR ( $\text{CDCl}_3$ ,  $22^\circ\text{C}$ ),  $\delta$ : 13.0, 19.4, 117.3, 118.2, 119.3, 128.6, 132.5, 158.7, 164.2, 167.0.

ESI MS of  $\text{H}_2\text{O}$  solution of **(49)** $\text{Na}^+$ ,  $m/z$  observed: 216.0593, Calculated for  $\text{C}_{10}\text{H}_{11}\text{NNaO}_3$ , 216.0637.

**Compound 51**

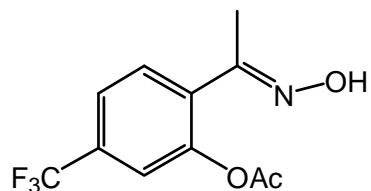


$^1\text{H}$  NMR ( $\text{CDCl}_3$ ,  $22^\circ\text{C}$ ),  $\delta$ : 2.21 (s, 3H), 2.29 (s, 3H), 2.30 (s, 3H), 7.12 (dd,  $J=8.1$ , 1.1 Hz, 1H), 7.26 (td,  $J=7.5$ , 1.1 Hz, 1H), 7.41 (td,  $J=7.9$ , 1.6 Hz, 1H), 7.46 (dd,  $J=8.0$ , 7.7, 1.6 Hz, 1H).

$^{13}\text{C}$  NMR ( $\text{CDCl}_3$ ,  $22^\circ\text{C}$ ),  $\delta$ : 16.9, 19.9, 21.3, 123.5, 126.3, 128.9, 129.8, 131.1, 148.3, 161.9, 168.6, 169.6.

ESI MS of  $\text{H}_2\text{O}$  solution of **(51)** $\text{Na}^+$ ,  $m/z$  observed: 258.0836. Calculated for  $\text{C}_{12}\text{H}_{13}\text{NNaO}_4$ , 258.0742.

**Compound 56**



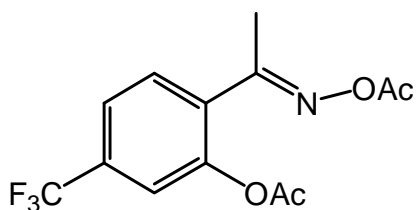
$^1\text{H}$  NMR ( $\text{CDCl}_3$ ,  $22^\circ\text{C}$ ),  $\delta$ : 2.26 (s, 3H), 2.46 (s, 3H), 7.13 (dd,  $J= 8.3, 1.3$  Hz, 1H), 7.27 (vs, 1H), 7.56 (d,  $J= 8.4$  Hz, 1H),

$^{13}\text{C}$  NMR ( $\text{CDCl}_3$ ,  $22^\circ\text{C}$ ),  $\delta$ : 13.2, 19.3, 115.6 (m), 120.2, 122.3, 125.0, 129.2, 134.1 (q), 158.9, 163.2, 166.7.

ESI MS of an aqueous solution of  $(\mathbf{56})\text{H}^+$ , positive mode,  $m/z$  observed; 262.0701, Calculated for  $\mathbf{56}\cdot\text{H}^+$ ,  $\text{C}_{11}\text{H}_{11}\text{F}_3\text{NO}_3 = 262.0691$ .

When the oxidation reaction was performed in the presence of acetic anhydride, a doubly acetoxyated acetophenone oxime was produced. However this reaction was slower and more  $\text{H}_2\text{O}_2$  was required for complete oxidation. 20 eq of  $\text{HOOH}$  was used.

**Compound 57**



$^1\text{H}$  NMR ( $\text{CDCl}_3$ ,  $22^\circ\text{C}$ ),  $\delta$ : 2.22 (s, 3H), 2.31 (s, 3H), 2.32 (s, 3H), 7.42 (s, 1H), 7.52 (d,  $J=8.7$  Hz, 1H), 7.59 (d,  $J=8.2$  Hz, 1H).

$^{13}\text{C}$  NMR ( $\text{CDCl}_3$ ,  $22^\circ\text{C}$ ),  $\delta$ : 16.8, 19.8, 21.2, 120.9 (q), 121.9, 123.1 (q), 124.7, 130.5, 132.4, 133.2 (q), 148.5, 160.9, 168.3, 169.1.

ESI MS of an aqueous solution of **57.H<sup>+</sup>**, positive mode, m/z observed = 304.0853: Calculated for C<sub>13</sub>H<sub>13</sub>F<sub>3</sub>NO<sub>4</sub>, 304.0797

#### 3.8.4 Kinetic experiments

*Activation parameters for C–O bond reductive elimination of acetic acid solutions of complex **31(OOCCF<sub>3</sub>)***

The following procedure was used for all kinetic experiments in acetic acid – *d*<sub>4</sub>.

10.0 μmol of **31(OOCCF<sub>3</sub>)** was dissolved in 1.0 ml of acetic acid-*d*<sub>4</sub> and 1.0 μl 1,4-dioxane was added as internal standard. The resulting yellow solution was transferred into a J. Young NMR tube and Teflon-sealed. <sup>1</sup>H NMR was taken before heating. The tube was then introduced into the NMR probe (500 MHz) at a pre-set temperature and <sup>1</sup>H NMR was taken at pre-set intervals. Clean formation of phenolic product **33**, and aryl acetate **35** was observed over a period of time. The disappearance of **31(OOCCF<sub>3</sub>)** was monitored, and was observed to follow first order kinetics. The spectra taken for the first 10 minutes were not used in the kinetic measurements because the solution takes approximately 5-10 minutes to equilibrate in the NMR probe. The color of the solution changed from deep yellow to colorless as the reaction progressed.

The graphs of  $\ln(c_0/c_x)$  vs. time for the C–O reductive elimination of **31**(OOCCF<sub>3</sub>) in AcOH-*d*<sub>4</sub> at various temperatures are given below.

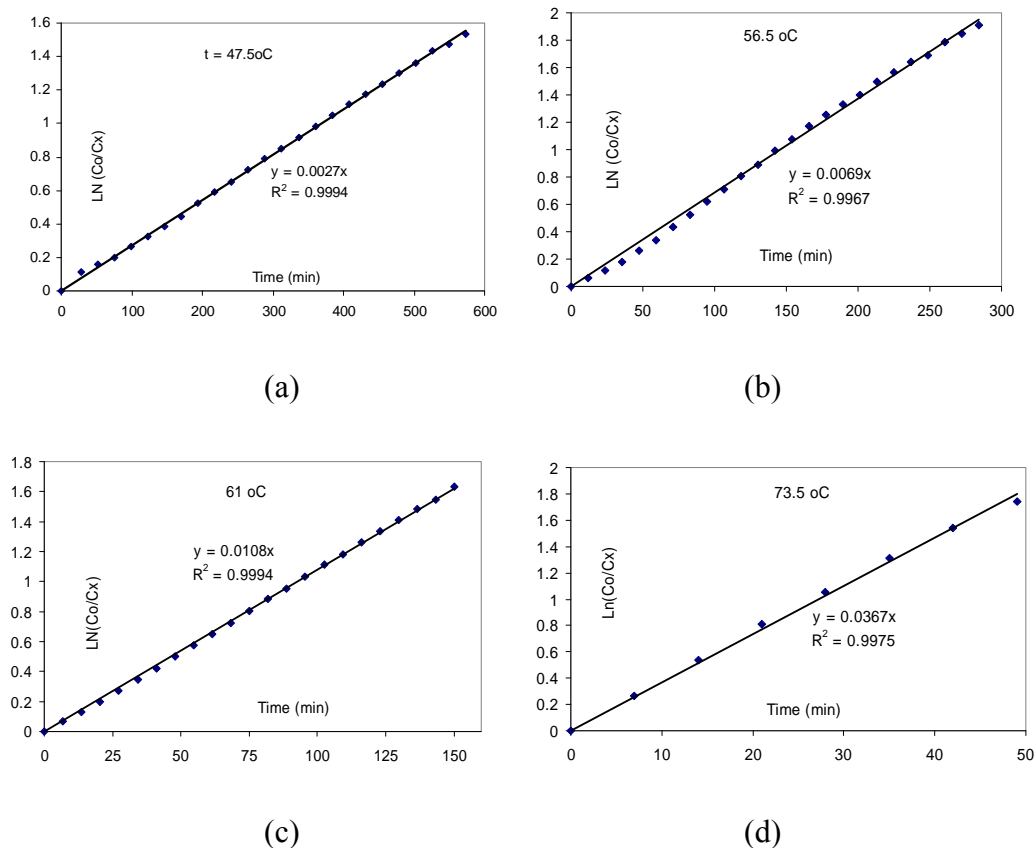


**Figure S3.1.** 1<sup>st</sup> order kinetic plots for the decomposition of acetic acid solutions of complex **31** at (a) 47.5 °C, (b) 56.5 °C, (c) 61.0 °C, (d) 73.5 °C.

*Kinetic experiments to probe electron-density on the rate of C–O reductive elimination in AcOH-*d*<sub>4</sub>*

The rate of reductive elimination from complex **31** and complex **32** was probed. 0.010 mmol of either **31**(OOCCF<sub>3</sub>) or **32**(OOCCF<sub>3</sub>) was dissolved in 1.0 ml of deuterated acetic acid and 1.0  $\mu\text{l}$  dioxane was added as internal standard. The resulting yellow solution was transferred into a J. Young NMR tube and Teflon-sealed. <sup>1</sup>H NMR was taken before heating. The tube was then introduced into the

NMR probe (500 MHz) set at 50 °C and consecutive  $^1\text{H}$  NMR spectra were taken at regular intervals. The disappearance of the starting complex was observed to follow first order kinetics. The concentrations of phenol and aryl acetate were determined by integration of a single peak that did not overlap with other peaks using dioxane as an internal standard, after addition of 5.0 eq pyridine to simplify the spectrum by freeing any coordinated products. The spectra taken for the first 10 minutes were not used in the kinetic analysis because the solution takes approximately 5-10 minutes to equilibrate in the NMR probe. The color of the solution changed from deep yellow to light yellow as the reaction progressed. At the end of the reaction, quantitative conversion to phenol and aryl acetate was observed. The product ratio for the reaction involving **31(OOCCF<sub>3</sub>)** was 58 % aryl acetate and 38 % phenol, while for the reaction involving **32(OOCCF<sub>3</sub>)** was ~ 59 % aryl acetate to 35 % phenol.

The plot of  $\ln([\text{Pd(IV)}]_0/[\text{Pd(IV)}]_x)$  vs. time for the C–O reductive elimination of **31(OOCCF<sub>3</sub>)** and **32(OOCCF<sub>3</sub>)** at 50 °C in AcOH-*d*<sub>4</sub> is given below.

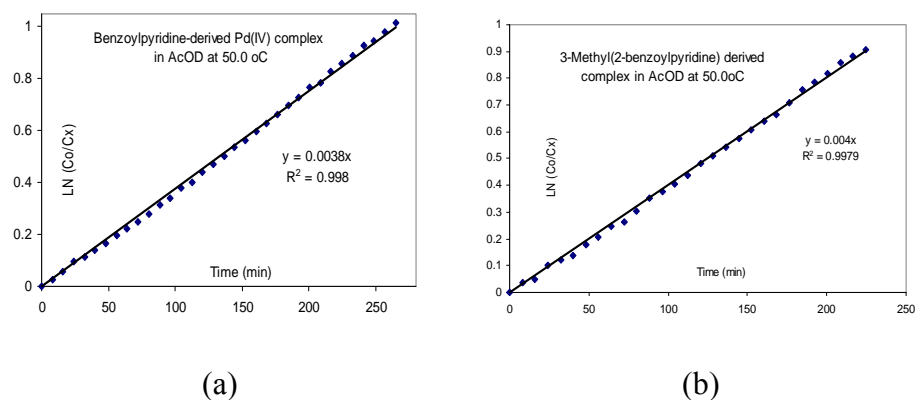


**Figure S3. 2.** First order kinetic plots for the decomposition of acetic acid solutions of complex **31** and **32** at 50°C.

*Effect of various additives on C–O reductive elimination from complex 31 in acetic acid in the presence of various additives:*

6.2 mg (0.01 mmoles  $\mu$ moles) of **31(OOCCF<sub>3</sub>)** was dissolved in 1.0 ml of deuterated acetic acid. 5 eq of additive was added to the solution followed by 1.0 ul dioxane as internal standard. The resulting yellow solution was transferred into a J. Young NMR tube and Teflon-sealed. <sup>1</sup>H NMR was taken before heating. The tube was then introduced into the NMR probe (500 MHz) set at 48°C and <sup>1</sup>H NMR was taken at pre-set intervals. Clean formation of phenolic product **33**, and aryl acetate **35** was observed over a period of time with a combined yield of > 95 %. The disappearance of **31(OOCCF<sub>3</sub>)** was observed to follow first order kinetics. The spectra taken for the first 10 minutes were not used in the kinetic measurements because the solution takes approximately 5-10 minutes to equilibrate in the NMR probe. The color of the solution changed from deep yellow to colorless as the reaction progressed. The product ratio was ~ 72 % aryl acetate to 24 % phenol.

The plot of  $\ln([\mathbf{31}]_0/[\mathbf{31}]_x)$  vs. time for the C–O reductive elimination reaction of **31(OOCCF<sub>3</sub>)** in AcOH-*d*<sub>4</sub> at 48°C in the presence of 5.0 eq pyridine is given below. The first order rate constant for the C–O reductive elimination was observed to be  $(4.3 \pm 0.1) * 10^{-4} \text{ min}^{-1}$  vs  $(2.7 \pm 0.3) * 10^{-3} \text{ min}^{-1}$  with no pyridine additive under the same conditions.

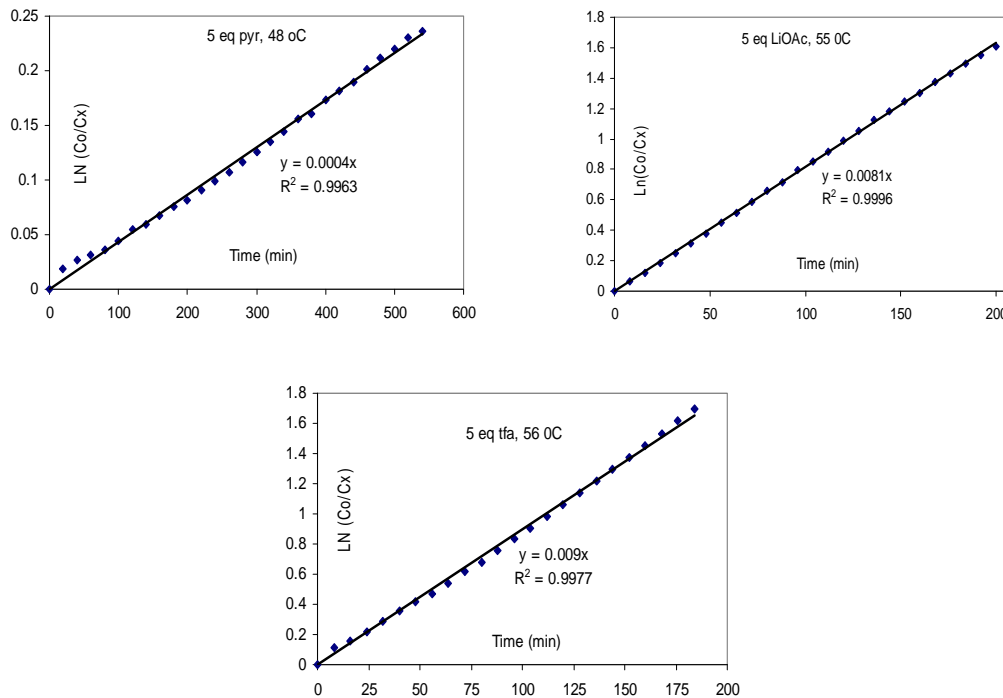


**Figure S3.3.** First order kinetic plots for the decomposition of acetic acid solutions of complex **31** at various temperatures in the presence of various additives.

#### *Kinetics experiments in the presence of NaOH additives*

In a small vial, 6.2 mg of **31(OOCCF<sub>3</sub>)** (10  $\mu\text{mol}$ ) was dissolved in 1.0 ml of D<sub>2</sub>O and 1.0  $\mu\text{l}$  1,4-dioxane was added as internal standard. Various equivalents (2-6) of NaOD were added to the solution, and the resulting yellow solution was transferred into a J. Young NMR tube and Teflon-sealed. In each case an <sup>1</sup>H NMR spectrum was taken before the start of the reaction. The tube was then placed into the NMR probe (500 MHz) set at 50°C and <sup>1</sup>H NMR spectra were taken at regular intervals. A single set of 16 multiplets was observed. The concentration of this complex which is presumed to be **44**, was monitored over a period of time. The spectra taken for the first 10 minutes were not used in the kinetics analyses because the solution takes

approximately 5-10 minutes to equilibrate to the pre-set temperature of the NMR probe.

The graphs of  $\ln(c_0/c_x)$  vs. time for the C–O reductive elimination reaction of **31(OOCCF<sub>3</sub>)** in D<sub>2</sub>O at 50 °C are given below.

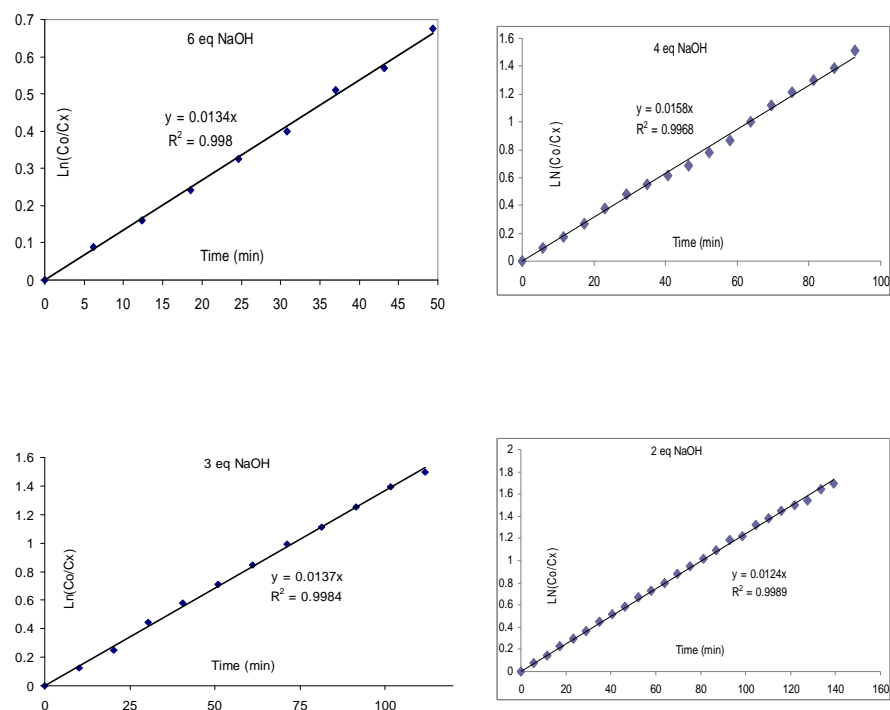
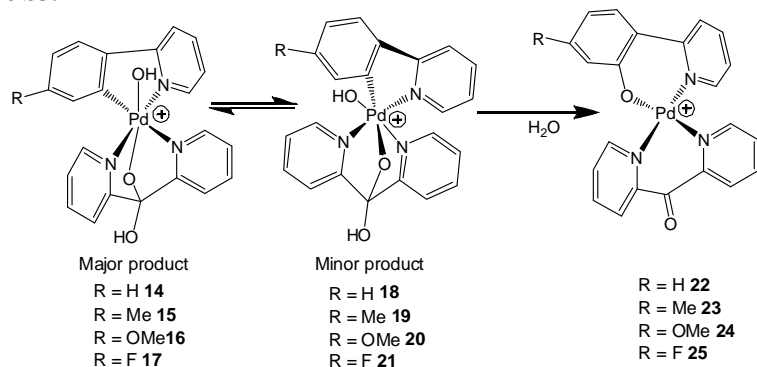


**Figure S3. 4.** First order kinetic plots for the decomposition of aqueous solutions of complex **31** at 50°C in the presence of various equivalents of NaOH.

When less than 2.0 eq of base was used, the reaction was heterogeneous and thus kinetics could not be studied.

*C-O reductive elimination reactivity from complexes 14-17 in water*

**Scheme S3. 1**



The C–O bond reductive elimination from complexes **14-17** in water was observed to generate the corresponding oxapalladacycles **22-25** in > 95 % yield. The solutions of complexes **14-17** were prepared *in-situ* by combining 0.010 M D<sub>2</sub>O solutions of complexes **10-13** with 5.0 equivalents of H<sub>2</sub>O<sub>2</sub> at 273 K since these complexes are too reactive to be isolated. In the preparation of these complexes, complexes **14-17** were prepared as major complexes while complexes **18-21** were also observed as minor complexes. At 273 K, no decomposition was observed for up to 2 hours, but when the temperature of these solutions was raised to 295 K, C–O reductive elimination was observed to cleanly generate the corresponding oxapalladacycles (see fig. S4 below).

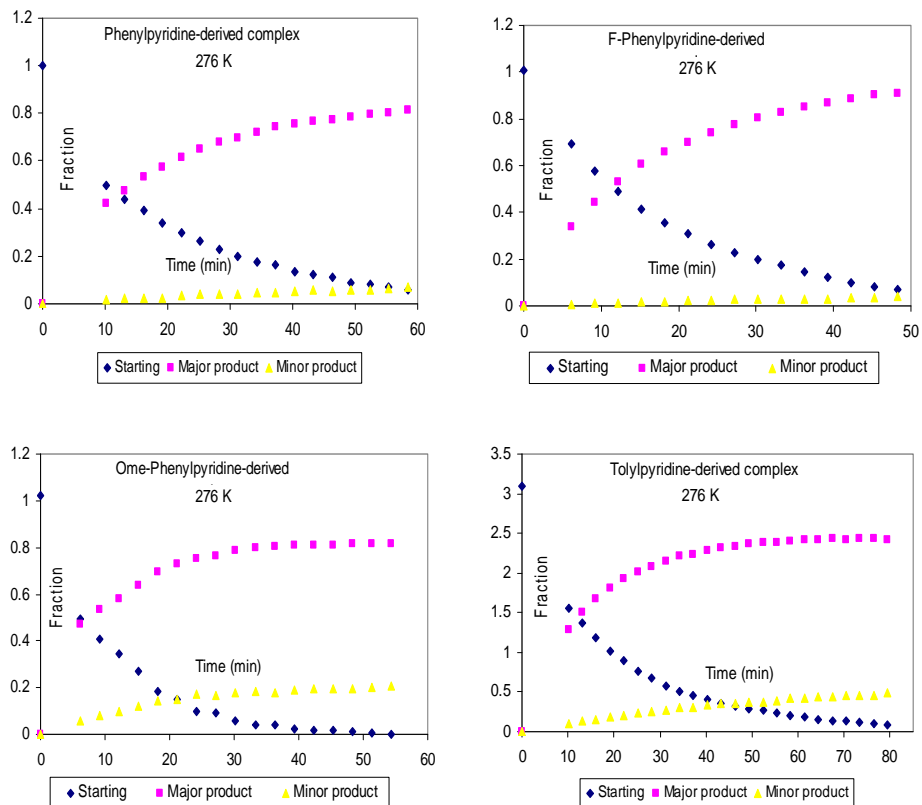
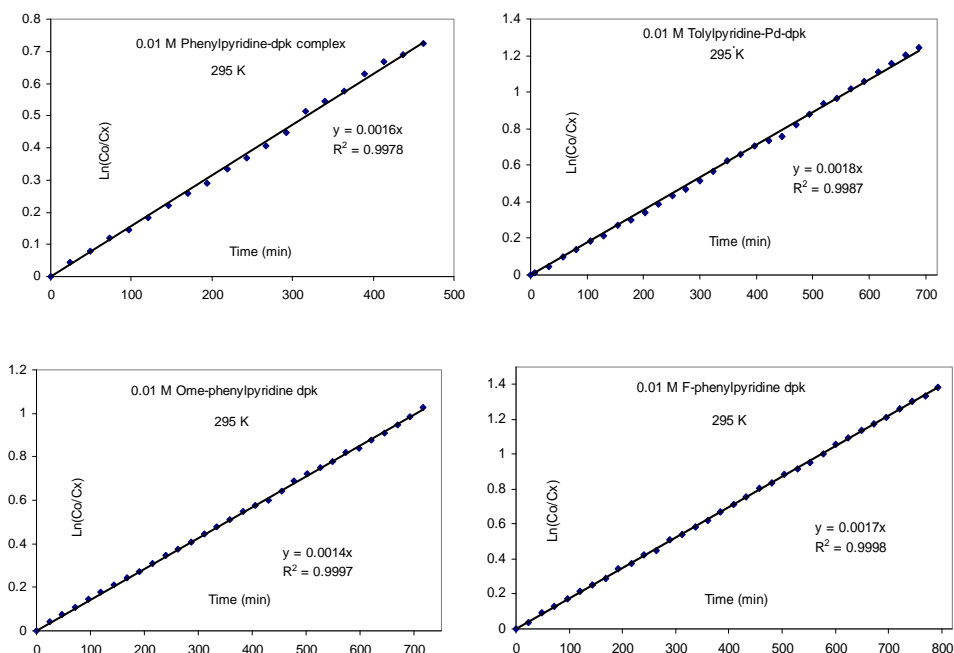


**Figure S3.4.** Plots for the C–O reductive elimination from 0.010 M D<sub>2</sub>O solutions of major products of oxidation **14-17** and minor products of oxidation **18-21** at 22°C showing the fraction of the major and minor Pd(IV) complexes as a function of time. *Kinetic study for the C-O reductive elimination reactivity from complexes 14-17 in water*

Reductive elimination from the total products of oxidation (major complexes **14-17** and minor complexes **18-21**) to oxapalladacycles **22-25** in D<sub>2</sub>O was studied by <sup>1</sup>H NMR. 0.010 ml of complexes **10-13** was dissolved in 1.0 ml of D<sub>2</sub>O and 1.0 μl of dioxane was added as internal standard. This solution was placed in ice-water bath for 10 minutes and 5.0 equivalents of H<sub>2</sub>O<sub>2</sub> were added. The resulting solution was placed in ice-water bath for 1 hour after which <sup>1</sup>H NMR was taken at 276 K to confirm complete conversion to the Pd(IV) product **14-17**. The NMR probe was warmed to 295 K and <sup>1</sup>H NMR was taken at regular intervals. The graphs of

$\ln([\text{Pd(IV)}]_0/[\text{Pd(IV)}]_x)$  vs. time for the C–O reductive elimination reaction of **14-17** in  $\text{D}_2\text{O}$  at 295 K are given below.



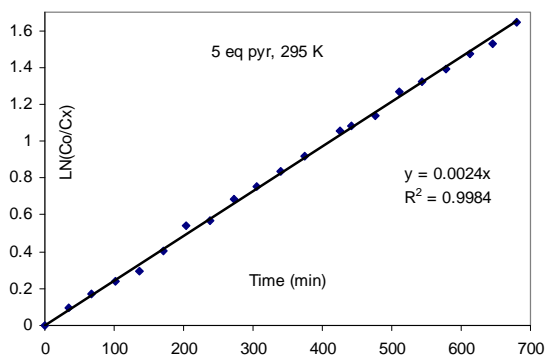
**Scheme S3. 2.** 1st order plots of  $\ln([\text{Pd(IV)}]_0/[\text{Pd(IV)}]_x)$  vs. time for the C–O reductive elimination reaction from the total products of oxidation from the oxidation of complexes **10-13** with 5.0 eq of  $\text{H}_2\text{O}_2$  in water, to the oxapalladacyclic complexes **22-25** in  $\text{D}_2\text{O}$  at 22°C.

The identity of the C–O bond forming elimination products was determined as the corresponding oxapalladacycles based on the isolation and complete characterization of complex **23**, including X–ray diffraction. However, the corresponding phenolic products were isolated via addition of HCl into the oxapalladacyclic reaction mixtures and subsequent heating at 70°C for 6 hours. The resulting reaction solution was neutralized with  $\text{NaHCO}_3$  and the product was extracted with diethyl ether. The identity of phenols **62**,<sup>21</sup> **63**,<sup>21</sup> and **64**<sup>21</sup> was confirmed by comparison of the NMR spectra to those reported in literature, while complex **25** was characterized by NMR spectroscopy and ESI–MS.

*C–O bond formation reactivity from complex 15 in H<sub>2</sub>O in the presence of various additives*

### 5.0 eq pyridine

5.2 mg **11(OAc)** was dissolved in 1.0 ml of D<sub>2</sub>O and 1.0 μl of dioxane was added as internal standard. The solution was placed in ice-water bath for 10 minutes, 5.0 eq of H<sub>2</sub>O<sub>2</sub> was added, and it was placed in ice-water bath for an additional 1 hour. <sup>1</sup>H NMR was taken at 3°C after 1 hour to confirm complete conversion to **15(OAc)**. After complete formation of **15(OAc)**, 5.0 eq of pyridine was added to the solution and <sup>1</sup>H NMR was taken at 22 °C at regular intervals. The plot of ln([**15**]<sub>0</sub>/[**15**]<sub>x</sub>) vs. time for the C–O reductive elimination reaction of complex **15** in D<sub>2</sub>O in the presence of 5.0 eq of pyridine at 22 °C is given below.

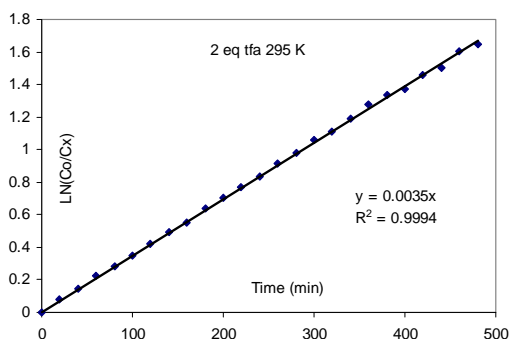


**Scheme S3. 3.** First order kinetic plot of ln([**15**]<sub>0</sub>/[**15**]<sub>x</sub>) vs. time for the depletion of **15(OAc)** to form the oxametallacyclic product **23(OAc)** in the presence of 5.0 eq of pyridine. The rate for the depletion at 22 °C is found to be  $(2.4 \pm 0.04) \times 10^{-3} \text{ min}^{-1}$ .

### 2.0 eq trifluoroacetic acid added

5.2 mg **11(OAc)** was dissolved in 1.0 ml of D<sub>2</sub>O and 1.0 μl of dioxane was added as internal standard. This solution was placed in ice-water bath for 10 minutes,

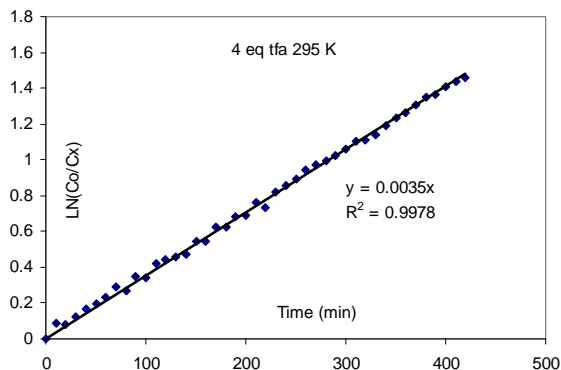
5.0 eq of H<sub>2</sub>O<sub>2</sub> was added, and it was placed back to ice-water bath for an additional 1 hour. <sup>1</sup>H NMR was taken at 3 °C to confirm complete conversion to the product. After complete formation of **15(OAc)**, 2.0 eq of deuterated trifluoroacetic acid was added to the solution and <sup>1</sup>H NMR was taken at 22 °C regular intervals. The graph of ln([**15**]<sub>0</sub>/[**15**]<sub>x</sub>) vs. time for the C–O reductive elimination reaction of complex **15** in D<sub>2</sub>O in the presence of 2.0 eq of tfa at 22 °C is given below.



**Scheme S3. 4.** First order kinetic plot of ln([**15**]<sub>0</sub>/[**15**]<sub>x</sub>) vs. time for the depletion of **15(OAc)** to form the oxametallacyclic product **23(OAc)** in the presence of 2.0 eq of tfa. The rate for the depletion at 22 °C is found to be  $(3.5 \pm 0.03) \times 10^{-3} \text{ min}^{-1}$

#### 4.0 eq trifluoroacetic acid added

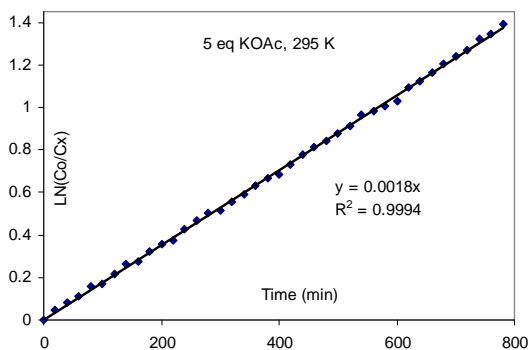
5.2 mg **11(OAc)** was dissolved in 1.0 ml of D<sub>2</sub>O and 1.0 µl of dioxane was added as internal standard. This solution was placed in ice-water bath for 10 minutes, 5.0 eq of H<sub>2</sub>O<sub>2</sub> was added, and it was placed back to ice-water bath for an additional 1 hour. <sup>1</sup>H NMR was taken at 276 K to confirm complete conversion to the product. After complete formation of **15(OAc)**, 4.0 eq of deuterated trifluoroacetic acid was added to the solution and <sup>1</sup>H NMR was taken at 22 °C at regular intervals. The graph of ln([**15**]<sub>0</sub>/[**15**]<sub>x</sub>) vs. time for the C–O reductive elimination reaction of complex **15** in D<sub>2</sub>O in the presence of 4.0 eq of tfa at 22 °C is given below.



**Scheme S3. 5.** First order kinetic plot of  $\ln([\mathbf{15}]_0/[\mathbf{15}]_x)$  vs. time for the depletion of  $\mathbf{15(OAc)}$  to form the oxametallacyclic product  $\mathbf{23(OAc)}$  in the presence of 4.0 eq of tfa. The rate for the depletion at 22 °C is found to be  $(3.5 \pm 0.04) \cdot 10^{-3} \text{ min}^{-1}$ .

### 5.0 eq KOAc added

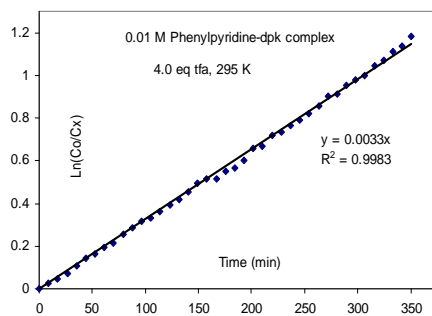
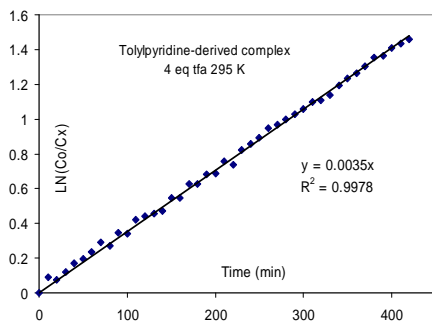
5.2 mg  $\mathbf{11(OAc)}$  was dissolved in 1.0 ml of  $\text{D}_2\text{O}$  and 1.0  $\mu\text{l}$  of dioxane was added as internal standard. This solution was placed in ice-water bath for 10 minutes, 5.0 eq of  $\text{H}_2\text{O}_2$  was added, and it was placed back to ice-water bath for an additional 1 hour.  $^1\text{H}$  NMR was taken at 3 °C to confirm complete conversion to the product. After complete formation of  $\mathbf{15(OAc)}$ , 5.0 eq of KOAc was added to the solution and  $^1\text{H}$  NMR was taken at 22 °C at regular intervals. The graph of  $\ln([\mathbf{15}]_0/[\mathbf{15}]_x)$  vs. time for the C–O reductive elimination reaction of complex  $\mathbf{15}$  in  $\text{D}_2\text{O}$  in the presence of 5.0 eq of KOAc at 22 °C is given below.



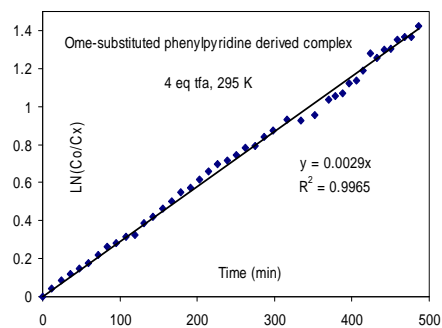
**Scheme S3. 6.** First order kinetic plot of  $\ln([\mathbf{15}]_0/[\mathbf{15}]_x)$  vs. time for the depletion of  $\mathbf{15(OAc)}$  to form the oxametallacyclic product  $\mathbf{23(OAc)}$  in the presence of 5.0 eq of KOAc. The rate for the depletion at 22 °C is found to be  $(1.76 \pm 0.01) \times 10^{-3} \text{ min}^{-1}$ .

*Effect of acid on C–O reductive elimination of complexes **14-17** in water*

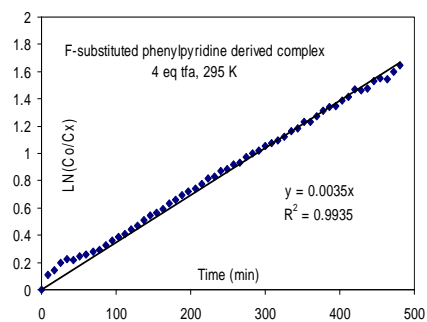
0.01 mmoles of the dpk-derived complex was dissolved in 1.0 ml of D<sub>2</sub>O and 1.0  $\mu\text{l}$  of dioxane was added as internal standard. This solution was placed in ice-water bath for 10 minutes, 5.0 eq of H<sub>2</sub>O<sub>2</sub> was added, and it was placed back to ice-water bath for an additional 1 hour. <sup>1</sup>H NMR was taken at 3 °C to confirm complete conversion to the product. After complete formation of the expected Pd(IV) adduct, 4.0 eq of deuterated trifluoroacetic acid was added to the solution and <sup>1</sup>H NMR was taken at 22 °C at regular intervals. The graphs of  $\ln([\text{Pd(IV)}]_0/[\text{Pd(IV)}]_x)$  vs. time for the C–O reductive elimination reaction of **14-17** in D<sub>2</sub>O at 22 °C in the presence of 4.0 equivalents of tfa are given below.



(a)



(b)



(c)

(d)

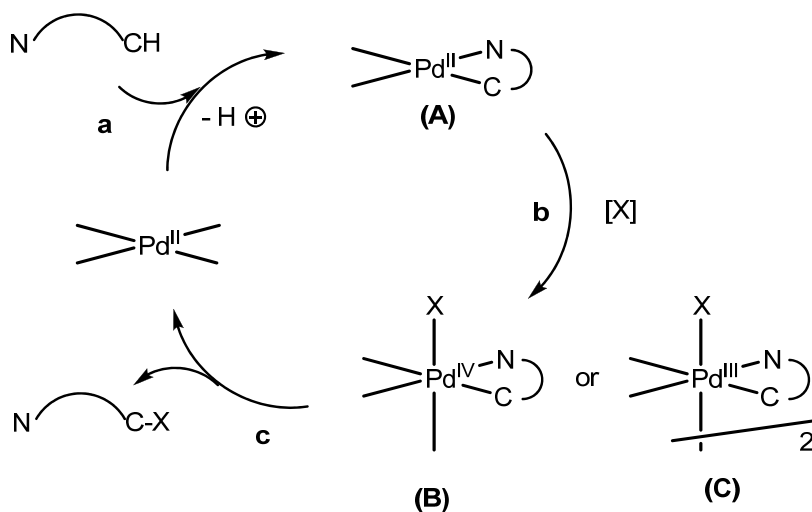
**Scheme S3. 7.** First order kinetic plots of  $\ln([\text{Pd(IV)}]_0/[\text{Pd(IV)}]_x)$  vs. time for the depletion of complexes **14-17** in  $\text{D}_2\text{O}$  at  $22^\circ\text{C}$  to form corresponding phenols in the presence of 4.0 eq of tfa. The rate for the depletion at  $22^\circ\text{C}$  is found to be  $(3.5 \pm 0.04) \times 10^{-3} \text{ min}^{-1}$ .

## Chapter 4: Synthesis and Reactivity of Monohydrocarbyl

### Pd(IV)–X in Water (X=Cl, Br, and I)

#### 4.1 Introduction

Scheme 4. 1



Palladium catalyzed processes for the functionalization of aromatic C–H bonds represent essential tools for synthetic organic chemistry. Mild and selective transformations of this type are essential in the synthesis of natural products, materials, pharmaceutical compounds, and other high value commercial products.<sup>178</sup> Recently, a variety of procedures that involve direct functionalization of aromatic C–H bonds have been developed.<sup>117</sup> Most of these procedures utilize N- or O-donor atoms as directing groups to selectively functionalize the *ortho* C–H bond. Of particular importance are the procedures for the selective halogenation of aromatic C–H bonds, given that aryl halides are important components of a variety of biologically

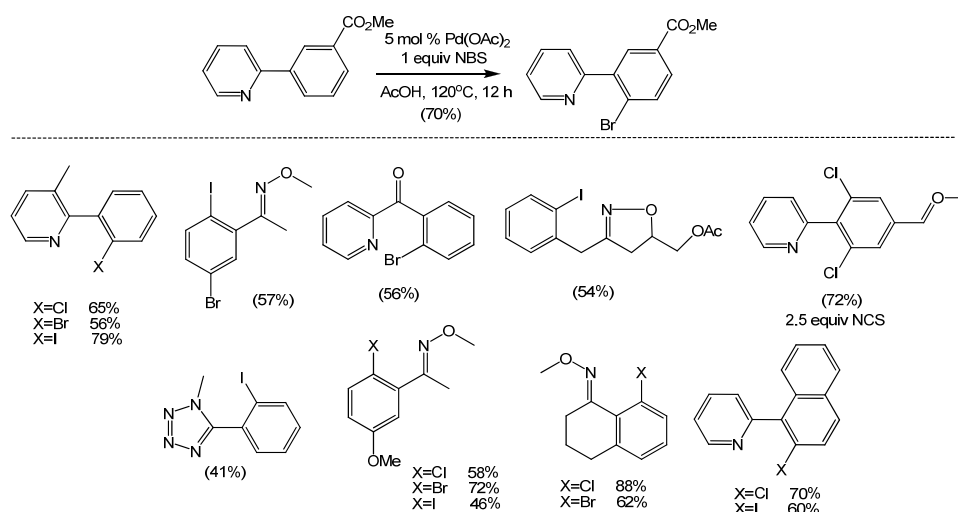
active molecules, natural products, and pharmaceuticals,<sup>87</sup> and also serve as precursors to organometallic reagents such as organolithium<sup>88</sup> and Grignard reagents.<sup>89</sup>

The most common synthetic approaches to halogenated arenes are electrophilic aromatic substitution reactions using reagents such as N-halosuccinimides,<sup>90-92</sup> X<sub>2</sub>,<sup>93</sup> peroxides/ HX,<sup>94,96</sup> peroxides/ MX,<sup>97-100</sup> or hypervalent iodine reagents/ MX (M= Li, Na, or K).<sup>101,102</sup> These transformations however suffer from several disadvantages including limited substrate scope due to the requirement for activated arenes, side reactions that include overhalogenation, and multiple regioisomeric products are usually obtained, resulting in decreased yields and the requirement for tedious separations.<sup>32,103,209,210</sup> Halogenated arenes are also prepared via directed *ortho*-lithiation followed by halogen quenching.<sup>104</sup> This technique is limited by the requirement for strong bases, which in turn results in low functional group tolerance, and a narrow scope of suitable directing groups.<sup>32</sup> As a result, the development of more efficient, selective, and environmentally friendly transition metal catalyzed procedures for halogenation of C–H bonds would be highly desirable.

An early result on the catalytic chlorination of aromatic C–H bonds with Cl<sub>2</sub> as oxidant was reported in 1970.<sup>114,115</sup> In this report, Fahey and co-workers carried out palladium catalyzed *ortho*-chlorination of azobenzenes with Cl<sub>2</sub> and generated a mixture of mono-, di-, tri-, and tetra-chlorinated products. The application of this system to organic synthesis was however limited due to the use of Cl<sub>2</sub> as oxidant, and the lack of selectivity. As a result, more practical electrophilic halogenating reagents have been the focus of current research efforts. In 2001, the N-iodosuccinimide was

applied as oxidant in the palladium catalyzed *ortho*-iodination of benzoic acids by Kodama and co-workers.<sup>116</sup> This system inspired Sanford and co-workers to develop a procedure for the palladium catalyzed *ortho* chlorination and bromination of benzo[*h*]quinoline utilizing *N*-chlorosuccinimide (NCS) and *N*-bromosuccinimide (NBS) as oxidants. These halogenation reactions have since been applied to a wide array of substrates with various directing groups such as pyridines, oxime ethers, isoquinolines, amides, and isoxazolines (Scheme 4.2).<sup>32,50</sup>

**Scheme 4.2**

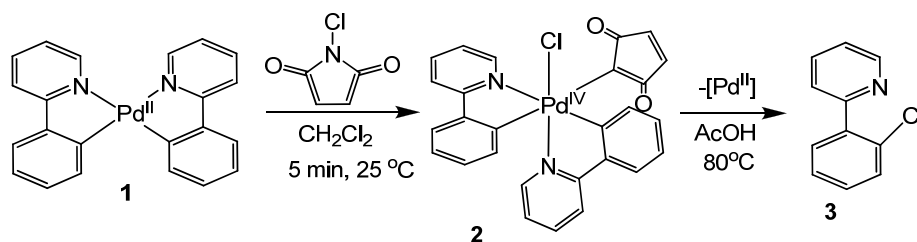


The mechanism of palladium catalyzed halogenation utilizing *N*-halosuccinimides as oxidants has recently been studied. Using 2-tolylpyridine as a model compound and NCS as oxidant, the palladium catalyzed chlorination of aromatic C–H bonds was found to be first order in [Pd] and zero order in NCS. A large intermolecular kinetic isotope effect ( $K_H/K_D = 4.4$ ) was also observed. On the basis of these experimental observations, C–H bond activation was proposed to be the rate-limiting step of this reaction. Consequently, it was not possible to determine the structure and oxidation state of the palladium intermediates involved in the

subsequent steps following the cyclopalladation reaction. As a result, model studies have been conducted in order to gain insight into the nature of intermediates involved in these steps.

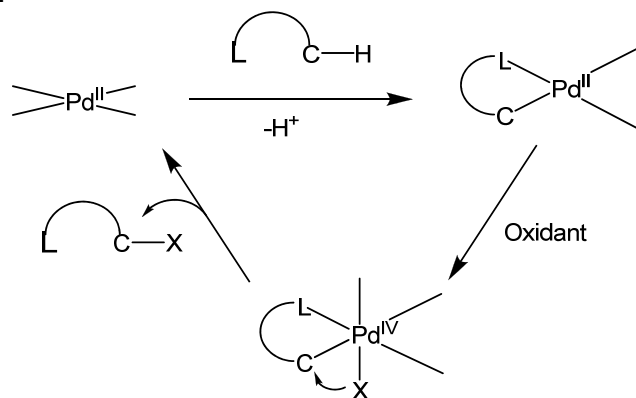
In the model studies, stoichiometric oxidation of a Pd(II) model complex (phpy)<sub>2</sub>Pd(II) **1** with NCS was performed to produce the corresponding Pd(IV) complex **2** (Scheme 4.3). Complex **2** underwent C–Cl reductive elimination upon thermolysis at 80°C to produce the corresponding aryl chloride **3** in high yield. These studies indicate that NCS is a sufficiently strong oxidant to promote oxidation of Pd(II) to Pd(IV) in this model system, and the viability of C–Cl bond-forming reductive elimination from Pd(IV) was also demonstrated.<sup>118</sup>

**Scheme 4.3**

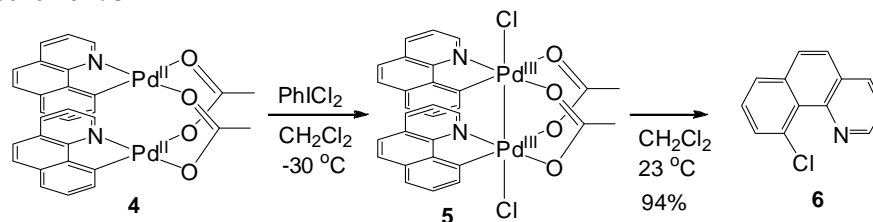


As a result of the model studies, Sanford and co-workers proposed a palladium catalyzed C–H halogenation mechanism that involves ligand-directed C–H bond activation to produce a cyclopalladated complex,<sup>50</sup> which undergoes two-electron oxidation with NCS to produce a Pd(IV) intermediate. This intermediate was proposed to undergo C–X reductive elimination to release the product and regenerate the catalyst (scheme 4.4).<sup>50</sup>

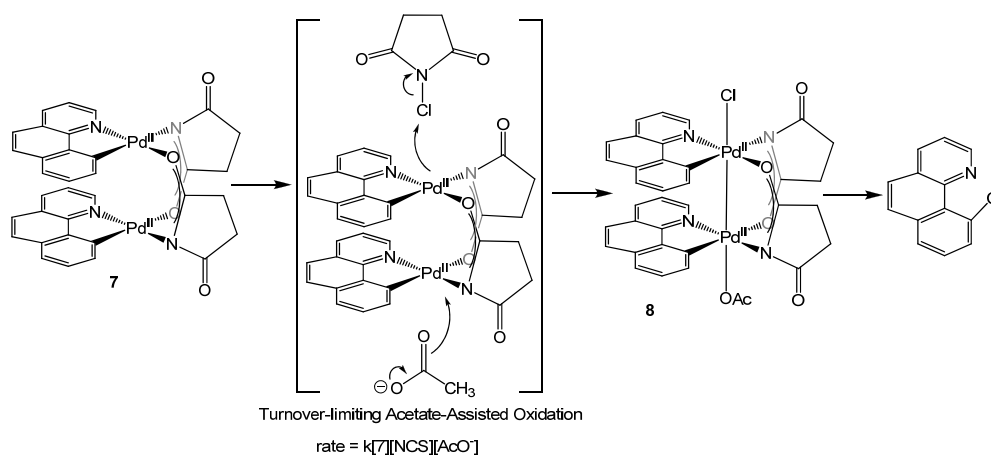
Scheme 4. 4



The intermediacy of Pd(III) complexes in the catalytic C–H bond chlorination reactions with NCS has also been considered. The reaction of the acetato-bridged palladacycle **4** with PhICl<sub>2</sub> at low temperature was observed to produce a dimeric Pd(III) complex **5** (Scheme 4.5).<sup>59</sup> Complex **5** underwent high yielding C–Cl reductive elimination when the temperature of the solution was raised to room temperature. This study indicates that NCS is a sufficiently strong oxidant to oxidize dimeric Pd(II) complexes to their Pd(III) analogues, and that the dimeric Pd(III) complexes are chemically viable intermediates in the catalytic chlorination reactions. The kinetic viability of dimeric Pd(III) complexes in the catalytic chlorination reactions was also demonstrated, where complex **5** was observed to catalyze the chlorination of benzo[*h*]quinoline in the presence of either PhICl<sub>2</sub> or NCS as oxidants. However in this system, it was not possible to determine the structure of the high valent palladium intermediate in the catalytic reactions due to a rate limiting C–H activation step.<sup>46</sup>

**Scheme 4. 5**

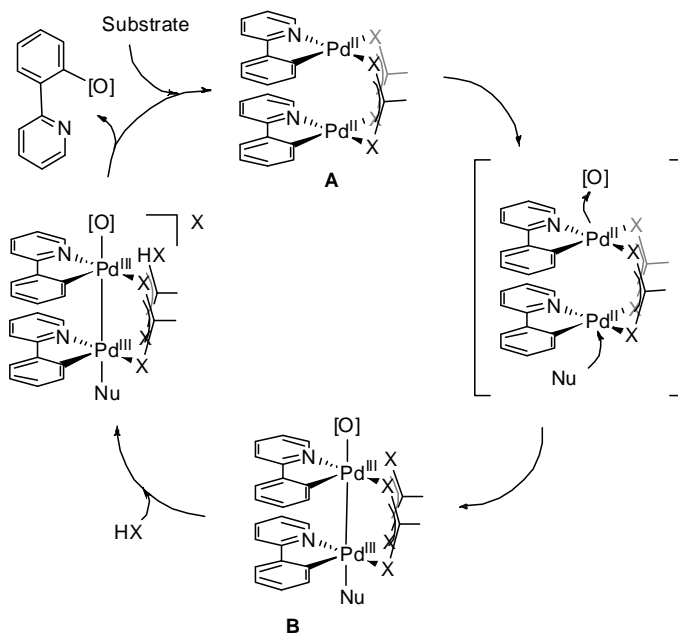
In 2010, Ritter and co-workers discovered a palladium catalyzed aromatic C–H bond chlorination reaction that takes place via rate limiting oxidation step, thus enabling characterization of the high valent palladium complexes (Scheme 4.6).<sup>46</sup> In this system, the succinamate bridged dimer **7** was proposed to be the resting state of the catalyst, while the rate law for this reaction was established as  $\text{rate} = k[\mathbf{7}][\text{NCS}][\text{OAc}^-]$ . On the basis of the rigid dinuclear structure of **7**, the measured first order dependence on the concentration of **7**, acetate, and NCS oxidant, a rate-limiting oxidation of **7** with nucleophilic assistance by acetate was proposed. This oxidation reaction was proposed to produce the dimeric  $\text{Pd}^{\text{III}}$  intermediate **8**.

**Scheme 4. 6**

Complex **8** was independently synthesized via oxidation of complex **7** with acetyl hypochlorite at  $-78\text{ }^\circ\text{C}$ , and characterized via  $^1\text{H}$  NMR at  $-90\text{ }^\circ\text{C}$ . Upon warming the solution to room temperature, C–Cl and C–O reductive elimination were observed

to generate the corresponding products in 84 % and 0.5 % yield respectively; a similar product distribution was observed during catalysis. As a result, the mechanism depicted in Scheme 4.7 was proposed for the palladium catalyzed chlorination of aromatic C–H bonds utilizing NCS as oxidant. This mechanism involves C–H bond activation to produce a dimeric Pd(II) complex **A**, which undergoes nucleophile assisted oxidation with NXS to produce a dimeric Pd(III) intermediate **B**. The intermediate undergoes acid catalyzed C–X reductive elimination to produce the functionalized product and regenerate the active catalyst **A**. This system allowed for the study of the structure of the intermediate complex, but the intermediate was not detected in solution due to its instability under the catalytic reaction conditions.

**Scheme 4.7**



As a result of the study of stoichiometric organometallic reactions described above, two mechanisms for the palladium catalyzed C–H halogenation reactions have been put forward; a mechanism involving Pd(II)/Pd(IV) redox couple and another involving Pd(II)/Pd(III) redox couple. Which of these cycles closely resembles the

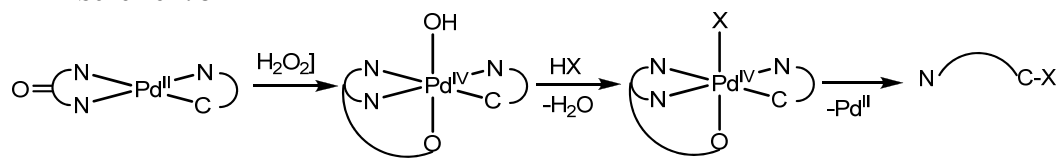
operative catalytic cycle has not been determined since most of these reactions operate via rate limiting C–H bond activation step. Thus, current research effort is aimed at understanding the mechanism of these C–H halogenation reactions with the aim of developing more selective and efficient catalysts. In addition, the study of these reaction mechanisms might enable the development of more environmentally friendly C–H bond halogenation reactions.

In an effort to develop more environmentally friendly procedures for the halogenation of aromatic C–H bonds, our research efforts have been focused on the synthesis of model halogeno-ligated monohydrocarbyl Pd(IV) complexes capable of undergoing C–halogen bond reductive elimination, utilizing environmentally friendly oxidants in water. Only a few halogeno-ligated monohydrocarbyl Pd(IV) complexes have been prepared to date and shown to undergo C–X reductive elimination.<sup>133</sup> This is because such complexes are usually too reactive to be isolated,<sup>106,201,211,212</sup> while most isolable halogeno-ligated Pd(IV) complexes possess multiple hydrocarbyl ligands, leading to fast competing C–C coupling processes.<sup>176,213,214</sup> In addition, the preparation of the halogeno-ligated monohydrocarbyl Pd(IV) complexes utilizing environmentally benign oxidants in water will allow for the substitution of the more common NXS and PhIX<sub>2</sub> oxidants, which are currently used in the catalytic C–H halogenation reactions, since these oxidants produce stoichiometric amounts of waste products. As such, our ultimate goal is to develop “green” palladium catalyzed C–H halogenations reactions utilizing environmentally benign oxidants in water.

A more atom-economical procedure for the preparation of model halogeno-ligated monohydrocarbyl Pd(IV) complexes involves ligand enabled oxidation of

organopalladium(II) complexes with H<sub>2</sub>O<sub>2</sub> in water, with subsequent reaction of the Pd(IV) hydroxo species with HX acids (X=Cl, Br, I, and F) (Scheme 4.8). We have previously reported the preparation of hydroxo-ligated monohydrocarbyl Pd(IV) complexes using H<sub>2</sub>O<sub>2</sub> in water (See Chapter 2). In order to prepare the halogeno-ligated Pd(IV) complexes, an acid assisted substitution of the hydroxo ligand by the halogeno ligand will be attempted. Upon formation of the halogeno-ligated Pd(IV) complex, we will investigate the C–X reductive elimination reactions.

**Scheme 4.8**



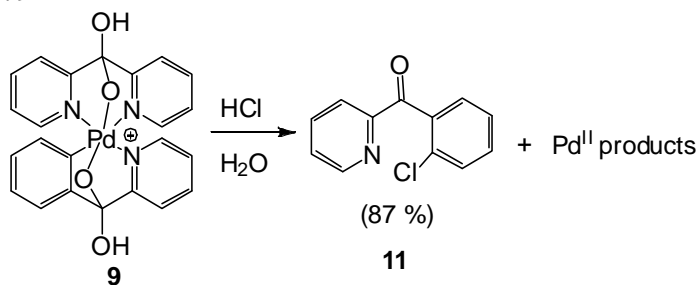
We started by preparing the alkoxy-ligated monohydrocarbyl Pd(IV) complexes derived from the 2-arylpyridine fragment, and studying their C–Cl reductive elimination reactivity in the presence of HCl.

#### 4.2 C–Cl Bond Formation at Monohydrocarbyl Pd(IV) Alkoxides in Water in the Presence of HCl

##### 4.2.1 C–Cl Bond Formation at 2-Arylpyridine-derived Monohydrocarbyl Pd(IV)

##### Alkoxides **9** and **15** in Water in the Presence of HCl.

**Scheme 4.9**

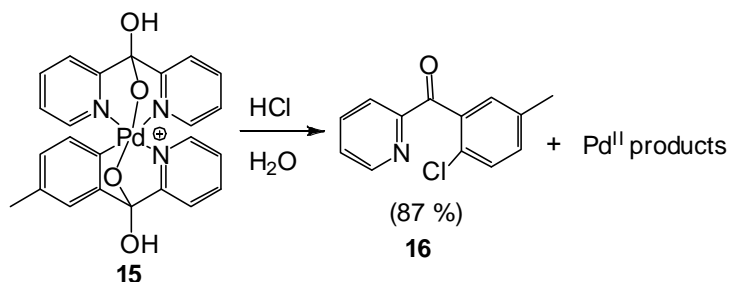


The procedure for the preparation of complex **9** and its characterization has been described in chapter 2. We started by studying the decomposition of the alkoxo-ligated Pd(IV) complex **9** in water in the presence of HCl to produce the corresponding aryl halide **11**. A 0.010 M D<sub>2</sub>O solution of complex **9** was prepared and 1.0 μl of 1,4-dioxane was added as internal standard. A <sup>1</sup>H NMR spectrum of this solution was taken, and 40.0 eq of HCl dissolved in D<sub>2</sub>O were added to the solution at room temperature. Upon addition of HCl, a yellow precipitate was gradually produced. <sup>1</sup>H NMR analysis of the reaction mixture upon addition of HCl revealed the presence of an additional minor set of signals in the aromatic region of the spectrum, which disappeared at the end of the reaction (Fig. 4.1). This reaction mixture was heated at 70°C for 6 hours, where a white precipitate was gradually produced as the reaction progressed. After 6 hours, pyridine-*d*<sub>5</sub> was added to the reaction mixture to free any coordinated products, and a <sup>1</sup>H NMR spectrum was collected. The spectrum revealed the presence of a major product in 89 % yield, with 8 multiplets in the aromatic region integrating as 1H each, and the corresponding phenol **13** in < 5 % yield. The ESI-MS analysis of this reaction mixture revealed a major mass envelope at *m/z* = 218.0410 (calculated for C<sub>12</sub>H<sub>9</sub>ClNO = 218.0373) which was assigned to the protonated aryl chloride **11.H**<sup>+</sup>, and a minor mass envelope at 200.0675 (calculated for C<sub>12</sub>H<sub>10</sub>NO<sub>2</sub> = 200.0712) which was assigned to the corresponding protonated phenol **13.H**<sup>+</sup>. The major compound **11** was isolated by extraction of the aqueous reaction mixture with diethyl ether. The major product was assigned as the corresponding Ar-Cl, **11**, by ESI-MS analysis and comparison of its <sup>1</sup>H NMR spectrum to that reported in literature.<sup>215</sup>



spectroscopy upon addition of HCl to an aqueous solution of complex **9**, which may be assigned to the chloro-ligated Pd(IV) complex **12** based on the ESI-MS analysis. C-Cl reductive elimination from complex **12** produces the corresponding chlorinated product **11** in high yields. The corresponding phenol **14** was also detected by ESI-MS.

**Scheme 4. 11**



C-Cl bond coupling from the 3-methyl(2-benzoyl)pyridine derived complex **15** was also investigated. In these studies, a 0.010 M D<sub>2</sub>O solution of complex **15** was prepared, 1.0 μl of 1,4 dioxane was added as internal standard, and <sup>1</sup>H NMR spectrum of this solution was collected at room temperature. 40.0 equivalents of HCl were added to the solution, leading to gradual formation of a yellow precipitate. This reaction mixture was heated at 70°C for 6 hours, where formation of a white precipitate was observed as the reaction progressed. Analysis of this reaction solution by <sup>1</sup>H NMR spectroscopy at the end of the reaction upon addition of pyridine-d<sub>5</sub> to free any Pd-coordinated products revealed the presence of a single product in 87 % yield relative to the internal standard, with seven multiplets in the aromatic region integrating as 1H each, and one singlet in the aliphatic region integrating as 3H. Analysis of this reaction mixture by ESI-MS revealed a mass envelope at 232.0499 (Calculated for C<sub>13</sub>H<sub>11</sub>ClNO = 232.0529) which was assigned to the protonated aryl

chloride compound **16.H<sup>+</sup>**. The product **16** was isolated by extraction of the aqueous reaction mixture with diethyl ether. The product was identified as the corresponding aryl chloride by ESI-MS analysis and comparison of its <sup>1</sup>H NMR spectrum to a commercially available sample.

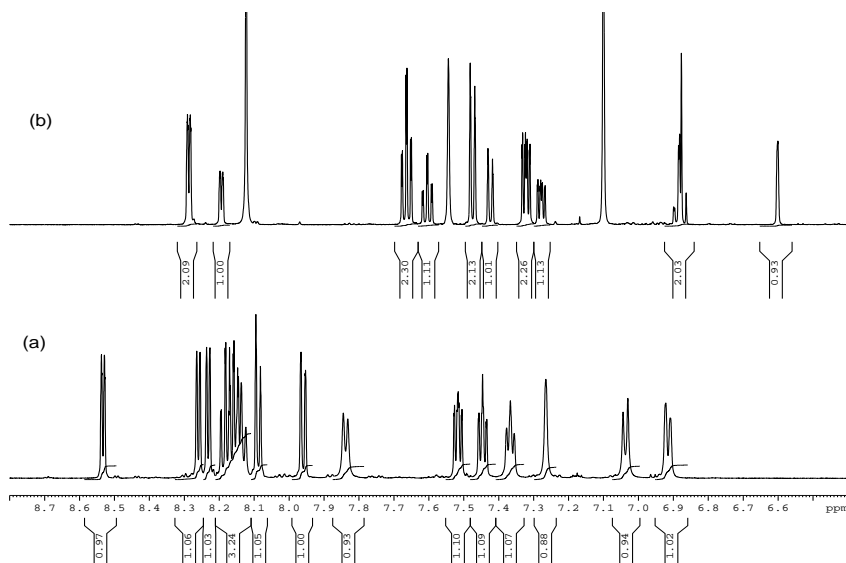
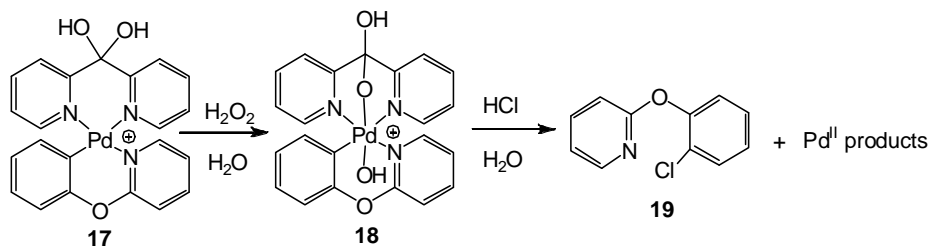


**Figure 4. 2.** Room temperature <sup>1</sup>H NMR spectra of (a) complex **15** in D<sub>2</sub>O, (b) the reaction mixture after C–Cl reductive elimination showing product **16** together with a symmetrical dpk-ligated Pd(II) product.

#### 4.2.2 C–Cl Bond Formation at 2-Phenoxyppyridine-derived Monohydrocarbyl Pd(IV)

##### Alkoxides **18** in Water in the Presence of HCl.

##### Scheme 4. 12



C–Cl bond formation at phenoxy-pyridine derived hydroxo-ligated monohydrocarbyl Pd(IV) complex **18** in the presence of HCl was also performed. A 0.010 M D<sub>2</sub>O solution of complex **18** was prepared *in-situ* by the oxidation of complex **17** with 0.95 equivalents of H<sub>2</sub>O<sub>2</sub> at 0°C, and 1,4 dioxane was added as internal standard. A <sup>1</sup>H NMR spectrum was collected and 40.0 equivalents of HCl were added to the solution at room temperature. Upon addition of HCl, another <sup>1</sup>H NMR spectrum was collected, where an additional minor set of signals was observed. Addition of HCl also led to gradual formation of a yellow precipitate. The resulting reaction mixture was heated at 70°C for 6 hours, where gradual formation of a white precipitate was observed. After 6 hours, a small amount of pyridine-d<sub>5</sub> was added to free any Pd-coordinated products, and a <sup>1</sup>H NMR spectrum was collected. The <sup>1</sup>H NMR spectrum of this reaction mixture revealed the presence of two species in solution. The first species displayed 8 multiplets in the aromatic region, integrating as 1H each, which was assigned to the organic product, while the second species displayed 4 multiplets in the aromatic region integrating as 2H each, which was assigned to a symmetrical dpk-ligated Pd(II) containing species. ESI–MS analysis of the reaction mixture revealed a mass envelope at m/z = 206.0408 (calculated for C<sub>11</sub>H<sub>9</sub>ClNO = 206.0373) which was assigned to the corresponding protonated aryl chloride **19.H<sup>+</sup>**. The organic compound **19** was isolated by extraction of the aqueous reaction mixture with diethyl ether, and its identity was confirmed as the corresponding aryl halide **19** by comparison of its <sup>1</sup>H NMR spectrum to that in literature.

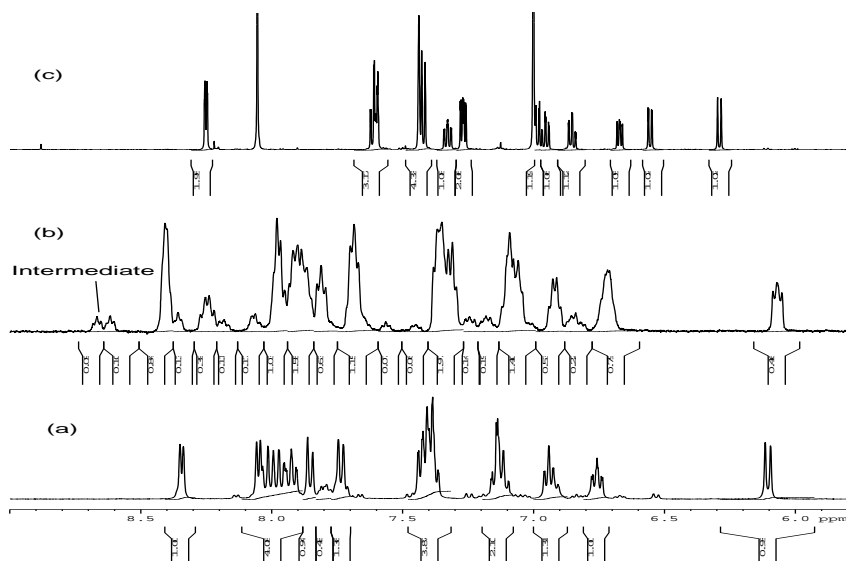
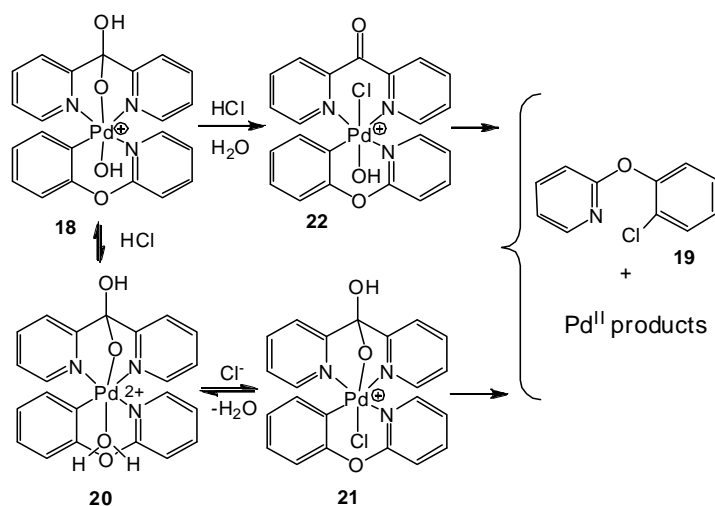


**Figure 4. 3.** Room temperature  $^1\text{H}$  NMR spectra of (a) complex **18** in  $\text{D}_2\text{O}$ , (b) complex **18** in  $\text{D}_2\text{O}$  upon addition of  $\text{HCl}$ , showing an additional set of signals belonging to an intermediate complex; (c)  $^1\text{H}$  NMR of the reaction mixture after decomposition, showing the C–Cl reductive elimination product **19** together with a symmetrical dpk-ligated Pd(II) product in the presence of pyridine- $\text{d}_5$ , which was added to free any Pd-coordinated products.

**Scheme 4. 13**



Analysis of the reaction solution by ESI–MS upon addition of  $\text{HCl}$  revealed a mass envelope at 511.9913 which may be assigned to the corresponding chloro-ligated Pd(IV) complex **22** or its isomer **21** (calculated for  $\text{C}_{22}\text{H}_{17}\text{ClN}_3\text{O}_3\text{Pd}^{106} =$

511.9993) (Scheme 4.13). Complex **22** might be produced by chelate opening of complex **18** in the presence of HCl, while complex **21** may be produced by protonation of complex **18** to produce an aqua-ligated Pd(IV) complex **20**, which may subsequently undergo ligand exchange in the presence of HCl. Protonation of a similar hydroxo-ligated Pd(IV) complex **24** to produce an aqua-ligated Pd(IV) complex **28** has been reported previously (Fig. 4.4). C–Cl reductive elimination from either **21** and/ or **22** produces the corresponding C–Cl bond coupling product **19**.

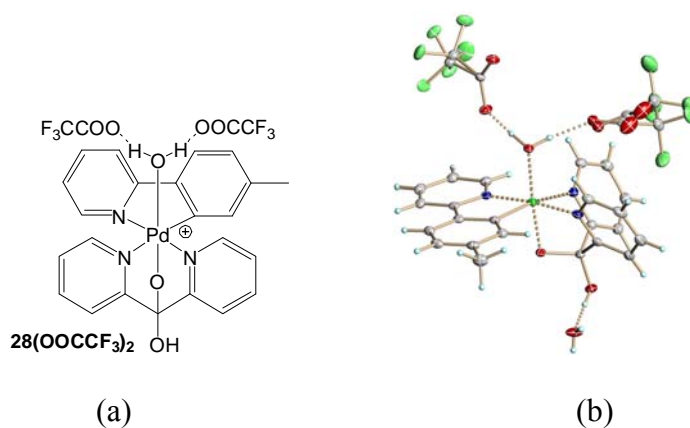


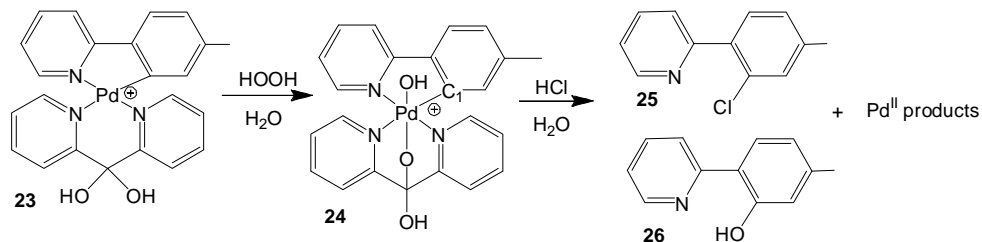
**Figure 4. 4.** (a) The aqua-ligated Pd(IV) complex **28** prepared via protonation of complex **24** with trifluoroacetic acid; (b) ORTEP drawing (50 % probability ellipsoid) of complex **30**.

Attempts to isolate the chloro-ligated Pd(IV) complexes from the reaction mixtures above were however not successful. Upon addition of HCl to an aqueous solution of complex **18**, a deep yellow precipitate is produced. This precipitate was filtered off and washed with a small amount of cold water. Analysis of the precipitate by  $^1\text{H}$  NMR in water, methanol and acetone produced complex spectra, indicative of multiple species in solution.

#### 4.2.3 C–Cl Bond Formation at 2-Tolylpyridine-derived Monohydrocarbyl Pd(IV)

##### Alkoxide **24** in Water in the Presence of HCl.

**Scheme 4. 14**



C–Cl reductive elimination was also attempted from the tolylpyridine derived hydroxo-ligated Pd(IV) complex **24** in water in the presence of HCl. A 0.010 M D<sub>2</sub>O solution of complex **24** was prepared *in-situ* by the oxidation of complex **23** with 0.95 equivalents of H<sub>2</sub>O<sub>2</sub> at 0°C, and 1,4 dioxane was added as internal standard. <sup>1</sup>H NMR was collected and 10.0–40.0 equivalents of HCl were added to this solution. Upon addition of HCl, a <sup>1</sup>H NMR spectrum was collected, where an additional minor set of signals was observed in the aromatic region (Fig. 4.5). Addition of HCl also led to gradual formation of a yellow precipitate. Heating the reaction mixture at 70°C for 6 hours led to gradual formation of a white precipitate. After 6 hours, a small amount of deuterated acetic acid was added to dissolve the products, and a small amount of pyridine-d<sub>5</sub> was added to free any coordinated products. A <sup>1</sup>H NMR spectrum was collected, where a mixture of two organic products was observed whose relative fractions were dependent on the amount of HCl used (Table 4.1). ESI–MS analysis the reaction mixture displayed a major mass envelope at *m/z* = 204.0538 (calculated for C<sub>12</sub>H<sub>11</sub>ClN = 204.0580) which was assigned to the corresponding protonated aryl chloride **25.H<sup>+</sup>**, and *m/z* = 186.0854 (calculated for C<sub>12</sub>H<sub>12</sub>NO = 186.0919) which was assigned to the corresponding protonated phenol **26.H<sup>+</sup>**. The major product

according to  $^1\text{H}$  NMR was identified as the corresponding aryl chloride via independent synthesis using literature procedures for palladium catalyzed chlorination of aromatic C–H bonds,<sup>32</sup> while the minor product was identified as the corresponding phenol via comparison of its  $^1\text{H}$  NMR to that of independently prepared compound. The highest selectivity for the aryl chloride **25** was observed when 40.0 equivalents of HCl were used, where the aryl chloride was produced as the only organic product, in 80 % yield relative to an internal standard. The aryl chloride was isolated by extraction of the aqueous reaction mixture with diethyl ether.

**Table 4. 1.**  $^1\text{H}$  NMR yields of the aryl chloride **25** and phenol **26** products relative to the amount of HCl used.

HCl (eq)	R-X (%)	R-OH (%)
10.0	38	51
20.0	51	37
40.0	> 80	0

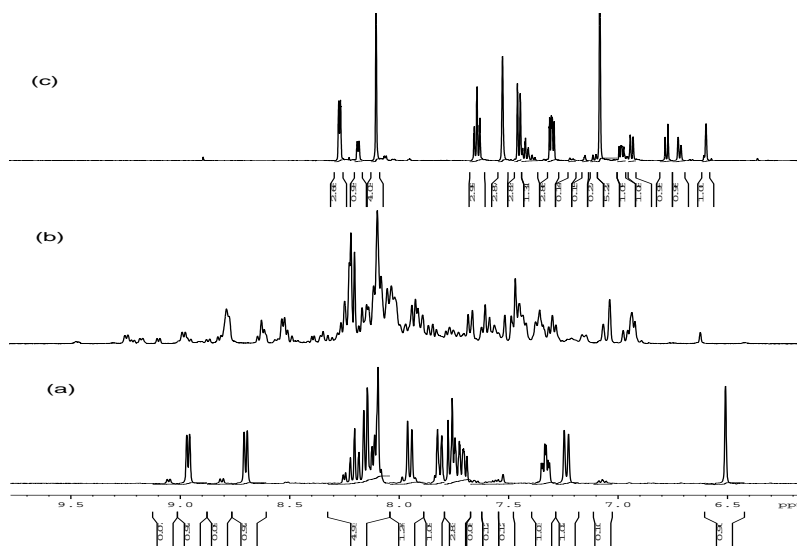
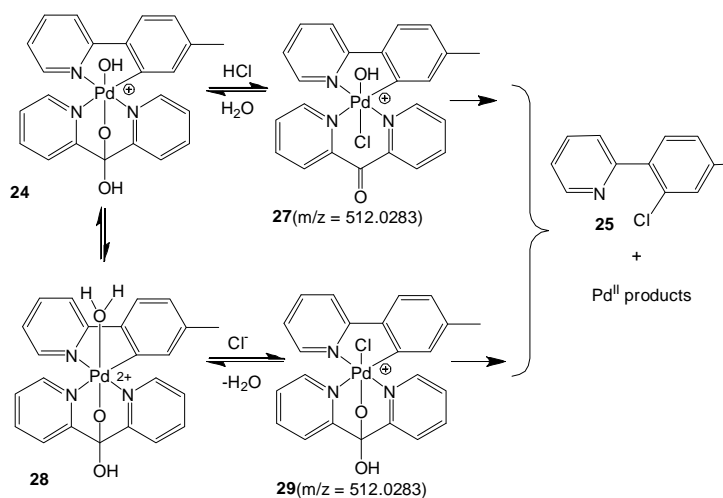


**Figure 4. 5.** Room temperature  $^1\text{H}$  NMR spectra of (a) complex **24** in  $\text{D}_2\text{O}$ , (b) complex **24** in  $\text{D}_2\text{O}$  upon addition of HCl; (c) the reaction mixture after

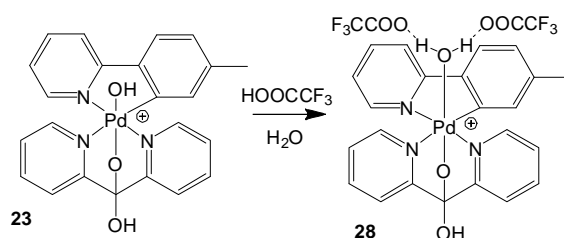
decomposition in the presence of pyridine-d<sub>5</sub>, showing C–Cl elimination product **25** and Pd(II) derived complexes.

**Scheme 4.15**



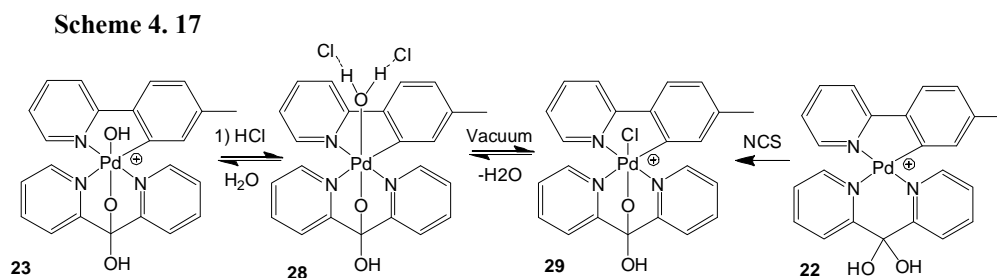
Analysis of the reaction mixture by ESI–MS upon addition of HCl revealed a major complex with a mass envelope at  $m/z = 512.0283$ , which may be assigned to the chloro-ligated Pd(IV) complex **27** or its isomer **29** (calculated for  $C_{23}H_{19}ClN_3O_2^{106}Pd = 512.0199$ ) (Scheme 4.15). Complex **27** could form via chelate opening of complex **24** in the presence of HCl, while complex **29** may be formed by protonation of complex **24** to produce the aqua ligated Pd(IV) complex **28** with chloride counterions. An aqua-ligated Pd(IV) complex **28** with trifluoroacetate counterions was isolated upon addition of trifluoroacetic acid to an aqueous solution of complex **24**, and this complex was characterized fully, including X-ray diffraction (Scheme 4.16). Complex **28** may undergo ligand substitution in the presence of chloride anions to produce the chloro-ligated Pd(IV) complex **29**. Based on the ESI–MS analysis, the intermediate detected by <sup>1</sup>H NMR spectroscopy may be assigned to complex **27** and/ or **28**, or their respective isomers.

Scheme 4.16



As a result, the C–Cl bond coupling reaction from the hydroxo-ligated Pd(IV) complex **24** in water in the presence of HCl to produce the aryl chloride **25** was proposed to take place via intermediate **27** and/ or **28** (Scheme 4.15), which have been detected by both <sup>1</sup>H NMR spectroscopy and ESI–MS.

In order to determine the structure of the intermediate complex produced upon addition of HCl to an aqueous solution of complex **24**, the reaction mixture was filtered and the orange precipitate was characterized by NMR spectroscopy and ESI–MS. The <sup>1</sup>H NMR chemical shifts of the orange solid in D<sub>2</sub>O were identical to that of complex **28**(OOCCF<sub>3</sub>)<sub>2</sub>, which was produced by protonation of complex **24** with trifluoroacetic acid in water, and was fully characterized, including X-ray diffraction. Consequently, the yellow solid was assigned to the corresponding aqua ligated Pd(IV) complex **28** with two chloride counterions.



When complex **28** was placed under high vacuum at room temperature to dry, an additional set of signals was observed to develop in the <sup>1</sup>H NMR spectrum of the residue in D<sub>2</sub>O, while signals belonging to complex **28** disappeared gradually.

Ultimately when complex **28** was left under high vacuum for 3 hours, the  $^1\text{H}$  NMR spectrum of this residue in  $\text{D}_2\text{O}$  was simple, displaying a pattern that was significantly different from that of complex **28**. This complex was observed to decompose at room temperature in water over 3 days to produce the C–Cl bond coupling product **24** in  $> 90\%$  yield. This reactivity indicates that the new complex is most likely a chloro-ligated Pd(IV) complex capable of undergoing C–Cl bond coupling. In addition, ESI–MS analysis of this complex in methanol exhibited a major mass envelope at  $m/z = 512.0283$  (calculated for  $\text{C}_{23}\text{H}_{19}\text{ClN}_3\text{O}_2^{106}\text{Pd} = 512.0199$ ). Consequently, the structure of this new species was assigned to the chloro-ligated Pd(IV) complex **29**.

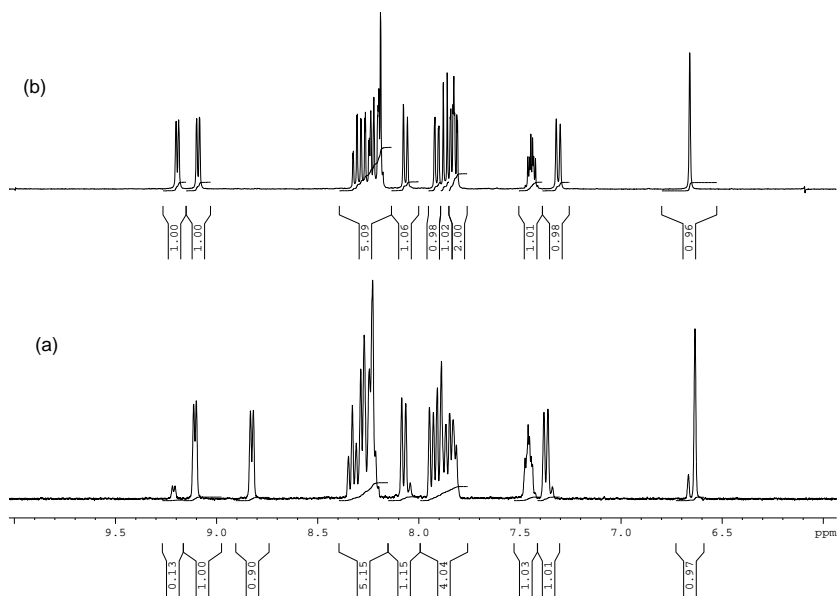
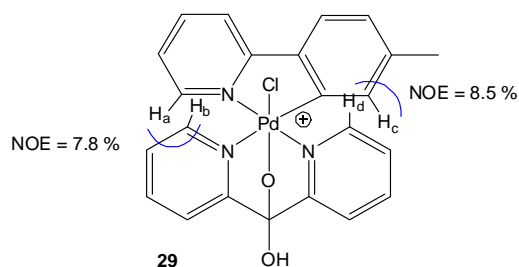


**Figure 4. 6.** (a)  $^1\text{H}$  NMR of aqua-ligated Pd(IV) complex **28** in  $\text{D}_2\text{O}$  at room temperature; (b)  $^1\text{H}$  NMR of chloro-ligated Pd(IV) complex **29** in  $\text{D}_2\text{O}$  at room temperature.

Although other isomers are possible in this reaction, the structure of complex **29** was assigned based on NOE analysis.



Given that irradiation of  $H_a$  results in NOE enhancement of  $H_b$  (7.8%), while irradiation of  $H_c$  results in NOE enhancement of  $H_d$  (8.5 %, mixing time of 0.6s, delay time 4s), this indicates that these sets of hydrogens are in close proximity, and thus an equatorial arrangement of the tolylpyridine and dpk fragments was considered. Although the NOE analysis cannot be used to differentiate between the structure of complexes **27** and **29**, complex **29** is favored because it is produced from the aqua ligated complex **28** under vacuum. Complex **28** was fully characterized, including X-ray diffraction studies, and the structure of complex **27** is expected to be similar to that of **28**. In addition, complex **29** is thermodynamically more stable than complex **27** as a result of the tridentate facial chelating mode of the ligand.

Complex **29** could also be independently prepared by combining the Pd(II) complex **23** with N-chlorosuccinimide (NCS) oxidant in water. The NMR analysis and reactivity of this complex is similar to that of complex (**29**)Cl, produced upon exposing the aqua-ligated Pd(IV) complex (**28**)Cl<sub>2</sub> to high vacuum. This analysis indicates that addition of HCl to an aqueous solution of complex **24** produces the aqua-ligated dicationic Pd(IV) complex (**28**)Cl<sub>2</sub>, which when placed under vacuum, undergoes ligand substitution to produce the chloro-ligated Pd(IV) complex (**29**)Cl. The substitution of the aqua for chloro ligand is probably driven by loss of a water molecule under vacuum.

Having prepared the chloro-ligated Pd(IV) complex **(29)Cl** in pure form, we investigated whether this complex is produced during the decomposition of complex **24** in water in the presence of HCl, since this reaction was observed to produce the corresponding aryl chloride in high yield. ESI-MS analysis of the aqueous solution of complex **24** upon addition of HCl revealed a mass envelope at  $m/z = 512.0283$ , corresponding to complex **29**. Additionally, the  $^1\text{H}$  NMR spectrum of the reaction mixture collected upon addition of 40.0 equivalents of HCl to an aqueous solution of complex **24** revealed the presence of an intermediate which was absent at the end of the reaction. Analysis of the  $^1\text{H}$  NMR spectrum of the intermediate revealed the presence of signals corresponding to complex **29**. Thus, this analysis indicates that complex **(29)Cl** is produced upon addition of HCl to an aqueous solution of complex **24**.

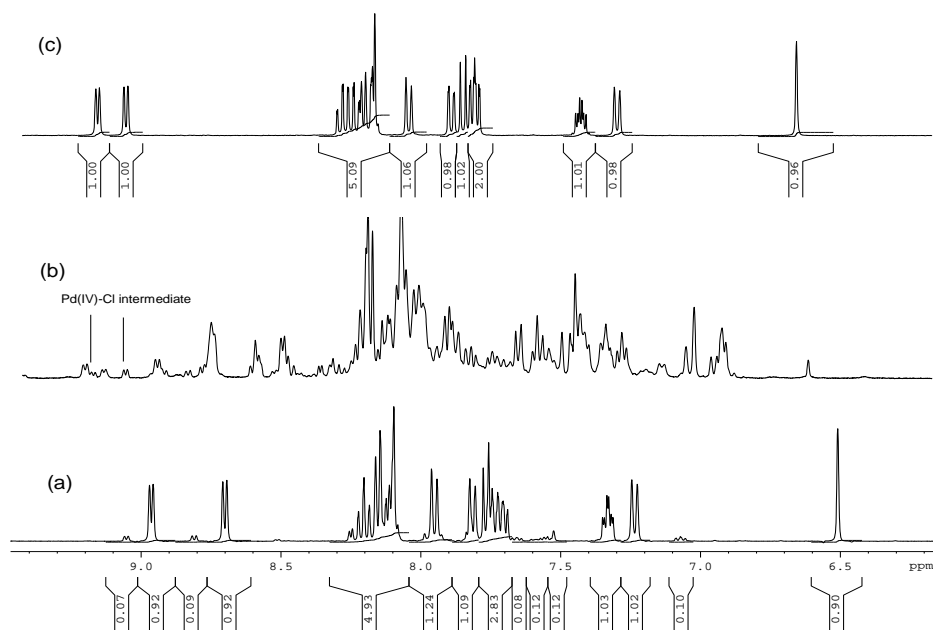
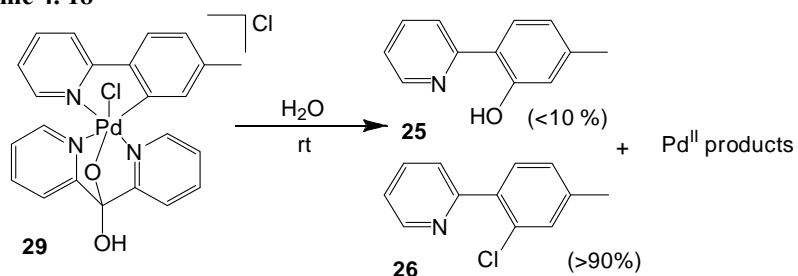


**Figure 4. 7.** Room temperature  $^1\text{H}$  NMR spectra of (a) complex **24** in  $\text{D}_2\text{O}$ , (b) complex **24** in  $\text{D}_2\text{O}$  upon addition of HCl; (c) complex **29** in  $\text{D}_2\text{O}$ .

Consequently, this analysis supports the mechanism of C–Cl bond coupling from complex **24** in water in the presence of HCl presented in Scheme 12 above, where the intermediacy of complex **29** has been proposed. However, given that multiple additional signals apart from those belonging to complex **29** are produced when HCl is added to an aqueous solution of complex **24**, other chloro-ligated Pd(IV) complexes may also be present in the solution such as **27**, and thus several complexes might be responsible for the C–Cl coupling reaction.

The kinetics study of C–Cl reductive elimination reaction from a D<sub>2</sub>O solution of complex **29** was also performed (Scheme 4.18).

Scheme 4.18



In the kinetics experiment, the decomposition of a ~ 0.010 M D<sub>2</sub>O solution of complex (**29**)Cl was monitored by <sup>1</sup>H NMR spectroscopy. C–Cl reductive elimination at this complex was observed to produce the corresponding aryl chloride **26** in > 90 % yield, along with a small amount of the corresponding C–O bond coupling product **25** in < 10 %. The first order kinetics plot of ln([**29**]<sub>0</sub>/[**29**]<sub>t</sub>) as a function of time is given below, where [**29**]<sub>0</sub> refers to the initial concentration of complex **29** while [**29**]<sub>t</sub> refers to the concentration of complex **29** at time *t*. The plot shows initial faster reaction which gradually slows down.

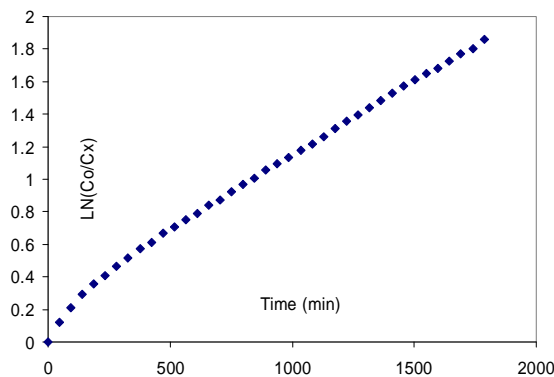
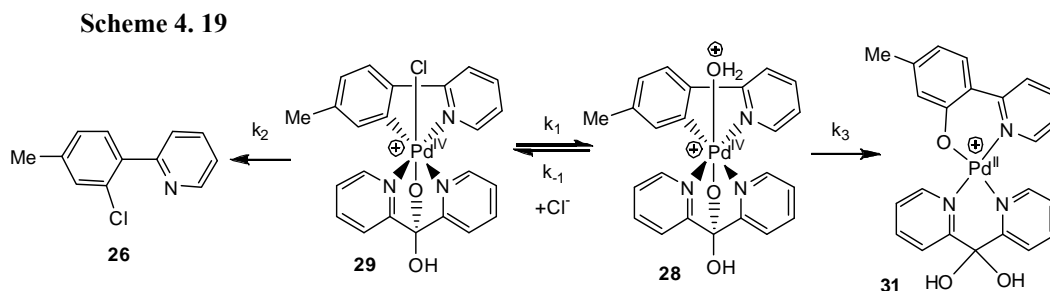


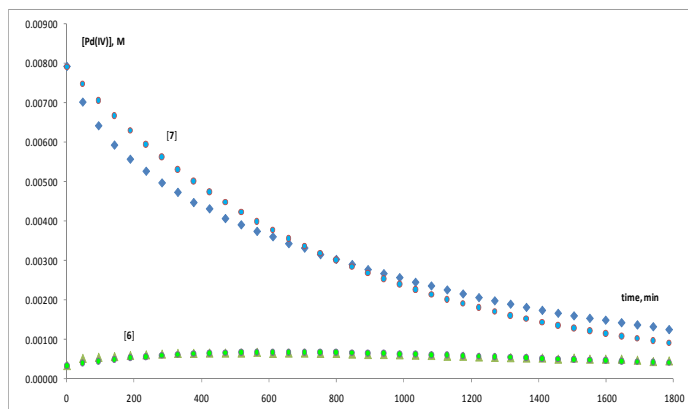
**Figure 4. 8.** A kinetic plot for the depletion of **29** in water at 22°C in  $\ln(C_0/C_x)$  vs. time coordinates.

*Kinetics modeling for the C-Cl elimination at complex **29***

This reaction kinetics was modeled by Dr. Vedernikov using the following reaction scheme.



The rate constants  $k_1$ ,  $k_{-1}$ ,  $k_2$  and  $k_3$  were varied to produce the best least-square fit to the experimental data. Numerical integration was used to find the desired concentrations of both **29** (diamonds in the plot below) and **28** (triangles in the plot below) based on the rate constant values guessed and initial concentrations of **29** and **28**. The quality of the final fit (circles) is shown below.



The rate constants values were optimized to

$$k_1 = (3.55 \pm 0.05) \cdot 10^{-6} \text{ s}^{-1},$$

$$k_{-1} = (4.90 \pm 0.06) \cdot 10^{-5} \text{ s}^{-1} \text{ M}^{-1},$$

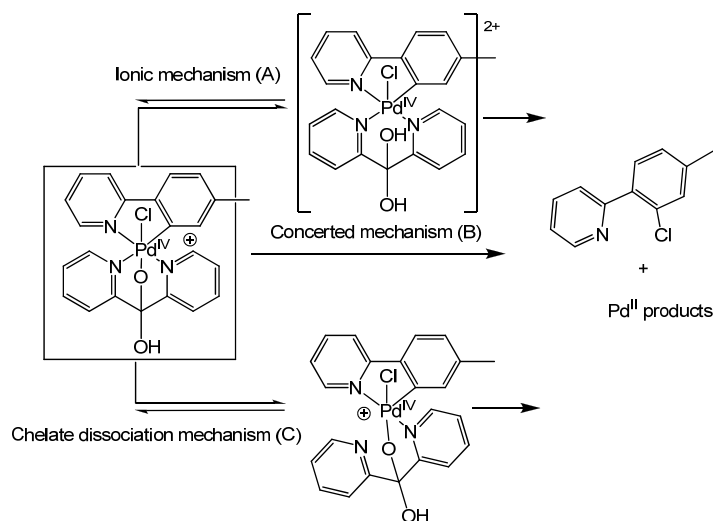
$$k_2 = (1.60 \pm 0.05) \cdot 10^{-5} \text{ s}^{-1}, \text{ and}$$

$$k_3 = (1.96 \pm 0.05) \cdot 10^{-5} \text{ s}^{-1}$$

Note that the  $k_3$  is close to the  $k_{\text{OH}}$  value,  $(2.52 \pm 0.03) \cdot 10^{-5} \text{ s}^{-1}$ , found for the C–O reductive elimination from **24** (Chapter 2).

### Study of the mechanism of C–X bond formation at complex **29**

Scheme 4. 20



The mechanism of C–Cl reductive elimination was also investigated, where three mechanisms were considered. The first, “ionic” mechanism involves preliminary dissociation of an alkoxide group from the Pd(IV) center to generate a dicationic, 5-coordinate Pd(IV) intermediate that undergoes faster C–Cl bond coupling. The second mechanism B involves concerted C–Cl coupling from a 6-coordinate palladium intermediate, while the third mechanism C involves preliminary dissociation of a pyridine group of the dpk chelate to generate a monocationic 5-coordinate species that subsequently undergoes C–Cl bond coupling. These mechanisms were considered because each has been observed in reductive elimination reactions involving group 10 transition metal centers.<sup>57</sup>

We started by determining whether acid accelerates the coupling reaction. Sanford and Goldberg observed acceleration of reactions that take place via preliminary dissociation of an ionic ligand by acids.<sup>179</sup> They proposed that acid accelerates the dissociation of the anionic ligand by hydrogen bonding to the OR ligand prior to dissociation. As a result, acceleration of the C–Cl bond reductive elimination reaction from complex **29** in water may indicate preliminary dissociation of an OR<sup>-</sup> ligand, followed by coupling from a 5-coordinate dicationic complex.

Thus the C–Cl reductive elimination reaction was performed in the presence of HCl to investigate the effect of acid on the C–Cl bond coupling reaction. A ~ 0.010 M D<sub>2</sub>O solution of complex **29** was prepared and 2.0 equivalents of HCl in D<sub>2</sub>O were added to the solution. The depletion of complex **29** was monitored by <sup>1</sup>H NMR spectroscopy in the presence of 1,4 dioxane as internal standard. The <sup>1</sup>H NMR spectra

revealed a fast disappearance of complex **29** and clean formation of aryl chloride **26** in > 95 % yield. The plot of  $\ln([\mathbf{29}]_0/[\mathbf{29}]_t)$  as a function of time is presented below.

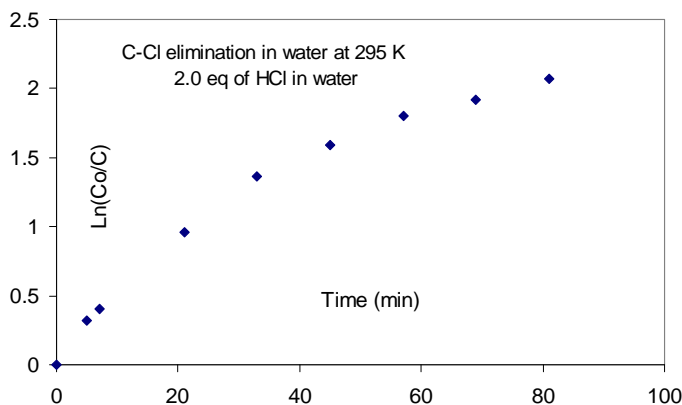


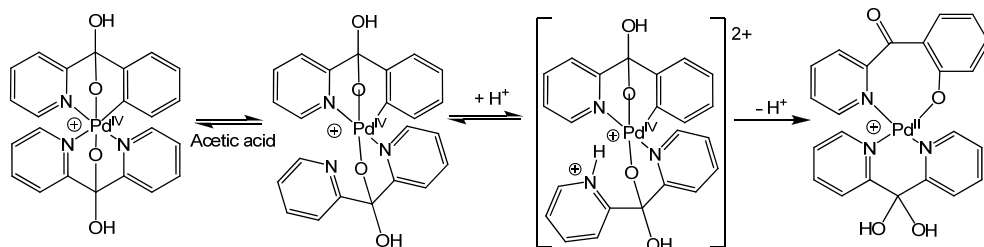
**Figure 4. 9.** A kinetic plot for the depletion of **29** in water in the presence of 2.0 equivalents of HCl at 22 °C in  $\ln(C_0/C)$  vs. time coordinates.

The plot was found to be non-linear, and the time for 50 % conversion to products was found to be ~ 19 minutes. Given that the time for 50 % conversion of complex **29** in water in the absence of HCl was 329 minutes, this indicates that reaction is significantly faster in the presence of 2.0 equivalents of HCl, suggesting that acid accelerates the rate of C–Cl reductive elimination. These results support an ionic mechanism, where the alkoxide ligand dissociates from the Pd(IV) center, followed by C–Cl bond coupling from a 5-coordinate Pd(IV) species.

These results however do not rule out the chelate dissociation mechanism. This is because the C–O reductive elimination reaction from 2-arylpdridine derived Pd(IV) complexes **9** and **14** was found to be significantly accelerated by acid, but these reactions were also significantly inhibited by pyridine additive (chapter 2). As a result, the C–O reductive elimination reaction was proposed to take place via preliminary dissociation of the pyridine group of the dpk chelate, followed by C–O

coupling from a 5-coordinate Pd(IV) species (Scheme 4.21). Acid was proposed to accelerate the reaction by protonating the dissociated pyridine group, thus inhibiting the coordination of the pyridine group back to the Pd(IV) center, and simultaneously generating a dicationic Pd(IV) species which is more reactive towards C–O coupling.

**Scheme 4. 21**



Therefore, we performed the C–Cl coupling reaction of complex **29** in the presence of 5.0 equivalents of pyridine additive. Thus, a ~ 0.010 M D<sub>2</sub>O solution of complex **29** was prepared and 5.0 equivalents of pyridine were added to the reaction solution. The depletion of complex **29** was monitored by <sup>1</sup>H NMR spectroscopy in the presence of 1,4 dioxane as internal standard. Upon addition of pyridine, disappearance of <sup>1</sup>H NMR signals belonging to complex **29** was observed accompanied by appearance of a new set of signals within 6 hours (see fig. 4.10 below). The <sup>1</sup>H NMR pattern of this new species was similar to that of complex **29** but not identical, indicating that this might be a product of pyridine coordination onto the Pd(IV) center, presumably resulting from dissociation of the pyridine group of the dpk chelate. Analysis of this solution by ESI–MS revealed a major mass envelope at  $m/z = 589.0585$  (calculated for C<sub>28</sub>H<sub>24</sub>ClN<sub>4</sub>O<sub>2</sub>Pd<sup>106</sup> = 589.0623), which was assigned to an adduct of pyridine coordination on to the Pd(IV) center upon dissociation of the pyridine group of the dpk chelate **32**. C–Cl reductive elimination from this reaction mixture was slow. In 24 hours, less than 30 % of the product of C–Cl coupling

product was observed and ~ 50 % conversion of the Pd(IV) species (**29** + the new species presumed to be a Pd(IV) species with an extra pyridine group coordinated onto the Pd(IV) center) was observed.

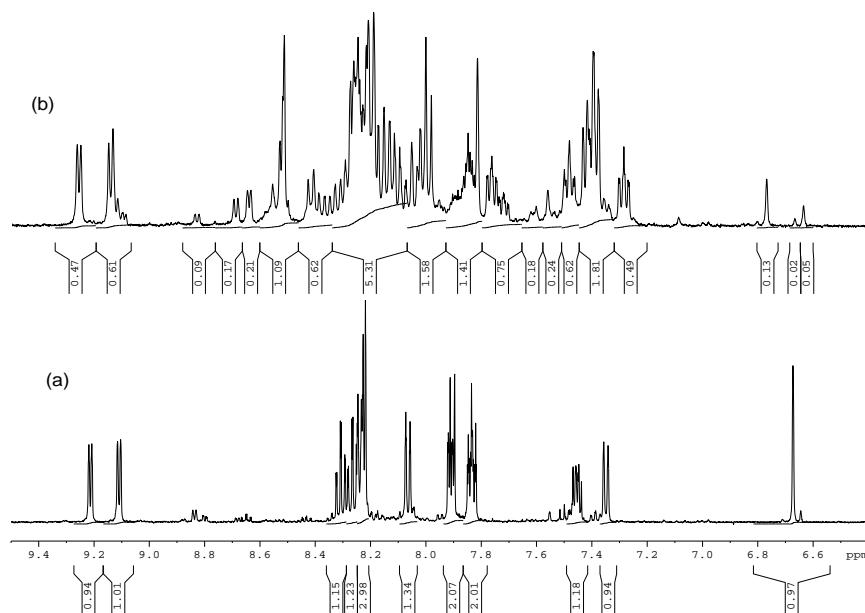
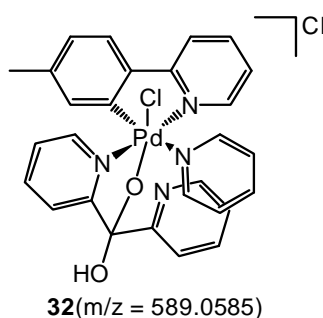


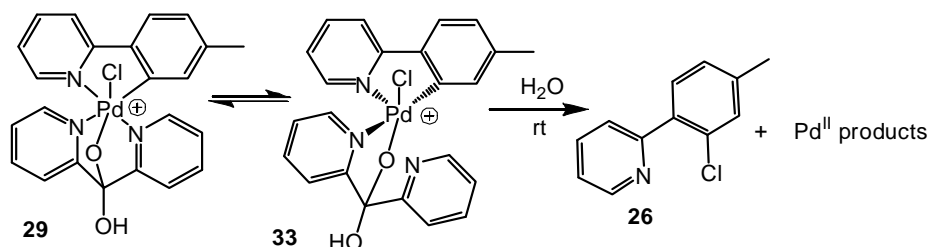
**Figure 4. 10.** Room temperature <sup>1</sup>H NMR spectra of (a) complex **29** in D<sub>2</sub>O, (b) complex **29** in D<sub>2</sub>O 6 hours after addition of 5.0 equivalents of pyridine, showing signals of a new species, presumably complex **32**.



Considering that the C–Cl reductive elimination reaction is slow in the presence of pyridine additive, where the time for 50 % conversion in the absence of any additive was ~ 329 minutes while the time for 50 % conversion in the presence of pyridine additive was ~ 1440 minutes, this indicates that C–Cl reductive elimination from complex **29** in water is inhibited by the pyridine additive, and thus takes place

via pyridine group dissociation of the dpk chelate to generate a reactive 5-coordinate palladium species. Bronsted acids may accelerate the reductive elimination by protonating the dissociated pyridine group, thus inhibiting the reverse coordination reaction, while at the same time producing a dicationic Pd(IV) species which is more reactive towards C–Cl bond coupling as shown in Scheme 4.22 below.

**Scheme 4. 22**

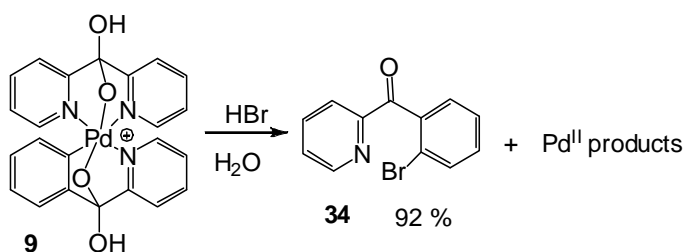


### 4.3 C–Br Bond Formation at Monohydrocarbyl Pd(IV) Alkoxides in Water in the Presence of HBr

#### 4.3.1 C–Br Bond Formation at 2-Aroylpyridine-derived Monohydrocarbyl Pd(IV)

##### Alkoxides **9** and **15** in Water in the Presence of HBr.

**Scheme 4. 23**



C–Br coupling from alkoxo-ligated Pd(IV) complex **9** in water in the presence of HBr was performed. A 0.010 M aqueous solution of complex **9** was prepared, 1,4 dioxane was added as internal standard and <sup>1</sup>H NMR spectrum was collected. 40.0 equivalents of HBr were added to the solution at room temperature and a <sup>1</sup>H NMR

spectrum was collected. The spectrum revealed formation of an additional minor set of signals in the aromatic region, with concomitant, gradual formation of an orange precipitate (Fig. 4.11). The reaction mixture was heated at 70°C for 6 hours, where a yellow precipitate was gradually produced. After 6 hours, pyridine-d<sub>5</sub> was added to free any coordinated products and a <sup>1</sup>H NMR spectrum was collected. The <sup>1</sup>H NMR spectrum displayed the presence of a new set of 8 multiplets in the aromatic region integrating as 1H each in ~ 92 % yield relative to the internal standard (Fig. 411), while the ESI-MS analysis of the reaction mixture exhibited a major mass envelope at m/z = 261.9770 (calculated for C<sub>12</sub>H<sub>9</sub>BrNO = 261.9868). This compound was isolated by extraction of the aqueous reaction mixture with diethyl ether, and its identity was confirmed as the corresponding aryl bromide **34** via ESI-MS and comparison of the <sup>1</sup>H NMR to that reported in literature.

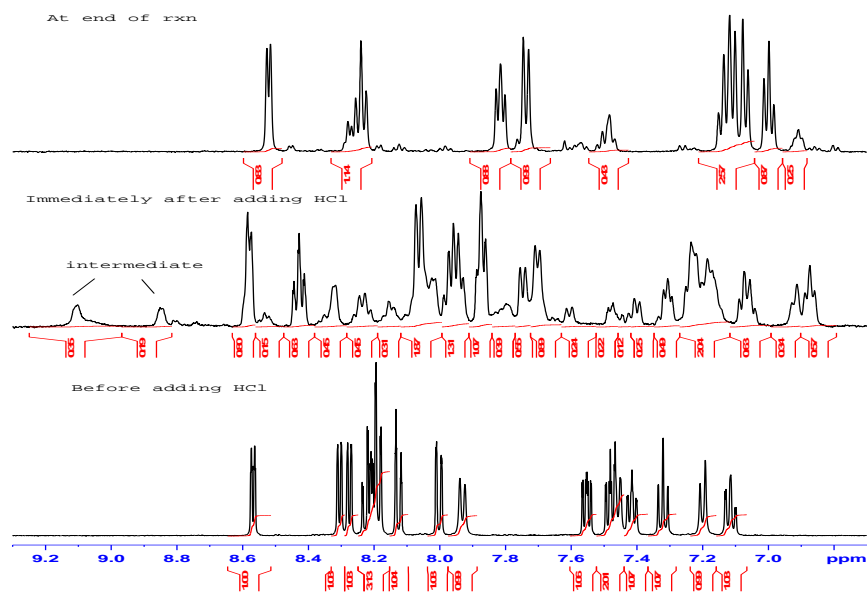
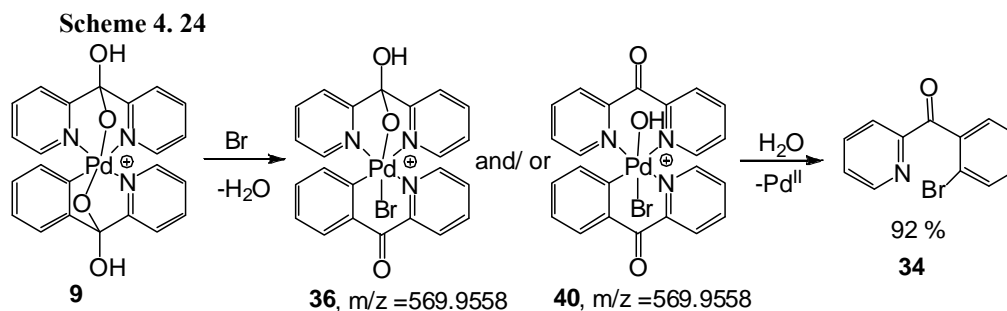
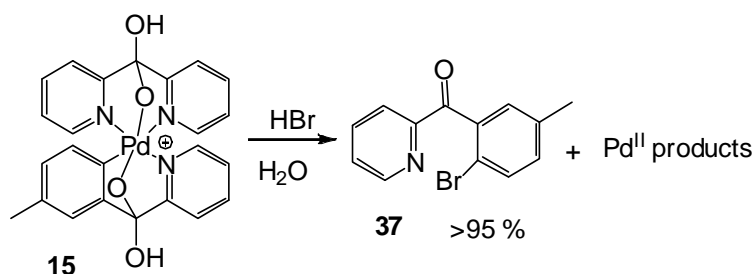


**Figure 4. 11.** Room temperature <sup>1</sup>H NMR spectra of (a)complex **9** in D<sub>2</sub>O, (b) complex **9** in D<sub>2</sub>O upon addition of HBr, showing additional signals belonging to an intermediate; (c) <sup>1</sup>H NMR of the reaction mixture after decomposition, showing the product of C-Br elimination, **34**.



Based on the decomposition of complex **9** in water in the presence of HBr to produce the corresponding aryl bromide **34**, we propose the intermediacy of a bromo-ligated Pd(IV) complex **36** and/ or **40** that undergoes C–Br bond coupling to produce the C–Br coupling product (Scheme 4.24). A mass envelope corresponding to the mass of complex **36** and/ or **40** was detected by ESI–MS at  $m/z = 569.9558$  (calculated for  $\text{C}_{23}\text{H}_{17}\text{N}_3\text{O}_3\text{Br}^{106}\text{Pd} = 569.9485$ ), upon addition of HBr to an aqueous solution of complex **9**. Additionally, an intermediate was detected in the  $^1\text{H}$  NMR spectrum of the reaction mixture upon addition of HBr to the aqueous solution of complex **9**. This intermediate may be assigned to complex **36** or **40** since a complex with a similar mass envelope was detected by ESI–MS analysis of this reaction mixture. The bromo-ligated Pd(IV) complex **36** may be produced via chelate opening of complex **9** in the presence of HBr. C–Br reductive elimination from complex **36** and/ or **40** produces the corresponding aryl bromide, **34**.

**Scheme 4. 25**



C–Br bond coupling was also attempted from the alkoxy-ligated Pd(IV) complex **15** in water in the presence of HBr (Scheme 4.25). A 0.010 M D<sub>2</sub>O solution of complex **15** was prepared and 40.0 equivalents of HBr in D<sub>2</sub>O were added to this solution. Addition of HBr led to gradual formation of an orange precipitate. The resulting reaction mixture was heated at 70°C for 6 hours, where gradual formation of a yellow precipitate was observed. After the reaction was complete, pyridine-d<sub>5</sub> was added to free coordinated products and a <sup>1</sup>H NMR spectrum was collected. The <sup>1</sup>H NMR spectrum exhibited 7 multiplets in the aromatic region, integrating as 1H each, as the only organic product. ESI–MS analysis of this reaction mixture revealed a mass envelope at 275.9928 (calculated for C<sub>13</sub>H<sub>11</sub>BrNO = 276.0024). The organic compound was isolated via extraction of the aqueous reaction mixture with diethyl ether, and its identity was confirmed as the corresponding aryl bromide **37**, by ESI–MS analysis and comparison of its <sup>1</sup>H NMR to that of commercially available compound **37**.

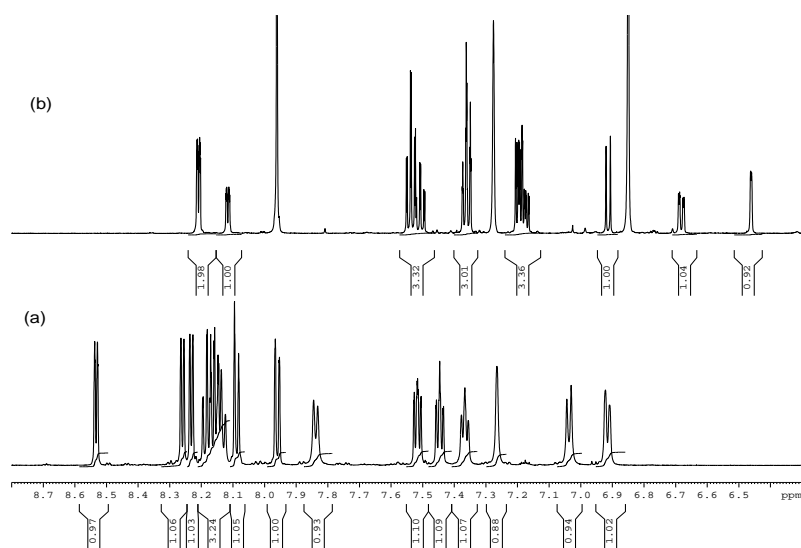


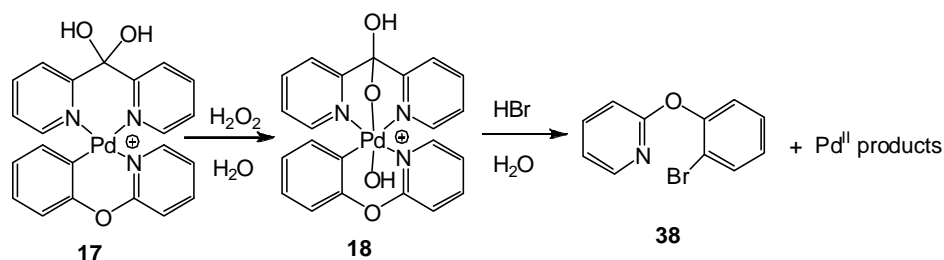
**Figure 4. 12.** Room temperature <sup>1</sup>H NMR spectra of (a) complex **15** in D<sub>2</sub>O, (b) the reaction mixture after decomposition, now in dms0-d<sub>6</sub> in the presence of pyridine-d<sub>5</sub>,

showing the presence of C–Br elimination product **37** and a symmetrical dpk-ligated Pd(II) product.

#### 4.3.2 C–Br Bond Formation at 2-Phenoxy-pyridine-derived Monohydrocarbyl Pd(IV)

##### Alkoxides **18** in Water in the Presence of HBr.

Scheme 4. 26



C–Br coupling from 2-phenoxy-pyridine derived Pd(IV) complex **18** was also performed in water in the presence of HBr. A 0.010 M  $\text{D}_2\text{O}$  solution of complex **18** was prepared *in-situ* by oxidation of complex **17** with  $\text{H}_2\text{O}_2$  in water as described previously, and  $^1\text{H}$  NMR spectrum was collected. 40.0 equivalents of HBr were added to the solution and a  $^1\text{H}$  NMR spectrum was collected. The  $^1\text{H}$  NMR spectrum revealed the presence of an additional minor set of signals, accompanied by gradual formation of an orange precipitate (Fig. 4.13). The resulting reaction mixture was heated at  $70^\circ\text{C}$  for 6 hours, where gradual formation of a yellow precipitate was observed. At the end of the reaction, the solvent was removed and the residue was dissolved in  $\text{dms}\text{-}d_6$  in the presence of a small amount of pyridine- $d_5$  to free any coordinated products. The  $^1\text{H}$  NMR spectrum revealed the presence of eight multiplets in the aromatic region, integrating as 1H each, while the ESI–MS of the reaction mixture revealed a major mass envelope at  $m/z = 249.9925$  which was assigned to the corresponding aryl bromide **38** (calculated for  $\text{C}_{11}\text{H}_9\text{BrNO} =$

249.9868). The organic product was isolated by extraction of the aqueous solution with diethyl ether and its identity was confirmed by both ESI–MS and comparison of the  $^1\text{H}$  NMR to that in literature.<sup>216</sup>

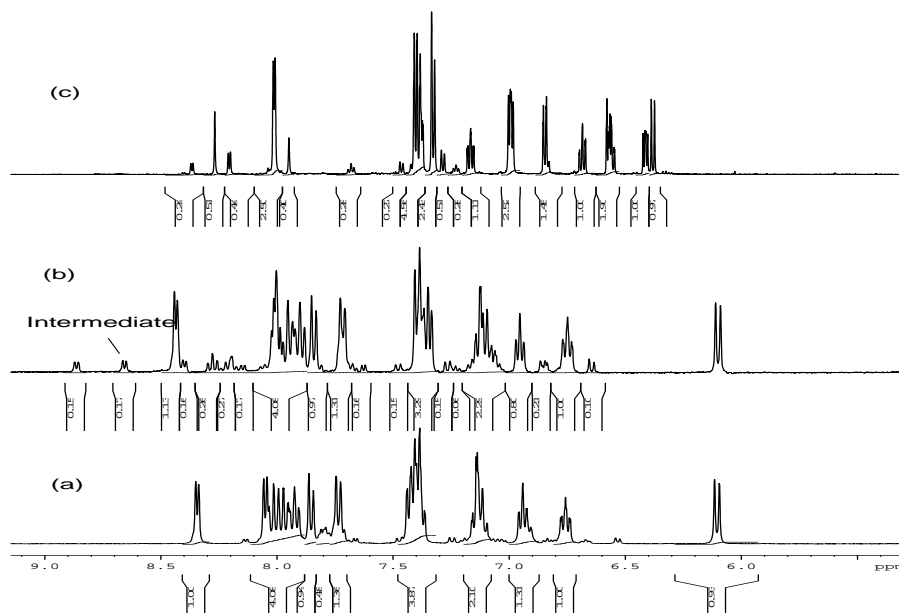
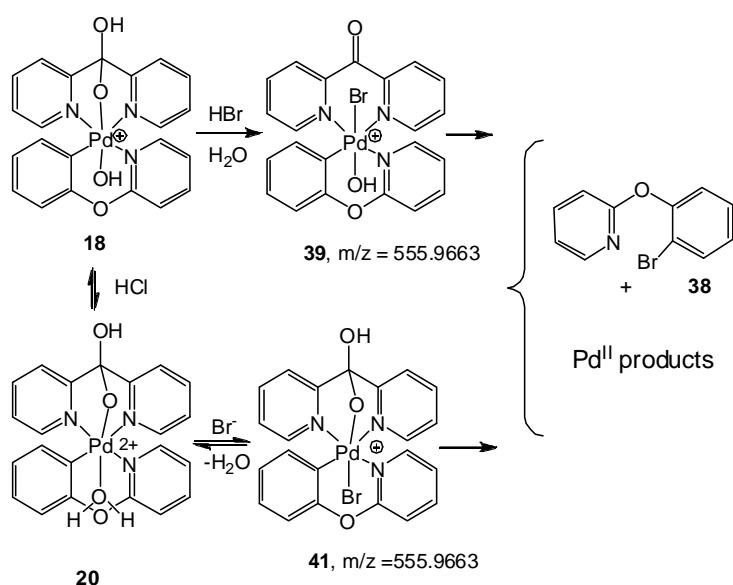


**Figure 4. 13.** Room temperature  $^1\text{H}$  NMR spectra of (a) complex **18** in  $\text{D}_2\text{O}$ , (b) complex **18** in  $\text{D}_2\text{O}$  upon addition of HBr showing additional signals belonging to an intermediate, (c)  $^1\text{H}$  NMR of the reaction mixture after decomposition, now in  $\text{dms}\text{-}d_6$  in the presence of pyridine- $d_5$ , showing the presence of C–Br elimination product **38** in the presence of (dpk)Pd(II) containing products

Considering the formation of the aryl bromide compound **38** from the decomposition of the hydroxo-ligated Pd(IV) complex **18** in water in the presence of HBr, we propose the intermediacy of bromo-ligated Pd(IV) complexes **39** and/ or **41** (Scheme 4.27). A complex with a matching mass envelope was detected by ESI–MS analysis of the reaction mixture produced upon addition of HBr to an aqueous solution of complex **18**, at  $m/z = 555.9663$  (calculated for  $\text{C}_{27}\text{H}_{17}\text{N}_3\text{O}_3\text{Br}^{106}\text{Pd} = 555.9488$ ). An intermediate was also detected by  $^1\text{H}$  NMR spectroscopy upon addition of HBr to an aqueous solution of complex **18**, which may be assigned to

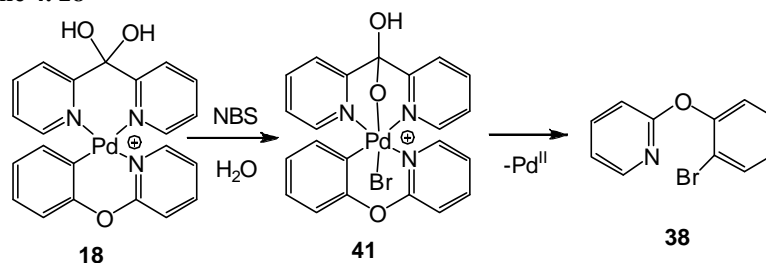
complex **39** and/ or **41** based on the ESI-MS analysis. Complex **39** may be formed via chelate opening of complex **18** in the presence of HBr, while complex **41** may be formed via protonation of complex **18** followed by ligand exchange from the aqua-ligated Pd(IV) complex **20** in the presence of bromide anions. C-Br reductive elimination from the bromo-ligated complexes **39** and/ or **41** produces the corresponding aryl bromide **38** as shown in the scheme below.

**Scheme 4. 27**



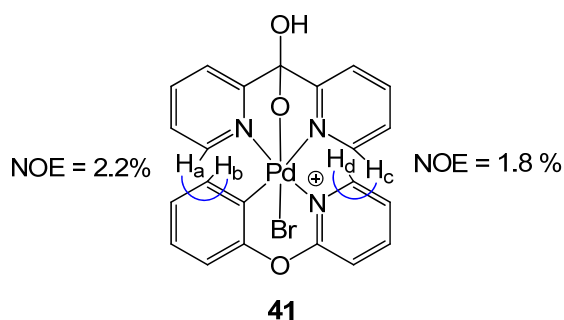
Attempts to isolate the bromo-ligated Pd(IV) complex by filtering the reaction mixture produced upon addition of HBr to an aqueous solution of complex **18** were not successful. The residue produced a complex  $^1\text{H}$  NMR spectrum in deuterated solvents such as methanol, acetone and dms $o$ .

**Scheme 4. 28**



Complex **41** was however independently prepared by oxidation of the Pd(II) complex **17** with NBS in water. Upon addition of NBS to an aqueous colorless solution of complex **17**, a deep orange precipitate was produced. This precipitate was filtered off and washed with a small amount of cold water. The precipitate produces a simple  $^1\text{H}$  NMR spectrum in deuterated methanol, where 16 multiplets are observed in the aromatic region, which integrate as 1H each. ESI-MS analysis of a methanolic solution of complex **41** displayed a mass envelope at  $m/z = 555.9221$  (Calculated for  $\text{C}_{22}\text{H}_{17}\text{BrN}_3\text{O}_3\text{Pd}^{106} = 555.9483$ ). When the methanolic solution of complex **41** is left at room temperature, an additional set of signals is observed after 12 hours corresponding to **38** produced in 60% yield. ESI-MS analysis of the reaction solution exhibits a mass envelope at 249.9871 (calculated for  $\text{C}_{11}\text{H}_9\text{BrNO} = 249.9868$ ), which was assigned to protonated **38**. After two days at room temperature, compound **38** is produced quantitatively. The identity of this compound as the corresponding aryl bromide was confirmed by comparison of its  $^1\text{H}$  NMR spectrum to that in literature.

The structure of complex **41** was assigned based on ESI-MS, and 1D difference NOE experiments.



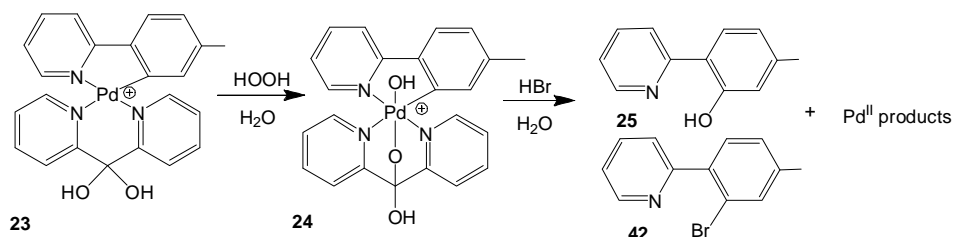
Given that irradiation of  $\text{H}_a$  results in NOE enhancement of  $\text{H}_b$  (2.2 %), while irradiation of  $\text{H}_c$  results in NOE enhancement of  $\text{H}_d$  (1.8 %, mixing time of 0.5s, delay time 4s), this indicates that these sets of hydrogens are in close proximity, and

thus an equatorial arrangement of the phenoxy pyridine and dpk fragments was considered. However, the NOE analysis cannot be used to differentiate between the structure of complexes **39** and **41**, and thus structure **41** is favored because it is thermodynamically more stable than **39** as a result of the tridentate facial chelating mode of the ligand.

#### 4.3.3 C–Br Bond Formation at 2-Tolylpyridine-derived Monohydrocarbyl Pd(IV)

##### Alkoxides **24** in Water in the Presence of HBr.

**Scheme 4. 29**



C–Br coupling from 2-tolylpyridine derived hydroxo-ligated Pd(IV) complex **24** was also performed. A 0.010 M D<sub>2</sub>O solution of complex **24** was prepared *in-situ* by the oxidation of the organopalladium(II) complex **23** with H<sub>2</sub>O<sub>2</sub> as described previously. 10.0-40.0 equivalents of HBr in D<sub>2</sub>O were added into this solution where gradual formation of an orange precipitate was observed. <sup>1</sup>H NMR spectrum of this reaction mixture revealed an additional minor set of signals which were absent at the end of reaction. The reaction mixture was heated at 70°C for 6 hours, where gradual formation of a yellow precipitate was observed. At the end of the reaction, a small amount of acetic acid and pyridine-d<sub>5</sub> were added to the reaction solution to free any coordinated products and increase solubility, and a <sup>1</sup>H NMR spectrum of the resulting reaction mixture was collected. The spectrum revealed the presence of three sets of aromatic signals. The first set included four multiplets integrating as 2H each, which

was assigned to a symmetrical dpk-ligated Pd(II) containing product. The second set consisted of seven aromatic multiplets integrating as 1H each, assigned to the major organic reaction product **42**, while the third set of multiplets was assigned to the corresponding phenol **25** by comparison to independently prepared compound. ESI-MS analysis of this reaction mixture revealed a major mass envelope at  $m/z = 248.0074$  (calculated for  $C_{12}H_{11}BrN = 248.0075$ ), while minor mass envelopes were detected at  $m/z = 264.0101$  (calculated for  $C_{12}H_{11}BrNO = 264.0024$ ), and  $186.0863$  (calculated for  $C_{12}H_{12}NO = 186.0919$ ). The major organic product was identified as the corresponding aryl bromide **42** via independent synthesis following literature procedures for palladium catalyzed bromination of aromatic C-H bonds using NBS as oxidant.<sup>32</sup> Thus, this reaction was observed to produce a mixture of C-Br and C-O coupling products **42** and **25**, depending on the amount of HBr used. However when 40.0 equivalents of HBr was used, only aryl bromide **42** was produced in ~ 93 % yield relative to the internal standard, no phenol was observed by <sup>1</sup>H NMR spectroscopy.

**Table 4. 2.** Fraction of the aryl bromide **42** and phenol **25** relative to the amount of HBr added according to <sup>1</sup>H NMR analysis.

HBr (eq)	Ar-Br	Ar-OH
10.0	59	31
20.0	68	24
40.0	93	0

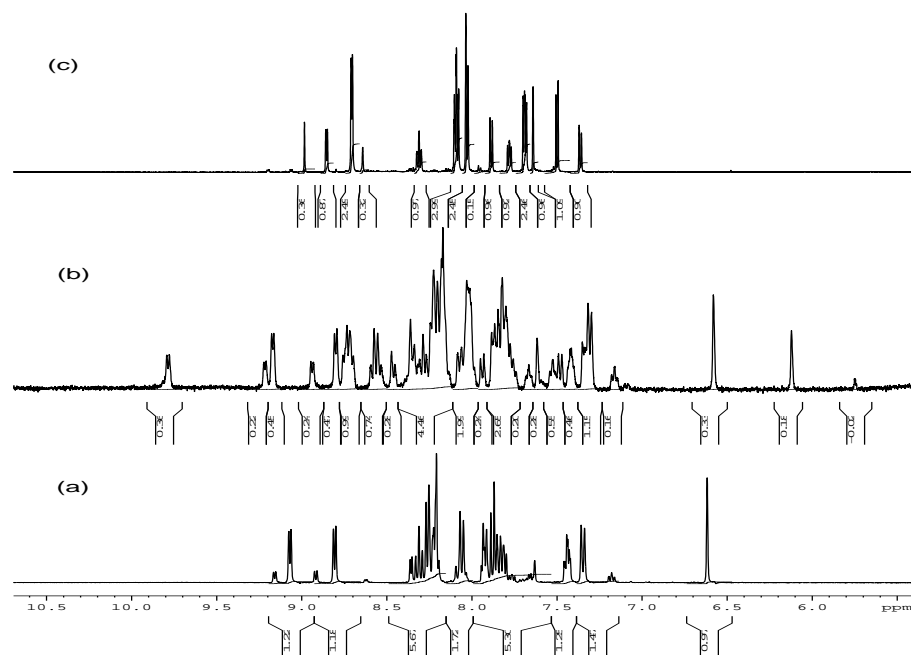
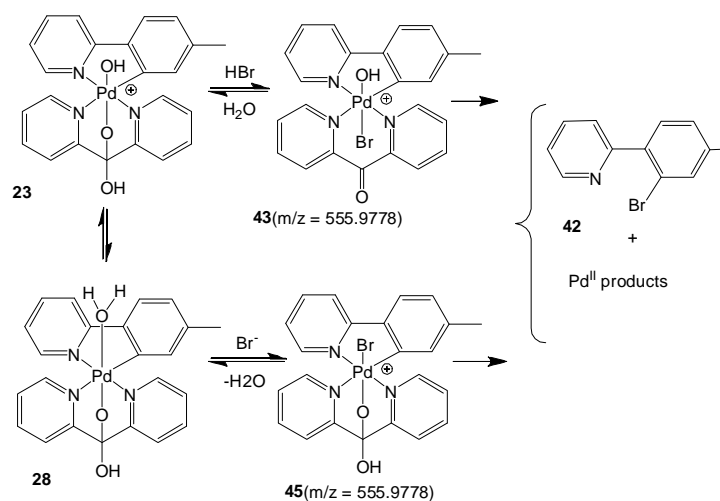


**Figure 4. 14.** Room temperature  $^1\text{H}$  NMR spectra of (a) complex **24** in  $\text{D}_2\text{O}$ , (b) complex **24** in  $\text{D}_2\text{O}$  upon addition of  $\text{HBr}$  showing the presence of additional set of signals belonging to an intermediate; (c)  $^1\text{H}$  NMR of the reaction mixture after decomposition, now in  $\text{dmsO-d}_6$  in the presence of  $\text{pyridine-d}_5$ , showing the presence of C–Br elimination product **42** in the presence of a symmetrical dpk-ligated  $\text{Pd(II)}$  product.

**Scheme 4. 30**



Considering the formation of the aryl bromide compound **42** from the decomposition of the hydroxo-ligated  $\text{Pd(IV)}$  complex **24** in water in the presence of

HBr, we propose the intermediacy of a bromo-ligated Pd(IV) complex **43** and/ or **45** (Scheme 4.30). A complex with a matching mass envelope was detected via ESI–MS of the reaction solution upon addition of HBr to an aqueous solution of complex **24** at  $m/z = 555.9778$  (calculated for  $C_{23}H_{19}BrN_3O_2Pd^{106} = 555.9695$ ). An intermediate was also detected by  $^1H$  NMR spectroscopy upon addition of HBr to an aqueous solution of complex **24**, which was assigned as the bromo-ligated Pd(IV) complex **43** or **45** based on the ESI–MS analysis of this reaction mixture. The bromo-ligated Pd(IV) complex **43** might be produced via acid assisted chelate opening of complex **24** in the presence of HBr, while complex **45** might be produced via protonation of complex **24**, followed by ligand exchange from the dicationic aqua-ligated Pd(IV) complex **28** in the presence of bromide anions. C–Br reductive elimination from either **43** and/ or **45** would produce the aryl bromide **42**.

In order to determine the identity of the intermediate complex, the solid produced upon combining an aqueous solution of complex **24** with HBr was filtered off and characterized by  $^1H$  NMR spectroscopy and ESI–MS. Analysis of this complex by  $^1H$  NMR exhibited an NMR pattern similar to that of aqua-ligated Pd(IV) complex **28** produced upon addition of either hydrochloric acid or trifluoroacetic acid to an aqueous solution of **24** (Fig. 4.15). As a result, this complex was assigned to **(28)Br<sub>2</sub>**, which is an aqua-ligated Pd(IV) dicationic complex with bromide counterions.

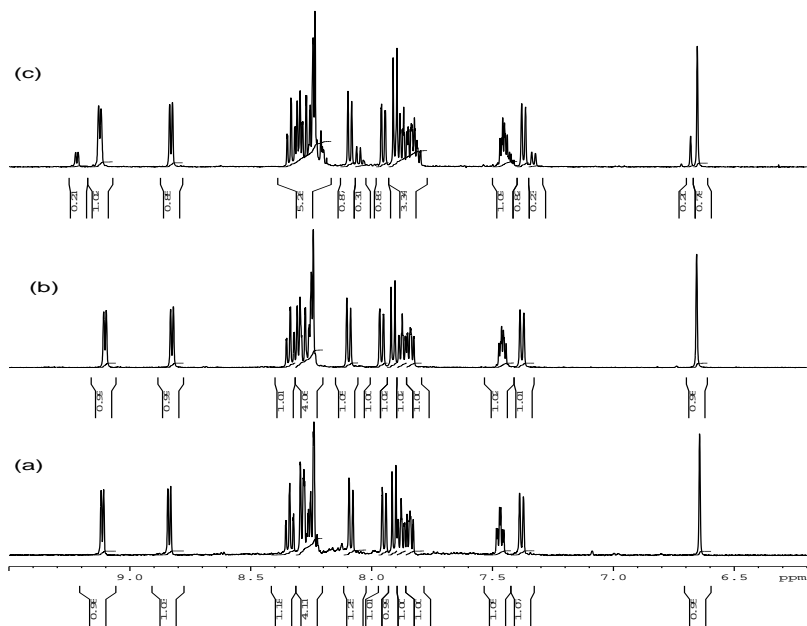
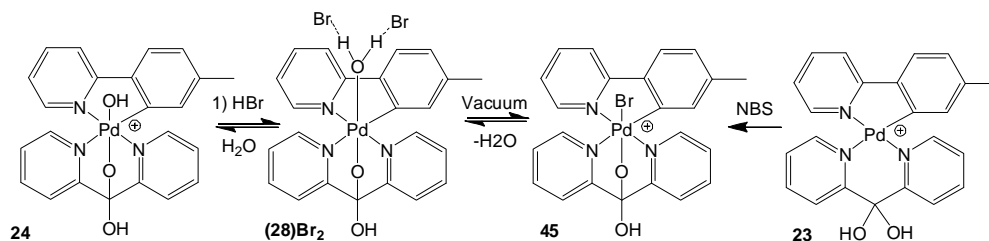


**Figure 4. 15.** Room temperature  $^1\text{H}$  NMR spectra of complexes (a)  $28(\text{OOCCF}_3)_2$ , (b)  $(28)\text{Br}_2$ , and (c)  $(28)\text{Cl}_2$ , in  $\text{D}_2\text{O}$ .

**Scheme 4. 31**



When the orange precipitate of complex  $(28)\text{Br}_2$  was placed under vacuum for 3 hours, analysis of the resulting solid by  $^1\text{H}$  NMR in  $\text{D}_2\text{O}$  at room temperature revealed a new set of signals with a pattern which was significantly different from that of the aqua-ligated complex  $(28)\text{Br}_2$  (Fig. 4.16). Analysis of a methanolic solution of this complex by ESI-MS revealed the major mass envelope at  $m/z = 555.9778$  (calculated for  $\text{C}_{23}\text{H}_{19}\text{BrN}_3\text{O}_2\text{Pd}^{106} = 555.9695$ ). As a result, this complex was assigned to **45**. Complex **45** could also be prepared via oxidation of the organopalladium(II) complex **23** with N-bromosuccinimide (NBS) oxidant.

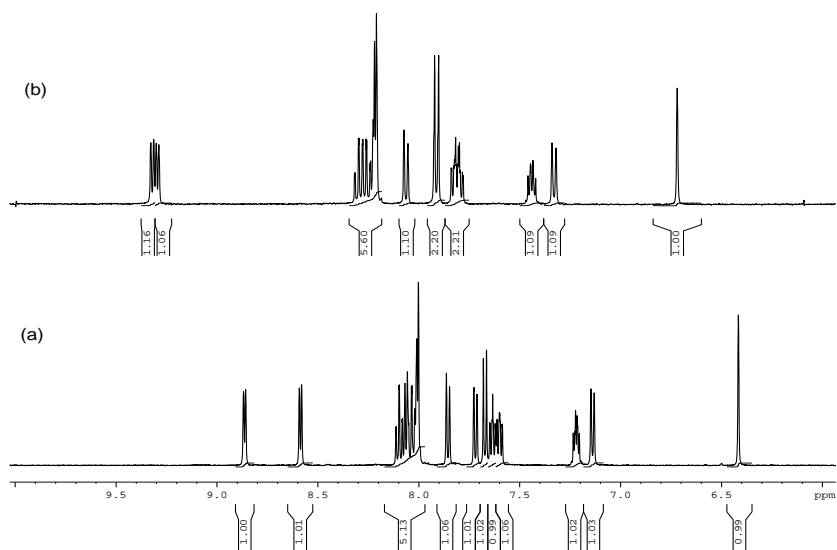
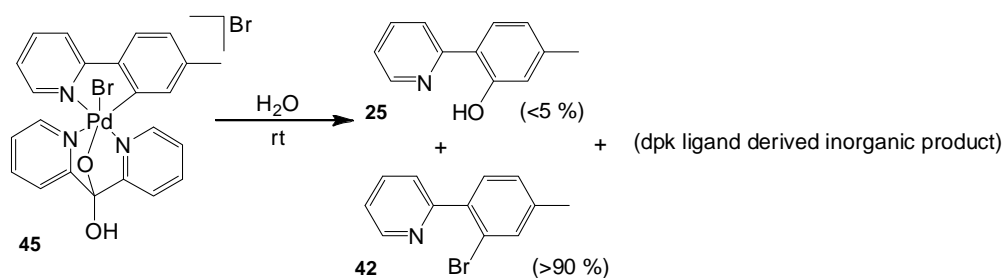


**Figure 4. 16.** (a) Room temperature  $^1\text{H}$  NMR spectrum of aqua-ligated Pd(IV) complex **(28)Br<sub>2</sub>** in  $\text{D}_2\text{O}$  at room temperature; (b)  $^1\text{H}$  NMR of bromo-ligated(IV) complex **45** in  $\text{D}_2\text{O}$  at room temperature.

Upon preparation of complex **45** in pure form, the kinetics study of the C–Br reductive elimination reactivity of this complex in water was performed.

**Scheme 4. 32**



Thus, 3.2 mg of complex **45** was dissolved in 1.0 ml of  $\text{D}_2\text{O}$ , and the depletion of complex **45** was monitored by  $^1\text{H}$  NMR in the presence of 1.0  $\mu\text{l}$  of 1,4-dioxane as an internal standard. After  $\sim 24$  hours, a small amount of acetic acid was added to dissolve the white precipitate formed, and the  $^1\text{H}$  NMR revealed formation of the corresponding phenol **25** (<5 %) and the aryl bromide **42** (>90 %) as the only organic

products. The first order kinetics plot of  $\ln([\mathbf{45}]_0/[\mathbf{45}]_t)$  as a function of time is given below. This plot was found to be linear.

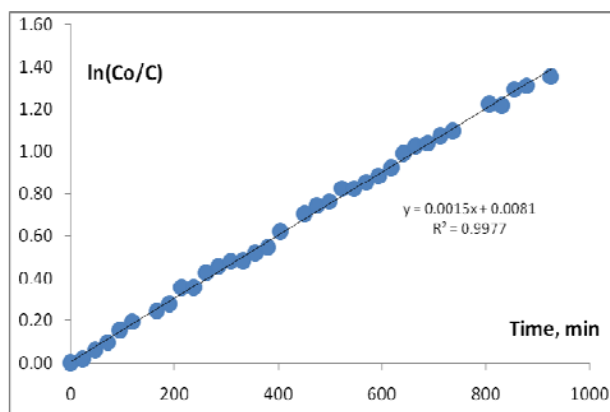


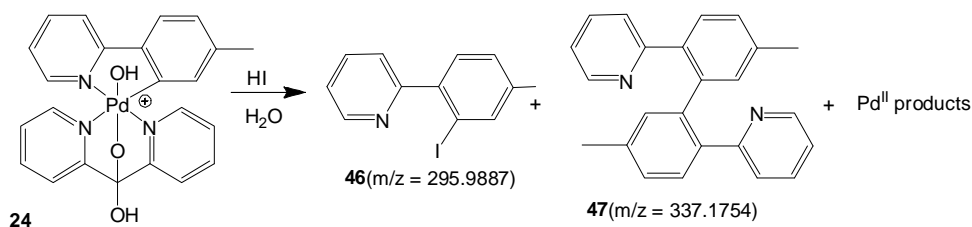
**Figure 4. 17.** Kinetic plot for the depletion of **45** in water at 22 °C in the coordinates  $\ln(C_0/C)$  vs. time.

#### 4.4 C–I Bond Formation at Monohydrocarbyl Pd(IV) Alkoxides in Water in the Presence of HI

##### 4.4.1 C–I Bond Formation at 2-Tolylpyridine-derived Monohydrocarbyl Pd(IV)

##### Alkoxide **24** in Water in the Presence of HI.

##### **Scheme 4. 33**



C–I coupling from 2-tolylpyridine derived hydroxo-ligated Pd(IV) complex **24** was performed in water in the presence of HI. 0.010 M D<sub>2</sub>O solution of complex **24** was prepared *in-situ* by the oxidation of the organopalladium(II) complex **23** with H<sub>2</sub>O<sub>2</sub> as described previously. 40.0 equivalents of HI in D<sub>2</sub>O were added into this solution where fast formation of a deep purple precipitate was observed. <sup>1</sup>H NMR

spectrum of this reaction mixture did not display any signals presumably due to poor solubility of the aqua-ligated Pd(IV) complex and/ or iodo-ligated Pd(IV) complexes with iodide counterions. The reaction mixture was heated at 70°C for 6 hours, where gradual formation of a deep red precipitate was observed. A small amount of acetic acid and pyridine-d<sub>5</sub> were added to the reaction solution to free coordinated products and improve the solubility. Analysis of this reaction mixture by <sup>1</sup>H NMR revealed the presence of three sets of signals. The first set was four multiplets integrating as 2H each, assigned to a symmetrical (dpk)Pd(II) containing product. The second major set consisted of seven multiplets integrating as 1H each, which was assigned to the major organic product, produced in ~ 78 % yield relative to an internal standard, while the third set was produced in ~ 15 % yield relative to an internal standard (the number of multiplets could not be determined due to significant overlap with other signals). ESI-MS analysis of this reaction mixture at the end of the reaction revealed a major mass envelope at m/z = 295.9887 (calculated for C<sub>12</sub>H<sub>11</sub>IN = 295.9936) which was assigned to the protonated product of C-I bond coupling **46** and a minor mass envelope at m/z = 337.1754 (calculated for C<sub>24</sub>H<sub>21</sub>N<sub>2</sub> = 337.1705) which was assigned to the protonated product of C-C bond coupling **47**. The organic products were isolated by extraction of the aqueous solution with diethyl ether. The major complex was assigned as the corresponding aryl iodide **46** via independent synthesis of this compound using literature procedures for palladium catalyzed iodination of aromatic C-H bonds utilizing N-iodosuccinimide as oxidant.<sup>32</sup>

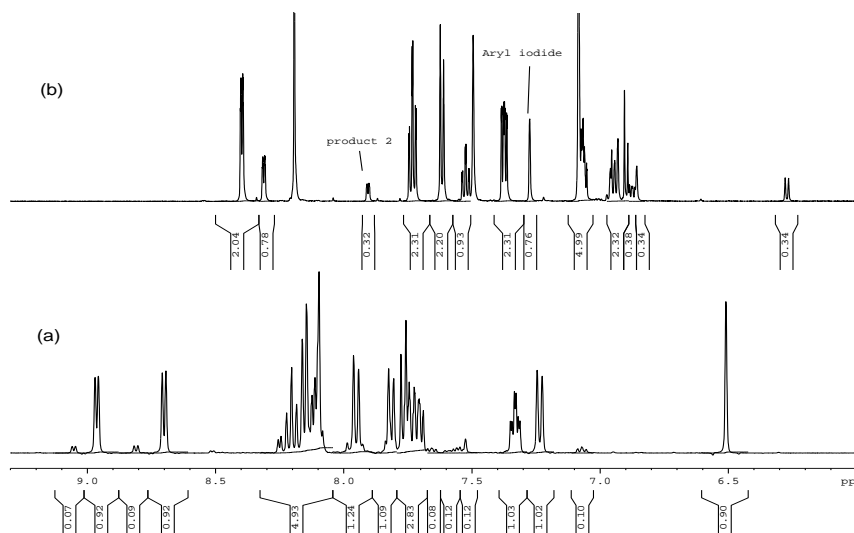
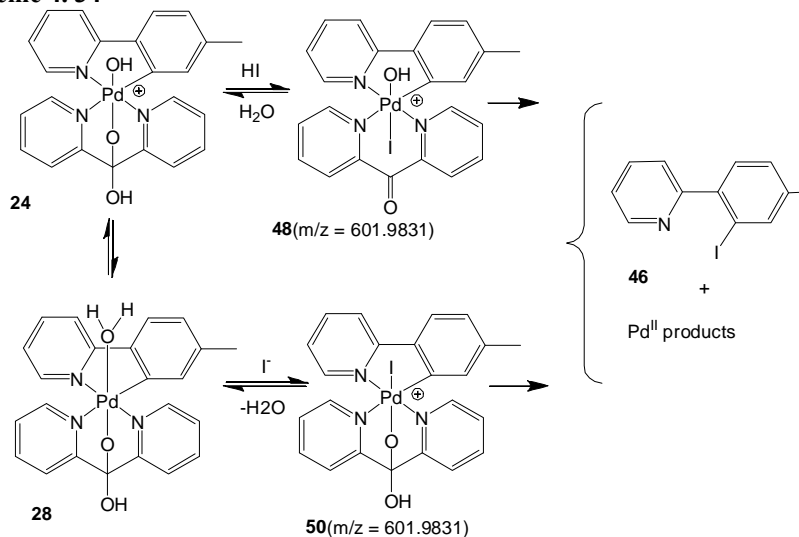


**Figure 4. 18.** Room temperature  $^1\text{H}$  NMR spectra of (a) the hydroxo-ligated Pd(IV) complex **24** in  $\text{D}_2\text{O}$ ; (b) the reaction solution upon decomposition of complex **24** in water in the presence of HI, now in  $\text{dmsO-d}_6$  in the presence of pyridine, showing the C–I elimination product **46**.

The formation of aryl iodide compound **46** from the decomposition of the hydroxo-ligated Pd(IV) complex **24** in water in the presence of HI was proposed to involve iodo-ligated Pd(IV) intermediates **48** and/ or **50** (Scheme 4.34). ESI–MS analysis of the reaction mixture upon addition of HI to an aqueous solution of complex **24** revealed a complex with a matching mass envelope at 601.9702 (calculated for  $\text{C}_{23}\text{H}_{19}\text{IN}_3\text{O}_2\text{Pd}^{106} = 601.9557$ ). Complex **48** could be formed via chelate opening of complex **24** in the presence of HI, while complex **50** might be formed via protonation of complex **24** to produce the aqua-ligated Pd(IV) complex **28(I)**<sub>2</sub>, which may undergo ligand exchange in the presence of HI to produce the iodo-ligated Pd(IV) complex **50**. C–I bond coupling from complex **48** and/ or **50** produces the aryl iodide product **46**.

**Scheme 4. 34**

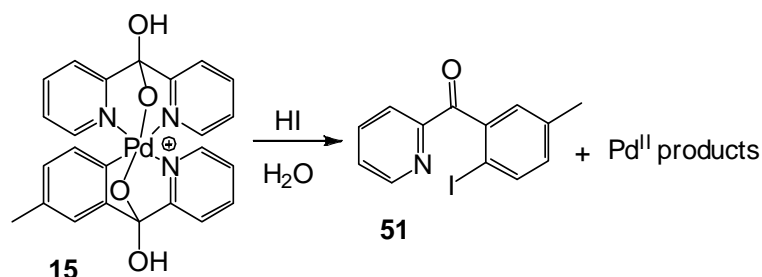


Considering that addition of HI into the aqueous solution of complex **24** leads to the formation of a deep red precipitate, this precipitate was filtered off and washed with a small amount of cold water. <sup>1</sup>H NMR analysis of this precipitate in various solvents such as deuterated acetone, methanol, and dimethyl sulfoxide resulted in complex <sup>1</sup>H NMR spectra, indicating the presence of multiple species in solution. These species could be a mixture of the corresponding aqua- and iodo-ligated Pd(IV) complexes. When this precipitate was placed under vacuum for several hours, a complex <sup>1</sup>H NMR still resulted. Thus the iodo-ligated Pd(IV) complex **50** could not be isolated in pure form using the techniques previously used for the isolation of bromo- and chloro-ligated Pd(IV) complexes. However since the bromo- and chloro-ligated Pd(IV) complexes could be prepared in pure form from the Pd(II) precursor **24** with either NBS or NCS, the next approach to synthesize the iodo-ligated Pd(IV) complex **50** might be via oxidation of complex **23** with N-iodosuccinimide.

#### 4.4.2 C–I Bond Formation at 2-Aroylpyridine-derived Monohydrocarbyl Pd(IV)

##### Alkoxides **15** in Water in the Presence of HI.

**Scheme 4. 35**



C–I bond coupling at the alkoxo-ligated Pd(IV) complex **15** in water in the presence of HI was also performed. 0.010 M aqueous solution of complex **15** was prepared, 1,4 dioxane was added as internal standard and a <sup>1</sup>H NMR spectrum was collected. 40.0 equivalents of HI in D<sub>2</sub>O were added to the solution at room temperature, leading to the formation of a deep red precipitate. It was not possible to collect a <sup>1</sup>H NMR spectrum of this reaction mixture to detect any intermediates due to the presence of a large amount of precipitate. ESI–MS analysis of this reaction mixture did not reveal a mass envelope corresponding to the iodo-ligated Pd(IV) complex, presumably due to poor solubility of this complex in water. The resulting reaction mixture was heated at 70°C for 6 hours, where a deep brown precipitate was gradually produced. After 6 hours, pyridine-d<sub>5</sub> was added to free any coordinated products and <sup>1</sup>H NMR spectrum was taken. The <sup>1</sup>H NMR spectra displayed the presence of the corresponding aryl iodide **51** in as the only organic product, which was also detected by ESI–MS at m/z = 323.9956 (calculated C<sub>13</sub>H<sub>11</sub>INO = 323.9885). This product was isolated by extraction of the aqueous reaction mixture with diethyl

ether, and characterized by NMR spectroscopy and electrospray ionization mass spectrometry.

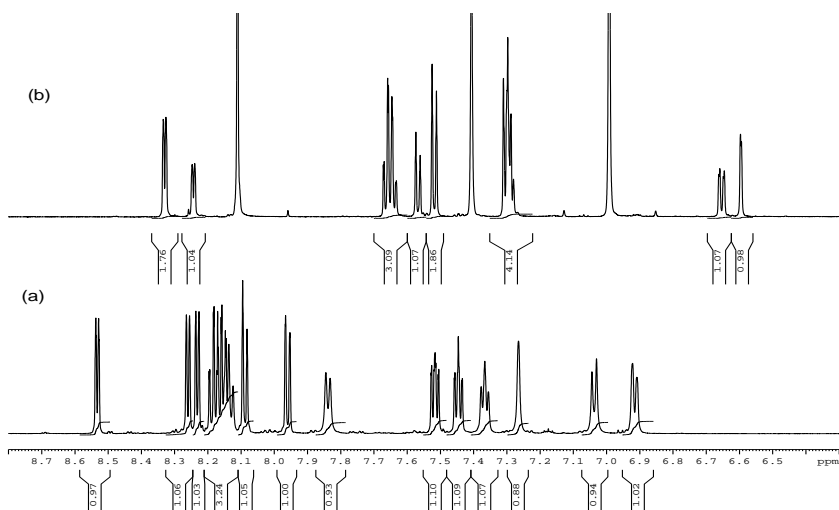
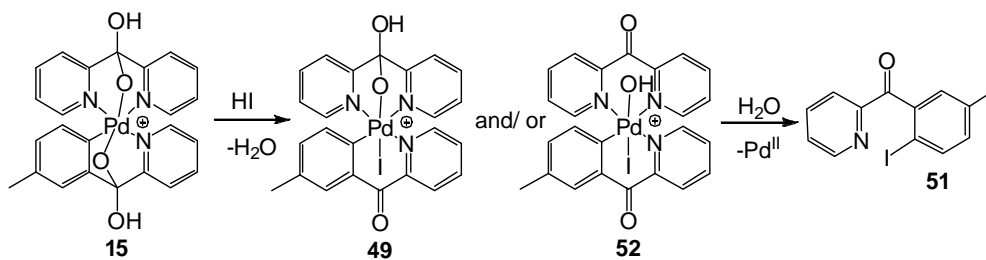


**Figure 4. 19.** Room temperature  $^1\text{H}$  NMR spectra of (a) the hydroxo-ligated Pd(IV) complex **15** in  $\text{D}_2\text{O}$ ; (b) the reaction solution upon decomposition of complex **25** in water in the presence of HI, now in  $\text{dmsO-d}_6$  in the presence of pyridine- $\text{d}_5$ , showing the aryl iodide **51** and  $(\text{dpk})\text{Pd}(\text{II})$  containing products.

**Scheme 4. 36**



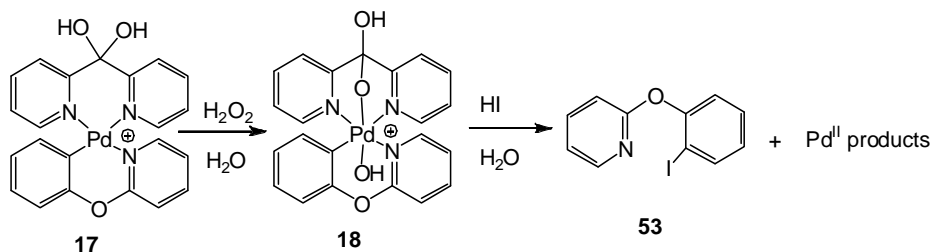
Given that decomposition of an alkoxo-ligated Pd(IV) complex **15** in water in the presence of HI led to quantitative formation of the corresponding aryl iodide, we propose the intermediacy of the iodo-ligated Pd(IV) complex **49** and/ or **52** in this reaction, which may be formed via chelate opening of complex **15** in the presence of HI (Scheme 4.36). Although the intermediate was not detected by either  $^1\text{H}$  NMR

spectroscopy or ESI-MS presumably due to its poor solubility in water, its presence is proposed because of the observed C-I coupling.

#### 4.4.3 C-I Bond Formation at 2-Phenoxy-pyridine-derived Monohydrocarbyl Pd(IV)

##### Alkoxides **15** in Water in the Presence of HI.

**Scheme 4. 37**



C-I coupling at 2-phenoxy-pyridine derived hydroxo-ligated Pd(IV) complex **18** was also performed in water in the presence of HI. A 0.010 M D<sub>2</sub>O solution of complex **18** was prepared *in-situ* by oxidation of complex **17** with H<sub>2</sub>O<sub>2</sub> in water as described previously, and a <sup>1</sup>H NMR spectrum was collected. 40.0 equivalents of HI were added to the solution and a deep brown precipitate was produced. <sup>1</sup>H NMR spectrum of the resulting reaction mixture could not be collected due to the presence of large amount of precipitate, while ESI-MS did not reveal the presence of a mass envelope corresponding to the iodo-ligated Pd(IV) complex presumably due to poor solubility of this complex in water. The resulting reaction mixture was heated at 70°C for 6 hours, where gradual formation of a deep red precipitate was observed. At the end of the reaction, a small amount of pyridine-d<sub>5</sub> was added to free coordinated products. The <sup>1</sup>H NMR spectrum revealed the presence of 8 aromatic multiplets which integrate as 1H each. The ESI-MS analysis of this reaction mixture revealed a major mass envelope at m/z = 297.9703 (calculated for C<sub>11</sub>H<sub>9</sub>INO = 297.9729). The

organic product was isolated via extraction of the aqueous solution with diethyl ether, and its identity as aryl iodide **53** was confirmed by NMR spectroscopy and electrospray ionization mass spectrometry.

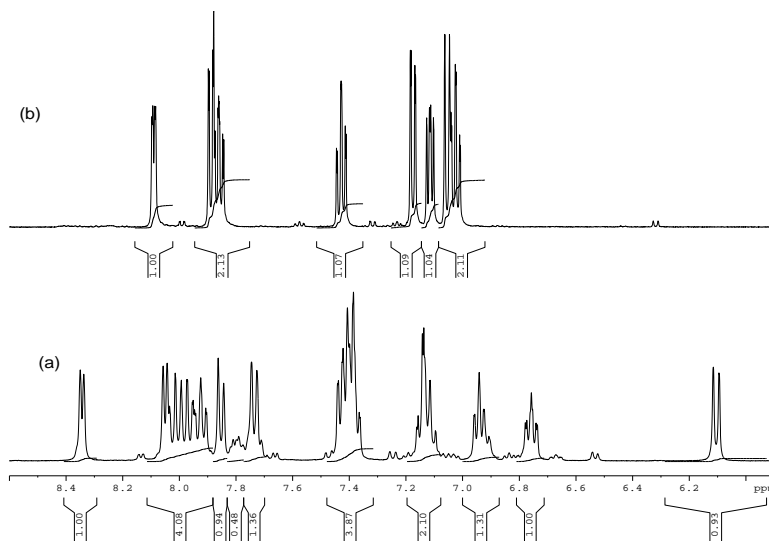


**Figure 4. 20.** Room temperature  $^1\text{H}$  NMR spectrum of (a) the hydroxo-ligated Pd(IV) complex **18** in  $\text{D}_2\text{O}$ , (b) the reaction solution upon decomposition of complex **18**, now in  $\text{dmsO-d}_6$  showing C–I elimination product **53**.

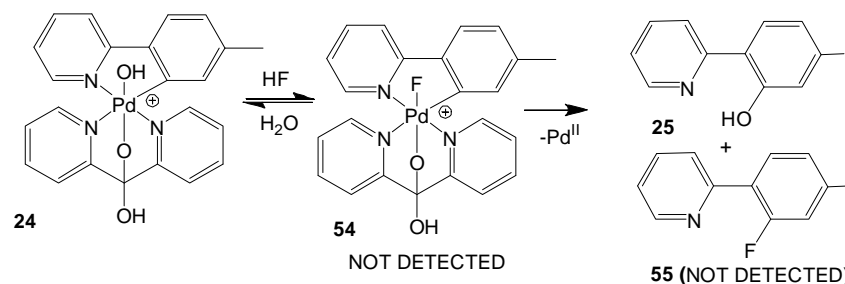
Attempts to isolate the intermediate complex were however unfruitful. When an aqueous solution of complex **18** was placed in ice-water bath and HI was added, a deep red precipitate was produced. This precipitate was filtered off and washed with a small amount of water. Analysis of the precipitate by  $^1\text{H}$  NMR in  $\text{CDCl}_3$  and deuterated acetic acid revealed the pure aryl iodide compound **53** as the only species in solution. This indicates that the C–I bond coupling reaction is too fast, complete within a few minutes after the addition of HI.

4.5 Attempted C–F Bond Formation at Monohydrocarbyl Pd(IV) Alkoxides in Water in the Presence of HCl

4.5.1 Attempted C–F Bond Formation at 2-Tolylpyridine-derived Monohydrocarbyl Pd(IV) Alkoxide **24** in Water, in the Presence of HF.

Given that C–X bond formation from hydroxo-ligated Pd(IV) complexes in water in the presence of HX (X=Cl, Br, and I) has been achieved, we next attempted C–F bond coupling from the hydroxo-ligated Pd(IV) complexes in the presence of HF.

**Scheme 4. 38**



We started our studies by investigating the decomposition of complex **24** in water in the presence of HF. Thus a 0.010 M D<sub>2</sub>O solution of complex **24** was prepared by oxidation of complex **23** with H<sub>2</sub>O<sub>2</sub> in water as previously described. 1,4 dioxane was added as internal standard and <sup>1</sup>H NMR spectrum was collected at room temperature. 40.0 equivalents of HF were added to the solution and another <sup>1</sup>H NMR was collected. This solution was heated at 70°C for 6 hours. Analysis of the <sup>1</sup>H NMR at the end of the reaction revealed the presence of the corresponding phenol **25** as the only product. No products of C–F bond coupling were detected by either <sup>1</sup>H NMR or ESI–MS analysis of the reaction solution.

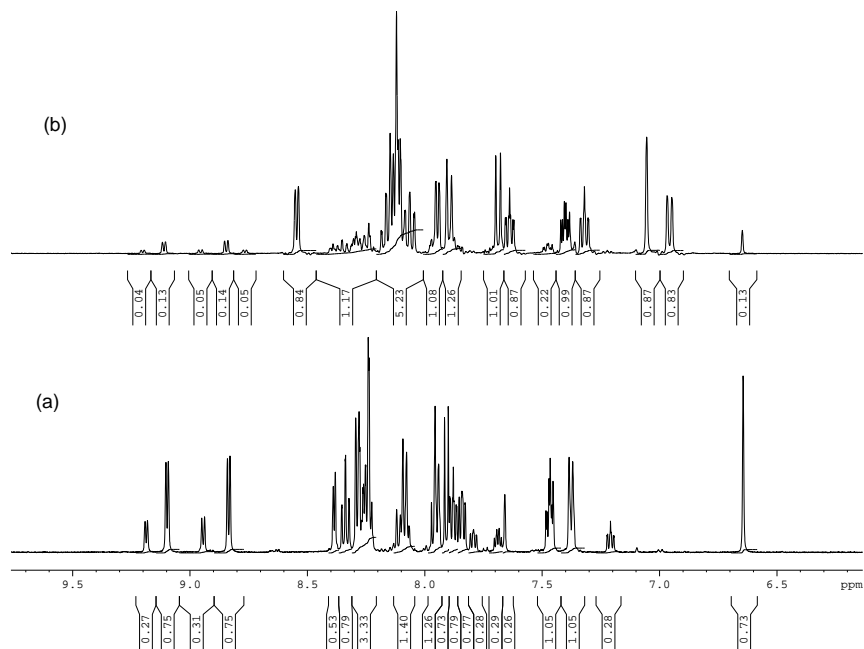


**Figure 4. 21.** Room temperature  $^1\text{H}$  NMR spectrum of (a) the hydroxo-ligated Pd(IV) complex **24** in  $\text{D}_2\text{O}$ , (b) the reaction solution upon decomposition of complex **24** in water in the presence of HF, showing oxapalladacycle **31**.

ESI–MS analysis of the solution upon addition of HF did not reveal fluoro-ligated Pd(IV) complex **54**, while analysis of the reaction solution at the end of the reaction did not reveal the presence of C–F bond coupling product **55** (Scheme 4.38). Only the corresponding oxapalladacycle **31** was observed by both  $^1\text{H}$  NMR and ESI–MS analysis of the solution at the end of the reaction. These results indicate that C–F bond coupling from complex **24** in water in the presence of HF was unsuccessful, and only the corresponding product of C–O coupling was produced.

We also attempted the decomposition of both complexes **15** and **18** in water in the presence of HF. Thus, when 40.0 equivalents of HF were added to 0.010 M aqueous solutions containing complexes **15** and **18**, no C–F coupling products were detected when these solutions were heated at  $70^\circ\text{C}$  for 6 hours by ESI–MS.

This reactivity is in contrast with the previously observed reactivity of the hydroxo-ligated Pd(IV) complexes in the presence of HX acids (X = Cl, Br, and I), where the X-ligated Pd(IV) complexes were detected by ESI-MS and were sometimes observed by  $^1\text{H}$  NMR spectroscopy, and these complexes underwent C-X bond coupling to produce the corresponding aryl halides in high yields. Given that the halogeno-ligated Pd(IV) intermediates may be produced via ligand exchange between the aqua-ligated Pd(IV) complexes with the halide ligand, the nucleophilicity of the ligand is important in the formation of the halogeno-ligated Pd(IV) complex. The fluoride ligand is however not as good a nucleophile compared to the chloro-, bromo-, and iodo- ligands. This might be the reason why C-F bond coupling was not observed in these reactions.

However since Pd(IV)-X complexes could be prepared by the oxidation of the Pd(II) complex **23** by NXS in water, future plans include preparation of Pd(IV)-F complexes via oxidation of complex **23** with N-fluoropyridinium salts, and study their reactivity in comparison to the Pd(IV)-X complexes (X=Cl, Br, and I).

#### 4.6 Mechanism of C-X Reductive Elimination From Monohydrocarbyl Pd(IV)

##### Alkoxides in Water, in the Presence of HX

C-X coupling from hydroxo-ligated Pd(IV) complexes in the presence of HX (X=Cl, Br, and I) is proposed to take place via initial protonation of the hydroxide ligand to produce aqua-ligated Pd(IV) complexes. Some aqua-ligated Pd(IV) complexes have been isolated and fully characterized, including X-ray diffraction. Substitution of the aqua ligand for the halide ligand is proposed to place in the presence of HX to produce the corresponding halogeno-ligated Pd(IV) complex. The

ligand exchange reaction has also been demonstrated, where isolated aqua-ligated Pd(IV) complexes have been observed to undergo ligand substitution under of vacuum. This reaction is presumably driven by the loss of a water molecule. C–X reductive elimination from the X–ligated Pd(IV) complexes produces the corresponding aryl halides. This reaction has also been demonstrated, where C–X bond coupling has been observed from isolated halogeno-ligated Pd(IV) complexes in water.

When the kinetics of C–X reductive elimination from isolated X–ligated Pd(IV) complexes (X=OH, Cl, and Br) in water at room temperature was investigated using <sup>1</sup>H NMR spectroscopy, the observed first order rate constants for these reactions were found to be similar (see table 3 below).

**Table 4. 3.** Observed first order rate constants for the C–X reductive elimination reactions in water at room temperature (X = OH, Cl, and Br).

Entry	Pd <sup>IV</sup> -X, X=	Ar-X (% yield)	K <sub>obs</sub> sec <sup>-1</sup>
1	OH	98	(2.52±0.03)·10 <sup>-5</sup>
2	Cl	95	(1.60±0.05)·10 <sup>-5</sup>
3	Br	90	(2.50±0.10)·10 <sup>-5</sup>

These results show that the reductive elimination reaction is not sensitive to the electronic effects of the halogeno ligand at the Pd(IV) center. These results are not unexpected since the C–O reductive elimination from complex **24** was also found to be insensitive to the electronics of the substituents on the aromatic ligand (Fig. 4.22).

Scheme 4. 39

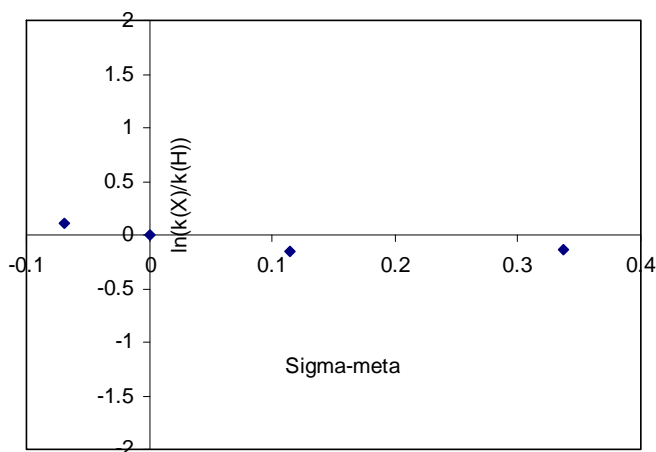
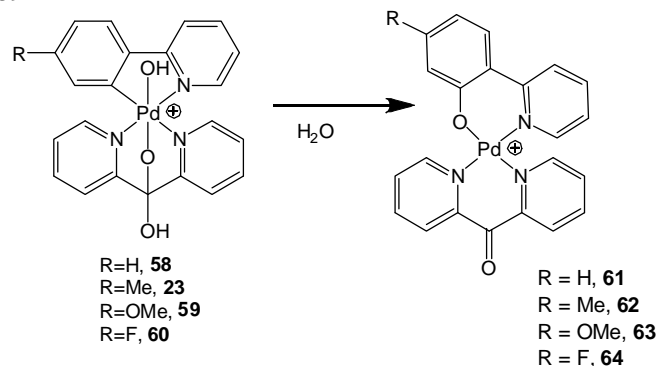


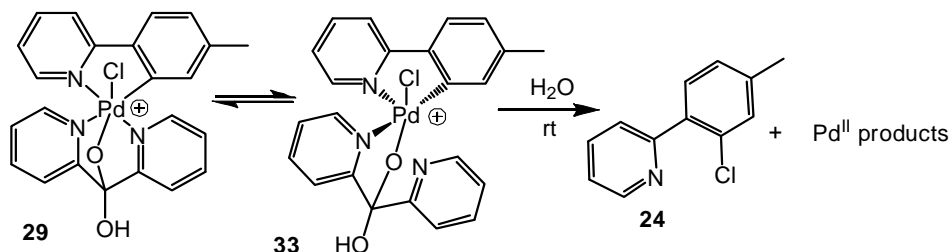
**Figure 4. 22.** Hammett plot for the decomposition of aqueous solutions of complexes **23**, **58-60** at 22 °C.

Given that the C–X reductive elimination reaction is insensitive to the electronics of the substituents on the aromatic ligand and that of the halide ligands, we propose that this reaction proceeds via a very early transition state, which results in a very exergonic reaction according to Marcus theory, leading to the insensitivity of the C–X reductive elimination process to the electronics of the substituents on the aromatic ligand and the halide ligands on the Pd(IV) center.

The mechanism of C–Cl bond coupling from complex **29** was investigated and was proposed to involve preliminary dissociation of the pyridine group of the dpk chelate, followed by C–Cl bond coupling from a 5-coordinate species (Scheme 4.40).

This mechanism was proposed based on inhibition of the C–Cl reaction in the presence of 5.0 equivalents of pyridine additive. The coupling reaction was also significantly accelerated in acid. Acid was proposed to protonate the dissociated pyridine group, thus inhibiting the reverse reaction.

Scheme 4. 40



#### 4.7 Summary and Conclusions

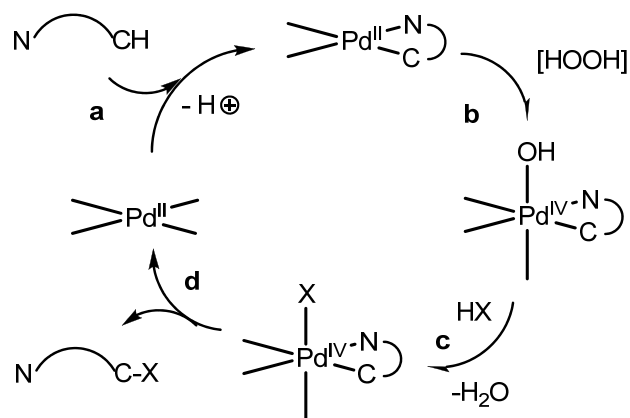
In summary, C–X bond formation has been observed from hydroxo-ligated Pd(IV) complexes in water in the presence of HX (X=Cl, Br, and I). These reactions are proposed to take place via the intermediacy of halogeno-ligated Pd(IV) complexes, which may be produced *in-situ* via chelate opening in the presence of HX, or protonation of the hydroxide ligand, followed by substitution of the aqua group by the halide ligand.

A number of chloro- and bromo-ligated Pd(IV) complexes have also been prepared and their reactivity towards C–X reductive elimination studied in water. The mechanism of C–X reductive elimination has been proposed to involve preliminary pyridine group dissociation of the dpk chelate, followed by C–X coupling from a 5-coordinate intermediate. The next goal of this work is to determine the solid state structure of the bromo- and chloro-ligated Pd(IV) complexes via X-ray diffraction analysis. In addition, iodo-ligated Pd(IV) complexes have not been isolated in pure

form. Future plans also involve preparation of iodo-ligated Pd(IV) complexes in pure form, complete characterization of the structure of these complexes, including X-ray diffraction, and characterization of their reactivity towards C–I reductive elimination.

Finally, fluoro-ligated Pd(IV) complexes have not been prepared. The next goal of this work will involve preparation of these complexes, complete characterization of the structures including X-ray diffraction studies, and characterization of their reactivity towards C–F bond coupling.

**Scheme 4. 41**



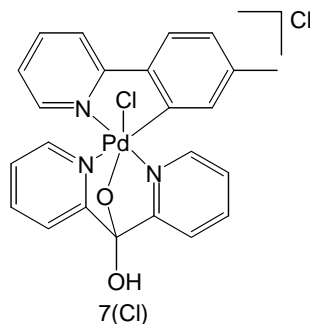
Ultimately, these studies will be employed towards catalytic C–X bond formation reactions utilizing  $\text{H}_2\text{O}_2$  as the terminal oxidant in water, in the presence of HX. As shown in Scheme 4.41, the catalytic reaction would involve C–H bond activation to produce organopalladium(II) complexes, oxidation of the Pd(II) complexes with  $\text{H}_2\text{O}_2$  to produce the corresponding hydroxo-ligated monohydrocarbyl Pd(IV) complexes, ligand exchange of the hydroxo-ligand for the halogeno-ligand in the presence of HX, followed by C–X coupling from the halogeno-ligated Pd(IV) complex. Towards this goal, the oxidation step b, the ligand substitution step c, and the C–X coupling d have been demonstrated. However the C–

H activation step a in water in the presence of HX has not been demonstrated, while oxidation of the organopalladium(II) species with H<sub>2</sub>O<sub>2</sub> in the presence of HX has not been investigated. Optimization of these steps will enable the development of the catalytic cycle depicted in Scheme 4.41. This catalytic reaction will make the palladium catalyzed halogenation of C–H bonds more environment friendly, since the H<sub>2</sub>O<sub>2</sub> oxidant will replace the currently applied NXS and PhIX<sub>2</sub> oxidants (X=Cl, Br, and I), which produce stoichiometric amounts of toxic waste products.

#### 4.8 Experimental

Compounds **11**,<sup>217</sup> **34**,<sup>218</sup> **14**,<sup>157</sup> **16**,<sup>158</sup> **37**,<sup>219</sup> **19**,<sup>220</sup> **38**,<sup>216</sup> and **26**,<sup>21</sup> have been reported in literature. The identity of these compounds was confirmed by their isolation and comparison of the <sup>1</sup>H NMR to those reported in literature.

#### **Complex 29(Cl)**



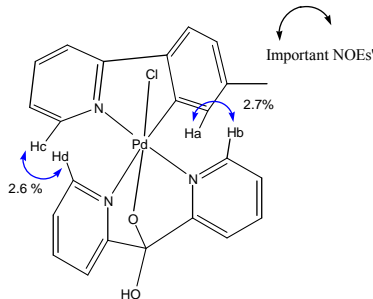
<sup>1</sup>H NMR (D<sub>2</sub>O, 3°C), δ: 2.31 (s, 3H), 6.66 (s, 1H), 7.29 (d, *J* = 7.9 Hz, 1H), 7.44 (td, *J* = 6.5, 2.7 Hz, 1H), 7.81-7.86 (m, 3H), 7.92 (d, *J* = 7.6 Hz, 1H), 8.07 (d, *J* = 7.7 Hz, 1H), 8.17-8.21 (m, 2H), 8.23 (d, *J* = 6.3 Hz, 1H), 8.27 (td, *J* = 7.7, 1.0 Hz, 1H), 8.31 (t, *J* = 7.6 Hz, 1H), 9.09 (d, *J* = 5.8 Hz, 1H), 9.19 (d, *J* = 5.2 Hz, 1H),

<sup>13</sup>C NMR (D<sub>2</sub>O, 3°C), δ: 24.3, 107.9, 124.8, 125.6, 125.9, 128.7, 130.0, 130.7, 131.7, 132.6, 132.9, 141.4, 145.2, 145.7, 146.7, 149.1, 150.4, 151.4, 151.6, 160.6, 161.6, 164.0, 164.5

ESI-MS of a solution of **29** in dmsO, *m/z* = 512.0135. Calculated for C<sub>23</sub>H<sub>19</sub>ClN<sub>3</sub>O<sub>2</sub><sup>106</sup>Pd = 512.0199.

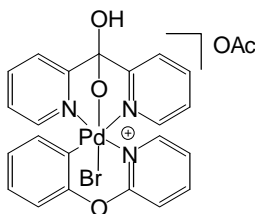
The complex is unstable and decomposes in the course of few days at room temperature.

Selective 1D-difference NOE experiments ( $D_2O$ ) for major intermediate **29(Cl)**



In the 1D difference NOE experiment, NOE was observed between the *ortho*-H<sub>a</sub> of the tolylpyridine ligand and *ortho*-H<sub>b</sub> of the dpk ligand and between the *ortho*-H<sub>c</sub> of the tolylpyridine and *ortho*-H<sub>d</sub> of the dpk ligand. Irradiation of a resonance at 6.66 ppm (*ortho*-H<sub>a</sub> of the tolylpyridine ligand) showed enhancement (positive NOE) of the doublet at 9.09 ppm (*ortho*-H<sub>b</sub> of the dpk ligand, 2.7 %) (mixing time of 0.5s, delay time 4s) and irradiation of a resonance at 9.19 ppm (*ortho*-H<sub>d</sub> of the dpk ligand) showed enhancement (positive NOE) of the doublet at 8.23 ppm (*ortho*-H<sub>c</sub> on the pyridyl fragment of tolylpyridine ligand, 2.6 %) (mixing time of 0.5s, delay time 4s).

**Complex 41(OAc)**

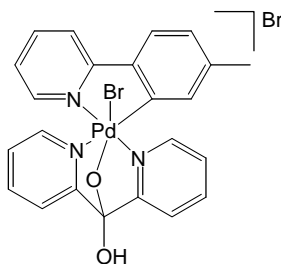


$^1\text{H}$  NMR (MeOD, 22°C),  $\delta$ : 6.67 (d,  $J = 8.0$  Hz, 1H), 7.11 (ddd,  $J = 8.4, 7.7, 2.1$  Hz, 1H), 7.34-7.43 (m, 3H), 7.71-7.77 (m, 3H), 7.97-7.99 (m, 2H), 8.13 (d,  $J = 8.0$  Hz, 1H), 8.26-8.32 (m, 2H), 8.34 (td,  $J = 7.8, 1.1$ Hz, 1H), 9.11 (d,  $J = 5.0$  Hz, 1H), 9.16 (d,  $J = 5.8$  Hz, 1H).

$^{13}\text{C}$  NMR (MeOD, 22°C),  $\delta$ : 29.1, 117.5, 119.7, 121.9, 122.1, 123.1, 126.5, 126.8, 127.8, 129.2, 130.7, 133.0, 141.9, 143.2, 145.3, 147.6, 147.8, 148.8, 151.0, 159.4, 159.6, 163.5, 180.2

ESI-MS of a solution of **41(OAc)** in methanol,  $m/z = 557.9184$ . Calculated for  $\text{C}_{22}\text{H}_{17}\text{BrN}_3\text{O}_3^{106}\text{Pd} = 557.9485$ .

**Complex 45(Br)**



$^1\text{H}$  NMR ( $\text{D}_2\text{O}$ , 3°C),  $\delta$ : 2.09 (s, 3H), 6.49 (s, 1H), 7.08 (d,  $J = 8.1$  Hz, 1H), 7.18 (td,  $J = 6.4, 2.6$  Hz, 1H), 7.52-7.58 (m, 2H), 7.66-7.68 (m, 2H), 7.81 (d,  $J = 8.0$  Hz, 1H), 7.96-8.01 (m, 4H), 8.04 (td,  $J = 7.7, 1.0$  Hz, 1H), 9.07 (d,  $J = 5.5$  Hz, 1H), 9.10 (d,  $J = 5.8$  Hz, 1H).

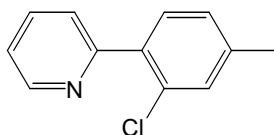
$^{13}\text{C}$  NMR (MeOD, 22°C),  $\delta$ : 22.3, 106.5, 123.2, 123.8, 123.9, 126.6, 128.1, 128.6, 129.8, 130.2, 131.6, 140.8, 143.1, 143.7, 144.6, 146.4, 149.1, 150.3, 151.4, 159.2, 161.7, 164.2, 165.4.

Anal. Found (Calcd. with 1.5 molecules of  $\text{H}_2\text{O}$  present) C, 41.97 (41.69); H, 3.46 (3.35); N, 5.98 (6.34)

ESI-MS of a solution of **45(Br)** in dmsO,  $m/z = 555.9704$ . Calculated for  $\text{C}_{23}\text{H}_{19}\text{BrN}_3\text{O}_2^{106}\text{Pd} = 555.9692$ .

Compounds **51**, **25**, **42** and **46** were prepared by literature procedures for directed palladium catalyzed halogenation of aromatic C–H bonds,<sup>117</sup> while compound **53** was isolated from the reaction mixture and characterized via NMR spectroscopy and ESI–MS.

**Compound 25**

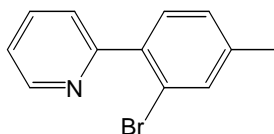


<sup>1</sup>H NMR (AcOH-d<sub>4</sub>, 22°C), δ: 2.43 (s, 3H), 7.29 (dq, *J*=7.9, 1.0 Hz, 1H), 7.42 (vs, 1H), 7.50 (d, *J*=7.8 Hz, 1H), 7.66 (dd, *J*=6.4, 1.2 Hz, 1H), 7.81 (d, *J*=7.8 Hz, 1H), 8.13 (td, *J*=7.8, 1.7 Hz, 1H), 8.92 (d, *J*=5.0, Hz, 1H).

<sup>13</sup>C NMR (AcOH-d<sub>4</sub>, 22°C), δ: 21.1, 124.9, 127.4, 129.1, 131.5, 132.4, 132.9, 134.2, 140.5, 142.7, 148.0, 155.6.

ESI-MS of solution of **25** in acetic acid, *m/z* = 204.0468; calculated for C<sub>12</sub>H<sub>11</sub>NCl = 204.0580

**Compound 42**

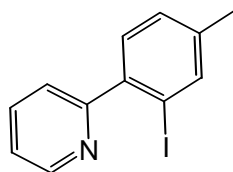


<sup>1</sup>H NMR (AcOH-d<sub>4</sub>, 22°C), δ: 2.41 (s, 3H), 7.32 (d, *J*=7.8 Hz, 1H), 7.46 (d, *J*=7.8 Hz, 1H), 7.59 (s, 1H), 7.73 (ddd, *J*=7.8, 5.4, 1.0 Hz, 1H), 7.83 (d, *J*=7.8 Hz, 1H), 8.22 (td, *J*=7.9, 1.6 Hz, 1H), 8.93 (dd, *J*=5.0, 0.7 Hz, 1H).

<sup>13</sup>C NMR (AcOH-d<sub>4</sub>, 22°C), δ: 21.0, 122.4, 125.4, 127.9, 129.7, 132.3, 134.8, 135.2, 141.8, 143.3, 147.1, 156.5.

ESI-MS of solution of **42**·H<sup>+</sup> in acetic acid, m/z = 248.0081; calculated for C<sub>12</sub>H<sub>11</sub>NCl = 248.0075.

**Compound 46**

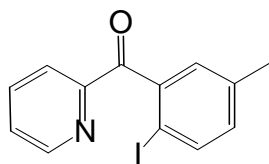


<sup>1</sup>H NMR (CDCl<sub>3</sub>, 22°C), δ: 2.33 (s, 3H), 7.20 (dd, *J*=7.7, 0.8 Hz, 1H), 7.25 (ddd, *J*=7.8, 4.9, 1.0 Hz, 1H), 7.31 (d, *J*=7.8 Hz, 1H), 7.46 (dt, *J*=7.8, 1.3 Hz, 1H), 7.72 (td, *J*=7.8, 1.8 Hz, 1H), 7.77(vs, 1H), 8.66 (dq, *J*=5.0, 0.8 Hz, 1H).

<sup>13</sup>C NMR (CDCl<sub>3</sub>, 22°C), δ: 20.7, 122.6, 124.7, 129.2, 130.1, 136.2, 140.1, 140.3, 142.2, 149.2, 160.8.

ESI-MS of solution of **46**·H<sup>+</sup> in acetic acid, m/z = 295.9887; calculated for C<sub>12</sub>H<sub>11</sub>IN = 295.9936

**Compound 51**

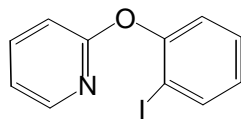


<sup>1</sup>H NMR (AcOH-d<sub>4</sub>, 22°C), δ: 2.33 (s, 3H), 7.07 (dd, *J*=8.2, 2.2 Hz, 1H), 7.24 (vs, 1H), 7.67 (ddd, *J*=7.8, 4.9, 0.8 Hz, 1H), 7.77 (d, *J*=8.2 Hz, 1H), 8.06 (td, *J*=7.6, 1.6 Hz, 1H), 8.11 (d, *J*=7.8 Hz, 1H), 8.74 (d, *J*=4.9 Hz, 1H).

<sup>13</sup>C NMR (AcOH-d<sub>4</sub>, 22°C), 20.9, 88.9, 126.1, 128.7, 131.3, 133.6, 139.4, 139.5, 140.4, 144.5, 149.9, 153.2, 197.2.

ESI-MS of solution of **51**·H<sup>+</sup> in acetic acid, m/z = 323.9956 (calculated C<sub>13</sub>H<sub>11</sub>INO = 323.9885).

**Compound 53**



$^1\text{H}$  NMR (dms $\text{o-d}_6$ , 22°C),  $\delta$ : 7.02 (td,  $J=7.6$ , 1.4 Hz, 1H), 7.05 (d,  $J=8.4$  Hz, 1H), 7.11 (dd,  $J=7.5$ , 4.9 Hz, 1H), 7.17 (dd,  $J=8.1$ , 1.2 Hz, 1H), 7.43 (td,  $J=7.7$ , 1.4 Hz, 1H), 7.87 (ddd,  $J=8.5$ , 6.6, 2.0 Hz, 1H), 7.89 (dd,  $J=7.8$ , 1.4 Hz, 1H), 8.09 (dd,  $J=5.1$ , 1.4 Hz, 1H).

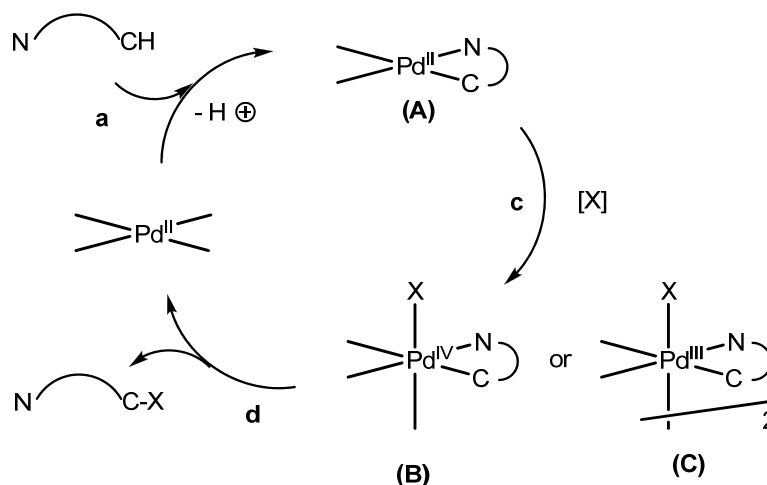
$^{13}\text{C}$  NMR (dms $\text{o-d}_6$ , 22°C),  $\delta$ : 111.2, 118.9, 123.1, 126.8, 129.6, 139.2, 140.1, 147.1, 162.3, 180.1.

ESI-MS of solution of **53.H<sup>+</sup>** in dms $\text{o}$ ,  $m/z = 297.9703$  (calculated for  $\text{C}_{11}\text{H}_9\text{INO} = 297.9729$ ).

## Chapter 5: PPC Ligand-enabled Functionalization of C–Pd Bonds With H<sub>2</sub>O<sub>2</sub> in Acetic Acid

### 5.1 Introduction

Scheme 5. 1

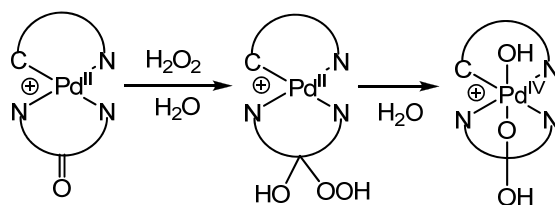


Palladium catalyzed oxidative C–H bond functionalization reactions have been proposed to take place through a three-step catalytic cycle as shown in scheme 5.1.<sup>24,132</sup> The first step (step a) involves C–H bond activation to generate organopalladium(II) intermediates, which undergo oxidation to produce either monomeric Pd(IV) or dimeric Pd(III) species (step b). C–O reductive elimination from these high oxidation palladium species generates the functionalized product and regenerates the catalyst (step c).

We have performed extensive studies on the oxidation of organopalladium(II) complexes utilizing H<sub>2</sub>O<sub>2</sub> as oxidant in both water and acetic acid solvents. In the absence of the 2-dipyridylketone (dpk) ligand, the reaction between acetato-bridged

palladacycles and  $\text{H}_2\text{O}_2$  is too slow in acetic acid solvent at room temperature. Among the substrates studied, only the 2-arylpyridine derived palladacycles bearing the  $\text{C}=\text{O}$  functional group undergoes functionalization of the  $\text{C}-\text{Pd}$  bond with  $\text{H}_2\text{O}_2$  to generate the corresponding phenol and aryl acetate products, underscoring the importance of the  $\text{C}=\text{O}$  functionality in these  $\text{C}-\text{Pd}$  functionalization reactions when  $\text{H}_2\text{O}_2$  is used as oxidant. The oxidation reactions become faster, cleaner, and applicable to more palladacycles when the dpk ligand is used. Dpk ligand-supported palladacycles derived from substituted phenylpyridine, benzoylpyridine, acetophenone oxime, and phenoxy pyridine were observed to undergo fast oxidation in water and acetic acid solvents to generate the corresponding monohydrocarbyl Pd(IV) complexes. These oxidation reactions were studied both experimentally and computationally, and a mechanism that involves addition of  $\text{H}_2\text{O}_2$  across the  $\text{C}=\text{O}$  bond of the dpk ligand, followed by nucleophilic attack of Pd(II) onto the hydroperoxide moiety resulting in heterolytic cleavage of the  $\text{O}-\text{O}$  bond was proposed (Scheme 5.2). In these reactions, the dpk ligand was proposed to assist in the oxidation reaction by bringing the electrophilic peroxy group in close proximity to the palladium(II) center.

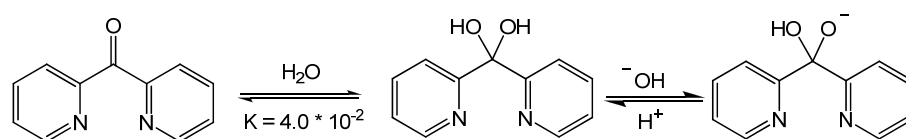
**Scheme 5. 2**



The dpk ligand was also found to be key in the stability of the resulting monohydrocarbyl Pd(IV) complexes. The ability of the hydrated dpk ligand to

undergo deprotonation and generate an anionic species is significant because this anionic form of the dpk hydrate stabilizes the Pd(IV) complex through coordination in a facial chelation mode (Scheme 5.3).<sup>123,154</sup> Arylpyridine derived Pd(IV) complexes bearing two anionic facially chelating ligands, derived from the hydrated 2-benzoylpyridine and 2-dipyridylketone fragments, were found to be the most stable among the substrates studied, such that they were isolated and stored in the solid state at room temperature for over two weeks without decomposition. In addition, aqueous solutions of the arylpyridine derived monohydrocarbyl Pd(IV) complexes are stable in water at room temperature for at least two days. In contrast, monohydrocarbyl Pd(IV) complexes bearing one tridentate facially chelating ligand undergo decomposition at room temperature, and thus have to be stored at  $-20^{\circ}\text{C}$ . Additionally, these complexes are not stable in water at room temperature, where they undergo C–O bond-forming decomposition to generate the corresponding oxapalladacycles.

**Scheme 5.3**



Given that monohydrocarbyl Pd(IV) complexes undergo clean C–O reductive elimination reactions in various solvents such as water and acetic acid, the mechanism of C–O reductive elimination was studied. Based on experimental and computational studies on the C–O reductive elimination reaction at 2-arylpyridine-derived monohydrocarbyl Pd(IV) complexes in water, a mechanism of C–O reductive elimination was proposed where the reaction takes place from a six-coordinate

palladium species. In contrast, C–O reductive elimination at monohydrocarbyl Pd(IV) complexes derived from 2-arylpyridine was proposed to take place from a 5-coordinate palladium intermediate generated via preliminary pyridine group dissociation in acidic solutions.

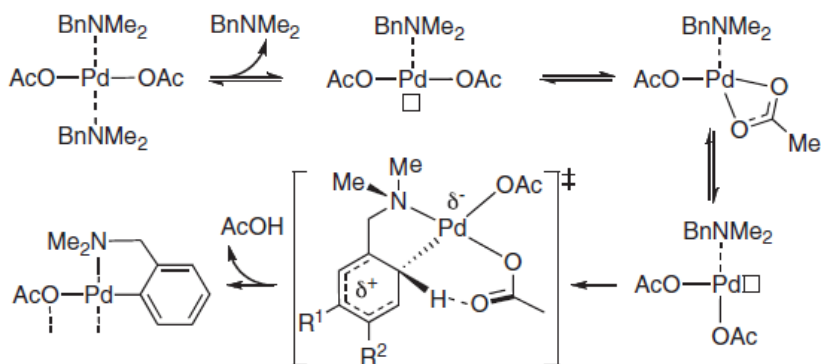
Thus, the dpk ligand was observed to enable oxidation of monohydrocarbyl Pd(II) complexes to their Pd(IV) analogues using H<sub>2</sub>O<sub>2</sub> as oxidant, and the subsequent C–O reductive elimination from the monohydrocarbyl Pd(IV) complexes to produce the corresponding oxapalladacycles, phenols, and/ or aryl acetates, depending on the solvent used. With successful oxidation (step b, Scheme 5.1) and reductive elimination (step c, Scheme 5.1) processes, an efficient palladium catalyzed C–H bond oxygenation reaction will be achieved upon optimization of the C–H activation reaction (step a) under similar conditions.

The transition metal-assisted C–H bond activation reaction has been studied for many years.<sup>119,221,222</sup> The earliest study of the mechanism of metal assisted C–H bond activation was performed by Winstein and Traylor in 1955.<sup>223</sup> In this report, the acetolysis of diphenyl mercury in acetic acid solvent was proposed to proceed via an electrophilic aromatic substitution mechanism, based on the electrophilic character of mercury.<sup>224-229</sup>

In 1985, Ryabov and co-workers studied the cyclopalladation reaction of N,N-dimethylbenzylamine in acetic acid.<sup>230</sup> Analysis of the reaction kinetics revealed a negative slope of the Hammet plot ( $\rho = -1.6$ ), which was proposed to indicate an electrophilic Pd(II) center, as well as an extremely negative entropy of  $-60 \text{ calK}^{-1} \text{ mol}^{-1}$  and high KIE ( $k_{\text{H}}/k_{\text{D}}$ ) of 2.2, which were interpreted to indicate a highly

ordered transition state in which the leaving proton is abstracted intramolecularly by the acetate ligand (see Scheme 5.4).

Scheme 5.4

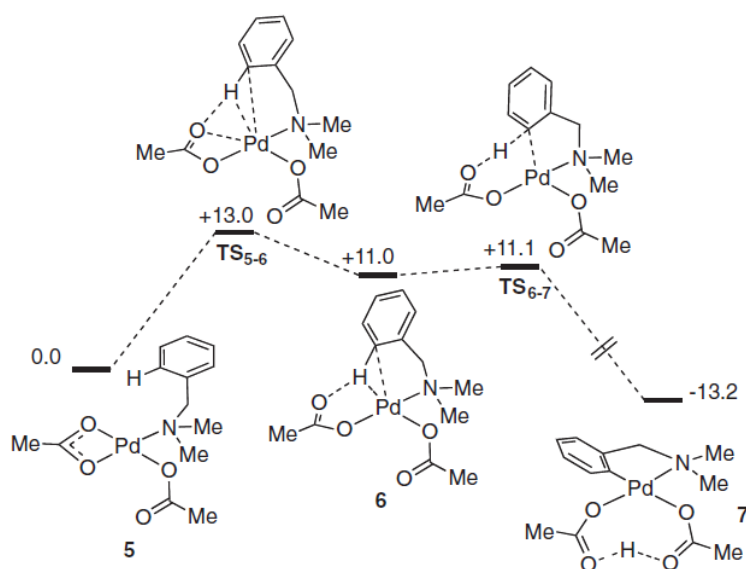


According to Scheme 5.4, the transition state depicted by Ryabov suggests deprotonation of a Wheland intermediate, although this intermediate was not explicitly mentioned in the report. In a later report, Ryabov stated that “the transition state of the orthopalladation of *N,N*-dimethylbenzylamine process involves concerted formation of the palladium–carbon bond and cleavage of the C–H bond with nucleophilic assistance by the coordinated acetate”.<sup>231</sup>

More recent computational studies on the *ortho*-palladation of *N,N*-benzylamine by Davis and co-workers showed that the lowest energy route proceeds via an agostic intermediate **6** (Scheme 5.5), followed by C–H bond deprotonation with acetate group through a six-membered cyclic transition state (**TS<sub>6-7</sub>**).<sup>232</sup> The agostic interaction is proposed to increase the acidity of the *ortho*-proton, facilitating its deprotonation by the acetate. In addition, hydrogen bonding between the acetate oxygen atom and the *ortho*-hydrogen of the aromatic group in **6** is proposed to orient the acetate for the C–H abstraction step, and to also increase the electron density of the C–H bond which in turn further strengthens the agostic interaction. As a result of

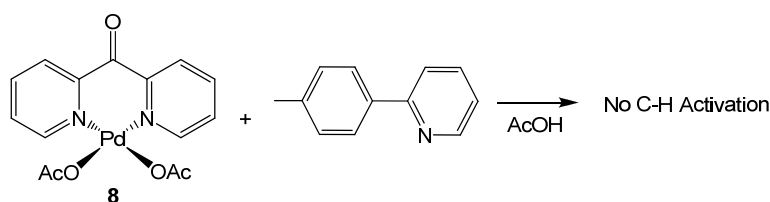
these combined effects, the C–H activation process is proposed to involve a near barrier-less proton transfer to yield the thermodynamically favored palladacycle **7**. The calculated atomic charges for **TS**<sub>6-7</sub> showed very little evidence for the contribution of a Wheland intermediate, which led to the conclusion that the deprotonation and metalation steps are concerted. These calculations were supported experimentally by KIE studies, where the calculated KIE ( $k_{\text{H}}/k_{\text{D}} = 1.2$ ) was close to the experimental value of ( $k_{\text{H}}/k_{\text{D}} = 2.2$ ).<sup>129</sup>

Scheme 5. 5



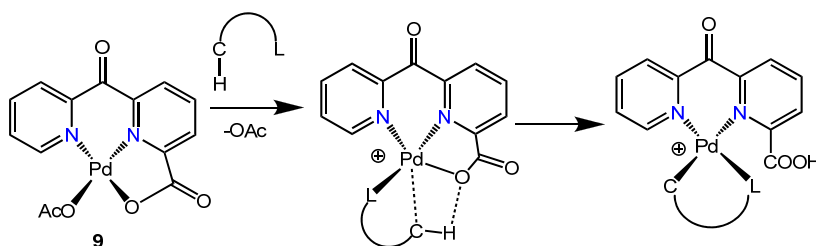
These studies indicate that carboxylate group may be important in the palladium assisted C–H activation processes. Therefore, activation of aromatic C–H bonds utilizing the dpk ligand in the presence of acetate groups was attempted. Complex **8** was prepared and used in stoichiometric quantities to activate the *ortho* C–H bond of the 2-tolylpyridine substrate in acetic acid solvent. These studies were performed by Vedernikov and Zhang, and no C–H bond activation was observed (Scheme 5.6).<sup>175</sup>

Scheme 5. 6

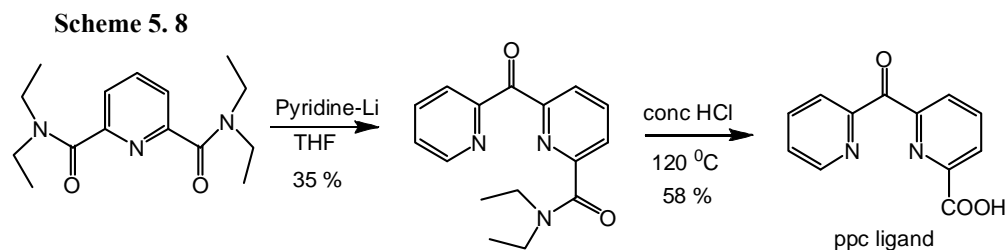


As a result, we designed a new ligand bearing an *ortho*-carboxylate group, the 6-(pyridin-2-ylcarbonyl)pyridine-2-carboxylic acid (ppc) ligand. This ligand was designed with an *ortho*-carboxylate group because the mechanism of C–H bond activation by palladium has been proposed to involve intramolecular deprotonation by the adjacent acetate ligand, where acetate acts as an intramolecular base. The *ortho*-carboxylate arm of the ppc ligand is expected to function as an intramolecular base in the C–H deprotonation step as shown in Scheme 5.7 below.

Scheme 5. 7



The ppc ligand was synthesized by the reaction of N,N,N',N'-tetraethylpyridine-2,6-dicarboxamide with pyridyl lithium in THF to afford the N,N-diethyl-6-(pyridin-2-ylcarbonyl)pyridine-2-carboxamide product (Scheme 5.8). Hydrolysis of this product in 6.0 M HCl generated the target ppc ligand. This ligand was characterized by NMR spectroscopy and electrospray ionization mass spectrometry (ESI-MS), while its purity was confirmed by elemental analysis.



Considering scheme 5.1 depicted above, our studies were aimed at determining whether the ppc ligand would enable palladium assisted C–H bond activation (step a), oxidation of the resulting organopalladium(II) complexes with H<sub>2</sub>O<sub>2</sub> (step b), and C–O reductive elimination from the resulting monohydrocarbyl Pd(IV) complexes (step c). With each step in the catalytic cycle demonstrated, we plan to develop a ppc ligand–enabled palladium catalyzed functionalization of aromatic C–H bonds utilizing H<sub>2</sub>O<sub>2</sub> as the terminal oxidant, in water or acetic acid.

Given that oxidation of organopalladium(II) complexes to their corresponding monohydrocarbyl Pd(IV) analogs with H<sub>2</sub>O<sub>2</sub> as oxidant was achieved using the dpk ligand, we started by determining whether the ppc ligand would enable the oxidation of similar organopalladium(II) complexes using H<sub>2</sub>O<sub>2</sub>. We anticipated this reaction to be facile because similar to the dpk ligand, the ppc ligand possesses a C=O functional group which is important for oxidation with H<sub>2</sub>O<sub>2</sub>. The C=O functional group was proposed to assist in oxidation of organopalladium(II) complexes by bringing the electrophilic oxidant in close proximity to the palladium center, since H<sub>2</sub>O<sub>2</sub> is capable of adding across the C=O bond to form a hydroperoxide adduct. The difference in reactivity of organopalladium(II) complexes supported by the ppc ligand and those supported by the dpk ligand towards H<sub>2</sub>O<sub>2</sub> will be discussed.

The C=O group of the ppc could undergo hydration and deprotonation to provide an alkoxide that can coordinate to the Pd(IV) center through the oxygen

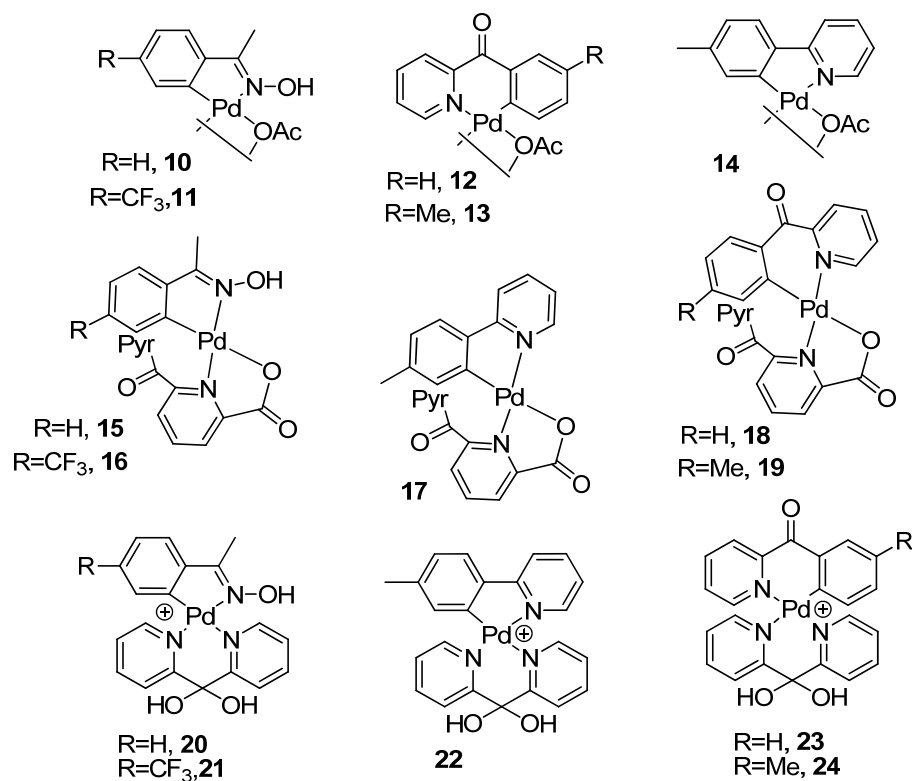
atom. The ppc ligand also possesses a carboxylic acid group that can undergo deprotonation and coordinate onto the Pd(IV) center. By coordination of the alkoxide, the ppc ligand might formally adopt a facially coordination mode that has been proposed to stabilize a variety of Pd(IV) complexes.<sup>184-188</sup> Alternatively, coordination of the carboxylate group would lead to either a facially or a meridional coordination geometry. As a result, the mode of binding of the ppc ligand in both the Pd(II) and Pd(IV) complexes will be studied, and the C–O bond forming reactivity of the ppc ligand–supported organopalladium Pd(IV) complexes will be compared to that of dpk ligand–supported organopalladium(IV) complexes.

Ultimately, the activation of aromatic C–H bonds will be investigated utilizing the ppc ligand. With successful C–H bond activation, oxidation of the resulting organopalladium(II) complexes with H<sub>2</sub>O<sub>2</sub>, and C–O reductive elimination from the resulting monohydrocarbyl Pd(IV) complexes to release the functionalized product, we envision to combine these steps into a catalytic cycle, and be able to perform a ligand enabled, palladium catalyzed functionalization of aromatic C–H bonds using H<sub>2</sub>O<sub>2</sub> as the terminal oxidant, in water or acetic acid.

We started our studies by preparing organopalladium(II) complexes supported by the ppc ligand, and studying their reactivity with H<sub>2</sub>O<sub>2</sub>.

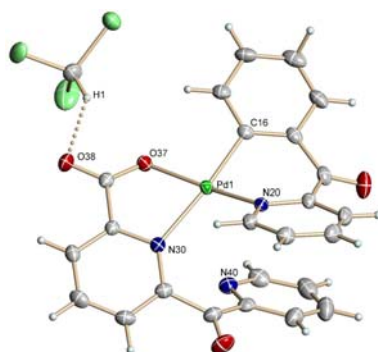
## 5.2 Preparation of Palladacycles Supported by ppc Ligand, 15–19

Chart 5.1



Preparation of the acetato-ligated hydrocarbyl Pd(II) complexes **10-14** has been described previously in chapter 2. The palladacyclic ppc ligand-supported complexes **15**, **16**, and **17** were prepared by stirring a mixture of acetato-ligated complexes **10**, **11**, and **12** respectively with the ppc ligand (1.05 eq.) in dichloromethane. These solutions were stirred under ambient conditions for several hours, concentrated and triturated with THF to produce white precipitate of the target complexes. Complexes **18** and **19** were also prepared using the procedure above, but benzene was used as solvent instead of dichloromethane, while diethyl ether was used to triturate the solutions. The precipitates were filtered off to afford complexes **15-19**, which were characterized by NMR spectroscopy and electrospray ionization mass

spectrometry, while complex **18** was also characterized by X-ray diffraction. The purity of these complexes was confirmed by elemental analysis.



**Figure 5. 1.** ORTEP drawing (50 % probability ellipsoids) of complex **18**

According to the crystal structure of complex **18**, the palladium center has a square planar geometry, as expected for  $d^8$  metal centers. The ppc ligand adopts a N,O binding mode that includes one oxygen atom from the carboxylate arm, and nitrogen from one pyridine group of the ppc ligand, while the benzoylpyridine fragment adopts the expected N,C chelation mode with the aryl and pyridine groups. The Pd–N bond length (2.135 Å) *trans* to the aryl ligand is elongated due the strong *trans* influence of the aryl group, while the Pd–N bond length (2.001 Å) *trans* to the carboxylate oxygen atom is shorter. The carboxylate group has C–O bond-lengths of 1.225 Å and 1.285 Å, which is indicative of charge localization.

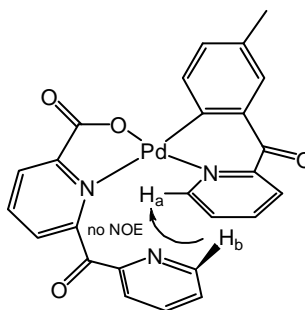
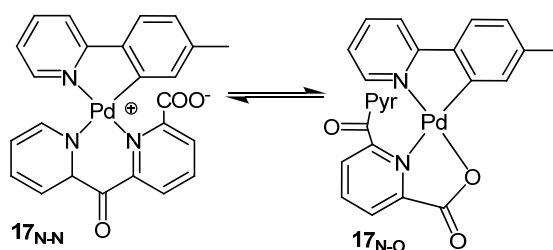


**Figure 5. 2.** Complex **19**, showing the hydrogen atoms  $H_a$  and  $H_b$ .

The solution structure of complex **19** was determined using selective 1D difference NOE experiments, where irradiation of the H<sub>a</sub> signal belonging to the *ortho*-Hydrogen of the pyridyl fragment of the 2-(3-methylbenzoyl)pyridine ligand and H<sub>b</sub> signal belonging to the *ortho*-Hydrogen of the pyridyl fragment of the ppc ligand did not result in enhancement of any hydrogen signals. These results suggest that the solid state structure of these complexes may be maintained in solution.

Complexes **15-19** display broad <sup>1</sup>H NMR signals in deuterated acetic acid solvent, indicative of fluxional behavior. This behavior might arise due to alternating coordination and dissociation of the carboxylate arm of the ppc ligand and the pyridine group of the ppc ligand, which are slow in the NMR time scale (Scheme 5.9). The <sup>1</sup>H NMR signals of these complexes are however sharp and narrow in CDCl<sub>3</sub> and dms<sub>o</sub>-d<sub>6</sub> solvents, indicative of no fluxional behavior. The enhanced fluxional behavior in protic solvents is consistent with the ability of protic solvents to stabilize charge separation, such as in the zwitterionic complex **17<sub>N-N</sub>** (Scheme 5.9).

**Scheme 5.9**

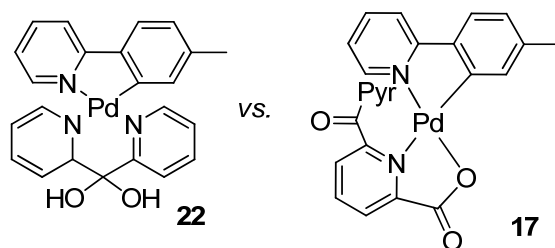


The assignment of complexes **15-19** as neutral compounds is supported by the absence of acetate ligand in the NMR spectra collected in dms<sub>o</sub>-d<sub>6</sub> or CDCl<sub>3</sub>, the X-ray structure of complex **19**, and by the elemental analysis of these complexes.

The N,O binding mode exhibited by ppc ligand-derived complexes **15-19** is different from that exhibited by the dpk ligand-supported complexes **20-24**, which

display a N,N binding mode (Scheme 5.10). This might be due to the preference of five-membered over six-membered chelates.

**Scheme 5.10**

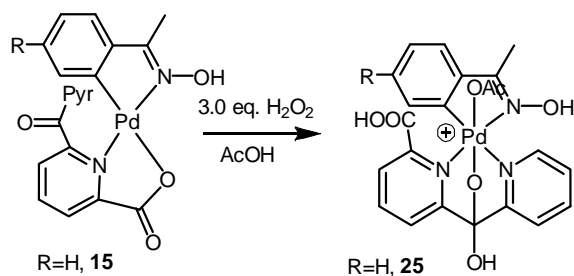


5.3 Reactivity of Palladacycles Supported by ppc Ligand, **15-19** with  $H_2O_2$  in Acetic Acid

Treatment of ppc-derived complexes **15-19** with dilute aqueous  $H_2O_2$  in acetic acid at room temperature resulted in exothermic reactions and immediate color change from colorless to brown or deep yellow.  $^1H$  NMR analysis of the reaction solutions revealed formation of intermediate products which gradually decomposed to produce the corresponding aryl acetate and sometimes phenol in total quantitative yield, and complex **30** as the only inorganic product of decomposition. The decomposition reaction was accompanied by color change from deep yellow to colorless or light yellow. The intermediates were not isolated and were characterized in solution by  $^1H$  NMR spectroscopy and electrospray ionization mass spectrometry, while the products were characterized by independent synthesis or comparison of the  $^1H$  NMR of known compounds to literature.

### 5.3.1 Reactivity of Complex **15** with H<sub>2</sub>O<sub>2</sub> in Acetic Acid at Room Temperature

Scheme 5. 11



In the reaction of a 0.01 M solution of complex **15** in acetic acid with 3 equivalents of H<sub>2</sub>O<sub>2</sub> at room temperature, <sup>1</sup>H NMR analysis revealed a fast and clean formation of a single product **25** within 10 minutes, accompanied by color change of the solution from colorless to deep brown (characterization of complex **25** will be discussed later). The <sup>1</sup>H NMR spectrum of this product exhibited 11 multiplets in the aromatic region with a pattern significantly different from both the starting complex and the final products. In particular, complex **25** exhibits narrow and sharp peaks, indicating loss of the fluxional behavior observed in the Pd(II) precursor **15**. The increased rigidity of **25** might arise due to coordination of both pyridine groups and the carboxylate arm of the ppc ligand upon reaction of complex **15** with H<sub>2</sub>O<sub>2</sub>. In the <sup>1</sup>H NMR spectrum of complex **25**, the singlet belonging to the methyl group of the oxime moiety is significantly shifted downfield to 2.50 ppm, relative to that of the Pd(II) precursor **15** whose methyl signal is observed at 2.17 ppm. A similar downfield shift is observed for the aromatic signals belonging to the oxime fragment of complex **25** relative to those of the Pd(II) precursor. The downfield shift of the <sup>1</sup>H NMR signals in the product of oxidation, complex **25** indicates a more electron deficient environment relative to that of the starting Pd(II) complex **15**.

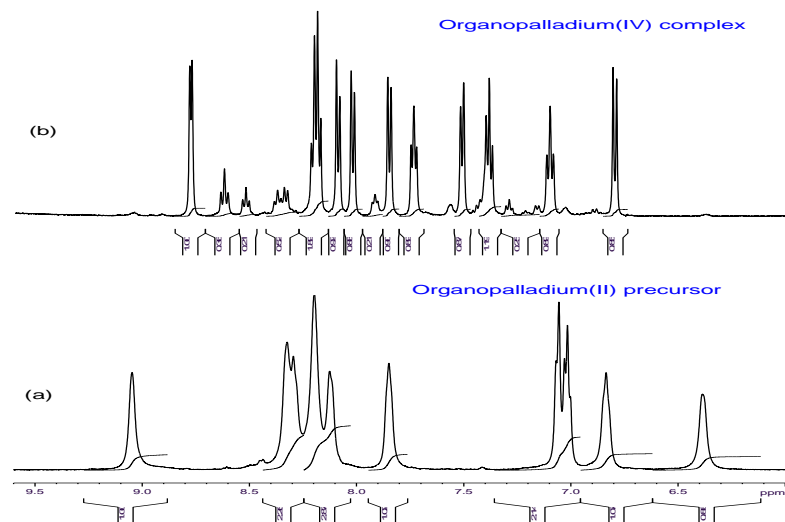


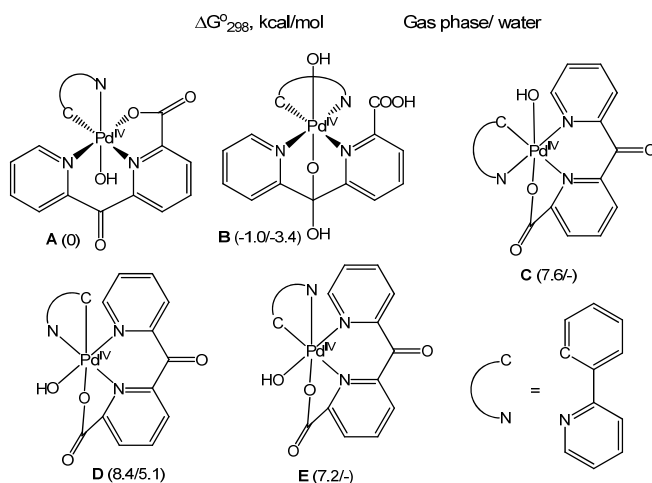
**Figure 5. 3.** Room temperature  $^1\text{H}$  NMR spectrum of (a) complex **15** in  $\text{AcOH-d}_4$  (b) complex **25** in  $\text{AcOH-d}_4$ . The minor signals belong to products of decomposition.

#### *Characterization of complex 25*

The ESI–MS analysis of the reaction solution after combining an acetic acid solution of complex **15** with 10.0 equivalents of  $\text{H}_2\text{O}_2$  displayed a major peak at  $m/z = 526.08683$  corresponding to the Pd(II) precursor + OAc group which was assigned to complex **25**, and  $m/z = 544.0984$  corresponding to the Pd(II) precursor + OAc +  $\text{H}_2\text{O}$  groups, which was assigned to complex **25** plus an additional water molecule. On the basis of ESI–MS analysis, the species observed by  $^1\text{H}$  NMR was assigned to monohydrocarbyl Pd(IV) complex **25**, with has an acetato-ligated palladium center. This assignment is consistent with the ESI–MS signals observed at  $m/z = 526.0868$  and 544.0984.

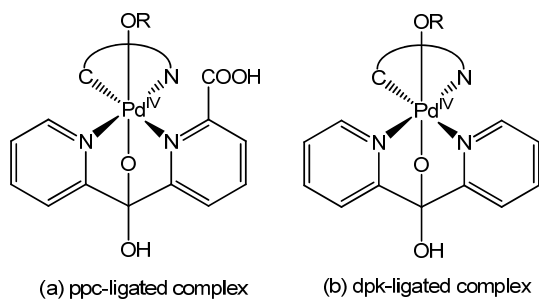
DFT calculations were used to find the lowest energy structure among a variety of possible structures (Scheme 5.12).

### Scheme 5. 12



In the DFT calculations, various possible structures were considered as presented in Scheme 5.12 above, with structure **A** used as the reference point. The energies are given both in the gas phase and aqueous phase. The lowest energy structure was calculated where the ppc ligand adopts a facial chelation mode, involving coordination of an alkoxide group, which is produced upon deprotonation of the hydrated C=O moiety. This binding mode is similar to that adopted by the dpk ligand as shown in Scheme 5.13 below.

### Scheme 5. 13



In the reaction involving complex **15** with H<sub>2</sub>O<sub>2</sub> in acetic acid, one intermediate complex is detected by <sup>1</sup>H NMR, while the ESI-MS analysis gives mass envelopes belonging to two species, at m/z = 526.0868 and 544.0984, with the mass envelope at 544.0498 being significantly larger relative to that at 526.0868. As a

result of the ESI-MS and  $^1\text{H}$  NMR analysis, together with the DFT calculations, the assigned structure of complex **25** (Scheme 5.11) includes a facially chelating ppc ligand using the pyridine nitrogen atoms, and the oxygen atom of the alkoxide group produced upon hydration and deprotonation of the C=O moiety. Facially chelating ligands have been found to stabilize Pd(IV)<sup>233</sup> and Pt(IV)<sup>123</sup> complexes. In addition, hydration of the C=O group of the dpk ligand becomes more facile upon coordination to a Pd(II) center, while subsequent deprotonation provides an alkoxide that coordinates and stabilizes the Pd(IV) center.<sup>123,154,233</sup> The assignment of complex **25** as an acetato-ligated organopalladium(IV) complex is also supported by its reactivity, where its decomposition in acetic acid solvent at room temperature produces the corresponding aryl acetate quantitatively. Since C–O reductive elimination from organopalladium(IV) complexes has been proposed to take place via a 3-center 4-electron transition state,<sup>45</sup> both the aryl and acetate ligands are required to be coordinated onto the palladium center for this process to take place, and this supports our assignment of complex **25** as an acetato-ligated monohydrocarbyl Pd(IV) complex. This reductive elimination reactivity will be discussed in more detail later. The structure of complex **25** in solution was studied using 1D difference NOE experiment.

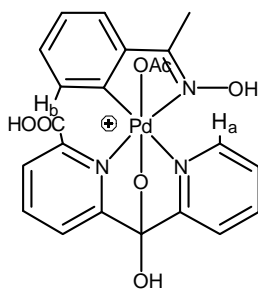
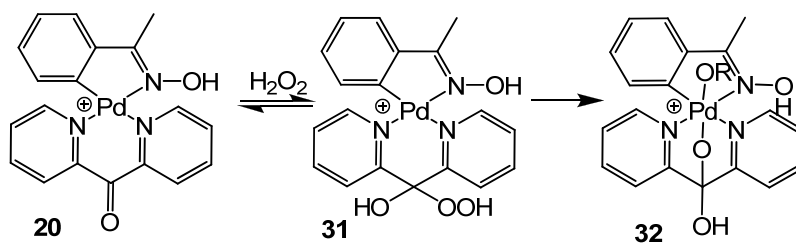


**Figure 5. 4.** NOE experiment of complex **25**, showing the hydrogen atoms  $\text{H}_a$  and  $\text{H}_b$ .

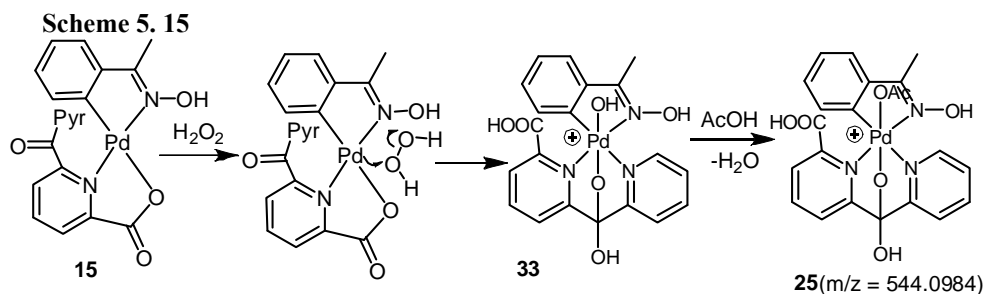
In the 1D difference NOE experiment of complex **25** in deuterated acetic acid at room temperature, no NOE was observed between any hydrogen atoms in the molecule. Irradiation of resonance H<sub>b</sub> at 6.96 ppm did not result in enhancement of any signals while irradiation of resonance H<sub>a</sub> at 9.13 did not show enhancement of any signals either. As a result, complex **25** was assigned to the structure above.

*Mechanism of oxidation of complex 15 to complex 25 with H<sub>2</sub>O<sub>2</sub>*

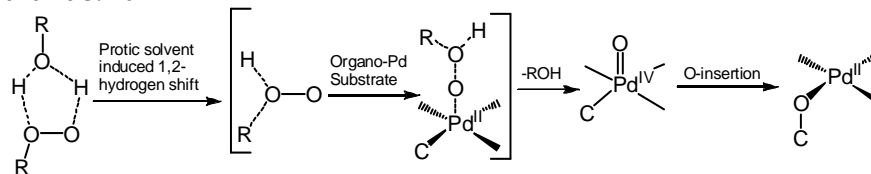
**Scheme 5. 14**



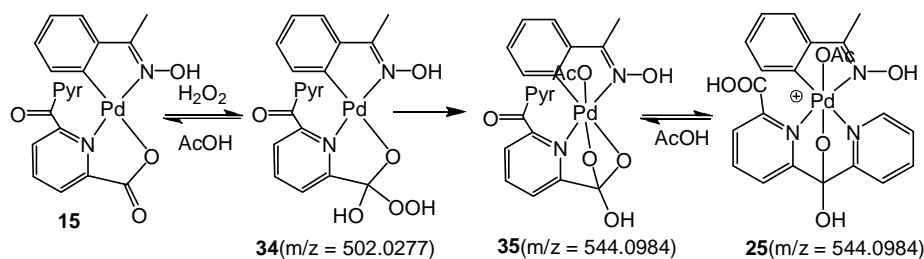
The mechanism of oxidation of the ppc ligand-supported complex **15** was compared to that of its dpk ligand-supported counterpart, **20**. The mechanism of oxidation of dpk ligand-supported Pd(II) complexes with H<sub>2</sub>O<sub>2</sub> was studied experimentally and computationally, and was proposed to involve addition of H<sub>2</sub>O<sub>2</sub> across the C=O bond of the dpk ligand to produce a hydroperoxide moiety. This is followed by nucleophilic attack by palladium onto the hydroperoxide group that results in heterolytic cleavage of the O–O bond and formation of an alkoxy-ligated Pd(IV) complex.



Considering the N,O binding mode of the neutral ppc ligated Pd(II) complexes relative to the cationic dpk ligated complexes, the Pd(II) center in the former is considerably more nucleophilic, and as a result, a direct nucleophilic attack of Pd(II) onto  $\text{H}_2\text{O}_2$  is possible. As a result, the reaction of the ppc ligated complex **15** with  $\text{H}_2\text{O}_2$  may involve a direct nucleophilic attack of Pd(II) onto  $\text{H}_2\text{O}_2$  as shown in Scheme 5.15 above, leading to heterolytic cleavage of the O–O bond and formation of a hydroxy ligated Pd(IV) complex **33**. Ligand substitution of this complex in acetic acid solvent may lead to formation of the acetato-ligated Pd(IV) complex **25** which was observed by  $^1\text{H}$  NMR spectroscopy and detected by electrospray ionization mass spectrometry. A similar mechanism for the oxygenation of cyclopalladated N,N-dimethylbenzylamine complexes by *tert*-butyl hydroperoxide was reported by Van Koten and co-workers (Scheme 5.16).<sup>120</sup> On the basis of kinetic studies where the oxygenation reaction was observed to be strongly enhanced by increasing the nucleophilicity of the metal center, a mechanism of oxygenation that involves nucleophilic attack of Pd(II) on a *tert*-butyl alcohol oxide was proposed. This attack leads to formation of a transient Pd(IV) oxo species and a neutral alcohol leaving group. Insertion of oxygen into the Pd–C bond produces the observed oxapalladacycle.

**Scheme 5.16**

However, given that the analogous neutral acetophenone oxime-derived acetato-bridged Pd(II) complexes do undergo oxidation with H<sub>2</sub>O<sub>2</sub> in acetic acid solvent, we propose that the carbonyl group present in the ppc ligand is important in the reactivity of the ppc ligated complexes with H<sub>2</sub>O<sub>2</sub>. As a result, the mechanism involving direct electrophilic attack of H<sub>2</sub>O<sub>2</sub> onto the central Pd(II) atom will not be considered, and a mechanism that involves addition of H<sub>2</sub>O<sub>2</sub> onto the C=O group of the ppc ligand will be considered (Scheme 5.17).

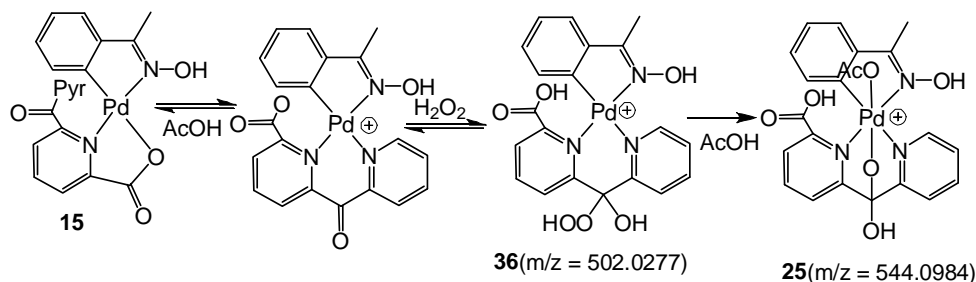
**Scheme 5.17**

We therefore propose that the reactivity of the ppc ligated Pd(II) complexes with H<sub>2</sub>O<sub>2</sub> may be similar to that of the dpk ligated Pd(II) complexes, where the C=O group of the ligand brings the peroxo oxidant in close proximity to the Pd(II) center. Thus, addition of H<sub>2</sub>O<sub>2</sub> to the C=O group of the ppc ligand in complex **15** produces the corresponding hydroperoxide adduct **34**, where a complex with a matching mass envelope at m/z = 502.0277 was detected by ESI-MS (calculated for C<sub>20</sub>H<sub>18</sub>N<sub>3</sub>O<sub>6</sub>Pd<sup>106</sup> = 502.0230). Nucleophilic attack of Pd(II) onto the hydroperoxide moiety results in heterolytic cleavage of the O–O bond and formation of alkoxo-

ligated Pd(IV) complex **35**. Isomerization of complex **35** in acetic acid produces complex **25**.

However, considering the strained nature of complex **35**, we propose that a different mechanism may be operative.

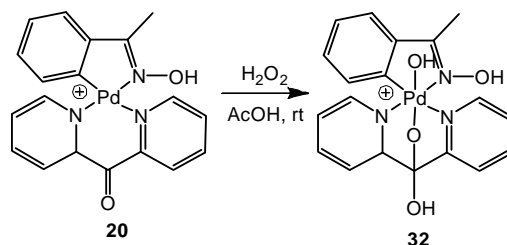
**Scheme 5. 18**



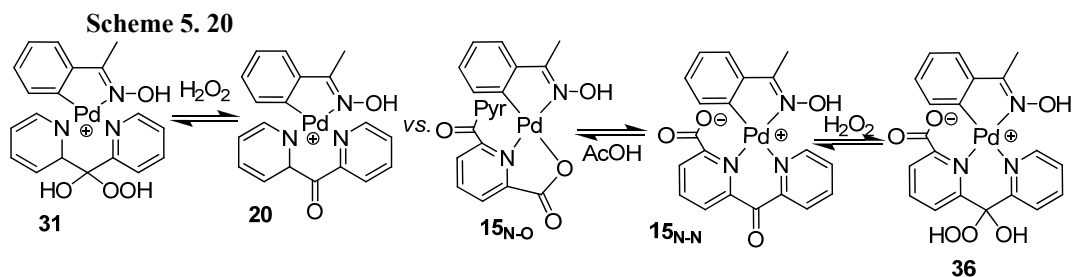
Given that complex **15** was observed to undergo a slow equilibrium between the N,O and the N,N coordination modes of the ppc ligand in protic solvents, the N,N coordination complex  $\text{15}_{\text{N-N}}$  may be more reactive towards addition of  $\text{H}_2\text{O}_2$  across the C=O bond because coordination of both pyridine groups onto the Pd(II) center enhances the electrophilicity of the central C=O group, relative to the N,O coordination mode. A similar enhanced electrophilicity of the C=O group of the 2-dipyridylketone ligand was reported upon N,N coordination onto M(II) (M=Pd or Pt).<sup>154</sup> Consequently, we propose a mechanism of oxidation that involves addition of  $\text{H}_2\text{O}_2$  across the C=O bond of the ppc ligand of complex **15** to produce the hydroperoxide adduct **36** (Scheme 5.18). Although this complex was not detected by  $^1\text{H}$  NMR spectroscopy, a complex with a matching mass envelope was detected via ESI-MS at  $m/z = 502.0277$  (calculated for  $\text{C}_{20}\text{H}_{18}\text{N}_3\text{O}_6\text{Pd}^{106} = 502.0230$ ). Moreover, addition of a molecule of methanol across the C=O bond of the ppc ligand in complex **15** has been observed by ESI-MS at  $m/z = 500.0585$  (calculated for  $\text{C}_{21}\text{H}_{20}\text{N}_3\text{O}_5\text{Pd}^{106}$

= 500.0438), indicating that the addition of nucleophiles across the C=O bond of the ppc ligand is possible. Nucleophilic attack of palladium(II) onto the hydroperoxide moiety leads to heterolytic cleavage of the O–O bond, and produces the acetato-ligated Pd(IV) complex **25**, which was observed by <sup>1</sup>H NMR and detected by ESI–MS.

**Scheme 5. 19**



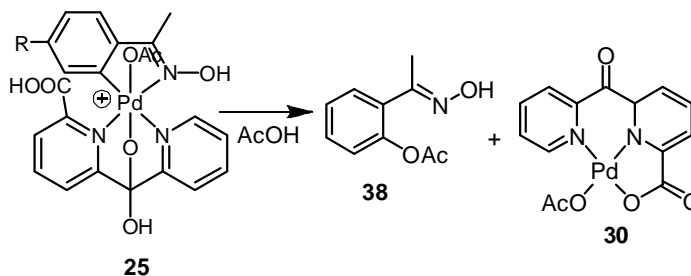
The reactivity of the ppc ligand-supported organopalladium(II) complex **15** towards oxidation with H<sub>2</sub>O<sub>2</sub> in acetic acid was compared to that of the dpk ligand-supported organopalladium(II) complex **20** under similar conditions. In contrast to the reactivity of ppc ligand-supported complex **15** with H<sub>2</sub>O<sub>2</sub> in acetic acid where the acetato-ligated organopalladium(IV) complex **25** was produced, the dpk ligand-supported organopalladium(II) analogue **20** reacts with H<sub>2</sub>O<sub>2</sub> in acetic acid to produce the hydroxo ligated organopalladium(IV) complex **32**. The reaction of complex **20** with 3.0 equivalents of H<sub>2</sub>O<sub>2</sub> in acetic acid to produce complex **32** at room temperature took ~ 4 minutes for complete conversion to take place. The characterization of complex **32** has been reported in chapter 2.<sup>233</sup>



Given that the ppc ligand-supported complex **15** reacts with 3.0 equivalents of  $\text{H}_2\text{O}_2$  in acetic acid at room temperature to produce the corresponding monohydrocarbyl Pd(IV) complex **25** in  $\sim 10$  minutes, while the dpk ligand-supported complex **20** reacts with 3.0 equivalents of  $\text{H}_2\text{O}_2$  to produce the corresponding monohydrocarbyl Pd(IV) complex **32** in under 4 minutes under similar conditions, this indicates that dpk-ligated Pd(II) complexes undergo oxidation with  $\text{H}_2\text{O}_2$  at a faster rate than analogous ppc-ligated complexes. The lower oxidation rate of the ppc ligated complex **15** may be due to the equilibrium between the N,O and the N,N ppc ligand coordination modes adopted by this complex in protic solvents. Given that the N,N ligated ppc complex **15<sub>N-N</sub>** is more reactive towards addition of  $\text{H}_2\text{O}_2$  relative to the N,O ligated complex **15<sub>N-O</sub>**, the overall oxidation rate of this complex depends on the fraction of **15<sub>N-N</sub>** in solution, which in turn depends on the equilibrium between the two complexes. On the other hand, the dpk-ligated complex **20** reacts faster because the complex is active towards  $\text{H}_2\text{O}_2$  addition.

*Decomposition of monohydrocarbyl Pd(IV) complex 25 in acetic acid*

**Scheme 5. 21**



The monohydrocarbyl Pd(IV) complex **25** gradually decomposes in acetic acid at room temperature in under 2 hours to generate the corresponding aryl acetate **38** quantitatively, with complex **30** as the only inorganic product of decomposition. The decomposition reaction was accompanied by gradual color change from deep brown to light yellow. The aryl acetate product **38** was isolated by removal of the solvent and extraction with diethyl ether. This compound was independently synthesized according to literature procedures for palladium catalyzed acetoxylation of aromatic C–H bonds using  $\text{PhI}(\text{OAc})_2$  oxidant.<sup>50</sup> Complex **30** was also independently synthesized and characterized fully, including NMR, ESI–MS, and X–ray diffraction, while its purity was confirmed by elemental analysis. The preparation of complex **30** will be described later.

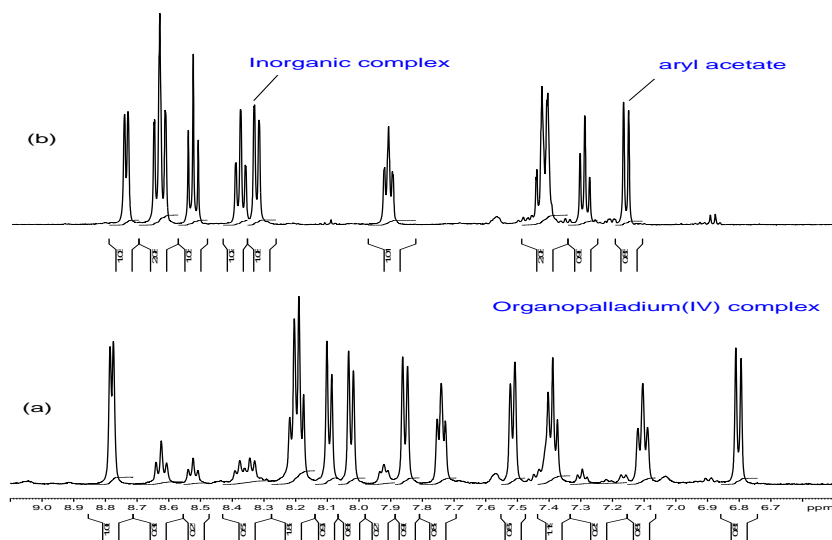
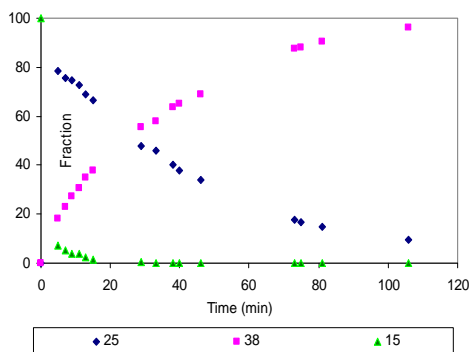
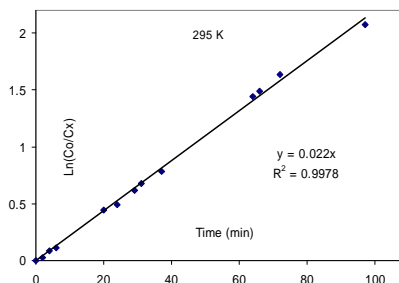


**Figure 5. 5.** Room temperature  $^1\text{H}$  NMR spectra of (a) Acetic solution of complex **25**, (b) acetic acid solution of a mixture of products of decomposition, aryl acetate **38** and inorganic product **30**.

The decomposition reaction of complex **25** in acetic acid at room temperature was monitored by  $^1\text{H}$  NMR. This complex was prepared in situ via the reaction of complex **15** with 5.0 equivalents of  $\text{H}_2\text{O}_2$ . The plot for the fraction of the organopalladium(II) precursor **15**, the organopalladium(IV) complex **25**, and the aryl acetate product **38**, as a function of time is given below. The plot for  $\ln([\mathbf{25}]_0/[\mathbf{25}]_t)$  as a function of time is also presented below, where  $[\mathbf{25}]_0$  refers to the initial concentration of complex **25**, while  $[\mathbf{25}]_t$  refers to the concentration of complex **25** at a time  $t$ . This plot was found to be linear, with observed rate constant of  $(2.21 \pm 0.07) \times 10^{-2} \text{ min}^{-1}$ .



(a)

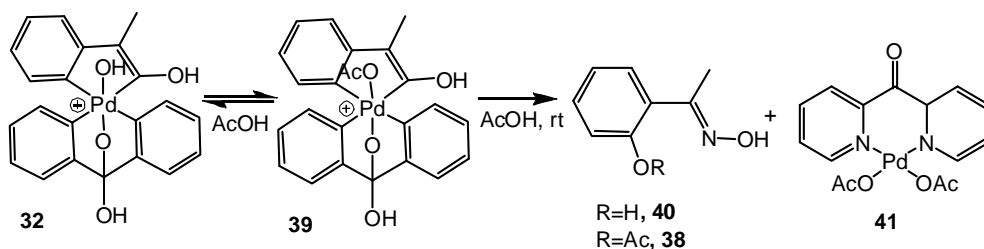


(b)

**Figure 5. 6.** (a) Kinetics plot for the reaction mixture containing 0.010 M acetic acid solution of complex **15** and 5 eq of H<sub>2</sub>O<sub>2</sub>, showing the fraction of the starting complex **15**, the organopalladium(IV) complex **25**, and aryl acetate product **38**, as a function of time; (b) Plot for the  $\ln([25]_0/[25]_t)$  vs. time in acetic acid at room temperature.

The decomposition of the ppc ligand-supported organopalladium(IV) complex **25** was compared to that of dpk ligand-supported organopalladium(IV) complex **32** in acetic acid.

**Scheme 5. 22**

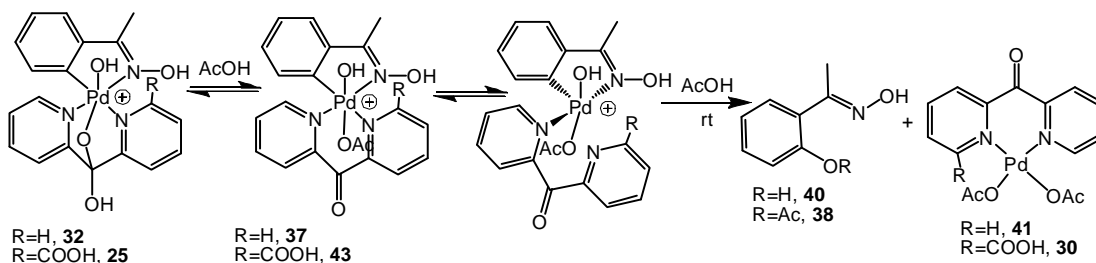


When the decomposition of an acetic acid solution of complex **32** was monitored by <sup>1</sup>H NMR at room temperature, ~ 60 % conversion of complex **32** was observed after 3 hours. At the end of the reaction, multiple new peaks appeared in the <sup>1</sup>H NMR indicating multiple products. ESI-MS analysis of the solution showed the presence of the corresponding phenol **40**, and the aryl acetate **38** products. This reaction was however simpler, generating the corresponding N-acetoxy aryl acetate

and Pd(II) complex **41** as the only products when performed in the presence of acetic anhydride.

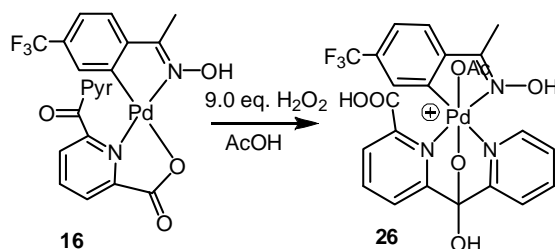
Given that quantitative decomposition of ppc ligand-supported organopalladium(IV) complex **25** in acetic acid at room temperature to produce the corresponding aryl acetate and the Pd(II) complex **30** took less than 2 hours, while only ~ 60 % decomposition of complex **32** was observed in 3 hours, this indicates that the ppc supported organopalladium(IV) complexes are kinetically less stable than their dpk supported counterparts. This might be due to the presence of the carboxylic acid functionality on the ppc ligand. Given that dpk-ligated Pd(IV) complexes have been proposed to undergo C–O reductive elimination in acetic acid from a 5-coordinate intermediate produced upon pyridine group dissociation (Scheme 5.23),<sup>233</sup> we propose that the enhanced reactivity of the ppc-ligated Pd(IV) complexes is due to the electron-withdrawing carboxylic acid functionality present on the ppc ligand, which accelerates pyridine group dissociation to generate the reactive 5-coordinate intermediate.

**Scheme 5. 23**



### 5.3.2 Reactivity of Complex **16** with H<sub>2</sub>O<sub>2</sub> in Acetic Acid at Room Temperature

Scheme 5. 24



The reaction of complex **16** with H<sub>2</sub>O<sub>2</sub> in acetic acid was similar to that of complex **15**. Addition of 3.0 equivalents of H<sub>2</sub>O<sub>2</sub> to a 0.010 M acetic acid solution of complex **16** led to an exothermic reaction and color change of the solution from colorless to deep red, but the reaction was too slow. Complete conversion of the organopalladium(II) complex **16** had not taken place after 30 minutes. Decomposition of the Pd(IV) complex **26** was simultaneously observed under the reaction conditions. As a result, 9.0 equivalents of H<sub>2</sub>O<sub>2</sub> were used to achieve a faster reaction in order be able to characterize the corresponding product of oxidation. When a 0.010 M acetic acid solution of complex **16** was combined with 9.0 equivalents of H<sub>2</sub>O<sub>2</sub> at room temperature, color change from a colorless to deep red solution was observed with cleaner generation of the product of oxidation, as determined by <sup>1</sup>H NMR, in ~ 10 minutes. The <sup>1</sup>H NMR resonances belonging to the new species are narrow and sharp relative to the Pd(II) precursor **16**, indicative of no fluxional behavior. In addition, <sup>1</sup>H NMR signal belonging to the methyl group of the new species is shifted downfield to 2.48 ppm, relative to that in the Pd(II) precursor **16** at 2.21 ppm. The same downfield shift is observed for the aromatic resonances belonging to the oxime moiety, indicating that the product of oxidation is in a more deshielded environment.

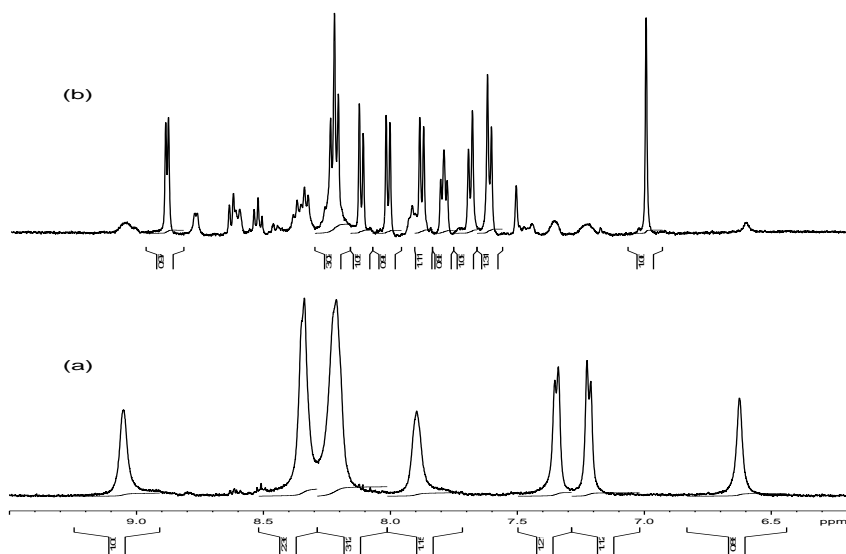


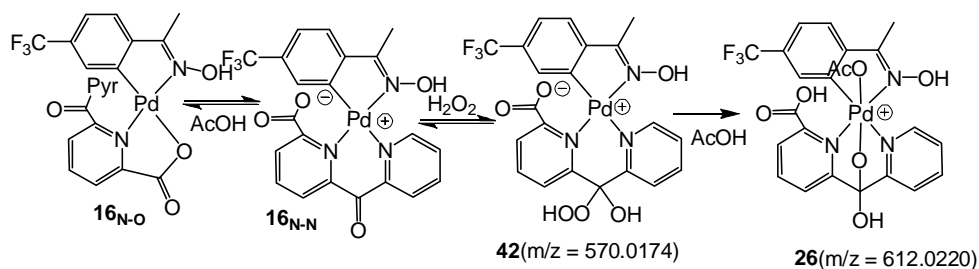
**Figure 5. 7.**  $^1\text{H}$  NMR spectra of acetic acid solution of (a) complex **16** and (b) complex **26** at room temperature. This spectrum also shows some products of decomposition.

The ESI-MS analysis of this reaction solution after combining an acetic acid solution of complex **16** with 20.0 equivalents of  $\text{H}_2\text{O}_2$  displayed major signals at  $m/z = 594.0907$ , which was assigned to complex **26**, and 612.0220 which was assigned to complex **26** with one  $\text{H}_2\text{O}$  molecule. Consequently, the product observed by  $^1\text{H}$  NMR upon combining an acetic acid solution of complex **16** with  $\text{H}_2\text{O}_2$  was assigned as organopalladium(IV) complex **26**. The structure of complex **26** is proposed to be similar to that of complex **25** due to the similar structure of the Pd(II) precursors **15** and **16**.

The mechanism of oxidation of this complex is similar to that of complex **15**, where addition of  $\text{H}_2\text{O}_2$  across the  $\text{C}=\text{O}$  bond of  $\mathbf{16}_{\text{N-N}}$  produces a hydroperoxo adduct **42** (Scheme 5.25). A matching mass envelope was detected by ESI-MS at  $m/z = 570.0174$  (calculated for  $\text{C}_{21}\text{H}_{17}\text{F}_3\text{N}_3\text{O}_6\text{Pd}^{106} = 570.0104$ ). Addition of MeOH across the  $\text{C}=\text{O}$  bond of the ppc ligand has also been observed by ESI-MS at  $m/z =$

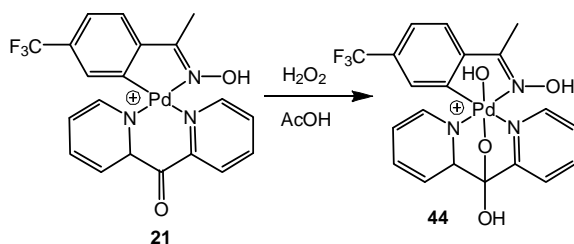
568.0379 (calculated for  $C_{22}H_{19}F_3N_3O_5Pd^{106} = 568.0312$ ), indicating that addition of nucleophiles across the C=O bond of the ppc ligand in this complex is possible. Nucleophilic attack of Pd(II) onto the hydroperoxide moiety results in heterolytic cleavage of the O–O bond and produces an alkoxide ligated Pd(IV) complex **26**, which was detected by both  $^1H$  NMR spectroscopy and ESI–MS.

**Scheme 5. 25**



The reactivity of the ppc ligand-supported organopalladium(II) complex **16** with  $H_2O_2$  in acetic acid was compared to that of dpk ligand-supported organopalladium(II) complex **21** under similar conditions. The reaction of an acetic acid solution of the dpk ligand-supported organopalladium(II) complex **21** with 3.0 equivalents of  $H_2O_2$  generates the corresponding organopalladium(IV) complex **44** in under 10 minutes. The characterization of complex **44** has been reported in chapter 2.<sup>233</sup>

**Scheme 5. 26**



Given that the reaction between the ppc-supported organopalladium(II) complex **16** with 3.0 equivalents of  $H_2O_2$  in acetic acid at room temperature does not

undergo full conversion in over 30 minutes, while the reaction of the dpk-supported Pd(II) complex **21** with 3.0 equivalents of H<sub>2</sub>O<sub>2</sub> under similar conditions undergoes full conversion in under 10 minutes, this indicates that the ppc ligated Pd(II) complexes are less reactive towards oxidation with H<sub>2</sub>O<sub>2</sub> relative to their dpk-ligated Pd(II) counterparts. This might be due to the equilibrium between the N–N and the N–O ppc-ligated complexes, where the overall rate of oxidation depends on the fraction of the reactive N–N isomer in solution as described previously (Scheme 5.25).

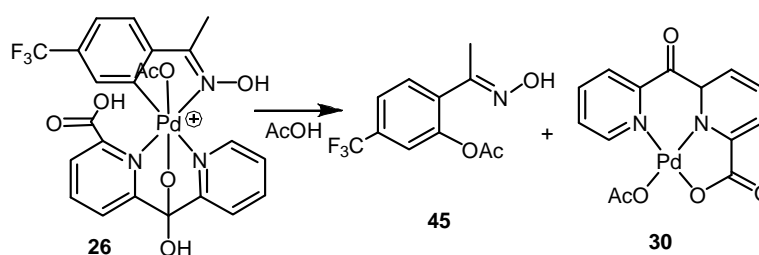
*Study of the electronics effects in the oxidation of complexes **15** and **16** with H<sub>2</sub>O<sub>2</sub> in acetic acid*

The electronics of the reaction between ppc ligated Pd(II) complexes and H<sub>2</sub>O<sub>2</sub> in acetic acid solvent were also investigated. Considering that the reaction between *para*-trifluoromethyl substituted acetophenone oxime-derived complex **16** with 3.0 equivalents of H<sub>2</sub>O<sub>2</sub> in acetic acid at room temperature does not reach full conversion in over 30 minutes, while that of the acetophenone oxime-derived complex **15** with 3.0 equivalents of H<sub>2</sub>O<sub>2</sub> under similar conditions takes ~ 10 minutes for complete conversion of the organopalladium(II) complex to take place, the slower rate of reaction of complex **16** may be a result of the electron-withdrawing trifluoromethyl substituent present in complex **16**. Since the oxidation reaction has been proposed to involve addition of H<sub>2</sub>O<sub>2</sub> across the C=O group of the ppc ligand, followed by nucleophilic attack of the Pd(II) center on the electrophilic HOOR group of the hydroperoxide adduct, the electron-withdrawing substituent –CF<sub>3</sub> decreases the

electron density of the Pd(II) center. This favors addition of H<sub>2</sub>O<sub>2</sub> across the C=O bond of the ppc ligand, while it inhibits the nucleophilic attack of the Pd(II) on the HOOR moiety. Since the trifluoromethyl substituted Pd(II) complex **16** is less reactive than the unsubstituted complex **15**, we propose that the nucleophilic attack of Pd(II) on the HOOR group has been inhibited to a greater extent by the presence of the -CF<sub>3</sub> group.

*Decomposition of complex 26 in acetic acid*

**Scheme 5. 27**



Similar to the decomposition of complex **25** in acetic acid at room temperature, complex **26** gradually decomposes in acetic acid at room temperature to produce the corresponding aryl acetate **45** as the only organic product and the Pd(II) complex **30** quantitatively, accompanied by color change from deep brown to pale yellow. This decomposition reaction was complete in less than 70 minutes. Compound **45** was isolated by removal of solvent and extraction with diethyl ether. The identity of compound **45** was confirmed by independent synthesis via literature procedures of palladium catalyzed acetoxylation of aromatic C-H bond using PhI(OAc)<sub>2</sub> as oxidant,<sup>50</sup> while the synthesis and characterization of complex **30** has been described.

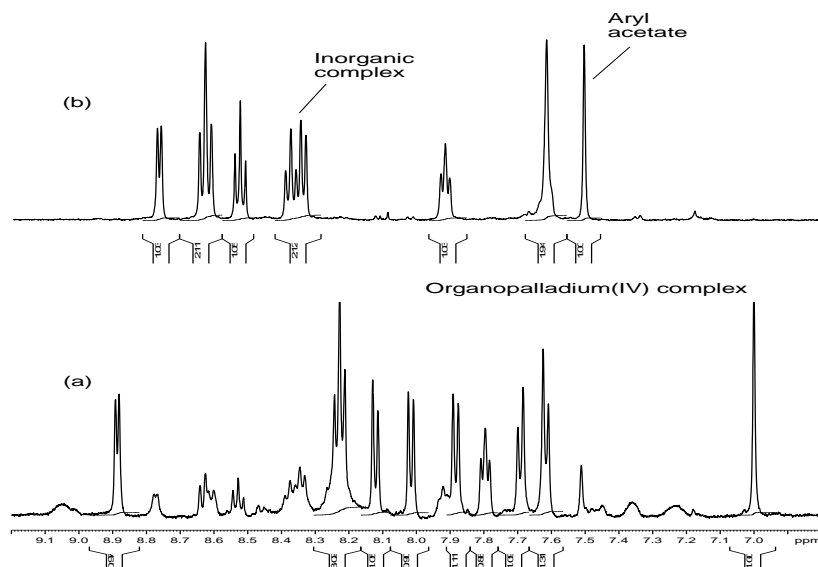
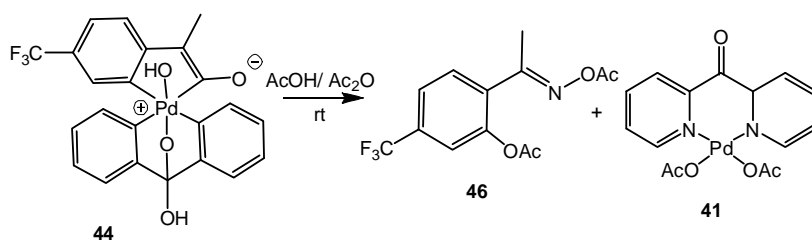


**Figure 5. 8.** Room temperature  $^1\text{H}$  NMR spectra for: (a) Acetic solution of complex **26** (b) acetic acid solution of products of decomposition, including aryl acetate **45** and inorganic product **30**.

**Scheme 5. 28**



The reactivity of the ppc ligand-supported organopalladium(IV) complex **26** towards C–O bond coupling in acetic acid was compared to that of dpk ligand-supported organopalladium(IV) complex **44** under similar conditions. Decomposition of an acetic acid solution of complex **44** at room temperature led to formation of multiple products by  $^1\text{H}$  NMR and ESI–MS, including the corresponding phenol and aryl acetate. However decomposition of an acetic acid solution of complex **44** at room temperature in the presence of 10 % acetic anhydride by volume led to clean formation of the corresponding N-acetylated aryl acetate **46** in > 95 % yield. This

reaction was however very slow, where 65 % conversion was observed in ~ 16 hours. This indicates that the decomposition of the dpk ligand-supported organopalladium(IV) complex **44** in acetic acid is slower than that of ppc ligand supported Pd(IV) complexes.

A similar high reactivity for analogous ppc ligated complex **25** relative to its dpk ligated analogue **32** was observed, and this was proposed to result from the electron-withdrawing carboxylic acid functionality of the ppc ligand, which accelerates dissociation of the pyridine group, and this in-turn accelerates the overall C–O reductive elimination reaction relative to the dpk-ligated complex **44**.

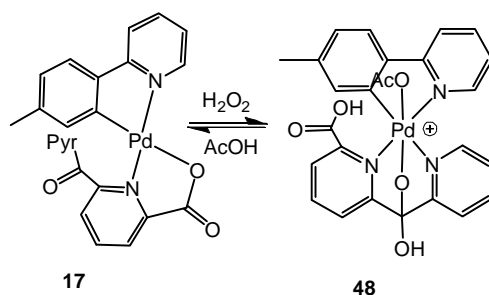
*Study of the electronic effects in the decomposition of complexes **25** and **26** at room temperature, in acetic acid*

The electronic effects of ppc-ligated organopalladium(IV) complexes towards decomposition were also studied. The unsubstituted acetophenone oxime derived Pd(IV) complex **25** was observed to undergo complete decomposition in 2 hours while the –CF<sub>3</sub> substituted acetophenone oxime derived Pd(IV) complex **26** was observed to undergo complete decomposition in under 70 minutes. This indicates that the more electron-deficient complex **26** is more reactive towards C–O reductive elimination than complex **25**, presumably as a result of the electron-withdrawing –CF<sub>3</sub> group on the aryl ring. In the study of C(sp<sup>2</sup>)–O reductive elimination at diaryl dicarboxylato Pd(IV) complexes,<sup>57,58</sup> Sanford and co-workers observed faster C–O reductive elimination reactions when electron-rich benzoate ligands and electron-poor arylpyridine fragments were employed, suggesting that the carboxylate ligands act as

nucleophilic coupling partners while the aryl rings act as electrophilic coupling partners in the C–O reductive elimination reaction. Similarly, the aryl ligand might act as electrophilic coupling partner while the carboxylate ligand might act as nucleophilic coupling partner in our system. As a result, the electron-withdrawing –CF<sub>3</sub> group increases the electrophilicity of the aryl ring, and this in turn increases the reaction rate of complex **26** relative to complex **25**.

### 5.3.3 Reactivity of Complex **17** with H<sub>2</sub>O<sub>2</sub> in Acetic Acid at Room Temperature

**Scheme 5. 29**



The reaction of complex **17** in acetic acid was slow when 3.0 eq of H<sub>2</sub>O<sub>2</sub> was used, where ~ 45 % conversion was observed in ~ 30 minutes, and as a result 20 equivalents of H<sub>2</sub>O<sub>2</sub> were used instead. Addition of 20.0 equivalents of H<sub>2</sub>O<sub>2</sub> to a 0.010 M acetic acid solution of complex **17** resulted in color change from light yellow to orange. <sup>1</sup>H NMR monitoring of this reaction several minutes after addition of H<sub>2</sub>O<sub>2</sub> revealed slow formation of one major product of oxidation whose structure was assigned as **48**. The <sup>1</sup>H NMR resonances belonging to the product of oxidation are narrow and sharp relative to the Pd(II) precursor, indicative of no fluxional behavior. The reaction was very slow however, where 65 % conversion of the organopalladium(II) complex was observed in ~ 8 hours, but the reaction was complete within two days at room temperature.

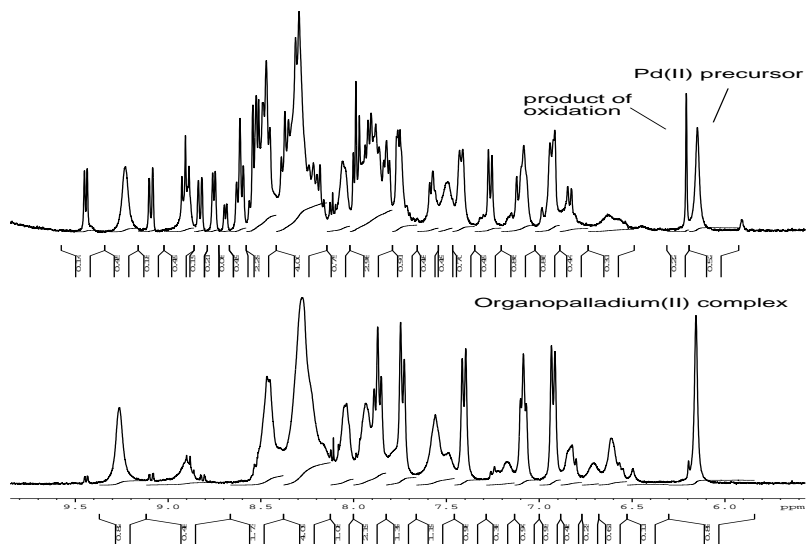


**Figure 5. 9.**  $^1\text{H}$  NMR spectra of acetic acid solution of (a) complex **17** and (b) a mixture of complexes **17** and **48** at room temperature.

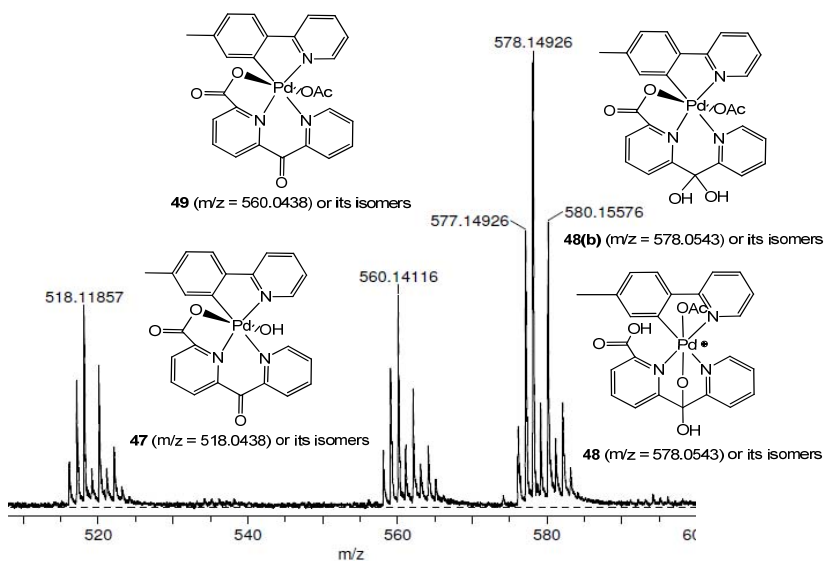
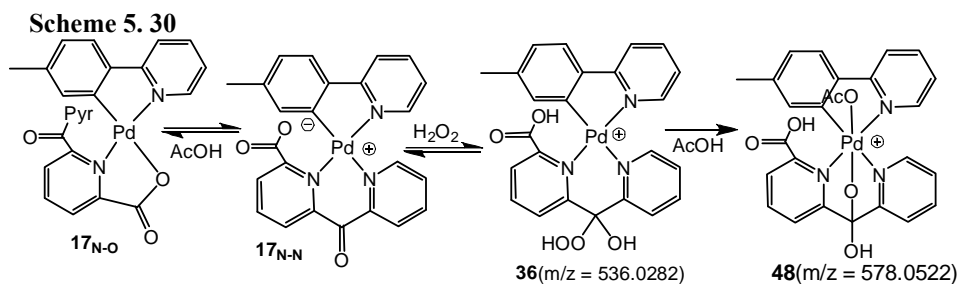


**Figure 5. 10.** ESI-MS spectrum of acetic acid solution of a mixture of complexes **17** and  $\text{H}_2\text{O}_2$  at room temperature.

The ESI-MS analysis of the solution produced upon combining a 0.010 M acetic acid solution of complex **17** with 20.0 equivalents of  $\text{H}_2\text{O}_2$  displayed major peaks at  $m/z = 518.0517$  which corresponds to the Pd(II) precursor plus OH and  $\text{H}_2\text{O}$

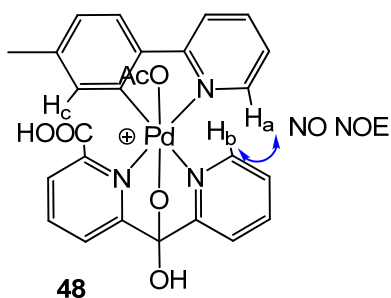
groups assigned to complex **47**,  $m/z = 560.0545$  corresponding to the Pd(II) precursor plus OAc group which was assigned to complex **49**, and  $m/z = 578.0436$  corresponding to the Pd(II) precursor plus OAc and H<sub>2</sub>O groups which was assigned to complex **48** (Fig. 5.10).

Given that one major product of oxidation was observed by <sup>1</sup>H NMR spectroscopy during the oxidation of complex **17** with H<sub>2</sub>O<sub>2</sub> in acetic, while three products were detected by ESI-MS of the same reaction solution, the product observed via <sup>1</sup>H NMR spectroscopy could either be a hydroxo-ligated Pd(IV) complex **47** or an acetato-ligated organopalladium(IV) complex **48** or **49**. Since similar ppc ligand-supported complexes **15** and **16** react with H<sub>2</sub>O<sub>2</sub> in acetic acid solvent to produce acetato-ligated Pd(IV) complexes **25** and **26** respectively as the major products, the major product of oxidation of complex **17** with H<sub>2</sub>O<sub>2</sub> in acetic acid, as observed via <sup>1</sup>H NMR spectroscopy is assigned to the acetato-ligated Pd(IV) complex **48** or **49**. In addition, formation of the hydroxo-ligated Pd(IV) complex **47** requires the presence of water in the reaction solution. However the concentration of water in this system is not sufficient to produce complex **47** as the major product. In order to distinguish between complexes **48** and **49**, DFT calculations were undertaken, where complexes with the structure of **48** were found to be lower in energy than complexes with the structure of **49** (this analysis was described previously). As a result, the product of oxidation of complex **17** with H<sub>2</sub>O<sub>2</sub> in acetic acid was assigned to **48**.



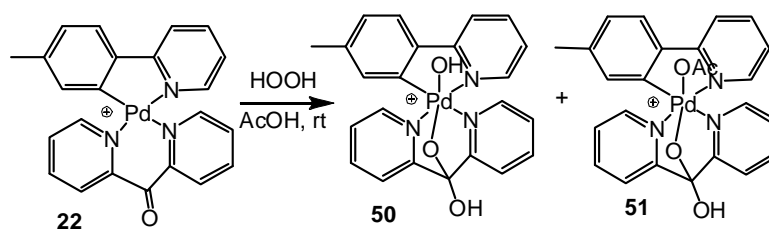
Similar to the mechanism proposed for the oxidation of acetophenone oxime derived Pd(IV) complexes **15** and **16** with H<sub>2</sub>O<sub>2</sub>, the oxidation of complex **17** with H<sub>2</sub>O<sub>2</sub> is proposed to involve addition of H<sub>2</sub>O<sub>2</sub> across the C=O group of the ppc ligand of the N<sub>2</sub>N ligated isomer **17**<sub>N-N</sub> to produce the hydroperoxide complex **36** (Scheme 5.30). A complex with a matching mass envelope was detected by ESI-MS at m/z = 536.0282 (calculated for C<sub>24</sub>H<sub>20</sub>N<sub>3</sub>O<sub>5</sub>Pd<sup>106</sup> = 536.0438), while addition of H<sub>2</sub>O across the C=O bond of the ppc ligand of complex **17** has also been observed by ESI-MS at m/z = 520.0528 (calculated for C<sub>24</sub>H<sub>20</sub>N<sub>3</sub>O<sub>4</sub>Pd<sup>106</sup> = 520.0489), indicating that addition of nucleophiles across the C=O bond of the ppc ligand is possible. The hydroperoxide adduct **36** could undergo nucleophilic attack by Pd(II), leading to heterolytic cleavage of the O–O bond, thereby giving the acetato-ligated Pd(IV) complex **48**, where a matching mass envelope was detected via ESI-MS at m/z = 578.0522 (calculated for C<sub>26</sub>H<sub>22</sub>N<sub>3</sub>O<sub>6</sub>Pd<sup>106</sup> = 578.0538). Nucleophilic attack of Pd(II) on the peroxy adduct in the presence of water might also produce complex **47**, which was detected by ESI-MS at m/z = 518.0438. Given that ~ 20.0 equivalents of 30% aqueous H<sub>2</sub>O<sub>2</sub> were used for this oxidation reaction, complex **47** might be produced from water added with the oxidant.

1D difference NOE experiments were performed to determine the structure of this complex in solution.



1D difference NOE experiment of complex **48** was performed in deuterated acetic acid at room temperature. No NOE was observed between any hydrogen atoms in the molecule. Irradiation of the singlet  $H_c$  at 6.21 ppm did not result in enhancement of any signals while irradiation of doublets  $H_b$  and  $H_a$  at 9.09 ppm and 9.45 ppm did not show enhancement of any signals either.

**Scheme 5. 31**

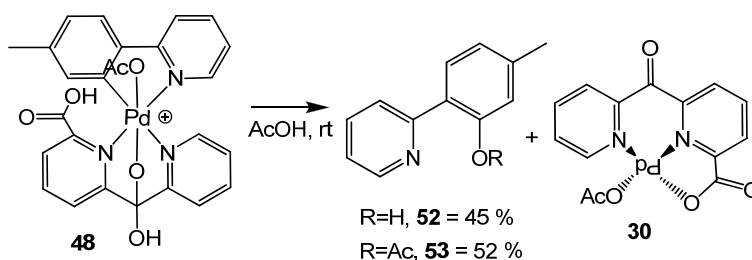


The reaction of the ppc ligand-supported, tolylpyridine-derived organopalladium(II) complex **17** with  $H_2O_2$  in acetic acid at room temperature was compared to the reaction of dpk ligand-supported organopalladium(II) complex **22** with  $H_2O_2$  under similar conditions. When a 0.010 M acetic acid solution of complex **22** was combined with 2.0 equivalents of  $H_2O_2$ , both hydroxo- and acetato-ligated organopalladium(IV) complexes **51** and **51** were produced, but the reaction was slow where  $\sim 60\%$  conversion was observed in  $\sim 30$  minutes. Ultimately, the corresponding phenol and aryl acetate products were produced in a 25 % and 71 % yields respectively.

Given that the reaction between 0.010 M acetic acid solution of the ppc ligand-derived complex **17** with 20.0 equivalents of H<sub>2</sub>O<sub>2</sub> at room temperature was very slow, where ~ 65 % conversion was observed in ~ 8 hours, while the reaction between a 0.010 M acetic acid solution of the dpk ligand-supported complex **22** with 3.0 equivalents of H<sub>2</sub>O<sub>2</sub> was faster, where 60 % conversion of the organopalladium(II) complex was observed in ~ 30 minutes, this indicates that dpk-ligated Pd(II) complexes undergo oxidation with H<sub>2</sub>O<sub>2</sub> at a faster rate relative to ppc-ligated Pd(II) complexes. The low reactivity of the ppc-ligated Pd(II) complexes has been proposed to result from the equilibrium between the N–N and the N–O ppc-ligated palladacycles, where the overall oxidation rate is dependent on the fraction of the N–N coordination isomer in solution; no such equilibrium exists in the dpk-ligated complexes leading to faster oxidation reaction as described previously.

*Decomposition of a mixture of complex 48 in acetic acid*

**Scheme 5. 32**



Complex **48** decomposed in acetic acid at room temperature to generate the corresponding phenol **52** in 45 % yield and aryl acetate **53** in 52 % yield. However due to the slow oxidation reaction, the kinetics of the C–O reductive elimination reaction could not be studied. This is due to the slow oxidation reaction, where the organopalladium(IV) complexes were produced in the presence of the products of C–

O bond coupling, and the Pd(II) precursor. Complete conversion of **17** to the corresponding aryl acetate and phenol products was observed after 2 days. At the end of the reaction, the color of the solution had changed from orange to colorless, after addition of pyridine to free coordinated products. The organic products **52** and **53** were isolated by removal of solvent under vacuum and extraction with diethyl ether. The identity of the phenol **52** was confirmed by comparison of the  $^1\text{H}$  NMR spectrum to literature publication,<sup>83</sup> while the identity of aryl acetate **53** was confirmed by independent synthesis.

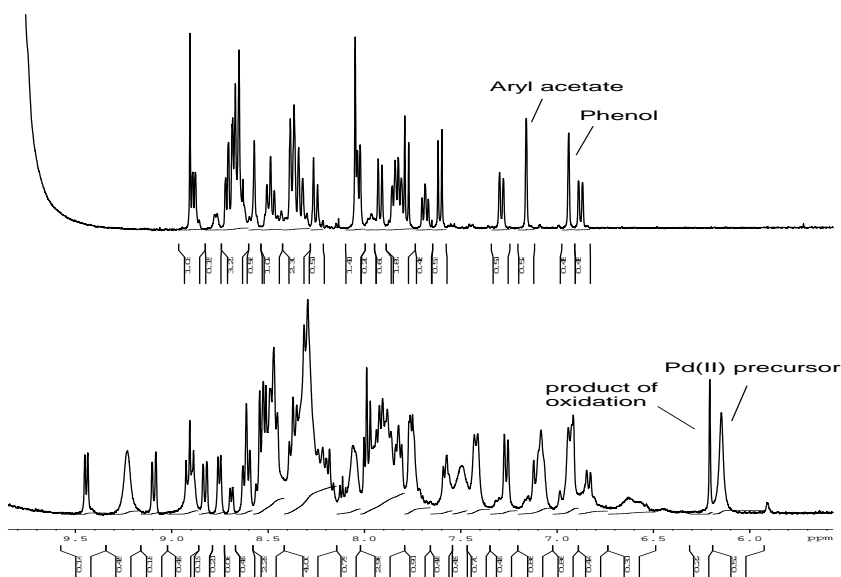
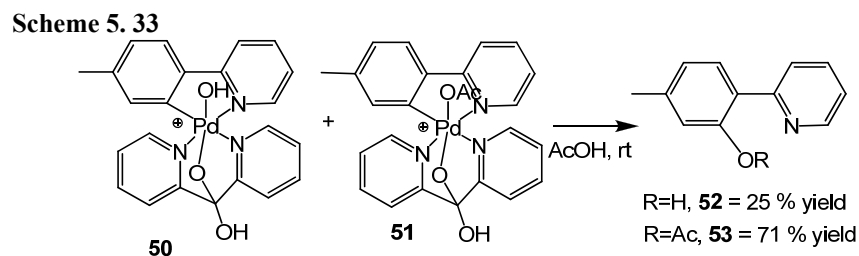


**Figure 5. 11.** Room temperature  $^1\text{H}$  NMR spectra for (a) Acetic solution of organopalladium(IV) complex **48** in the presence of organopalladium(II) precursor **17**; (b) acetic acid solution of the products of decomposition, including the aryl acetate **53**, phenol **52**, and inorganic product **30**, in the presence of pyridine- $d_5$  added to free coordination products.

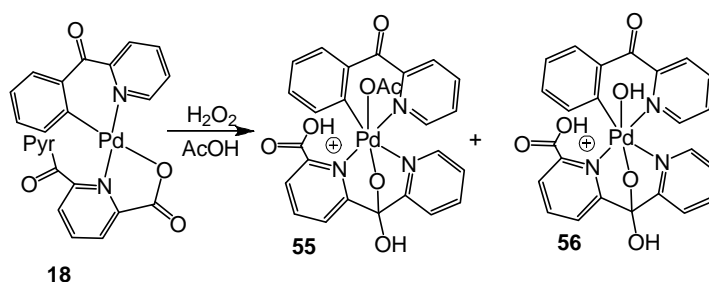


The C–O reductive elimination reactivity of organopalladium(IV) complexes supported by the ppc ligand were compared to the reactivity of the dpk ligand supported counterparts under similar conditions. The reaction between the organopalladium(II) complex **22** with  $\text{H}_2\text{O}_2$  in acetic acid at room temperature generates the hydroxo- and the acetato-ligated organopalladium(IV) complexes **50** and **51**, which were both observed by  $^1\text{H}$  NMR and detected by ESI–MS. The oxidation reaction is slow, and thus the Pd(IV) complexes **50** and **51**, and the organopalladium(II) complex **22** were observed simultaneously in comparable amounts. As a result, the Pd(IV) complexes could not be characterized cleanly, and the reductive elimination kinetics could not be studied. However the decomposition of complexes **50** and **51** in acetic acid solvent produced the corresponding products of C–O reductive elimination, **52** and **53** in 25 % and 71 % yield respectively after two days.

Consequently, the C–O reductive elimination reactivity from ppc ligand-supported organopalladium(IV) complexes and dpk ligand-supported organopalladium(IV) complexes could not be compared because these complexes are not produced cleanly.

### 5.3.4 Reactivity of Complex **18** with H<sub>2</sub>O<sub>2</sub> in Acetic Acid at Room Temperature

Scheme 5. 34



In the reaction between an acetic acid solution of complex **18** and 4.0 eq of H<sub>2</sub>O<sub>2</sub>, 28 % conversion of complex **18** was observed in 10 minutes. In order to increase the reaction rate, 27 equivalents of H<sub>2</sub>O<sub>2</sub> were used. The combination of a 0.010 M acetic acid solution of complex **18** with 27.0 equivalents of H<sub>2</sub>O<sub>2</sub> led to color change of the solution from light yellow to deep yellow, accompanied by gradual formation of a brown precipitate. When this reaction was monitored by <sup>1</sup>H NMR, two products of oxidation were observed upon addition of H<sub>2</sub>O<sub>2</sub> in ~ 70 % and 20 % yields relative to an internal standard. The <sup>1</sup>H NMR resonances belonging to these products are narrow and sharp relative to the Pd(II) precursor. The aromatic resonances belonging to the major product of oxidation are shifted downfield relative to the Pd(II) precursor, indicating a more deshielded environment. However the resonances belonging to the minor product of oxidation are not significantly shifted downfield relative to the Pd(II) precursor, indicative of less deshielding. In order to determine the identity of these products of oxidation, ESI-MS analysis was performed.

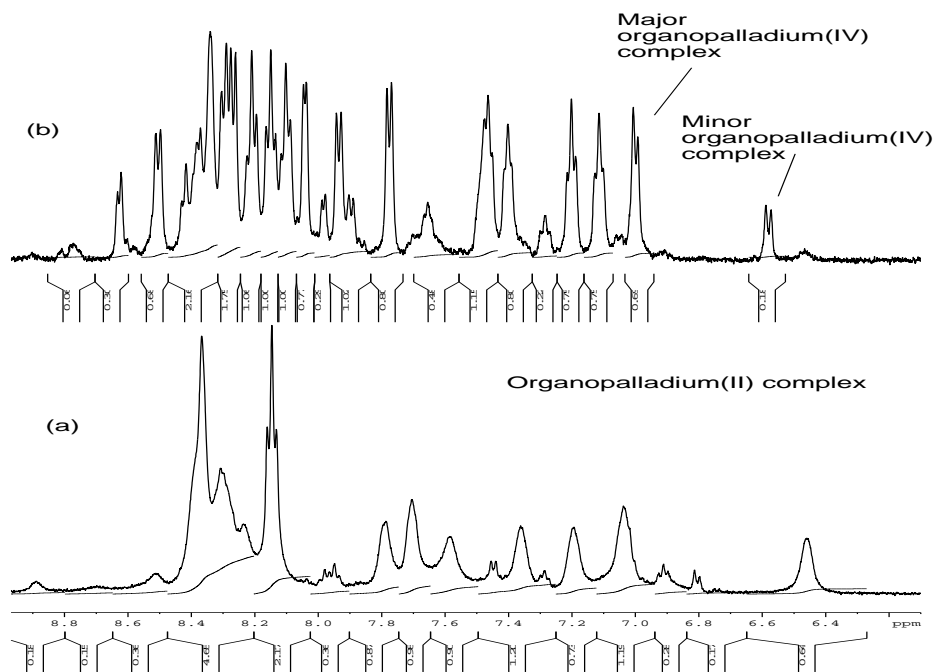


**Figure 5. 12.** Room temperature  $^1\text{H}$  NMR spectra of acetic acid solution of (a) complex **18** and (b) a mixture of complexes **54** and **55** at room temperature.

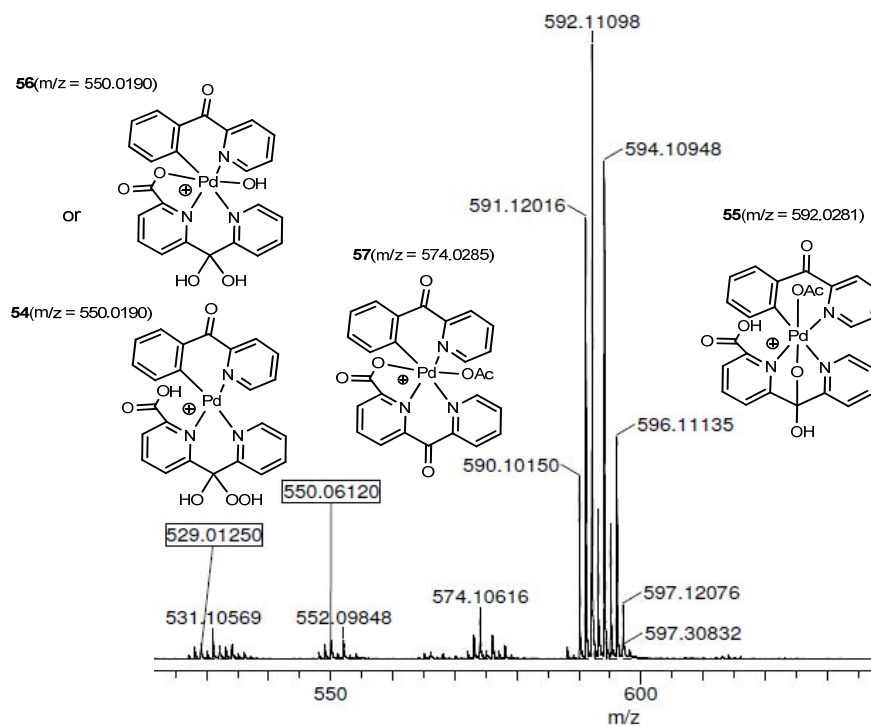
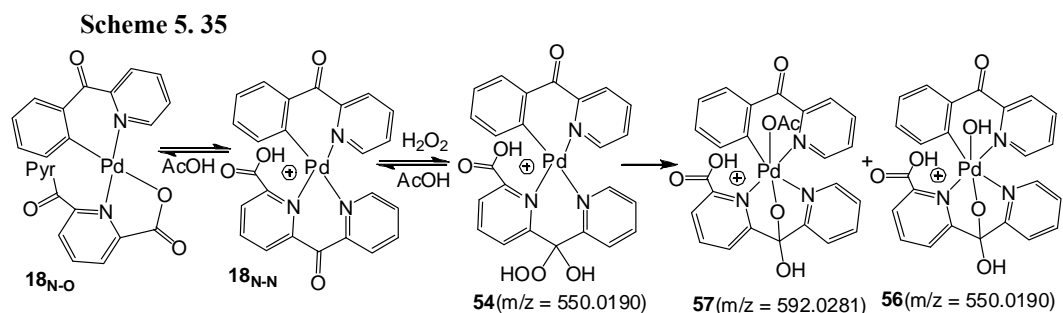


**Figure 5. 13.** ESI-MS analysis of an acetic acid solution of complex **18** upon addition of  $\text{H}_2\text{O}_2$ .

ESI-MS analysis of the reaction solution produced upon addition of H<sub>2</sub>O<sub>2</sub> to an acetic acid solution of complex **18** displayed a major mass envelope at  $m/z = 592.0281$ , which corresponds to the Pd(II) precursor plus additional OAc<sup>-</sup> and H<sub>2</sub>O molecules assigned to complex **55**, and minor mass envelopes at  $m/z = 550.0190$ , which corresponds to the mass of the Pd(II) precursor **18** plus additional OH<sup>-</sup> and H<sub>2</sub>O groups assigned to complex **56**, and  $m/z = 574.0285$  which corresponds to the Pd(II) precursor **18** plus additional OAc<sup>-</sup>, assigned to complex **57** (Fig. 5.13). The ESI-MS analysis indicates that both hydroxo-ligated Pd(IV) complex **56** and acetato-ligated Pd(IV) complexes **55** and **57** are produced when an acetic acid solution of complex **18** is combined with H<sub>2</sub>O<sub>2</sub> in acetic acid at room temperature. As a result, the two products of oxidation detected via <sup>1</sup>H NMR are assigned to organopalladium(IV) complexes **56**, **55** and/ or **57**. This assignment is supported by the reactivity of these complexes, where decomposition of these products of oxidation in acetic acid at room temperature produces the corresponding phenol **60** and aryl acetate **61**, indicating the presence of hydrocarbyl and -OR ligands on the palladium coordination sphere, since C-O reductive elimination reactions are proposed to take place via a 3-center, 4-electron transition state (the decomposition reaction will be discussed in greater details in the following sections). The major oxidation product was assigned to the acetato-ligated complex **55** or **57** based on the ESI-MS, where the major mass envelope detected at  $m/z = 592.0281$  corresponds to the acetoxy-ligated complex (Fig. 5.13). In addition, formation of the hydroxo-ligated Pd(IV) complex **56** requires the presence of water in the reaction solution. However the concentration of water in this system is not sufficient to produce complex **56** as the

major product. Still, similar ppc-ligated Pd(II) complexes **15-17** react with H<sub>2</sub>O<sub>2</sub> in acetic acid to produce the acetato-ligated Pd(IV) complexes as major products of oxidation. The structure of the acetato-ligated Pd(IV) complex was assigned to **55** based on DFT calculations on similar ppc-ligated Pd(IV) complexes, where complexes with the structure of **55** were found to be lower in energy than complexes with the structure of **57**. (this analysis was described previously).

Therefore in summary, the oxidation of complex **18** with H<sub>2</sub>O<sub>2</sub> in acetic acid at room temperature produces the acetato-ligated Pd(IV) complex **55** as the major product and the hydroxo-ligated Pd(IV) complex **56** as the minor product.



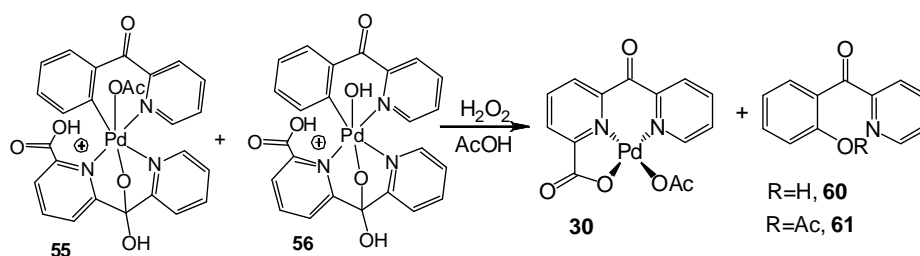
Similar to the oxidation of complex **15**, **16**, and **17** discussed previously, the oxidation of complex **18** with H<sub>2</sub>O<sub>2</sub> could proceed via addition of H<sub>2</sub>O<sub>2</sub> across the C=O bond of the ppc ligand of the N,N coordinated complex to produce the hydroperoxo adduct **54**; this intermediate was not observed by <sup>1</sup>H NMR, but a matching mass envelope was detected by ESI-MS at m/z = 550.0190 (calculated for C<sub>24</sub>H<sub>18</sub>N<sub>3</sub>O<sub>6</sub>Pd<sup>106</sup> = 550.0230). In addition, the C=O group of the ppc ligand of complex **18** has been observed to undergo nucleophilic attack by H<sub>2</sub>O to generate the corresponding hydrated complex observed by ESI-MS at m/z = 534.0340 (calculated for C<sub>24</sub>H<sub>18</sub>N<sub>3</sub>O<sub>5</sub>Pd<sup>106</sup> = 534.0281). Nucleophilic attack of the hydroperoxide moiety by the Pd(II) center leads to heterolytic cleavage of the O-O bond to produce the



supported complex **18** undergoes oxidation at a slower rate than the dpk ligand-supported complex **23**. As has been discussed previously, the slower reactivity of the ppc-ligated complexes might be due to the equilibrium between the reactive N–N vs. the less reactive N–O ligated isomers, while no such equilibrium exists for the dpk-ligated complexes.

*Decomposition of the organopalladium(IV) complexes 55 and 56*

**Scheme 5. 37**



When an acetic acid solution of complexes **55** and **56** was left at room temperature, formation of the corresponding phenol **60** and aryl acetate **61** was observed in 56 % and 41 % respectively within two days (Scheme 5.37). The generation of phenol and aryl acetate products from the decomposition of complexes **55** and **56** supports our assignment of the two intermediates as hydroxo- and acetato-ligated organopalladium(IV) complexes, given that C–O reductive elimination from Pd(IV) complexes has been proposed to take place via a 3-center, 4-electron transition state,<sup>45</sup> indicating that the hydroxo, acetato, and hydrocarbyl groups ought to be present on the palladium coordination sphere for this reaction to take place.

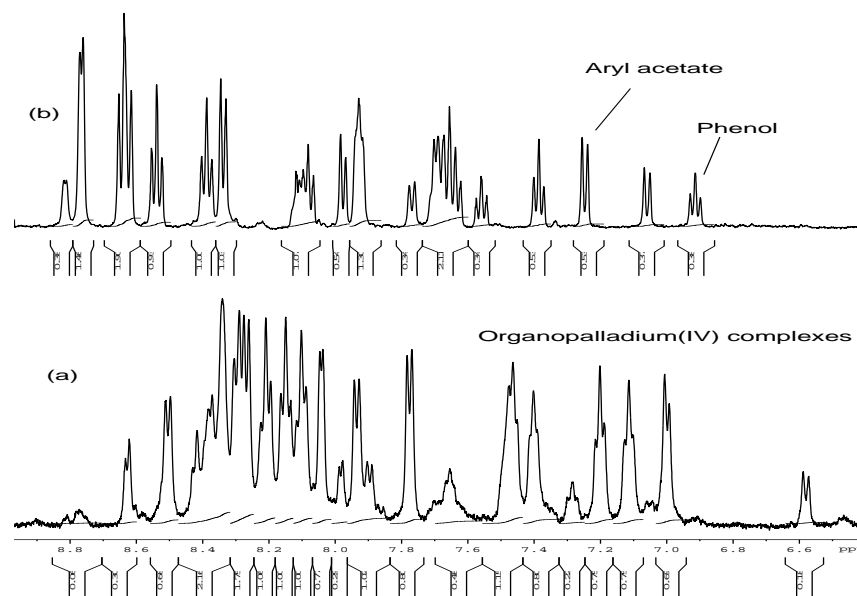
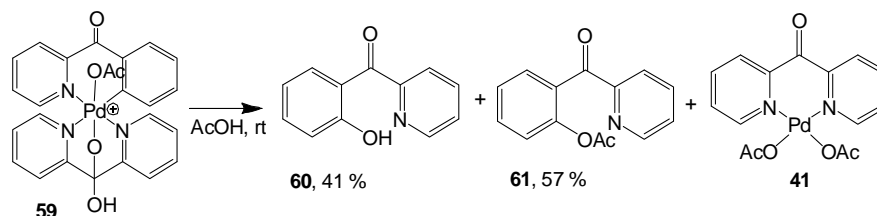


**Figure 5. 14.** Room temperature  $^1\text{H}$  NMR spectra for the, (a) Acetic solution of complex **55** and **56**; (b) acetic acid solution of products of decomposition, including the aryl acetate **61**, phenol **60**, and inorganic product **30**.

**Scheme 5. 38**



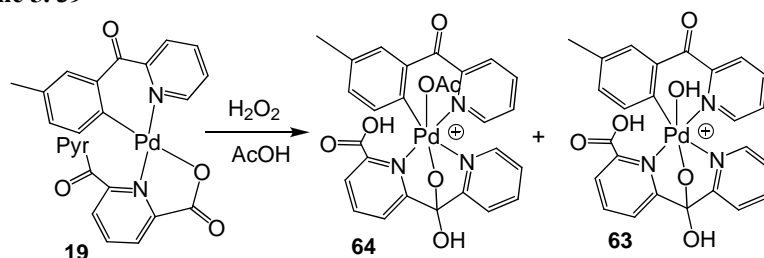
The decomposition of ppc ligand-supported organopalladium(IV) complexes **56** and **58** was compared to that of dpk ligand-supported Pd(IV) complexes **59**. When an acetic acid solution of complex **81** was left at room temperature, products of C–O bond coupling **60** and **61** were observed in 41 % and 57 % yield respectively, together with complex **41** as the only inorganic product after two days.

The reactivity of ppc ligand-supported organopalladium(IV) complexes towards C–O bond coupling could be compared to that of the dpk ligand-supported Pd(IV) complex only qualitatively. This is because a heterogeneous reaction mixture

was produced during the reaction of the Pd(II) complex **18** with H<sub>2</sub>O<sub>2</sub> in acetic acid, and thus the decomposition of this heterogeneous mixture could not be monitored, although the corresponding C–O bond coupling products were ultimately produced in a total quantitative yield after two days. Since oxidation of **18** is slower than that of **23**, we presume that reductive elimination from the ppc ligated complexes **55** and **56** takes place at a faster rate than from the dpk ligated Pd(IV) complex **59**.

### 5.3.5 Reactivity of Complex **19** with H<sub>2</sub>O<sub>2</sub> in Acetic Acid at Room Temperature

Scheme 5. 39



The reaction between complex **19** and H<sub>2</sub>O<sub>2</sub> in acetic acid was similar to that of complex **18** under similar conditions. Upon addition of 20.0 equivalents of H<sub>2</sub>O<sub>2</sub> into a 0.010 M acetic acid solution of complex **19**, the light yellow solution changed color to deeper yellow, followed by gradual formation of a brown precipitate. When this reaction was monitored by <sup>1</sup>H NMR, two products of oxidation were observed in 55 % to 20 % yields upon combination of the acetic acid solution of complex **19** with H<sub>2</sub>O<sub>2</sub>. The <sup>1</sup>H NMR resonances belonging to these products are narrow and sharp relative to the Pd(II) precursor **19**. The resonances belonging to the major product of oxidation are collectively shifted downfield relative to the Pd(II) precursor, indicating a more deshielded environment. However the low-field shift of the resonances belonging to the minor product of oxidation relative to the Pd(II) precursor is not significant, indicative of less deshielding.

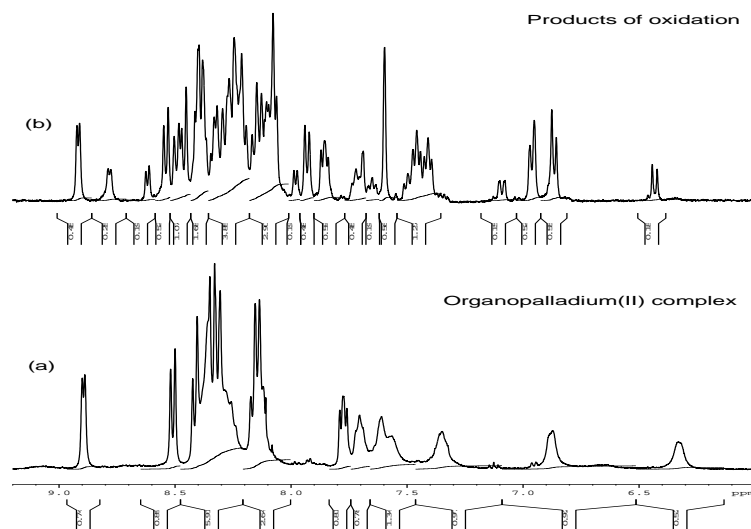


**Figure 5.15.**  $^1\text{H}$  NMR spectra of acetic acid solution of (a) complex **19** and (b) a mixture of complexes **62** and **63** at room temperature.

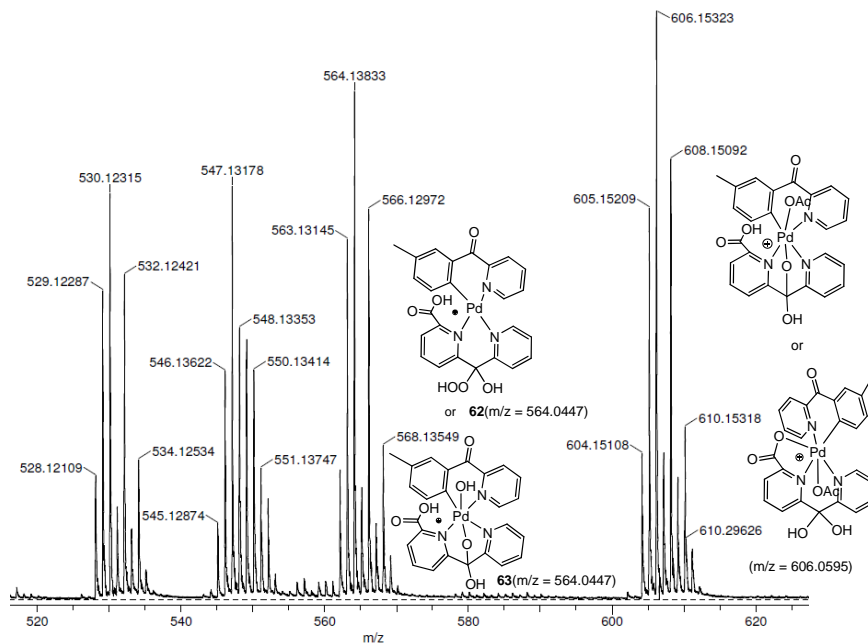
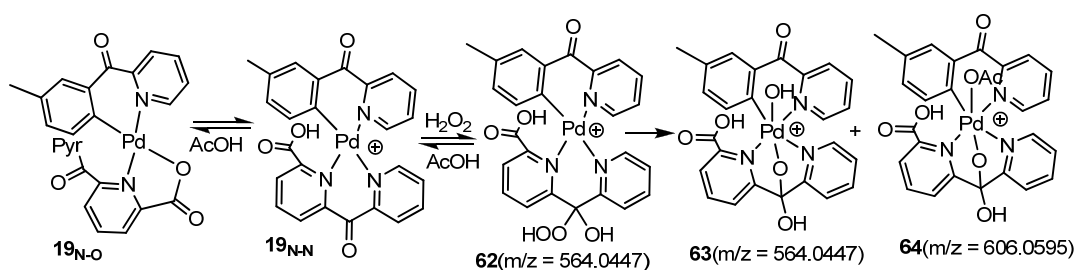


**Figure 5.16.** ESI-MS analysis of an acetic acid solution of complex **19** upon addition of  $\text{H}_2\text{O}_2$ .

The ESI-MS analysis of the reaction solution after combining an acetic acid solution of complex **19** with 20.0 equivalents of  $\text{H}_2\text{O}_2$  displayed major peaks at  $m/z = 564.0447$  corresponding to the mass of the Pd(II) precursor plus OH and  $\text{H}_2\text{O}$  groups, which was assigned to complex **63**, and  $m/z = 606.0595$  corresponding to the Pd(II) precursor with an additional OAc and  $\text{H}_2\text{O}$  groups, which was assigned to complex

**64.** Given that complex **18**, which is a near identical analogue of **19** reacts with  $\text{H}_2\text{O}_2$  in acetic to produce both hydroxo- and acetato-ligated Pd(IV) complexes, where the acetato-ligated complex was identified as the major product, we propose that the two products generated in this reaction are the hydroxo- and acetato-ligated Pd(IV) complexes, as has also been revealed by ESI–MS. Similarly, we propose that the major product is the acetato-ligated Pd(IV) complex **64** while the minor product is the hydroxo-ligated complex **63**. The structures of these complexes was proposed based on DFT calculations on similar ppc-ligated Pd(IV) complexes, described previously.

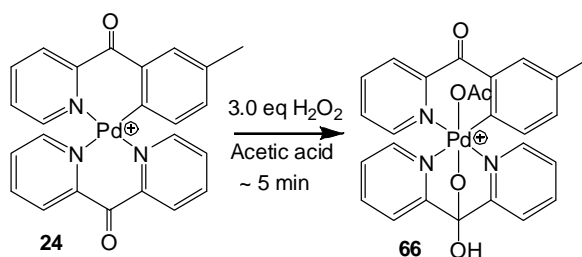
**Scheme 5. 40**



The mechanism of oxidation of complex **19** is proposed to be similar to that of complex **18**, where addition of  $\text{H}_2\text{O}_2$  across the C=O bond of the ppc ligand of the N,N ligated complex **19<sub>N-N</sub>** produces the hydroperoxo adduct **62**. A complex with a matching mass envelope at  $m/z = 564.0447$  was observed (calculated for  $\text{C}_{25}\text{H}_{20}\text{N}_3\text{O}_6\text{Pd}^{106} = 564.0387$ ). The addition of water molecule across the C=O bond of the ppc ligand in complex **19** has also been observed via ESI–MS, at  $m/z = 548.0549$  (calculated for  $\text{C}_{25}\text{H}_{20}\text{N}_3\text{O}_5\text{Pd}^{106} = 548.0432$ ). Nucleophilic attack of Pd(II) on the hydroperoxide moiety leads to heterolytic cleavage of the O–O bond, resulting in formation of the acetato ligated Pd(IV) complex **64**, where a matching mass envelope was detected by ESI–MS at  $m/z = 606.0595$  (calculated for

$C_{27}H_{22}N_3O_7Pd^{106} = 606.0493$ ). Nucleophilic attack of Pd(II) on the hydroperoxide moiety of complex **62** in the presence of water produces the hydroxo-ligated Pd(IV) complex **63**, where complex with a matching mass envelope at  $m/z = 564.0447$  was detected (calculated for  $C_{25}H_{20}N_3O_6Pd^{106} = 564.0387$ ). Thus, formation of complex **63** requires the presence of water in the solution. In this reaction, water came from  $H_2O_2$ , where 20.0 equivalents of 30% aqueous  $H_2O_2$  was used as oxidant.

**Scheme 5. 41**



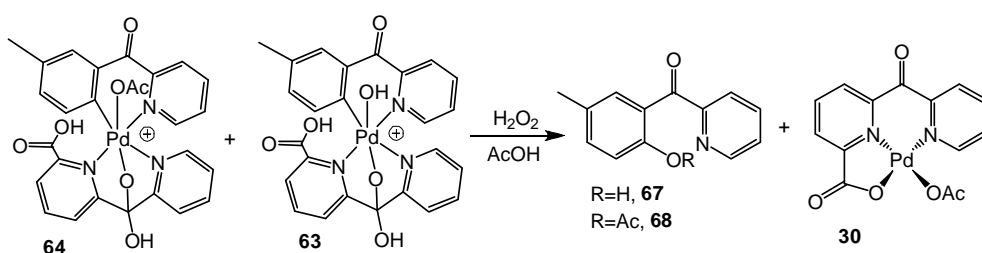
The reactivity of the ppc ligand-derived organopalladium(II) complex **19** was compared to that of dpk ligand-supported organopalladium(II) complex **24** under similar conditions. The combination of a 0.010 M acetic acid solution of complex **24** with 3.0 equivalents of  $H_2O_2$  produced the corresponding organopalladium(IV) complex **66** within 5 minutes at room temperature.

Given that the ppc ligand-supported complex **19** undergoes a very slow reaction with 3.0 equivalents of  $H_2O_2$ , and requires 20.0 equivalents of  $H_2O_2$  to generate the corresponding organopalladium(IV) complexes fast enough, while the dpk ligand-supported complex **24** reacts with 3.0 equivalents of  $H_2O_2$  in acetic acid solvent at room temperature to produce the corresponding organopalladium(IV) complex **66** within 5 minutes, this indicates that organopalladium(II) complexes supported by the dpk ligand react with  $H_2O_2$  faster than Pd(II) complexes supported by the ppc ligand. As discussed previously, the slower reactivity of ppc-ligated

complexes relative to dpk-ligated complexes may be due to the equilibrium between the N–N and the N–O ligated complexes, where the reaction rate is dependent on the fraction of the more reactive N–N ligated complex in the solution; this equilibrium is absent in the solutions of dpk-ligated complexes.

*Decomposition of complexes 157 and 158 in acetic acid*

**Scheme 5. 42**



After several hours, <sup>1</sup>H NMR analysis of the reaction solution containing organopalladium(IV) complexes **63** and **64** revealed the presence of the corresponding phenol **67** and aryl acetate **68** in 71 % and 20 % yields respectively relative to an internal standard (Fig. 5.17)). The organic products were isolated by removal of the solvent, and extraction of the residue with diethyl ether. The decomposition of the products of oxidation upon combining an acetic acid solution of complex **19** with H<sub>2</sub>O<sub>2</sub> supports our assignment of these complexes as hydroxo- and acetato-ligated organopalladium(IV) complexes **63** and **64**.

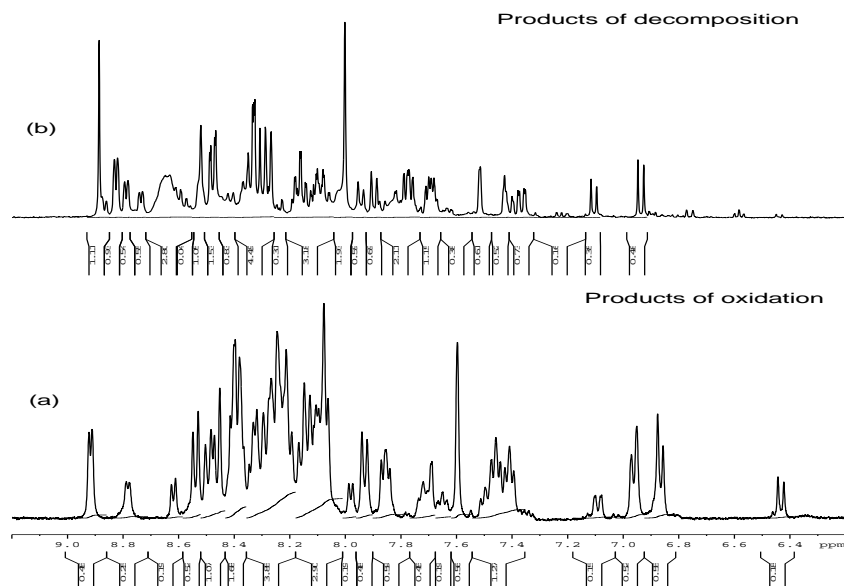
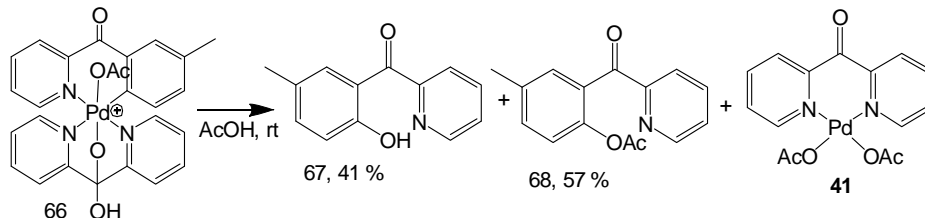


**Figure 5. 17.** Room temperature  $^1\text{H}$  NMR spectra for (a) Acetic solution of complex **63** and **64**; (b) acetic acid solution of products of decomposition, including the aryl acetate **68**, phenol **67**, after addition of pyridine- $\text{d}_5$  to the reaction solution.

**Scheme 5. 43**



The decomposition of the ppc ligand-derived organopalladium(IV) complexes **63** and **64** at room temperature in acetic acid was compared to that of dpk ligand-derived organopalladium(IV) complex **66** under similar conditions. Complex **66** was observed to undergo decomposition to produce the corresponding phenolic and aryl acetate products in 39 % and 57 % respectively after 2 days. Given that a heterogenous reaction mixture is produced during the oxidation of complex **19** to produce the ppc-ligated Pd(IV) complexes **63** and **64**, only qualitative comparison

could be performed, where the decomposition of complex **66** was qualitatively slower than that for complexes **63** and **64** in acetic acid at room temperature.

#### 5.4 Summary and Conclusions

In summary, Pd(II) complexes supported by the ppc ligand were prepared. These complexes were found to exist in a slow equilibrium between the N,O and the N,N coordination modes of the ppc ligand, and this equilibrium was found to be more significant in protic solvents than aprotic solvents. This may be due to the fact that protic solvents stabilize the charged N,N chelated zwitterion better than aprotic solvents.

The reaction between organopalladium(II) complexes **15-19** supported by the ppc ligand with H<sub>2</sub>O<sub>2</sub> in acetic acid solvent was investigated. These reactions were observed to produce the corresponding acetato- and sometimes hydroxo-ligated monohydrocarbyl Pd(IV) complexes. The structures of these Pd(IV) complexes were proposed based on ESI-MS, NMR experiments, DFT calculations, and the reactivity of these complexes. In particular, the observation of intermediates by both <sup>1</sup>H NMR spectroscopy and ESI-MS, and the reactivity of these intermediates to generate the corresponding C-O bond-coupling products enabled the assignment of the intermediates as acetato- and/ or hydroxo-ligated Pd(IV) complexes. The chelation mode of the ppc ligand in these complexes was computed using the DFT, where a facially chelating mode involving the hydrated, deprotonated ppc adduct with a N,O,N binding mode was the lowest energy conformation found, after optimizing for various possible geometries.

These oxidation reactions were proposed to take place via preliminary addition of  $\text{H}_2\text{O}_2$  onto the  $\text{C}=\text{O}$  group of the N,N-ligated ppc ligand, where mass envelopes matching the hydroperoxide adducts were detected by ESI-MS. Nucleophilic attack of Pd(II) onto the hydroperoxide moiety results in heterolytic cleavage of the  $\text{O}-\text{O}$  bond, leading to the formation of acetato-ligated organopalladium(IV) complexes in acetic acid solvent, and hydroxo-ligated Pd(IV) complexes in the presence of water; matching mass envelopes were detected by ESI-MS. The acetato-ligated Pd(IV) complexes were usually produced as major complexes.

In the study of electronic effects in the oxidation reactions, complexes with electron-withdrawing substituents were found to be less reactive towards oxidation with  $\text{H}_2\text{O}_2$  than those with electron rich substituents. Given that two overall steps are involved in the oxidation reaction, including addition of  $\text{H}_2\text{O}_2$  across the  $\text{C}=\text{O}$  bond of the ligand, and nucleophilic attack of Pd(II) on to the HOOR moiety of the hydroperoxide adducts, the overall reactivity depends on which of these steps is affected to a greater extent. In this case, the more electron-rich palladacycles were found to be more reactive than the electron-poor palladacycles towards oxidation with  $\text{H}_2\text{O}_2$ , indicating that the energy associated with the nucleophilic attack of Pd(II) on the HOOR moiety of the hydroperoxide adducts is lowered to a greater extent.

The reactivity of the ppc ligand-supported Pd(II) complexes towards oxidation with  $\text{H}_2\text{O}_2$  was also compared to that of the dpk ligand-supported counterparts, where the ppc supported complexes were found to be less reactive. This was proposed to result from the slow equilibrium between the N,O and the N,N ppc-supported

chelates. Given that the N,N chelated complexes are more reactive towards H<sub>2</sub>O<sub>2</sub> addition across the C=O bond of the ppc ligand than the N,O chelated complexes, the relative fraction of the N,N ligated complex determines the rate of the oxidation reaction. Since no such equilibrium exists in the dpk-ligated Pd(II) complex, these complexes react faster than ppc ligated complexes.

Decomposition of the ppc-supported organopalladium(IV) complexes was also studied, where C–O reductive elimination in acetic acid produced the corresponding aryl acetate, and sometimes phenolic products in a total quantitative yield, together with complex **30** as the only inorganic product of decomposition. In these studies, complexes with electron-withdrawing substituents on the aromatic rings were found to undergo decomposition at a faster rate compared to those containing electron-donating substituents on the aromatic rings. For example the ppc-supported complex **25** underwent complete decomposition to produce the corresponding aryl acetate product in 2 hours while complex **26** which contains a trifluoromethyl substituted aromatic ligand underwent decomposition in 70 minutes. Given that aryl ligands act as electrophilic coupling partners while carboxylate ligands act as nucleophilic coupling partners in the C–O reductive elimination reactions,<sup>58</sup> the electron-withdrawing groups on the aromatic rings were proposed to increase the electrophilicity of the aryl ligands, which in turn increases the rate of the C–O coupling reaction.

Decomposition of the ppc ligand supported organopalladium(IV) complexes was compared to that of their dpk counterparts, where the ppc supported complexes were observed to be more reactive. The higher reactivity of the ppc-ligated complexes

was attributed to the electron-withdrawing carboxylic acid group present on the ppc ligand. Given that the mechanism of C–O reductive elimination at dpk-ligated Pd(IV) complexes in acetic acid was proposed to involve pyridine dissociation followed by reductive elimination from a 5-coordinate intermediate, the electron-withdrawing carboxylic acid group on the ppc ligand increases the rate of dissociation of the pyridine group, which in turn increases the overall reaction rate.

In conclusion, the ppc ligand has been observed to enable oxidation of organopalladium(II) complexes with H<sub>2</sub>O<sub>2</sub> in acetic acid, and the subsequent C–O reductive elimination at ambient conditions. Organopalladium(II) complexes supported by the ppc ligand were found to be less reactive towards oxidation with H<sub>2</sub>O<sub>2</sub> and more reactive towards C–O reductive elimination relative to their dpk counterparts under similar conditions.

With successful oxidation and reductive elimination reactions of organopalladium(II) complexes enabled by the ppc ligand, we next sought to establish whether the ppc ligand would enable C–H bond activation of aromatic substrates. Successful C–H bond activation would complete the catalytic cycle shown in Scheme 5.1 and enable the development of a ligand enabled, palladium catalyzed C–H oxygenation reaction using H<sub>2</sub>O<sub>2</sub> as the terminal oxidant.

### 5.5 Application of the ppc Ligand Towards C–H Bond Activation

In order to determine whether C–H activation is possible using the ppc ligand, the ppc derived palladium(II) complex **30** was prepared. This complex was prepared by the reaction between ppc ligand and Pd(OAc)<sub>2</sub> in acetic acid at 50°C under ambient conditions, where the target complex **30** precipitated out of the solution as a yellow

solid and was filtered off. The complex could also be prepared by the reaction of the N,N-diethyl-6-(pyridin-ylcarbonyl)pyridine-2-carboxamide with Pd(OAc)<sub>2</sub> in acetic acid as shown below. It was characterized fully by NMR spectroscopy, ESI-MS, and X-ray diffraction, while its purity was confirmed by elemental analysis.

**Scheme 5. 44**

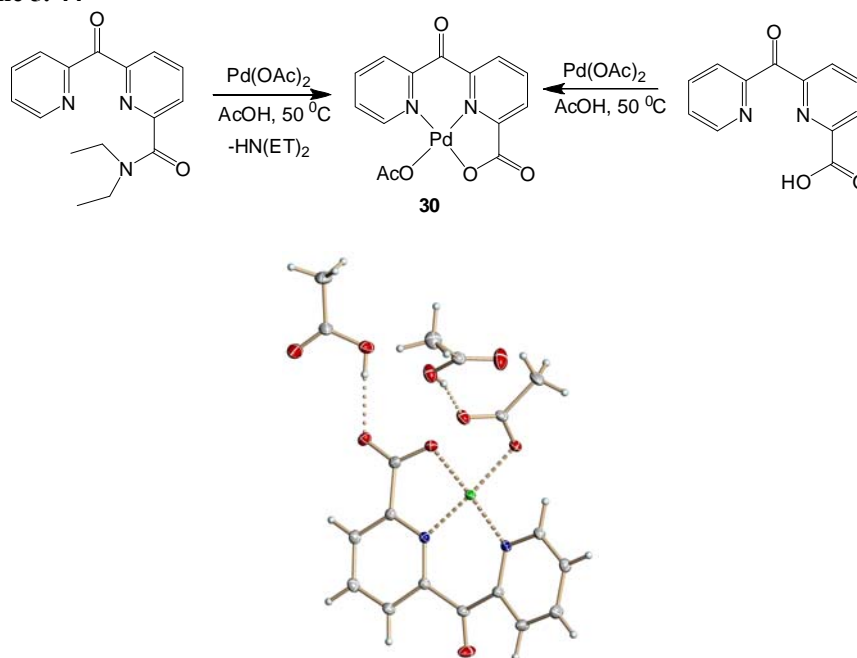
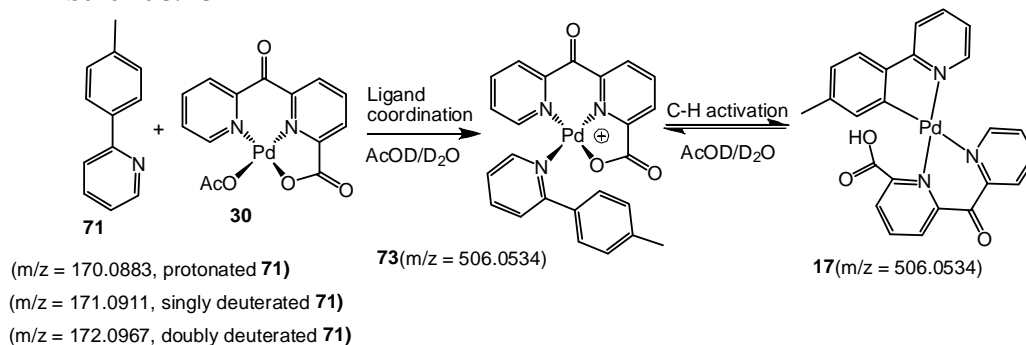


**Figure 5. 18.** ORTEP drawing (50 % probability ellipsoids) of complex **30**

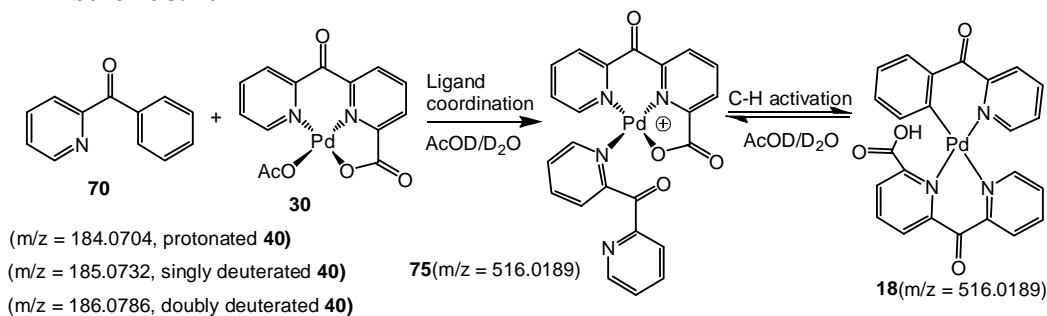
In order to determine whether C–H bond activation of aromatic substrates is possible using complex **30**, an AcOD/D<sub>2</sub>O (1:1) solution of this complex was combined with either 2-tolylpyridine or 2-benzoylpyridine substrates in stoichiometric quantities and heated at 100°C under an argon atmosphere. After 2 days, the <sup>1</sup>H NMR spectra of these solutions were examined to determine the possibility of H/D exchange.

**Scheme 5. 45**



Indeed, in the  $^1\text{H}$  NMR analysis of the solution containing compound **71**, the integration of the *ortho* C–H bonds had decreased to 1.81/2.0, indicating  $\sim 10\%$  deuteration. Analysis of this reaction solution by ESI–MS revealed major peaks at  $m/z = 170.0883$  which was assigned to the protonated compound **71**, 171.0911 assigned to singly deuterated **71**, 172.0967 assigned to doubly deuterated **71**, and 506.0534 which could be assigned to either complex **17** which is the product of C–H bond activation, or complex **73** which is a cationic product of coordination of tolylpyridine onto complex **30** upon dissociation of the acetate ligand. The ESI–MS mass envelope at 506.0534 indicates that coordination of tolylpyridine onto the palladium complex **30** is possible upon dissociation of the acetate ligand, and it also indicates that C–H activation may be possible, since coordination of tolylpyridine brings the *ortho* C–H bond of this substrate in close proximity to the palladium center. In this reaction, C–H bond activation was confirmed by the presence of the singly and doubly deuterated tolylpyridine molecules in the reaction solution by ESI–MS, where the deuteration indicates a reversible *ortho* C–H activation of 2-tolylpyridine in the presence of deuterated solvents. This analysis indicates that complex **30** enables C–H bond activation, but this reaction is not favorable thermodynamically.

**Scheme 5. 46**

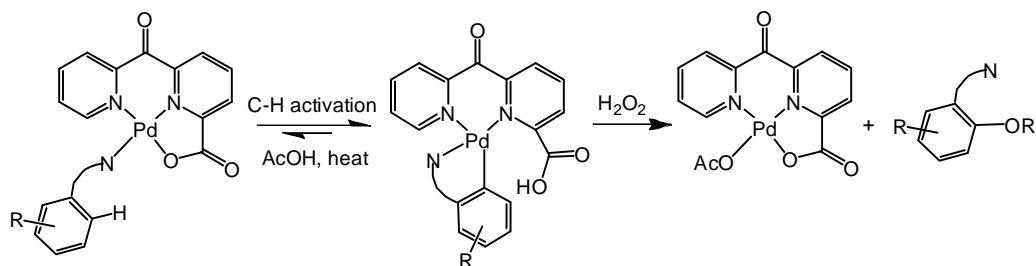


Similarly, in the  $^1\text{H}$  NMR analysis of the solution containing compound **70**, the integration of the ortho C–H bonds had decreased to 1.9/2.0, indicating a 5 % deuteration. Analysis of the reaction mixture by ESI–MS revealed major signals at  $m/z = 184.0704$  which was assigned to protonated benzoylpyridine **70**, 185.0732 which was assigned to singly deuterated **70**, 186.0786 which was assigned to doubly deuterated **70**, and 516.0189 which could be assigned to cationic complex **75** which is product of coordination of 2-benzoylpyridine onto complex **30** upon dissociation of an acetato ligand, or complex **18** which is a product of C–H activation of benzoylpyridine by complex **30**. The mass envelope at 516.0189 indicates that coordination of 2-benzoylpyridine onto complex **30** upon dissociation of an acetato ligand is possible, and this also indicates that C–H bond activation may be possible. Indeed, C–H bond activation was also confirmed by observation of singly and doubly deuterated molecules of 2-benzoylpyridine by ESI–MS, where the deuteration indicates a reversible C–H bond activation reaction in the presence of deuterated solvents. This analysis also indicates that complex **30** enables C–H bond activation of aromatic substrates, although this reaction is not favorable thermodynamically.

Given that the C–H bond activation reaction was found to be reversible and the equilibrium lies towards the reactants, we attempted to drive this equilibrium

forward by adding H<sub>2</sub>O<sub>2</sub> into the reaction solutions. The oxidant was expected to oxidize the product of C–H bond activation, thus driving the equilibrium forward as shown below.

**Scheme 5. 47**

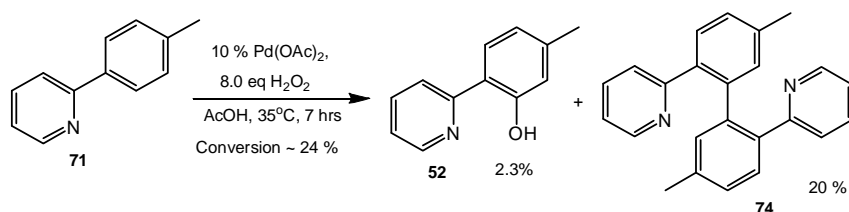


Thus a mixed AcOD/D<sub>2</sub>O (2:1) reaction solution containing complex **30** and 2-benzoylpyridine substrate **70** was prepared by combining a 0.010 M aqueous solution of complex **30** with a 0.010 M acetic acid solution of 2-benzoylpyridine substrate **70**.<sup>234</sup> 10.0 equivalents of H<sub>2</sub>O<sub>2</sub> were added and the resulting solution was stirred at room temperature for several days. 10.0 equivalents of H<sub>2</sub>O<sub>2</sub> were added to the reaction solution after every 8 hours, for a total of 40.0 equivalents of H<sub>2</sub>O<sub>2</sub>. After 2 days, <sup>1</sup>H NMR analysis of reaction mixture revealed the presence of the corresponding phenol in 3 % yield. This indicates that complex **30** enables C–H bond activation of 2-benzoylpyridine, and subsequent functionalization of the resulting organopalladium(II) complex. However these reactions are too slow leading to only 3 % product yield. Analysis of the reaction solution by ESI–MS indicated the presence of the corresponding phenol, together with singly and doubly deuterated 2-benzoylpyridine molecules. Control reactions in the absence of palladium did not yield any phenol.

In summary, the ppc ligand has been found to enable C–H bond activation of aromatic molecules, oxidation of the corresponding organopalladium(II) complex with H<sub>2</sub>O<sub>2</sub>, and C–O reductive elimination from the resulting monohydrocarbyl Pd(IV) complexes under similar reaction conditions. With all these steps enabled by the ppc ligand, we next sought to develop a ppc ligand-enabled palladium catalyzed C–H bond functionalization of aromatic molecules with H<sub>2</sub>O<sub>2</sub> as the sole oxidant.

### 5.6 Application of the ppc Ligand Towards Catalytic C–H Bond Functionalization

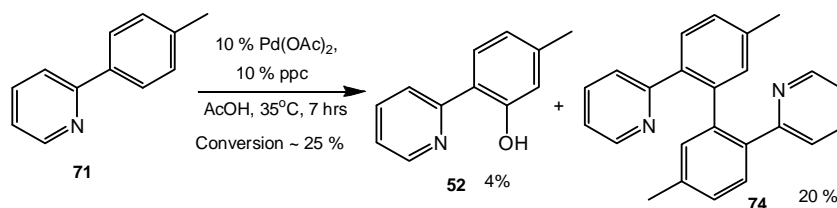
**Scheme 5. 48**



We began by attempting *ortho* oxygenation of tolylpyridine using 10 % of Pd(OAc)<sub>2</sub> in acetic acid solvent using H<sub>2</sub>O<sub>2</sub> as oxidant at 35°C. In this reaction, 0.1 mmoles of tolylpyridine were combined with 0.01 mmoles of Pd(OAc)<sub>2</sub> in 1.0 ml of deuterated acetic acid, and 1.0 μl of 1,4 dioxane was added as internal standard. <sup>1</sup>H NMR was taken, and 20.0 eq of H<sub>2</sub>O<sub>2</sub> was added into the reaction solution. The resulting solution was placed in oil bath at 35°C, one more batch of 20.0 equivalents H<sub>2</sub>O<sub>2</sub> was added to the solution after 1 hr, and 2 more batches were added after every 2 hours for a total of 8.0 equivalents of H<sub>2</sub>O<sub>2</sub>. After 7 hours, the <sup>1</sup>H NMR spectrum of the reaction solution revealed the presence of 20 % biphenyl product **74** and 2.3 % of the corresponding phenol **52**. The presence of phenol was also confirmed by ESI-MS with m/z = 186.0964 (Calculated for protonated phenol C<sub>12</sub>H<sub>12</sub>NO<sup>+</sup> = 186.0919) while the presence of the corresponding biphenyl product was confirmed by ESI-MS

at  $m/z = 337.1691$  (Calculated for protonated biphenyl product  $C_{24}H_{21}N_2^+ = 337.1705$ ). These products were also confirmed by independent synthesis, where the phenol **52** was synthesized according to literature procedures,<sup>21</sup> where the biphenyl product was isolated from the reaction solution and its  $^1H$  NMR was compared to that published in literature.<sup>207</sup>

**Scheme 5. 49**



This reaction was repeated in the presence of 10 % ppc ligand. Thus 0.1 mmoles of 2-tolylpyridine was dissolved in 1.0 ml of deuterated acetic acid, and 0.010 mmoles of Pd(OAc)<sub>2</sub> and ppc ligand were added. 1.0 μl of 1,4 dioxane was added to the solution as internal standard and  $^1H$  NMR spectrum was taken. 20.0 eq of H<sub>2</sub>O<sub>2</sub> was added and the resultant solution was placed in oil bath at 35°C. 20.0 more equivalents of H<sub>2</sub>O<sub>2</sub> were added, and 2 more batches of 20.0 equivalents of H<sub>2</sub>O<sub>2</sub> were added after every two hours for a total of 8.0 equivalents of H<sub>2</sub>O<sub>2</sub>. The  $^1H$  NMR spectrum of the reaction solution after 7 hours revealed the presence of the corresponding phenol **52** in ~ 4 % yield, and biphenyl **74** in ~ 20 % yield. Considering that a similar product distribution is observed in the absence of the ppc ligand, this indicates that the ppc ligand does not affect this reaction. However given that 2.3 % phenol is produced in the absence of the ppc ligand, while ~ 4 % phenol is produced in the presence of the ligand, this suggests that it may be possible to optimize the reaction conditions and increase the yield of the phenol **52**.

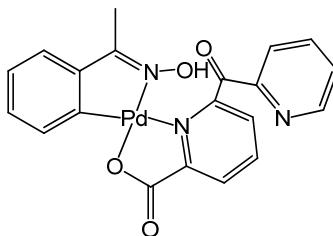
The unsuccessful C–H bond functionalization reaction led us to design a new ligand which would enable catalytic oxygenation of the aromatic C–H bonds utilizing H<sub>2</sub>O<sub>2</sub> as oxidant.

## 5.6 Experimental

Preparation of the acetato-ligated hydrocarbyl Pd(II) complexes **10-14** has been described previously in chapter 2. The palladacyclic ppc ligand-supported complexes **15** and **16** were prepared by dissolving 0.10 mmol of the ppc ligand in dichloromethane and addition of 1.0 eq of the corresponding acetato-bridged palladacycle **10** or **11** to the dichloromethane solution. A clear solution was formed upon stirring the reaction mixture for a few minutes, but further stirring resulted in precipitation of a white solid. The reaction mixture was stirred for a total of 3 hours, after which it was concentrated and filtered off. The residue was washed with a small amount of cold thf and dried under vacuum at room temperature to afford the pure target complexes **15** and **16**. These complexes were characterized by NMR spectroscopy and electrospray ionization mass spectrometry, while their purity was confirmed by elemental analysis. Complex **17** was prepared following a similar procedure, but further stirring of the reaction solution did not lead to precipitation of the product, and therefore the solution was concentrated and triturated with thf to afford white precipitate of the target compound **17**. The reaction mixture was filtered off, washed with a small amount of cold diethyl ether, and dried under high vacuum at room temperature to afford the pure target complex. Complex **17** was characterized by NMR spectroscopy and electrospray ionization mass spectrometry, while its purity was confirmed by elemental analysis. Complexes **18** and **19** were also prepared and isolated using the procedure above, but benzene was used as solvent instead of dichloromethane. Diethyl ether or hexanes could also be used instead of tetrahydrofuran to precipitate the products. Complexes **18** and **19** were characterized

by NMR spectroscopy and electrospray ionization mass spectrometry, while complex **18** was also characterized by X-ray diffraction. The purity of these complexes was confirmed by elemental analysis.

### Complex 15



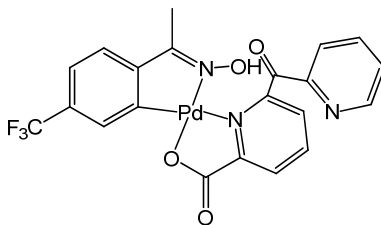
$^1\text{H}$  NMR (AcOH- $\text{d}_4$ , 22°C),  $\delta$ : 2.16 (s, 3H), 6.39 (br s, 1H), 6.84 (br s, 1H), 7.00 to 7.05 (m, 2H), 7.85 (br s, 1H), 8.13 (br s, 1H), 8.20 (br s, 2H), 8.29 to 8.32 (m, 2H), 9.05 (br s, 1H).

$^{13}\text{C}$  NMR not obtained due to poor solubility in common NMR solvents.

Anal. Found: C, 50.23; H, 3.55; N, 8.63. Calculated for  $\text{C}_{20}\text{H}_{16}\text{N}_3\text{O}_{4.5}^{106}\text{Pd}$  (+ 0.5  $\text{H}_2\text{O}$  molecule); C, 50.38; H, 3.38; N, 8.81.

ESI-MS of solution of **15** in aqueous acetic acid, positive mode,  $m/z$  = 468.0197 and 486.0140. Calculated for  $(\mathbf{15}+\text{H})^+$   $\text{C}_{20}\text{H}_{16}\text{N}_3\text{O}_4\text{Pd}^{106+}$  = 468.0176 and  $(\mathbf{15}+\text{H}_3\text{O})^+$  (hydrated ketone group)  $\text{C}_{20}\text{H}_{18}\text{N}_3\text{O}_5^{106}\text{Pd}^+$  = 486.0281.

### Complex 16



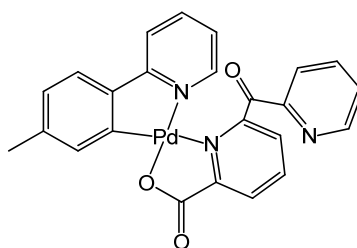
$^1\text{H}$  NMR (AcOH- $\text{d}_4$ , 22°C),  $\delta$ : 2.21 (s, 3H), 6.62 (s, 1H), 7.21 (d,  $J=7.7$  Hz, 1H), 7.34 (d,  $J=7.8$  Hz, 1H), 7.89 (s, 1H), 8.22 (s, 3H), 8.34 (s, 2H), 9.05 (s, 1H).

$^{13}\text{C}$  NMR not obtained due to poor solubility in common NMR solvents.

Anal. Found: C, 46.90; H, 2.33; N, 7.78. Calculated for  $\text{C}_{21}\text{H}_{14}\text{F}_3\text{N}_3\text{O}_4^{106}\text{Pd}$ ; C, 47.08; H, 2.63; N, 7.84.

ESI-MS of solution of **16** in aqueous acetic acid, positive mode,  $m/z = 536.0056, 554.0053$ . Calculated for  $(\mathbf{16}+\mathbf{H})^+ \text{C}_{21}\text{H}_{15}\text{F}_3\text{N}_3\text{O}_4^{106}\text{Pd}^+$ : 536.00494, with  $(\mathbf{16}+\mathbf{H}_3\mathbf{O})^+$  hydrated ketone fragment  $\text{C}_{21}\text{H}_{17}\text{F}_3\text{N}_3\text{O}_5^{106}\text{Pd}^+$ : 554.0155

### Complex 17



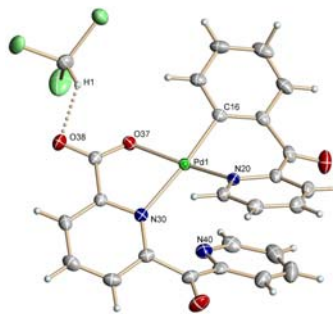
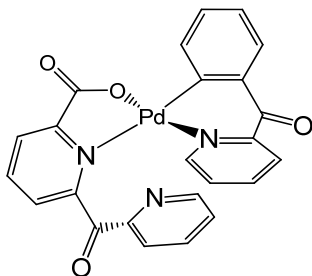
$^1\text{H}$  NMR (dms $\text{o-d}_6$ , 22°C),  $\delta$ : 1.86-1.90 (m, 3H), 6.81 (bs, 2H), 7.16 (bs, 1H), 7.45 (bs, 1H), 7.70 (dd,  $J=7.9, 5.3$  Hz 1H), 7.92-8.04 (m, 4H), 8.13 (d,  $J=5.9$  Hz 1H), 8.25 (bs, 2H), 8.35 (bs, 1H), 8.75 (bs, 1H).

$^{13}\text{C}$  NMR (dms $\text{o-d}_6$ , 22°C),  $\delta$ : 20.8, 119.0, 122.2, 123.6, 124.6, 125.6, 127.2, 127.5, 129.0, 134.2, 137.6, 138.5, 139.4, 140.2, 142.4, 149.1, 149.3, 151.6, 152.9, 154.1, 155.4, 164.4, 168.6, 191.4

ESI-MS of solution of **17** in aqueous acetic acid, positive mode,  $m/z = 502.0397$  and  $520.0436$ . Calculated for  $(\mathbf{17}+\mathbf{H})^+ \text{C}_{24}\text{H}_{18}\text{N}_3\text{O}_3^{106}\text{Pd}^+$ : 502.0383, with  $(\mathbf{17}+\mathbf{H}_3\mathbf{O})^+$  hydrated ketone fragment  $\text{C}_{24}\text{H}_{20}\text{N}_3\text{O}_4^{106}\text{Pd}^+$ : 520.0489

Anal. Found: C, 53.57; H, 3.75; N, 7.69. Calculated for hydrated complex with one additional molecule of  $\text{H}_2\text{O}$ ;  $\text{C}_{26}\text{H}_{21}\text{N}_3\text{O}_5^{106}\text{Pd}$ ; C, 53.59; H, 3.94; N, 7.81.

## Complex 18



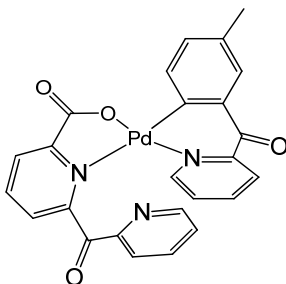
$^1\text{H}$  NMR ( $\text{CDCl}_3$ ,  $22^\circ\text{C}$ ),  $\delta$ : 6.78 (s, 1H), 6.97 (s, 1H), 7.03 (d,  $J=7.6$  Hz 1H), 7.31 (d,  $J=7.4$  Hz, 1H), 7.40 to 7.45 (m, 2H) 7.54 (t,  $J=6.0$  Hz, 1H), 7.71 (t,  $J=7.7$  Hz, 1H), 7.98 (d,  $J=7.6$  Hz, 1H), 8.03 (t,  $J=7.6$  Hz, 1H), 8.13 (d,  $J=7.6$  Hz, 1H), 8.22 (t,  $J=7.7$  Hz, 1H), 8.52 (d,  $J=7.8$  Hz, 1H), 8.60 (d,  $J=4.1$  Hz, 1H), 9.26 (d,  $J=5.2$  Hz, 1H).

$^{13}\text{C}$  NMR ( $\text{CDCl}_3$ ,  $22^\circ\text{C}$ ),  $\delta$ : 124.2, 125.4, 125.8, 127.6, 127.7, 128.4, 129.1, 130.3, 131.4, 133.2, 136.8, 137.2, 139.8, 140.1, 147.0, 148.5, 150.3, 152.1, 152.9, 156.3, 156.9, 169.3, 190.1, 190.6

Anal. Found: C, 50.17; H, 3.51; N, 7.23. Calculated for doubly hydrated complex with 1.3 additional  $\text{H}_2\text{O}$  molecules; C, 50.06; H, 3.79; N, 7.30.

ESI-MS of solution of **18** in acetic acid, positive mode,  $m/z = 516.0089$ , 534.0368. Calculated for  $(\mathbf{18}+\mathbf{H})^+$   $\text{C}_{24}\text{H}_{16}\text{N}_3\text{O}_4^{106}\text{Pd}^+$ : 516.0176, with  $(\mathbf{18}+\mathbf{H}_3\mathbf{O})^+$  hydrated ketone fragment  $\text{C}_{24}\text{H}_{18}\text{N}_3\text{O}_5^{106}\text{Pd}^+$ : 534.0281.

### Complex 19



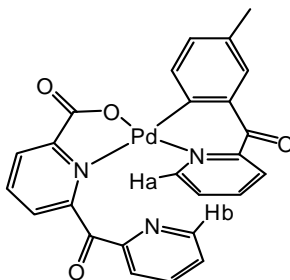
$^1\text{H}$  NMR (dms $\text{-d}_6$ , 22°C),  $\delta$ : 2.12 (s, 3H), 6.60 (bs, 1H), 7.09 (bs, 1H), 7.26 (s, 1H), 7.33 (d,  $J=7.7$  Hz, 1H), 7.50 (bs, 1H), 7.63 (dd,  $J=7.7, 5.0$  Hz, 1H), 7.88 (td,  $J=7.9, 0.9$  Hz, 1H), 8.02-8.06 (m, 2H), 8.15 (t,  $J=7.1$  Hz, 1H), 8.29 (dd,  $J=7.7, 0.9$  Hz, 1H), 8.38 (t,  $J=7.7$  Hz, 1H), 8.68 (d,  $J=4.5$  Hz, 1H), 8.86 (d,  $J=4.5$  Hz, 1H).

$^{13}\text{C}$  NMR (dms $\text{-d}_6$ , 22°C),  $\delta$ : 19.9, 123.5, 125.6, 127.4, 128.0, 128.1, 128.3, 130.1, 131.4, 132.5, 134.1, 135.4, 137.4, 140.6, 140.7, 142.8, 148.7, 149.5, 151.2, 152.2, 154.7, 168.7, 190.0, 190.2.

Anal. Found: C, 54.13; H, 3.51; N, 7.52. Calculated for singly hydrated complex with 0.5 additional  $\text{H}_2\text{O}$  molecule; C, 53.92; H, 3.62; N, 7.55.

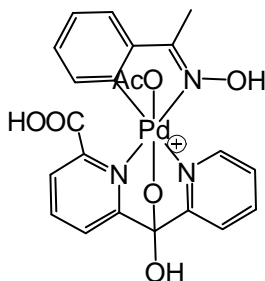
ESI-MS of solution of **19** in acetic acid, positive mode,  $m/z = 530.0343$  and 548.0459. Calculated for  $(\mathbf{19}+\mathbf{H})^+$   $\text{C}_{24}\text{H}_{16}\text{N}_3\text{O}_4^{106}\text{Pd}^+$ : 530.0332, with  $(\mathbf{19}+\mathbf{H}_3\mathbf{O})^+$  hydrated ketone fragment  $\text{C}_{24}\text{H}_{18}\text{N}_3\text{O}_5^{106}\text{Pd}^+$ : 548.0438.

*Selective 1D-difference NOE experiments ( $\text{D}_2\text{O}$ ) for **19***



In the 1D difference NOE experiment, irradiation of the *ortho*-H<sub>a</sub> doublet at 8.86 ppm belonging to the pyridyl fragment of the 2-(3-methylbenzoyl)pyridine ligand, and *ortho*-H<sub>b</sub> doublet at 8.68 ppm belonging to the pyridyl fragment of the ppcp ligand, did not result in any NOE effect (mixing time of 0.6s, delay time 4s).

### Complex 25



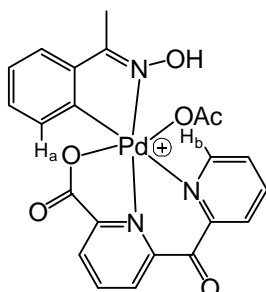
<sup>1</sup>H NMR (AcOH-d<sub>4</sub>, 22°C), δ: 2.34 (s, 3H), 6.96 (d, *J*=7.7 Hz, 1H), 7.00 (t, *J*=7.6 Hz, 1H), 7.32 (t, *J*=7.2 Hz, 1H), 7.37 (d, *J*=7.2 Hz, 1H), 7.61 (t, *J*=6.2 Hz, 1H), 7.76 (t, *J*=6.2 Hz, 1H), 7.89 (t, *J*=7.2 Hz, 2H), 8.06 (t, *J*=7.6 Hz, 1H), 8.17 (t, *J*=7.2 Hz, 1H), 9.09 (d, *J*=4.8 Hz, 1H), 9.13 (d, *J*=4.8 Hz, 1H). (the acetoxy group attached to palladium could not be observed in the AcOH-d<sub>4</sub> solution, this complex could not be isolated either.)

<sup>13</sup>C NMR couldn't be obtained because the complex was not stable.

ESI-MS of solution of **25** in acetic acid, positive mode, *m/z* = 544.349.

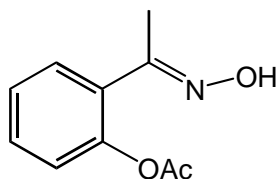
Calculated for **25**<sup>+</sup> C<sub>22</sub>H<sub>20</sub>N<sub>3</sub>O<sub>7</sub>Pd<sup>106+</sup>: 544.0336.

### Selective 1D-difference NOE experiments (AcOD) for 25



In the 1D difference NOE experiment, no NOE was observed between any hydrogen atoms in the molecule. Irradiation of a resonance  $H_a$  at 6.96 ppm (*ortho*- $H_b$  on the dpk ligand) did not show enhancement of any other signals (positive NOE) while irradiation of resonance  $H_b$  at 9.13 did not show enhancement of any signals either (positive NOE) (mixing time of 0.3-0.8s, delay time 5s).

### Compound 38



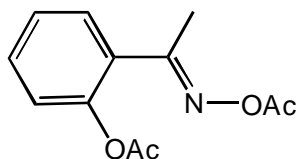
$^1\text{H}$  NMR ( $\text{CDCl}_3$ ,  $22^\circ\text{C}$ ),  $\delta$ : 2.22 (s, 3H), 2.41 (s, 3H), 6.89 (td,  $J=7.6$ , 1.2 Hz, 1H), 7.00 (dd,  $J=8.4$ , 1.3 Hz, 1H), 7.31 (td,  $J=7.8$ , 1.5 Hz, 1H), 7.44 (dd,  $J=8.0$ , 1.5 Hz, 1H), 11.2 (s, 1H).

$^{13}\text{C}$  NMR ( $\text{CDCl}_3$ ,  $22^\circ\text{C}$ ),  $\delta$ : 13.0, 19.4, 117.3, 118.2, 119.3, 128.6, 132.5, 158.7, 164.2, 167.0.

ESI MS of  $\text{H}_2\text{O}$  solution of  $(\mathbf{38})\text{Na}^+$ ,  $m/z$  observed: 216.0593, Calculated for  $\text{C}_{10}\text{H}_{11}\text{NNaO}_3$ , 216.0637.

### Compound 41

This compound was prepared by acetoxylation of compound **38** in acetic anhydride. Compound **38** was dissolved in acetic anhydride solvent and stirred at  $60^\circ\text{C}$  for 6 hours. The solvent was removed under vacuum, and pure **41** was obtained.

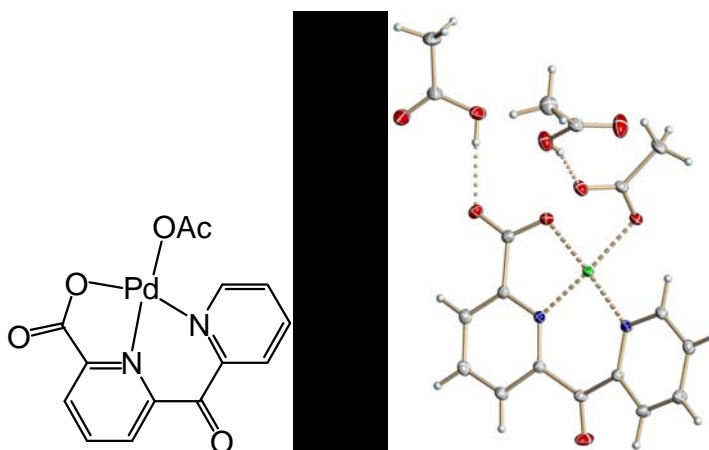


$^1\text{H}$  NMR ( $\text{CDCl}_3$ ,  $22^\circ\text{C}$ ),  $\delta$ : 2.21 (s, 3H), 2.29 (s, 3H), 2.30 (s, 3H), 7.12 (dd,  $J=8.1$ , 1.1 Hz, 1H), 7.26 (td,  $J=7.5$ , 1.1 Hz, 1H), 7.41 (td,  $J=7.9$ , 1.6 Hz, 1H), 7.46 (dd,  $J=8.0$ , 7.7, 1.6 Hz, 1H).

$^{13}\text{C}$  NMR ( $\text{CDCl}_3$ ,  $22^\circ\text{C}$ ),  $\delta$ : 16.9, 19.9, 21.3, 123.5, 126.3, 128.9, 129.8, 131.1, 148.3, 161.9, 168.6, 169.6.

ESI MS of  $\text{H}_2\text{O}$  solution of **(41)** $\text{Na}^+$ ,  $m/z$  observed = 258.0768. Calculated for  $\text{C}_{12}\text{H}_{13}\text{NNaO}_4 = 258.0742$ .

### Compound 30

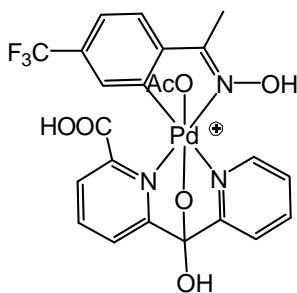


$^1\text{H}$  NMR ( $\text{AcOH-d}_4$ ,  $22^\circ\text{C}$ ),  $\delta$ : 1.95 (s, 3H), 7.55 (ds,  $J=1.1$  Hz 1H), 7.65 (dd,  $J=8.1$ , 1.1 Hz, 1H), 7.74 (d,  $J=8.2$  Hz, 1H).

$^{13}\text{C}$  NMR ( $\text{AcOH-d}_4$ ,  $22^\circ\text{C}$ ),  $\delta$ : 21.0, 23.2, 128.8, 129.8, 129.9, 130.5, 141.1, 142.6, 144.8, 145.9, 150.1, 151.4, 170.2, 171.9, 175.6, 182.1

ESI-MS of solution in acetic acid:  $m/z = 392.9770$ : Calculated for  $\text{C}_{14}\text{H}_{11}\text{N}_2\text{O}_5^{106}\text{Pd}^+$ : 392.9703

### Complex 26



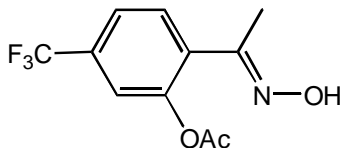
<sup>1</sup>H NMR (AcOH-d<sub>4</sub>, 22°C), δ: 2.48 (s, 3H), 7.00 (s, 1H), 7.62 (d, *J*=7.8 Hz, 1H), 7.69 (d, *J*=7.9 Hz, 1H), 7.80 (t, *J*=6.4 Hz, 1H), 7.88 (d, *J*=7.8 Hz, 1H), 8.01 (d, *J*=7.6 Hz, 1H), 8.12 (d, *J*=7.7 Hz, 1H), 8.21-8.24 (m, 2H), 8.89 (d, *J*=5.32 Hz, 1H). (The acetoxy group attached to palladium could not be observed in the AcOH-d<sub>4</sub> solution.)

<sup>13</sup>C NMR couldn't be obtained because the complex was not stable.

ESI-MS of solution of **26.H<sup>+</sup>** in acetic acid, positive mode, *m/z* = 612.0220.

Calculated for C<sub>23</sub>H<sub>19</sub>F<sub>3</sub>N<sub>3</sub>O<sub>7</sub><sup>106</sup>Pd<sup>+</sup> = 612.0210

### Compound 45



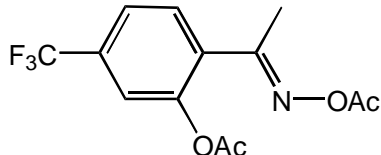
<sup>1</sup>H NMR (CDCl<sub>3</sub>, 22°C), δ: 2.26 (s, 3H), 2.46 (s, 3H), 7.13 (dd, *J*= 8.3, 1.3 Hz, 1H), 7.27 (vs, 1H), 7.56 (d, *J*= 8.4 Hz, 1H),

<sup>13</sup>C NMR (CDCl<sub>3</sub>, 22°C), δ: 13.2, 19.3, 115.6 (m), 120.2, 122.3, 125.0, 129.2, 134.1 (q), 158.9, 163.2, 166.7.

ESI MS of an aqueous solution of (**45**)H<sup>+</sup>, positive mode, *m/z* observed; 262.0701,

Calculated for **45.H<sup>+</sup>**, C<sub>11</sub>H<sub>11</sub>F<sub>3</sub>NO<sub>3</sub> = 262.0691.

### Compound 46



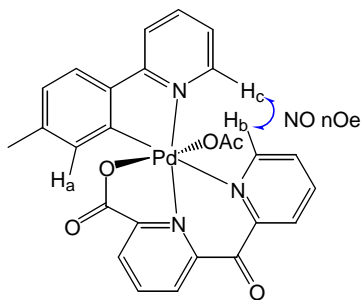
$^1\text{H}$  NMR ( $\text{CDCl}_3$ ,  $22^\circ\text{C}$ ),  $\delta$ : 2.22 (s, 3H), 2.31 (s, 3H), 2.32 (s, 3H), 7.42 (s, 1H), 7.52 (d,  $J=8.7$  Hz, 1H), 7.59 (d,  $J=8.2$  Hz, 1H).

$^{13}\text{C}$  NMR ( $\text{CDCl}_3$ ,  $22^\circ\text{C}$ ),  $\delta$ : 16.8, 19.8, 21.2, 120.9 (q), 121.9, 123.1 (q), 124.7, 130.5, 132.4, 133.2 (q), 148.5, 160.9, 168.3, 169.1.

ESI MS of an aqueous solution of  $(46+\text{Na})^+$ , positive mode,  $m/z = 326.0593$ .

Calculated for  $46\cdot\text{Na}^+$ ,  $\text{C}_{13}\text{H}_{12}\text{F}_3\text{NNaO}_4 = 326.0616$ .

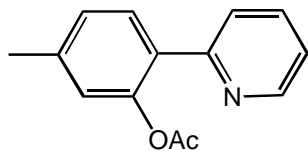
#### Selective 1D-difference NOE experiments (AcOD) for 48



In the 1D difference NOE experiment, no NOE was observed between any hydrogen atoms in the molecule. Irradiation of a resonance  $\text{H}_a$  at 6.21 ppm (*ortho*- $\text{H}_a$  on the tolylpyridine ligand) did not show enhancement of any other signals (positive NOE) while irradiation of resonances  $\text{H}_b$  and  $\text{H}_c$  9.09 ppm and 9.45 ppm did not show enhancement of any signals either (positive NOE) (mixing time of 0.3-0.8 s, delay time 5s).

The phenolic product **23** is a known compound.<sup>21</sup>

### Compound 28



Compound **28** was prepared by acetoxylation of phenol **23** in acetic anhydride. Compound **23** was dissolved in acetic anhydride, and the resulting solution was heated at 60°C for 6 hours. Removal of the solvent afforded pure compound **28**.

$^1\text{H}$  NMR (AcOD, 22°C),  $\delta$ : 2.13 (s, 3H), 2.42 (s, 3H), 7.10 (s, 1H), 7.24 (d,  $J=7.8$  Hz, 1H), 7.57 (d,  $J=7.8$  Hz, 1H), 7.60 (t,  $J=6.6$  Hz, 1H), 7.73 (d,  $J=7.8$  Hz, 1H), 8.11 (td,  $J=7.8, 1.5$  Hz, 1H), 8.88 (d,  $J=5.2$  Hz, 1H).

$^{13}\text{C}$  NMR (AcOD, 22°C),  $\delta$ : 20.9, 21.3, 124.6, 124.7, 126.4, 128.3, 128.5, 131.7, 141.0, 142.9, 148.1, 149.1, 154.8, 170.8.

ESI-MS of solution of **29** in methanol,  $m/z$  observed: 228.1108, Calculated for  $\text{C}_{14}\text{H}_{14}\text{NO}_2$ ,  $m/z = 228.1025$ .

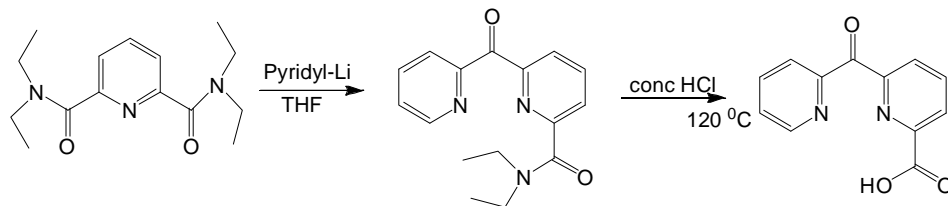
The phenols **60** and **67** and aryl acetates **61** and **68** are known compounds (See Chapter 3 for the preparation and characterization of these compounds).

### Synthesis of *N,N,N',N'*-tetraethylpyridine-2,6-dicarboxamide

The *N,N,N',N'*-tetraethylpyridine-2,6-dicarboxamide was synthesized according to literature.<sup>235</sup>

## Synthesis of 6-(pyridine-2-ylcarbonyl)pyridine-2-carboxylic acid (ppc) ligand

Scheme S5. 1



5.50 g (35.0 mmoles) of bromopyridine was added to a 150.0 ml of dry THF under argon and the solution stirred to  $-78^{\circ}\text{C}$ . 14.0 ml of 2.5 M n-Buli (35.0 mmoles) in hexanes was added slowly to the solution, and the resulting dark red solution was stirred at  $-78^{\circ}\text{C}$  for an additional 1.25 hours.

Another solution of 9.3 g of pyridyl dicarboxamide (33.6 mmoles) was dissolved in 250.0 ml THF and cooled to  $-78^{\circ}\text{C}$ . The pyridyl lithium solution was slowly cannulated to the pyridyl dicarboxamide/ THF solution over 30 minutes. The resulting dark red solution was stirred at  $-78^{\circ}\text{C}$  for 30 minutes and stirred overnight as it slowly warmed up to room temperature.

Water (12.6 mL) was added to quench the solution and remove the inorganic products. The resulting red organic solution was transferred to another container and dried with anhydrous  $\text{MgSO}_4$ . Solvent was removed under vacuum and the product was obtained by column chromatography (hexane/ethyl acetate 70:30 to 60:40), together with excess pyridine dicarboxamide. The solvent was removed and the resulting residue was dissolved in diethyl ether because the impurity, pyridyl dicarboxamide is more soluble in ether than our target compound, dpk carboxamide. Continuous removal of solvent and dissolution in ether increased the yield. Removal of solvent under vacuum gave the analytically pure dpk carboxamide product in  $\sim 35\%$ .

Hydrolysis of the DPK carboxamide in refluxing concentrated hydrochloric acid for 7 days afforded the DPK carboxylic acid ligand. The solution was concentrated by distillation and diluted with NaOH to a pH of ~ 3-4 to give white crystals of dpk carboxylic acid. Removal of solvent under vacuum gave a yield of 58.5 %.

***N,N-diethyl-6-(pyridin-2-ylcarbonyl)pyridine-2-carboxamide***

$^1\text{H NMR}$  (AcOH- $d_4$ , 22°C),  $\delta$ : 0.91 (t,  $J=7.0$  Hz, 3H), 1.21 (t,  $J=7.2$  Hz, 3H), 3.39 (q,  $J=7.0$  Hz, 2H), 3.53 (q,  $J=7.1$  Hz, 2H), 7.67 to 7.70 (m, 1H), 7.99 (dd,  $J=7.5$ , 1.4 Hz, 1H), 8.08 to 8.19 (m, 4H), 8.81 (td,  $J=4.9$ , 1.2 Hz, 1H).

$^{13}\text{C NMR}$  (AcOH- $d_4$ , 22°C),  $\delta$ : 12.1, 13.4, 41.2, 44.0, 125.9, 126.0, 127.4, 138.7, 139.0, 148.5, 152.9, 153.1, 153.8, 168.5, 192.2

Anal. Found: C, 67.69; H, 6.30; N, 14.61. Calculated for  $\text{C}_{16}\text{H}_{17}\text{N}_3\text{O}_2$ ; C, 67.83; H, 6.05; N, 14.83.

***ppc ligand***

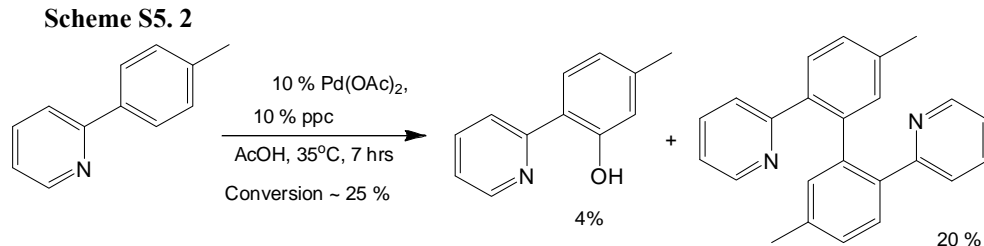
$^1\text{H NMR}$  ( $\text{CDCl}_3$ , 22°C),  $\delta$ : 7.58 (dd,  $J=4.8$ , 1.2 Hz, 1H), 7.98 (dt,  $J=7.7$ , 1.7 Hz, 1H), 8.15-8.20 (m, 2H), 8.34 (dd,  $J=7.8$ , 1.0 Hz 1H), 8.42 (dd,  $J=7.8$ , 1.0 Hz, 1H), 8.75 (dd,  $J=4.7$ , 1.2 Hz, 1H).

$^{13}\text{C NMR}$  ( $\text{DMSO}-d_6$ , 22°C),  $\delta$ : 124.5, 126.7, 127.1, 127.2, 137.3, 138.2, 148.0, 149.0, 153.3, 154.7, 165.6, 192.9

Anal. Found: C, 62.83; H, 3.07; N, 12.08. Calculated for  $\text{C}_{12}\text{H}_8\text{N}_2\text{O}_3$ ; C, 63.16; H, 3.53; N, 12.28.

ESI-MS of solution of ppc ligand in methanol, positive mode,  $m/z = 229.08696$ . Calculated for  $\text{C}_{12}\text{H}_9\text{N}_2\text{O}_3^+$ : 229.06132.

## Application of the ppc ligand towards catalytic C-H bond oxidation



4.6 mg (0.01 mmol) of Pd(OAc)<sub>2</sub> and 4.8 mg of ppc ligand were placed in a vial and 1.0 ml of either deuterated methanol or acetic acid was added. 17.0 mg (0.1 mmol) of 2-*p*-tolylpyridine substrate was added and the reaction mixture was transferred to a NMR tube and 1.0  $\mu$ l of 1,4-dioxane standard was added. <sup>1</sup>H NMR spectrum was taken, and 2.0 eq of HOOH was added and the NMR tube was placed in an oil-bath set at 35°C. Additional 2 eq HOOH were added 1 hr later and 2 more portions of 2.0 eq of HOOH were added every 2 hours. <sup>1</sup>H NMR was taken after 5 hours, 7 hours and 10 hours. <sup>1</sup>H NMR analysis reveal the presence of phenol in ~ 5 % yield in both methanol and acetic acid, among other products. The presence of phenol was also confirmed by ESI-MS with  $m/z = 186.0964$  (Calculated for protonated phenol C<sub>12</sub>H<sub>12</sub>NO<sup>+</sup> = 186.0919).

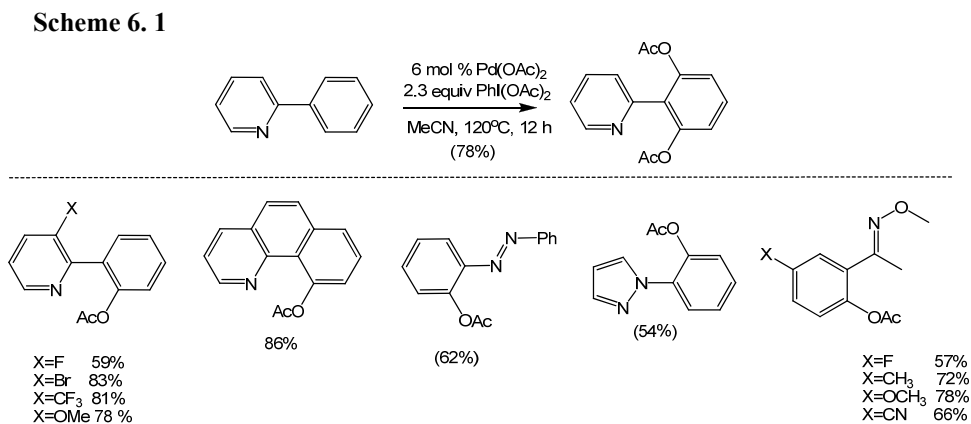
## Chapter 6: Ligand-Enabled Oxidative Palladium Catalyzed Functionalization of Aromatic C–H Bonds

### 6.1 Introduction

The development of palladium catalyzed processes for selective, direct functionalization of C–H bonds remains a significant challenge in organic chemistry. Mild and selective transformations of this type will find widespread application in the synthesis of pharmaceuticals, natural products, polymers, and feedstock commodity chemicals. Traditional approaches for such functionalization reactions rely on prefunctionalized starting materials for both reactivity and selectivity, thus adding costly steps to the overall functionalization of a molecule. As such, procedures for the direct functionalization of C–H bonds will improve atom economy, and also increase the overall efficiency of multistep synthetic sequences.<sup>24</sup>

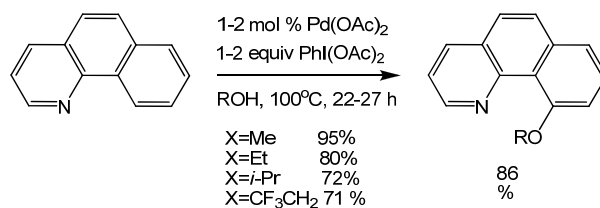
Palladium catalyzed C–H bond oxygenation reactions have undergone significant development during the past 17 years, although such reactions have been known for a very long time.<sup>45,127</sup> The catalytic acetoxylation of benzene with Pd(OAc)<sub>2</sub> was first reported in 1966 by Triggs and co-workers.<sup>47</sup> In 1971, another example of aromatic C–H acetoxylation using K<sub>2</sub>Cr<sub>2</sub>O<sub>7</sub> as oxidant was reported by Henry and co-workers, where the intermediacy of Pd(IV) complexes was proposed.<sup>48</sup> Crabtree<sup>49</sup> also reported a palladium catalyzed acetoxylation of benzene using PhI(OAc)<sub>2</sub> as the terminal oxidant, where he proposed the intermediacy of Pd(IV) complexes. In 2004, Sanford optimized the procedure developed by Crabtree for the acetoxylation of aromatic C–H bonds using PhI(OAc)<sub>2</sub> as oxidant.<sup>50</sup> Since then, a

variety of aromatic compounds bearing nitrogen-based directing groups such as imines, oxime ethers, azobenzene derivatives, and nitrogen heterocycles (eg pyrazoles and isoxazolines) have undergone palladium catalyzed *ortho* C–H bond acetoxylation using  $\text{PhI}(\text{OAc})_2$  as oxidant (Scheme 6.1).<sup>33,236</sup>



When the solvent of these reactions was changed from acetic acid to alcohol, aryl ether products were produced in high yields. Sanford proposed that in situ reaction of the alcohol solvent with  $\text{PhI}(\text{OAc})_2$  affords  $\text{PhI}(\text{OR})_2$  which functions as the oxidant in these transformations.<sup>50</sup>

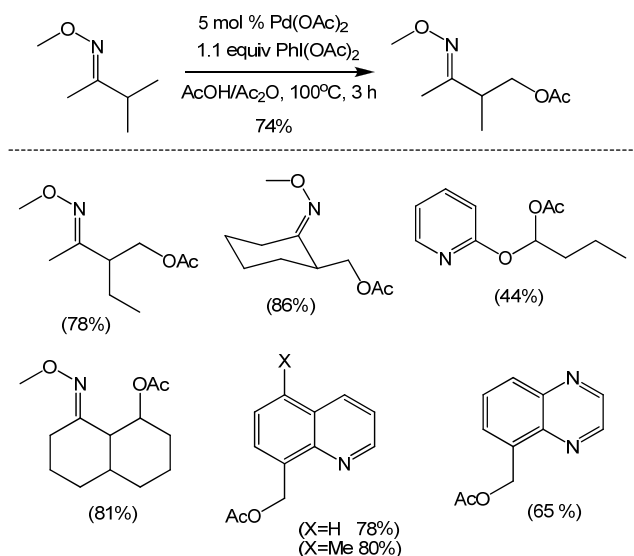
**Scheme 6.2**



The palladium catalyzed acetoxylation reaction using  $\text{PhI}(\text{OAc})_2$  as the terminal oxidant has also been applied to aliphatic C–H bonds as shown in Scheme 3 below.<sup>33,50,128</sup> In this transformation, both benzylic and unactivated  $\text{sp}^3$  C–H bonds were converted to the corresponding alkyl acetates, and no products from  $\beta$ -hydride elimination were observed. The reactions also proceeded with high selectivity for

primary vs. secondary C–H bonds, and compounds that form 5-membered palladacycles were favored over those that form 6-membered palladacycles. Although the functionalization of secondary and tertiary C–H bonds was not efficient in this system, secondary C–H bonds adjacent to activating groups were acetoxylation (Scheme 6.3).

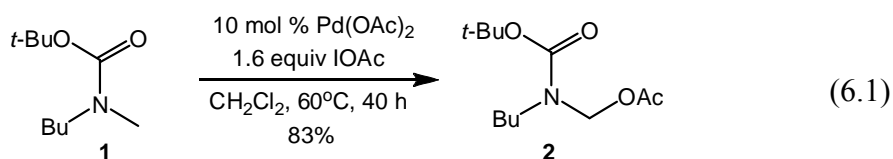
**Scheme 6.3**



The palladium catalyzed transformations using PhI(OR)<sub>2</sub> as oxidant were proposed to involve the Pd(II)/Pd(IV) redox couple. The mechanism proposed involves ligand-directed cyclometalation at Pd(II) to produce cyclopalladated intermediate, which undergoes two-electron oxidation to produce a monomeric Pd(IV) species. Subsequent C–O reductive elimination from the Pd(IV) species releases the product and regenerates the catalyst.<sup>50,57,58</sup> The intermediacy of dimeric Pd(III) intermediates in these reactions has also been considered by Ritter and co-workers.<sup>46,59,127</sup>

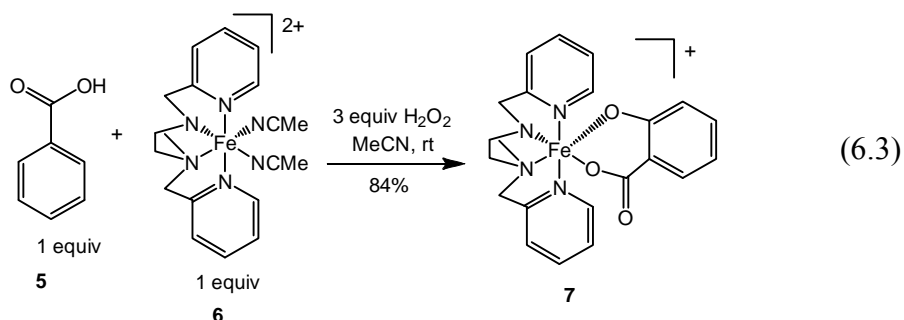
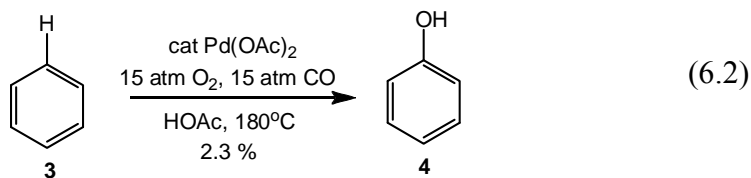
Iodine(I) oxidants have also been applied as oxidants in the acetoxylation of sp<sup>3</sup> C–H bonds. The IOAc oxidant was used in the palladium catalyzed acetoxylation

of Boc-protected *N*-methylamine derivatives (eq. 6.1).<sup>62</sup> This oxidant is generated in situ by the reaction of I<sub>2</sub> with either PhI(OAc)<sub>2</sub> or AgOAc. In this system, no reaction was observed when either PhI(OAc)<sub>2</sub> or I<sub>2</sub> was used independently. High selectivity was observed for the functionalization of N-CH<sub>3</sub> over N-aryl substituents. The mechanism of this reaction was proposed to involve amide directed C-H activation, followed by oxidation by IOAc to Pd(IV), C-I bond-forming reductive elimination, and ultimately nucleophilic displacement of I<sup>-</sup> by OAc<sup>-</sup> under the reaction conditions. Direct C-OAc elimination to generate the acetoxyated products was not ruled out.

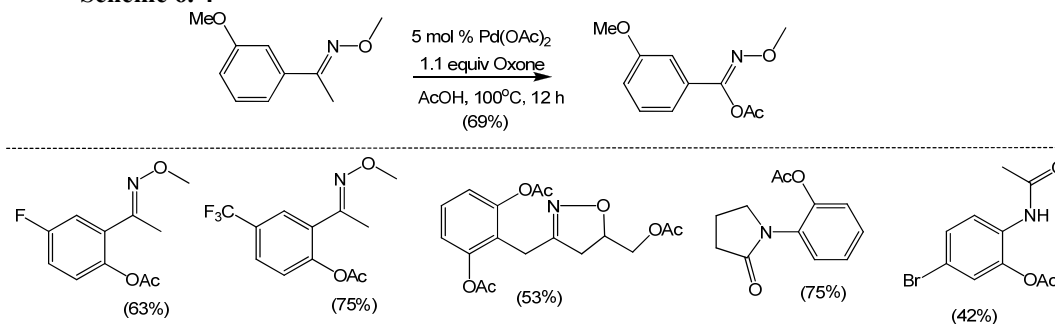


Given that the iodine based oxidants are relatively expensive and also produce stoichiometric amount of waste products, it would be more attractive to develop C-H functionalization reactions that utilize dioxygen and hydrogen peroxide, since these oxidants are inexpensive and benign to the environment. In addition, dioxygen and peroxide based oxidants will make the resulting transformations “greener” and more practical for large scale synthesis.<sup>33</sup> Such transformations however remain a significantly challenging task in both chemical industry and organic synthesis.<sup>63-67</sup> An early result on the palladium catalyzed hydroxylation of benzene using molecular oxygen was reported by Fujiwara and co-workers in 1990.<sup>68</sup> This transformation was however conducted under harsh reaction conditions and low yields were produced (eq. 6.2). In another study, Rybak-Akimova and Que reported the *ortho*-

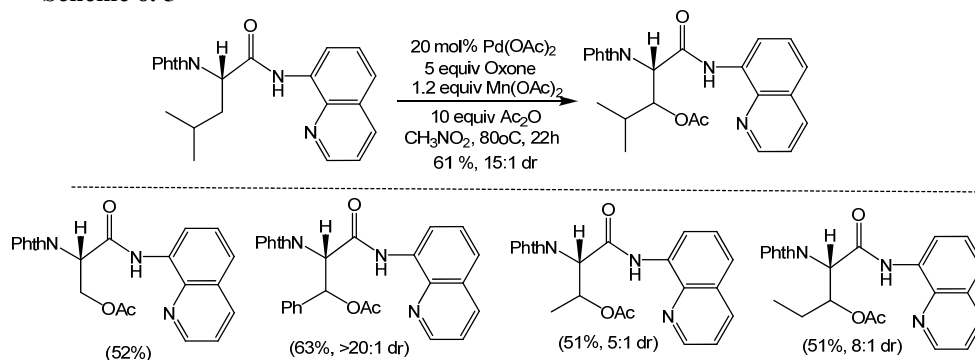
hydroxylation of benzoic acid with  $\text{H}_2\text{O}_2$  in the presence of a stoichiometric amount of a reactive iron complex  $[\text{Fe}(\text{II})(\text{BPMEN})(\text{CH}_3\text{CN})_2](\text{ClO}_4)_2$  **7** (eq. 6.3).<sup>69</sup>



Recently, more efficient palladium catalyzed reactions have been developed for the oxygenation of  $\text{sp}^3$  and  $\text{sp}^2$  C–H bonds using various peroxide-based oxidants. In 2006, Sanford and co-workers reported a palladium catalyzed acetoxylation of aromatic C–H bonds using Oxone as terminal oxidant in acetic acid solvent.<sup>33</sup> The inorganic peroxides were proposed to oxidize Pd(II) to Pd(IV) while the solvent was proposed to be the source of oxygen functionality. Substrates with a variety of directing groups including oxime ethers, amides, and isoxazolines reacted in acetic acid solvent to afford aryl esters,<sup>70</sup> and in alcohol solvents to afford aryl ethers (Scheme 6.4).<sup>33</sup>

**Scheme 6.4**

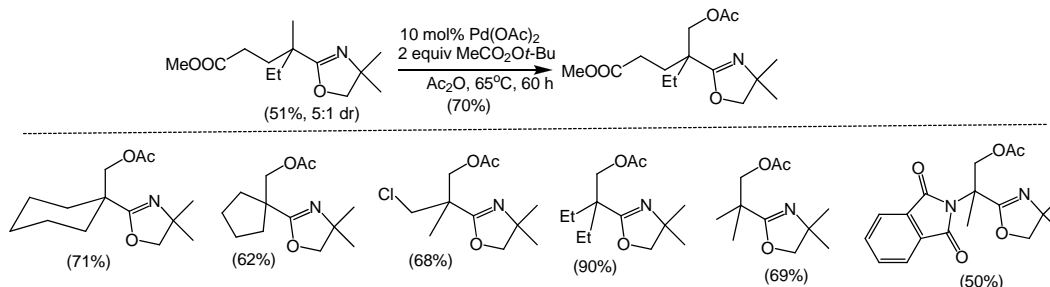
While Oxone and K<sub>2</sub>S<sub>2</sub>O<sub>8</sub> were effective oxidants for the oxygenation of aromatic C–H bonds, only modest activity was observed when these oxidants were used for the oxygenation of aliphatic C–H bonds.<sup>33</sup> The combination of Oxone with Mn(OAc)<sub>2</sub> however promoted efficient oxygenation of secondary sp<sup>3</sup> C–H bonds in amidoquinolines (Scheme 6.5).<sup>71</sup> The authors proposed that the reaction between Mn(OAc)<sub>2</sub> and Oxone affords Mn<sub>3</sub>O(OAc)<sub>7</sub>, which then functions as a Lewis acid to increase the reactivity of the Pd(II) catalyst.

**Scheme 6.5**

*Tert*-butyl peroxyacetate has also been used as terminal oxidant for the palladium catalyzed oxygenation of aliphatic C–H bonds (Scheme 6.6).<sup>72</sup> Acetic anhydride was an important additive in this reaction, where it was proposed to increase the catalytic turnover. Oxazolines were used as directing groups, and the

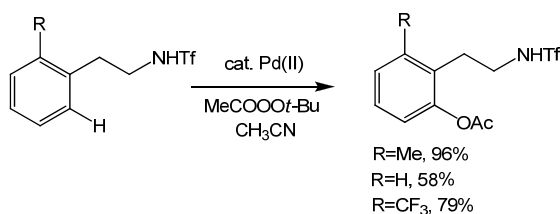
reaction conditions applied were compatible with ketals, imides, esters, and alkyl chlorides. A Pd(II)/Pd(IV) catalytic cycle was proposed.

**Scheme 6.6**



The *tert*-butyl peroxyacetate oxidant has also been utilized for the acetoxylation of aromatic C–H bonds.<sup>73</sup> In 2010, Jin-Quan Yu and co-workers reported a palladium catalyzed acetoxylation of phenylalanine and ephedrine derivatives with *tert*-butyl peroxyacetate as terminal oxidant in dichloroethane solvent (Scheme 6.7). In this transformation, additives such as DMF, acetonitrile, acetic acid and acetic anhydride were used to increase the yields. The role of these additives was however not discussed.

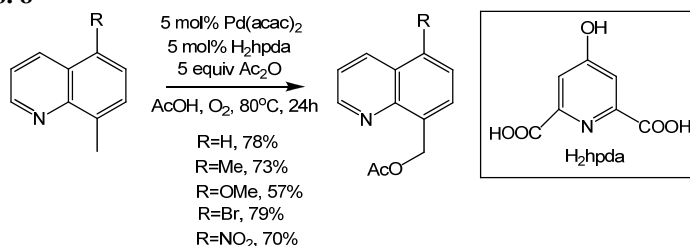
**Scheme 6.7**



Dioxygen has also been used as a terminal oxidant in palladium catalyzed oxygenation of both aliphatic and aromatic C–H bonds. In the acetoxylation of aliphatic C–H bonds, our group reported a quinoline-directed transformation using dioxygen as the terminal oxidant (Scheme 6.8).<sup>82</sup> This transformation proceeded with Pd(acac)<sub>2</sub> as the catalyst in conjunction with a 2,6-pyridinedicarboxylate ligand in

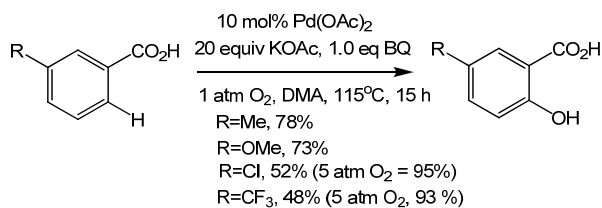
AcOH/Ac<sub>2</sub>O under an atmosphere of oxygen. This transformation was compatible with a wide array of substituents, including all aryl halides. The possibility of Pd(II)/Pd(IV) catalytic cycle where dioxygen acts as a terminal oxidation for the oxidation of Pd(II) to Pd(IV) was suggested.

**Scheme 6. 8**



Palladium catalyzed *ortho*-hydroxylation of potassium benzoates with dioxygen as the terminal oxidant in DMF, DMA and DMP was recently reported by Yu and co-workers (Scheme 6.9).<sup>83</sup> In this transformation, benzoquinone and bases such as KOAc and K<sub>2</sub>HPO<sub>4</sub> were found to increase the product yields. Labeling studies using <sup>18</sup>O<sub>2</sub> and H<sub>2</sub><sup>18</sup>O supported a direct oxygenation of the arylpalladium intermediates instead of an acetoxylation/hydrolysis sequence.

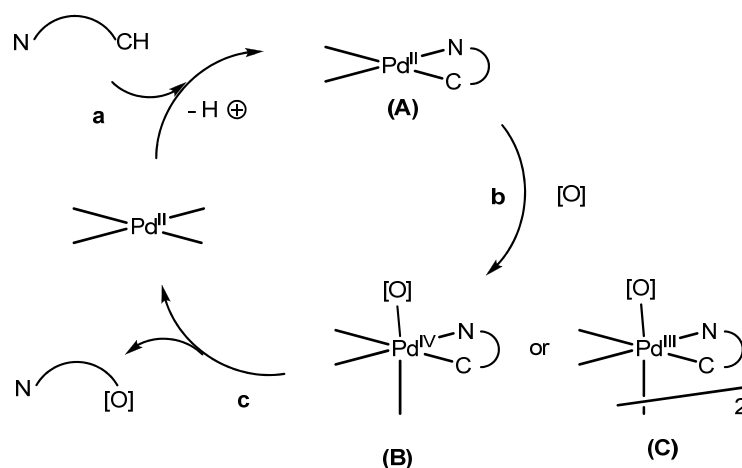
**Scheme 6. 9**



Given that very few palladium catalyzed C–H functionalization reactions utilizing molecular oxygen and/ or hydrogen peroxide oxidants have been developed, our ultimate goal has been to develop mild, efficient, and environmentally friendly catalytic C–H functionalization reactions utilizing molecular oxygen or hydrogen peroxide as terminal oxidants. Our approach involves the use of facially chelating

tridentate ligands to aid in these transformations. Stoichiometric studies have shown that bidentate ligands which can adopt a tridentate, facially chelating mode such as the 2-dipyridylmethanesulfonate (dpms) or 2-dipyridylketone (dpk) ligands enable functionalization of C–Pd bonds using hydrogen peroxide as oxidant.<sup>233</sup> These organometallic reactions have been shown to proceed via the Pd(II)/Pd(IV) redox cycle, and thus the corresponding palladium catalyzed C–H functionalization reactions in the presence of such ligands may also proceed via the Pd(II)/Pd(IV) catalytic cycle. This is important because under the Pd(IV) catalysis, common problems associated with the Pd(II) catalysis such as  $\beta$ -hydride elimination and the decomposition of Pd black from Pd(II) are usually eliminated. In addition, many functional groups are tolerated such as aryl halides, which are generally not usually tolerated under the Pd(0)/Pd(II) catalysis.<sup>43</sup>

**Scheme 6.10**



We aim to develop efficient aromatic C–H bond oxygenation reactions by conducting each of the steps depicted in Scheme 6.10 above, under similar reaction conditions. According to this Scheme, the C–H bond functionalization reaction is proposed to proceed via (a) C–H activation to produce cyclopalladated species **A**.

Stoichiometric ligand-directed C–H activation reactions to produce cyclopalladacyclic complexes have been demonstrated in literature.<sup>17</sup> The following step (b) involves oxidation of the palladacycle to produce a high-valent palladium intermediate **B** or **C**. The oxidation of organopalladium(II) compounds to generate monomeric Pd(IV)<sup>118</sup> or dimeric Pd(III)<sup>127</sup> complexes has been demonstrated using strong oxidants such as NCS or PhIX<sub>2</sub>. The functionalization of C–Pd bonds using peroxide based oxidants such as MCPBA,<sup>74-77</sup> tert-butylhydroperoxide in the presence of a vanadium catalyst,<sup>120</sup> and hydrogen peroxide in the presence of an iron catalyst<sup>121</sup> have also been demonstrated. Most of these reactions were proposed to proceed via Pd(IV) intermediates, although these species were not detected in the solution. The final step in the catalytic cycle involves C–O reductive elimination from the high valent palladium complexes (step c) to release the product and regenerates the catalyst. This step has also been demonstrated.<sup>132</sup>

Given that we aim to develop palladium catalyzed C–H functionalization reactions using hydrogen peroxide as the terminal oxidant, we started our work by exploring the oxidation of C–Pd bonds using H<sub>2</sub>O<sub>2</sub>, and the subsequent C–O reductive elimination step. Since very few examples of C–Pd bond functionalization using hydrogen peroxide as oxidant have been reported in literature,<sup>81,121</sup> we started by investigating the oxidation reaction of monohydrocarbyl Pd(II) complexes to their Pd(IV) analogues using the di(2-pyridyl)ketone (dpk) and 6-(pyridin-2-ylcarbonyl)pyridine-2-carboxylic acid (ppc) ligands (see chapters 2 and 5). In these studies, dpk- and ppc-ligated organopalladium(II) complexes were observed to undergo oxidation with H<sub>2</sub>O<sub>2</sub> in water and acetic acid solvents to generate the

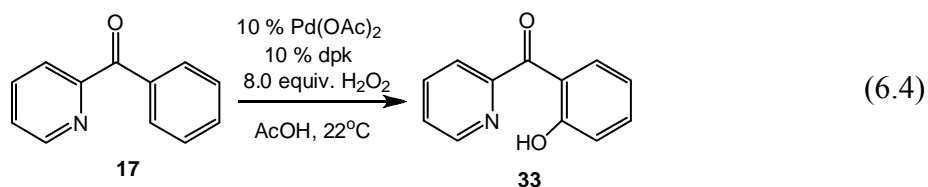
corresponding hydroxy-ligated monohydrocarbyl Pd(IV) species. These complexes were observed to undergo C–O bond-forming reductive elimination in acidified water to produce the corresponding phenol or a mixture of phenol and aryl acetate in acetic acid solvent. In the absence of the dpk and ppc ligands, the oxidation reaction of the analogous acetato-bridged palladacycles was too slow, indicating that the dpk and ppc ligands are required for efficient functionalization of C–Pd bonds.

As a result, our goal is to perform C–H functionalization reactions with Pd(OAc)<sub>2</sub> as catalyst in the presence of potentially tridentate, facially chelating ligand such as dpk, ppc, and dpms with H<sub>2</sub>O<sub>2</sub> as oxidant. This catalytic reaction will combine the C–H activation ability of Pd(OAc)<sub>2</sub> and the C–Pd bond functionalization ability of the dpk ligand with H<sub>2</sub>O<sub>2</sub> as oxidant.

## 6.2 Results and Discussion

We started by attempting C–H bond oxygenation of the 2-benzoylpyridine substrate **17** with Pd(OAc)<sub>2</sub> in the presence of the di(2-pyridyl)ketone (dpk) ligand and H<sub>2</sub>O<sub>2</sub> as oxidant (eq. 6.4). This ligand was used because it had enabled C–Pd bond functionalization of palladacycles derived from 2-benzoylpyridine using H<sub>2</sub>O<sub>2</sub> in acetic acid. We combined 0.10 mmoles of compound **17**, 0.010 mmoles of Pd(OAc)<sub>2</sub> and 0.010 mmoles of the dpk ligand in 1.0 ml of deuterated acetic acid. 1,4-dioxane was added and a <sup>1</sup>H NMR spectrum of the resulting solution was collected at room temperature. 1.0 equivalents of H<sub>2</sub>O<sub>2</sub> oxidant were added and the resulting solution was stirred at room temperature. 1.5 more equivalents of H<sub>2</sub>O<sub>2</sub> were added after 2 hours, and 3 more batches of 1.5 equivalents of H<sub>2</sub>O<sub>2</sub> were added after every 4 hours. The solution was stirred at room temperature for a total of ~24 hours and a <sup>1</sup>H

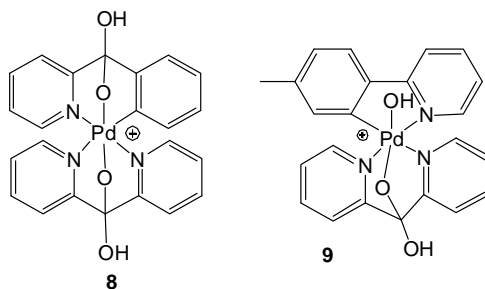
NMR spectrum was collected at the end of the reaction. The spectrum revealed the presence of the corresponding phenol **33** in 2.5 %  $^1\text{H}$  NMR yield relative to the internal standard. The identity of the phenol **33** was confirmed by comparison of the  $^1\text{H}$  NMR spectrum to literature.<sup>237</sup> The reaction was repeated in acetic acid in the presence of 5 equivalents of acetic anhydride in order to simplify the spectrum. The corresponding aryl acetate **34** was observed by  $^1\text{H}$  NMR in  $\sim 5\%$   $^1\text{H}$  NMR yield relative to an internal standard. The identity of compound **34** was confirmed by independent synthesis via acetoxylation of compound **33** in AcOH/Ac<sub>2</sub>O (1:1) solvent mixture. The compound was characterized by NMR spectroscopy and electrospray ionization mass spectrometry techniques.



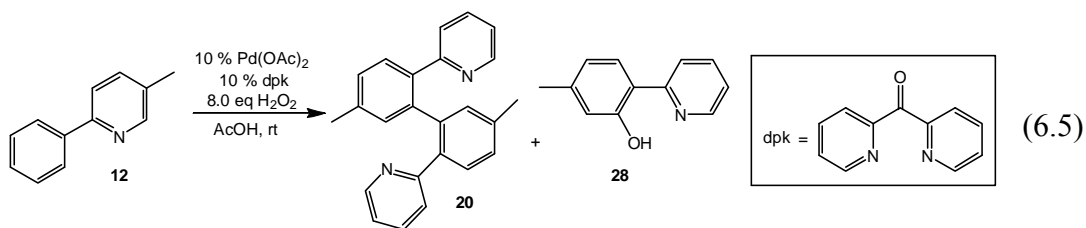
These results indicate that oxygenation of C–H bonds using Pd(OAc)<sub>2</sub> catalyst in the presence of dpk ligand is possible, but the reaction is slow under the present reaction conditions. The slow reactivity of the 2-benzoylpyridine compound **17** towards functionalization with Pd(OAc)<sub>2</sub> in the presence of the dpk ligand might result from the ability of both benzoylpyridine and dpk ligand to produce tridentate facially chelating ligands that would stabilize a Pd(IV) intermediate species. Hydrocarbyl Pd(IV) complexes stabilized by bis-anionic facially chelating ligands such as complex **8** (chart 6.1) have been observed to be very stable, such that they can be stored at room temperature for more than two weeks without decomposition.<sup>233</sup> In contrast, analogous Pd(IV) complexes stabilized by a single

tridentate facially chelating ligand such as complex **9** (chart 1) have been found to be less stable, where they undergo decomposition at room temperature in the solid state, and are thus stored at  $-20^{\circ}\text{C}$  in the solid state.

Chart 6.1

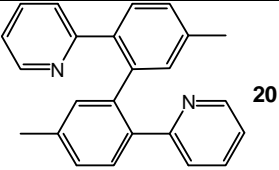
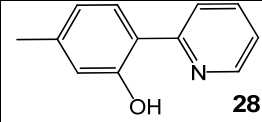
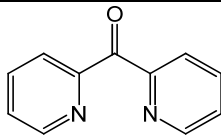
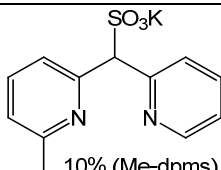
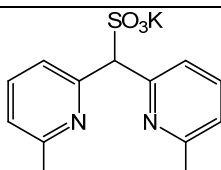


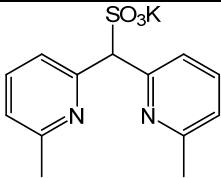
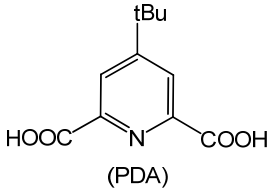
As a result, we attempted palladium catalyzed oxygenation of 2-tolylpyridine compound **12** in order to determine whether this compound would react faster than compound **17**, given that this substrate can only bind palladium via a bidentate coordination mode. A 0.10 M AcOD solution of complex **12** with 10 % dpk and 10 % Pd(OAc)<sub>2</sub> catalyst was prepared in the presence of 1,4 dioxane as internal standard, 8.0 equivalents of H<sub>2</sub>O<sub>2</sub> were added as described previously, and the reaction was monitored at room temperature over a period of 22 hours via <sup>1</sup>H NMR. At the end of the reaction, the C–C coupling compound 2-(5,5'-dimethyl-2'-pyridin-2-yl-1,1'-biphenyl-2-yl)pyridine **20** was produced as the major reaction product in 12.1 % yield and the C–O coupling compound 5-methyl-2-pyridine-2-ylphenol **28** was generated as a minor product in 2.0 % yield (eq. 6.5), while a 17% conversion of compound **12** was observed relative to the internal standard. The major product was identified as **20** while the minor product was identified as **28** by comparison of their <sup>1</sup>H NMR spectra to literature.<sup>21,207</sup>



Given the successful C–H functionalization of compound **12** to give **20** and **28**, we aimed to increase the yield of product **28** by using ligands that kinetically stabilize Pd(IV) intermediates to a lesser extent than the dpk ligand. A variety of ligands were examined (See table 6.1 below).

**Table 6. 1.** Palladium catalyzed C–H bond functionalization using H<sub>2</sub>O<sub>2</sub> as terminal oxidant in the presence of various ligands.

Entry	Ligand		
1	NONE	17 %	3 %
2	 10 % (dpk)	12 %	2 %
3	 10% (Me-dpms)	2 %	~1 %
4	 10% (Me <sub>2</sub> -dpms)	58 %	8 %

5	 5% (Me <sub>2</sub> -dpms)	29 %	4 %
5	 (PDA)	60 %	8 %

\*Reaction conditions applied include 0.10 mol of compound 12, 1.0 ml of AcOD, 10 mol % Pd(OAc)<sub>2</sub>, 10 mol % ligand, 8.0 equivalents of H<sub>2</sub>O<sub>2</sub>, 22°C, and 24 hours reaction time. <sup>1</sup>H NMR yields are reported relative to an internal standard.

The most efficient ligands are the Me<sub>2</sub>-dpms and PDA, which give the C–C coupling product **20** in 58 % and 60 % yields respectively and the C–O coupling product **28** in 8 % yields each. As a result, the Me<sub>2</sub>-dpms ligand was used in the subsequent transformations.

In order to increase the reaction rate, the temperature of the reaction solution was raised. The reaction solutions were prepared as described before. The solutions were placed in constant temperature oil baths set at either 35°C or 50°C in order to determine the optimum temperature for the catalytic reaction. Into these solutions, 2.0 equivalents of H<sub>2</sub>O<sub>2</sub> were added immediately, another 2.0 equivalents were added after 1 hour, and after every two hours for a total of 8.0 equivalents of H<sub>2</sub>O<sub>2</sub>. The results are presented in the table 6.2 below.

**Table 6. 2.** Palladium catalyzed *ortho* C–H bond functionalization of compound **12** in acetic acid using H<sub>2</sub>O<sub>2</sub> as terminal oxidant in the presence of Me<sub>2</sub>-dpms ligand, showing relative fractions of C–C and C–O coupling products as a function of temperature.

Entry	Conversion of <b>12</b>	R–R ( <b>20</b> )	R–OH ( <b>28</b> )	Temp
1	68.0 ± 1	58 ± 0.5	8.0 ± 0.5	25°C
2	70 ± 0.5	57.0 ± 0.5	9.0 ± 0.5	35°C
3	55 ± 0.5	46 ± 0.5	6.0 ± 0.5	50°C

\*The reactions were carried out using 0.10 M AcOD solutions of **12**, 10 % Pd(OAc)<sub>2</sub>, 10% Me<sub>2</sub>-dpms ligand, and 8.0 equivalents of H<sub>2</sub>O<sub>2</sub> at 22°C, 35°C, and 50°C.

According to table 6.2 above, the highest conversion was obtained at 35°C, while a lower conversion was observed at 50°C. As a result, 35°C was used for the subsequent reactions.

The catalyst loading was also optimized. The reaction solution was prepared as described previously but different amounts of Pd(OAc)<sub>2</sub> and Me<sub>2</sub>-dpms were used as shown on the table below.

**Table 6. 3.** Palladium catalyzed *ortho* C–H bond functionalization of compound **12** in acetic acid using H<sub>2</sub>O<sub>2</sub> as terminal oxidant in the presence of Me<sub>2</sub>-dpms ligand, showing the conversion of compound **12** and yield of compound **20** as a function of catalyst loading.

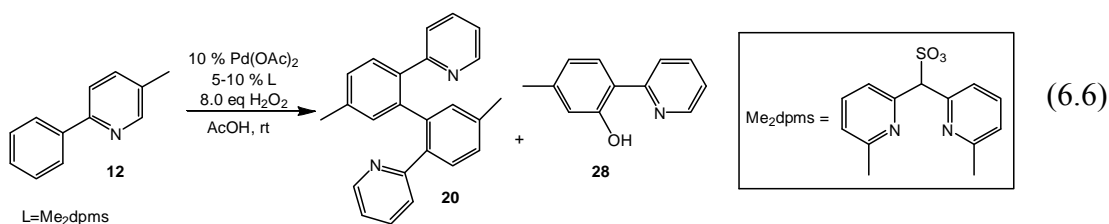
Pd(OAc) <sub>2</sub> = Me <sub>2</sub> -dpms (%)	% yield of <b>20</b>	Conversion of <b>12</b> (%)
5	18	32
10	47	65
15	38	62
20	42	65

\*The reactions were carried out using 0.10 M AcOD solutions of **12**, 5-20 % Pd(OAc)<sub>2</sub>, 5-20% Me<sub>2</sub>-dpms ligand, and 8.0 equivalents of H<sub>2</sub>O<sub>2</sub> at 35°C.

According to table 6.3, use of 5% catalyst gives a conversion of 32 %, while 10% catalyst loading gives a conversion of 65%. Increase of the catalyst loading from 10-20 % does not significantly change the conversion. As a result, 10 % catalyst loading was used for the subsequent transformations.

Therefore, the optimized conditions include the use of 10 % Pd(OAc)<sub>2</sub> as catalyst, 10 % Me<sub>2</sub>-dpms ligand in acetic acid solvent, the oxidant is added in 2.0 equivalent batches immediately upon combining the reagents, 1 hour later, and after every 2.0 hours for a total of 8.0 equivalents. The reactions were also be conducted for 7 hours.

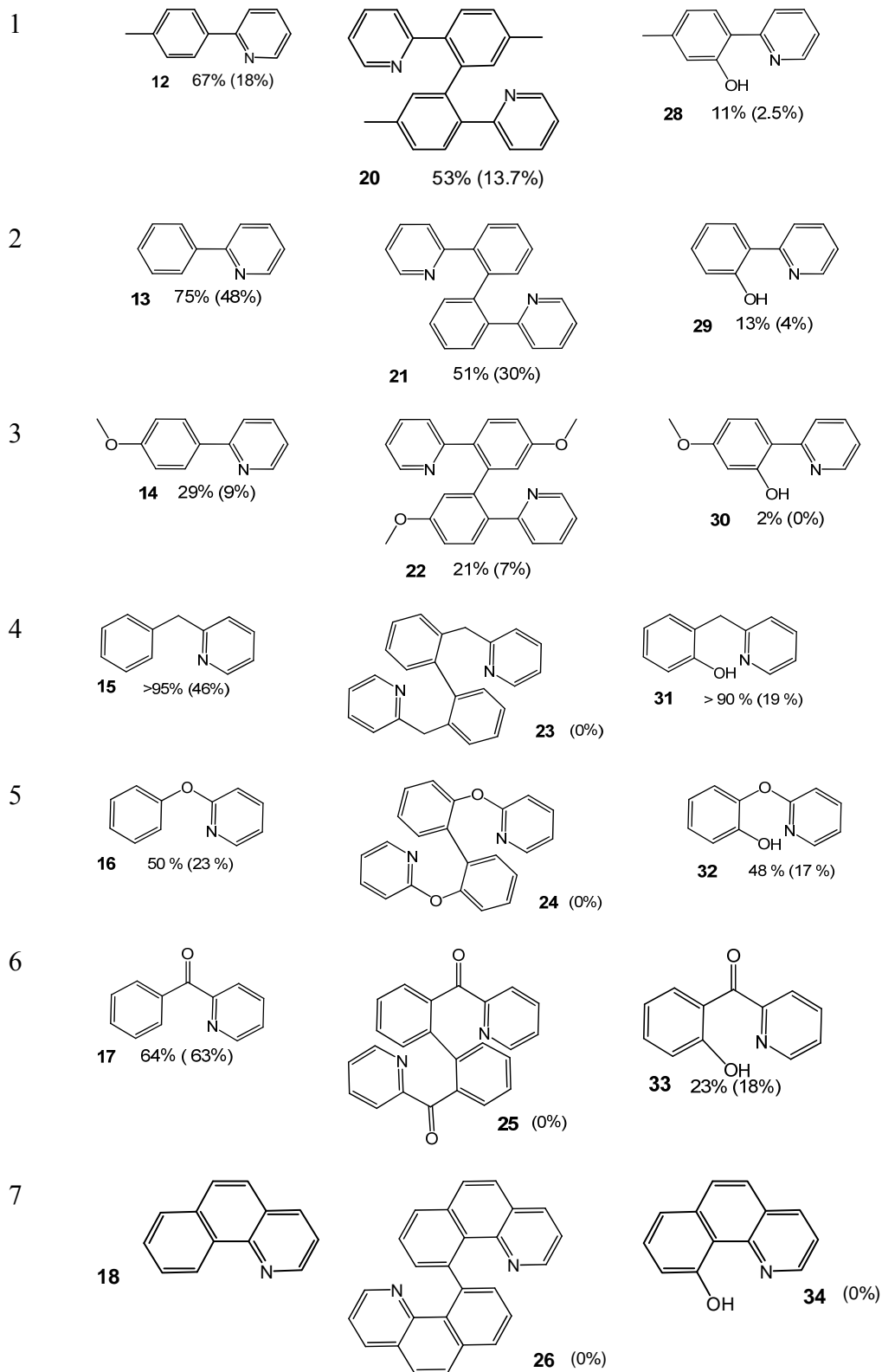
The scope and selectivity of the oxidative C–H bond functionalization reaction with 10 % Pd(OAc)<sub>2</sub> in the presence of Me<sub>2</sub>-dpms ligand, in acetic acid, with H<sub>2</sub>O<sub>2</sub> as oxidant was investigated for a wider array of substrates with N-donor directing groups. As summarized in table 6.4, the functionalization of phenylpyridine-derived substrates yielded predominantly C–C bond coupling products, while substrates which can form 6-membered rings with palladium produced the corresponding C–O bond coupling products predominantly.

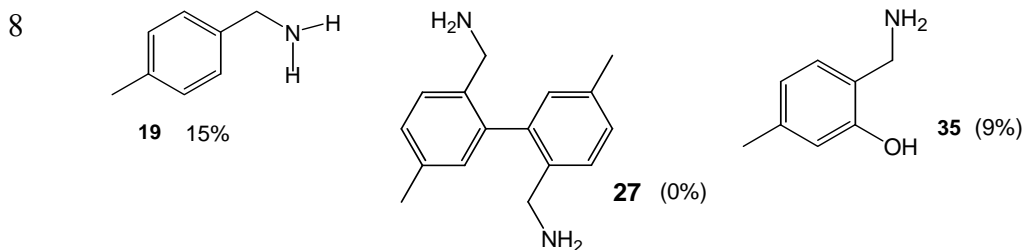


**Table 6. 4.** Palladium catalyzed *ortho* C–H bond functionalization in acetic acid using H<sub>2</sub>O<sub>2</sub> as terminal oxidant in the presence of Me<sub>2</sub>-dmps ligand

Substrate	% R-R	% R-OH
-----------	-------	--------

Entry





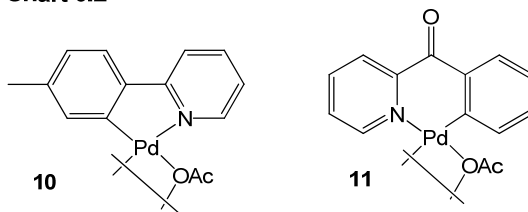
\* Reaction conditions include 0.10 M AcOD solution, 10 mol % Pd(OAc)<sub>2</sub>, 10 mol % Me<sub>2</sub>-dpms ligand, 8.0 equivalents of H<sub>2</sub>O<sub>2</sub>, 35°C for entries 1-3, 50°C for entries 4-8, 7 hours reaction time each. The conversions and yields in the parentheses represent reactions in the absence of the ligand. The entries below compounds **12-19** represent the <sup>1</sup>H NMR % conversions relative to an internal standard while the entries below the products **20-34** represent the <sup>1</sup>H NMR % product yield relative to an internal standard.

The substituted phenylpyridine compounds **12-14** produce the corresponding C–C coupling products **20-22** predominantly, while phenols **28-30** are produced as minor products. The identity of compounds **20-22** and **28-30** was confirmed by isolation of the compounds and comparison of the <sup>1</sup>H NMR to literature reports. No doubly hydroxylated products are observed by ESI–MS.

The preference of C–C over C–O coupling in the reaction of compounds **12-14** indicates that a different mechanism might be operative in this reaction relative to that involving compounds **15-17**, where the C–O coupling product was preferred. The formation of C–C coupling products requires both hydrocarbyl ligands to be coordinated onto the palladium center, since reductive elimination from Pd(II) and Pd(IV) has been proposed to take place via 3-center, 4-electron transition state.<sup>45</sup> Consequently, the size of the metacycle produced upon C–H activation might play an important role in this reaction. In contrast, the C–O reductive elimination reaction requires the hydrocarbyl and the alkoxy ligands to be coordinated on the palladium center, and considering the small size of the alkoxy ligand, the size of the metacycle might not be important in this case. Given that compounds **12-14** form 5-membered

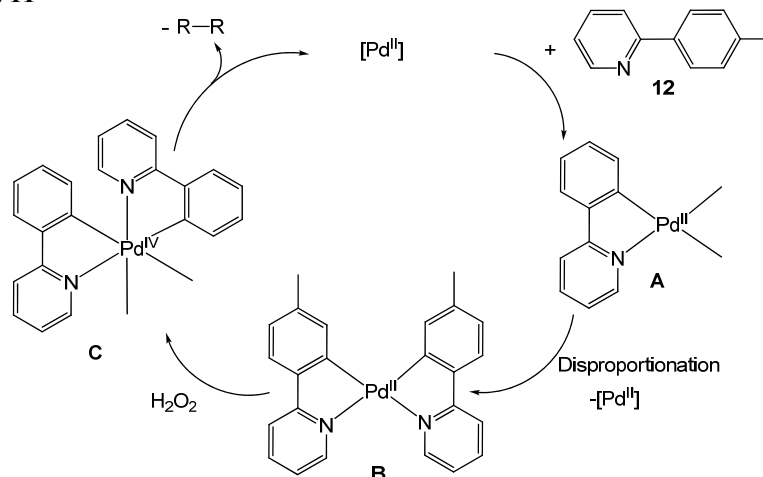
palladacycles upon cyclometalation while compounds **15-17** produce 6-membered palladacycles, the smaller size of the 5-membered palladacycles such as **10** might allow for two hydrocarbyls to be coordinated onto the palladium center at the same time, thus allowing for C–C coupling to take place, while the larger size of 6-membered palladacycles such as **11** might not allow for another hydrocarbyl to be coordinated onto the palladium center, thus preventing the C–C coupling reaction.

**Chart 6.2**



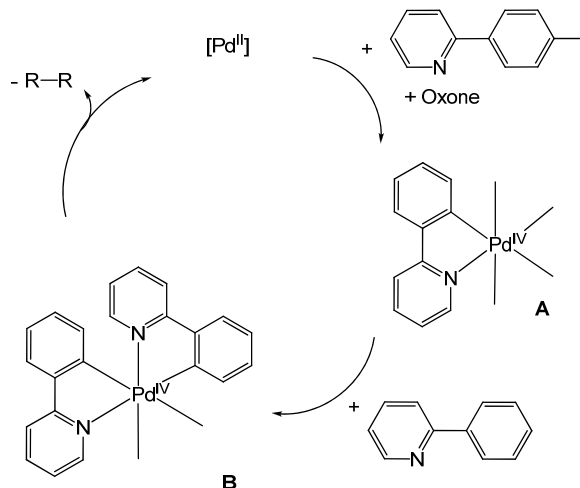
We thus propose a C–C coupling mechanism depicted in Scheme 6.11 below, where cyclometalation of compound **12** produces a palladacyclic complex of structure **A**. This complex is not reactive towards  $\text{H}_2\text{O}_2$  in acetic acid, given that no reaction was observed in the stoichiometric oxidation of complex **10** with 8.0 equivalents of  $\text{H}_2\text{O}_2$  in acetic acid in over 12 hours at room temperature.<sup>233</sup> Disproportionation of complex **A** produces a bis-hydrocarbyl Pd(II) complex of structure **B**. Given that complex **B** is more electron-rich than **A**, oxidation of **B** with  $\text{H}_2\text{O}_2$  is more facile, to generate a Pd(IV) complex with structure **C**. The oxidation of **B** with  $\text{PhI}(\text{OAc})_2$  to generate Pd(IV) complexes of structure **C** has been reported, and both C–C and C–O reductive elimination from this Pd(IV) complex have also been reported,<sup>57,58</sup> where C–C reductive elimination was proposed to take place via the 6-coordinate Pd(IV) complex while C–O reductive elimination was proposed to take place from a cationic 5-coordinate intermediate produced upon dissociation of an  $\text{OR}^-$  ligand.

Scheme 6.11



The C–C bond-forming reaction might also proceed through a mechanism similar to the palladium catalyzed arylation of aromatic C–H bonds using Oxone as oxidant, reported by Sanford and co-workers (Scheme 6.12).<sup>42</sup> This reaction was proposed to take place via C–H activation to generate a cyclopalladated intermediate, followed by oxidation of the palladacycle to a Pd(IV) species. This was followed by a second C–H activation reaction at the Pd(IV) center, and ultimately C–C bond-coupling reductive elimination to release the product and regenerate the catalyst (see Scheme 6.12). C–H activation at Pt(IV) centers<sup>63</sup> and other metals<sup>238</sup> have been reported. Given that C–C coupling products are generated in our system, a similar mechanism might be operative. However no detailed mechanistic studies were conducted for the C–C coupling reactions.

Scheme 6. 12

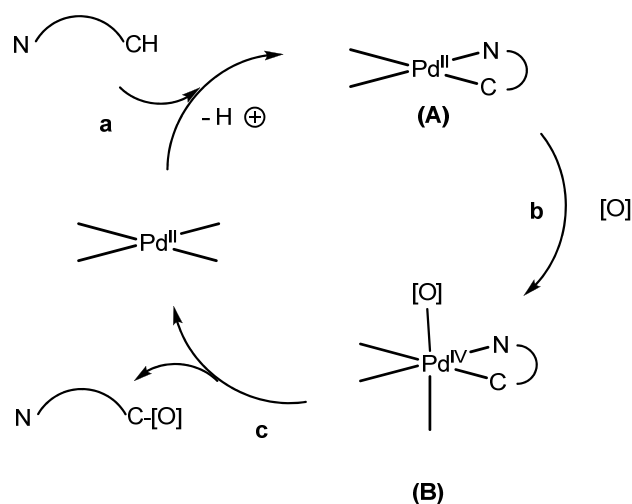


The palladium catalyzed functionalization of compounds **15-17** in the presence of the Me<sub>2</sub>-dpms ligand produces the corresponding phenolic **31-33** as the only products. The identity of these products was confirmed by ESI-MS, and comparison of their <sup>1</sup>H NMR data with literature reports. No C-C coupling products were detected in these reactions by either <sup>1</sup>H NMR spectroscopy or ESI-MS. In addition, no products of double C-H bond hydroxylation are detected in the ESI-MS analysis of the reaction solutions after the reaction. Products of double hydroxylation are however detected when the reaction of compound **15** is carried out in the absence of the ligand. In the absence of the Me<sub>2</sub>-dpms ligand, compound **15** undergoes C-H functionalization to produce the corresponding phenol in 19 % <sup>1</sup>H NMR yield, while another product is detected in 19 % yield. ESI-MS analysis of this reaction solution exhibits mass envelopes at m/z = 186.0874 which was assigned to the corresponding phenol **30** (calculated for C<sub>12</sub>H<sub>12</sub>NO = 186.0919), and m/z = 202.0834 which was assigned to the corresponding doubly *ortho*-hydroxylated compound **35** (Calculated for C<sub>12</sub>H<sub>12</sub>NO<sub>2</sub> = 202.0868). Thus, the second product may be a doubly hydroxylated

product **35**. The ligand is observed to increase the reaction rate, indicating that it is involved in the rate-limiting step.

We propose that the mechanism of C–O bond coupling is different from the mechanism of C–C coupling presented above (Scheme 6.13). According to Scheme 6.13, the proposed mechanism of C–H bond oxygenation begins by cyclopalladation of the aromatic compound to yield a dimeric acetato-bridged palladacycle of structure **A**.<sup>50,127</sup> Ligand enabled oxidation of complex **A** with H<sub>2</sub>O<sub>2</sub> produces Pd(IV) intermediate **B**. Ligand enabled oxidation of palladacycle **A** is proposed because stoichiometric reactions between the dimeric acetato-bridged palladacycle derived from phenoxy pyridine and H<sub>2</sub>O<sub>2</sub> in acetic at room temperature did not result in any reaction. The intermediate **B** undergoes C–O reductive elimination to release the product, and regenerate the catalyst.

**Scheme 6. 13**



For the benzoquinoline compound **17**, no changes were observed in the <sup>1</sup>H NMR spectrum, and no product of C–C or C–O coupling was detected by ESI–MS, indicating that the palladium catalyzed functionalization of this substrate is not facile.

The para-tolylbenzylamine compound **18** produced the corresponding monohydroxylated product **35** according to both <sup>1</sup>H NMR and ESI-MS.

### 6.3 Summary and Conclusion

In conclusion, we have achieved ligand-directed palladium catalyzed functionalization of aromatic C-H bonds using H<sub>2</sub>O<sub>2</sub> as oxidant, which are significantly accelerated by the Me<sub>2</sub>-dpms ligand. The substituted phenylpyridine compounds **12-14** underwent C-H bond functionalization to afford the corresponding C-C bond-coupling compounds **20-22** as major products while the C-O bond-coupling compounds **28-30** were produced as minor products. Complexes **15-17** underwent C-H bond functionalization to produce the corresponding C-O bond-coupling products **31-33**; no C-C bond-coupling products were detected in these reactions. Compound **18** did not undergo functionalization while **19** underwent oxygenation to give the corresponding phenol; no C-C coupling product was detected in this reaction.

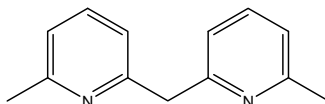
The mechanism of these reactions was not studied. The future goal will involve studying the mechanism of the C-C and C-O bond formation reactions, and optimize these catalytic transformations further. In addition, the substrate scope of these reactions needs to be increased.

## 6.4 Experimental

### 6.2

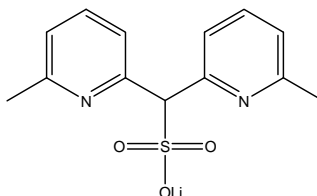
The identity of the compounds **20**,<sup>207</sup> **21**,<sup>207</sup> and **22**, and **28**,<sup>21</sup> **29**,<sup>239</sup> **30**,<sup>21</sup> **31**,<sup>240</sup> **32**,<sup>241</sup> and **33**<sup>157</sup> was confirmed by comparison of their <sup>1</sup>H NMR data to that reported in literature.

### Preparation of Li(Me<sub>2</sub>-dpms)



**Bis(6-methyl-2-pyridyl)methane, Me<sub>2</sub>-dpm**, was prepared as described previously.<sup>10</sup>

### Lithium bis(6-methyl-2-pyridyl)methanesulfonate



1.98g Me<sub>2</sub>-dpm (10 mmol) were dissolved in dry THF (20 mL) under argon in a Schlenk flask and cooled to -78°C. 1 eq of 2.5M *n*-BuLi was added dropwise to the solution while stirring. The solution temperature was raised to room temperature and after 2h 1 eq of SO<sub>3</sub>·NMe<sub>3</sub> was added. The Schlenk flask was then closed with a Teflon seal and the mixture was heated for 1 day at 120°C in an oil bath. After cooling to 0°C, the reaction was quenched with water. Ether was added and the remaining solid was filtered off. The solid was dissolved in water and the solution

neutralized with H<sub>2</sub>SO<sub>4</sub>. The solid resulting upon removal of water was extracted with ethanol. The product can be isolated from the ethanol solution and recrystallized from H<sub>2</sub>O to obtain 1.4 g of Li(Me<sub>2</sub>-dpms) (50% yield) as a crystalline, white solid.

<sup>1</sup>H NMR (22°C, D<sub>2</sub>O), δ: 8.12 (t, 2H, *J*=7.9Hz), 7.81 (d, 2H, *J*=7.9Hz), 7.61 (d, 2H, *J*=7.9Hz), 5.93 (s, 1H), 2.76 (s, 6H).

<sup>13</sup>C NMR (22°C, CD<sub>3</sub>OD), δ: 156.8, 150.3, 143.1, 126.4, 125.5, 66.9, 22.19.

ESI-MS of solution of **Li(Me<sub>2</sub>-dpms)** in water, negative mode: *m/z* = 277.0681; calculated for C<sub>13</sub>H<sub>13</sub>N<sub>2</sub>O<sub>3</sub>S = 277.0647.

## Chapter 7: Conclusion

### 7.1 Summary and Conclusion

In summary, the functionalization of C–Pd bonds enabled by dpk and ppc ligands using H<sub>2</sub>O<sub>2</sub> in various media to produce the corresponding oxapalladacycles, phenols, aryl acetates, and aryl halides has been demonstrated.

In particular, both the dpk and ppc ligands have been shown to enable oxidation of Pd(II) hydrocarbyls to the corresponding monohydrocarbyl Pd(IV) complexes in water and acetic acid solvents. These complexes were characterized in solution, and sometimes isolated in pure form and characterized fully, including X-ray diffraction. Pd(IV) monohydrocarbyls bearing two facially chelating tridentate ligands were observed to be significantly stable, where they could be stored at room temperature in the solid state for over two weeks without decomposition, while those bearing one facially tridentate ligand are less stable and have to be stored at –20°C.

The mechanism for the oxidation of Pd(II) monohydrocarbyls with H<sub>2</sub>O<sub>2</sub> was studied experimentally and computationally, and a mechanism that involves addition of H<sub>2</sub>O<sub>2</sub> across the C=O bond of the ligand, followed by nucleophilic attack by Pd(II) onto the hydroperoxide moiety leading to heterolytic cleavage of the O–O bond was proposed. Oxidation of ppc-supported organopalladium(II) complexes was proposed to take place via a similar mechanism, but these complexes were observed to undergo oxidation at a lower rate compared to their dpk-supported counterparts.

C–O reductive elimination from the monohydrocarbyl Pd(IV) complexes was conducted in both water and acetic acid solvents. Pd(IV) complexes bearing two

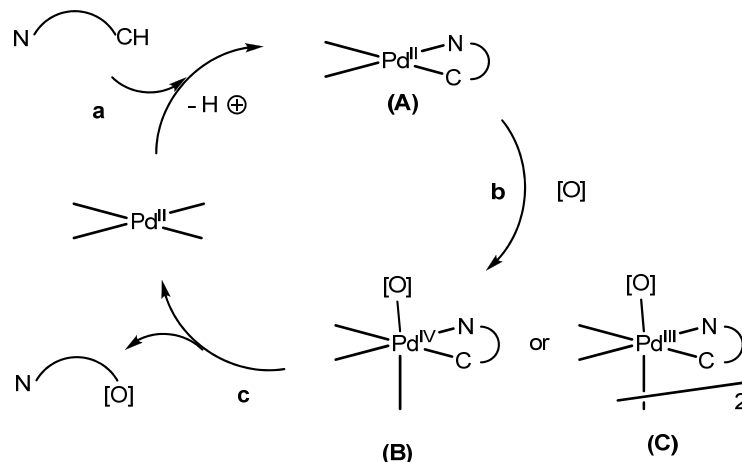
facially chelating tridentate ligands were less reactive towards C–O reductive elimination in water, where no reaction was observed in over two days at room temperature, while those bearing one facially chelating tridentate ligand were more reactive with formation of the corresponding oxapalladacycle quantitatively in under 24 hours. Both complexes however underwent clean C–O reductive elimination in acetic acid to produce the corresponding phenols and aryl acetates quantitatively in under two days. The mechanism of C–O reductive elimination in water was studied experimentally and computationally, and a mechanism that involves reductive elimination from a 6-coordinate Pd(IV) complex was proposed. This reaction was found to be insensitive to the substituents on the aromatic ring. Mechanistic studies on C–O reductive elimination in acetic acid were also performed, and a mechanism that involves pyridine group dissociation from the Pd(IV) coordination sphere, followed by reductive elimination from a 5-coordinate complex was proposed. Ppc-ligated Pd(IV) complexes were proposed to undergo C–O reductive elimination in acetic acid via a similar mechanism. These complexes were found to undergo faster reductive elimination reaction than their dpk-supported Pd(IV) counterparts.

When the hydroxy-ligated Pd(IV) complexes were dissolved in aqueous HX solutions ( $X = \text{Cl}, \text{Br}, \text{and I}$ ), the corresponding aryl halides were produced in high yields. The rates of C–X ( $X = \text{OH}, \text{Cl}, \text{and Br}$ ) reductive elimination from the corresponding Pd(IV)–X complexes were found to be similar, indicating that this process is not sensitive to the nature of the –X ligand. Given that the C–X reductive elimination process is not sensitive to the nature of the substituents on the aromatic

ring and the halide ligand, it was proposed that the transition state in these reactions is too early, leading to a near barrierless, exergonic reaction.

Ppc-ligand enabled C–H bond activation with Pd(II) was also demonstrated in neat and aqueous acetic acid solutions.

**Scheme 7. 1**



Consequently, each step in the oxidative palladium catalyzed C–H bond functionalization reaction depicted in Scheme 7.1, including (a) C–H bond activation, (b) oxidation of Pd(II) complexes using  $\text{H}_2\text{O}_2$ , and (c) C–X reductive elimination, has been demonstrated under similar reaction conditions. These steps were combined to produce environmentally benign, palladium catalyzed C–C and C–O bond-forming reactions utilizing  $\text{H}_2\text{O}_2$  as oxidant, and  $\text{Me}_2\text{-dpms}$  ligand. Substrates that form 5-membered palladacycles produced predominantly C–C coupling products while substrates which form 6-membered palladacycles predominantly produced C–O coupling products.

## 7.2 Future Work

The mechanism of the palladium catalyzed C–H bond functionalization reactions will be studied in order to improve the efficiency of these reactions, and increase the substrate scope.

The C–X bond-forming reductive elimination reactions will also be studied. The structure of the Pd(IV) complexes bearing various X ligands will be determined unambiguously using X-ray diffraction studies. The mechanism of C–X reductive elimination will also be studied, and palladium catalyzed C–X bond-forming reactions utilizing H<sub>2</sub>O<sub>2</sub> in aqueous HX solutions will be explored.

# Appendices

## NMR Spectra

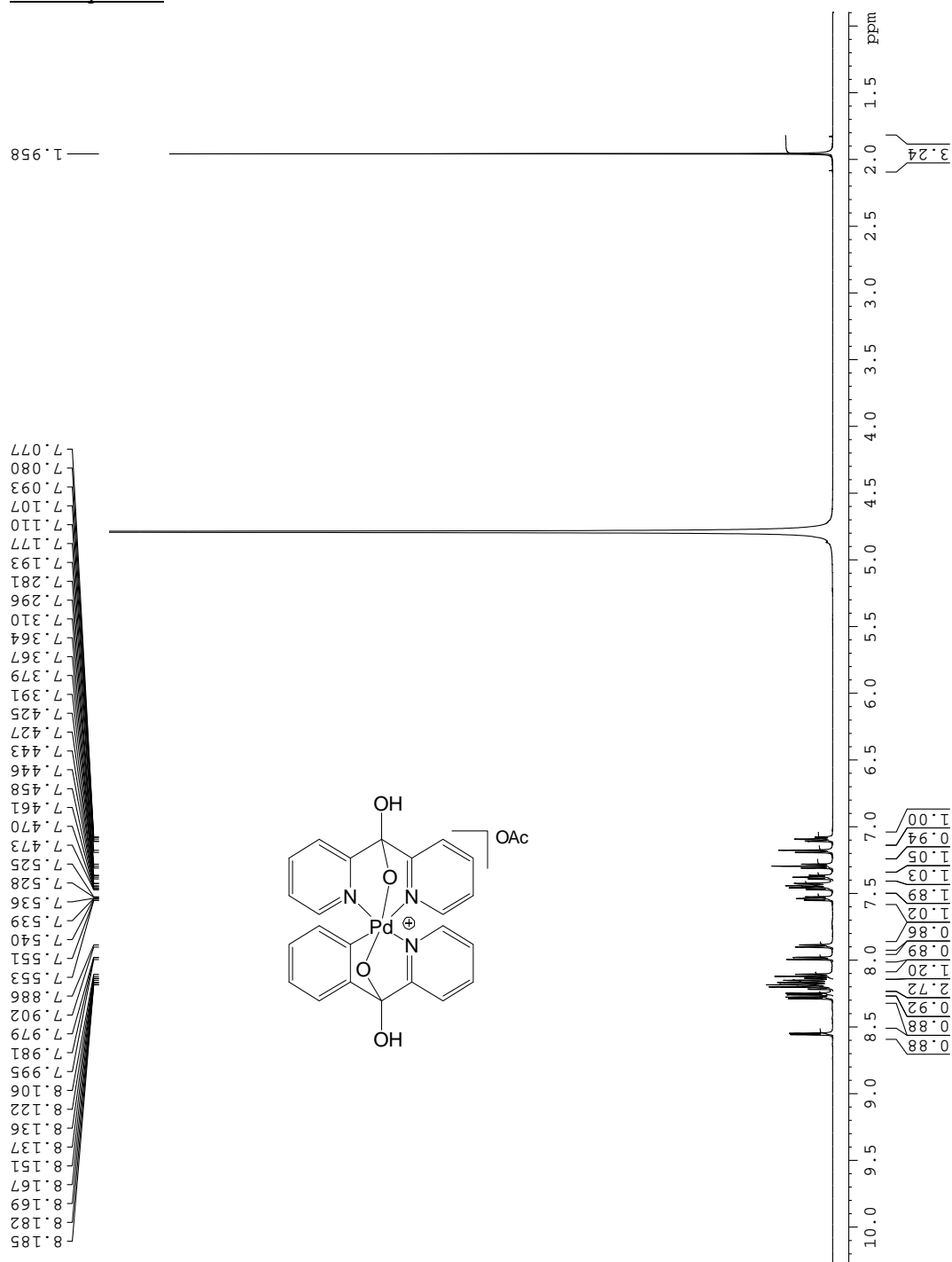


Fig. A1.  $^1\text{H}$  NMR spectrum of **75(OAc)** in  $\text{D}_2\text{O}$  at  $22\text{ }^\circ\text{C}$

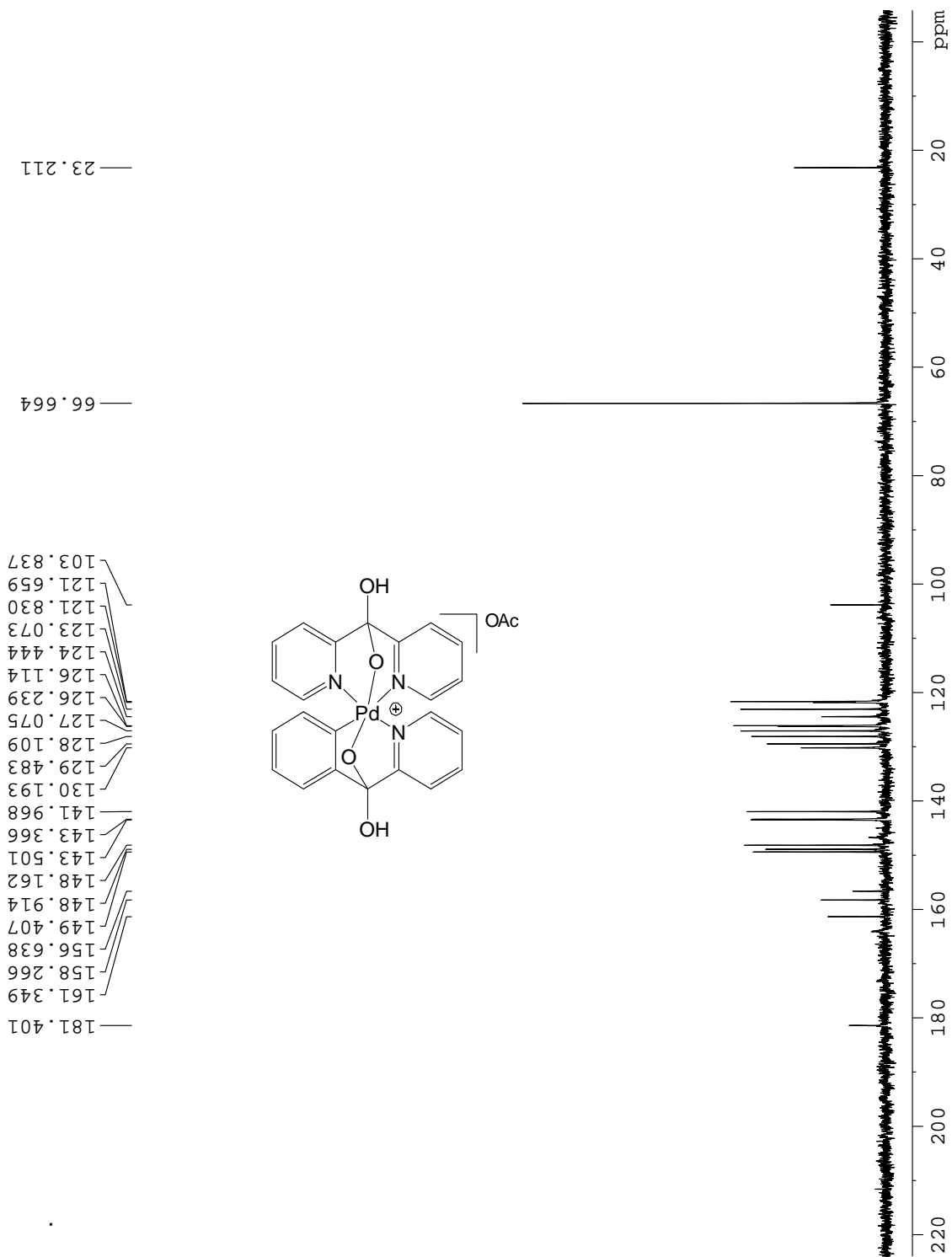


Fig. A2.  $^{13}\text{C}$  NMR spectrum of **75(OAc)** in  $\text{D}_2\text{O}$  at  $22^\circ\text{C}$

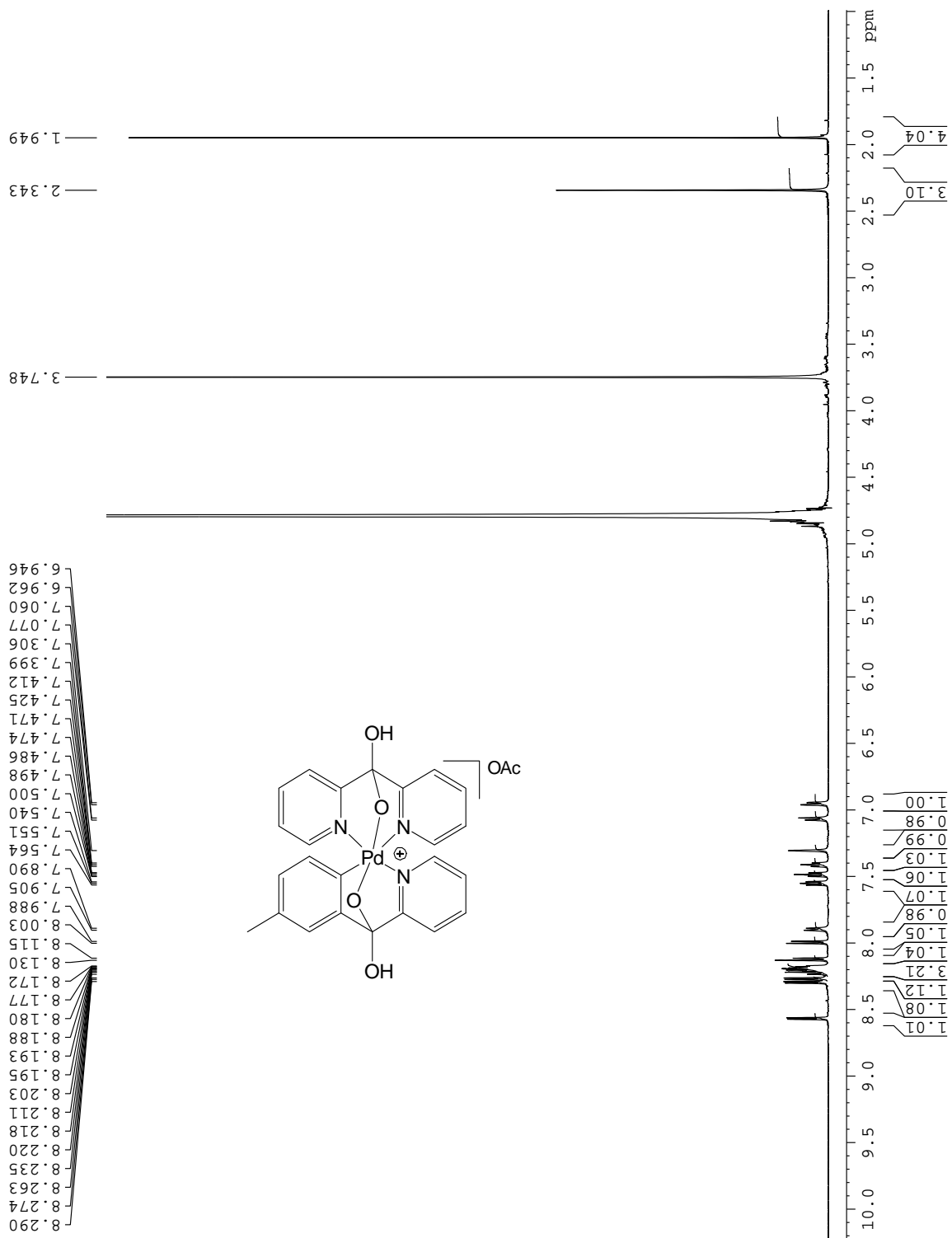


Fig. A3.  $^1\text{H}$  NMR of **76(OAc)** in  $\text{D}_2\text{O}$  at  $22^\circ\text{C}$

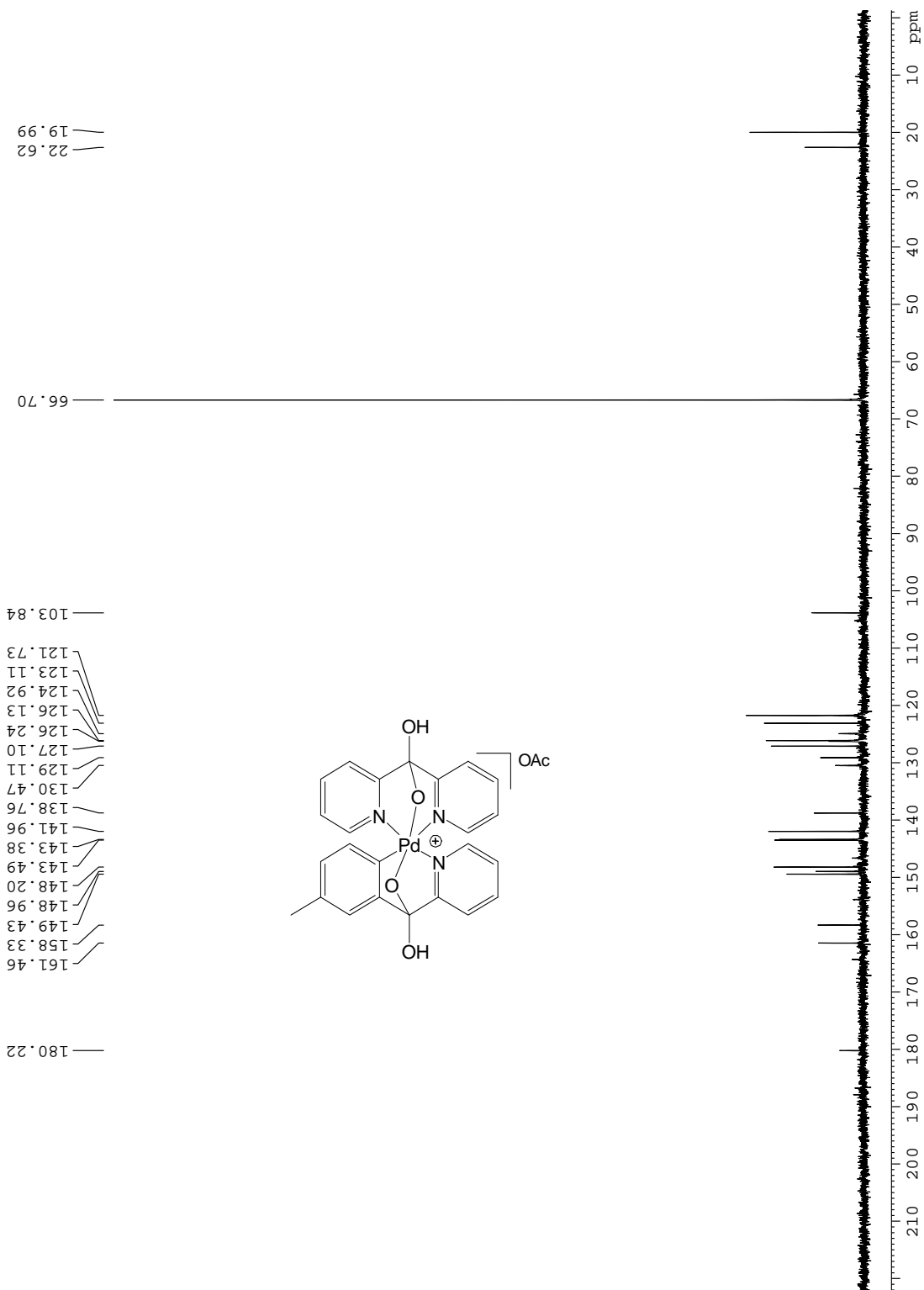


Fig. A4.  $^{13}\text{C}$  NMR of **76(OAc)** in  $\text{D}_2\text{O}$  at  $22^\circ\text{C}$

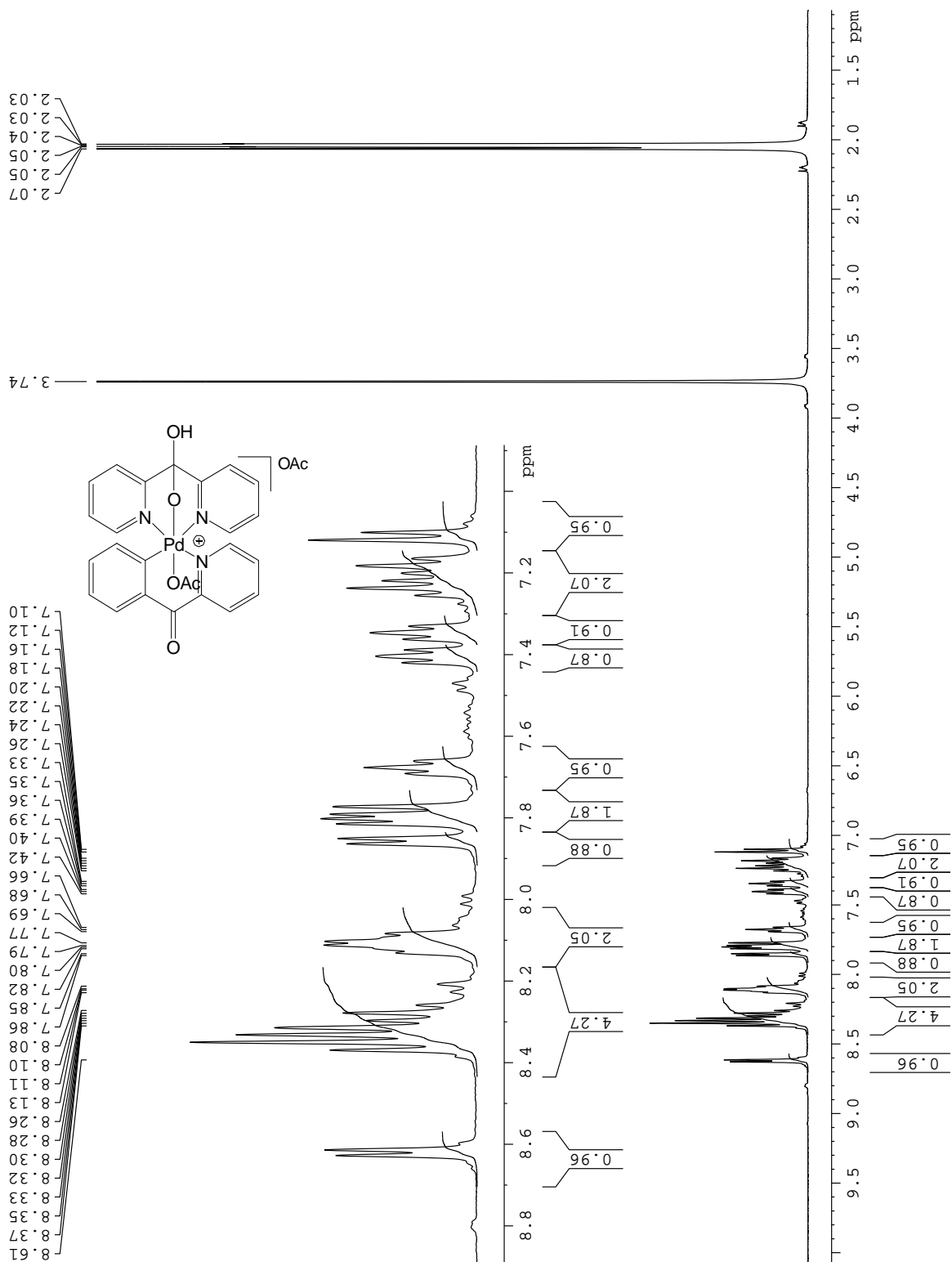


Fig. A5.  $^1\text{H NMR}$  of **81(OAc)** in  $\text{AcOH-d}_4$  at 295 K

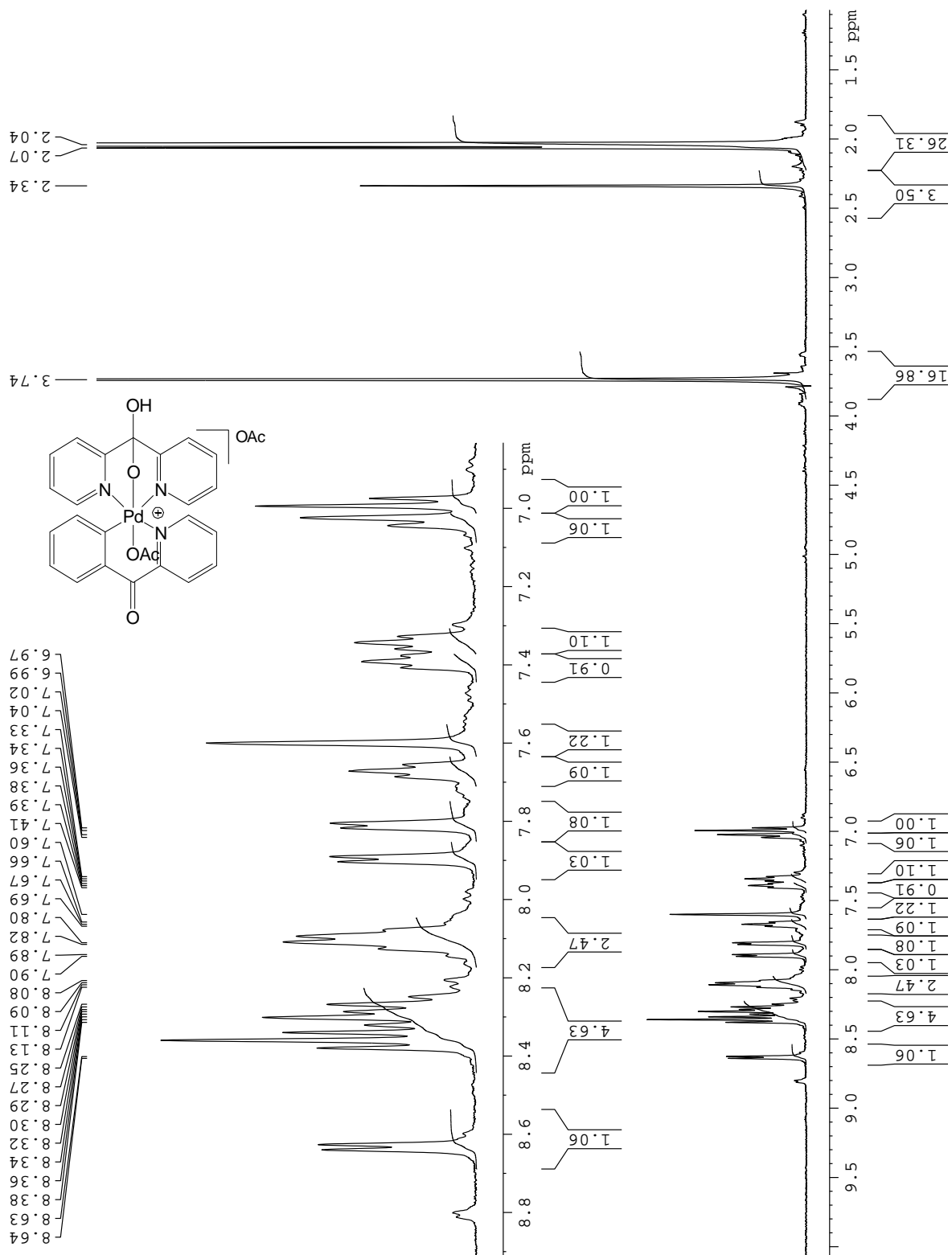


Fig. A6. <sup>1</sup>H NMR of **82(OAc)** in AcOH-d<sub>4</sub> at 295 K

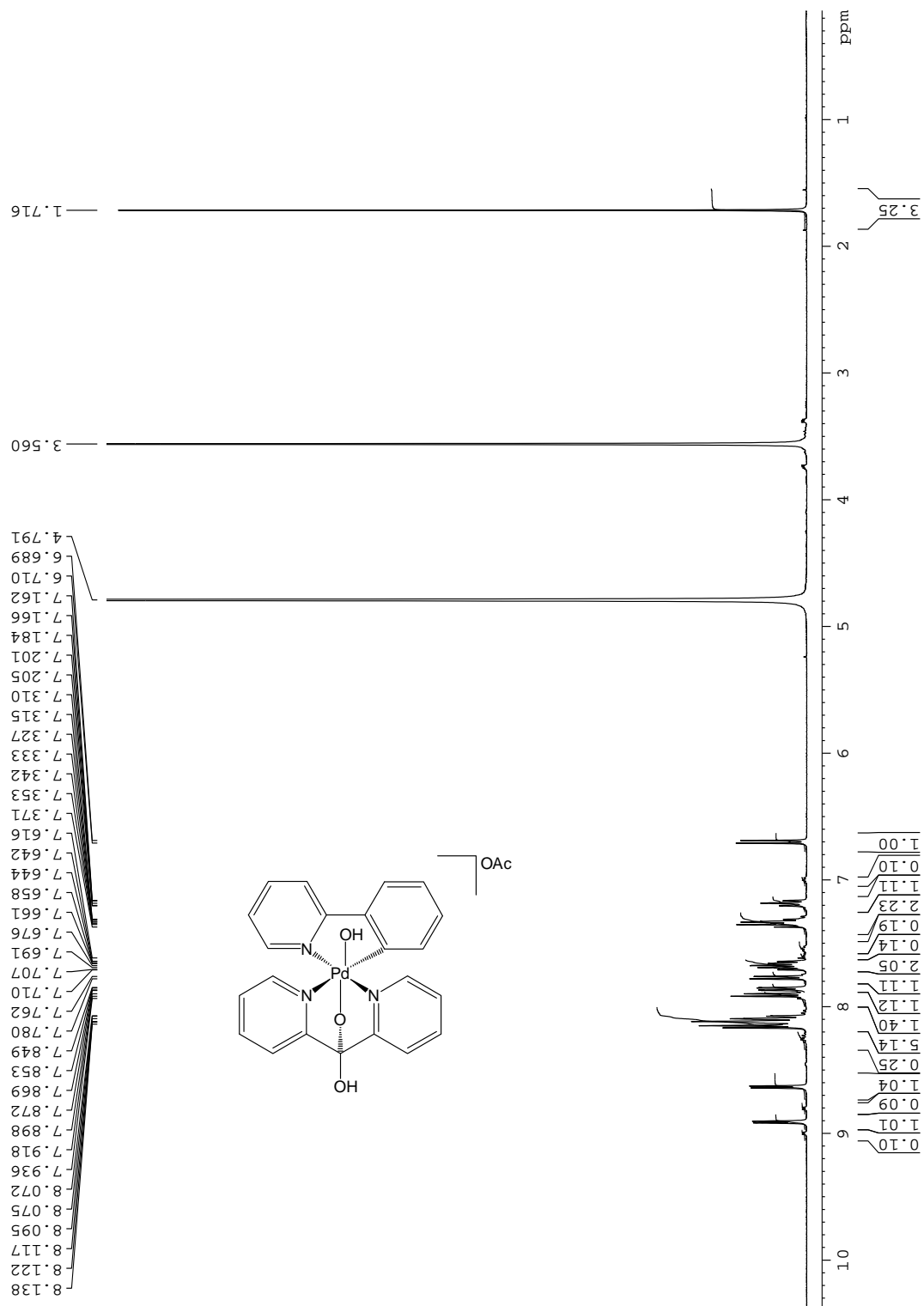


Fig. A7. <sup>1</sup>H NMR of **83(OAc)** in D<sub>2</sub>O at 5°C

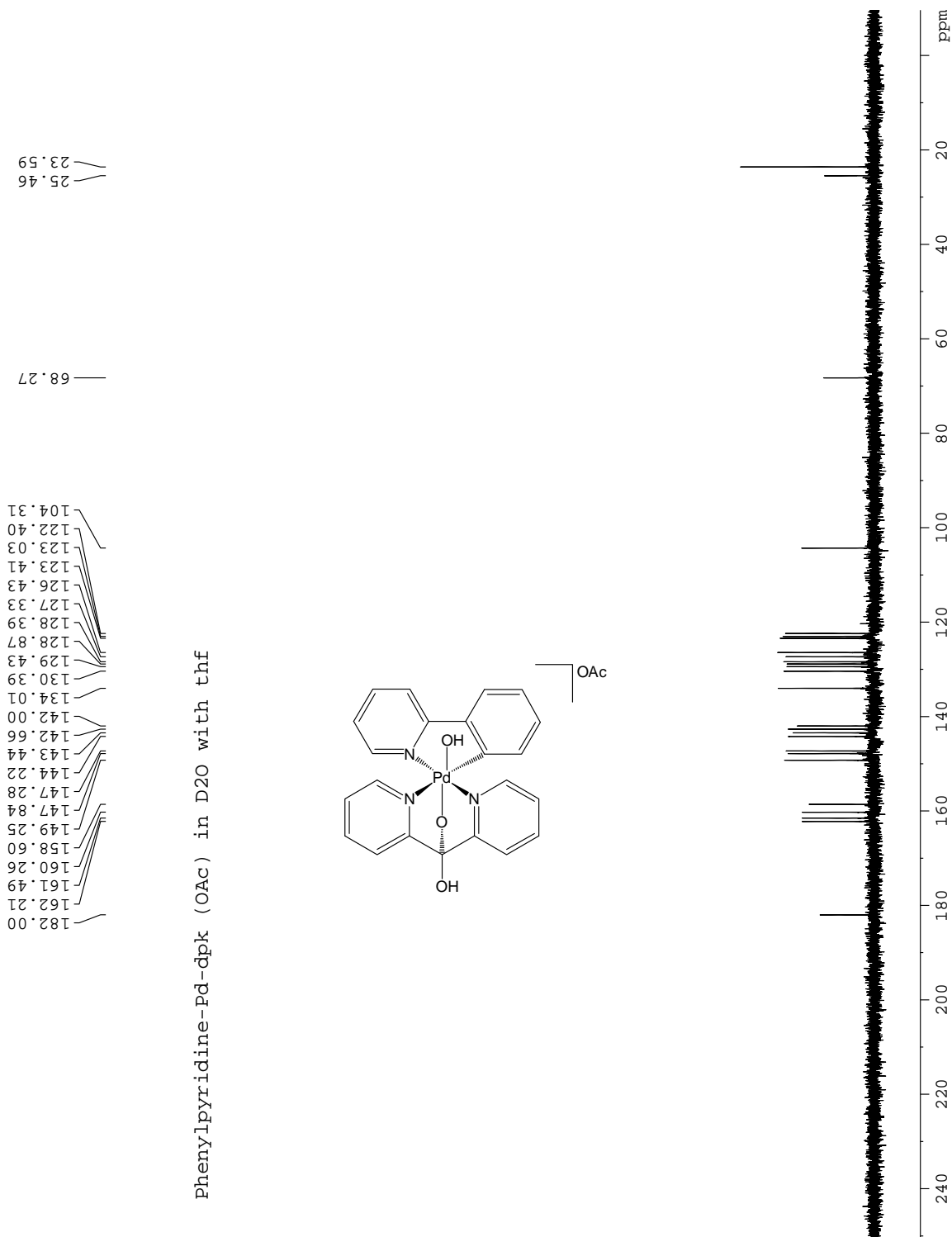


Fig. A8. <sup>13</sup>C NMR of **83**(OAc) in D<sub>2</sub>O at 5°C

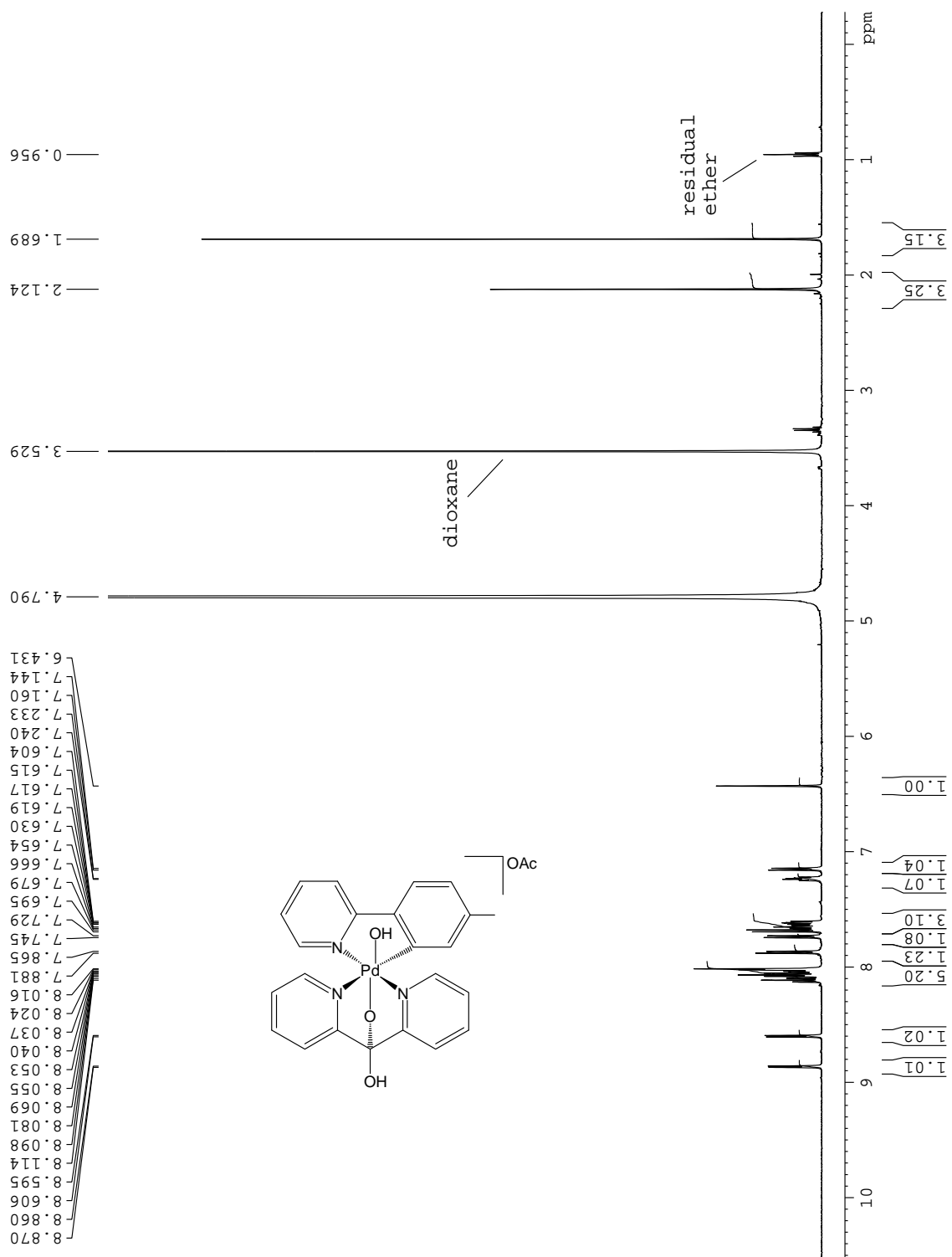


Fig. A9.  $^1\text{H}$  NMR spectrum of **84(OAc)** at  $5^\circ\text{C}$  in  $\text{D}_2\text{O}$ .

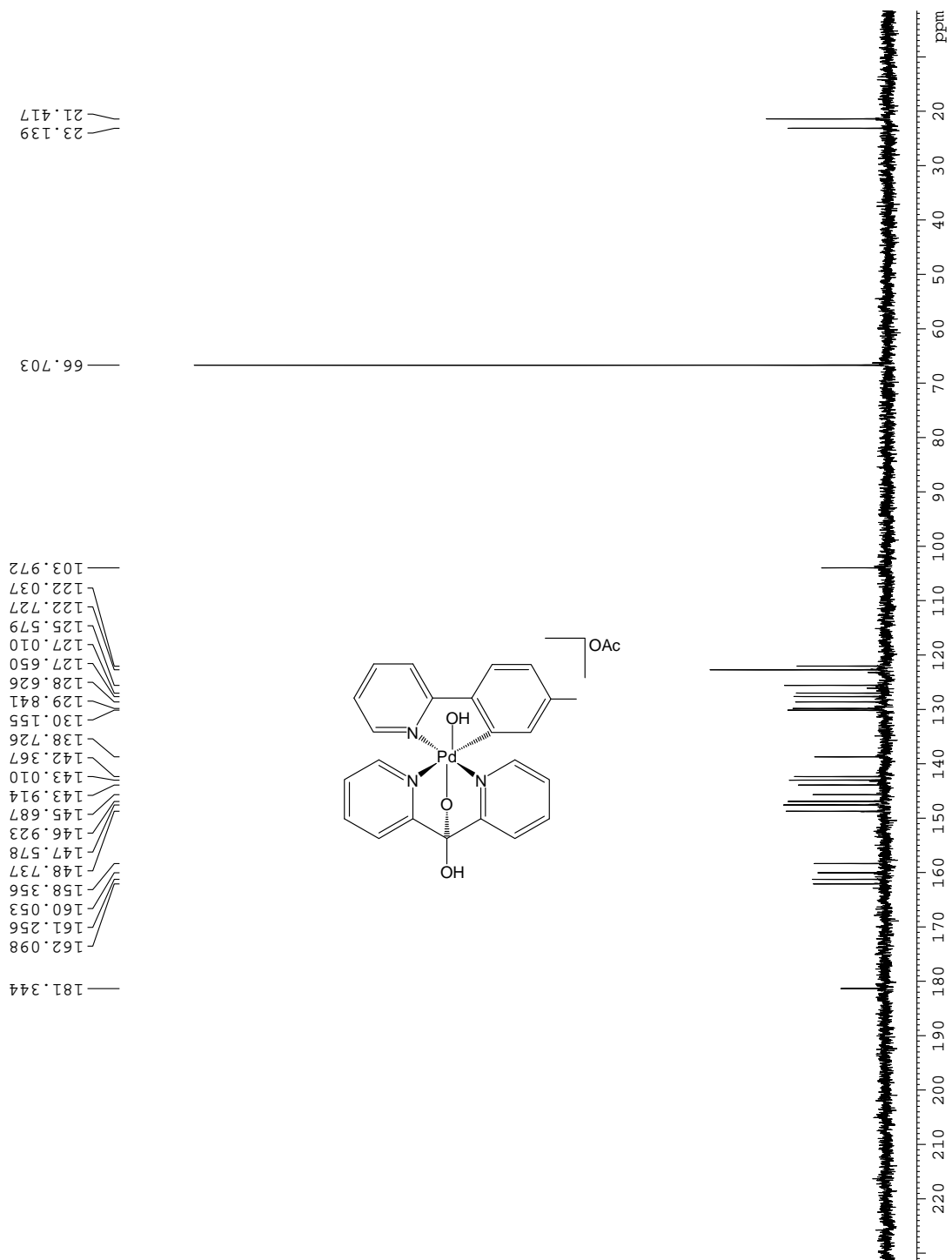


Fig. A10.  $^{13}\text{C}$  NMR spectrum of **84(OAc)** at  $5^\circ\text{C}$  in  $\text{D}_2\text{O}$

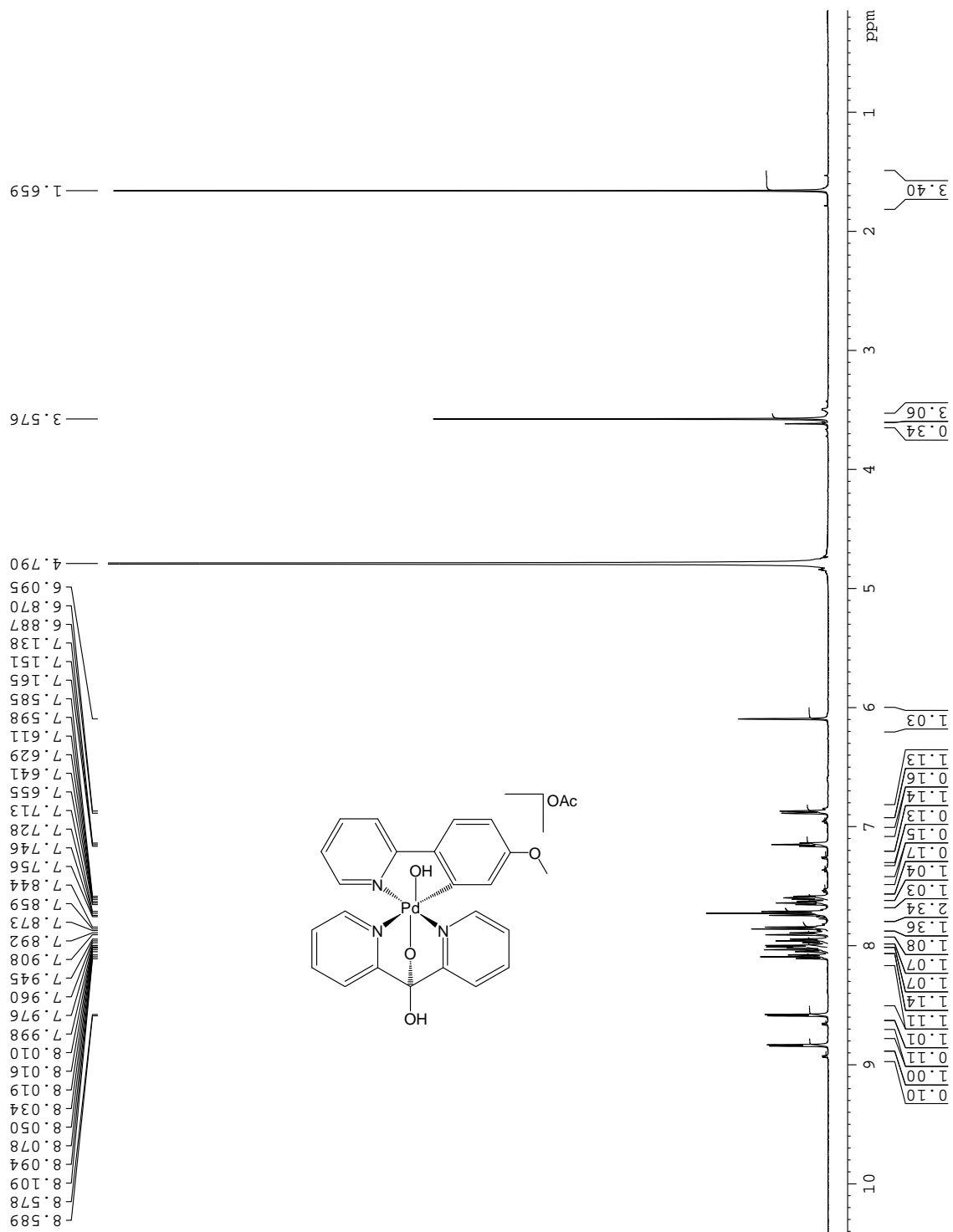


Fig. A11.  $^1\text{H}$  NMR spectrum of **85(OAc)** at  $5^\circ\text{C}$  in  $\text{D}_2\text{O}$ .

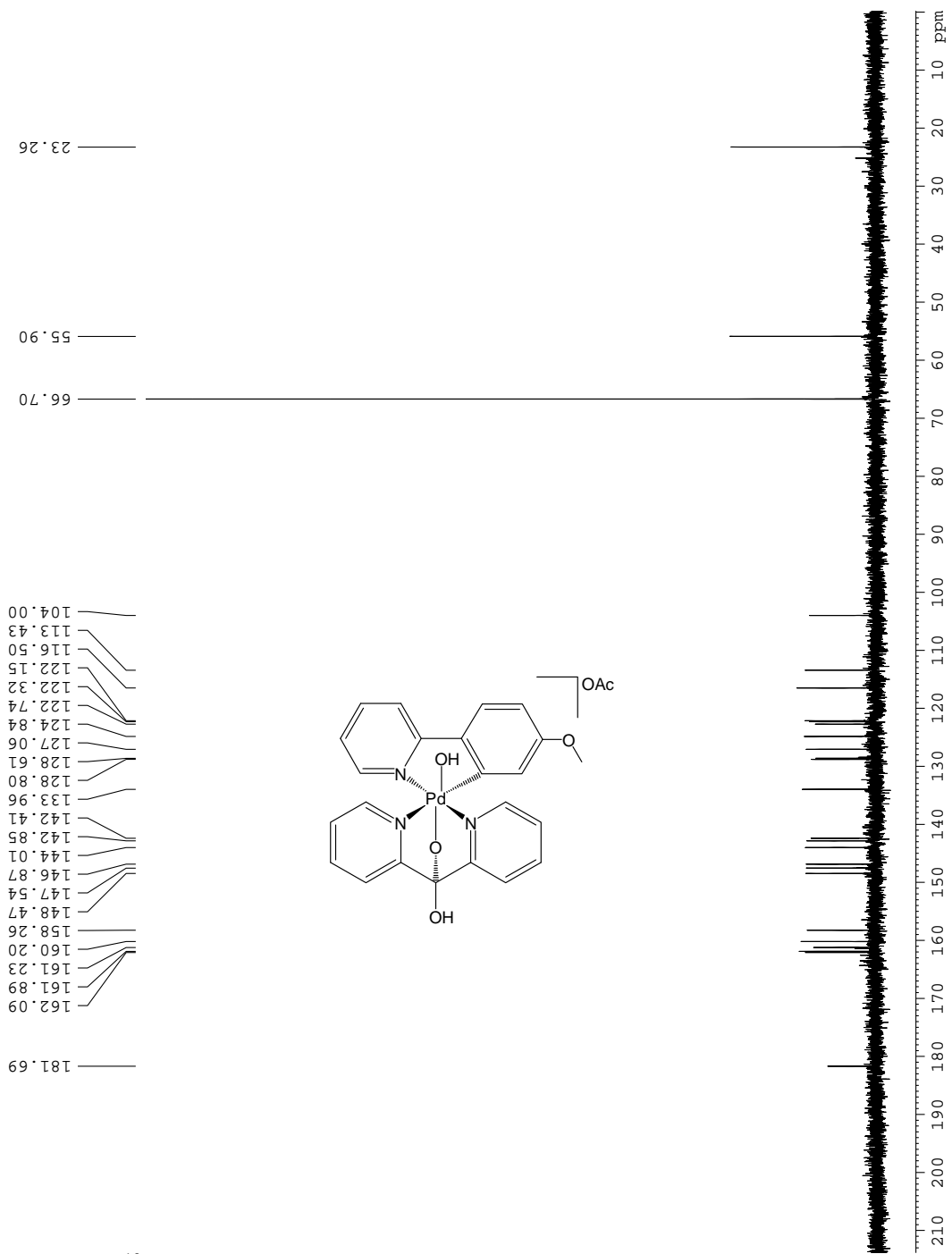
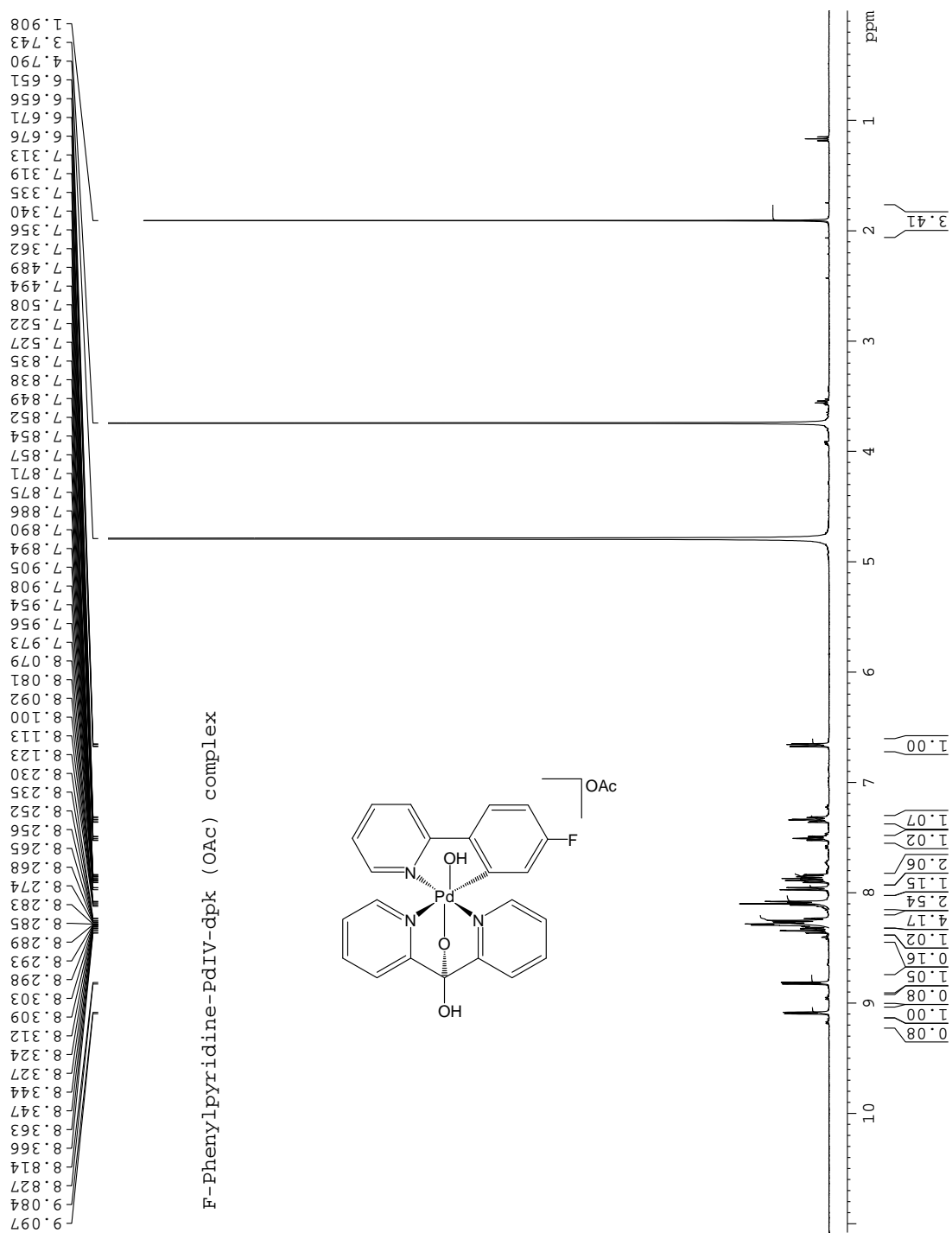


Fig. A12. <sup>13</sup>C NMR spectrum of **85(OAc)** at 5°C in D<sub>2</sub>O



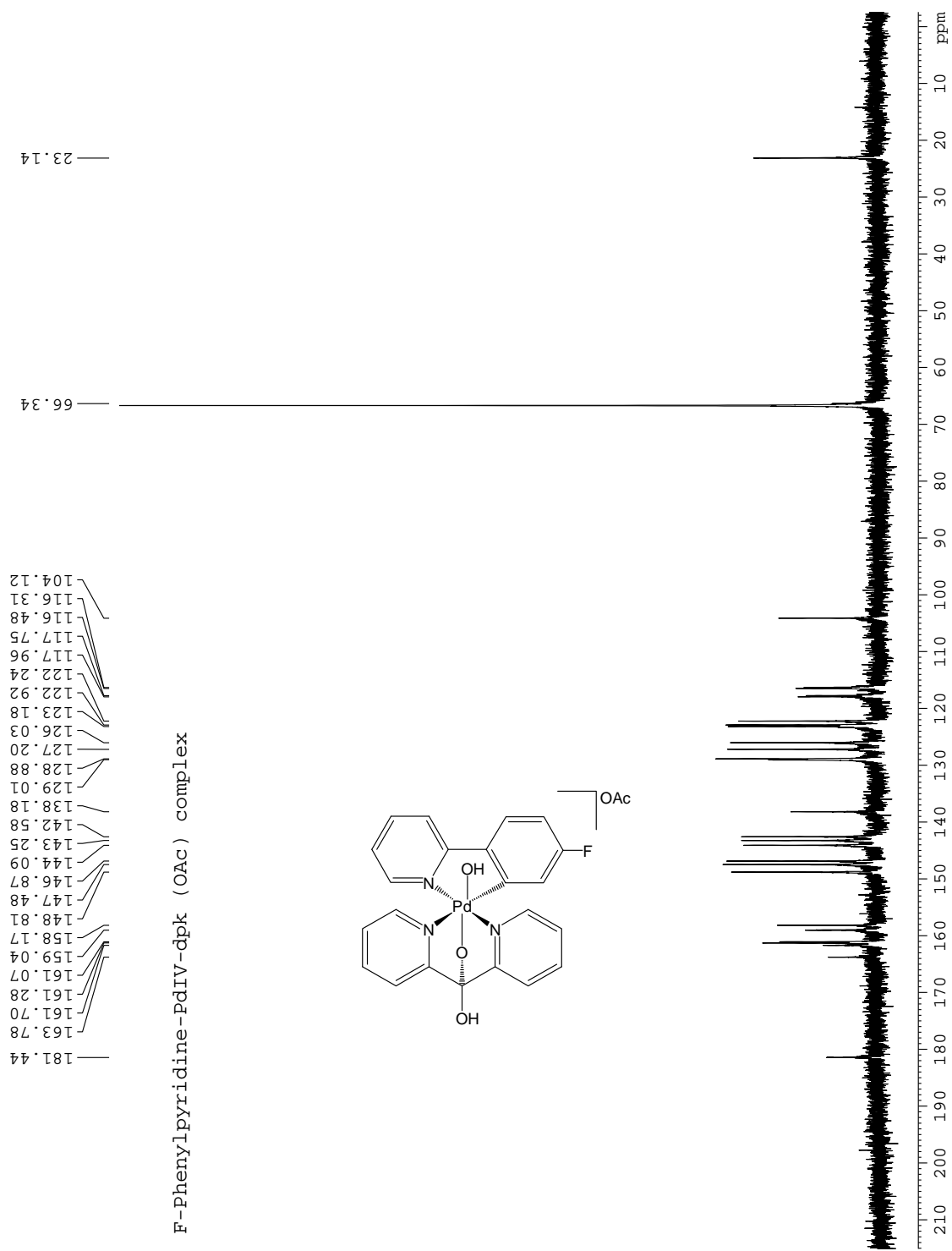


Fig. A14.  $^{13}\text{C}$  NMR spectrum of **86(OAc)** at  $5^\circ\text{C}$  in  $\text{D}_2\text{O}$

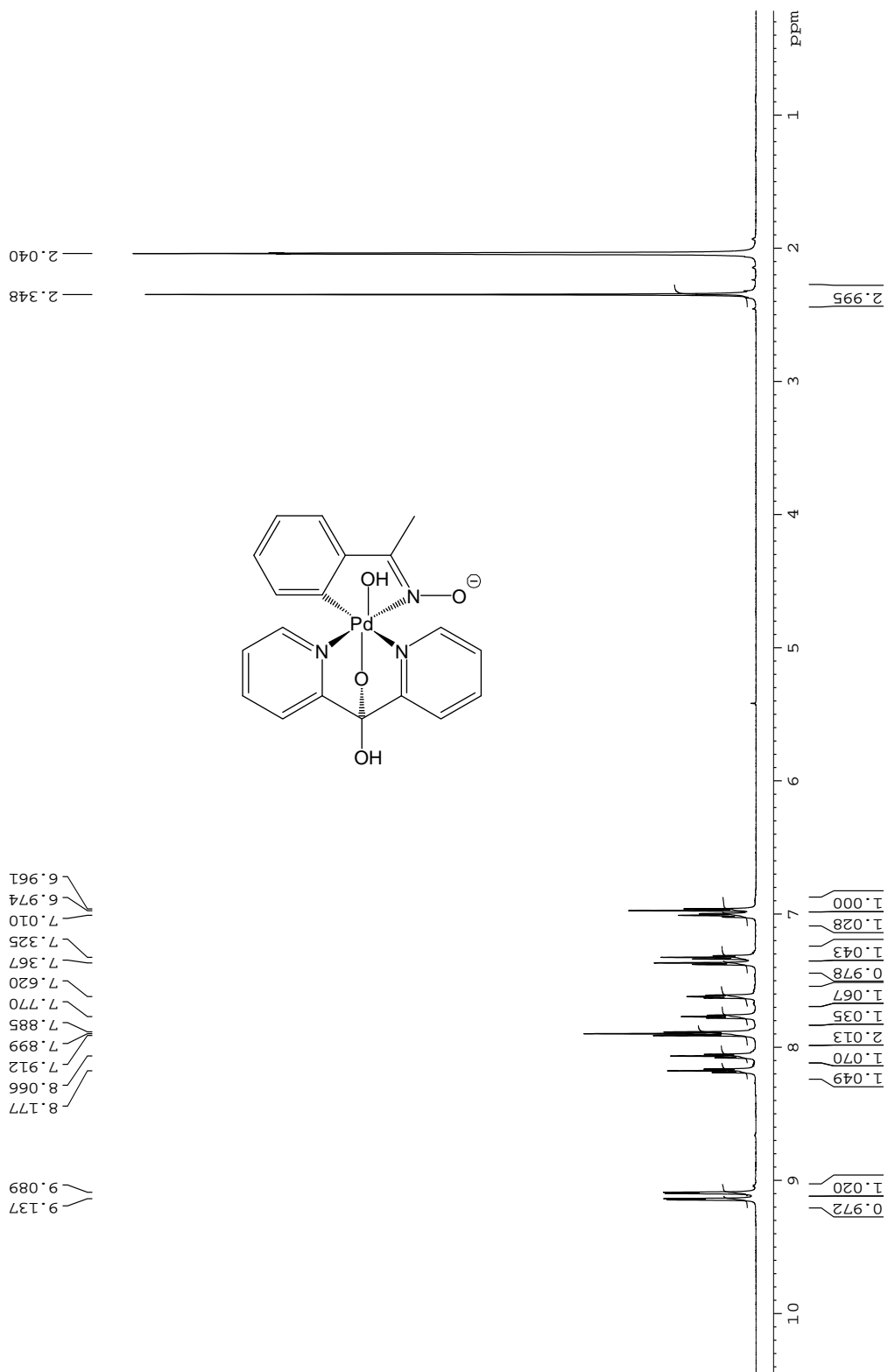


Fig. A15; <sup>1</sup>H NMR of **93** in AcOH-d<sub>4</sub> at 22°C

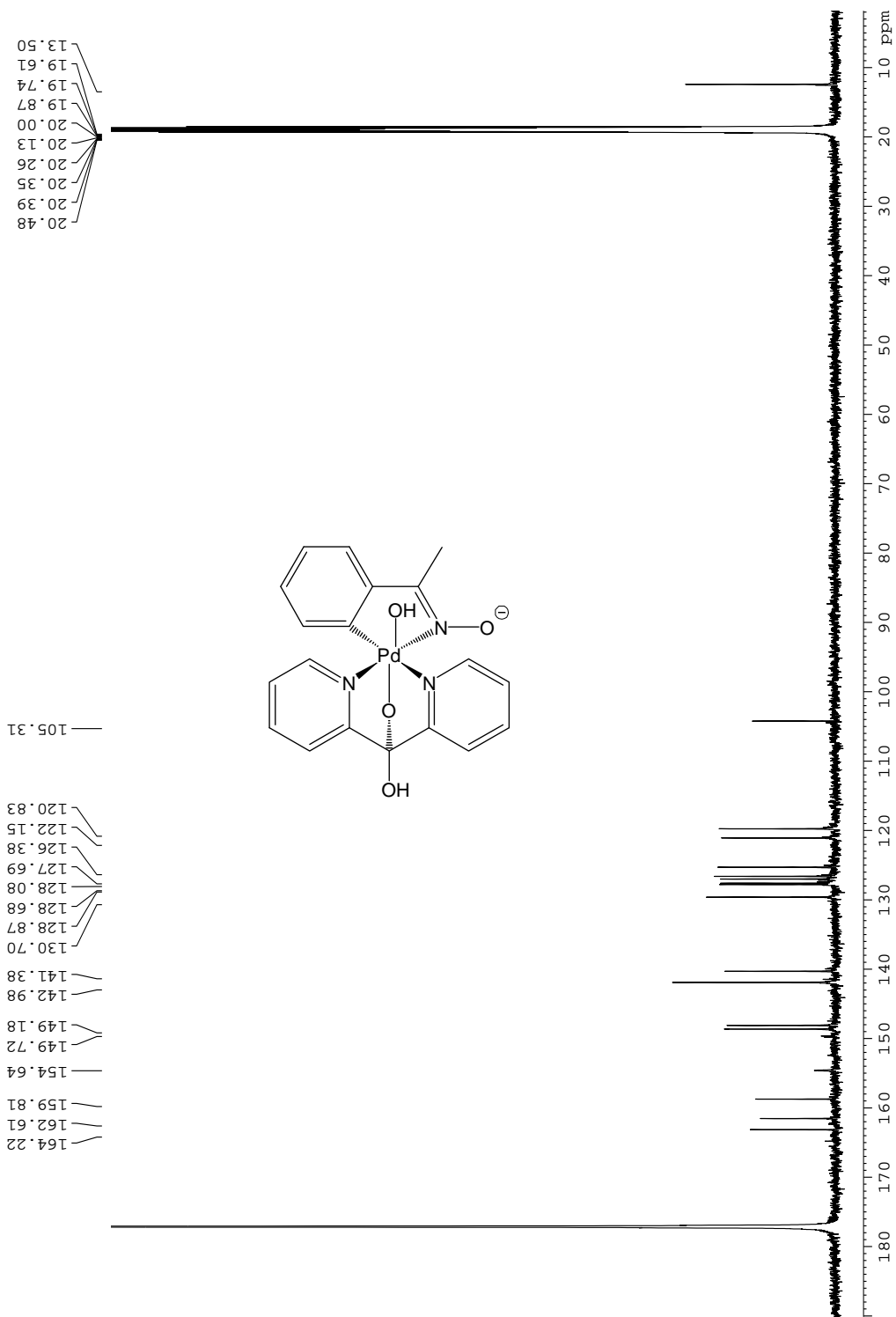


Fig. A16; <sup>13</sup>C NMR of **93** in AcOH-d<sub>4</sub> at 22°C

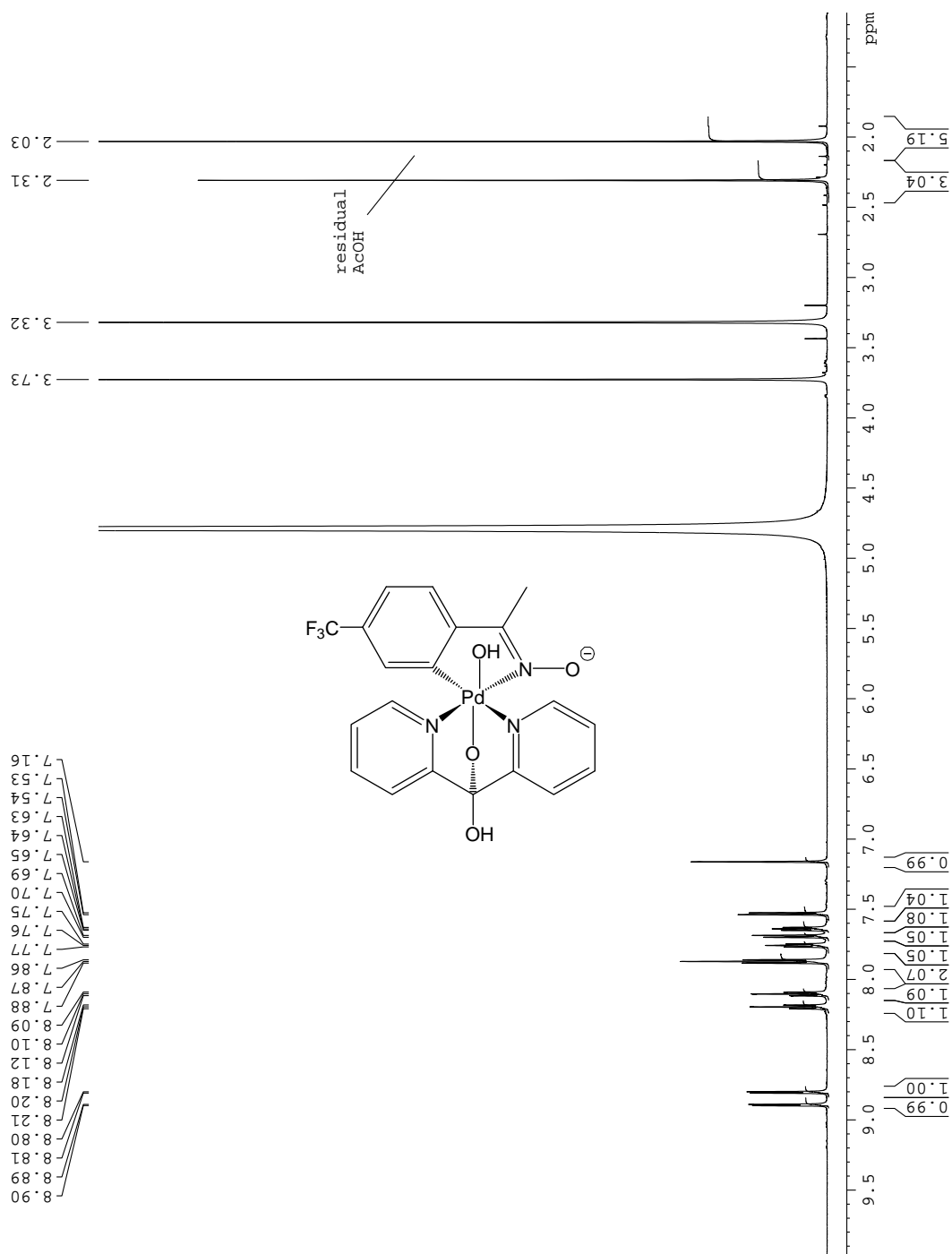


Fig. A17;  $^1\text{H}$  NMR of **94** in  $\text{MeOH-d}^4$  at  $22^\circ\text{C}$

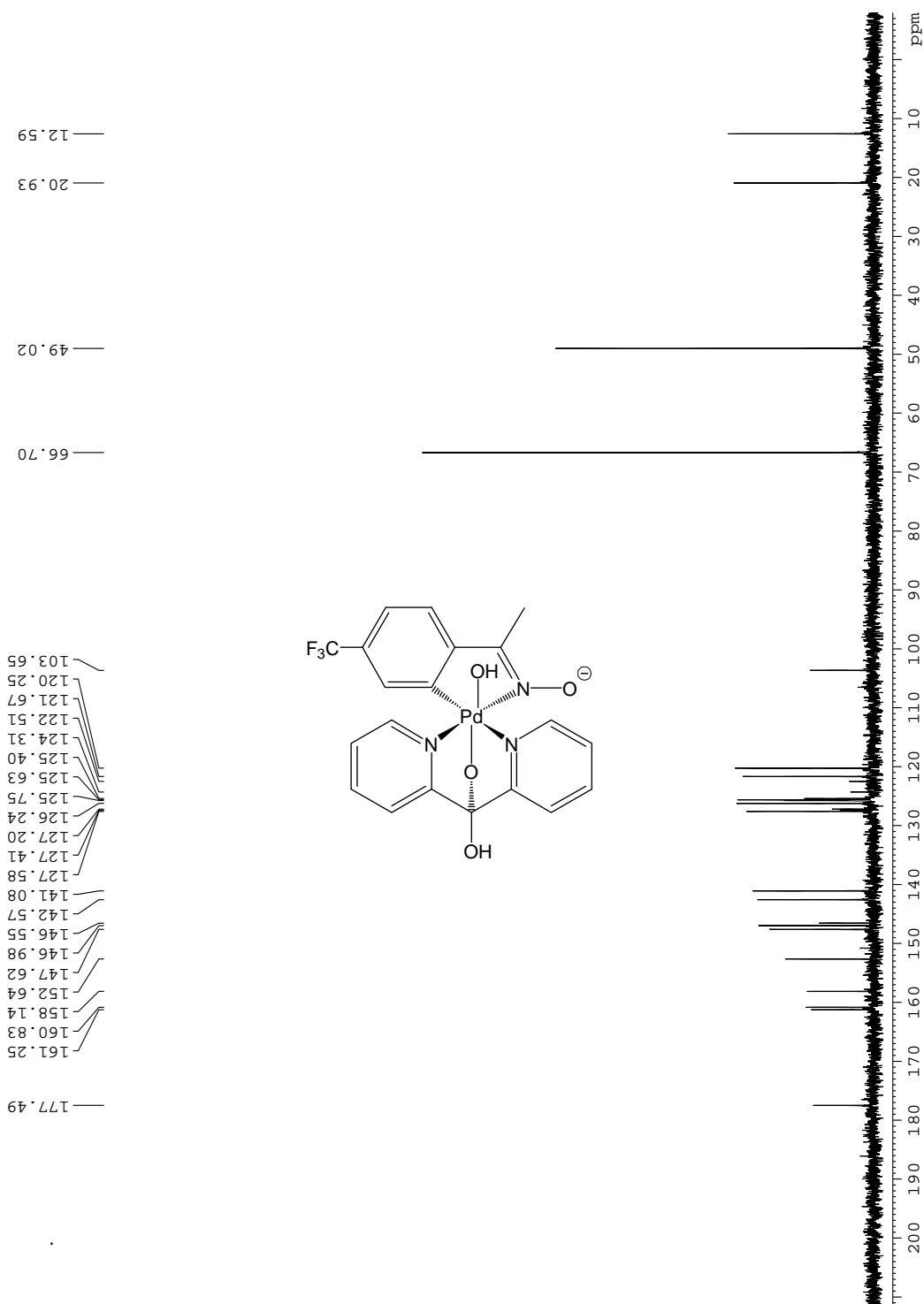


Fig. A18;  $^{13}\text{C}$  NMR of **94** in MeOH- $\text{d}_4$  at 22°C

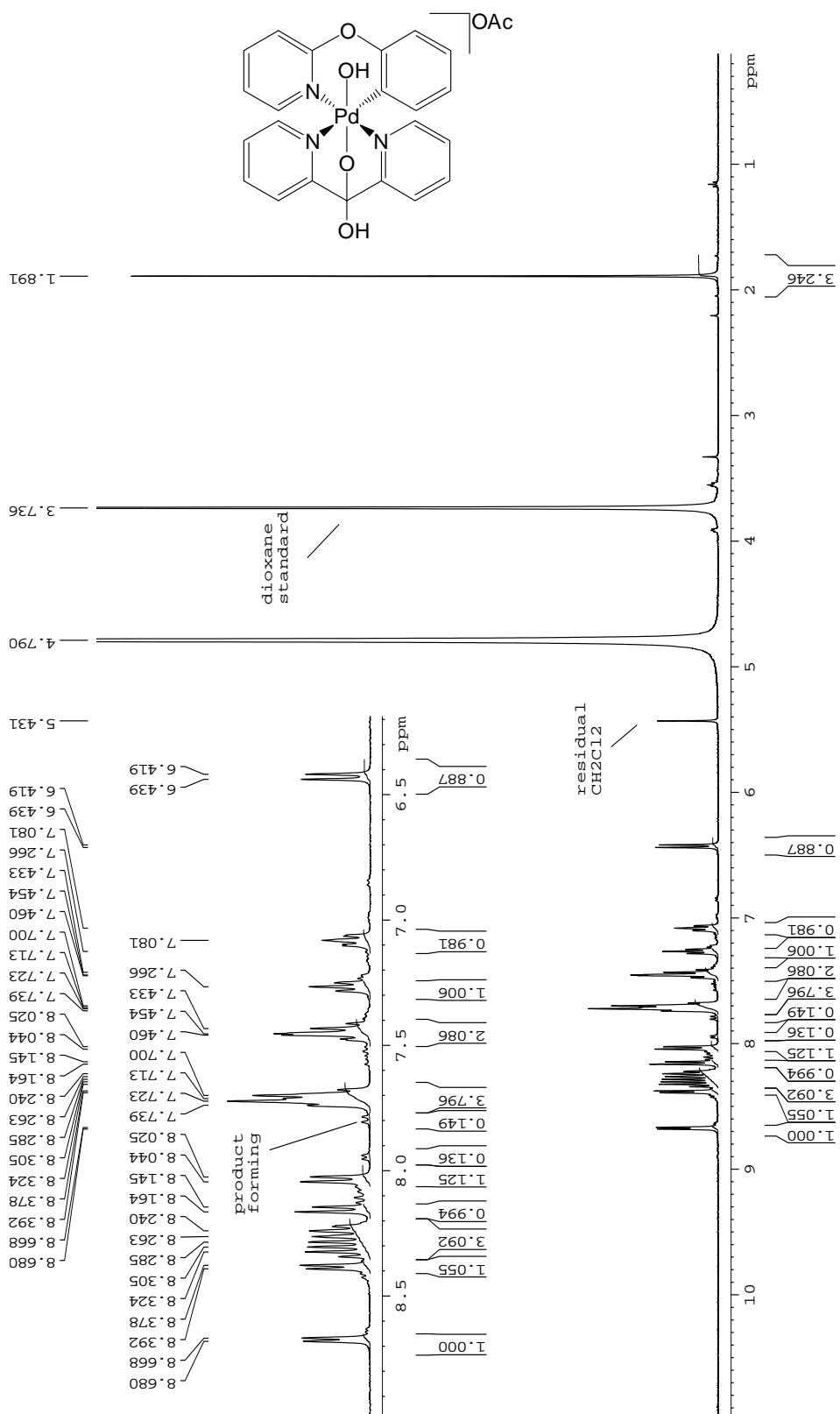


Fig. A19;  $^1\text{H NMR}$  of **96** in  $\text{D}_2\text{O}$  at  $5^\circ\text{C}$

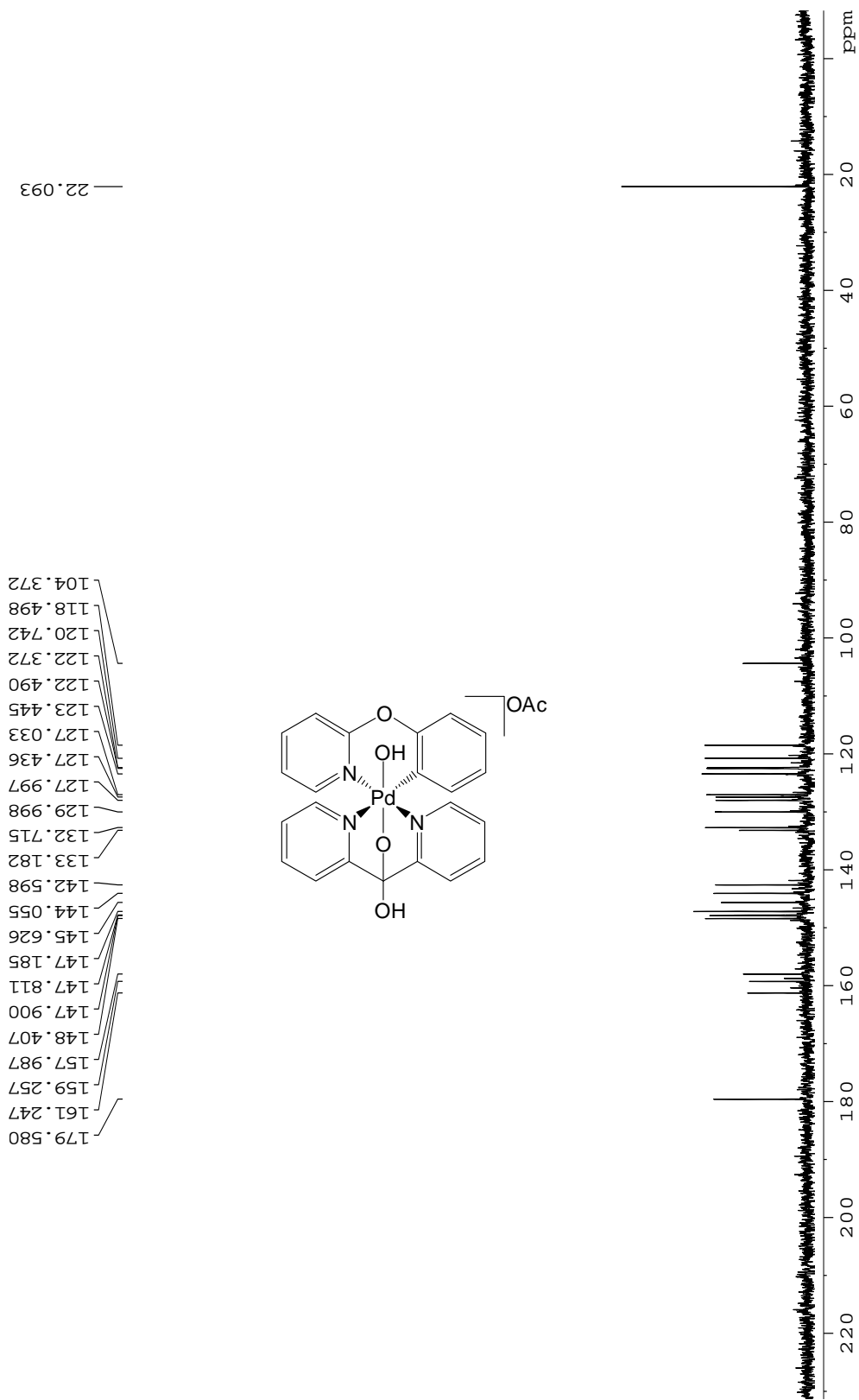


Fig. A20;  $^{13}\text{C}$  NMR of **96** in  $\text{D}_2\text{O}$  at  $5^\circ\text{C}$

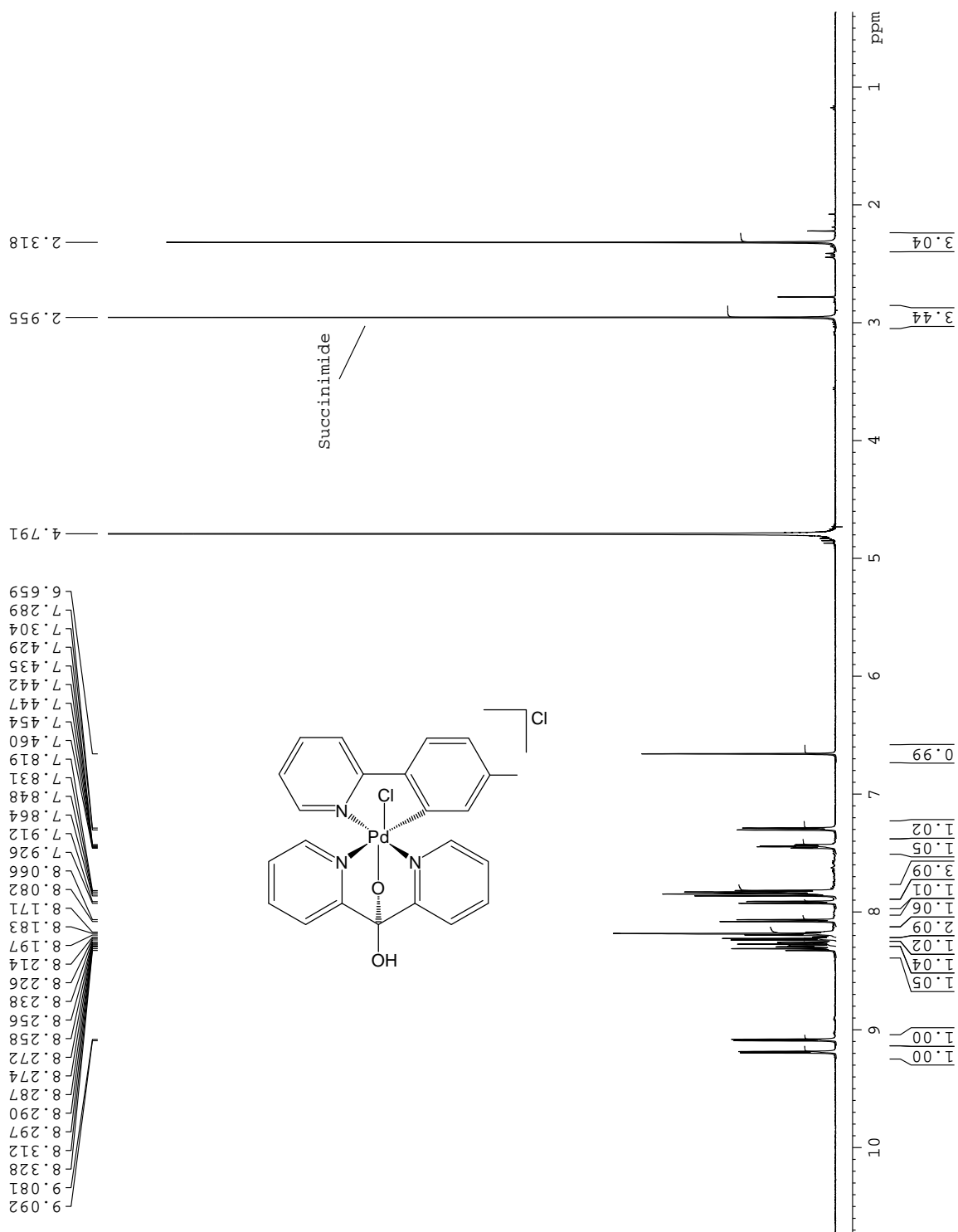


Fig. A21; <sup>1</sup>H NMR of **29(Cl)** in D<sub>2</sub>O at 5°C

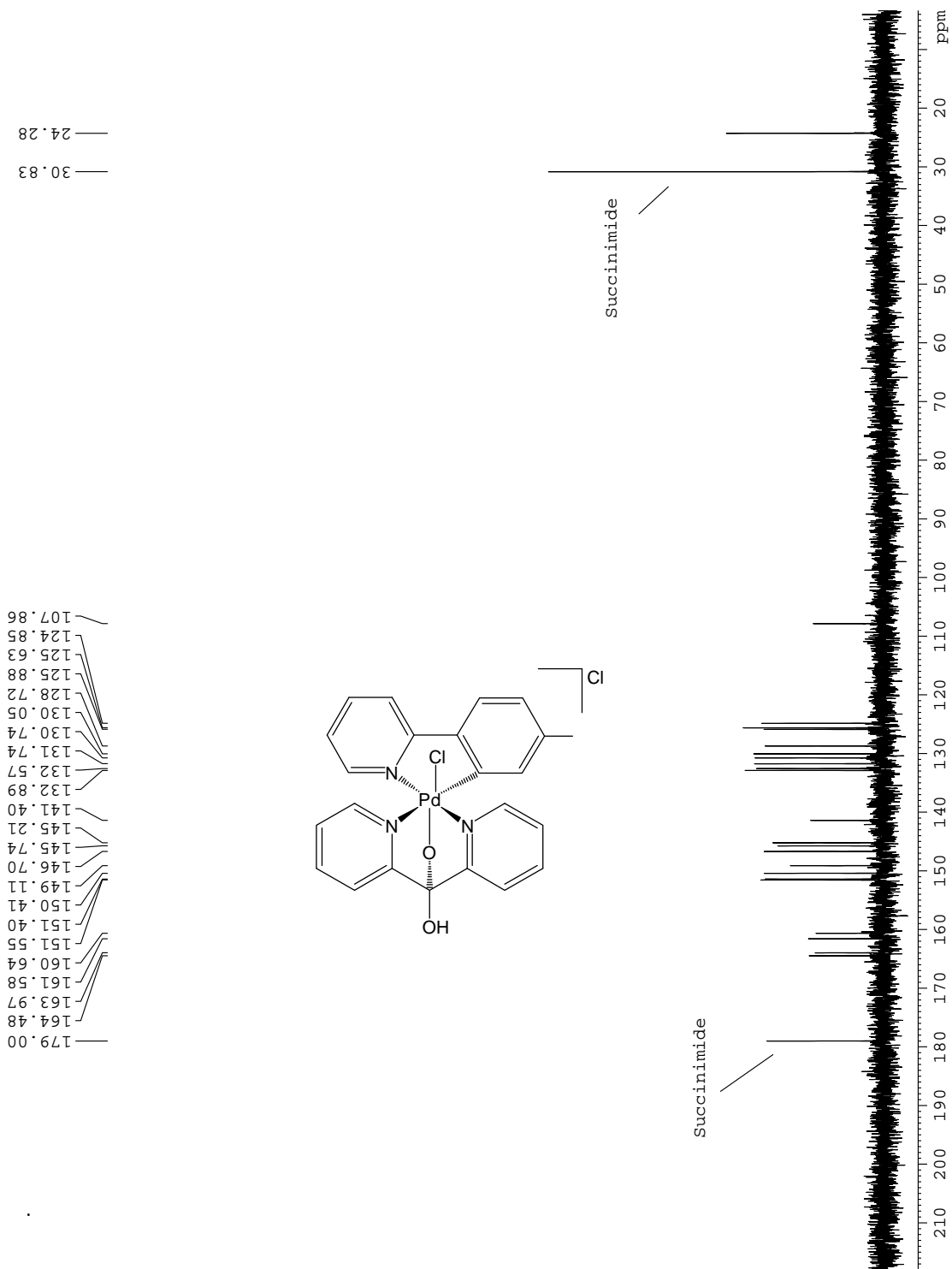


Fig. A22; <sup>13</sup>C NMR of **29(Cl)** in D<sub>2</sub>O at 5°C

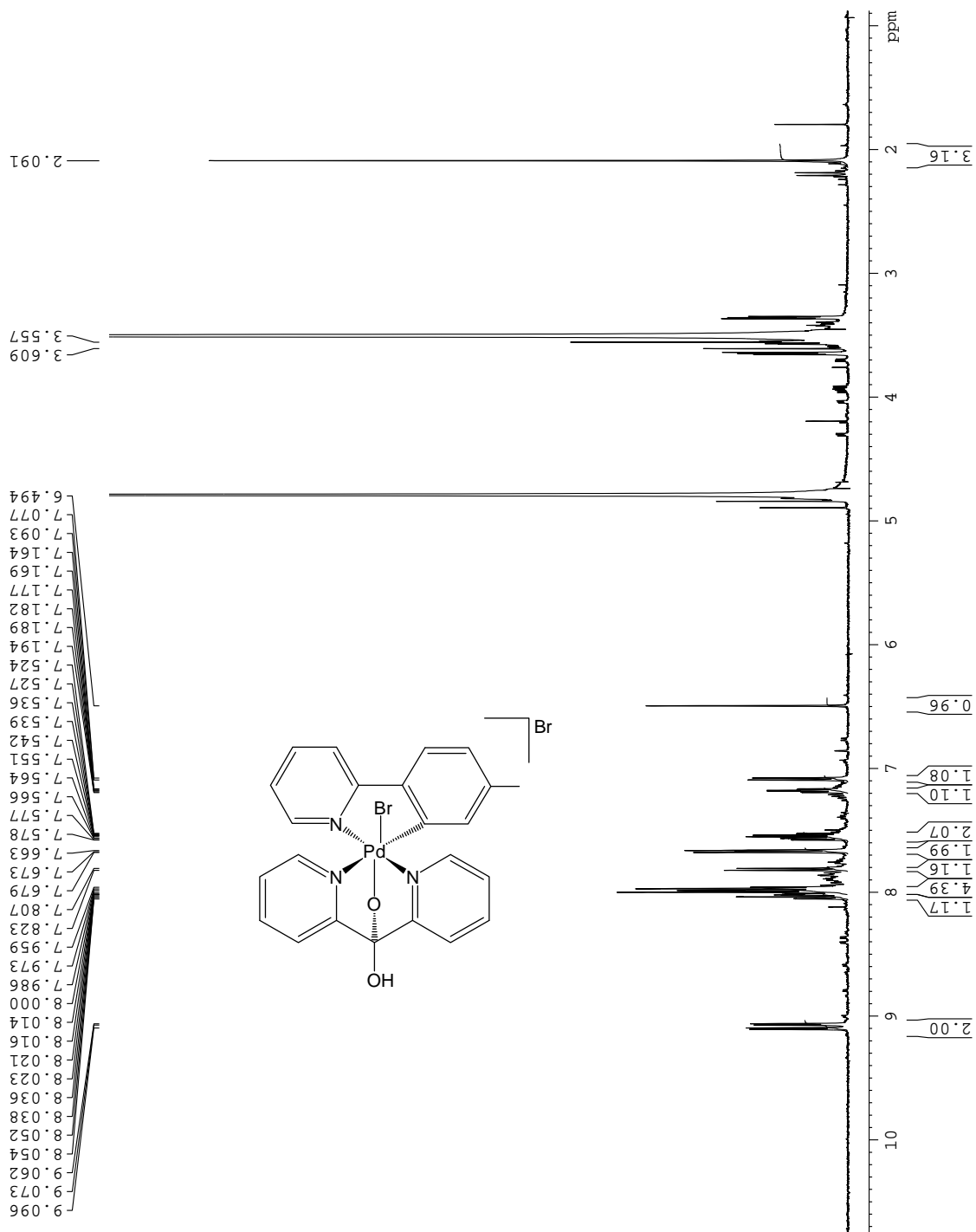


Fig. A23;  $^1\text{H}$  NMR of **45(Br)** in  $\text{D}_2\text{O}$  at  $5^\circ\text{C}$

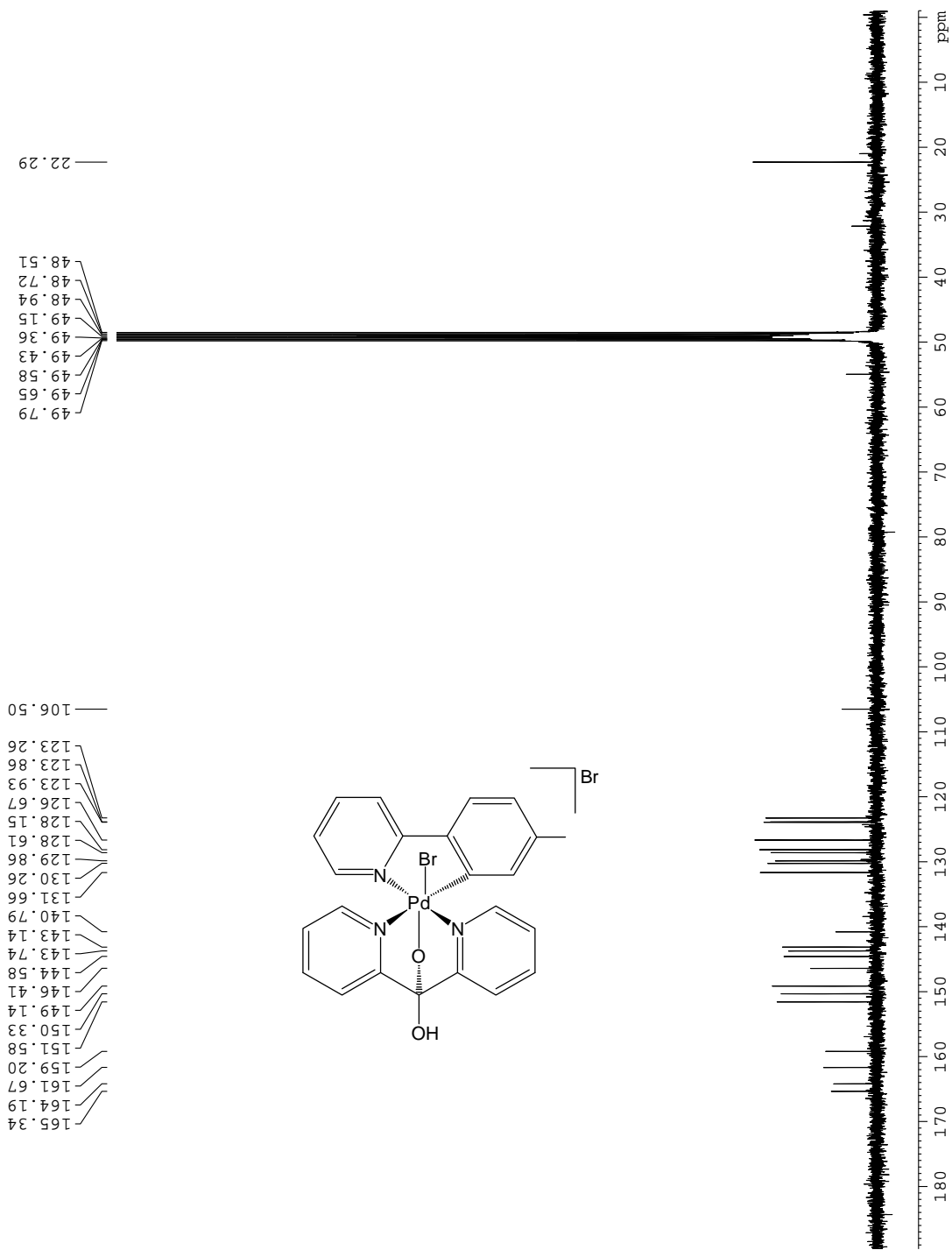


Fig. A24;  $^{13}\text{C}$  NMR of **45(Br)** in  $\text{D}_2\text{O}$  at  $5^\circ\text{C}$

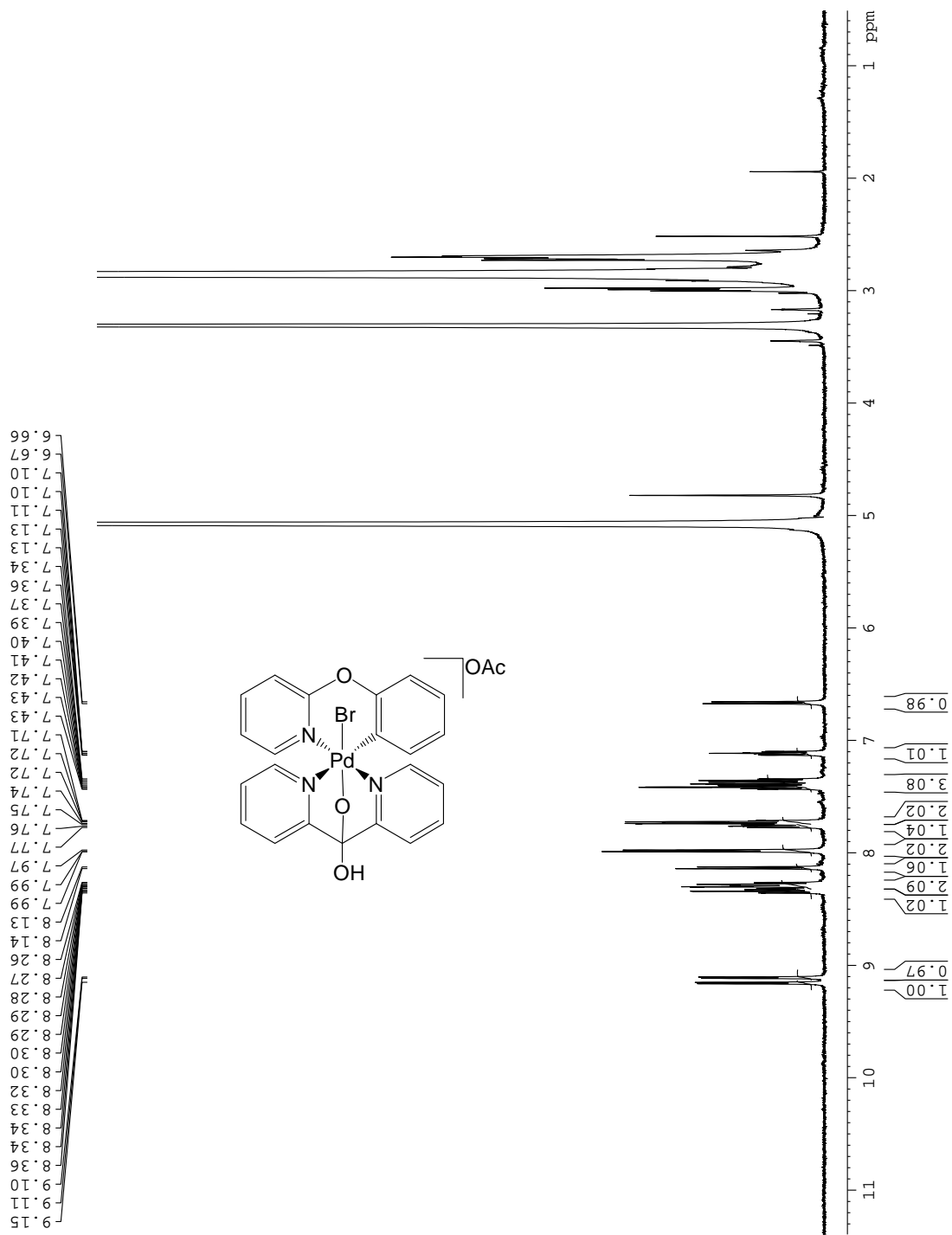


Fig. A25;  $^1\text{H NMR}$  of **41(Br)** in  $\text{MeOH-d}_4$  at  $22^\circ\text{C}$

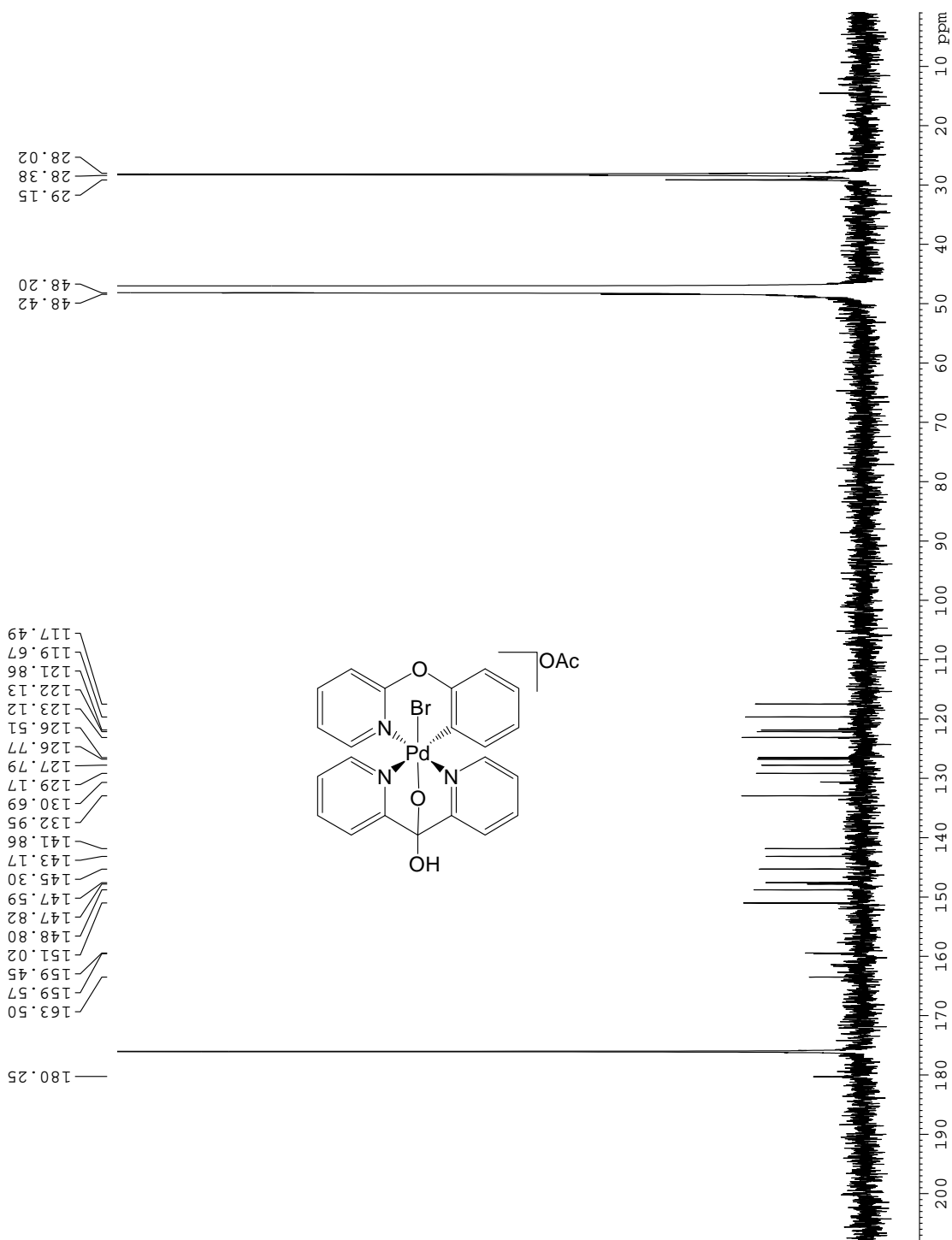


Fig. A26;  $^{13}\text{C}$  NMR of **41(Br)** in  $\text{MeOH-d}_4$  at  $22^\circ\text{C}$

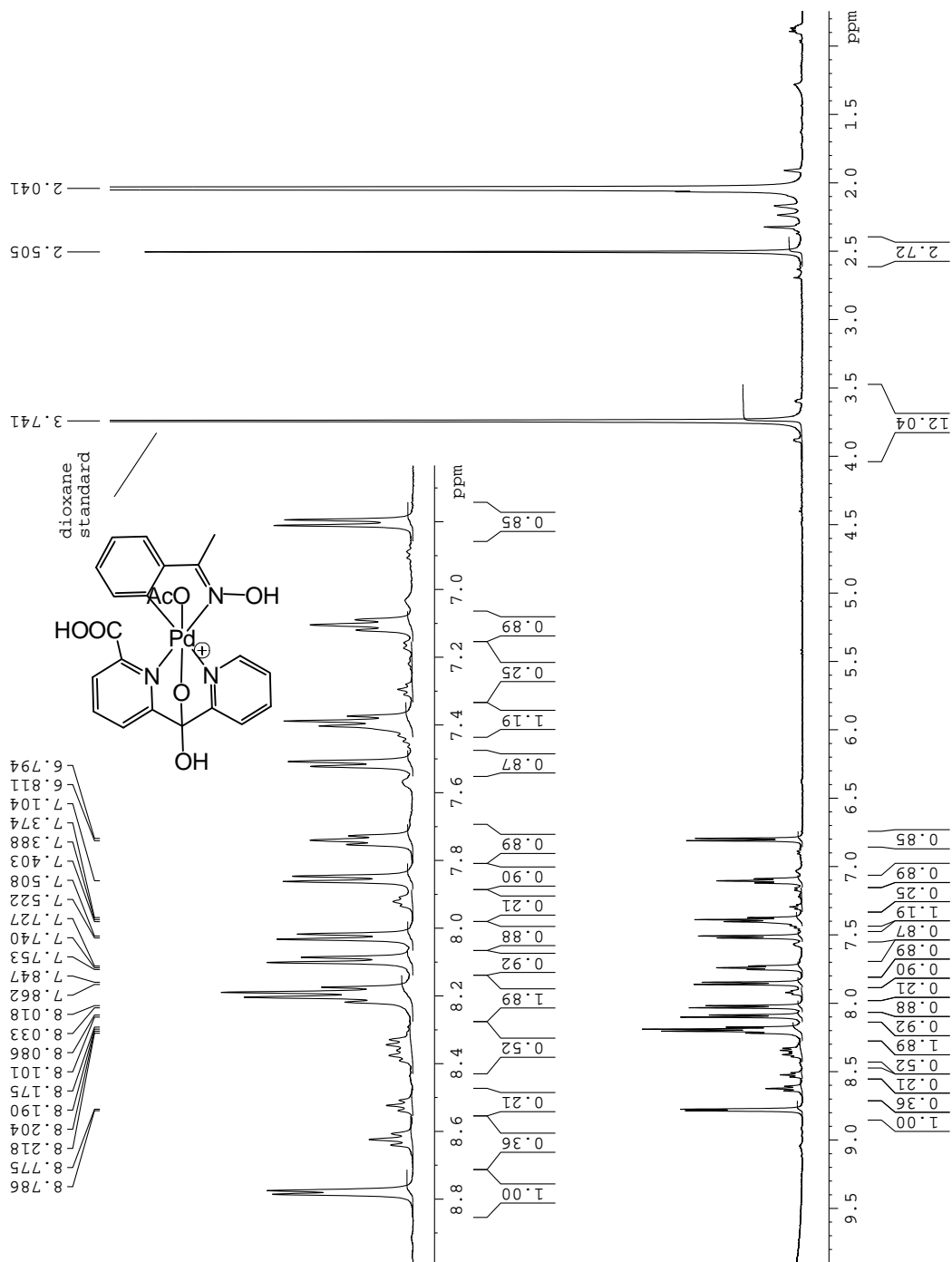


Fig. A27,  $^1\text{H}$  NMR of **25** in  $\text{AcOH-d}_4$  at  $22^\circ\text{C}$

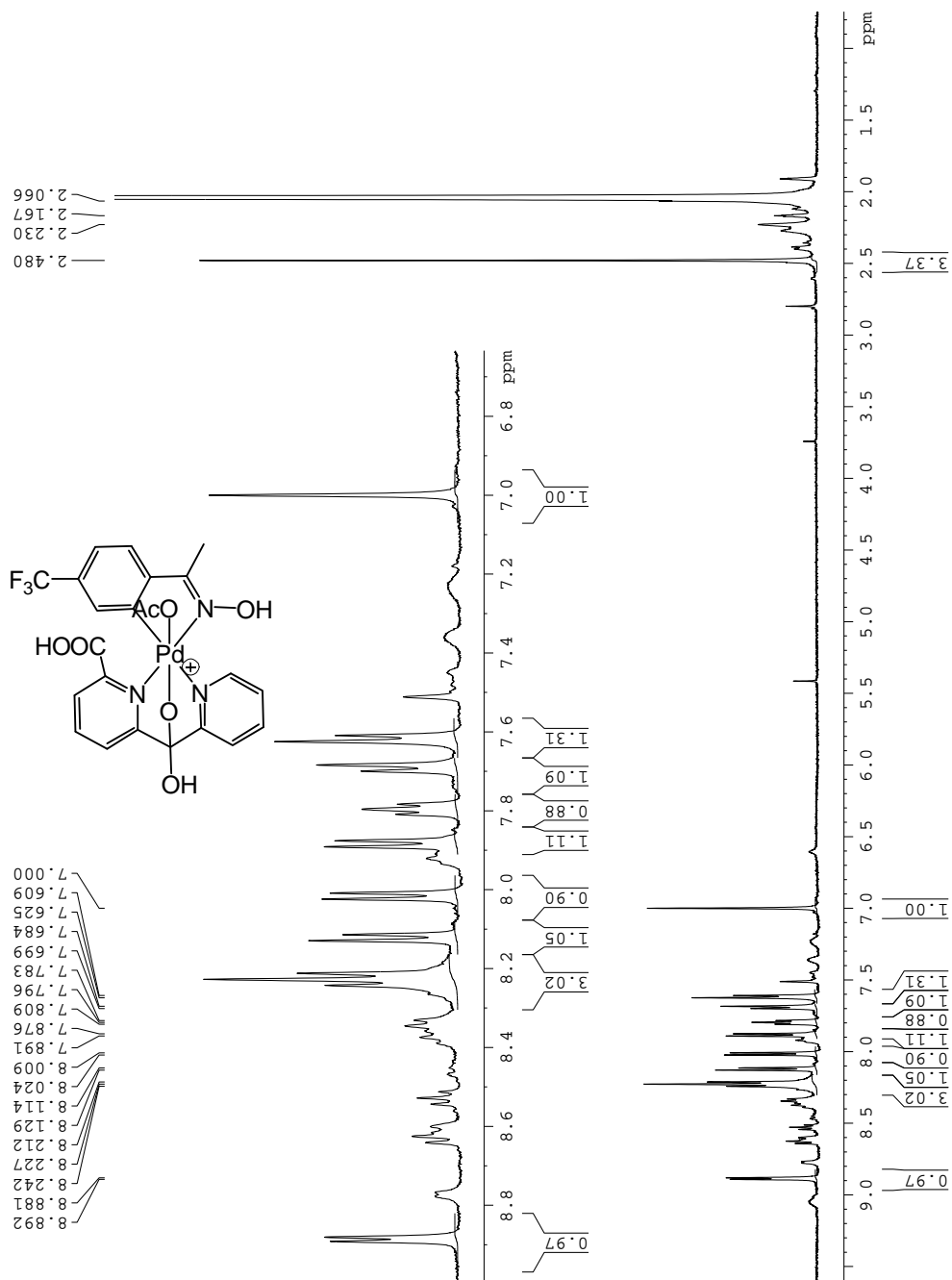


Fig. A28,  $^1\text{H NMR}$  of 17 in  $\text{AcOH-d}_4$  at  $22^\circ\text{C}$

NMR Spectra of Organic Compounds

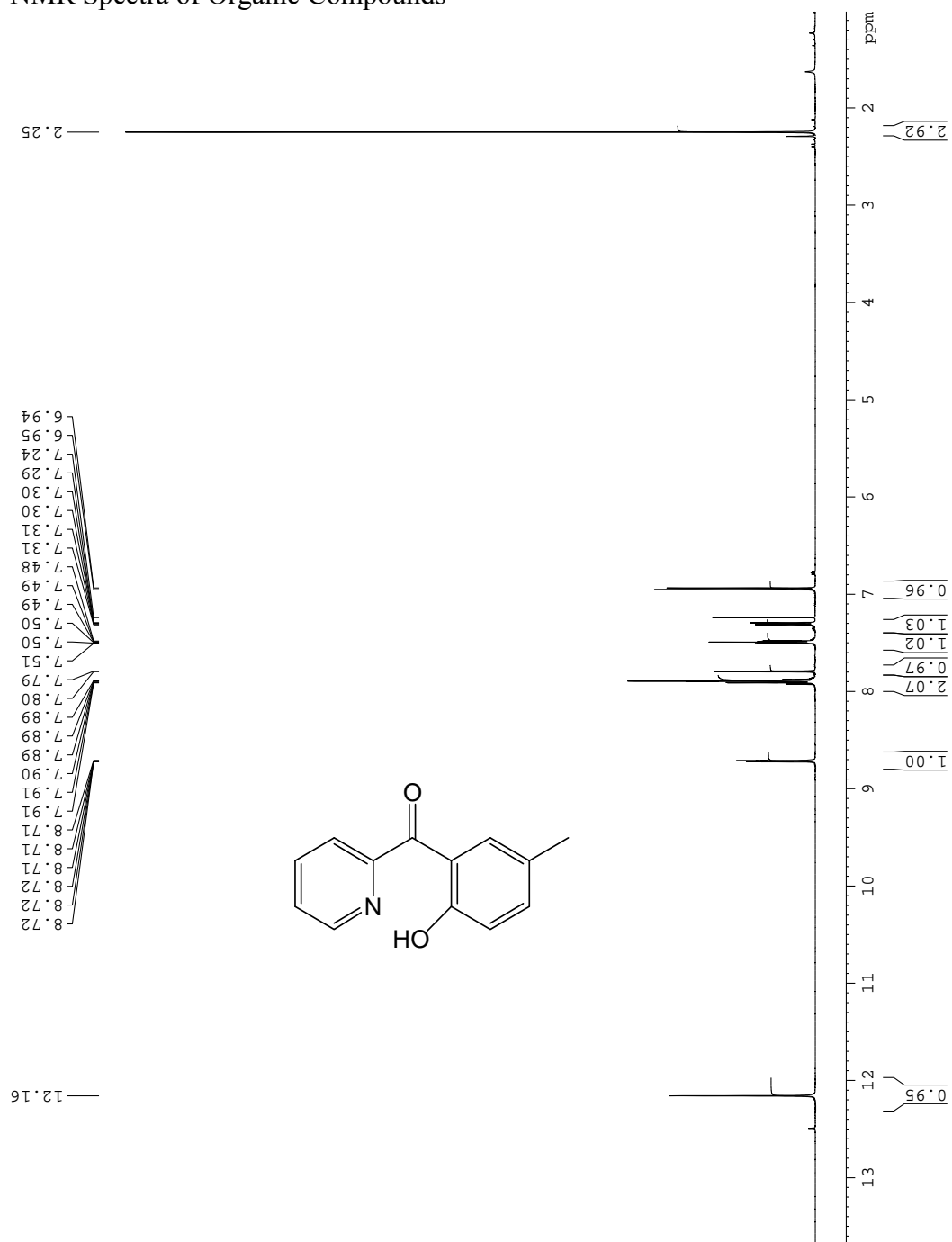


Fig. A29, <sup>1</sup>H NMR of **34** in CDCl<sub>3</sub> at 22°C



Fig. A30,  $^{13}\text{C}$  NMR of **34** in  $\text{CDCl}_3$  at  $22^\circ\text{C}$

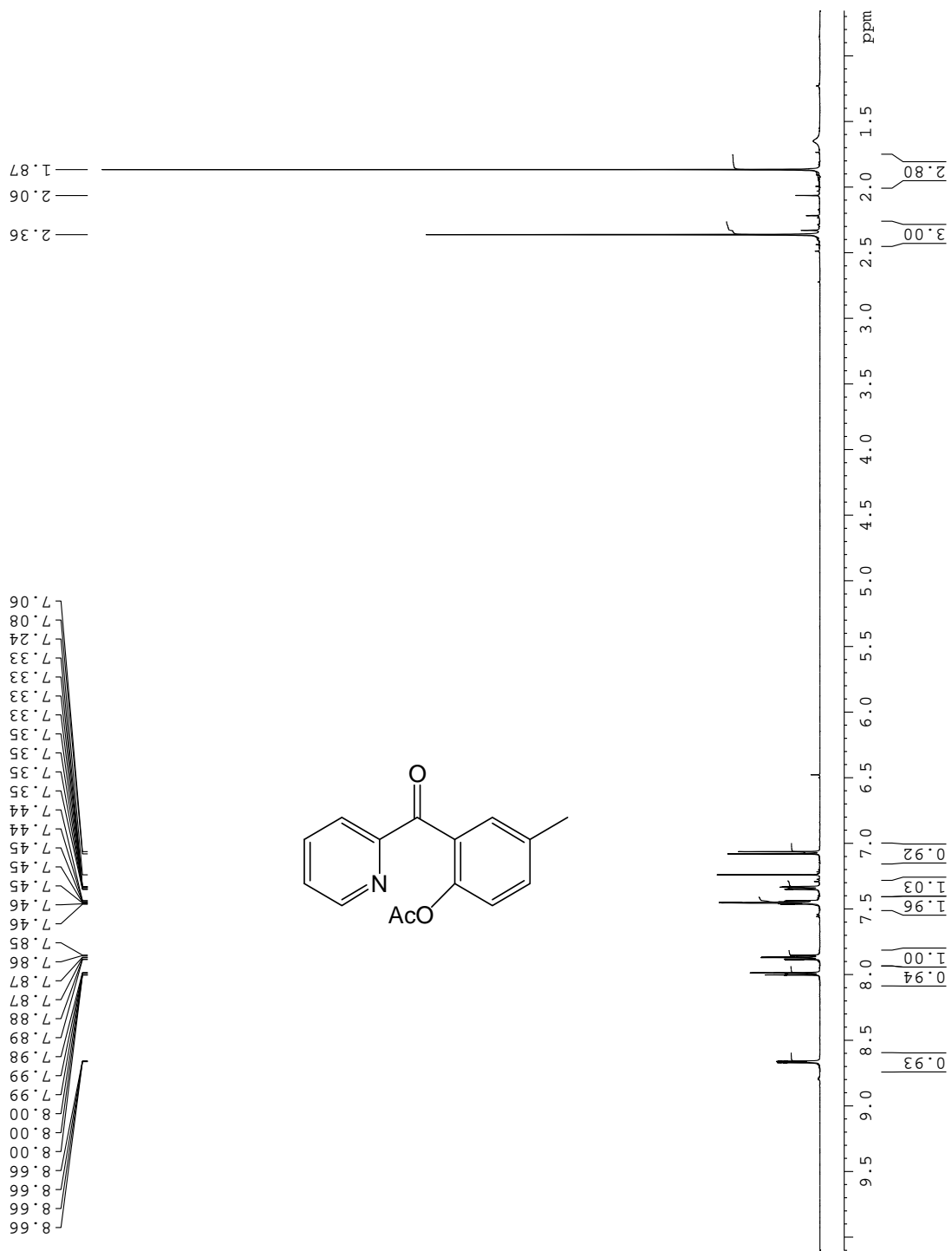


Fig. A31,  $^1\text{H NMR}$  of **36** in  $\text{CDCl}_3$  at  $22^\circ\text{C}$

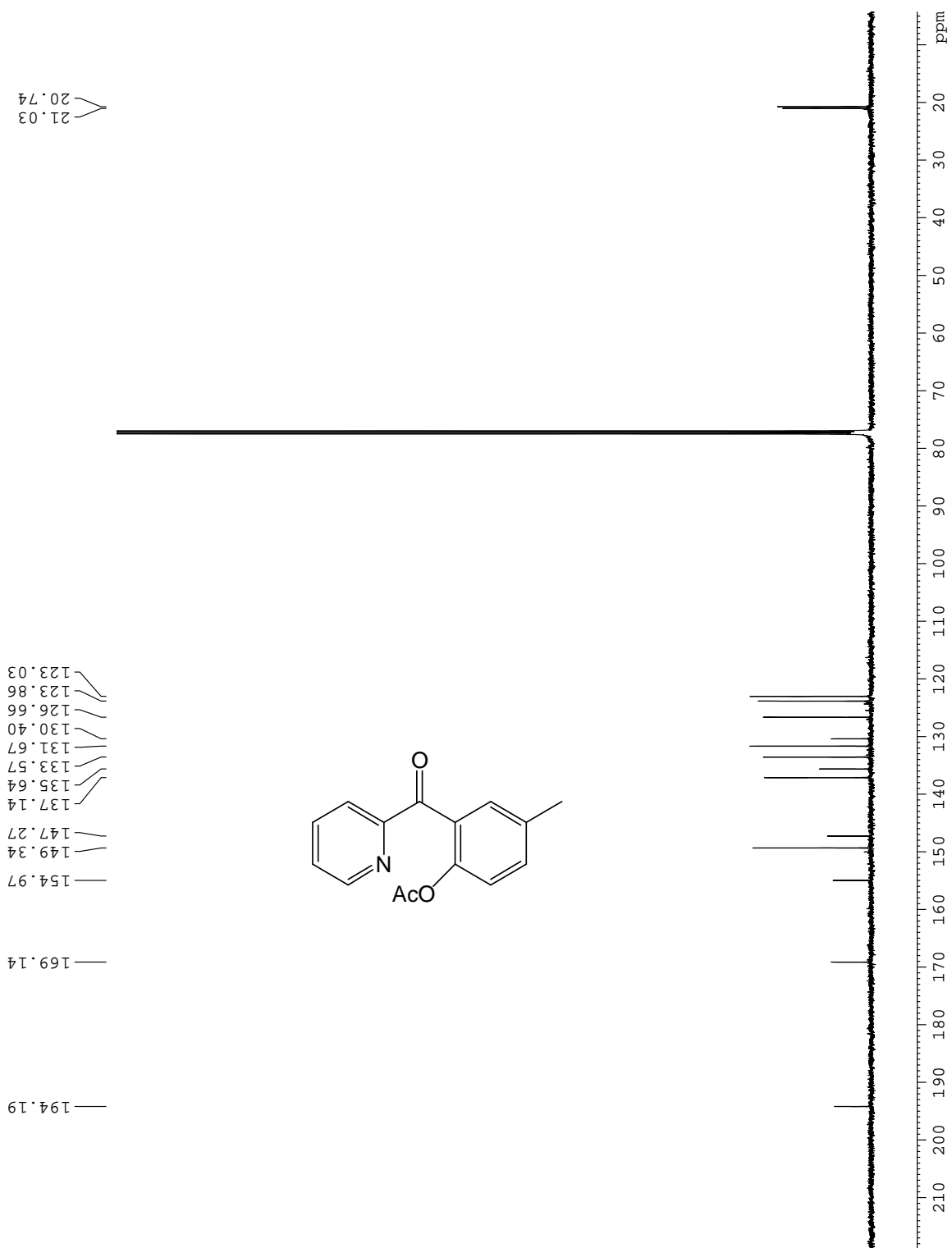


Fig. A32, <sup>13</sup>C NMR of **36** in CDCl<sub>3</sub> at 22°C

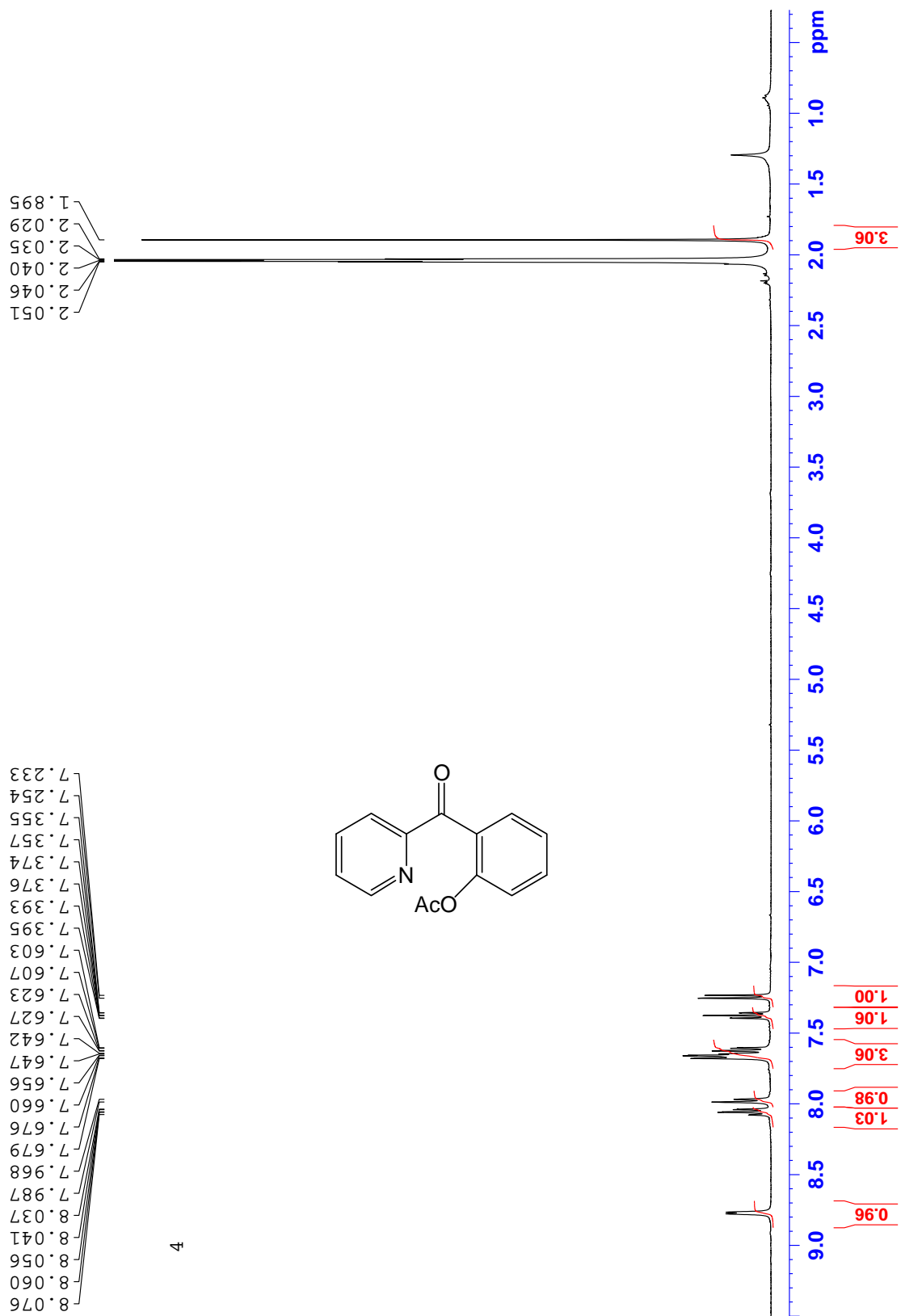


Fig. A33,  $^1\text{H}$  NMR of **35** in AcOH- $d_4$  at 22°C

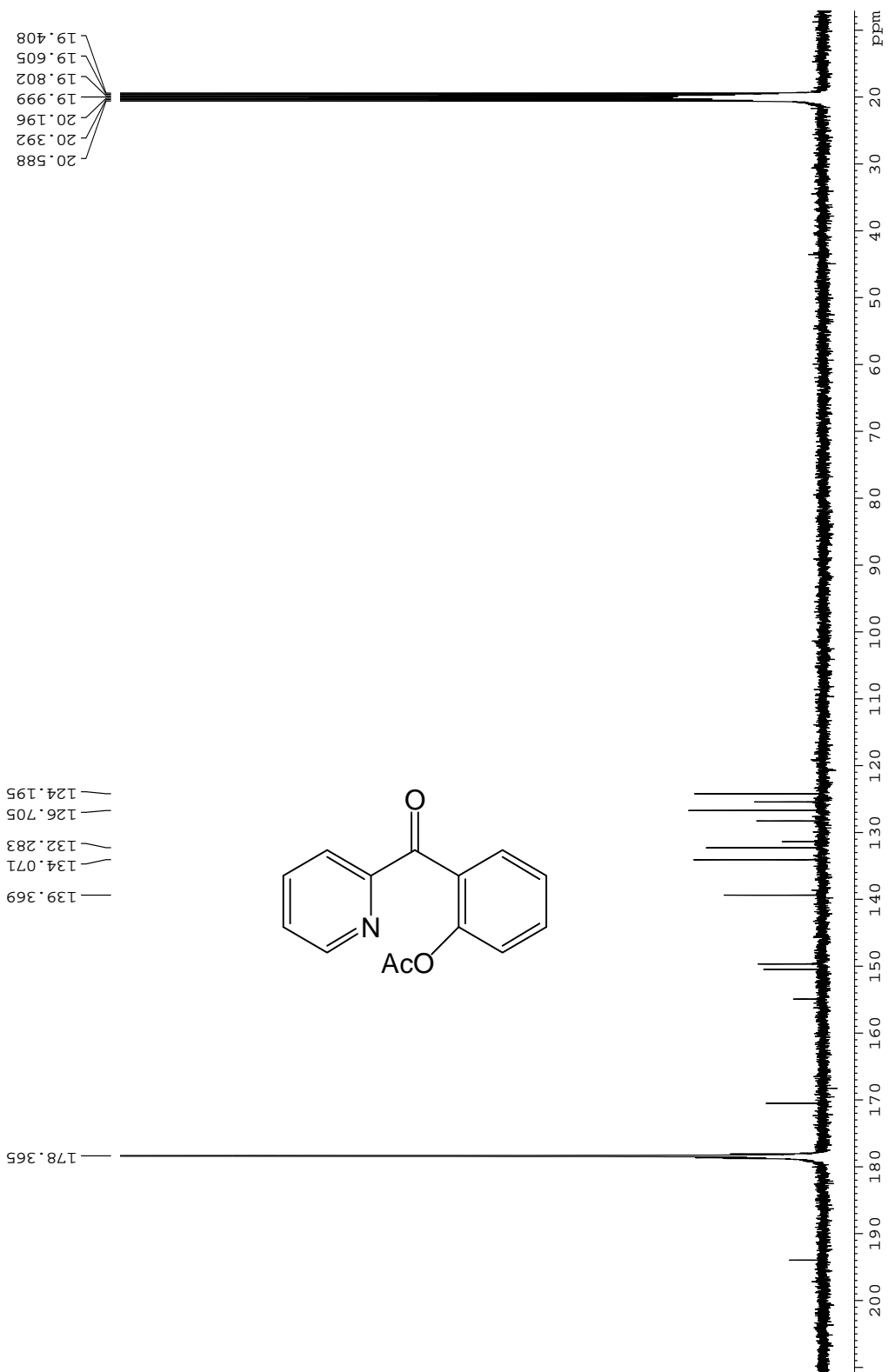


Fig. A34,  $^{13}\text{C}$  NMR of **35** in  $\text{AcOH-d}_4$  at  $22^\circ\text{C}$

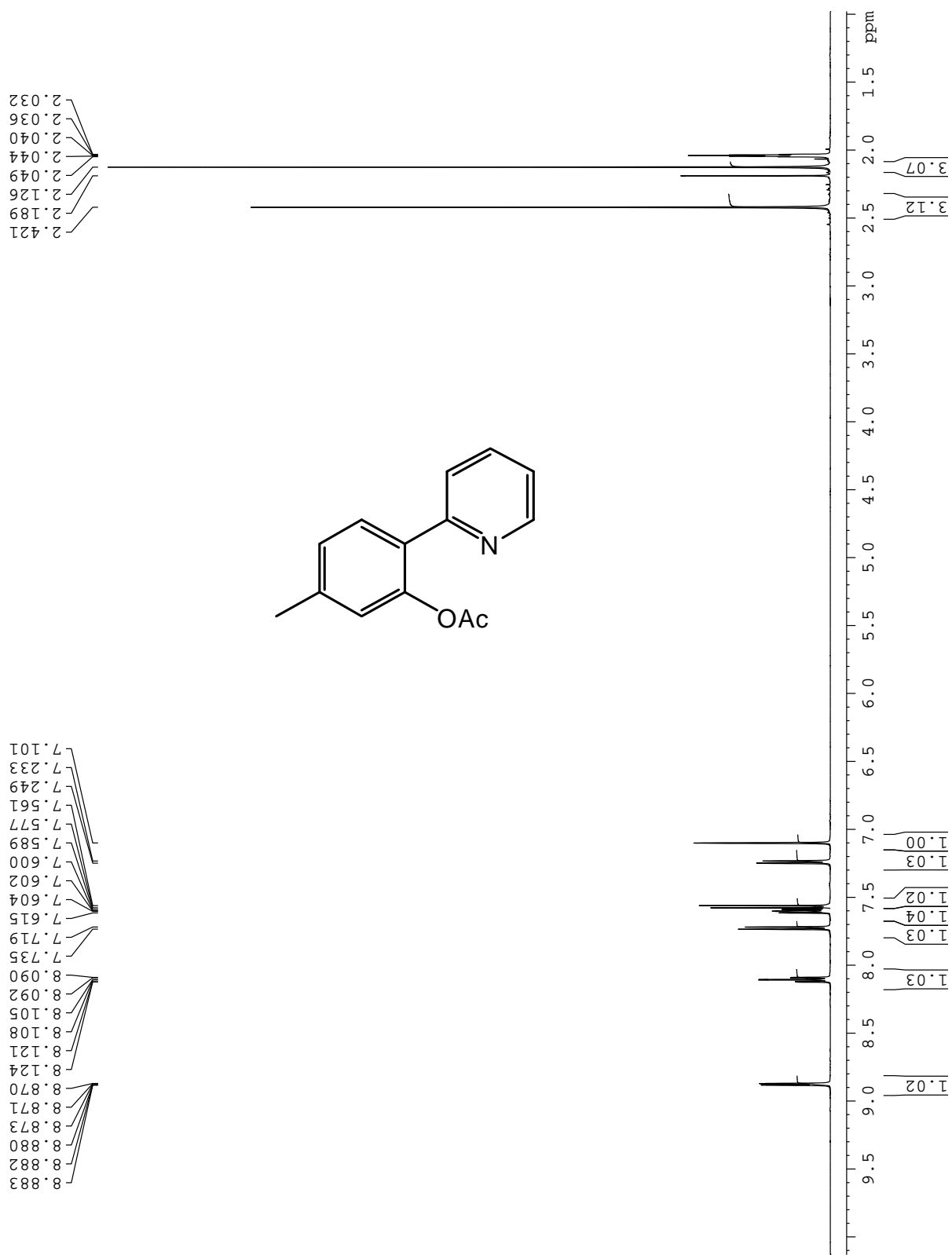


Fig. A35, <sup>1</sup>H NMR of **29** in AcOH-d<sub>4</sub> at 22°C

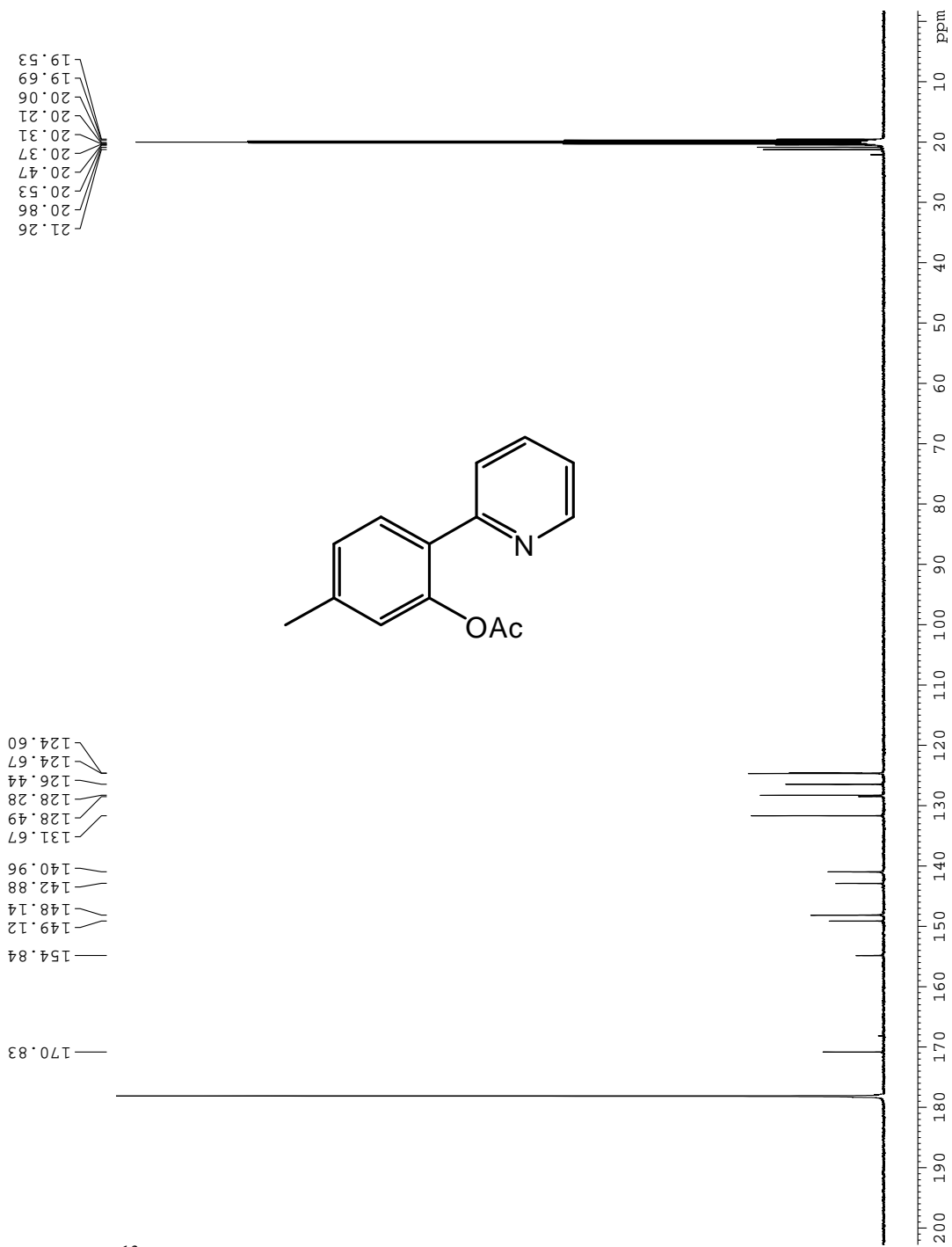


Fig. A36,  $^{13}\text{C}$  NMR of **29** in  $\text{AcOH-d}_4$  at  $22^\circ\text{C}$

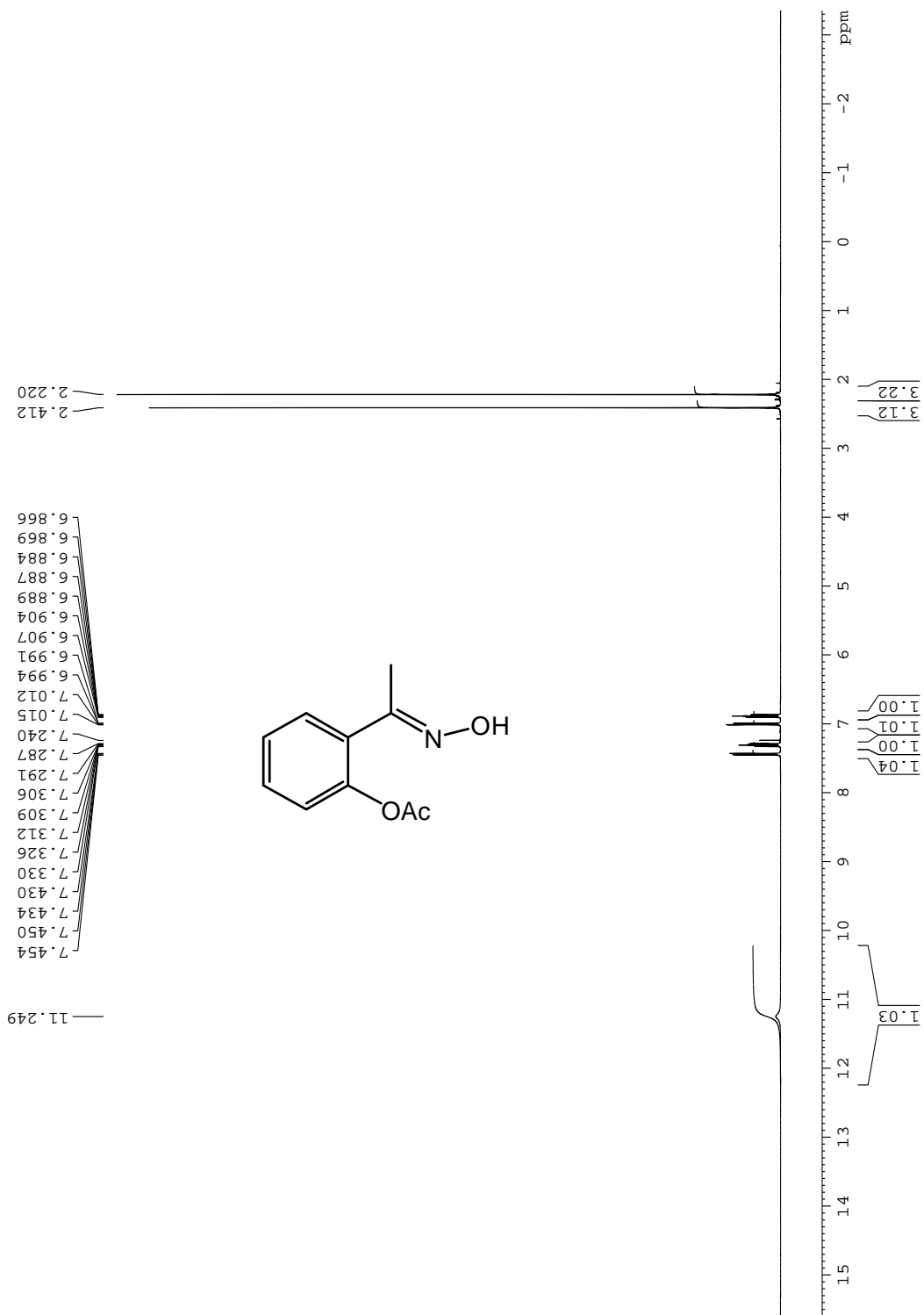


Fig. A37, <sup>1</sup>H NMR of complex **49** in CDCl<sub>3</sub> at 22°C

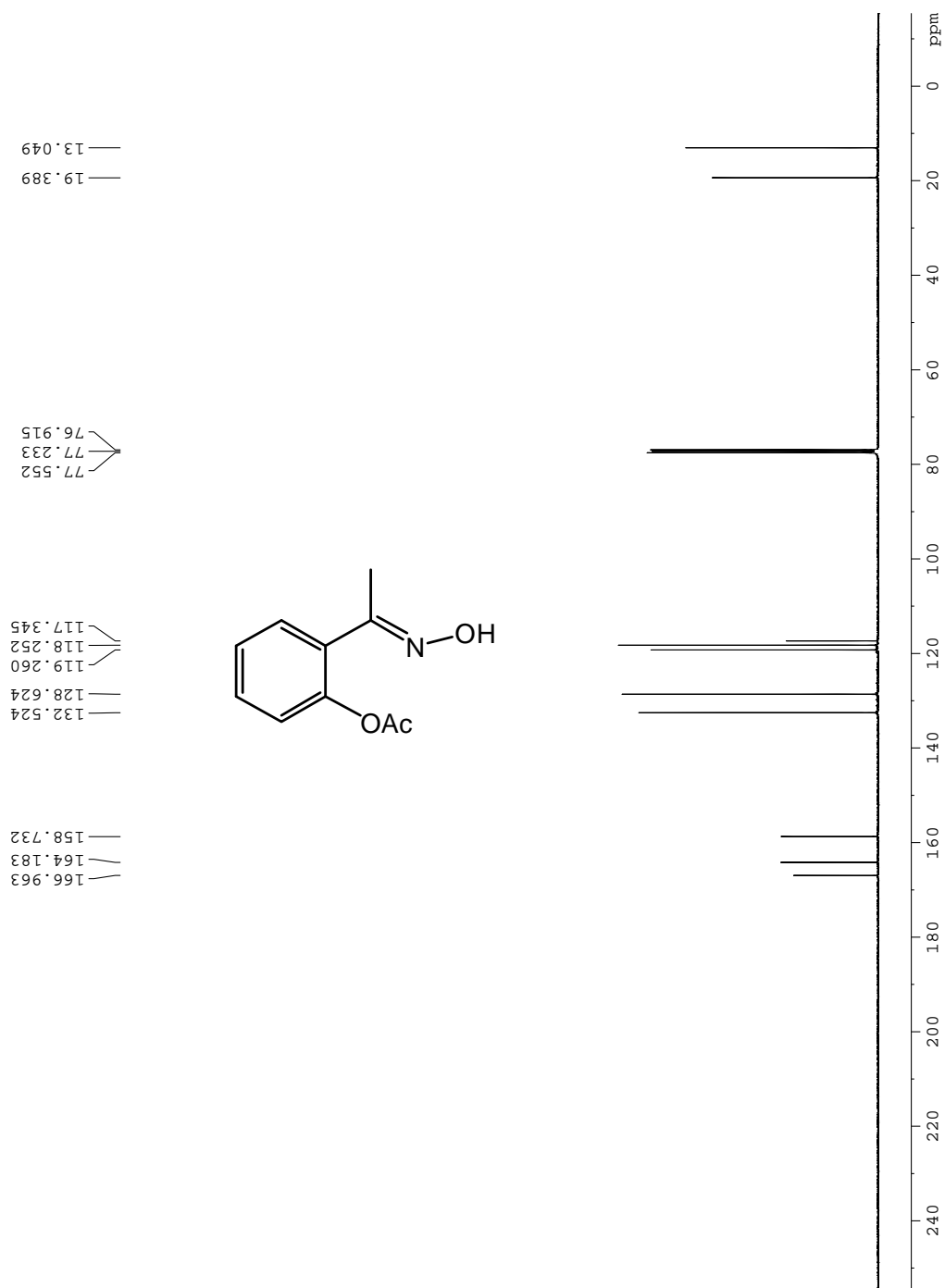


Fig. A38, <sup>13</sup>C NMR of complex **49** in CDCl<sub>3</sub> at 22°C

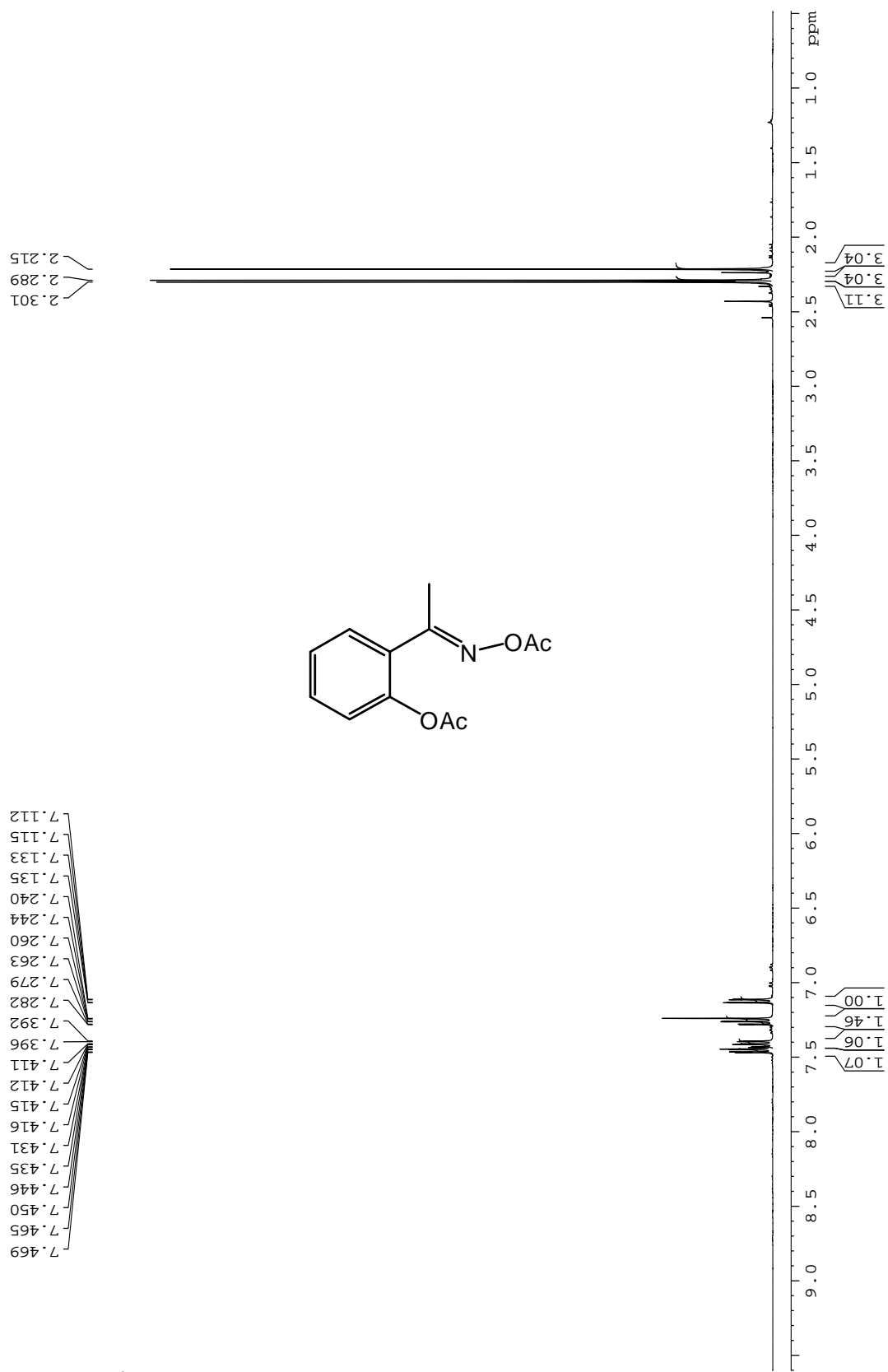


Fig. A39; <sup>1</sup>H NMR of complex **51** in CDCl<sub>3</sub> at 22°C

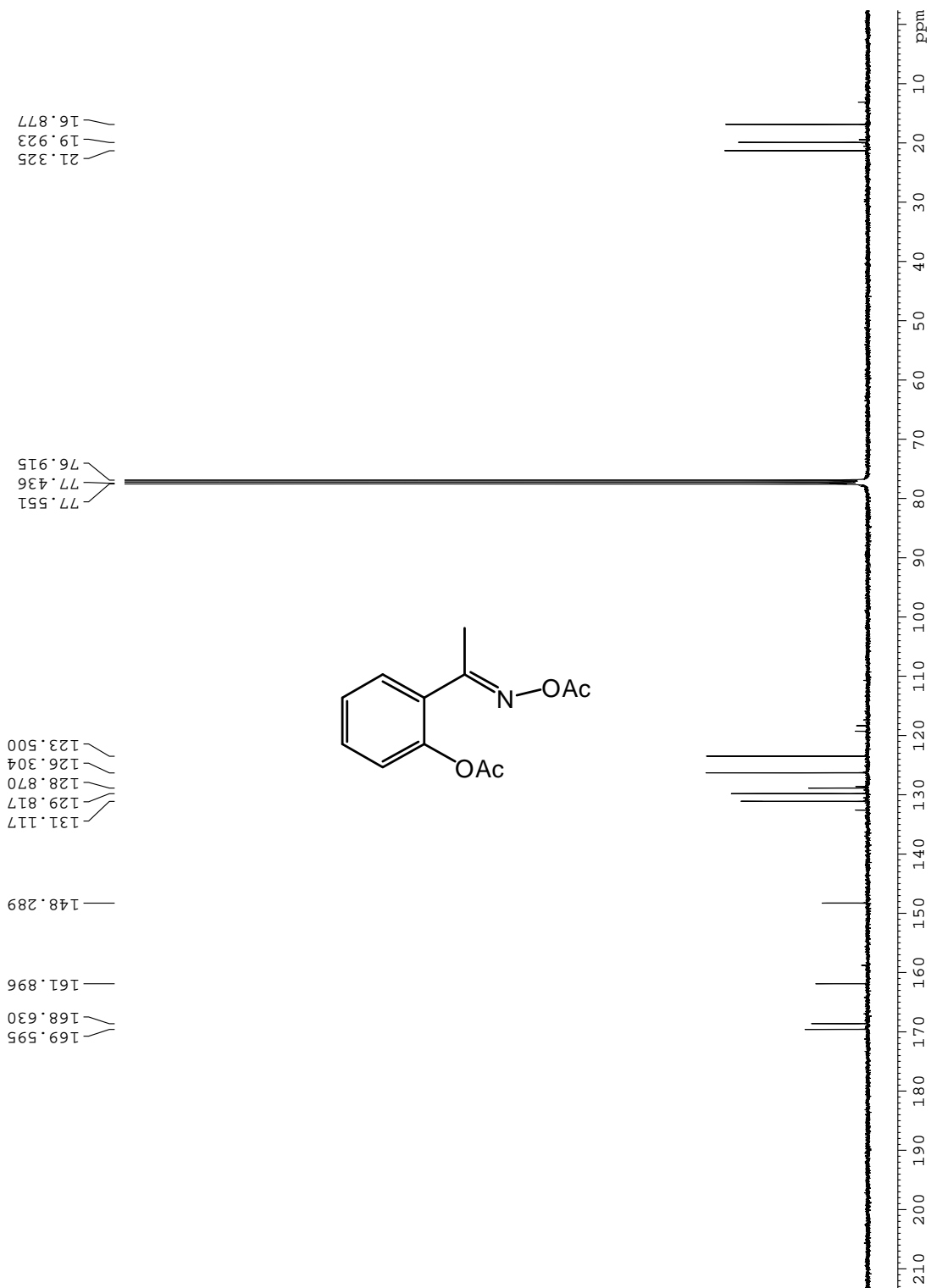


Fig. A40; <sup>13</sup>C NMR of complex **51** in CDCl<sub>3</sub> at 22°C

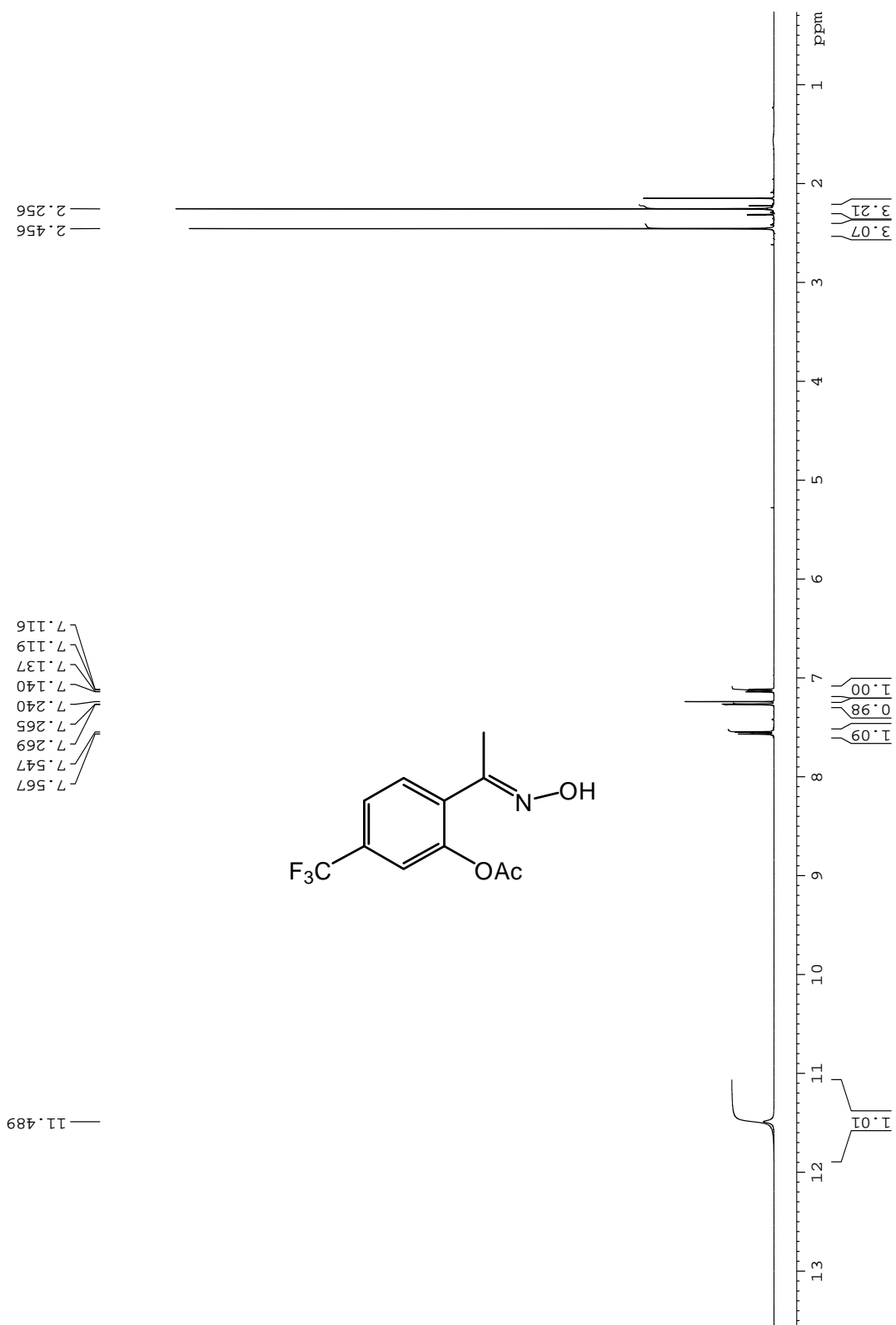


Fig. A41; <sup>1</sup>H NMR of complex **56** in CDCl<sub>3</sub> at 22°C

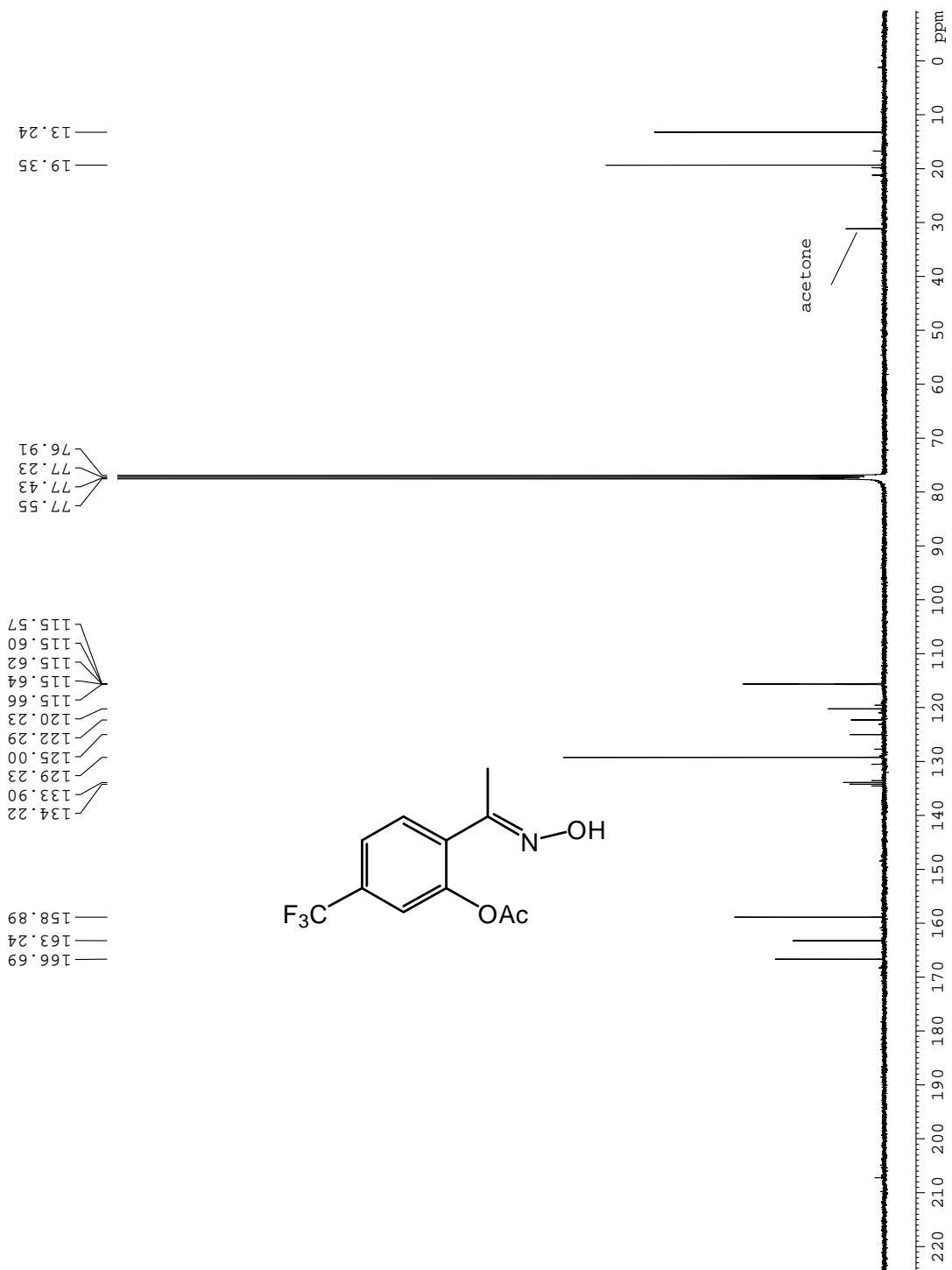


Fig. A42, <sup>13</sup>C NMR of complex **56** in CDCl<sub>3</sub> at 22°C

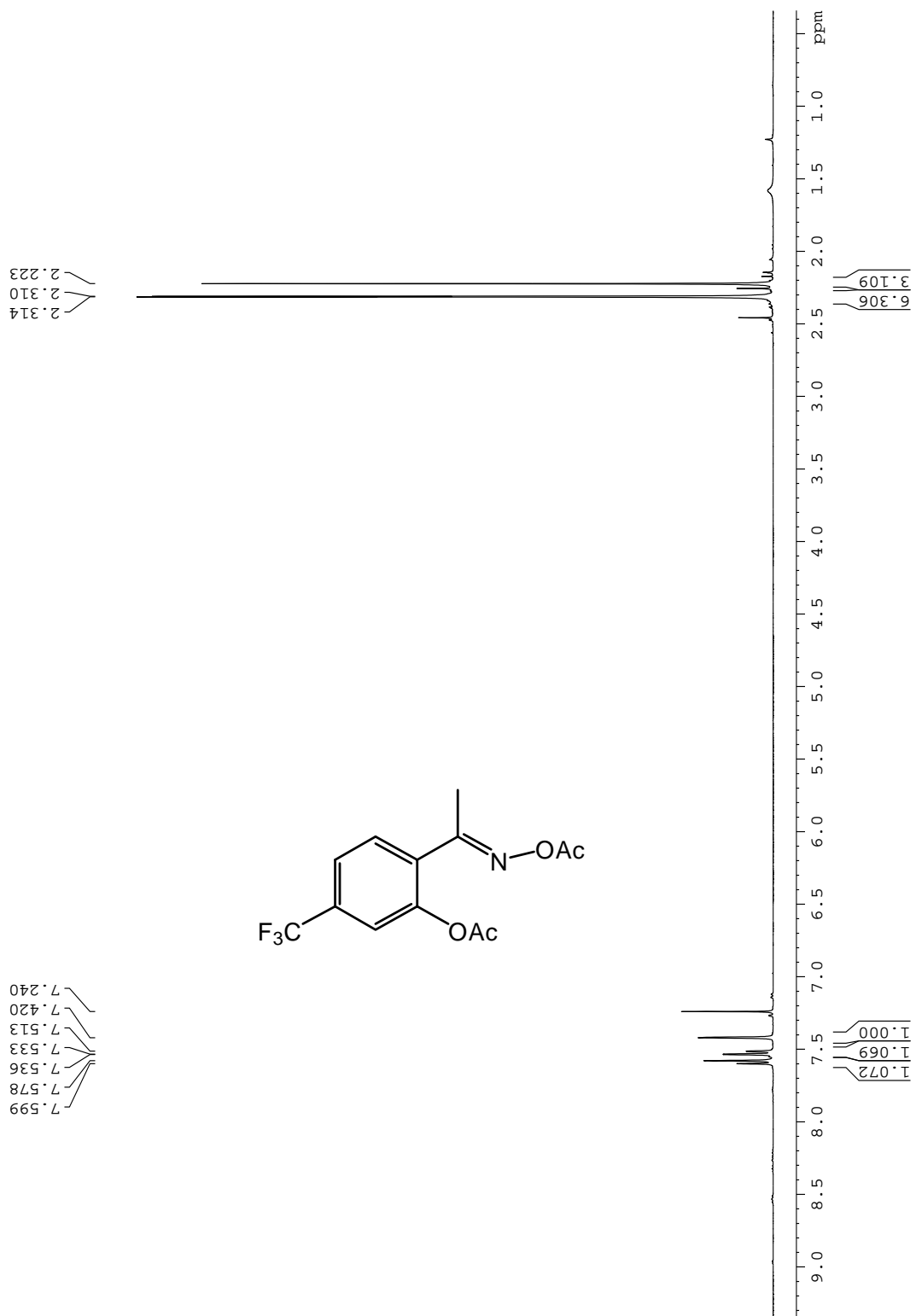


Fig. A43, <sup>1</sup>H NMR of complex **57** in CDCl<sub>3</sub> at 22°C

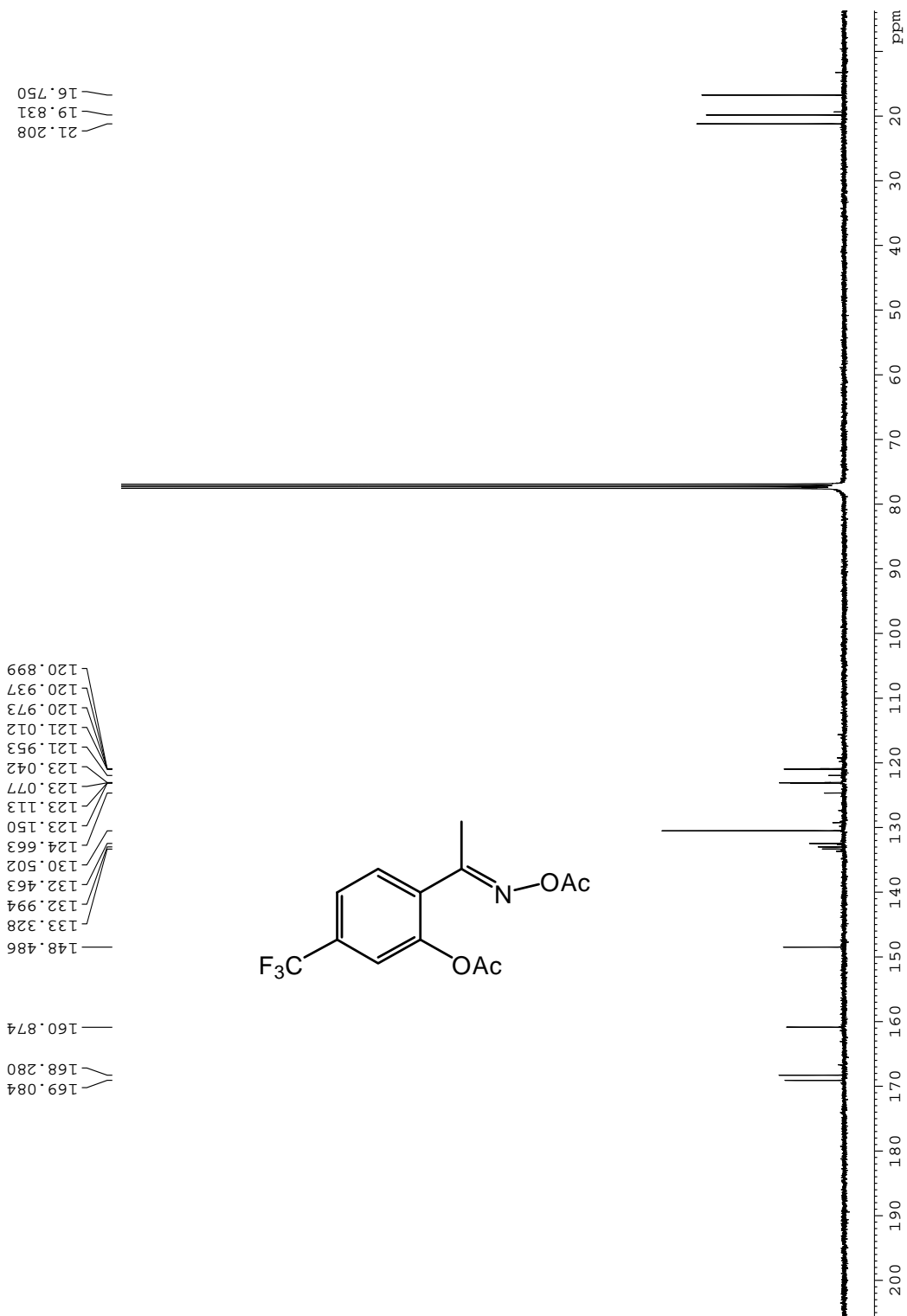


Fig. A44;  $^{13}\text{C}$  NMR of complex **57** in  $\text{CDCl}_3$  at  $22^\circ\text{C}$

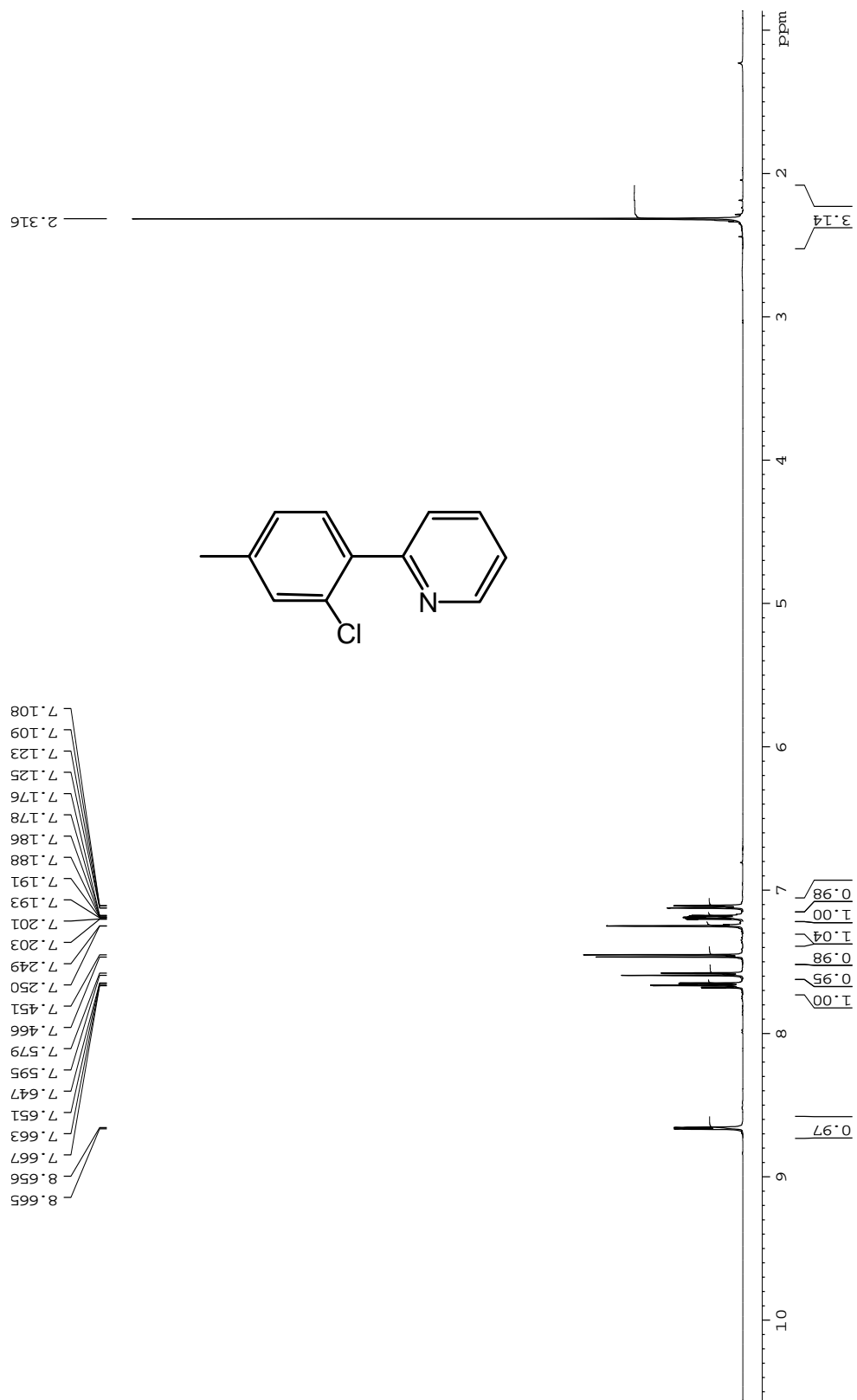


Fig. A45; <sup>1</sup>H NMR spectrum of **25** in CDCl<sub>3</sub>, 22°C.

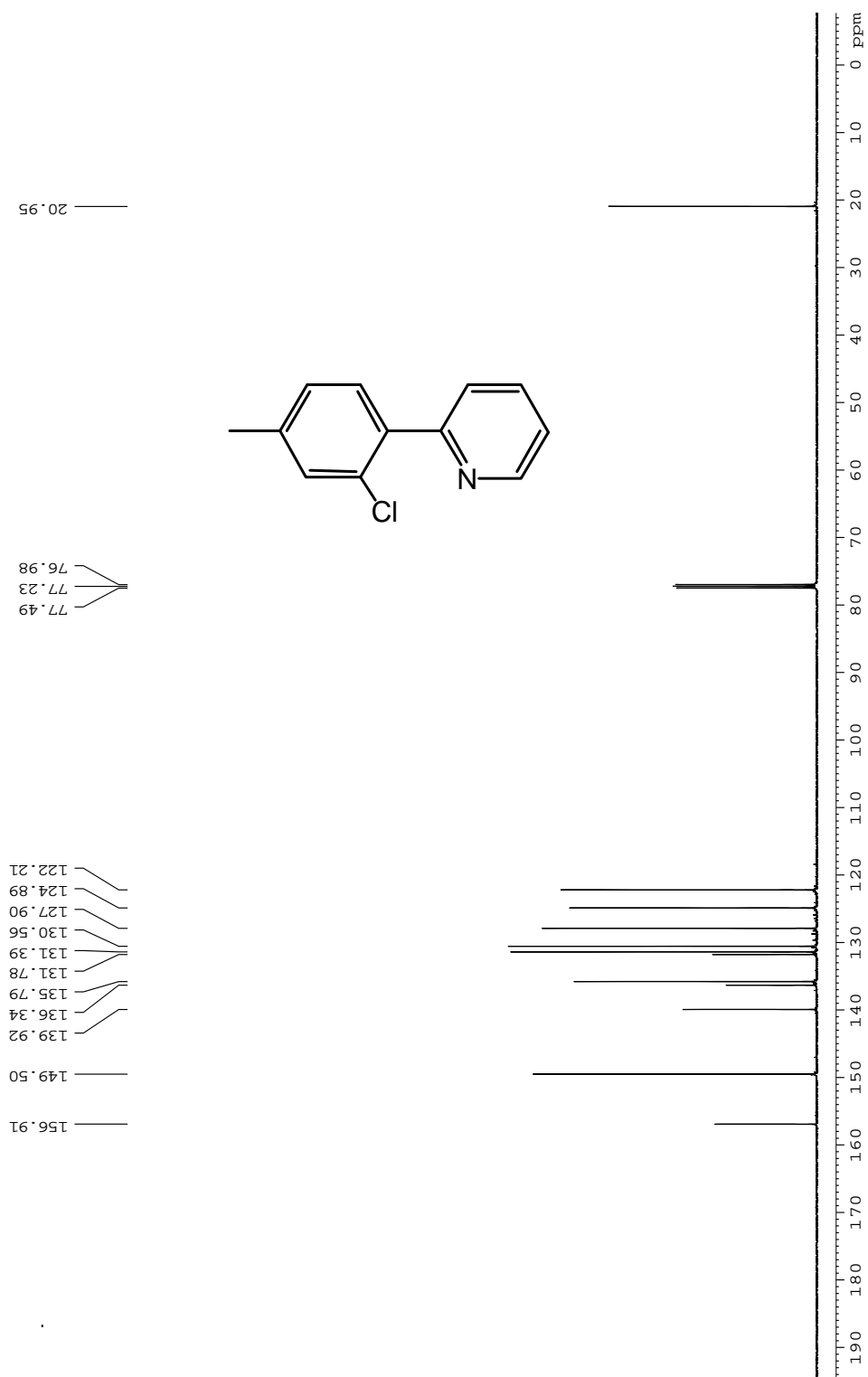


Fig. A46;  $^{13}\text{C}$  NMR spectrum of **25** in  $\text{CDCl}_3$ ,  $22^\circ\text{C}$ .

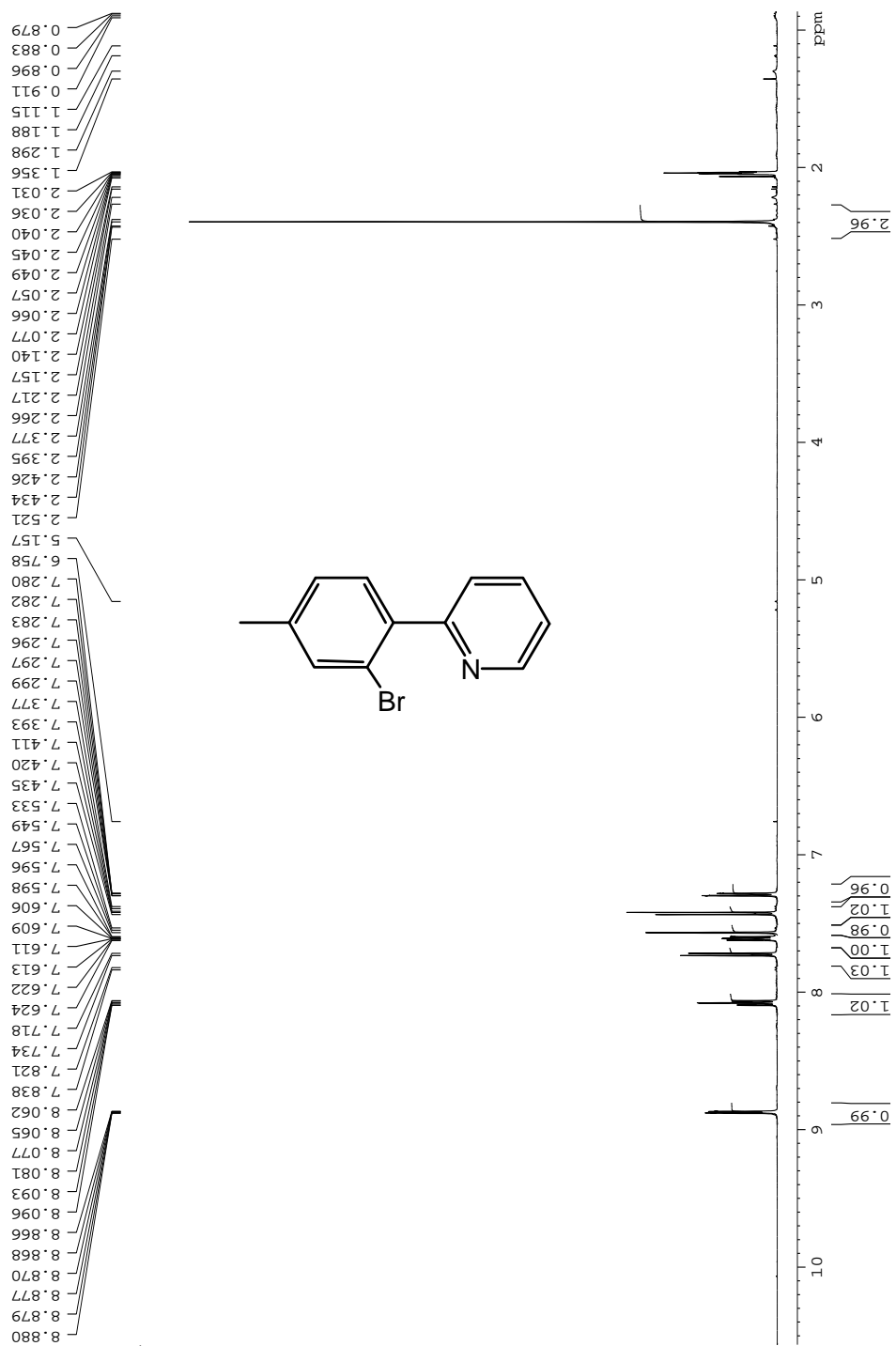


Fig. A47; <sup>1</sup>H NMR spectrum of **42** in CD<sub>3</sub>COOD, 22°C.

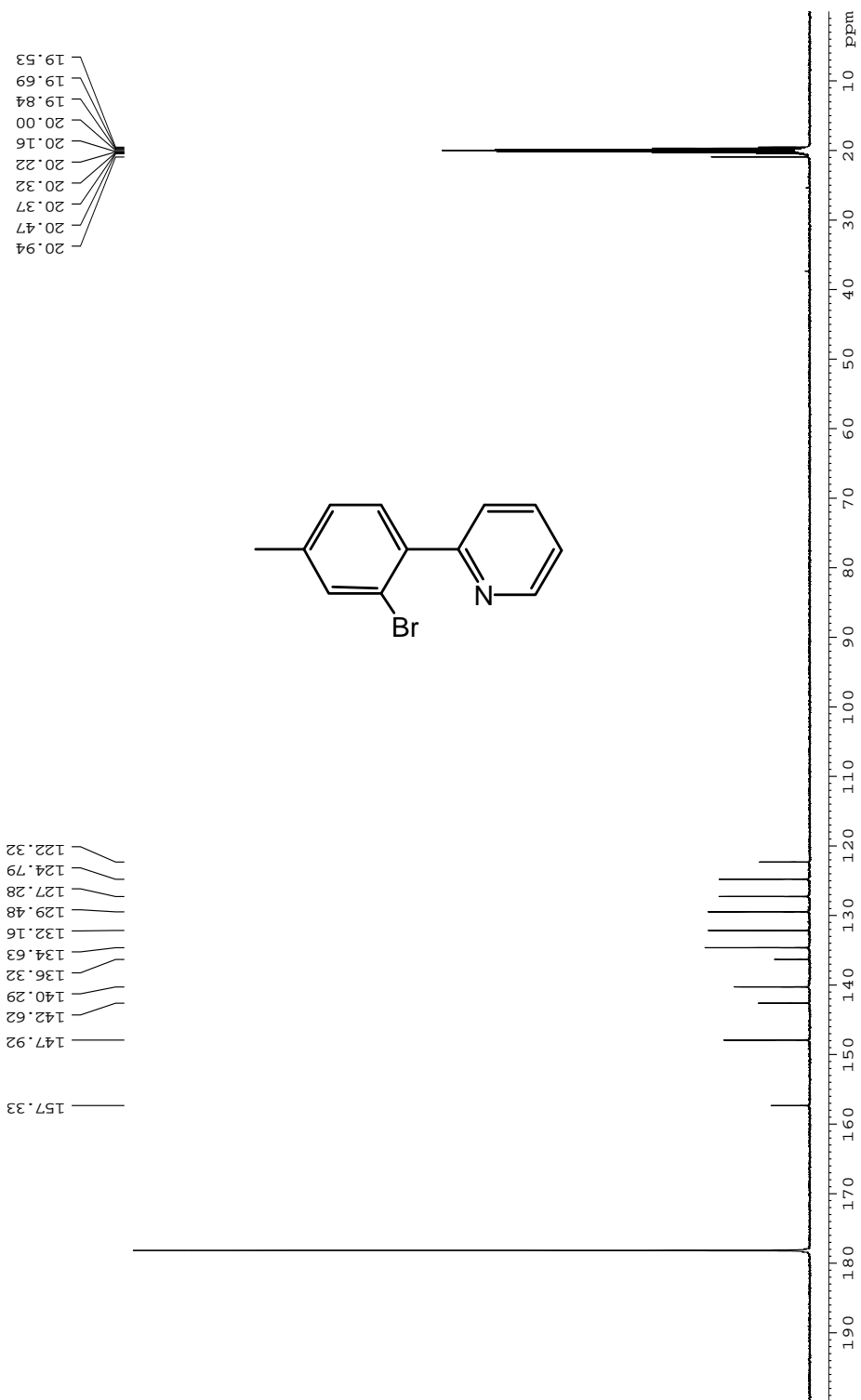


Fig. A48;  $^{13}\text{C}$  NMR spectrum of **42** in  $\text{CD}_3\text{COOD}$ ,  $22^\circ\text{C}$ .

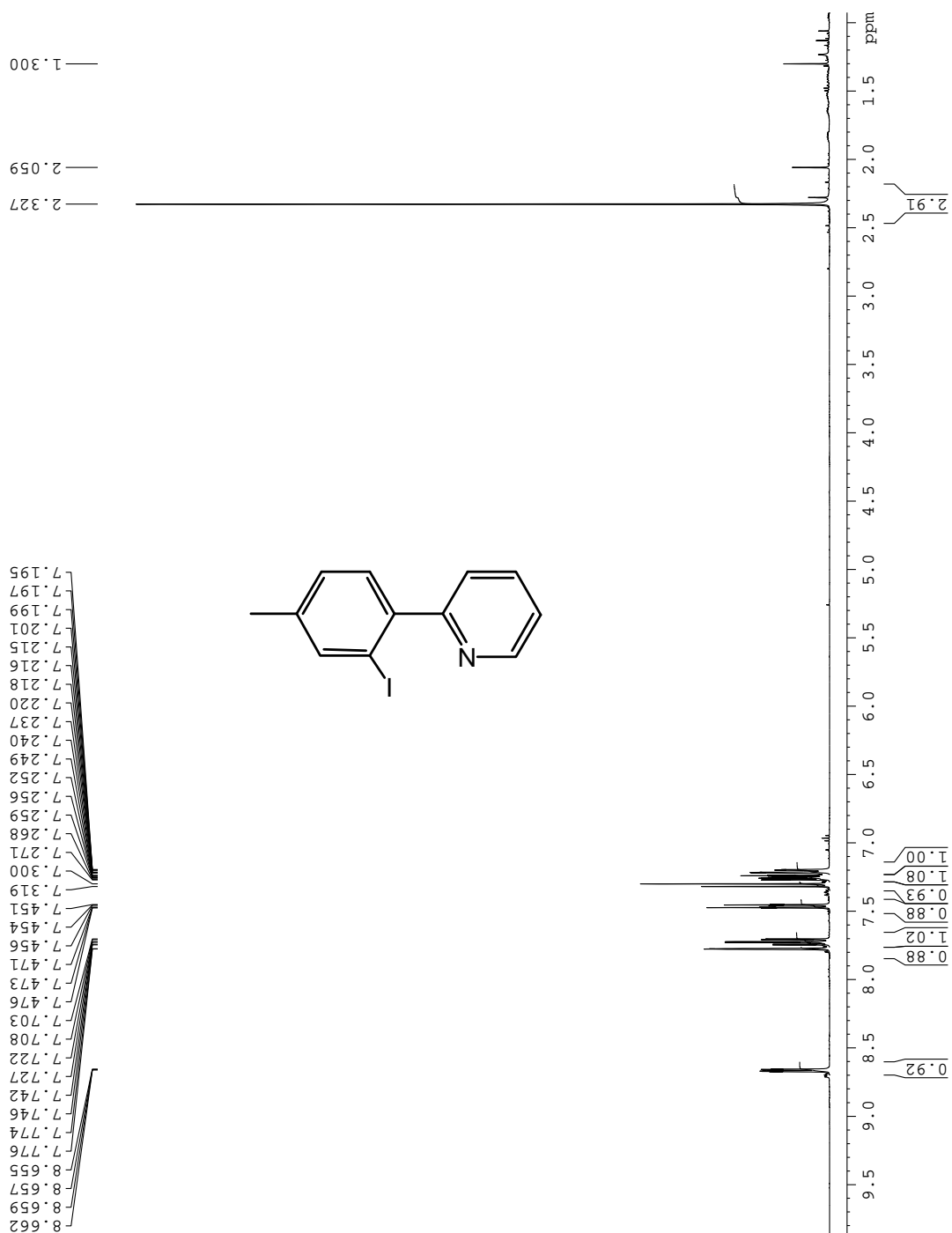


Fig. A49; <sup>1</sup>H NMR spectrum of **46** in CDCl<sub>3</sub>, 22°C.

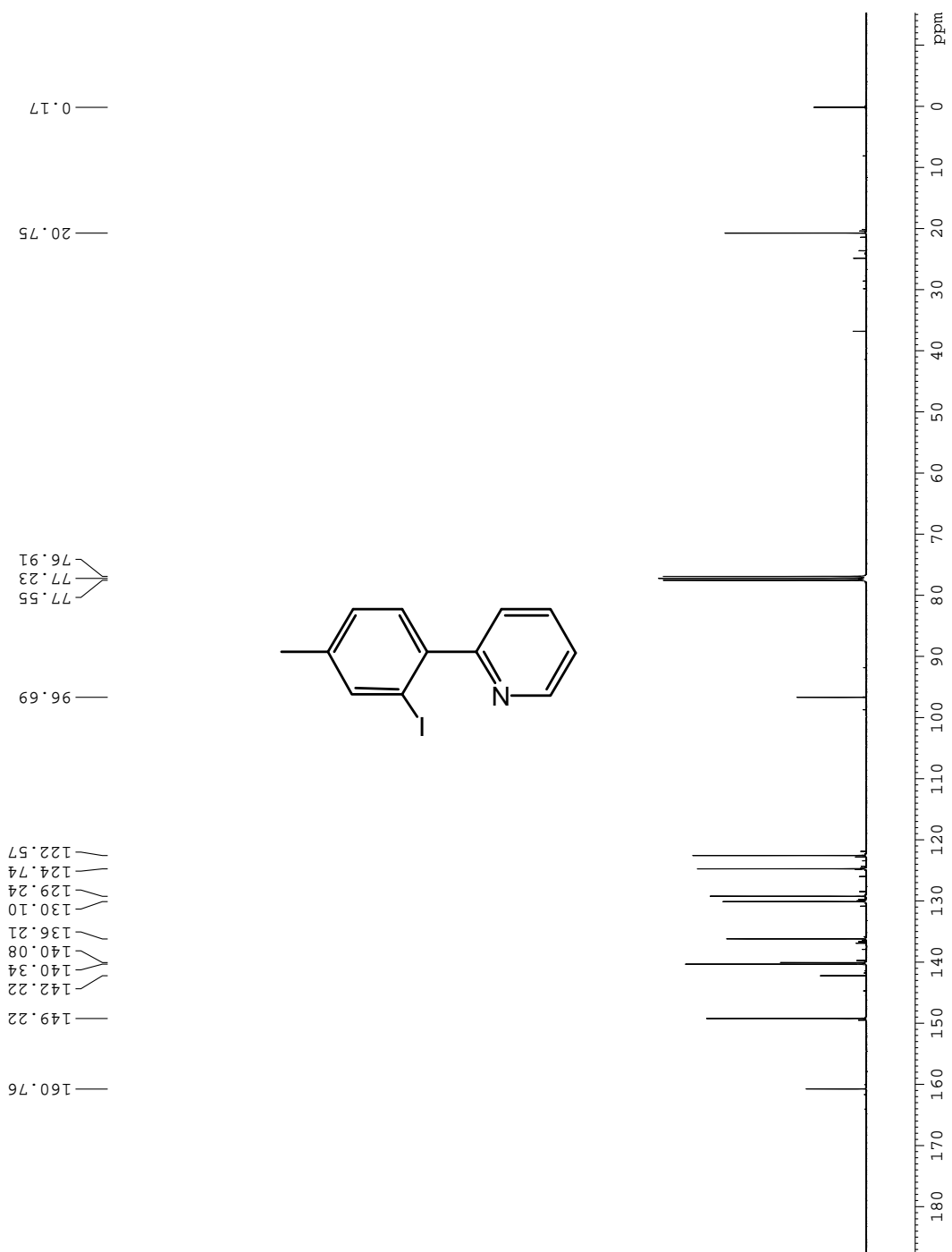


Fig. A50;  $^{13}\text{C}$  NMR spectrum of **46** in  $\text{CDCl}_3$ ,  $22^\circ\text{C}$ .





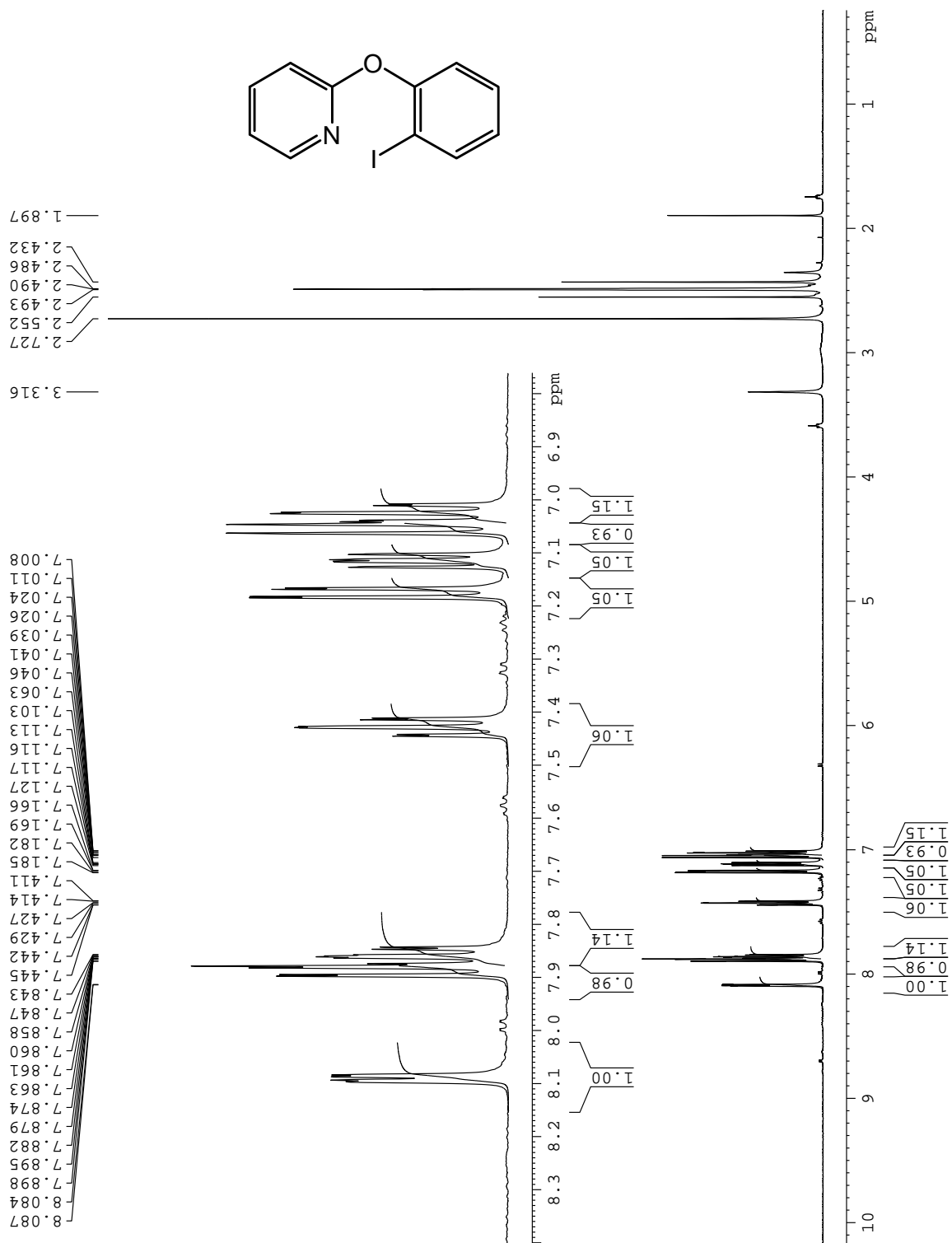


Fig. A53; <sup>1</sup>H NMR spectrum of **53** in dms0-d<sub>6</sub>, 22°C.

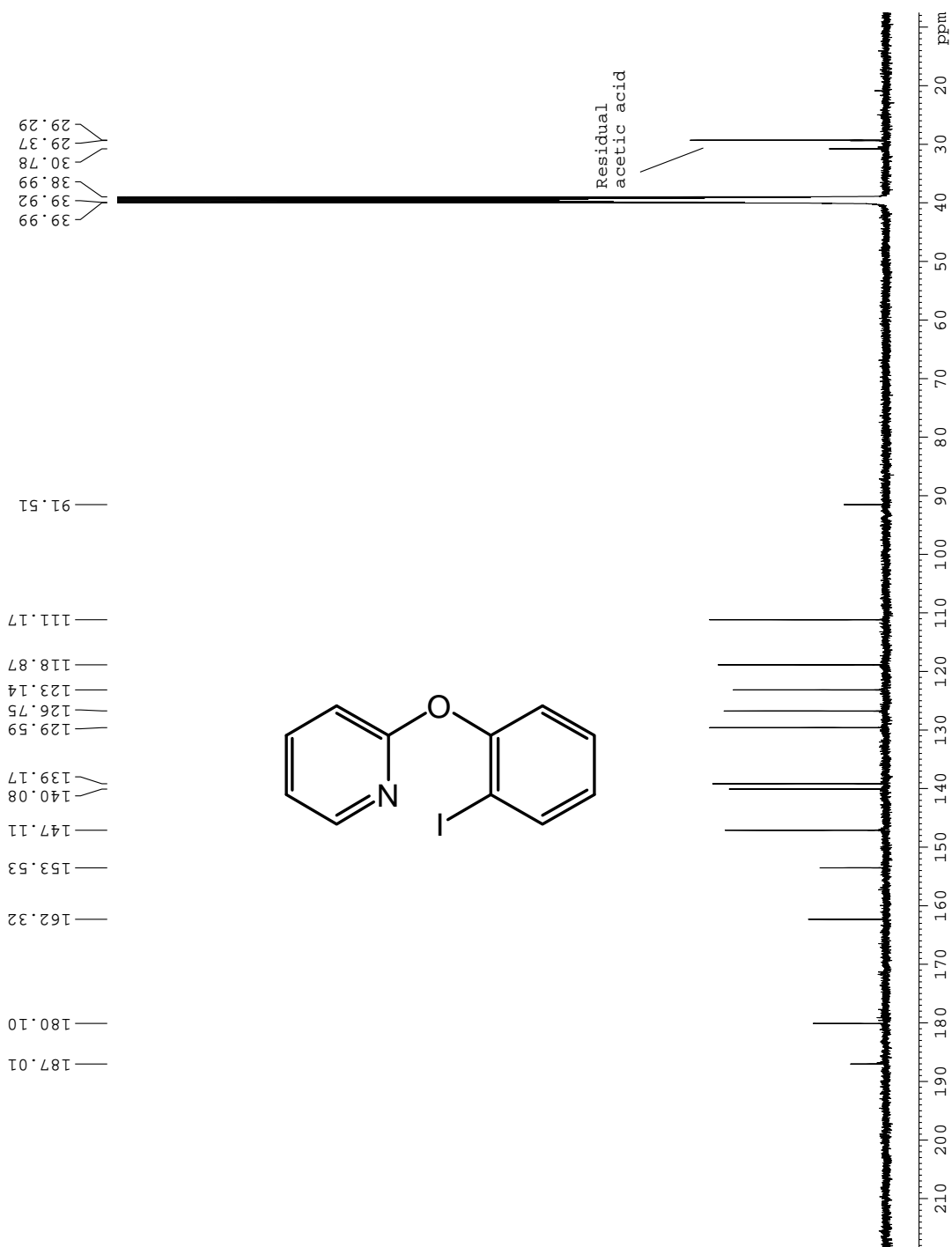


Fig. A54; <sup>13</sup>C NMR spectrum of **53** in dms0-d<sub>6</sub>, 22°C.

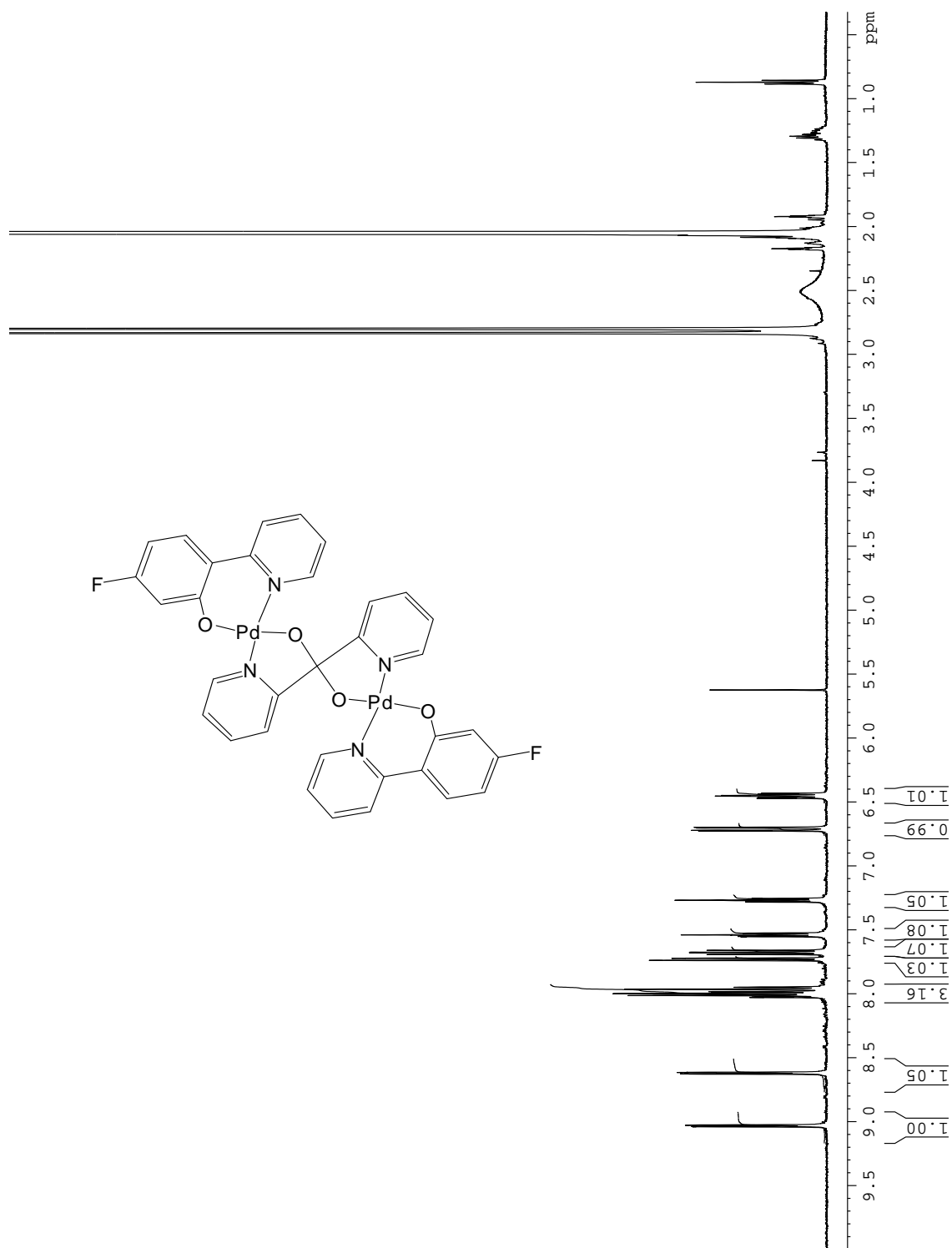


Fig. A55;  $^1\text{H}$  NMR spectrum of **25** in  $\text{acetone-d}_6$ ,  $22^\circ\text{C}$ .

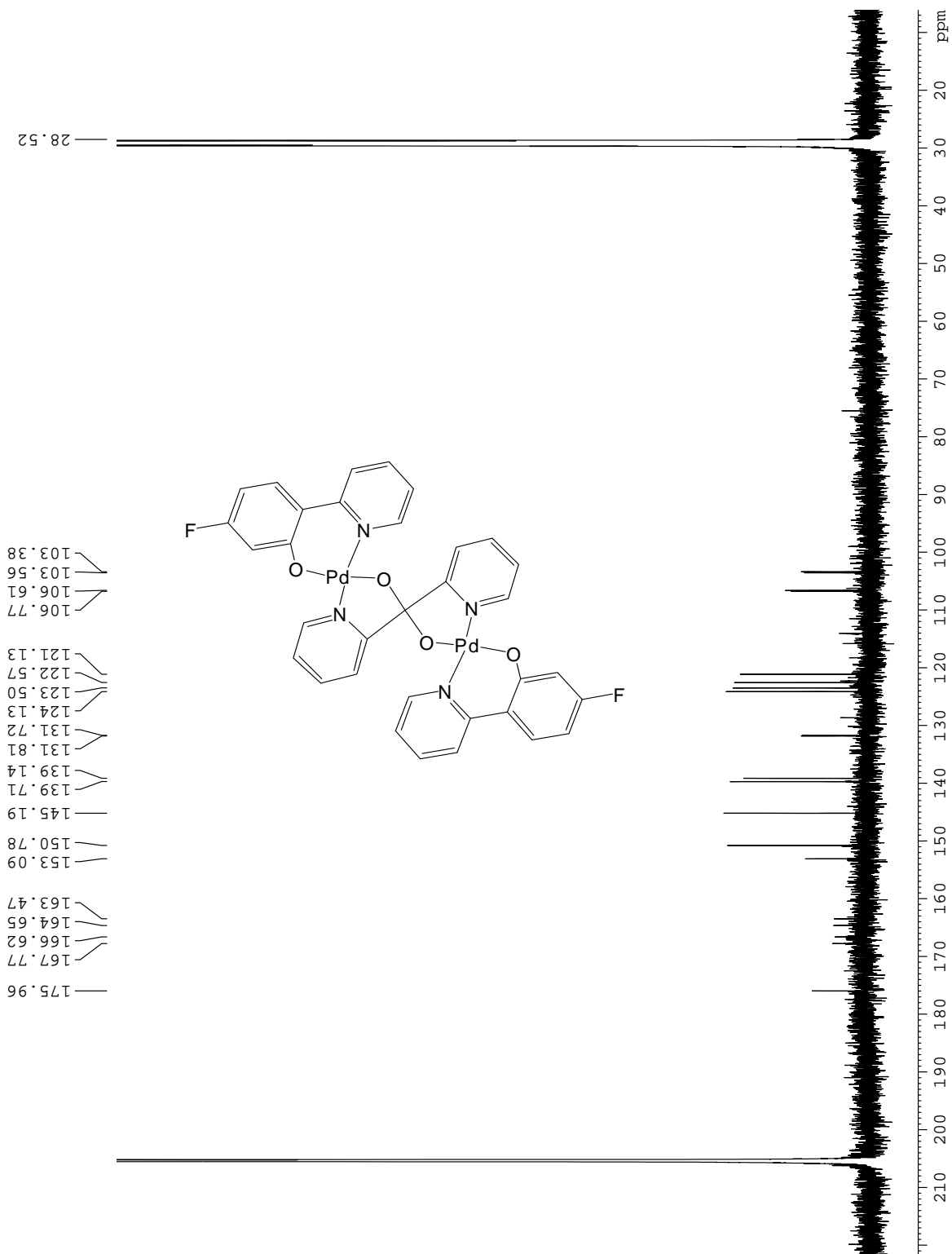


Fig. A56;  $^{13}\text{C}$  NMR spectrum of **25** in acetone- $d_6$ , 22°C.

## Bibliography

- (1) Alonso, D. A.; Najera, C.; Pacheco, M. C. *Organic Letters* **2000**, *2*, 1823.
- (2) Backvall, J. E. *Modern Oxidation Methods*; Wiley\_VCH: Weinheim, 2004.
- (3) Crabtree, R. H. *Chemical Reviews* **1985**, *85*, 245.
- (4) Arndtsen, B. A.; Bergman, R. G.; Mobley, T. A.; Peterson, T. H. *Accounts of Chemical Research* **1995**, *28*, 154.
- (5) Dick, A. R.; Sanford, M. S. *Tetrahedron* **2006**, *62*, 2439.
- (6) Nakao, Y.; Idei, H.; Kanyiva, K. S.; Hiyama, T. *Journal of the American Chemical Society* **2009**, *131*, 15996.
- (7) Nakao, Y.; Kanyiva, K. S.; Hiyama, T. *Journal of the American Chemical Society* **2008**, *130*, 2448.
- (8) Shi, F.; Larock, R. C. In *C-H Activation* 2010; Vol. 292, p 123.
- (9) Campeau, L. C.; Fagnou, K. *Chemical Communications* **2006**, 1253.
- (10) Beck, E. M.; Gaunt, M. J. In *C-H Activation* 2010; Vol. 292, p 85.
- (11) Ackermann, L.; Vicente, R.; Kapdi, A. R. *Angewandte Chemie-International Edition* **2009**, *48*, 9792.
- (12) Bandini, M.; Eichholzer, A. *Angewandte Chemie-International Edition* **2009**, *48*, 9608.
- (13) Bellina, F.; Rossi, R. *Tetrahedron* **2009**, *65*, 10269.
- (14) Lewis, J. C.; Bergman, R. G.; Ellman, J. A. *Accounts of Chemical Research* **2008**, *41*, 1013.
- (15) Hickman, A. J.; Sanford, M. S. *Acs Catalysis* **2011**, *1*, 170.

- (16) Dunina, V. V.; Zalevskaya, O. A.; Potapov, V. M. *Uspekhi Khimii* **1988**, *57*, 434.
- (17) Ryabov, A. D. *Chemical Reviews* **1990**, *90*, 403.
- (18) Dyker, G. *Angewandte Chemie-International Edition* **1999**, *38*, 1699.
- (19) Dupont, J.; Consorti, C. S.; Spencer, J. *Chemical Reviews* **2005**, *105*, 2527.
- (20) Cope, A. C.; Siekman, R. W. *Journal of the American Chemical Society* **1965**, *87*, 3272.
- (21) Chen, X.; Hao, X. S.; Goodhue, C. E.; Yu, J. Q. *Journal of the American Chemical Society* **2006**, *128*, 6790.
- (22) Sen, A. *Accounts of Chemical Research* **1998**, *31*, 550.
- (23) Dangel, B. D.; Johnson, J. A.; Sames, D. *Journal of the American Chemical Society* **2001**, *123*, 8149.
- (24) Lyons, T. W.; Sanford, M. S. *Chemical Reviews* **2010**, *110*, 1147.
- (25) Stahl, S. S. *Angewandte Chemie-International Edition* **2004**, *43*, 3400.
- (26) Beccalli, E. M.; Broggini, G.; Martinelli, M.; Sottocornola, S. *Chemical Reviews* **2007**, *107*, 5318.
- (27) Huheey, J. E. *Inorganic Chemistry: Principles of Structure & reactivity*; 5th ed.; Addison-Wesley, 2009.
- (28) James, A. M.; Lord, M. P. *Macmillan's Chemical and Physical Data*; Macmillan: London, 1992.
- (29) Ballhausen, C. J. *Introduction to Ligand Field Theory*; McGraw-Hill: New York, 1962.
- (30) Pope, W. J.; Peachey, S. J. *Proc. Chem. Soc.* **1907**, *23*, 86.

- (31) Deprez, N. R.; Sanford, M. S. *Inorganic Chemistry* **2007**, *46*, 1924.
- (32) Kalyani, D.; Dick, A. R.; Anani, W. Q.; Sanford, M. S. *Organic Letters* **2006**, *8*, 2523.
- (33) Desai, L. V.; Malik, H. A.; Sanford, M. S. *Organic Letters* **2006**, *8*, 1141.
- (34) Alexanian, E. J.; Lee, C.; Sorensen, E. J. *Journal of the American Chemical Society* **2005**, *127*, 7690.
- (35) Desai, L. V.; Sanford, M. S. *Angewandte Chemie-International Edition* **2007**, *46*, 5737.
- (36) Li, Y.; Song, D.; Dong, V. M. *Journal of the American Chemical Society* **2008**, *130*, 2962.
- (37) Streuff, J.; Hovelmann, C. H.; Nieger, M.; Muniz, K. *Journal of the American Chemical Society* **2005**, *127*, 14586.
- (38) Streuff, J.; Muniz, K. *Journal of Organometallic Chemistry* **2005**, *690*, 5973.
- (39) Welbes, L. L.; Lyons, T. W.; Cychosz, K. A.; Sanford, M. S. *Journal of the American Chemical Society* **2007**, *129*, 5836.
- (40) Schroeder, K.; Tong, X.; Bitterlich, B.; Tse, M. K.; Gelalcha, F. G.; Bruckner, A.; Beller, M. *Tetrahedron Letters* **2007**, *48*, 6339.
- (41) Desai, L. V.; Stowers, K. J.; Sanford, M. S. *Journal of the American Chemical Society* **2008**, *130*, 13285.
- (42) Hull, K. L.; Lanni, E. L.; Sanford, M. S. *Journal of the American Chemical Society* **2006**, *128*, 14047.
- (43) Fu, Y.; Li, Z.; Liang, S.; Guo, Q. X.; Liu, L. *Organometallics* **2008**, *27*, 3736.
- (44) Hartwig, J. F. *Inorganic Chemistry* **2007**, *46*, 1936.

- (45) Muniz, K. *Angewandte Chemie-International Edition* **2009**, *48*, 9412.
- (46) Powers, D. C.; Xiao, D. Y.; Geibel, M. A. L.; Ritter, T. *Journal of the American Chemical Society* **2010**, *132*, 14530.
- (47) Davidson, J. M.; Triggs, C. *Chemistry & Industry* **1966**, 457.
- (48) Henry, P. M. *Journal of Organic Chemistry* **1971**, *36*, 1886.
- (49) Yoneyama, T.; Crabtree, R. H. *Journal of Molecular Catalysis a-Chemical* **1996**, *108*, 35.
- (50) Dick, A. R.; Hull, K. L.; Sanford, M. S. *Journal of the American Chemical Society* **2004**, *126*, 2300.
- (51) Canty, A. J.; Denney, M. C.; Skelton, B. W.; White, A. H. *Organometallics* **2004**, *23*, 1122.
- (52) Canty, A. J.; Denney, M. C.; van Koten, G.; Skelton, B. W.; White, A. H. *Organometallics* **2004**, *23*, 5432.
- (53) Canty, A. J.; Jin, H. *Journal of Organometallic Chemistry* **1998**, *565*, 135.
- (54) Valk, J. M.; Boersma, J.; vanKoten, G. *Organometallics* **1996**, *15*, 4366.
- (55) Canty, A. J.; Jin, H.; Skelton, B. W.; White, A. H. *Inorganic Chemistry* **1998**, *37*, 3975.
- (56) Yamamoto, Y.; Kuwabara, S.; Matsuo, S.; Ohno, T.; Nishiyama, H.; Itoh, K. *Organometallics* **2004**, *23*, 3898.
- (57) Dick, A. R.; Kampf, J. W.; Sanford, M. S. *Journal of the American Chemical Society* **2005**, *127*, 12790.
- (58) Racowski, J. M.; Dick, A. R.; Sanford, M. S. *Journal of the American Chemical Society* **2009**, *131*, 10974.

- (59) Powers, D. C.; Ritter, T. *Nature Chemistry* **2009**, *1*, 302.
- (60) Powers, D. C.; Geibel, M. A. L.; Klein, J.; Ritter, T. *Journal of the American Chemical Society* **2009**, *131*, 17050.
- (61) Yamamoto, Y.; Ohno, T.; Itoh, K. *Angewandte Chemie-International Edition* **2002**, *41*, 3662.
- (62) Wang, D. H.; Hao, X. S.; Wu, D. F.; Yu, J. Q. *Organic Letters* **2006**, *8*, 3387.
- (63) Shilov, A. E.; Shul'pin, G. B. *Chemical Reviews* **1997**, *97*, 2879.
- (64) Baik, M. H.; Newcomb, M.; Friesner, R. A.; Lippard, S. J. *Chemical Reviews* **2003**, *103*, 2385.
- (65) Lucke, B.; Narayana, K. V.; Martin, A.; Jahnisch, K. *Advanced Synthesis & Catalysis* **2004**, *346*, 1407.
- (66) Que, L.; Tolman, W. B. *Nature* **2008**, *455*, 333.
- (67) Hartwig, J. F. *Nature* **2008**, *455*, 314.
- (68) Jintoku, T.; Nishimura, K.; Takaki, K.; Fujiwara, Y. *Chemistry Letters* **1990**, 1687.
- (69) Taktak, S.; Flook, M.; Foxman, B. M.; Que, L.; Rybak-Akimova, E. V.; Akimova, R. *Chemical Communications* **2005**, 5301.
- (70) Wang, G. W.; Yuan, T. T.; Wu, X. L. *Journal of Organic Chemistry* **2008**, *73*, 4717.
- (71) Reddy, B. V. S.; Reddy, L. R.; Corey, E. J. *Organic Letters* **2006**, *8*, 3391.
- (72) Giri, R.; Liang, J.; Lei, J. G.; Li, J. J.; Wang, D. H.; Chen, X.; Naggar, I. C.; Guo, C. Y.; Foxman, B. M.; Yu, J. Q. *Angewandte Chemie-International Edition* **2005**, *44*, 7420.

- (73) Vickers, C. J.; Mei, T. S.; Yu, J. Q. *Organic Letters* **2010**, *12*, 2511.
- (74) Mahapatra, A. K.; Bandyopadhyay, D.; Bandyopadhyay, P.; Chakravorty, A. *Journal of the Chemical Society-Chemical Communications* **1984**, 999.
- (75) Mahapatra, A. K.; Bandyopadhyay, D.; Bandyopadhyay, P.; Chakravorty, A. *Inorganic Chemistry* **1986**, *25*, 2214.
- (76) Sinha, C.; Bandyopadhyay, D.; Chakravorty, A. *Inorganic Chemistry* **1988**, *27*, 1173.
- (77) Sinha, C. R.; Bandyopadhyay, D.; Chakravorty, A. *Journal of the Chemical Society-Chemical Communications* **1988**, 468.
- (78) Pal, C. K.; Chattopadhyay, S.; Sinha, C.; Chakravorty, A. *Journal of Organometallic Chemistry* **1992**, *439*, 91.
- (79) Bhawmick, R.; Biswas, H.; Bandyopadhyay, P. *Journal of Organometallic Chemistry* **1995**, *498*, 81.
- (80) Bhawmick, R.; Bandyopadhyay, P. *Transition Metal Chemistry* **1995**, *20*, 415.
- (81) Milet, A.; Dedieu, A.; Canty, A. J. *Organometallics* **1997**, *16*, 5331.
- (82) Zhang, J.; Khaskin, E.; Anderson, N. P.; Zavalij, P. Y.; Vedernikov, A. N. *Chemical Communications* **2008**, 3625.
- (83) Zhang, Y. H.; Yu, J. Q. *Journal of the American Chemical Society* **2009**, *131*, 14654.
- (84) Rostovtsev, V. V.; Labinger, J. A.; Bercaw, J. E.; Lasseter, T. L.; Goldberg, K. I. *Organometallics* **1998**, *17*, 4530.
- (85) Rostovtsev, V. V.; Henling, L. M.; Labinger, J. A.; Bercaw, J. E. *Inorganic Chemistry* **2002**, *41*, 3608.

- (86) Vedernikov, A. N.; Binfield, S. A.; Zavalij, P. Y.; Khusnutdinova, J. R. *Journal of the American Chemical Society* **2006**, *128*, 82.
- (87) Butler, A.; Walker, J. V. *Chemical Reviews* **1993**, *93*, 1937.
- (88) Sotomayor, N.; Lete, E. *Current Organic Chemistry* **2003**, *7*, 275.
- (89) Silverman, G. S.; Rakita, P. E. *Handbook of Grignard Reagents*, 1996.
- (90) Zhang, Y. H.; Shibatomi, K.; Yamamoto, H. *Synlett* **2005**, 2837.
- (91) Prakash, G. K. S.; Mathew, T.; Hoole, D.; Esteves, P. M.; Wang, Q.; Rasul, G.; Olah, G. A. *Journal of the American Chemical Society* **2004**, *126*, 15770.
- (92) Tanemura, K.; Suzuki, T.; Nishida, Y.; Satsumabayashi, K.; Horaguchi, T. *Chemistry Letters* **2003**, *32*, 932.
- (93) Firouzabadi, H.; Iranpoor, N.; Shiri, M. *Tetrahedron Letters* **2003**, *44*, 8781.
- (94) Vyas, P. V.; Bhatt, A. K.; Ramachandraiah, G.; Bedekar, A. V. *Tetrahedron Letters* **2003**, *44*, 4085.
- (95) Widenhoefer, R. A.; Buchwald, S. L. *Journal of the American Chemical Society* **1998**, *120*, 6504.
- (96) Lee, K. J.; Cho, H. K.; Song, C. E. *Bulletin of the Korean Chemical Society* **2002**, *23*, 773.
- (97) Iskra, J.; Stavber, S.; Zupan, M. *Synthesis-Stuttgart* **2004**, 1869.
- (98) Dewkar, G. K.; Narina, S. V.; Sudalai, A. *Organic Letters* **2003**, *5*, 4501.
- (99) Tamhankar, B. V.; Desai, U. V.; Mane, R. B.; Wadgaonkar, P. P.; Bedekar, A. V. *Synthetic Communications* **2001**, *31*, 2021.
- (100) Roche, D.; Prasad, K.; Repic, O.; Blacklock, T. J. *Tetrahedron Letters* **2000**, *41*, 2083.

- (101) Braddock, D. C.; Cansell, G.; Hermitage, S. A. *Synlett* **2004**, 461.
- (102) Evans, P. A.; Brandt, T. A. *Journal of Organic Chemistry* **1997**, *62*, 5321.
- (103) Merkushev, E. B. *Synthesis-Stuttgart* **1988**, 923.
- (104) Snieckus, V. *Chemical Reviews* **1990**, *90*, 879.
- (105) Roy, A. H.; Hartwig, J. F. *Organometallics* **2004**, *23*, 1533.
- (106) van Belzen, R.; Elsevier, C. J.; Dedieu, A.; Veldman, N.; Spek, A. L. *Organometallics* **2003**, *22*, 722.
- (107) Alsters, P. L.; Engel, P. F.; Hogerheide, M. P.; Copijn, M.; Spek, A. L.; Vankoten, G. *Organometallics* **1993**, *12*, 1831.
- (108) Kubota, M.; Boegeman, S. C.; Keil, R. N.; Webb, C. G. *Organometallics* **1989**, *8*, 1616.
- (109) Wong, P. K.; Stille, J. K. *Journal of Organometallic Chemistry* **1974**, *70*, 121.
- (110) Alsters, P. L.; Boersma, J.; Smeets, W. J. J.; Spek, A. L.; Vankoten, G. *Organometallics* **1993**, *12*, 1639.
- (111) Lagunas, M. C.; Gossage, R. A.; Spek, A. L.; van Koten, G. *Organometallics* **1998**, *17*, 731.
- (112) Backvall, J. E. *Tetrahedron Letters* **1977**, 467.
- (113) Backvall, J. E. *Accounts of Chemical Research* **1983**, *16*, 335.
- (114) Fahey, D. R. *Journal of the Chemical Society D-Chemical Communications* **1970**, 417.
- (115) Fahey, D. R. *Journal of Organometallic Chemistry* **1971**, *27*, 283.
- (116) Kodama, H.; Katsuhira, T.; Nishida, T.; Hino, T.; Tsubata, K. *Chem. Abstr.* **2001**, 135.

- (117) Kalyani, D.; Dick, A. R.; Anani, W. Q.; Sanford, M. S. *Tetrahedron* **2006**, *62*, 11483.
- (118) Whitfield, S. R.; Sanford, M. S. *Journal of the American Chemical Society* **2007**, *129*, 15142.
- (119) Balcells, D.; Clot, E.; Eisenstein, O. *Chemical Reviews* **2010**, *110*, 749.
- (120) Alsters, P. L.; Teunissen, H. T.; Boersma, J.; Spek, A. L.; Vankoten, G. *Organometallics* **1993**, *12*, 4691.
- (121) Wadhwani, P.; Bandyopadhyay, D. *Organometallics* **2000**, *19*, 4435.
- (122) Canty, A. J.; Dedieu, A.; Jin, H.; Milet, A.; Richmond, M. K. *Organometallics* **1996**, *15*, 2845.
- (123) Zhang, F. B.; Broczkowski, M. E.; Jennings, M. C.; Puddephatt, R. J. *Canadian Journal of Chemistry-Revue Canadienne De Chimie* **2005**, *83*, 595.
- (124) Wieghardt, K.; Koppen, M.; Swiridoff, W.; Weiss, J. *Journal of the Chemical Society-Dalton Transactions* **1983**, 1869.
- (125) Vedernikov, A. N.; Pink, M.; Caulton, K. G. *Inorganic Chemistry* **2004**, *43*, 3642.
- (126) Vedernikov, A. N. *Chemical Communications* **2009**, 4781.
- (127) Powers, D. C.; Benitez, D.; Tkatchouk, E.; Goddard, W. A.; Ritter, T. *Journal of the American Chemical Society* **2010**, *132*, 14092.
- (128) Desai, L. V.; Hull, K. L.; Sanford, M. S. *Journal of the American Chemical Society* **2004**, *126*, 9542.
- (129) Lapointe, D.; Fagnou, K. *Chemistry Letters* **2010**, *39*, 1119.

- (130) Ye, Y. D.; Ball, N. D.; Kampf, J. W.; Sanford, M. S. *Journal of the American Chemical Society* **2010**, *132*, 14682.
- (131) Powers, D. C.; Ritter, T. *Nature Chemistry* **2009**, *1*, 419.
- (132) Vedernikov, A. N. In *C-X Bond Formation* 2010; Vol. 31, p 101.
- (133) Arnold, P. L.; Sanford, M. S.; Pearson, S. M. *Journal of the American Chemical Society* **2009**, *131*, 13912.
- (134) Ball, N. D.; Sanford, M. S. *Journal of the American Chemical Society* **2009**, *131*, 3796.
- (135) Furuya, T.; Ritter, T. *Journal of the American Chemical Society* **2008**, *130*, 10060.
- (136) Shabashov, D.; Daugulis, O. *Journal of the American Chemical Society* **2010**, *132*, 3965.
- (137) Hull, K. L.; Anani, W. Q.; Sanford, M. S. *Journal of the American Chemical Society* **2006**, *128*, 7134.
- (138) Wang, X. S.; Mei, T. S.; Yu, J. Q. *Journal of the American Chemical Society* **2009**, *131*, 7520.
- (139) Kaspı, A. W.; Yahav-Levi, A.; Goldberg, I.; Vigalok, A. *Inorganic Chemistry* **2008**, *47*, 5.
- (140) Vigalok, A. *Chemistry-a European Journal* **2008**, *14*, 5102.
- (141) Furuya, T.; Kaiser, H. M.; Ritter, T. *Angewandte Chemie-International Edition* **2008**, *47*, 5993.
- (142) Boisvert, L.; Denney, M. C.; Hanson, S. K.; Goldberg, K. I. *Journal of the American Chemical Society* **2009**, *131*, 15802.

- (143) Khusnutdinova, J. R.; Zavalij, P. Y.; Vedernikov, A. N. *Organometallics* **2007**, *26*, 2402.
- (144) Khaskin, E.; Zavalij, P. Y.; Vedernikov, A. N. *Angewandte Chemie-International Edition* **2007**, *46*, 6309.
- (145) Byers, P. K.; Canty, A. J.; Skelton, B. W.; White, A. H. *Organometallics* **1990**, *9*, 826.
- (146) Trofimenko, S. *Chemical Reviews* **1993**, *93*, 943.
- (147) Sobanov, A. A.; Vedernikov, A. N.; Dyker, G.; Solononov, B. N. *Mendeleev Communications* **2002**, 14.
- (148) Bennett, M. A.; Canty, A. J.; Felixberger, J. K.; Rendina, L. M.; Sunderland, C.; Willis, A. C. *Inorganic Chemistry* **1993**, *32*, 1951.
- (149) Gulliver, D. J.; Levason, W. *Journal of the Chemical Society-Dalton Transactions* **1982**, 1895.
- (150) Klaui, W.; Glaum, M.; Wagner, T.; Bennett, M. A. *Journal of Organometallic Chemistry* **1994**, *472*, 355.
- (151) Fuchita, Y.; Hiraki, K.; Kage, Y. *Bulletin of the Chemical Society of Japan* **1982**, *55*, 955.
- (152) de Geest, D. J.; O'Keefe, B. J.; Steel, P. J. *Journal of Organometallic Chemistry* **1999**, *579*, 97.
- (153) Annibale, G.; Canovese, L.; Cattalini, L.; Natile, G.; Biaginicini, M.; Manottilanfredi, A. M.; Tiripicchio, A. *Journal of the Chemical Society-Dalton Transactions* **1981**, 2280.

- (154) Khutia, A.; Miguel, P. J. S.; Lippert, B. *Inorganica Chimica Acta* **2010**, *363*, 3048.
- (155) Sommerer, S. O.; Jircitano, A. J.; Westcott, B. L.; Abboud, K. A.; Bauer, J. A. K. *Acta Crystallographica Section C-Crystal Structure Communications* **1997**, *53*, 707.
- (156) Crabtree, R. H. *The Organometallic Chemistry of the Transition Metals*; 4 ed., 2005.
- (157) Thienthong, N.; Bergman, Y. E.; Perlmutter, P. *Synthetic Communications* **2009**, *39*, 2683.
- (158) Shah, R. C.; Raman, P. V.; Shah, B. M.; Vora, H. H. *Drug Development Communications* **1976**, *2*, 393.
- (159) Glasoe, P. K.; Long, F. A. *Journal of Physical Chemistry* **1960**, *64*, 188.
- (160) Beyer, H.; Lassig, W.; Schudy, G. *Chemische Berichte-Recueil* **1957**, *90*, 592.
- (161) Stowers, K. J.; Sanford, M. S. *Organic Letters* **2009**, *11*, 4584.
- (162) Whitfield, S. R.; Sanford, M. S. *Organometallics* **2008**, *27*, 1683.
- (163) Kamaraj, K.; Bandyopadhyay, D. *Organometallics* **1999**, *18*, 438.
- (164) Rashidi, M.; Nabavizadeh, M.; Hakimelashi, R.; Jamali, S. *Journal of the Chemical Society-Dalton Transactions* **2001**, 3430.
- (165) Yassin, A. A.; Elreedy, A. M. *European Polymer Journal* **1973**, *9*, 657.
- (166) Parr, R. G.; Yang, W. *Density-functional Theory of Atoms and Molecules*; Oxford University Press: Oxford, 1989.
- (167) Perdew, J. P.; Burke, K.; Ernzerhof, M. *Physical Review Letters* **1996**, *77*, 3865.

- (168) Laikov, D. N. *Chemical Physics Letters* **1997**, *281*, 151.
- (169) Anslyn, E. A.; Dougherty, D. A. *Modern Physical Organic Chemistry*; University Science Books, 2006.
- (170) Cundari, T. R.; Stevens, W. J. *Journal of Chemical Physics* **1993**, *98*, 5555.
- (171) Stevens, W. J.; Krauss, M.; Basch, H.; Jasien, P. G. *Canadian Journal of Chemistry-Revue Canadienne De Chimie* **1992**, *70*, 612.
- (172) Stevens, W. J.; Basch, H.; Krauss, M. *Journal of Chemical Physics* **1984**, *81*, 6026.
- (173) Inc., S.; 7.6 ed.; Shrodinger Inc.: Portland, OR, 2009.
- (174) Bercaw, J. E.; Durrell, A. C.; Gray, H. B.; Green, J. C.; Hazari, N.; Labinger, J. A.; Winkler, J. R. *Inorganic Chemistry* **2010**, *49*, 1801.
- (175) Zhang, J.; Vedernikov, A.; University of Maryland: College Park, 2008.
- (176) Canty, A. J.; Traill, P. R.; Skelton, B. W.; White, A. H. *Journal of Organometallic Chemistry* **1992**, *433*, 213.
- (177) Canty, A. J.; Jin, H.; Roberts, A. S.; Skelton, B. W.; White, A. H. *Organometallics* **1996**, *15*, 5713.
- (178) Sehnal, P.; Taylor, R. J. K.; Fairlamb, I. J. S. *Chemical Reviews* **2010**, *110*, 824.
- (179) Williams, B. S.; Holland, A. W.; Goldberg, K. I. *Journal of the American Chemical Society* **1999**, *121*, 252.
- (180) Williams, B. S.; Goldberg, K. I. *Journal of the American Chemical Society* **2001**, *123*, 2576.

- (181) Luinstra, G. A.; Labinger, J. A.; Bercaw, J. E. *Journal of the American Chemical Society* **1993**, *115*, 3004.
- (182) Khusnutdinova, J. R.; Zavalij, P. Y.; Vedernikov, A. N. *Organometallics* **2007**, *26*, 3466.
- (183) Khusnutdinova, J. R.; Newman, L. L.; Zavalij, P. Y.; Lam, Y. F.; Vedernikov, A. N. *Journal of the American Chemical Society* **2008**, *130*, 2174.
- (184) Canty, A. J. *Accounts of Chemical Research* **1992**, *25*, 83.
- (185) Vanasselt, R.; Rijnberg, E.; Elsevier, C. J. *Organometallics* **1994**, *13*, 706.
- (186) Canty, A. J.; Vankoten, G. *Accounts of Chemical Research* **1995**, *28*, 406.
- (187) Suginome, M.; Kato, Y.; Takeda, N.; Oike, H.; Ito, Y. *Organometallics* **1998**, *17*, 495.
- (188) Campora, J.; Palma, P.; del Rio, D.; Lopez, J. A.; Alvarez, E.; Connelly, N. G. *Organometallics* **2005**, *24*, 3624.
- (189) Smythe, N. A.; Grice, K. A.; Williams, B. S.; Goldberg, K. I. *Organometallics* **2009**, *28*, 277.
- (190) Mann, G.; Hartwig, J. F. *Journal of the American Chemical Society* **1996**, *118*, 13109.
- (191) Widenhofer, R. A.; Zhong, H. A.; Buchwald, S. L. *Journal of the American Chemical Society* **1997**, *119*, 6787.
- (192) Mann, G.; Incarvito, C.; Rheingold, A. L.; Hartwig, J. F. *Journal of the American Chemical Society* **1999**, *121*, 3224.
- (193) Komiyama, S.; Akai, Y.; Tanaka, K.; Yamamoto, T.; Yamamoto, A. *Organometallics* **1985**, *4*, 1130.

- (194) Shelby, Q.; Kataoka, N.; Mann, G.; Hartwig, J. *Journal of the American Chemical Society* **2000**, *122*, 10718.
- (195) Mann, G.; Shelby, Q.; Roy, A. H.; Hartwig, J. F. *Organometallics* **2003**, *22*, 2775.
- (196) Stambuli, J. R.; Weng, Z. Q.; Incarvito, C. D.; Hartwig, J. F. *Angewandte Chemie-International Edition* **2007**, *46*, 7674.
- (197) Crumpton, D. M.; Goldberg, K. I. *Journal of the American Chemical Society* **2000**, *122*, 962.
- (198) Crumpton-Bregel, D. M.; Goldberg, K. I. *Journal of the American Chemical Society* **2003**, *125*, 9442.
- (199) Arthur, K. L.; Wang, Q. L.; Bregel, D. M.; Smythe, N. A.; O'Neill, B. A.; Goldberg, K. I.; Moloy, K. G. *Organometallics* **2005**, *24*, 4624.
- (200) Goldberg, K. I.; Yan, J. Y.; Winter, E. L. *Journal of the American Chemical Society* **1994**, *116*, 1573.
- (201) Goldberg, K. I.; Yan, J. Y.; Breitung, E. M. *Journal of the American Chemical Society* **1995**, *117*, 6889.
- (202) Pawlikowski, A. V.; Getty, A. D.; Goldberg, K. I. *Journal of the American Chemical Society* **2007**, *129*, 10382.
- (203) Yahav-Levi, A.; Goldberg, I.; Vigalok, A.; Vedernikov, A. N. *Journal of the American Chemical Society* **2008**, *130*, 724.
- (204) Driver, M. S.; Hartwig, J. F. *Journal of the American Chemical Society* **1997**, *119*, 8232.

- (205) Baranano, D.; Hartwig, J. F. *Journal of the American Chemical Society* **1995**, *117*, 2937.
- (206) Mann, G.; Baranano, D.; Hartwig, J. F.; Rheingold, A. L.; Guzei, I. A. *Journal of the American Chemical Society* **1998**, *120*, 9205.
- (207) Chen, X.; Döbereiner, G.; Hao, X. S.; Giri, R.; Mangel, N.; Yu, J. Q. *Tetrahedron* **2009**, *65*, 3085.
- (208) Higgs, A. T.; Zinn, P. J.; Sanford, M. S. *Organometallics* **2010**, *29*, 5446.
- (209) Taylor, R. *Electrophilic Aromatic Substitution*, 1990.
- (210) De La Mere, P. B. *Electrophilic Halogenation*.
- (211) Yahav-Levi, A.; Goldberg, I.; Vigalok, A. *Journal of the American Chemical Society* **2006**, *128*, 8710.
- (212) Ettore, R. *Inorganic & Nuclear Chemistry Letters* **1969**, *5*, 45.
- (213) Canty, A. J.; Hoare, J. L.; Davies, N. W.; Traill, P. R. *Organometallics* **1998**, *17*, 2046.
- (214) Canty, A. J.; Watson, A. A.; Skelton, B. W.; White, A. H. *Journal of Organometallic Chemistry* **1989**, *367*, C25.
- (215) Archer, G. A.; Stempel, A.; Ho, S. S.; Sternbach, L. *Journal of the Chemical Society C-Organic* **1966**, 1031.
- (216) Ames, D. E.; Opalko, A. *Tetrahedron* **1984**, *40*, 1919.
- (217) Lee, C. T.; Lipshutz, B. H. *Organic Letters* **2008**, *10*, 4187.
- (218) Kim, S. H.; Rieke, R. D. *Tetrahedron* **2010**, *66*, 3135.
- (219) Limited, H. E. C. C.

- (220) Fujikawa, K. I.; Kondo, K.; Yokomich.I; Kimura, F.; Haga, T.; Nishiyam.R  
*Agricultural and Biological Chemistry* **1970**, *34*, 68.
- (221) Lin, Z. Y. *Coordination Chemistry Reviews* **2007**, *251*, 2280.
- (222) Boutadla, Y.; Davies, D. L.; Macgregor, S. A.; Poblador-Bahamonde, A. I.  
*Dalton Transactions* **2009**, 5820.
- (223) Winstein, S.; Traylor, T. G. *Journal of the American Chemical Society* **1955**,  
*77*, 3747.
- (224) Corwin, A. H.; Naylor, M. A. *Journal of the American Chemical Society*  
**1947**, *69*, 1004.
- (225) Klapproth, W. J.; Westheimer, F. H. *Journal of the American Chemical*  
*Society* **1950**, *72*, 4461.
- (226) Brown, H. C.; McGary, C. W. *Journal of the American Chemical Society*  
**1955**, *77*, 2300.
- (227) Brown, H. C.; McGary, C. W. *Journal of the American Chemical Society*  
**1955**, *77*, 2306.
- (228) Brown, H. C.; McGary, C. W. *Journal of the American Chemical Society*  
**1955**, *77*, 2310.
- (229) Brown, H. C.; Nelson, K. L. *Journal of the American Chemical Society* **1953**,  
*75*, 6292.
- (230) Ryabov, A. D.; Sakodinskaya, I. K.; Yatsimirsky, A. K. *Journal of the*  
*Chemical Society-Dalton Transactions* **1985**, 2629.
- (231) Kurzeev, S. A.; Kazankov, G. M.; Ryabov, A. D. *Inorganica Chimica Acta*  
**2002**, *340*, 192.

- (232) Davies, D. L.; Donald, S. M. A.; Macgregor, S. A. *Journal of the American Chemical Society* **2005**, *127*, 13754.
- (233) Williamson, O., 2011.
- (234) Oloo, W. 2011.
- (235) Fabien, R.; Claude, P.; Gerald, B.; Jean-Claude, G.; Gerard, H. *European Journal of Chemistry* **1997**, *3*.
- (236) Kalyani, D.; Sanford, M. S. *Organic Letters* **2005**, *7*, 4149.
- (237) Basil, B.; Coffee, E. C. J.; Gell, D. L.; Maxwell, D. R.; Sheffield, D.; Wooldrid, K. *Journal of Medicinal Chemistry* **1970**, *13*, 403.
- (238) Labinger, J. A.; Bercaw, J. E. *Nature* **2002**, *417*, 507.
- (239) Uemura, T.; Imoto, S.; Chatani, N. *Chemistry Letters* **2006**, *35*, 842.
- (240) Sammes, P. G.; Serraerrante, G.; Tinker, A. C. *Journal of the Chemical Society-Perkin Transactions 1* **1978**, 853.
- (241) Friedle, S.; Lippard, S. J. *European Journal of Inorganic Chemistry* **2009**, 5506.